# Proceedings of the 1st Plant biomechanics International conference

Bernard Thibaut, Joseph Gril, Bernard Chanson, Caroline Loup, Jeronimidis Georges

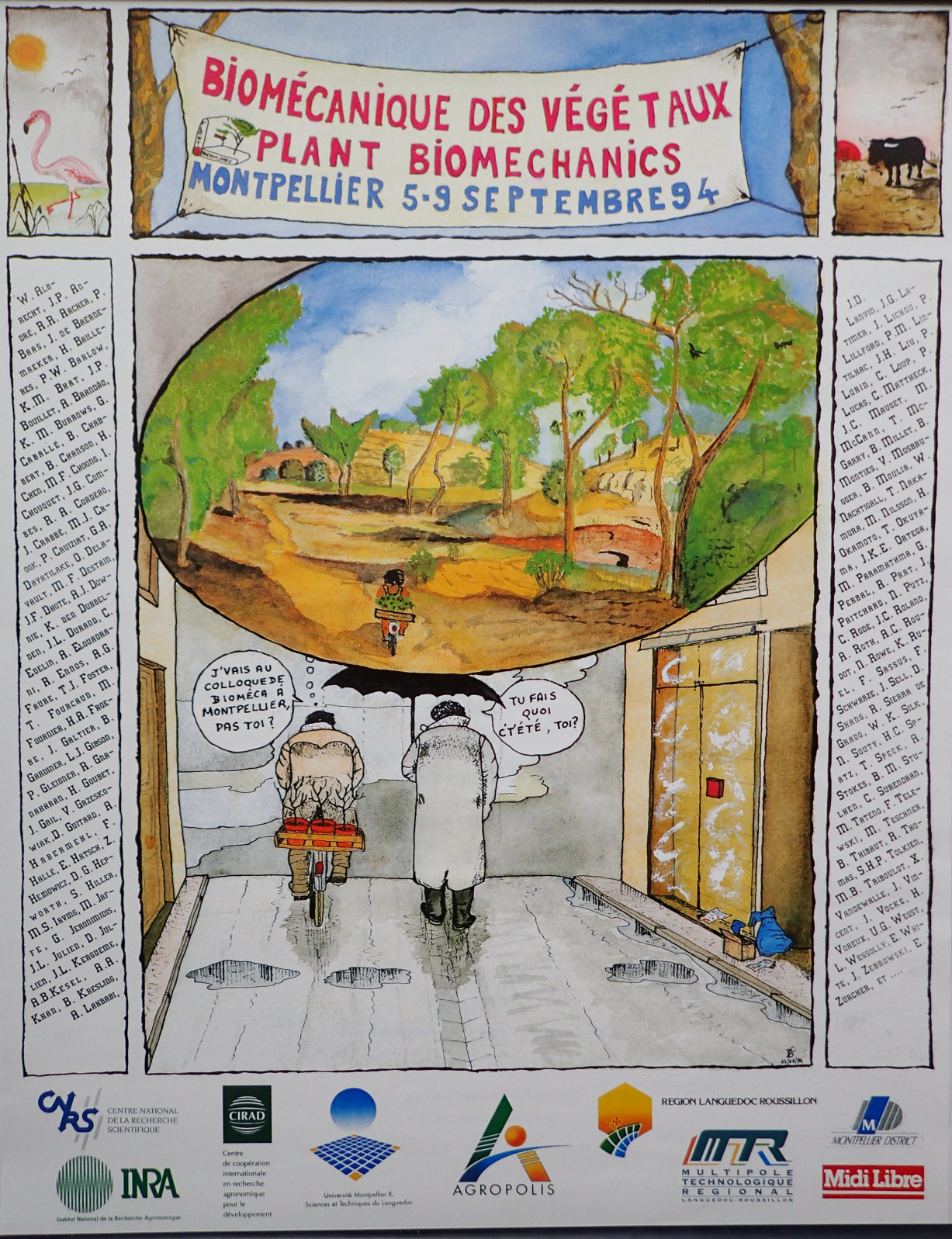


Conference poster by Bernard CHANSON - 1994
*(the name of participants is indicated on both sides)*

PLANT BIOMECHANICS • Septembre 1994 • Résumés •

CENTRE NATIONAL DE LA RECHERCHE SCIENTIFIQUE

INRA
Institut National de la Recherche Agronomique

CIRAD

Université Montpellier II, Sciences et Techniques du Languedoc

ELSEVIER

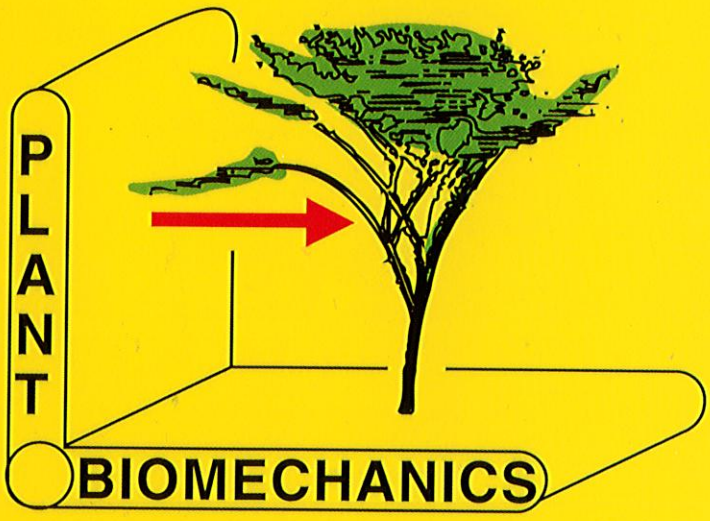


**Actes - *Proceedings***

# 5-9 septembre 1994

## Colloque interdisciplinaire du Comité national de la recherche scientifique

## Montpellier – France

Le colloque de biomécanique des végétaux est organisé sous l'égide du Centre national de la recherche scientifique (CNRS).

Avec la participation de :

- ✓ Institut national de la recherche agronomique (INRA)
- ✓ Université de Montpellier II (UM II)
- ✓ Centre de coopération internationale de recherche agronomique pour le développement (CIRAD).

Et le soutien de :

- ✓ Agropolis
- ✓ Conseil régional du Languedoc-Roussillon
- ✓ Multipôle technologique régional du Languedoc-Roussillon.

AGROPOLIS

REGION Languedoc Roussillon

MULTIPOLE TECHNOLOGIQUE REGIONAL LANGUEDOC-ROUSSILLON

# Biomécanique des végétaux
# *Plant biomechanics*

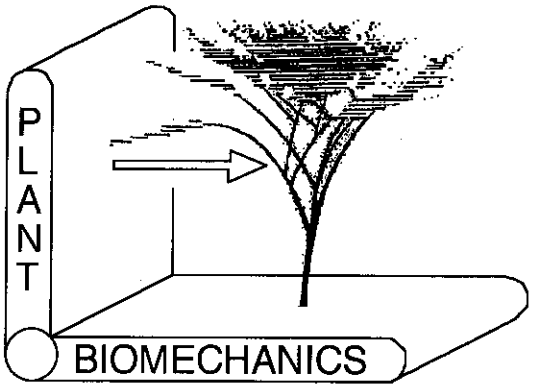


**RÉSUMÉS - *SUMMARIES***

Colloque interdisciplinaire
du Comité national de la recherche scientifique
Montpellier (France) du 5 au 9 Septembre 1994

# PRÉFACE

Ce colloque est le résultat d'une volonté affichée par le Comité national de la recherche scientifique : promouvoir l'interdisciplinarité, c'est-à-dire la rencontre et la mise en commun des compétences de disciplines différentes pour aborder des grands problèmes de la recherche actuelle.

La biomécanique des végétaux est typiquement un champ de recherches qui nécessite la synergie entre des scientifiques de la biologie végétale, de la modélisation des systèmes complexes et de la mécanique des matériaux et des structures.

Elle a pour objectif :

- une meilleure compréhension de la morphogenèse et du fonctionnement des organes de soutien chez les plantes,
- une contribution à l'analyse des relations entre fonctionnement des plantes cultivées et qualité de la production,
- une analyse de la croissance, du développement, de la structure et particulièrement de la tenue mécanique des plantes modifiées par l'homme ou son environnement,
- le développement, grâce à l'étude des végétaux, de procédés et de types de constructions originaux, inspirés des phénomènes biologiques (bionique ou biomimétique).

Depuis quelques années cette thématique nouvelle a connu un développement important en Amérique du Nord, au Japon et en Europe, notamment en Grande-Bretagne, en Allemagne et en France.

L'intiative du Comité national a donc permis d'organiser le premier colloque international entièrement dédié à la biomécanique des végétaux et l'ensemble des résumés de communications volontaires[1] ci-après reflète bien les principaux axes de recherches développés actuellement. A côté des préoccupations fondamentales sur la morphogenèse et la croissance des végétaux, se retrouvent des recherches plus finalisées visant à répondre aux demandes des forestiers, du monde agricole, des industries agroalimentaires ou des gestionnaires de parcs et jardins. Ces aller-retours entre la connaissance et les applications constituent le deuxième point fort de ce colloque qui se veut d'abord un moment de rencontre entre les uns et les autres.

Bernard THIBAUT
Président du Comité d'organisation

[1] L'ensemble des textes des communications invitées fait l'objet d'une publication séparée dans 2 numéros spéciaux de la revue *Biomimetics*.

# FOREWORD

This congress is the result of a voluntary policy of the French National Committee for Scientific Research to promote interdisciplinarity. Some of the major problems encountered by present research require the collaboration and association of abilities from various disciplines.

Plant biomechanics is a typical case, since it requires a synergy between scientists involved in plant biology, the modelling of complex systems, and the mechanics of materials and structures.

This field aims at improving the understanding and analysis of:

- morphogenesis and function of supporting organs in plants;
- relationships between mechanical functions of cultivated plants and the quality of crops;
- growth, development, structure and mechanical strength of plant systems relative to modifications imposed by man and the environment;
- plant mechanical, structural and responsive designs as paradigms, in a biomimetic sense, for man-made applications.

During the last few years, this new theme has been developed in North America, Japan and Europe, particularly in Great Britain, Germany and France.

The first international congress entirely devoted to plant biomechanics is thus due to the initiative of the national committee. The following collection of voluntary contributions[2] reflects the main axes of the research under development, either basic approaches to morphogenesis and plant growth, or applied research aiming to meet the needs of foresters, the agricultural sector, the food industry and park managers. The level of interaction between specialists in basic and applied knowledge is another strong feature of this congress, which should be, primarily, an occasion to meet others.

Bernard THIBAUT
President of the Organising Committee

[2] The text of invited papers has been published separately in two special issues of *Biomimetics*.

## COMITÉ SCIENTIFIQUE - *SCIENTIFIC COMMITTEE*

| | |
|---|---|
| R.R. ARCHER | Univ. of Massachusetts (USA) |
| P. BAAS | Hortus Botanicus (N) |
| J. CRABBE | Univ. Gembloux (B) |
| P. CRUIZIAT | INRA Clermont-Ferrand (F) |
| A.R. ENNOS | Univ. Manchester (UK) |
| B. GARDINER | Forestry Commission (UK) |
| D. GUITARD | Univ. Bordeaux (F) |
| F. HALLE | Univ. Montpellier (F) |
| M. JAFFE | Wake Forest Univ. (USA) |
| G. JERONIMIDIS | Univ. Reading (UK) |
| B. MONTIES | INRA Grignon (F) |
| V. MOSBRUGGER | Univ. Tübingen (D) |
| J.C. ROLAND | Univ. Paris VI (F) |
| K. RUEL | CNRS Grenoble (F) |
| W. SILK | Univ. Davis (USA) |
| T. SPECK | Univ. Freiburg (D) |
| H.-Ch. SPATZ | Univ. Freiburg (D) |
| B. THIBAUT | CNRS Montpellier (F) |
| J. VINCENT | Univ. Reading (UK) |

## COMITÉ D'ORGANISATION - *ORGANISING COMMITTEE*

| | |
|---|---|
| B. CHANSON | CNRS Bordeaux (F) |
| J.L. DURAND | INRA Lusignan (F) |
| M. FOURNIER | ENGREF Paris (F) |
| J. GRIL | CNRS Montpellier (F) |
| G. JERONIMIDIS | Univ. Reading (UK) |
| C. LOUP | Univ. Montpellier II (F) |
| B. MOULIA | INRA Grignon (F) |
| T. SPECK | Botanical Garden Freiburg (D) |
| B. THIBAUT | CNRS Montpellier (F) |

Pour des renseignements complémentaires contacter - *For additional information please contact*

Bernard THIBAUT
LMGC "Bois", CP 081
Université Montpellier II - Place E.-Bataillon
34095 MONTPELLIER CEDEX 5 - FRANCE
Tel : (33) 67 14 34 31 - Fax : (33) 67 54 48 52
E-mail : jgril@lmgc.univ-montp2.fr

# SOMMAIRE

## Optimized distribution of lateral strength in trees.

Albrecht, W., Bethge, K., Mattheck, C.

Kernforschungszentrum Karlsruhe
Institut für Materialforschung II
Postfach 3640
76021 Karlsruhe
Germany

### Summary

Through evolution and competition with other living forms, trees had to optimize themselves. Metzger [1] was the first who found a relationship between tree design and mechanical loading. He showed that the stem of spruce trees taper in a manner which leads to a constant mechanical stress along the surface. This principle of even load distribution was generalized to biological load carriers and was called "Constant Stress Axiom" by Mattheck and co-workers. [2,3,4] The constant stress axiom is limited to the surface of the tree. Nevertheless, even intact trees could fail by the failure mode described in Fig. 1. This failure mode is caused by internal lateral stress.

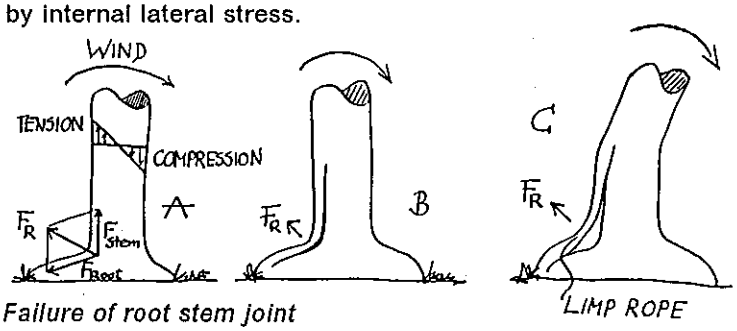


Fig. 1: *Failure of root stem joint*

If a curved beam is bent in order to be straightened,lateral tensile stresses in the radial direction could not be avoided [5]. These tensile stresses are zero on the surface and have their maximum inside the structure. In trees a lot of curved beams are hidden and are called hazard beams. Every curved stem, every curved branche or root stem joint could act as a hazard beam. If they were straightened they often fail by delamination of the wood fibres. In order to find out whether there is some reaction in the tree to avoid this failure mode, more than 15 different trees have been studied. A side-view photograph was taken from each of them and a 2-dimensional finite element calculation was done under bending load, in order to get the stress distribution perpendicular to the grain inside the tree. A sample of drilling cores where taken out of the tree with a 5mm diameter increment borer. At the Karlsruhe Nuclear Research Center a small wood testing device called Fractometer [6] (see Fig. 2) was developed to measure the bending strength of increment cores. The cylindrical samples had been broken successively along their length with the Fractometer. Strength distribution within the core and from core to core within the stem was recorded. In any case there was an evident increase in lateral strength in the same zone where highest lateral stresses perpendicular to the grain were computed in the previously calculated FE-model (see Fig. 3).

In simple words: the measured splitting resistance is highest where the greatest splitting stresses are computed.

So there is further evidence to suggest that strength of wood is controlled by local mechanical stress.

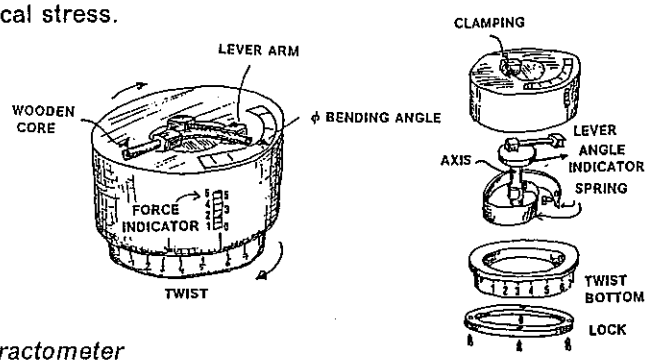


Fig 2: *Fractometer*

Wood rays run into the direction in which lateral splitting stress is acting. So it is very easy to imagine that the wood ray system is mainly responsible for lateral strength. Also there must be an adaptive mechanism which enables the tree to detect laterally highly loaded zones and prevent tree splitting by increasing the wood quality, i.e. the lateral strength which is the resistance against splitting.

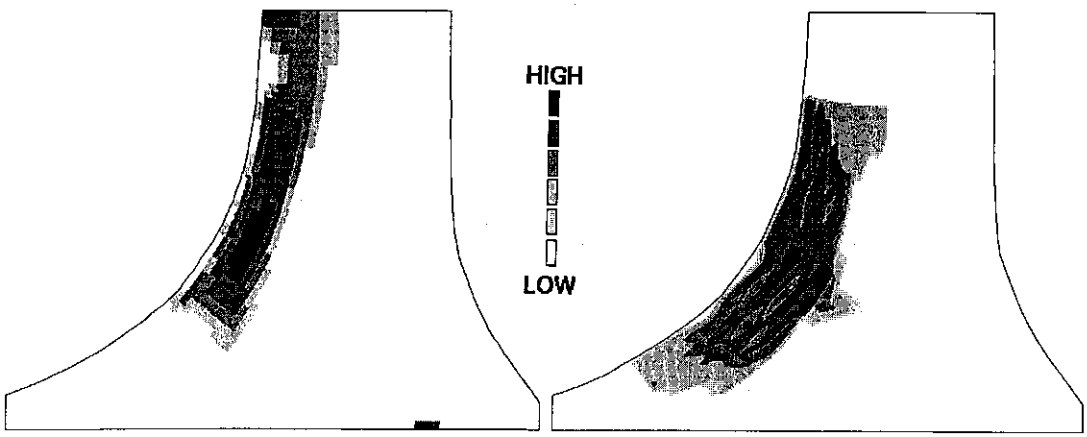


Fig. 3: *Stress and strength distribution perpendicular to the grain*

**References**

[1] *Metzger, K.* Der Wind als maßgeblicher Faktor für das Wachstum der Bäume, Mündener forstliche Hefte, Springer Verlag, Berlin 1893

[2] *Mattheck, C.* Trees- the mechanical design, Springer Verlag, Heidelberg 1991

[3] *Mattheck, C.* Design in der Natur, Rombach Verlag, Freiburg 1992

[4] *Mattheck, C., Breloer, H.,* Handbuch der Schadenskunde von Bäumen - der Baumbruch in Mechanik und Rechtsprechung, Rombach Verlag, Freiburg 1993

[5] *Young, W.,* Roark's Formulas for Stress & Strain, McGraw-Hill Book Company, New York, 6th edition

[6] *Mattheck, C., Bethge, K.,* Das Fractometer: Ein Prüfgerät für Holz im Taschenformat, Allg. Forst Zeitschrift, Nr.3, 1993

# ETUDE PAR MICROMOULAGE DE L'ARCHITECTURE VASCULAIRE DE LA PLANTE ENTIERE

J.P. ANDRÉ - INRA - ANTIBES

On entend ici par architecture vasculaire de la plante entière la disposition des vaisseaux d'origine procambiale (xylème primaire), puis d'origine cambiale (xylème secondaire), dans les faisceaux qui relient les axes de la plante à leurs organes adjacents. Elle est en grande partie déterminée par la phyllotaxie de l'espèce.

L'examen des connexions vasculaires dans les zones nodales et le suivi des trajets longitudinaux des vaisseaux de grande longueur présentent des difficultés d'ordre histologique bien connues.

Une technique récente consistant à matérialiser la lumière des vaisseaux par remplissage avec un polymère réticulable, puis à dégager ces moulages internes par destruction totale ou partielle des parois du xylème, fournit une vision nouvelle de ce tissu et un utile complément aux techniques histologiques classiques.

Plus généralement, la technique permet le moulage de la lumière de toute cellule du xylème (fibre, trachéide, parenchyme) et d'autres tissus, à la condition qu'elle soit vide et que sa paroi primaire soit, en un point, poreuse au polymère.

L'excellente définition de surface du moulage paraît être de l'ordre de 0,1 $\mu$m.

L'architecture vasculaire du plant de tomate est choisie ici pour illustrer les possibilités nouvelles d'investigation de la technique des micromoulages.

## BIBLIOGRAPHIE :

ANDRÉ, J.P., 1993 - Micromoulage des espaces vides intra et intercellulaires dans les tissus végétaux. C.R. Ac. Sc. Paris, 316, 1336-41.
FUJII, T., 1993 - Application of a resin casting method to wood anatomy of some japanese Fagacae species. IAWA J. 14 (3) 273-288.

ARCHITECTURE VASCULAIRE DU PLANT DE TOMATE

*Lycopersicum esculentum, Mill.*

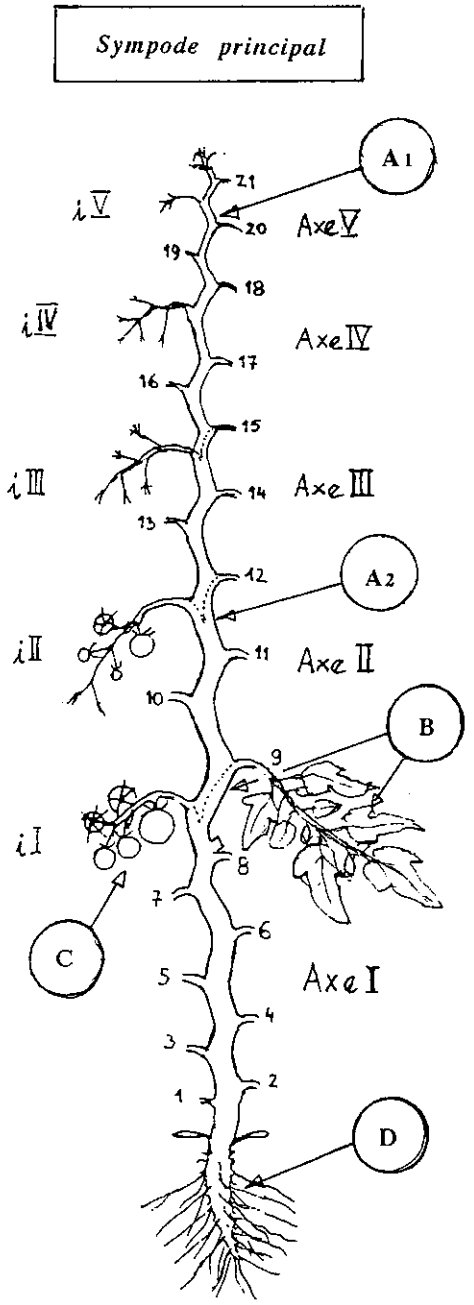


A1 A2
*Vascularisation primaire et secondaire de l'axe*

B
*Vascularisation foliaire trace foliaire*

C
*Vascularisation du fruit zone d'abscission*

D
*Vascularisation racinaire Connexion pivot-racine*

# Induction of reaction wood : the loop experiment revisited

R.R. ARCHER
University of Massachusetts
Amherst, Mass. U.S.A.

## Introduction

For a more complete discussion of the induction of reaction wood, see the review article Wilson & Archer 1977. The literature contains a lerge number of experiments where branches or stems are tilted or bent into various configurations. Most of these experiments are designed to prove or disprove various hypotheses with the goal of showing that a single stimulus is involved.

Many of these experiments involved bending stems into partial and full loops. In some cases, conclusions as to the role of compressive or tensile stresses in the induction of reaction wood were made. For example, Sinnott (1952) reports the observation by Ewart & Mason-Jones (1906) that for the vertical loop experiment, compression wood "did not develop on the inside of the entire loop, as it should have done if compression were the factor chiefly involved, but formed on the lower side of both the upper and lower portions of the loop, as if gravity determined its position". In the course of bending the stem into a loop, the initial stress state is indeed compressive on the inside of the entire loop. Cells in the cambial zone on the inside of the loop are developing adjacent to mature cells that have been compresses. Cells either attempt to expand in place or to contract depending upon whether they are compression or normal wood cells. These growth strains can produce considerable stresses and deformation of the loop. Depending upon how the loop is supported, a new increment of stress is produced in the new layer of cells (Archer, 1987). This new stress state can be very different from the initial stress state, and as this process is reprated in layer after layer, one can test the stress hypothesis that cells that develop in cambial zones adjacent to xylem in a state of compression become compression wood. In the present paper, our objective is to present the analysis which would seem to be necessary in order to apply the stress hypothesis to a given problem where mechanical action of reaction wood is involved.

## Analysis

The stem is modeled as a tapered elastic rod which is subjected to a set of loads to deform it into some desired state and then it is supported so as to remain fixed at one or more points. For a given time interval, a small increment of radial growth takes place. Where radially adjacent xylem cells in a state of compression/tension then compression/tension wood cells develop elsewhere around the periphery of the stem normal wood cells develop. Using methods presented in Archer (1987), it is possible to calculate the increment of new stresses in the entire stem due to the mechanical action of each new increment of growth. The associated deformation of the stem is also calculated.

A particular stem experiment is studied for which experiments were carried out by Sinnott (1952). Comparisons with the results of his experiments can only be qualitative since there are too many parameters which need to be estimated and which are not avalaible. The purpose of the present work is to show the potential of this kind of analysis for problems where more quantitative data are avalaible.

## Results

In one set of the many experiments with young trees of *Pinus strobus*, Sinnott (1952, Fig.3) pulled down the tree leader until the tip had undergone a rotation of 180° and was parallel to its basal portion (Fig.1). A tie held the tip^in this position. The xylem stresses and the bent shape shown in Fig.1 for the half loop were calculated using a theory for the elastic bending of tapered rods (Archer 1987). A simplified model for the compression wood (CW) action was

used. Growth increments each corresponding to 10% of the annual growth were added to the stem. If the newly developing wood in the cambial zone was adjacent to wood in compression, the CW cells are assumed to be formed and the resulting mechanical action of the CW will stress and deform the stem including the new layer of wood. Repeated application of these rules for CW induction provides an algorithm for the formation of CW according to the stess hypothesis. In Fig.3, typical stress distributions in newly grown layers (for layers 9 and 10, the last two layers in the annual growth) are presented.

A summary of the induction of CW based upon the stress hypothesis is given in Fig.2. A vertical section through the stem is made and the stem is shown as straight. Portions of growth layers shown as shaded represent CW. The initial compression zones at the periphery of the newly bent stem are indicated by lower case letters "c" (Fig.2). The experiments carried out by Sinnott (1952) result in CW located over the first 70% of the inside of the bent stem and then over the last 30% of the outside as shown by shading in Fig.1 and marked by arrows in Fig2.

According to the above analysis, starting with the initial compressive stress state in the newly bent stem on through most of the stress states induced in the new growth layers but CW action, there is a tendancy to create CW in the general regions of the stem where Sinnott (1952) observed CW.

## References

ARCHER, R.R. (1987). Growth stresses and strains in trees. Springer Verlag, 240p.
EWART, A.W. & MASON-JONES, A.J. (1906). The formation of red wood in conifers. Ann. Bot. **20** : 201-204.
SINNOTT, E.W. (1952). Reaction wood and the regulation of tree form. Am. J. Bot. **39** : 69-78
WILSON, B.F. & ARCHER, R.R. (1977). Reaction wood : Induction and mechanical action. Ann. Rev. Plant Physiol. **28** : 23-43.

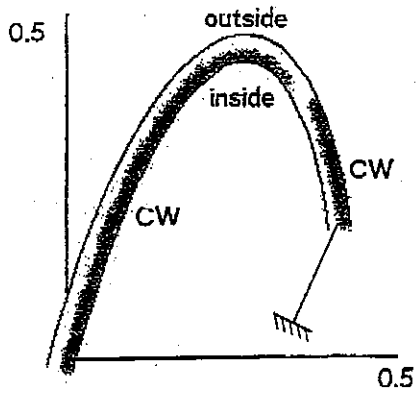


Figure 1 : Computed shape of a tapered tree pulled into a half loop and tied so that the tip is rotated through 180°. Shaded portions on the inside and outside correspond to CW induced in the trees (*Pinus strobus)* in the Sinnott (1952) 's experiments.

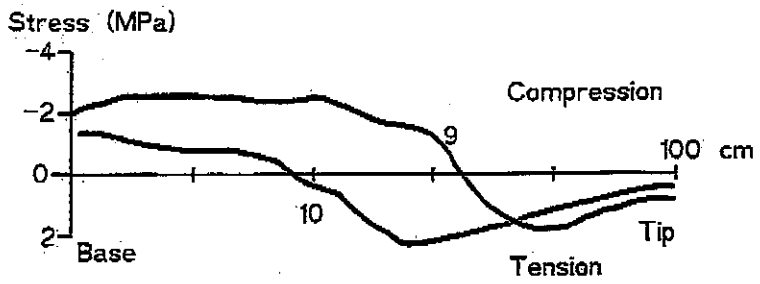


Figure 2 : CW zones (shaded) as shown in a vertical section of the 100cm (straightened) stem. Growth before bending (normal wood) indicated by "+" while "*" indicates the 10 growth layers defined for purposes of analysis and occuring after the initial bending. The arrows indicate the limits of the CW zones as found by Sinnott (1952) for the inside and outside portions of the stem. [Note : CW results for growth layers 3,7 and 8 are interpolated from the calculated CW results for neighboring layers since computer results for those layers were found to be unreliable.]

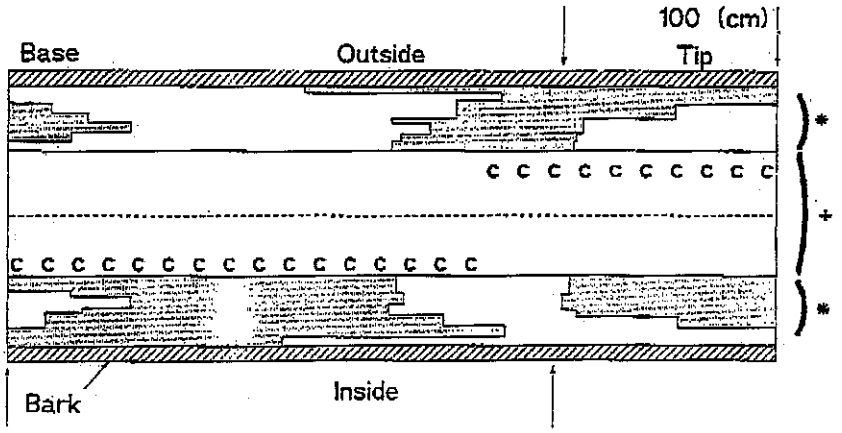


Figure 3. Typical bending stress increments induced in growth layers of a stem due to CW action in the layer. Results for layers 9 and 10 [ The last two growth layers in the annual growth] are given.

# WOOD STRUCTURE, CHEMICAL COMPOSITION AND GROWTH STRAINS IN *EUCALYPTUS* CLONES. INTERPRETATION OF THE NOTICED PHENOMENONS

H. BAILLÈRES[1]; B. CHANSON[2]; M. FOURNIER[2]; M.T. TOLLIER[3]; B. MONTIES[3]

(1) CIRAD-Forêt - 45 bis av. de la Belle Gabrielle - 94736 Nogent / Marne Cedex - FRANCE
(2) Laboratoire de Rhéologie du Bois de Bordeaux - BP 10 - 33610 Cestas Gazinet - FRANCE
(3) Laboratoire de Chimie Biologique (INRA) - 78850 Thiverval Grignon - FRANCE

The longitudinal residual growth strains at the stem surface, named Longitudinal Residual Strain of Maturation (**LRSM**), is appraised by stresses ("growth stresses") release on stem periphery by means of cutting in the wood [1], [4], [5]. The measurement of Longitudinal Residual Strain of Maturation allowed a continuous and quantitative classification of wooden samples coming from hybrid clones of *Eucalyptus* (Congo, Africa). This kind of measurements allows a mechanical identification of tension wood. In *Eucalyptus* species, it is not characterised by G-fibres, it can be however characterised by its growth strains [1].

The relationships between wood structure and mechanical properties were studied by ultrastructural (MicroFibril Angle = **MFA**) and chemical (quantitative investigation of the monomeric compound of lignines by thioacidolysis [6]).

The results presented in this study show :

- an important variation of the LRSM with high values, in spite of the weak eccentricity, the good verticality and the absence of G-fibre of our trees (Fig 1)
- a negative correlation between the level of the LRSM, the lignin content (Klason lignin) and the MFA (Fig 2 and 3)
- a positive correlation between the level of the LRSM and the ratio of the lignin monomeric units rates: syringyl on guaiacyl (S/G ratio) (Fig 4).

The weak knowledge about the effects of quantitative and qualitative variations of lignins on the phenomenons involve in physical and mechanical caracteristics of wood don't allow us an interpretation of this observation.

The signification of these correlations can be discussed as a biochemical problem: are there direct mechanical causality or more intricate correlations between structural variables ?

Some micro-mechanical models allow the expression of the longitudinal deformation of maturation at the scale of the cell wall in terms of two biochemical phenomenons (Fig 5 et 6) :

- The swelling of amorphous matrix typical of the lignification [3], the deposition of encrusting lignins between cellulose fibrils causes transverse expansion, because of the lateral links between fibrils, the transverse expansion is associated with longitudinal contraction.
- The contraction of the microfibrils typical of the crystallisation process of cellulose with simultaneous polymerisation due to a high degree of lateral order in the crystals [2].

## BIBLIOGRAPHY :

[1] BAILLERES H., CHANSON B., FOURNIER M., TOLLIER M.T., MONTIES B., **1994**. Structure, composition chimique et retraits de maturation du bois chez des clones d'Eucalyptus. Accepted by the *Annales des Sciences Forestières*.

[2] BAMBER R.K., **1987**. The origin of growth stresses : A rebutal, *IAWA Bulletin n.s.* **8**(1), 80-84.

[3] BOYD J.D., **1985**. The key factor in growth stress generation in trees : lignification or crystallisation. *IAWA Bulletin* **6**(2), 139-150.

[4] FOURNIER M., CHANSON B., THIBAUT B., GUITARD D., **1994**. Mesure des déformations résiduelles de croissance à la surface des arbres, en relation avec leur morphologie. Observations sur différentes espèces. *Ann. Sci. For.* **51**(3), 10 p.

[5] FOURNIER M., GUITARD D., **1994**. Les contraintes de croissance générées par la différenciation cellulaire. *Acta bot. Gallica* **140**(4), 12 p.

[6] MONTIES B., **1991**. *Lignins in Methods in Plant Biochemistry Vol. 1.* p 113-153. Harbone J.B. Ed.

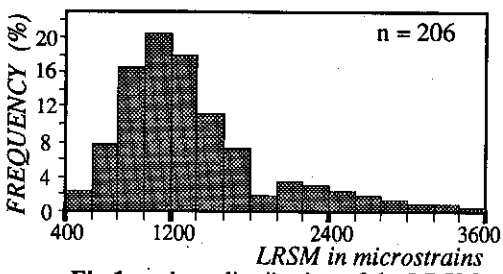


**Fig 1** : values distribution of the LRSM
(LRSM are shrinkages expressed here in absolute value)

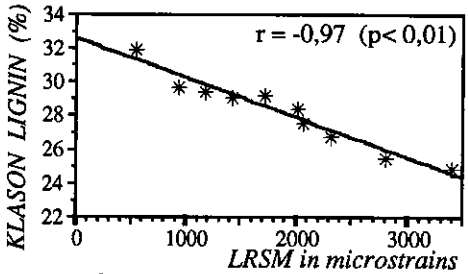


**Fig 2** : relationship between Klason lignin rate and LRSM

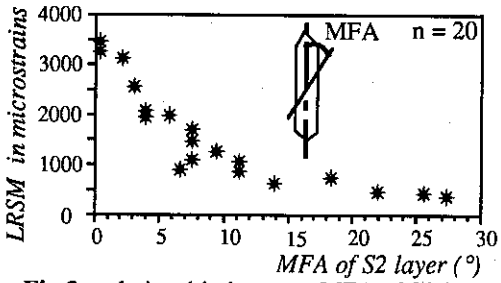


**Fig 3** : relationship between MFA of S2 layer and LRSM

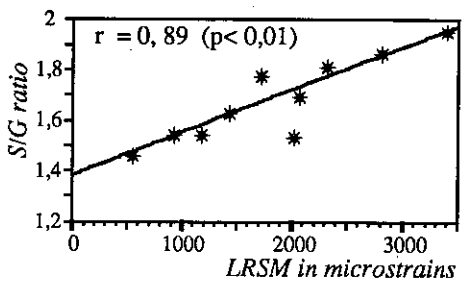


**Fig 4** : relationship between S/G ratio and LRSM

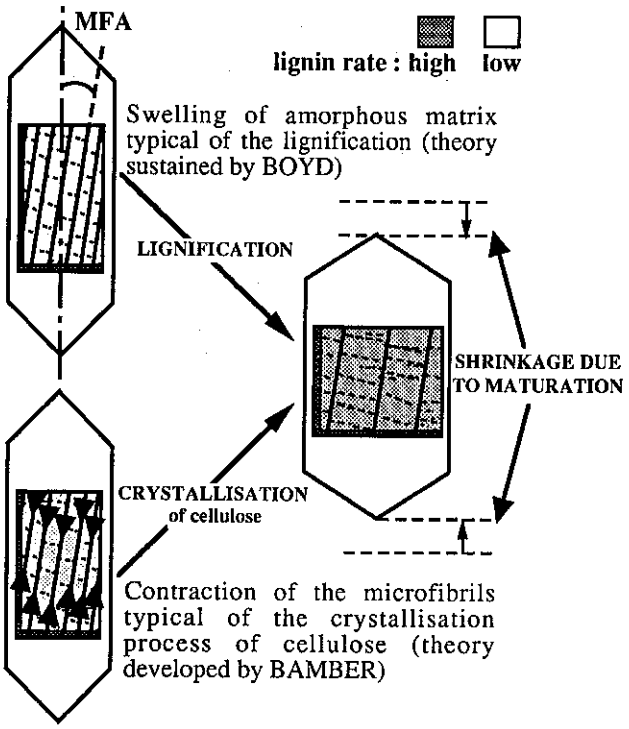


**Fig 5** : the origin of the longitudinal deformation of maturation at the scale of the cell wall can be expressed in terms of two biochemical phenomenons.

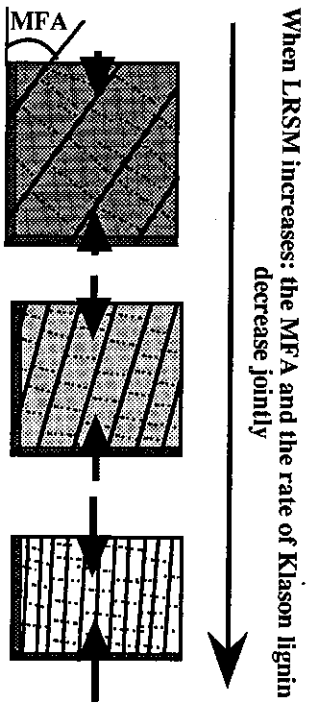


**Fig 6** : Schematic representation of the mechanical and histological observations.

# TWO FIELD MEASUREMENT TECHNIQUES FOR APPRAISING THE LONGITUDINAL GROWTH STRAINS AT THE STEM SURFACE.

H. BAILLÈRES[1]; B. CHANSON[2]; M. FOURNIER[2]

[1] CIRAD-Forêt - 45 bis av. de la Belle Gabrielle - 94736 Nogent / Marne Cedex - FRANCE
[2] Laboratoire de Rhéologie du Bois de Bordeaux - BP 10 - 33610 Cestas Gazinet - FRANCE

Growth stresses originate in surface growth strains (= maturation strains), induced in cambial layers during the differentiation and maturation of new cells, impeded by the mass of the whole trunk. The longitudinal residual growth strains at the stem surface, named **L**ongitudinal **R**esidual **S**train of **M**aturation (**LRSM**), is appraised by stresses ("growth stresses") release on stem periphery by means of cutting in the wood located under the cambium. This cutting is supposed to release locally, in the measured spot, existing stresses in the stem, and thus, the observed strains are proportional and have opposite signs to the initial stresses.

Two different methods using special sensors are used for the determination of the longitudinal residual strain of maturation :

**1> The single drilled hole method, using CIRAD sensor (Fig 1).** It's a classical technique for measuring residual stresses in elastic materials [1], [2], [3]. The metrological principle consists in measuring dimensional changes in fibre direction near a single drilled hole. The recorded value is a displacement ($\delta$) that is proportional to the LRSM ($\alpha_L$) :

$$\alpha_L = - \phi \, \delta$$

where $\phi$ is a variable that depend on : hole diameter, reference distance of measurement, moduli of elasticity ($E_L$ and $E_T$), shear modulus parallel to the grain ($G_{LT}$) and Poisson coefficient ($\nu_{LT}$).

**2> The two grooves method, using Wap's sensor (Fig 2).** This method uses a classical extensometric sensor (manufactured by HBM - Germany) [2], [3], [4]. The total longitudinal stress is relieved by sawing two grooves above and below the sensor. After this operation we achieve the longitudinal residual strain of maturation.

In spite of the difference between the position of the measurement spots (it's impossible to realise two measurements on the same place), there is a highly significant correlation between the values achieved by the two methods (Fig 3).

## BIBLIOGRAPHY

[1] ARCHER R.R., **1986**. *Growth Stresses and strains in trees*. Springer Verlag, Springer series in wood science, Editor : E. Timell, 240 p.
[2] BAILLÈRES H., **1994**. Précontraintes de croissance et propriétés mécano-physiques de clones d'Eucalyptus (Pointe Noire - Congo) : hétérogénéités, corrélations et interprétations histologiques. *Thèse en Sciences du Bois de l'université de Bordeaux I*, 161 p.
[3] FOURNIER M., CHANSON B., THIBAUT B., GUITARD D., **1994**. Mesure des déformations résiduelles de croissance à la surface des arbres, en relation avec leur morphologie. Observations sur différentes espèces. *Ann. Sci. For.* **51**(3), 10 p.
[4] FOURNIER M., GUITARD D., **1994**. Les contraintes de croissance générées par la différenciation cellulaire. *Acta bot. Gallica* **140**(4), 12 p.

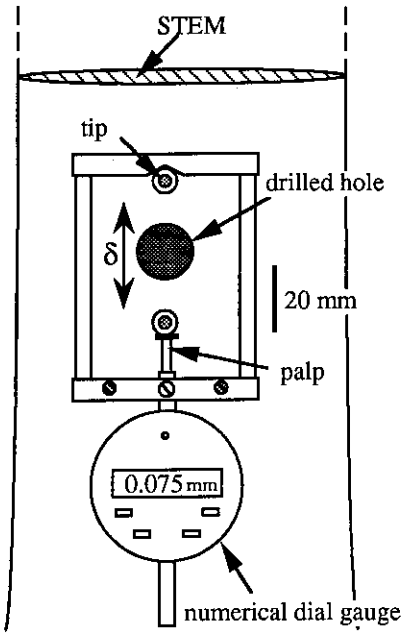


**Fig 1** : single drilled hole method
**(CIRAD sensor)**

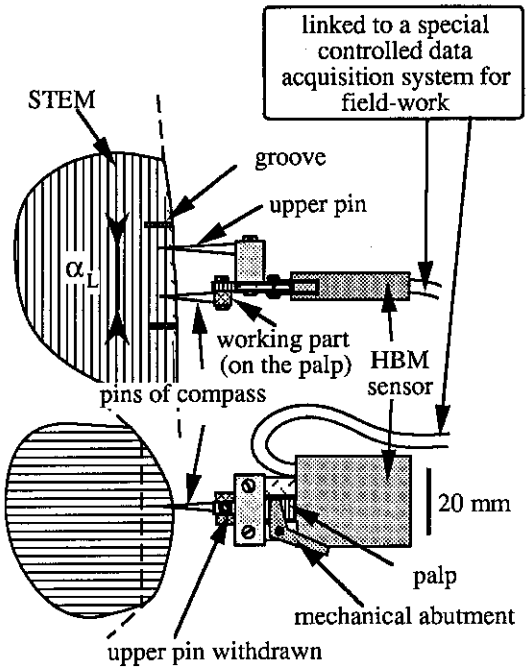


**Fig 2** : two grooves method
**(Wap's sensor)**

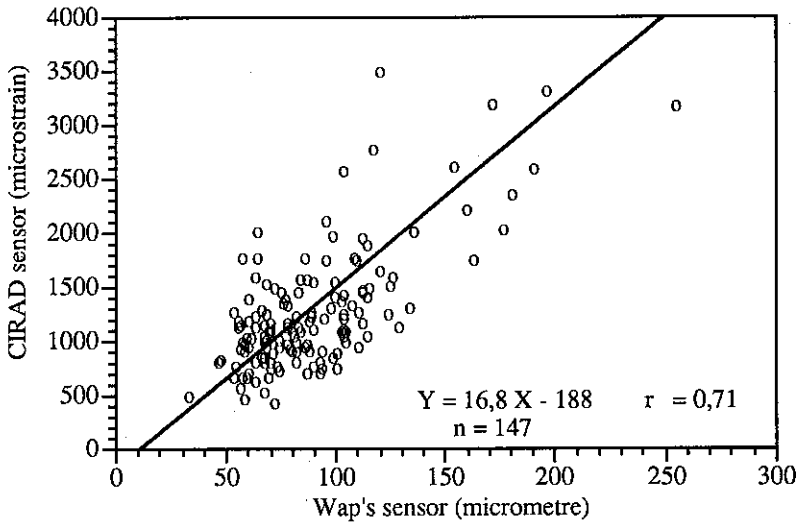


**Fig 3** : correlation between the values achieved by the two methods on *Eucalyptus* clones.
For each point the sensors are situated on the same generatrix with a distance of about 20 cm one from the other.

# LODGING : THE DEVELOPMENT OF A RISK ASSESSMENT TECHNIQUE BASED ON A MECHANICAL MODEL

C.J.BAKER
*Dept. of Civil Engineering, University Park, Nottingham, NG7 2RD, UK*

J.M.GRIFFIN & R.K.SCOTT
*Dept. of Agriculture & Horticulture, Sutton Bonington Campus, University of Nottingham, Loughborough, LE12 5RD, UK*

R.SYLVESTER-BRADLEY
*ADAS Soil & Water Research Centre, Anstey Hall, Cambridge, CB2 2LF, UK*

Lodging is a serious problem for cereal growers and when extensive lodging occurs in seasons such as 1980, 1985, 1987 and 1992, costs to the industry are large, through lower yields and poor grain quality.

Our aim is to reduce lodging and in order to achieve this, the development of a better predictive system of lodging risk in wheat is of paramount importance. The vast majority of lodging is caused by two basic modes of failure ; buckling at the stem base or uprooting in the soil. The basis of the prediction system evolves around a mechanical model which encompasses both of these types of lodging.

The model outlined for wheat consists of a double 'lumped mass' (representing the ear and the root ball respectively) on a weightless stem (see Fig. 1), which forms a two degree of freedom system. Preliminary calculations to determine the transfer functions for the system indicate that the model can be simplified to a one degree of freedom system, which is assumed to act as a second order harmonic oscillator. Wind engineering technology was used to formulate the model. In simple terms, the model descibes how the transfer functions can be used to form a spectrum of base bending moment of a wheat stem. From the incident wind spectrum values for the extreme base bending moment can then be extrapolated, in order to determine the plants failure criteria.

The ultimate objective is to develop a method of identifying individual wheat crops at high risk then to control lodging at least cost. Experimentally, this will involve the measurement of various parameters in the spring, which include identification of loose tilth, or weakly binding soil, few or weak roots, thin or weakened stems and the potential for dense wind- and rain-trapping canopies and heavy heads. If these measurements can be shown to predict vulnerability in July (when highest lodging risk occurs), as a result of fulfilling the failure criteria derived from the model, then the percentage probability of lodging occurring can be predicted. If anchorage is thought at fault then the best option may be to roll the crop. If stem buckling is expected then a plant growth regulator can be applied or less nitrogen fertilizer can be used, to control lodging.

Fig. 1 - *The basic mechanical model of a wheat stem*

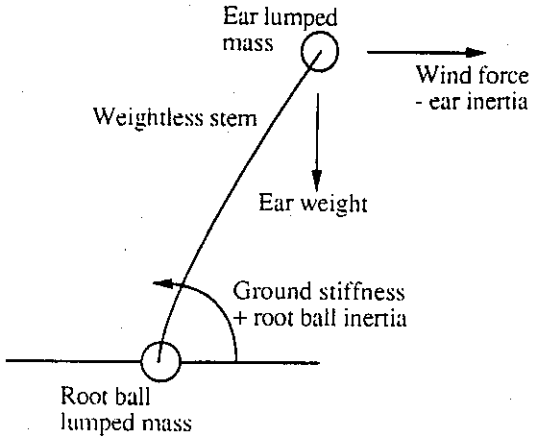


*References*

BAKER, C.J. (1993) Engineering approaches to aspects of the wheat lodging problem. *Nottingham University, Dept. of Civil Engineering, Report Number* **FR93036**.

EASSON, D.L., WHITE, E.M. and PICKLES, S.J. (1992) A study of lodging in cereals. *Home-Grown Cereals Authority, Report Number* **52**.

ENNOS, A.R. and CROOK, M.J. (1993) The mechanics of root lodging in winter wheat, *Triticum aestivum L. Journal of Experimental Botany* **44**, 1219-1224.

FINNIGAN, J.J. (1979) Turbulence in waving wheat I and II. *Boundary-Layer Meteorology* **16**, 2, 181-236.

GRAHAM, J. (1983) Crop lodging in British wheats and barleys. PhD thesis, *Reading University*.

# PATTERNS AND PROGRAMS OF CELL DIVISION IN ROOT MERISTEMS OF MAIZE AND TOMATO

P W Barlow[1], J Lück[2] and HB Lück[2]
[1]Dept of Agricultural Sciences, University of Bristol, Long Ashton Research Station, Bristol BS18 9AF, UK, [2]Laboratoire de Botanique analytique et Structuralisme végétal, Faculté des Sciences et Techniques de St-Jérôme, 13397 Marseille cedex 13, France.

Besides their importance as units of growth and differentiation, cells, by virtue of their turgidity and the rigidity of their walls, are units of structural support for plant tissues and organs. Presumably, the network of cell walls (cellworks)[1], which can be seen in histological sections, has evolved to provide an optimal internal scaffold for the maintenance of form and the differentiation of metabolic functions. In the root, most of this cellwork results from the continuous growth and division of cells within the apical meristem. We have found that relatively simple algorithms will develop the cellworks seen within the meristem of maize (*Zea mays* L.) roots and attempts are being made to extend these algorithms to account for the cellworks of the tomato (*Lycopersicon esculentum* Mill.) root apex.

In the primary root of maize, the distal part of the meristem maintains a recurrent pattern of periclinal, longitudinal-radial, and anticlinal divisions (formative divisions) which develops the basic cellwork. In the proximal (and major) part of the meristem the cellwork expands and shows ordered sequences of anticlinal divisions (proliferative divisions). We analysed in detail the relative elongation growth and sequence of mitoses of cells participating in the first four rounds of division following germination[2,3] and, in a more general way, the relative lengths of cells resulting from two further rounds of division. In this post-germination period it was possible to recognize cell packets (groups of cells of common descent) containing from 1 to 16 cells and, later, up to 64 cells. At this latter stage, many cells were then emigrating from the meristem into the non-meristematic elongating zone.

Although a large number of division pathways are theoretically possible, each pathway being defined by a particular sequence of divisions within a growing packet, observation shows that relatively few are actually used[2]. This suggests that there may be some inherent polarity of growth or division which limits their number. In fact, the pathways that do operate result from inherited sequences of asymmetric division that lead to sister cells of unequal length. However, as root growth proceeds the asymmetry becomes less noticeable. The unequal divisions are a regular feature of the germinating primary root. Their significance is obscure; divisional asymmetry may have some consequence for countering the physical resistance that roots experience as they penetrate the soil, or it could ensure that cell cycle phases are asynchronous and thereby minimizes the sensitivity of the cell population to potentially damaging effects from the environment. Asymmetry may even, in some way, anticipate further cell differentiation[4]: *viz.* the case of trichoblasts, for example.

All possible pathways, not just those actually found, can be generated by deterministic 'bootstrap' L-systems which assign different lifespans to sister cells of successive generations and hence specify the sequence of divisions[2]. The two pathways most frequently found in the maize root meristem are shown in Fig. 1. Further analysis has shown that these minimal pathways can be expanded (Fig. 2) to represent the division pattern occurring later in development, following which the cell packets pass from the meristem into the elongation zone. At the same time, the relative values for the lifespans can be related to those described earlier[5] and by more direct analysis from the kinetics of $^3$H-thymidine-labelled mitoses[6].

Programmes of formative divisions have been further investigated in clones of *in-vitro*-grown tomato roots and have provided material for studies of cell genealogies in the three major histogenetic zones of stele, cortex and cap/epidermis[7]. The lifespans and genealogies

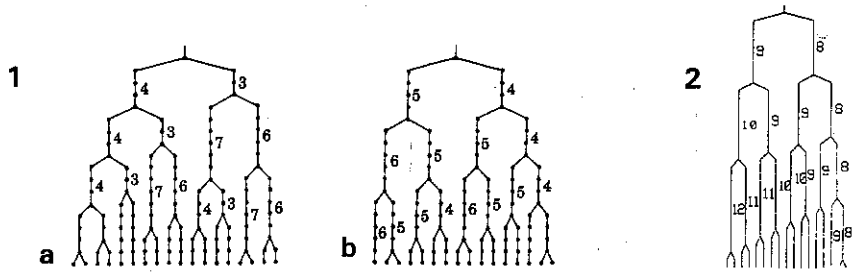


Fig. 1. Genealogical trees illustrating two cell populations simulated by a bootstrap device which follow (a) pathway $P_{14}$ and (b) pathway $P_{21}$, these two pathways being the most frequent in the early stages of cell development in the meristem of the maize root cortex.

Fig. 2. Genealogical tree illustrating pathway $P_{E2}$, this being a pathway that represents cell growth and division as cells migrate through the proximal part of the meristem.

---

of each cell in each histogen are coordinated, the genealogy of the cap being the most complex and its development is related to the genealogy of the cortex. For analytical purposes, the cap is considered as being sub-divided into three zones: a central columella, a flank zone that extends up the side of the root and abuts the outer face of the cortex, and an intermediate zone wedged between these other two zones. The fate of each cell in each zone can be traced both spatially and temporally, from its inception by a functional initial cell until it 'dies' and is shed from the surface of the root. Remarkably, cells from each zone of the cap are shed simultaneously as a coherent peel of senescent tissue, all cells having the same age since their birth from an initial.

Again, three types of formative division initiate the cellwork of the cap and each type can be mapped to specific sites in each zone. The columella zone, however, is constructed from transverse divisions only. Zones change their boundaries as the root grows. For example, the columella zone increases its diameter at a rate of 1 new cell-file being added every 4.5 days, or in the time that 1.8 cells are added to a pre-existing columella cell-file. The new files are derived from initials in the former intermediate zone; their diverse types of division give way to transverse only, this being brought about by radial growth of the cortical tissue.

Algorithms are being constructed that will formalize the coordinated development of all three histogens and the divisional lifespans of their component cells.

References

1. Liu, H.L. & Fu, K.S., 1981. *Information Sciences* 24, 93-109.
2. Lück, J, Barlow, P.W. & Lück, H.B., 1993. *Cell Proliferation* 27, 1-21.
3. Lück, J, Barlow, P.W. & Lück, H.B., 1993. *Annals of Botany* 73, 1-11.
4. Barlow, P.W., 1984. In *Positional Controls in Plant Development* (eds P.W. Barlow & D.J. Carr), pp. 281-318 Cambridge University Press, Cambridge.
5. Barlow, P.W. & Macdonald, P.D.M. (1973). *Proceedings of the Royal Society* B 183, 385-398.
6. Barlow, P.W., 1987. *New Phytologist* 105, 27-56.
7. Barlow, P.W., 1993. In *Molecular and Cell Biology of the Plant Cell Cycle* (eds J.C. Ormrod & D. Francis), pp. 179-199. Kluwer Academic Publishers, Dordrecht.

# STRUCTURAL BASIS FOR THE BIOMECHANICAL BEHAVIOUR OF RATTAN MATERIAL

**K. M. Bhat**
Division of Wood Science
Kerala Forest Research Institute
Peechi 680 653
India

With the recent concept of property manipulation in wood and non-wood forest products, rattans - the climbing palms of the tropics will soon find a place in material science. Rattan competes with numerous other materials like wood, plastics and metals. As a material, its versatility is evident from the unique aesthetic value of its furniture products, high strength to weight ratio, durability, ease in workability, pliability, bio-degradability and natural renewability as crop. Based on the study of more than 25 species of Indian rattans, representing three genera, *viz. Calamus, Daemonorops* and *Korthalsia,* attempts are made in this paper to establish the definite structure-property relationships to interpret the biomechanical behaviour of rattans.

Based on the mechanical properties such as bending (modulus of rupture - MOR) and tensile stresses (UTS), three classes recognised are: (a) strong to very strong (MOR and UTS > 70 N/mm$^2$), (b) moderately strong (45-70 N/mm$^2$) and (c) weak (< 45 N/mm$^2$) rattans. , With the MOR of 65 N/mm$^2$, the average bending strength of rattans is close to that of wood (65.5 N/mm$^2$) or even greater than that of bamboo (55 N/mm$^2$) although the maximum compressive stress (parallel to grain) is low (28 N/mm$^2$).

With the greater range of mechanical property values, rattan appears to be more heterogeneous material than wood. This is possibly due to the different pattern of structural variability at the tissue/cellular level as evident from the following:

- The mechanical tissues (sclerenchyma fibres), confined to the scattered vascular and non-vascular bundles, generally account for only 1/3rd of the total stem tissues of rattans in contrast to the relatively high fibre content of wood.
- The percentage of fibres within the vascular bundles and the polylamellate fibre wall thickness show more definite patterns of variation than the vascular bundle size and number per unit area.
- Instead of fibres, non-mechanical cortical and ground parenchyma constitute as the major component (up to 58-60%) of stem tissues.
- The conducting tissues *viz.* xylem and phloem often contribute to 30-35% void volume of the material.
- At the ultrastructural level, it is observed that new lamellae are added with the aging of fibres, thereby increasing both the wall thickness and density of the material.
- The fibre wall structure/thickness appears to be the single most important factor that determines the mechanical behaviour under bending and tensile stresses. The fracture mode of individual fibres follows the fibril angle and is in opposite direction from broad to narrow lamellae. The broad lamellae appear to govern the fracture behaviour more than the narrow lamellae.

# REGULATION DE LA FORME DU TRONC DE *PINUS KESIYA* DANS LA REGION DU MANGORO (MADAGASCAR): INDEPENDANCE ENTRE LA FORME DE LA SECTION DROITE ET LA COMPETITION INTER-INDIVIDUS

JP Bouillet, Mission CIRAD-Forêt, BP 745, Antananarivo, Madagascar

## INTRODUCTION

L'impact des éclaircies fortes et précoces sur les Pinus kesiya du Mangoro (≈ 50000 ha) est connu: très forte réaction individuelle sans modifications notables des propriétés technologiques du bois (mesurées sur des éprouvettes sans défaut, ni bois de compression). Mais pour donner un avis définitif sur l'effet d'une telle sylviculture sur la qualité des arbres, on doit aussi connaître l'influence des éclaircies sur l'anisotropie radiale, qui entraîne la production de bois de moins bonne qualité technologique.
C'est pourquoi une étude a été engagée pour répondre aux questions suivantes:
- les éclaircies entraînent-elles une activité cambiale plus importante dans la direction des arbres partant en éclaircie, sous l'hypothèse avancée par ZIMMERMANN et BROWN (1971) d'un flux vertical de sève élaborée avec peu de transferts latéraux?
- est-il possible de proposer un schéma de régulation de la forme du tronc?

## RÉSULTATS

*Caractérisation de l'irrégularité d'une section et de son évolution au cours du temps*
Celle-ci repose sur l'identification des accroissements radiaux annuels à des vecteurs et sur l'évolution de leur somme.

*Effet de la compétion aérienne sur l'anisotropie radiale*
L'échantillon comporte 56 individus dominants/codominants âgés de 14 à 20 ans: 21 arbres témoins et 35 ayant subi 1, 2 ou 6 éclaircies pour lesquels sont construits 10 indices de libération de la concurrence qui tiennent compte de l'orientation des arbres enlevés en éclaircie. De 4 à 11 niveaux sont pris en compte par individu (limite du tronc: diamètre fin bout de 15cm sur écorce).
On aboutit aux résultats suivants: **(1)** l'orientation de l'excentricité ne dépend pas de celle des voisins enlevés en éclaircie, **(2)** l'amplitude de l'excentricité, assez marquée, est comparable pour les arbres témoins et ceux enlevés en éclaircie, **(3)** l'excentricité est globalement orientée le long du tronc dans une direction NW, **(4)** une forme de la section bonne prédictrice de la forme finale apparaît précocement (3-5 ans), **(5)** le méplat ne présente pas d'orientation privilégiée et est assez marqué.

*Correspondance excentricité et distribution des branches le long de l'axe principal*
Afin de préciser les résultats précédents, on a étudié la correspondance pouvant exister entre l'excentricité et la distribution (orientation et grosseur) des branches le long de l'axe principal. L'étude a porté sur 54 individus âgés de 5 à 22 ans et a pris en compte 2 types de correspondance (stricte ou sur une partie limitée du périmètre) et 2 types d'influence des branches (locale ou sur une longue distance).
On observe que: **(1)** l'excentricité des sections ne dépend pas de la distribution des branches le long de l'axe principal, tant pour le tronc que pour la partie sommitale de l'arbre,

correspondant au houppier participant de manière prépondérante à la croissance,
**(2)** l'excentricité est toujours globalement orientée vers le NW.
L'étude complémentaire de 14 individus élagués sur la moitié de leur périmètre, et ceci sur toute leur hauteur, conduit aux mêmes conclusions.

*Causes possibles*
Les phénomènes ne peuvent être expliqués par:
- une disposition particulière du système racinaire,
- des conditions spéciales au Mangoro; les mêmes observations sont faites sur Pinus kesiya à Manankazo,
- une caractéristique propre à Pinus kesiya; au Mangoro, Pinus caribaea est excentré aussi dans une direction NW.
L'influence des températures n'a pas été testée mais est une cause peu probable.

Le vent semble être la cause principale car: **(1)** le vent souffle de SE-->NW au Mangoro et à Mankazo (régime des alizés), **(2)** une excentricité se développant sous le vent d'intensité, comme au Mangoro, faible à modérée s'observe sur d'autres résineux et dans d'autres pays, **(3)** du bois de compression est noté dans la direction de l'excentricité.

## CONCLUSION - SCHÉMA DE RÉGULATION

On ne peut véritablement définir le chemin suivi par le flux de sève élaborée et plus généralement la connaissance de celui-ci ne suffit pas pour expliquer les phénomènes observés. L'alimentation du cambium semble sous la dépendance de relations de type source-puits, la partie N-W du tronc jouant le rôle d'un puits attirant de manière préférentielle les nutriments. L'excentricité du tronc est expliquée principalement par l'influence des alizés du S-E bien que leur intensité soit faible à modérée.
Un schéma de régulation de la forme du tronc est proposé (d'après LOUP *et al.*, 1991, modifié): les arbres réagissent de manière continuelle à l'action du vent de SE pour maintenir la forme de consigne, droite, en formant du bois de compression et des cernes plus larges dans la direction opposée au vent.

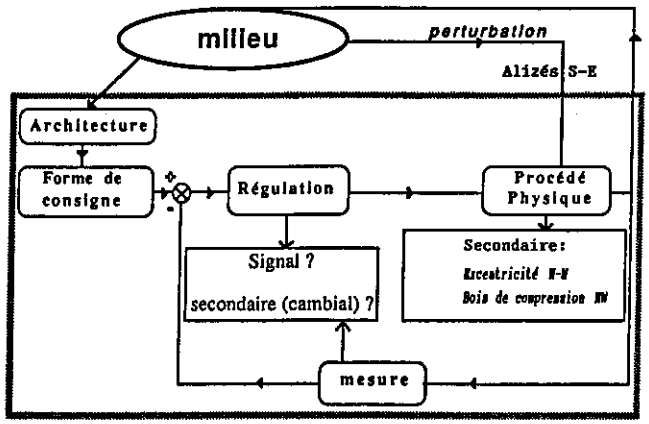


LOUP, FOURNIER, CHANSON, 1991. Relations entre architecture, mécanique et anatomie de l'arbre - Cas d'un pin maritime. In: L'arbre, Biologie et Développement (EDELIN éd.)
ZIMMERMANN, BROWN, 1971. Trees structure and function. Berlin: Springer

**Mots-clés**: forme des arbres, éclaircies, fonctionnement du cambium, Pinus kesiya

# FINITE ELEMENT ANALYSIS OF THE MECHANICAL PROPERTIES OF PLANT CELLS

**K.M. BURROWS**

UNILEVER RESEARCH LABORATORY
COLWORTH HOUSE
SHARNBROOK
BEDFORDSHIRE MK44 1LQ

During standard materials testing, assumptions such as material continuity, isotropy and homogeneity are generally made. When testing biological materials these assumptions are not valid due to the cellular nature of the tissue. As a result of this, a structural analysis is necessary.

It is difficult to relate the stress or strain applied to the tissue sample to the stress in the cell-wall. Models are needed to give relations between the properties of the material and the properties of individual cell components. A number of models have been developed, most use analytical techniques to define the relationship between cell-wall properties and turgor pressure, and the gross mechanical properties of the tissue. [1-3]

Finite element techniques hold out the promise of modelling the structure of fruits and vegetables using reasonable materials constants to model the type of behaviour expected from plant tissue under general mechanical loading. It should be possible to include the effects of varying cell size, shape and wall thickness in the calculation of the response of the tissue to external loading.

Current finite element techniques use software packages that model either solids or fluids. In modelling plant tissue, we need to combine the behaviour of a solid with that of a fluid. In this poster we examine the behaviour of a single, fluid-filled cell under compressive, flat plate loading. For simplicity, the cell-wall and cell fluid are assumed to be homogeneous and isotropic during the current investigation. The presence of cell fluid is modelled using two different techniques. One method involves representing the fluid as a solid with fluid-like properties; in the other the fluid is represented as a pressure load normal to the internal surface of the cell-wall, with compression taking place at constant cell volume. The relative merits of the two techniques are considered and assessed.

[1] R.S. GATES, R.E. PITT, A. RUINA AND J.R. COOKE. Cell Wall Elastic Constitutive Laws and Stress-Strain Behaviour of Plant Vegetative Tissue. *Biorheology*, **23**, 1986, 453-466.

[2] Q. GAO, R.E. PITT AND A. RUINA. A Mechanics Model of the Compression of Cells with Finite Initial Contact Area. *Biorheology*, **27**, 1990, 225-240.

[3] Q. GAO, R.E. PITT. Mechanics of Parenchyma Tissue Based on Cell Orientation and Microstructure. *Transactions of the ASAE*, **34**, 1991, 232-238.

# AUTOPORTANCE vs NON AUTOPORTANCE: SES EXPRESSIONS ANATOMIQUES ET MORPHOLOGIQUES CHEZ LES LIANES.

**Guy Caballé et Francis Hallé**

Ecole Pratique des Hautes Etudes, Laboratoire de Botanique, 163 rue Auguste Broussonnet, 34000-Montpellier, France.

Les lianes tropicales réalisent des ontogenèses anatomiques variées. Cette radiation anatomique dans le groupe des lianes est la conséquence directe de l'accomplissement d'une gamme étendue de processus de croissance secondaire.

Dans leurs phases expansives de développement en forêt, les lianes tropicales adoptent un mode de vie non autoportant et grimpant. Juvéniles, contraintes ou piégées dans un environnement ouvert, ces mêmes lianes prennent de préférence un mode de vie autoportant. Cette dualité de mode de vie est toujours sous-jacente, même si elle peut être très affirmée chez certaines espèces et familles (ex. Connaraceae et Dichapetalaceae) ou au contraire plus diffuse chez d'autres (ex. Mimosaceae).

Le passage d'un mode de vie à l'autre s'accompagne le plus souvent de transformations biomorphologiques radicales, rapides et durables: principalement en anatomie, architecture et morphologie, dynamique de croissance et physiologie. Les changements anatomiques sont à la fois qualitatifs et quantitatifs, d'ordres structurel et fonctionnel: nouveaux modes de fonctionnement du cambium, néoformation d'assises cambiales, fractionnement de la charpente primaire, assemblage des tiges en plusieurs cylindres, richesse accrue en fibres, réduction des tissus de soutien, fort développement des parenchymes, augmentation sensible des dimensions des vaisseaux conducteurs, etc. Les études de terrain révèlent que c'est à partir du moment où les lianes ne se conforment plus à un mode de vie autoportant que leur énorme potentiel de diversité anatomique s'extériorise le mieux.

Sur un plan évolutif, les lianes pourraient représenter une forme ligneuse particulière qui aurait conservé (ou acquis) deux modes de vie, un autoportant, l'autre non. Dans ses exemples les plus représentatifs, l'intégration anatomie-mode de vie serait parfaite: une dualité anatomique correspondrait à la dualité des ports. Ailleurs, la diversité des situations et tendances s'inscrirait dans un large continuum. Quelques rares exemples d'espèces arborescentes qui ont la possibilité de modifier leur port ou leur maintien mériteraient une étude approfondie.

**Bibliographie sommaire:**

-Bhambie S. 1972. Correlation between form, structure and habit in some lianas. Proc. Indian Acad. Sci. 75(5): 246-256.

-Caballé G. 1986. Sur la biologie des lianes ligneuses en forêt gabonaise. Thèse de Doctorat d'Etat, Université de Montpellier II Sciences et Techniques du Languedoc.

-Caballé G. 1993. Liana structure, function and selection: a comparative study of xylem cylinders of tropical rainforest species in Africa and America. Bot. J. Linn. Soc. 113(1): 41-60.

-Chiu S.-T. & F.W. Ewers 1992. Xylem structure and water transport in a twiner, a scrambler, and a shrub of *Lonicera* (Caprifoliaceae). Trees 6: 216-224.
-Coudurier T. 1992. Sur la place des lianes dans la forêt guyanaise. Une approche qui utilise l'architecture végétale. Thèse de Doctorat, Université de Montpellier II Sciences et Techniques du Languedoc.
-Cremers G. 1973. Architecture de quelques lianes d'Afrique Tropicale.1. Candollea 28/2: 249-280.
-Cremers G. 1974. Architecture de quelques lianes d'Afrique Tropicale.2. Candollea 29/1: 57-110.
-Ewers F.W. 1985. Xylem structure and water conduction in conifer trees, dicot trees, and lianas. IAWA Bull. 6(4): 309-317.
-Gartner B.L. 1991. Is the climbing habit of poison oak ecotypic? Funct. Ecol. 5: 696-704.
-Gasson P. & D.R. Dobbins 1991. Wood anatomy of the Bignoniaceae, with a comparison of trees and lianas. IAWA Bull. 12(4): 389-417.
-Givnish T.J. & G.J. Vermeij 1976. Sizes and shapes of lianas leaves. Am. Nat. 110: 743-778.
-Lee D.W. & J.H. Richards 1991. Heteroblastic development in vines. In: Putz F.E. & H.A. Mooney eds. The Biology of Vines. Cambridge University Press, pp. 205-243.
-Putz F.E. 1984. The natural history of lianas on Barro Colorado Island, Panama. Ecology 65: 1713-1724.

**Coupes transversales de tiges de lianes:**

Les parties en noir uni correspondent aux phases autoportantes.
1.*Millettia duchesnei* .2.*Machaerium leiophyllum.* 3.*Strychnos* sp. 4.*Icacinaceae.* 5.*Griffonia physocarpa.* 6.*Anacolosa uncifera.* 7.*Uncaria africana.* 8.*Salacia* sp. 9.*Salacia staudtiana.* 10.*Verbenaceae.* 11.*Loeseneriella clematoides.*

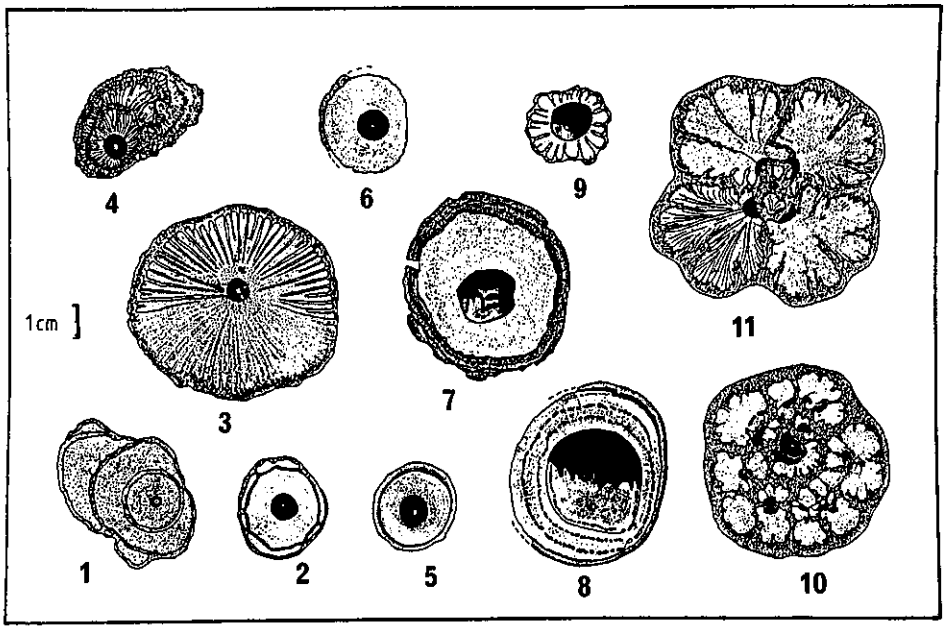

# CHANGES IN LIGNIFICATION IN ROSE FLOWER PEDUNCLES DIFFERING BY THEIR RESISTANCE TO BENDING

**B Chabbert, B Monties**
Laboratoire de Chimie Biologique, INRA, INA-PG, 78850 Thiverval Grignon, FRANCE

**N Zieslin, R Ben-Zaken**
The Hebrew University of Jerusalem, Faculty of Agriculture, PO Box 12, Rehovot, 76-100 ISRAEL

Bending of rose stems (bent-neck) during ageing is one important characteristic determining the post- harvest quality of rose peduncles (1). The tendency to bend is dependent on cultivar and stage of flower bud development. The upper part of the peduncles further shows the least resistance to bending as compared to basal part (2).

Anatomical differences have been reported between the strong flower peduncles of cv. Mercedes and the weak peduncles of cv. Nubia (3). The resistance to bending has also been related to highest peroxidase activity in strong cultivar(4). Peroxidases are implicated in various plant processes among which polymerisation of cinnamyl alcohol polymerisation into lignin. Apart from others functions, lignin in association with the cell wall components is assumed to contribute to the cell wall rigidity and plant support (5).

Both quality and quantity of lignin polymer displays large variations under genetic and physiological factors (6). These changes are mainly correlated to the variations in:

-proportions of the main monomers, syringyl and guaiacyl corresponding to the di- and monomethoxylated units,

-frequency and nature of intermonomeric linkages, the alkyl aryl ether bonds referred to non-condensed ones are prominent as compared to the C-C linkages (condensed).

This study was designed to evaluate the possible variations in lignification in relation to the resistance of bending of peduncles from strong cultivar (cv. Mercedes) and weak cultivar (cv. Nubia). Monomeric composition of lignin was determined by depolymerisation of the phenolic network using thioacidolysis (7) which allows specific determination of the non-condensed monomeric units.

Largest changes in lignin content were observed in xylem tissues as compared to phloem tissues. Upper parts of both cultivars and tissues of the weak cultivar are less lignified (figure 1). Lignin from phloem and xylem of cv. Mercedes contains larger amounts of non-condensed structures than corresponding tissues of the weak peduncle. In addition, enriched syringyl lignin fractions are deposited in the stronger peduncles, especially in the distal parts (table 1 & 2).

The variations observed in content and composition of lignin from strong and weak peduncles suggest that lignin may have a tissue specific function in the resistance of these cultivars to bending (8). Such modifications under genetic control might also be related to specific syringyl deposition in secondary wall differenciation of fiber cells, regarded as the main supporting cells in plants.

1-Burnett A N (1970) J. Am. Soc. Hort. Sci. 95: 427-431.
2-Zieslin N, Starkman F & Zamski E (1989) Pl. Growth Regul. 8: 65-67.
3-Zamski E, Starkman F & Zieslin N (1991) Israel J. Bot. 40: 1-6.
4-Zieslin N &Ben-Zaken R (1991) Pl. Physiol. Biochem. 29: 147-151.
5-Lewis N G & Yamamoto E (1990) An. Rev. Pl. Physiol. Pl. Molec. Biol. 41: 455-496.
6-Monties B (1989) Methods in Plant Biochemistry 1: 113-145.
7-Lapierre C, Monties B & Rolando C. (1986) Holzforschung 40: 113-119.
8-Chabbert B, Monties B, Zieslin N & Ben-Zaken R (1993) Plant Physiol. Biochem. 31: 241-247.

**Figure 1: LIGNIN CONTENT OF PHLOEM AND XYLEM CELL-WALL RESIDUE (CWR) FROM ROSE PEDUNCLE**

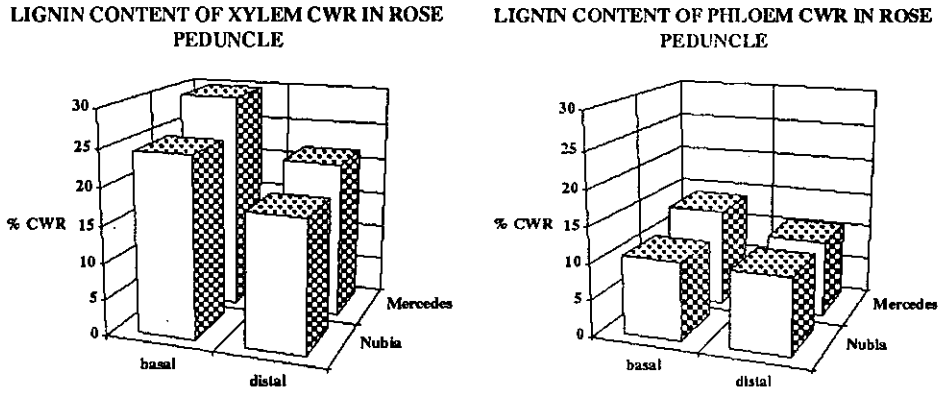


**Table 1: MONOMERIC COMPOSITION OF LIGNIN FROM XYLEM CWR IN ROSE PEDUNCLE**
( as $\mu$ mole G or S / $g^{-1}$ )

| Part of the peduncle | Cultivar | Guaiacyl G | Syringyl S | Total S+G | Ratio S/G |
|---|---|---|---|---|---|
| Basal | Nubia | 306 +/- 4 | 453 +/- 2 | 759 +/- 6 | 1.48 |
| | Mercedes | 432 +/- 25 | 745 +/- 46 | 1177 +/- 71 | 1.70 |
| Distal | Nubia | 96 +/- 12 | 75 +/- 7 | 171 +/- 19 | 0.78 |
| | Mercedes | 266 +/- 16 | 580 +/- 34 | 846 +/- 50 | 2.18 |

**Table 2: MONOMERIC COMPOSITION OF LIGNIN FROM PHLOEM CWR IN ROSE PEDUNCLE**
( as $\mu$mole G or S / $g^{-1}$ )

| Part of the peduncle | Cultivar | Guaiacyl G | Syringyl S | Total S+G | Ratio S/G |
|---|---|---|---|---|---|
| Basal | Nubia | 53 +/- 4 | 93 +/- 7 | 146 +/- 11 | 1.75 |
| | Mercedes | 152 +/- 8 | 253 +/- 4 | 405 +/- 12 | 1.66 |
| Distal | Nubia | 14 +/- 4 | 11 +/- 2 | 25 +/- 6 | 0.78 |
| | Mercedes | 25 +/- 2 | 66 +/- 6 | 91 +/- 8 | 2.64 |

## Influence of the inhomogeneity of the apple on the response spectra during nondestructive acoustic sensing of fruit firmness

H. Chen, F. Duprat, M. Grotte, D. Loonis, E. Pietri
INRA-LAMPE, Domaine Saint Paul, B.P.91, 84143 Montfavet, France

### Introduction

Nondestructive acoustic sensing of fruit firmness has been based on the derivation of the resonant frequency from the response spectrum of the fruit under vibration. The frequency is used in the stiffness factor $f^2m^{2/3}$, with f the resonant frequency and m the fruit mass, for the firmness evaluation. The reliability of this technique depends on whether a representative frequency can be correctly obtained. The response spectrum of an apple is influenced by some factors such as the shape and the inhomogeneity of the apple. The objective of this work is to investigate the influence of the inhomogeneity on the frequency spectrum.

### Experimental technique

Several Granny apples recently harvested and imported from Chile were used. The apples were first measured for their frequency response spectra and mode shapes. The reagent HCl of 18% Vol. was then injected into different parts of the apples to create the internal defects. Thirty minutes to two hours after the injection, the apples were measured again for their frequency spectra and mode shapes.

As shown in Fig.1, 20 points around the equator of each apple were measured. The apple was excited by impact at point 1. Two small condense type MCE-2500 microphones, with one fixed at point 1 and another placed in sequence from point 1 to 20, were used to measure the response signals. The signals were then fed into a Nicolet-310 digital oscilloscope which was connected via a IEEE-488 interface to a SX386 personal computer where the time-domain signals were transferred into the frequency spectra by using a program coded in Quick Basic. All the spectra were saved and further calculated in the same way as used by Huarng et al. (1992) for mode shapes.

### Results

Fig. 2 shows three spherical mode shapes measured for Granny apples, where the dotted circles represent the base circles and the solid lines the mode shape at one extreme deformation of the apple equator. The mode (a), (b) and (c), having respectively 2, 3 and 4 nodal lines, are referred to as $S_{20}$, $S_{30}$ and $S_{40}$. In previous research, the $S_{20}$ mode was found the most important in reflecting the fruit firmness, and its resonant frequency was therefore used in the stiffness factor $f^2m^{2/3}$ for calculating the fruit firmness.

Fig. 3(a) shows the frequency response spectrum of an apple without internal defect. The highest peak around 700-760 Hz corresponds to the $S_{20}$ mode, the peak around 1120-1140 to the $S_{30}$ mode and the peak around 1460-1480 Hz to the $S_{40}$ mode. Thirty minutes after 0.88g of HCl was injected into a part of the core, about 2.5% of the total weight of the apple in this region became very soft. In this case, the highest peak in Fig.3(a) is split into two peaks with one at around 580 to 600 Hz and another around 720 to 760 Hz (Fig.3(b)). Both peaks correspond to the $S_{20}$ mode. Using the lower frequency in the stiffness factor may cause an error of about 25 to 30% in firmness evaluation.

In comparison with the first apple, another apple was injected with half amount of HCl at an outer layer, which causes the same effect. It seems that the inhomogeneity in the outer part of an apple influences more on the response spectrum.

It was observed that some apples after a few months of storage display more peaks. This could probably be an indication of the existence of the inhomogeneity inside the apple.

**Conclusions**

Inhomogeneity inside the apple may split the main resonant peaks in the frequency spectrum into two or even more, this may cause considerable error in the firmness evaluation. On the other side, the increase in the peaks during the storage of the apple can possibly be used as an indication of the internal defect.

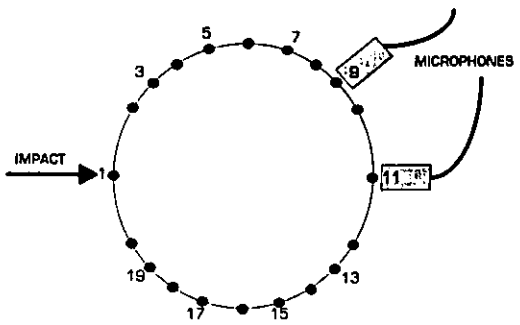


Fig.1 Relative positions of the impact, microphones and 20 measurement points along the equator of an apple

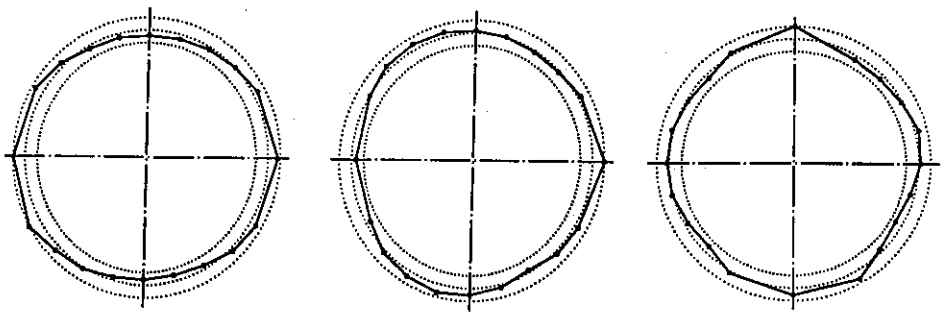

(a) $S_{20}$ mode (b) $S_{30}$ mode (c) $S_{40}$ mode

Fig.2 Spherical mode shapes of the apple

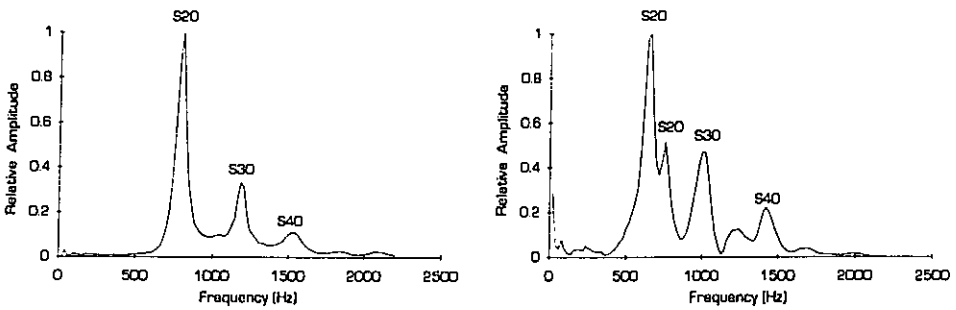


(a) without internal defect (b) with internal defect near the core

Fig.3 Frequency response spectra of an apple

# Predictability of leaf toughness from anatomical studies

Ms Mei Fun Choong

Botany Department,
University of Hong Kong,
Pokfulam Road,
Hong Kong

Toughness, a term which is here used to mean the work required to make unit area of crack, has been postulated to be one of the mechanisms that a plant uses to defend its leaves against herbivores. There is, however, little agreement in the ecological literature over the definition of leaf toughness (most authors consider it to be the force required to push a rod through the lamina) and also about what causes it - various suggestions include the presence of silica, the thickness of the cuticles and the proportion of lignin in the cell wall. In addition, toughness is often confused with stiffness - increasing the stiffness of a leaf may aid its photosynthetic function. This study is designed (a) to attempt to determine which parts of a dicotyledonous leaf provide it with toughness, (b) to use this information to predict the toughness of other leaves and (c) to establish whether the distribution of tough tissue is optimal to defend leaves from herbivores or instead to act in some other capacity, such as to prevent wind damage, for example.

The anatomy of the leaf of *Castanopsis fissa* (Fagaceae) was studied as part of a wider investigation into the leaf structure of the oak family in relation to herbivory. This leaf has been observed being eaten by herbivores external to the leaf and also by those living inside it (leaf miners). Using confocal images, the relative thicknesses of the layers of the leaf - upper and lower epidermis, palisade, spongy mesophyll, vascular tissue (both xylem and phloem), sclerenchyma bundle sheath and also the parenchyma bundle sheath extension - were estimated. In addition, anatomical features of the cell wall thickness and cell shape were quantified. A distinction was made between heavily-lignified on the one hand and lightly- or non-lignified tissue on the other, lignification being judged both by natural fluorescence and by phloroglucinol staining. These measurements have been manipulated into an index which could predict the toughness of a leaf and which could also help to estimate the energy expended by an invertebrate herbivore in feeding on various tissue layers of the leaf.

# RELATIONSHIPS BETWEEN TREE MORPHOLOGY AND LONGITUDINAL GROWTH STRESS MEASURED AT STEM LEVEL: INSTANCE OF PIN MARITIME (*Pinus pinaster* Ait.).

COMBES J.-G.
Laboratoire de Rhéologie du Bois de Bordeaux - B.P. 10 - 33610 Cestas Gazinet - FRANCE.

During tree growth, two major accidents can happen inducing some after-effects on morphogenesis:

- a change of the tree initial orientation involving the recovery of the growth direction by a stem deformation, in case studied a basal sweep (Fig. 1).
- a loss of apical dominance involving the putting of a traumatic reiteration complex under fork appearance (Fig. 2).

In any cases, there will be an elaboration of typical wood (reaction wood named compression wood in gymnosperms and tension wood in angiosperms) in peculiar angular sector of stem. This wood presence allows a reorientation movement of the stem, sometimes important. Peripheral measurements of Longitudinal Residual Strain of Maturation (LRSM) show a strain peak associated with the presence of réaction wood.

After cambial division, daugthter cells go into a differenciation and maturation stage. During the formation of secondary wall, cells have a tendancy to shrink longitudinally (and to swell tangentially) but the presence of anciently formed and rigid cells prevent this shrinkage. Thus, wood is pre-stessed in tree.

In the case of compression wood, there is a tendency to longitudinal expansion cell caused by a swelling matrix associated with a high microfibril angle. But this phenomenom being prevented by the bioenvironnement rigidity and compression wood is under compressive longitudinal stress (easily estimable at experimental level by the measurement of two points displacement after maturation strains relaxation). Those LRSM measured in stem surface, when stem longitudinal continuity is interrupted (by making tapping, drilling... in xylem under cambium area), are usually linked with tree morphology and peculiar wood anatomy.

The used method for the determination of LRSM is the single drilled hole method (Mitutoyo sensor on CIRAD structure, Fig. 3). Studied trees (22 years old pinus -*Pinus pinaster* Ait-) are morphologicaly different and show typical strain peaks, those peaks are correlated with the phenomenom of stem orientation.

The basal sweep and the fork are schematized in figure 1 and 2 with the principal localisations of measurements and values given by the sensor.

## BIBLIOGRAPHY.

Baillères H., 1994. Précontraintes de croissance et propriétés mécano-physiques de clones d'Eucalyptus (Pointe-Noire, Congo): hétérogénéité, corrélations et interprétations histologiques. *Thèse en Sciences du Bois de l'Université de Bordeaux I*, 161p.

Chanson B., 1993. déformation de maturation: hétérogéinétés angulaires en fonction du plan d'organisation des arbres. *Acta Botanica Gallica* **140**(4), 395-401

Fournier M., Guitard D., 1993. Les contraintes de croissance générées par la différenciation cellulaire. *Acta Botanica Gallica* **140**(4), 389-394

Timell T.E., 1986. *Compression Wood in Gymnosperms*. Springer-Verlag, 3 volumes,2150p.

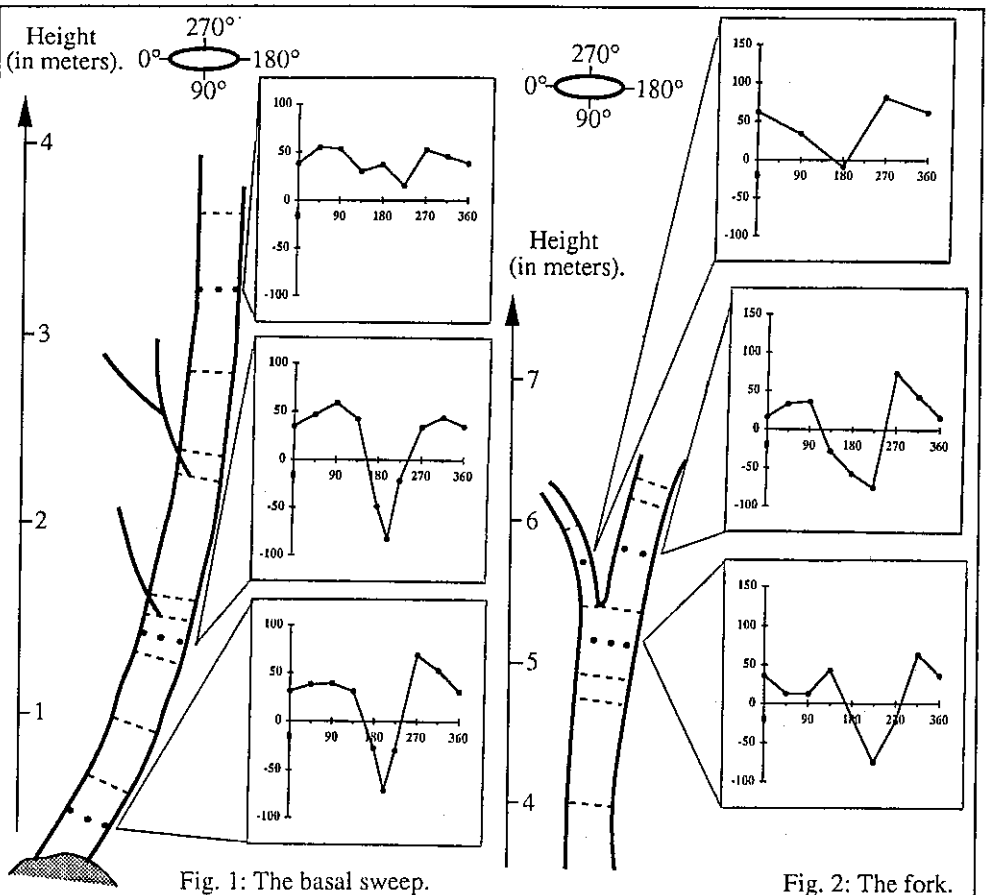


Fig. 1: The basal sweep.




Fig. 2: The fork.

(Angular sectors in abscissa, valors given by the sensor in ordinate)

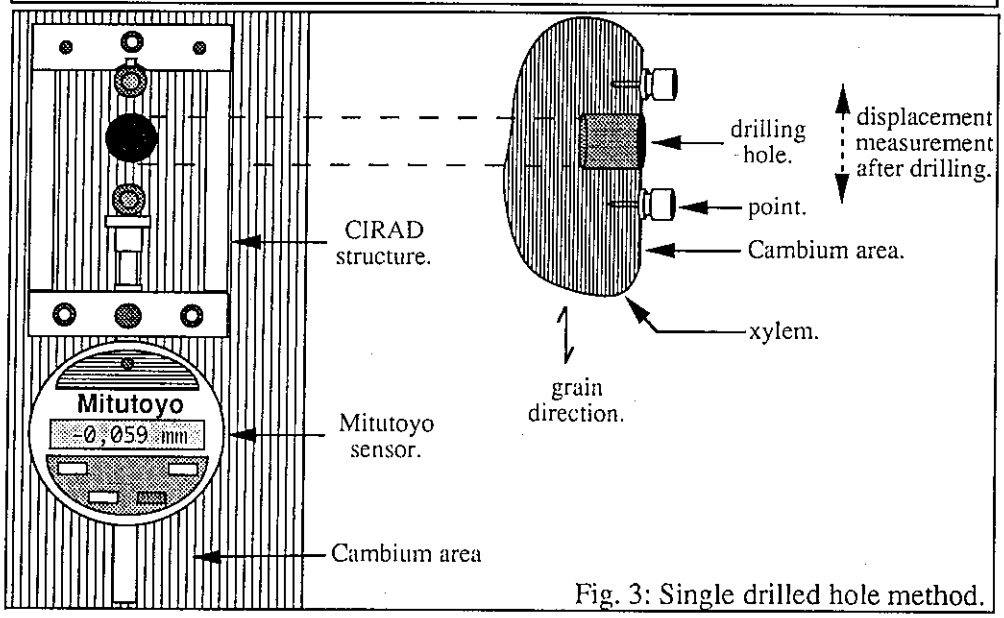


Fig. 3: Single drilled hole method.

# EFFECT OF WIND ON SOME ALLOMETRIC RELATIONSHIPS OF TWO PLANT SPECIES OF AN ELFIN SUBTROPICAL FOREST

*CORDERO Roberto A., VOLTZOW Janice and FETCHER Ned*
Department of biology, University of Puerto Rico,
PoBox 23360 Rio Pedras, PR 00931

Exposure to wind typically produces a reduction in organ length in plants. For plants growing in the cloud "elfin" forest, we hypothesized an increase in structures for mechanical support at the expense of growth in height and length. This hypothesis was tested in a transplant experiment in Pico del Este cloud forest, in the Luquillo Experimental Forest, in Northern Puerto Rico. This forest is also subjected to disturbances produced by high wind speeds. Plants of *Clibadium erosum* (a shrubby Compositae) and saplings of *Prestoea montana* (a mountain tree palm, Arecaceae) were grown from cuttings and seedlings, respectively, during almost three years. Barriers were used to protect randomly selected individuals from the wind.

For *Clibadium*, we used regression to examine the relationship between basal diameter of branches and branch length, in order to compare the slope with the one predicted by the power law model. We found a significant effect of barrier on the slope of the relationship indicating that exposure to wind produced overbuilt structures. We also found an effect of the barrier on the slope of the relationship between basal diameter of branches and total area of leaves on the branch.

For *Prestoea*, we studied the effect of wind on the leaf allometric relationships by considering the petiol as a columnar structure supporting a laminar load. We used the same analysis performed with *Clibadium*. We also consider the leaf type. As seedlings, this species presents simple laminar structures as leaves. Later, plants developes pinnately compound leaves. We found that the slope of the relationship between petiol diameter and leaf lamina area was significantly different between leaf types. This relationship seems to be influenced by the wind treatment. Other parameters like leaf dimensions related to petiol relative sizes did not changes between leaf types.

These results indicate that wind could be an important factor influencing plant form in cloud forest and may contribute to the dwarfed structure of the plants.

Actually, we are beginning to test some biomechanical properties of trees and shrubs trunks by mean of field bending tests. Also, we are interested in obtain relationships between growth patterns and field biomechanical properties for these trees, that help us to understand the "elfin" structure of this forest association.

TITLE: **The structural development of the stems and anchorage roots of winter wheat, *Triticum aestivum* L**

M.J.Crook, A.R.Ennos & E.K.Sellers: School of Biological Sciences, University of Manchester, Williamson Building, Oxford Road, Manchester M13 9PL.

## SUMMARY

The structural development of the stems and basal anchorage roots of two winter wheat cultivars (*Triticum aestivum* L) were investigated and related to their mechanical function. Stem and root morphology, anatomy and mechanical properties were examined from tillering (March) up to maturity (August), together with plant weight distribution. This allowed us to calculate a "factor of safety" against root and stem failure throughout development.

As the plants grew taller the stem and the anchorage "coronal roots" increased in bending strength countering the increasing mechanical demands. The bending strength, in turn, was correlated with the amount of lignified material around the stem and root perimeter. Structural development ceased by ear emergence, when the plant was at its tallest, but because the ear weight continued to rise the "self-weight" moment pushing the plant over continued to increase. This meant that the "Safety Factors" of both cultivars against both root and stem mechanical failure decreased throughout development (Figure 1). In both cultivars the safety factors against root failure were lower than for stem failure, and Galahad had lower factors of safety than Hereward. All these findings were consistent with results of field trials; failure tends to occur late in development, during grain filling, and is localised to the root system, whilst Galahad is more prone to failure than Hereward.

The pattern of mechanical development of winter wheat seems to be one which would maximise its reproductive success, maintaining its structural integrity especially early in development while investing in a minimum of structural material.

Figure 1: "Safety Factors" against mechanical failure: stem breakage (closed symbols) and anchorage failure (open symbols). Bars represent ± SE of the mean for stem safety factors (n=10).

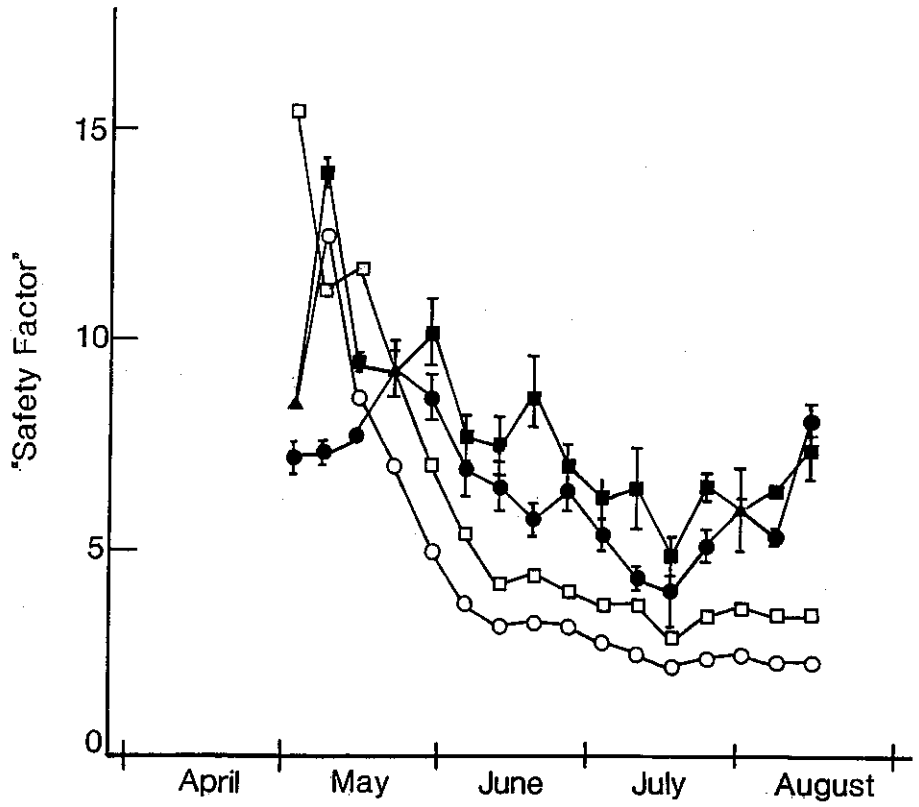
"Safety Factor"
15
10
5
0
April
May
June
July
August

# FLUORESCENCE MICROSCOPIC STUDIES OF SECONDARY WALL DEPOSITION PATTERNS IN TRACHEARY ELEMENT (TE) DIFFERENTIATION IN *ZINNIA ELEGANS* LEAF MESOPHYLL CELL SUSPENSION CULTURES

*DAYATILAKE, G.A.* and RAJAGOPAL, R.***

* Dept. of Crop Science, Faculty of Agric., Univ. of Ruhuna, Mapalana, Kamburupitiya, Sri Lanka, corresponding author
** Dept. of Plant Biol., Royal Vet. & Agric. Univ., Thorvaldesnsveg 40, Frederiksberg C, DK 1871 Denmark

Tracheary element (TE) differentiation of isolated mesophyll cells of *Zinnia elegans* (L) CV Envy was studied in cell suspension cultures. Changes in the secondary cell wall band deposition sequence and patterns were observed using calcoflour white (CW) fluorescent brightener. Using this procedure, the initiation of secondary cell wall deposition was observed 10-12 hrs earlier than that of phase contrast light (PCL) microscopy. At 48 hrs, the primary walls of the expanded mesophyll cells, faintly stained with CW, were only visible. In contrast, clearly stained cell plates were detected in dividing cells. Initial stages of depostion of the cell wall material, in an annular pattern was observed at 52 hrs. TEs which had been differentiated following initial cell division or directly were recognized, with brightly stained annular/spiral wall bands, at 64 hrs of incubation. However, under phase contrast light (PCL), only the reticulate, scalariform and pitted as well as some irregular patterns were noted in the cell suspension. During the course of TE differentiation, transition of the patterns were observed indicating that there was a continuing cell wall deposition which resulted in the transformation of annular or spiral patterns into scalariform or pitted patterns. In partially plasmolyzed cells with sorbitol, it was noted that the cell wall thickenings followed the contour of the protoplast and were not associated with the primary cell wall at the beginning.

Key words : Tracheary elements, Differentiation, *Zinnia elegans*, Secondary wall depositions.

# BOIS JUVENILE ET BOIS ADULTE : RECHERCHE DE DIFFERENCES CARACTERISTIQUES A TRAVERS L'ETUDE DU BOIS DE TENSION DU WAPA, *Eperua falcata* Aubl. (CAESALPINIACEAE)

Olivia DELAVAULT
LMGC, Université Montpellier II, place Eugène Bataillon, Case courrier 081
34095 MONTPELLIER Cédex 5

Sur de jeunes Wapas ou sur des Wapas adultes, la recherche de la signification anatomique des mesures de relaxation des contraintes dans l'arbre sur pied, nous a conduit vers une approche du bois tant au niveau pariétal qu'au niveau cellulaire.

Cette étude vise plus particulièrement à identifier les évolutions entre le bois normal et le bois de tension à l'état juvénile et adulte. Des photos de **coupes transversales** observées en microscopie électronique à balayage (MEB) d'après lesquelles nous avons mesuré l'épaisseur des parois secondaires (S) et celle des couches gélatineuses (G), ainsi que les **diagrammes** de type nuages de points (Fig. A, B, C) qui expriment en µm l'épaisseur de S en fonction de celle de G, constituent le support matériel de cette analyse comparative.

L'observation et la superposition de ces figures montrent que :

* d'une **manière générale**, l'épaisseur de la paroi S des fibres du bois normal est nettement supérieure à celle des fibres de bois de tension, et ceci dans tous les cas envisagés (bois d'un jeune plant, bois juvénile prélevé dans le duramen d'un arbre adulte, aubier d'arbres adultes).

* dans le **bois normal**, l'épaisseur de la paroi secondaire des fibres d'un arbre adulte ([1,8-3,4µm]) recouvre celle des fibres d'un jeune plant ([1,8-2,25µm], photo 1) ainsi que celle des fibres du bois juvénile ([2,1-3µm]).

* dans le **bois de tension**, il existe pour les **parois secondaires**, vers les valeurs inférieures, un décalage du diagramme obtenu pour l'individu jeune (épaisseur de S comprise entre 0,5 et 1,5 µm) par rapport aux 2 autres diagrammes (épaisseur de S comprise entre 0,9 et 1,9 µm), alors que l'étalement relatif des valeurs de l'épaisseur pariétale est sensiblement identique dans tous les cas de figure (environ 1 µm).

* l'épaisseur de la **couche G** du bois de tension d'un jeune arbre (photo 2) ou celle du bois juvénile prélevé dans le duramen d'un arbre adulte (photo 3), s'étend sur une plage de valeurs plus grande que celle couverte par l'épaisseur de la couche G dans le bois de tension situé en périphérie du tronc d'arbres adultes (photo 4). Il existe donc, dans le bois à l'état jeune, des fibres dont la couche G est très fine (de 1 à 1,6 µm) qui sont absentes dans le bois à l'état adulte.

Des fibres gélatineuses qui diffèrent par l'épaisseur de leur couche G et/ou par celle de leurs parois secondaires mettent en évidence des différences caractéristiques entre le bois juvénile et le bois adulte. Mais il reste à comprendre la signification mécanique de ces différents faciès de bois de tension dans les phases successives de croissance de l'arbre.

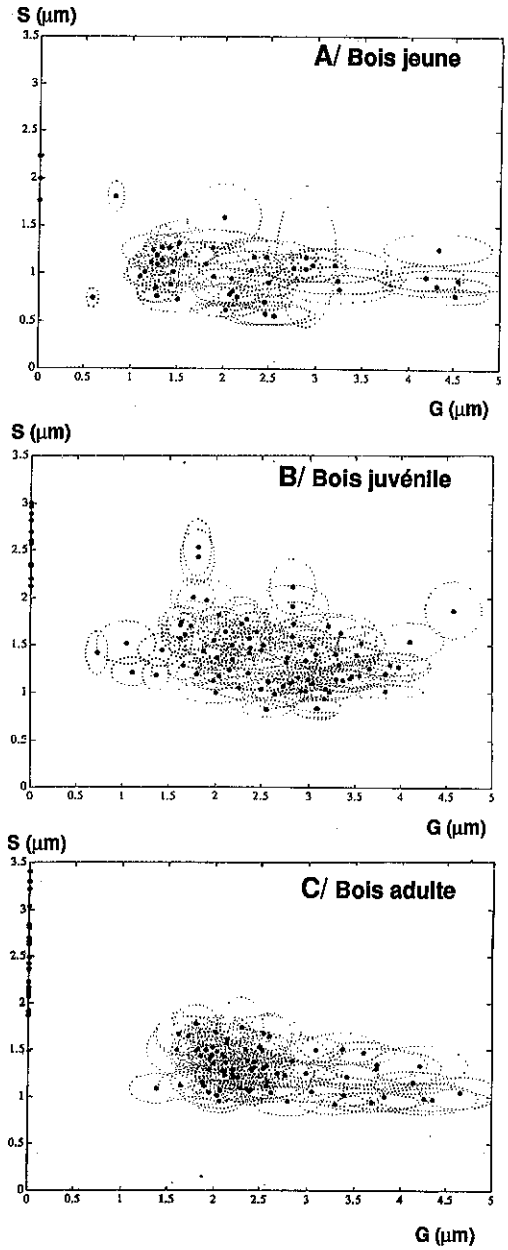


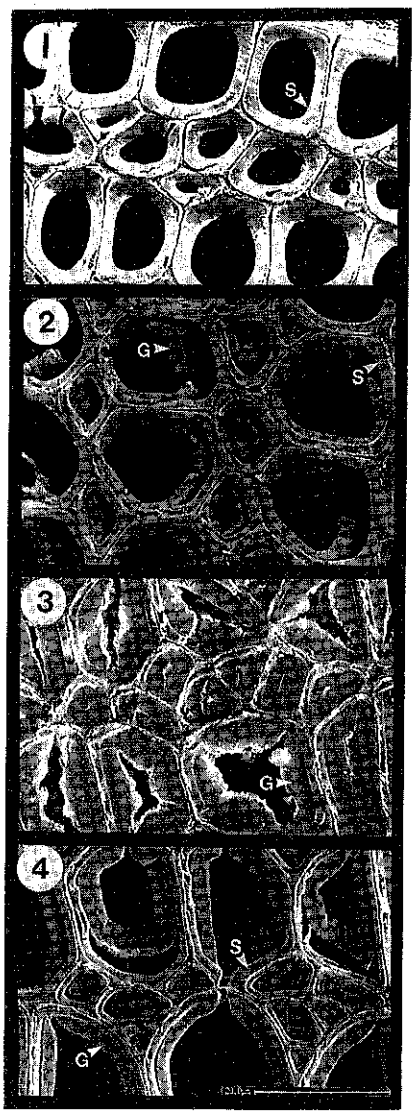


Légende :
S=paroi secondaire; G=couche gélatineuse;
• =moyenne des mesures pour chaque photo;
.....= écart type sur S et sur G

**Figures A, B, et C :** Diagrammes représentant l'épaisseur de la paroi S en fonction de celle de la couche G (en µm) pour le jeune plant, le bois juvénile et le bois adulte.

**Photos 1 et 2** : Bois de l'individu jeune. **1)** bois normal (l'épaisseur de la couche S est de 2 µm); **2)** bois de tension (les épaisseurs de G et de S mesurées sur cette photo sont respectivement 1,28 et 1,2µm).

**Photo 3 :** Bois de tension de la partie juvénile (duramen) d'un 'individu adulte (les épaisseurs de G et de S mesurées sur cette photo sont respectivement 3,31 et 1,30µm).

**Photo 4** : Fibres de bois de tension prélevées dans l'aubier d'un individu adulte (S=1,12µm et G=2,56µm).

**The effect of the availability of external support on allocation patterns in herbaceous climbing plants.**

Koen C. den Dubbelden and Bertjan Oosterbeek.

Department of Plant Ecology and Evolutionary Biology, Utrecht University, P.O. Box 80084, 3508 TB Utrecht, The Netherlands.

Climbing plants differ from non-climbing plants in their morphology, anatomy and physiology mainly as a result of differences in biomechanical constraints. Climbers utilize external structures as support. Although this enables them to use stem biomass for stem length rather than for rigidity (Darwin, 1876; den Dubbelden & Verburg, in press) it also makes them dependent on the availability of structures upon which to climb. Lacking the capacity to hold themselves upright, the growth of climbers will be restricted by their capacity to encounter suitable structures for climbing, and by their efficiency in ascending these structures (Putz & Holbrook, 1991).

In a greenhouse experiment we studied the effects of the availability of external support on the allocation of plant biomass to main stems and branches in herbaceous climbing plants from temperate zones. The experiment included three species of climbers from grasslands and verges that climb by means of tendrils, and three twining species from verges and forest-edges. Plants were germinated from seeds and grown for three months in pots containing a river sand medium that was regularly watered with a non-limiting nutrient supply. Simulating the success and failure of encountering and ascending external supporting structures, one third of all plants was supplied with support directly at the start of the experiment, one third was refrained from support during the whole experimental period and the remaining third was offered support halfway the experiment.

At the end of the experiment, all three treatments resulted in the same total amount of plant biomass for a given species. However, supported plants allocated relatively more aboveground biomass to their climbing main stem, while unsupported plants invested more plant mass in basal branches. The main stem of supported plants grew to be much taller than that of unsupported plants (Fig 1.). The latter stopped growing after a few weeks, which was associated with the number of internodes formed. The number of basal branches was higher in unsupported than in supported individuals (Fig. 1). When the main stem of unsupported plants was supplied with support halfway the experiment, they were no longer able to climb, while the branches of these plants could climb into the support. Once the branches ascended the support, the branching frequency declined in comparison with plants that remained unsupported branching during the whole experimental period.

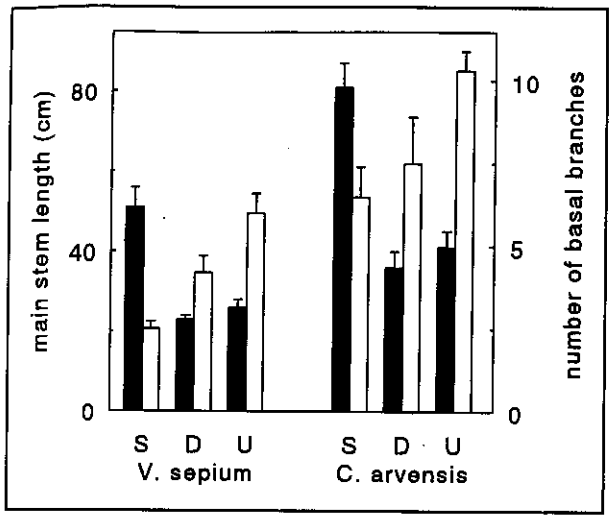


Figure 1. Mean (±se) length of main stem (black bars) and mean (±se) number of branches (white bars) of a typical tendril climber *Vicia sepium* and a typical twiner *Convolvulus arvensis* as affected by support availability (S, supported, and U, unsupported during whole experiment; D, support was offered halfway the experimental period).

Our results show that the availability of external supporting structures, both in space and time, is an important resource that determines plant height and branching patterns in herbaceous climbing plants. A large number of branches, that can grow in any direction, enhances the possibility that external support is encountered. The number of branches seems to be determined by the ability of the main stem to locate support and in case of failure by the successful support attachment of branches.

*References*

- Darwin, C. 1876. The Movements and Habits of Climbing Plants. - John Murray, London.
- den Dubbelden, K.C. & Verburg, R.W. Allocation patterns and growth rates in herbaceous climbing plants. - Oecologia (in press).
- Putz, F. E. & Holbrook, N. M. 1991. Biomechanical studies of vines. - In: The Biology of Vines (eds. F.E. Putz & H.A. Mooney). Cambridge University Press, Cambridge, pp. 73-97.

# DYNAMIC MECHANICAL THERMAL ANALYSIS AND ITS APPLICATION TO THE INVESTIGATION OF TEXTURAL DEFECTS OF LEGUMES

Andy J. DOWNIE, Dominique M.R. Georget, Andrew C. Smith and Keith W. Waldron.
BBSRC Institute of Food Research, Norwich Laboratory, Norwich Research Park, Colney, Norwich NR4 7UA

The sensory texture of foods is the consumer's interpretation of the mechanical properties of that food. Any processing or storage of food, altering the chemistry of the commodity, may influence these properties and affect the demand for that commodity.
Legumes are an important source of dietary protein, especially in the developing countries. However, this specific commodity is underutilised. A major reason for this is the tendency for certain seeds to develop textural defects; the main one being the storage-induced defect known as the hard-to-cook defect.

The defect results in a lack of cell separation upon cooking (Jones and Boulter, 1983). This behaviour has been widely attributed to an increase in the rigidity of the middle lamella of the cell wall as a result of pectin insolubilisation. The insolubilisation may itself be the consequence of pectin-cation binding in the middle lamella, or other forms of cross-linking. In preliminary trials we are investigating the influence of water content and temperature upon the mechanical properties of the bean cotyledonary tissue. In the past a number of techniques have been used to characterise the mechanical properties of hard-to-cook beans, including the Mattson bean cooker (Mattson, 1946) and use of a puncture test (Bourne, 1972); trials with these apparatus are performed in parallel to those with the DMTA.

The present study uses broad beans as a model system for beans stored under tropical conditions, and employs the DMTA to assess the stiffness of cotyledonary sections at different initial water contents. Artificial conditions of high temperature and high humidity are employed to reproduce the tropical storage conditions. This procedure is employed as a general procedure has been shown to yield legumes which are hard-to-cook.
A comparative analysis is drawn between the results of the DMTA work and that of the other mechanical analyses.
Figures 1 and 2 show preliminary data on the effect of initial water content on the bending modulus- and tan $\delta$-temperature scan.

## REFERENCES

Bourne, M.C. (1972). Texture measurement of individual cooked dry beans by the puncture test. *J. Food Sci.*, **37**, 751

Jones. P.M.B., Boulter, D. (1983). The cause of reduced cooking rate in *Phaseolus vulgaris* following adverse storage conditions. *J. Food Sci.*, **48**, 623

Mattson, S (1946). The cookability of yellow peas: A colloid chemical and biochemical study. *Acta. Agric. Suec.* **2**, 185

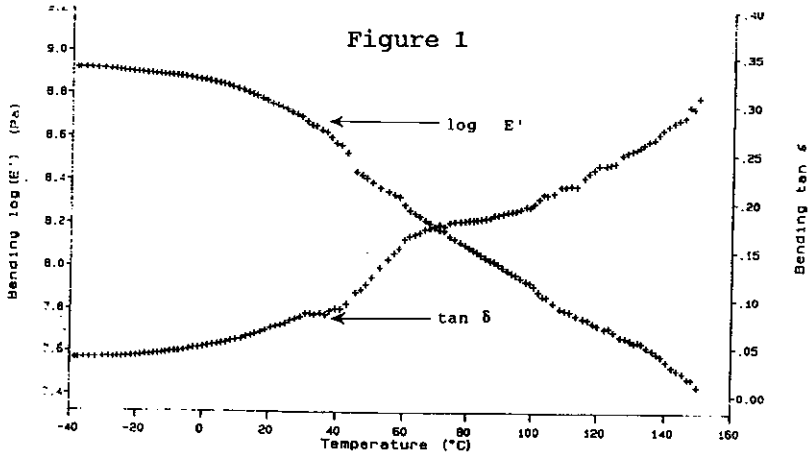


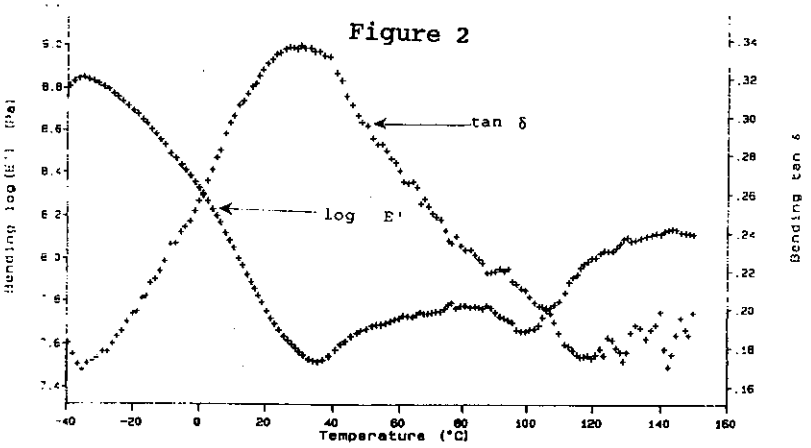


Figure 1 represents the data obtained when using beans of an initial water content of 7.69 %. Whilst figure 2 represents a higher initial water content of 20.66%.

# TURGOR IN THE GROWTH ZONE OF TALL FESCUE LEAVES AT LOW WATER AND NITROGEN AVAILABILITY: DRIVING OR DRIVEN FORCE ?

Jean-Louis Durand, Bertrand Onillon, François Gastal.
Station d'Ecophysiologie des Plantes Fourragères. INRA. F-86600 Lusignan, France.

## INTRODUCTION.

In grasses, leaf elongation is highly sensitive to nitrogen and water shortage. The leaf elongation rate (L) depends on the length (z) and the relative elongation rate (R) of the tissues situated in the growth zone. Turgor in the growth zone ($P_{zc}$) is the origin of the force inducing irreversible tissue elongation (Lokhart 1965):

$$R = L/z = \Phi (P_{zc} - Y) \qquad (1)$$

where Y is the yield turgor and $\Phi$ is the extensibility. The aim of the work reported here was to determine the combined effects of nitrogen and water deficits on the length, the relative elongation rate and turgor of growing tissues.

## MATERIAL AND METHODS.

After two regrowth cycles from cutting at 5 cm, tall fescue plants (cv *Clarine)* were grown in growth cabinet. Half of the pots received a high nitrogen solution and the other half received a low nitrogen solution. Irrigation was stopped in half of the plants, the other receiving nutrient solution as before. L was determined by regression of daily measurements of leaf length on time. Water and osmotic potentials were determined at the end of the dark period on mature leaves (pressure chamber) and in the growth zone (psychrometry on sampled 5 mm long leaf segments). On a separate set of plants the length of the growth zone was measured using the pin hole technique described by Schnyder and Nelson (1988).

## RESULTS.

Nitrogen deficiency induced a large decrease of L at well watered conditions. With time after withholding water nitrogen deficient leaves elongated faster (Fig 1a). However the effect of drought, as measured by the leaf water potential of mature leaves, was the same under both nitrogen situations (Fig 1b). Both z and R declined during drought at high and low nitrogen (Fig. 2). Growth zone turgor ($P_{zc}$ = water potential - osmotic potential) in well watered plants was 0.5 MPa whatever the nitrogen level (Fig 3). Under drought, in the low nitrogen treatment, turgor increased continuously from 0.5 MPa to 1 MPa. In the high nitrogen treatment, $P_{zc}$ reached the same value after a transient decline.

## DISCUSSION.

The decline of z explained only one part of the effect of nitrogen deficiency on L. As $P_{zc}$ was unaffected by nitrogen nutrition under well watered conditions $\Phi$ or Y also were affected. Both z and R decreased due to water deficit and $P_{zc}$ declined only transiently in high N treatment. The stability of $P_{zc}$ during the first 5 days of water deficit indicates that $\Phi$ or Y had changed. This was also true for the local growth rate at 7.5 mm where

turgor was computed. For slow permanent alterations of L with constant $P_{zc}$ (for instance N effects) structural changes in the growing tissues such as cell size or wall thickness could explain the changes of Φ (or Y). Cell wall properties were more likely involved in the faster changes of L as during the first steps of a drying cycle at constant $P_{zc}$. The constancy of $P_{zc}$ under contrasted circumstances suggests that it was regulated and that L variations were part of the regulation, which could be expressed by rearranging equation (1):

$$P_{zc} = L/(z \times \Phi) + Y \qquad L>0 \qquad (2)$$

$P_{zc}$ only increased when water deposition in the growing tissues was nil (L=0 and Φ=0) probably as a result of a continuing solute deposition associated to an interrupted water deposition in the growth zone.

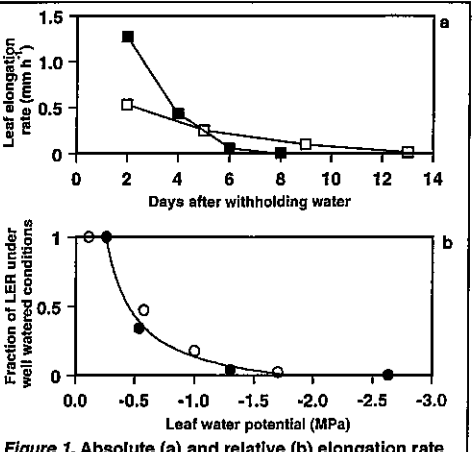


*Figure 1.* Absolute (a) and relative (b) elongation rate of tall fecue leaves after withholding water versus time (a) or water potential of mature leaves (b). ■, ●: high nitrogen □, ○: low nitrogen.

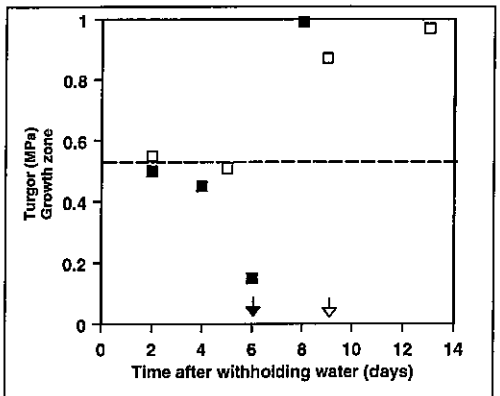


*Figure 3.* Turgor of the growth zone at 7.5 mm from leaf base. ■: High N □: Low N. The arrows indicate the time at which elongation stopped. The dashed line indicates the turgor in well watered leaves.

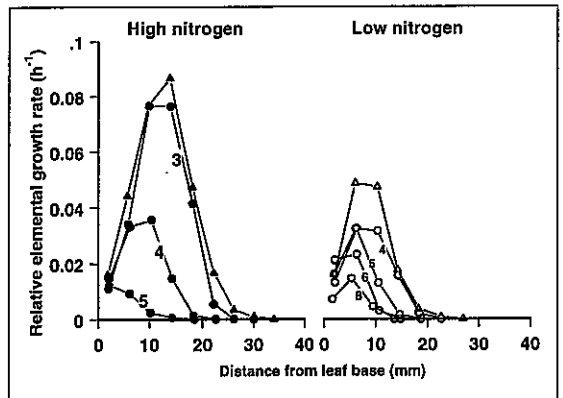


*Figure 2.* Spatial distribution of growth in the base of tall fescue leaves submitted to increasing water deficit at two levels of nitrogen nutrition. ▲,△: well watered; numbers indicate the time from withholding water.

## LITTERATURE CITED

Lokhart 1965. An analysis of irreversible plant cell elongation. J. Theor. Biol., 8, 264-275.

Schnyder H, Nelson CJ. 1988. Diurnal growth of tall fescue leaf blades. I.Spatial distribution of growth, deposition of water, and assimilate import in the elongation zone. Plant Physiol., 86, 1070-76.

# LE SAPIN ET L'EPICEA FRANÇAIS
# PROPRIETES TECHNOLOGIQUES & IMPACT SUR LA SYLVICULTURE

**A. EL OUADRANI**
**C. de LAFOND**
**J.D. LANVIN**
**F. ROUGER**

Centre Technique du Bois et de l'Ameublement, CTBA
Département Structure
Unité Etudes et Recherche
10, avenue de St Mandé 75012 PARIS

L' importance des reboisements réalisés en France depuis une cinquantaine d'années situe la forêt française aujourd'hui parmi les plus productives d'Europe. Dans ce contexte, les essences résineuses en particulier, doivent trouver des débouchés valorisants, notamment en structure (charpente et ossature). Mais cette valorisation passe par une connaissance précise des caractéristiques technologiques, et notamment mécaniques. C'est pour pallier ce manque de connaissances que le CTBA a lancé en 1990 un vaste programme de qualification du sapin et de l' épicéa français.

Les objectifs sont multiples, puisqu'il s'agit à la fois :

- de conseiller utilement les politiques de boisement et les sylvicultures à développer.
- de renseigner les concepteurs d'ouvrage sur les performances du matériau.
- de proposer des systèmes "classement- résistance" garantissant la sécurité d'emploi des essences concernées, tout en assurant la valorisation optimale du potentiel forestier actuel et futur.

L'échantillonnage des placettes et des arbres est réalisé selon une méthode statistique intégrant les facteurs sylvicoles les plus pertinents : structure forestière (régulière ou irrégulière), classe de diamètre , classe de fertilité et altitude.
Au total, 1022 arbres ont été prélevés dans 206 placettes. Cet échantillonnage, validé par un groupe d'experts forestiers, est basé sur les données de l'Inventaire Forestier National et a été réalisé à l'aide des différents services forestiers régionaux (O.N.F, C.R.P.F, SERFOB).

Des pièces de dimensions commerciales sont débitées de façon à identifier précisément leur origine : région, placette (type de sylviculture et altitude), arbre (environnement dans la placette), billon (hauteur de prélèvement dans l'arbre), position de la pièce dans la section transversale de l'arbre.

Deux familles d'éprouvettes sont testées: éprouvettes de bois sans défaut de petites dimensions testées en flexion, traction longitudinale et perpendiculaire, compression axiale, cisaillement et fendage et éprouvettes en dimensions commerciales sollicitées en flexion et en traction longitudinale pour déterminer le module d'élasticité et la contrainte de rupture.

La largeur des cernes, la masse volumique et la nodosité locale sont mesurées avant de réaliser ces tests mécaniques. Au total plus de 4 300 pièces en grandeur d'emploi et 900 éprouvettes de bois sans défaut sont testés. La masse de données ainsi acquise fournit environ 43 000 informations d'ordre forestière et 23 000 données sur le matériau bois.

L'analyse des résultats d'essais conduit à énoncer les principales conclusions sylvicoles suivantes:

☞ La masse volumique de l'épicéa est plus sensible à une variation de largeur de cernes que celle du sapin.
A largeur de cerne égale, et au delà de 3 mm, la masse volumique du sapin devient plus forte que celle de l'épicéa.

**Il n'est pas recommandé de favoriser une trop forte croissance de l'épicéa en veillant à la régularité et à l'intensité des éclaircies des plantations .**

☞ La texture du sapin est environ 1,5 fois plus forte que celle de l'épicéa, et ceci quel que soit l'âge de formation du bois.
Quelle que soit l'essence, la texture augmente avec l'âge de végétation jusqu'à 80 ans puis elle a tendance à se stabiliser .

**Cette caractéristique anatomique pourrait expliquer le comportement au séchage et à l'imprégnation de ces deux essences.**

☞ Globalement, la rigidité et la résistance en flexion sont identiques pour les deux essences. Cependant l'épicéa est plus résistant mécaniquement quand il présente une largeur de cerne inférieure au millimètre.
Planter de l'épicéa à très faible altitude et hors de son aire naturelle conduit à produire du bois à très faible propriétés mécaniques .
Les propriétés physiques et mécaniques sont très différentes selon les régions d'approvisionnement.

**La diversité de comportement mécanique relevé dans les différents massifs doit permettre d'orienter les politiques sylvicoles vers un choix judicieux d'une essence en fonction des caractéristiques stationnelles existantes et de l'utilisation finale des produits forestiers.**

# Champ de contraintes développé dans le sol par la croissance des racines: Considérations théoriques.

Auteur: A.G. Faure

Unité de Science du Sol
Domaine Saint-Paul
Institut National de la Recherche Agronomique
BP 91 - 84143 Montfavet Cédex

**Résumé du poster.**

La méthode des éléments finis est utilisée pour déterminer la distribution des contraintes développées dans le sol, au voisinage d'une racine, lors de sa croissance. L'étude porte sur l'influence de l'état physique du sol sur cette distribution en prenant en compte les modifications qu'il entraîne sur le développement morphologique de la racine. Ces lois sont fournies par lès expériences de N'Guyen sur le maïs placé en conditions contrôlées de croissance.

Lorsque la racine se développe, des zones de plasticité de forme quasi circulaire apparaissent autour de l'apex et la méthode des éléments finis permet d'en déterminer l'évolution en fonction du développement de la racine.

Ce modèle théorique permet de changer les paramètres des lois morphologiques lorsque la réaction du sol devient importante ou lorsque ses propriétés mécaniques évoluent. Il établit ainsi les possibilités de prendre en compte simultanément les diverses interactions mécaniques développées entre le sol et la racine.

Cette méthode paraît plus performante que les hypothèses basées sur l'expansion cylindrique ou circulaire du champ de contraintes autour de la racine.

Il devrait rendre possible une meilleure simulation de la croissance des racines que ne le fait l'analogie de l'action du pénétromètre.

Actuellement le modèle fonctionne sous les hypothèses de contraintes planes, avec un sol élasto plastique répondant au critère de Drucker-Prager.

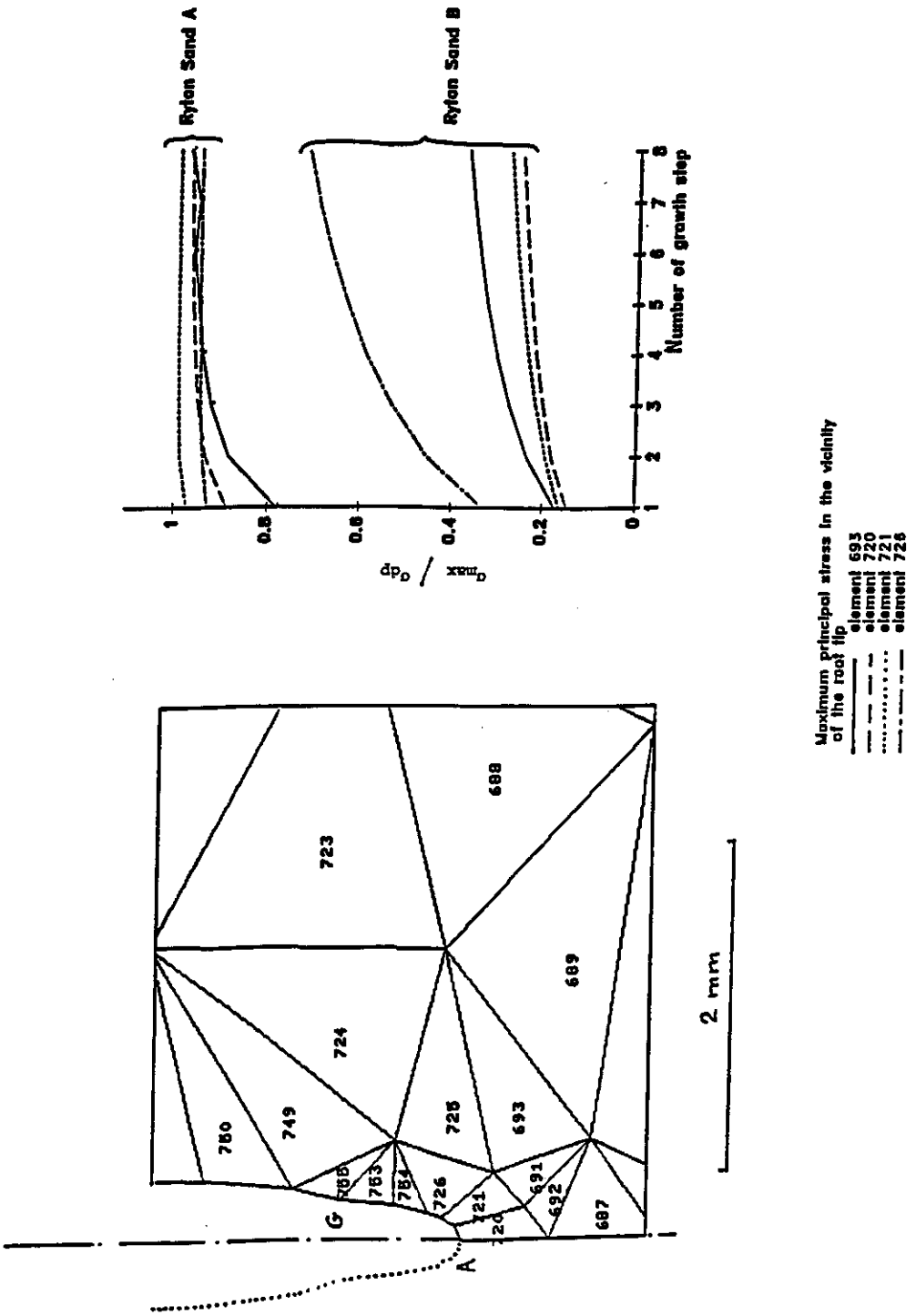
Rylan Sand A
Rylan Sand B
Number of growth step
$\sigma_{max}$ / $\sigma_{dp}$
Maximum principal stress in the vicinity of the root tip
element 693
element 720
element 721
element 726
2 mm
G
A

# Mechanical Properties of Plant Tissue, Isolated Cells and Isolated Cell Wall Material.

**T.J.Foster, M.J.Gidley, B.J.Briscoe*, D.R.Williams*, A.J.Barraclough, and P.J.Lillford.**

*Unilever Research, Colworth Laboratory, Colworth House, Sharnbrook, Bedford, MK44 1LQ, UK.*
**Dept. Chemical Engineering, Imperial College, Prince Consort Road, Kensington, London, SW7 2BY, UK.*

## ABSTRACT

Aspects of the mechanical and material properties of plant tissue, cells and cell wall material have been studied. Cell wall material and individual cells have been isolated from the pericarp tissue of a processing variety of *Lycopersicon esculentum* in order to study the properties of the cell wall matrix and the turgor pressure of cells individually. Techniques used in such analyses are mechanical spectroscopy (at Colworth) and individual particle upsetting technology (at Imperial College).

Cell wall material was produced by homogenising tomato pericarp tissue. After washing, it had a rather gelatinous appearance. The mechanical spectra obtained from such material were similar to those of biopolymer networks with G' and G" almost independent of frequency, and $\eta^*$ decreasing as frequency increased with a slope $\sim 1$.

*In vitro* enzyme hydrolysis of plant tissue has been difficult to study in the past because of uncontrollable enzyme diffusion. However, enzyme incubation with cell wall material provides direct access to substrates, and the hydrolysis of cell wall material by a variety of cell wall acting enzymes has been followed by mechanical spectroscopy.

Tomato cells are isolated by soaking pieces of pericarp in calcium chelating (50mM CDTA) solution. Most of the cells retained their viability and it proved possible to alter turgor pressures by soaking in a range of mannitol solutions. The mechanical properties of cells at varying stages of turgor may then be tested, both as concentrated dispersions (mechanical spectroscopy) and as isolated cells (force deformation behaviour).

# Simulation d'un arbre en croissance : relations architecture / mécanique.

Th. FOURCAUD[1], F. BLAISE[2], P. LAC[1]
1 - Laboratoire de Rhéologie du Bois de Bordeaux - UMR 123 CNRS, INRA, Univ. Bordeaux I Domaine de l'Hermitage BP 10 33610 Cestas Gazinet.
2 - Unité de Modélisation des Plantes CIRAD BP 5035 34032 Montpellier CEDEX 01

## Modélisation et simulation de la croissance des arbres.

**.Mise en place de l'architecture aérienne.** Une méthode originale de modélisation et de simulation de la croissance et de l'architecture des végétaux a été développée au CIRAD. Elle s'appuie sur les connaissances qualitatives apportées par l'école de Hallé [1] en architecture végétale et sur les méthodes quantitatives mises au point au CIRAD dans le cadre de l'AMAP [2] (fig.1). Ces méthodes sont basées sur la description du fonctionnement des bourgeons (croissance, mort, ramification) par des processus stochastiques. La simulation du modèle est assurée par le logiciel AMAPpara. Ce dernier permet d'établir l'architecture d'un arbre à un âge donné en faisant fonctionner parallèlement tous ses bourgeons selon leurs lois propres de croissance, de mort et de ramification. La gestion en parallèle des bourgeons actifs permet d'obtenir, à tout moment de la croissance, une topologie cohérente de l'arbre [3]. Le résultat de la simulation est une description géométrique en 3D de l'arbre qui est utilisée pour la visualisation, mais qui peut servir de base à d'autres applications tel le calcul des transferts radiatifs.

**.Modèle de simulation de la grosseur des axes.** La cohérence topologique de l'arbre permet de connaître le nombre d'unités de croissances feuillées susceptibles de produire des assimilats par photosynthèse. La quantité d'assimilats déposée le long des axes dépend du mode de diffusion utilisé (uniforme, non uniforme avec dépôt binomial ...). La simulation de ces modèles de diffusion permet de calculer la largeur des cernes internes résultant de la migration des assimilats (fig.2) [4].

## Couplage architecture / biomécanique de l'arbre.

**.Calcul des structures par pas.** L'utilisation d'un algorithme de simulation du parallélisme dans AMAPpara permet de déterminer l'évolution du comportement mécanique d'une plante à chaque étape de son élaboration. A cet effet, un module de calcul mécanique utilisant la Méthode des Eléments Finis est actuellement développé au Laboratoire de Rhéologie du Bois de Bordeaux. Cette méthode s'appuie sur l'écriture d'une formulation incrémentale d'équilibre originale adaptée aux structures de volume variable [5]. Deux types de chargement sont pris en compte à chaque pas de croissance :

- l'incrément de poids propre de la structure (croissances primaire et secondaire);
- les précontraintes induites par les déformations de maturation du bois dans les cernes périphériques [6], [7]. Un différentiel de ces déformations dans une section droite entraîne une flexion des axes permettant à l'arbre de se réorienter (tropismes, recherche de la lumière ...) (fig.3).

**.Applications.** Ce module de calcul est totalement interactif avec le moteur de croissance AMAPpara. Il permet d'une part de calculer la géométrie des branches, d'autre part de déterminer l'évolution des contraintes mécaniques dans chaque cerne du tronc d'un arbre tout au long de sa croissance (fig.4), ceci en relation avec son architecture (répartition des

charges, largeur des cernes). Les applications de ce logiciel sont nombreuses et couvrent différents domaines de recherche. En particulier, il permet d'étudier l'influence des arcures des branches sur le mode de ramification chez certains arbres fruitiers (phénomènes d'épitonie). Il est aussi un outil pouvant permettre d'analyser la qualité du bois chez un arbre en peuplement (influence de la compétition sur le champ de contraintes dans la grume, influence de la présence de fourches etc. ...).

**Références :**

[1] Hallé F., Oldeman R.A.A. et Tomlinson P.B., 1978. *Tropical Trees and Forest.* Springer-Verlag, Berlin, Heidelberg, New-York, 44 p.

[2] Reffye (de) Ph., Blaise F. et Guedon Y., 1993. *Modélisation et simulation de l'architecture et de la croissance des plantes.* Revue du Palais de la Découverte, Vol.21, N°209, pp 22-48.

[3] Blaise F., 1991. *Simulation du parallélisme dans la croissance des plantes et application.* Nouvelle thèse N°1071, Université Louis Pasteur, Strasbourg, France.

[4] Reffye (de) Ph. *et al.*, 1994. *Essai sur les relations entre l'architecture d'un arbre et la grosseur de ses axes végétatifs.* Publication INRA (à paraître).

[5] Fourcaud Th. et Lac P., 1993. *Modélisation mécanique de la croissance des végétaux.* Actes du Colloque National en Calcul des Structures, Giens, Var 11-14 mai 1993, Edition Hermès, Vol.1:131-140.

[6] Archer R.R., 1986, *Growth stresses and strains in trees.* Springer Verlag series in Wood Science, Edited by E. Timell, 240p.

[7] Fournier M., 1989. *Mécanique de l'arbre sur pied : maturation, poids propre, contraintes climatiques dans la tige standard.* Thèse de l'Institut National Polytechnique de Lorraine.

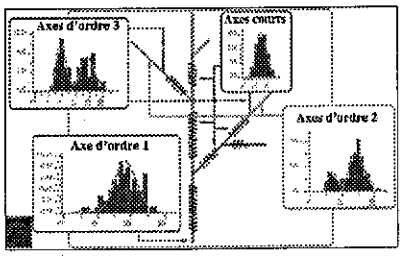


**Figure 1 :** Evolution des Unités de Croissance dans une architecture de type Merisier.

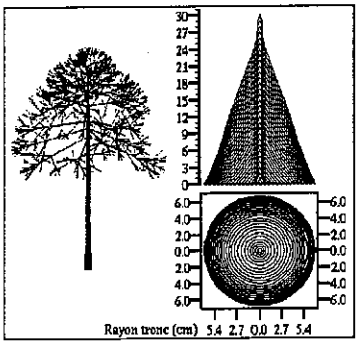


**Figure 2 :** Largeurs des cernes du tronc pour une diffusion uniforme des assimilats.

**Figure 3 :** Déséquilibre et redressement d'un pin.

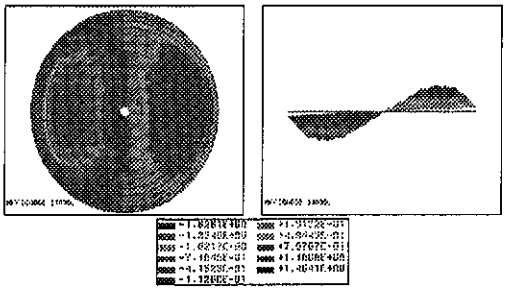

**Figure 4 :** Contraintes longitudinales dans une section droite du tronc.

# The impact of the ramification on the architecture of Tilia during its development phases

Peter GLEIßNER

Institute of Botany, Dep. Plant Morphology, RWTH Aachen, Worringer Weg, D-52056 Aachen

The crown habit of the linden (*Tilia platyphyllos SCOP.* und *T. cordata MILL.*) is well characterized by two symptoms in winter state. Firstly the twigs in the peripheral layers of the crown are of planar construction as well as those of the orthotropic tree top. Secondly the persistent frame branches at the crown center are nearly orthotropic, the thickest ones forming monoaxial (in a straigth line) stems. It is shown which morphological processes are responsible for branching and to what extent it is possible to understand the architecture of the whole tree by these insights. It is an essential part of the examination to take into account important changes in branching during different stages of crown development (the vegetative, adult and senescent phases). These alterations in tree structure are considered to be innate to the genetic model because they occur independent of environmental influences.

1. Branching in peripheral layers of the crown

During the vegetative phase the branching system arises from a succession of renewal axes each beginning on top of each other (sympodial shoot connection) resulting in a monoaxial twig or branch. Distal lateral shoots are smaller turning off at an angle of 80°. In accordance with this the extension mode of the lateral shoots is acrotonic. The planar construction of twigs is formed by the interaction of distichous leaf arrangement and a local torsion at the beginning of each lateral shoot. Its first leaves are transverse to its descendent axis, but only by turning 90° the branching plane of the preceding axis is adjusted again. Lamma shoots arising sympodially are of the same structure as the spring shoot.

During the adult age (from 15 to 25 years) planar branching arises from other morphological processes because two shoot generations differing in structure are produced in succession each year. The first one is vegetative being homologous to the shoot before adult stage. The second one is the inflorescence axis. The latter unfold sylleptic ly on the vegetative shoot each having again a basal innovation bud[1].
Branching in one plane comes about by the interaction of two processes: The flowering axis with frail extension is inserted obligately between two vegetative axes and it is placed transversely to them with regard to the two orthostichies. The innovation buds at the base of the inflorescence axes are, moreover, the winter buds of the tree and are not homologous to those of the vegetative phase. The top innovation bud is not excluded from this way of branching.
By the extension mode of lateral shoots - here acrotony - we can also predict which axes of the peripheral layers become frame branches and which are shed by abscission: The apical lateral axes descending in a straight line are persistent, the smaller proximal ones are shed from the 4th to the 10th (15th) year of their lives. The latter can be recognized by their wide angle of turning off.

2. The architecture of the linden and its metamorphoses

During its lifespan three different models of correlating the frame branches can be characterized. During the initial phase of the first ten years several nearly upright frame branches arise competing in building the crown - called the **polyaxial-orthotropic** model (Fig. A). The further crown enlargement is based on them resulting in monoaxial stems by the above mentioned shoot connection. Each of these dominating stems forms a **monoaxial-orthotropic** unit together with thinner frame branches which turn off in a oblique direction (Fig. B). Such a subsystem is striking within the crown as a whole and, moreover, in later adult stage it is visible in the retuse hem line of the crown.

---

in the ß-prophyllum, see EICHLER, A.W. (1878): Blüthendiagramme. Bd.II. Leipzig, p. 270

In this way the linden gains its maximum spreading at the age of 120 - 130 years (Fig. c). Then senescence has already started at lower sections of the crown: Reiteration shoots arise from proventitious buds on the upper side of the plagiotropic frame branches after their apical parts go out of operation or have already been broken off. Finally the innovation also wanes in the peripheral layers of the crown. The original region of the tree top is obviously thinned by the tree itself. Larger sections of the framework break off leaving gaps which are no longer compensated by reiterations also arising here. Over the age of about 300 years the lime tree has only a half or a third of the original crown volume (Fig. D). Often only the trunk and the base of lower main branches remain. Then all other twigs and branches are produced by series of reiterations lined up plagiotropically with their distal segments. This is why the architecture of old age is called **polyaxial-plagiotropic**.

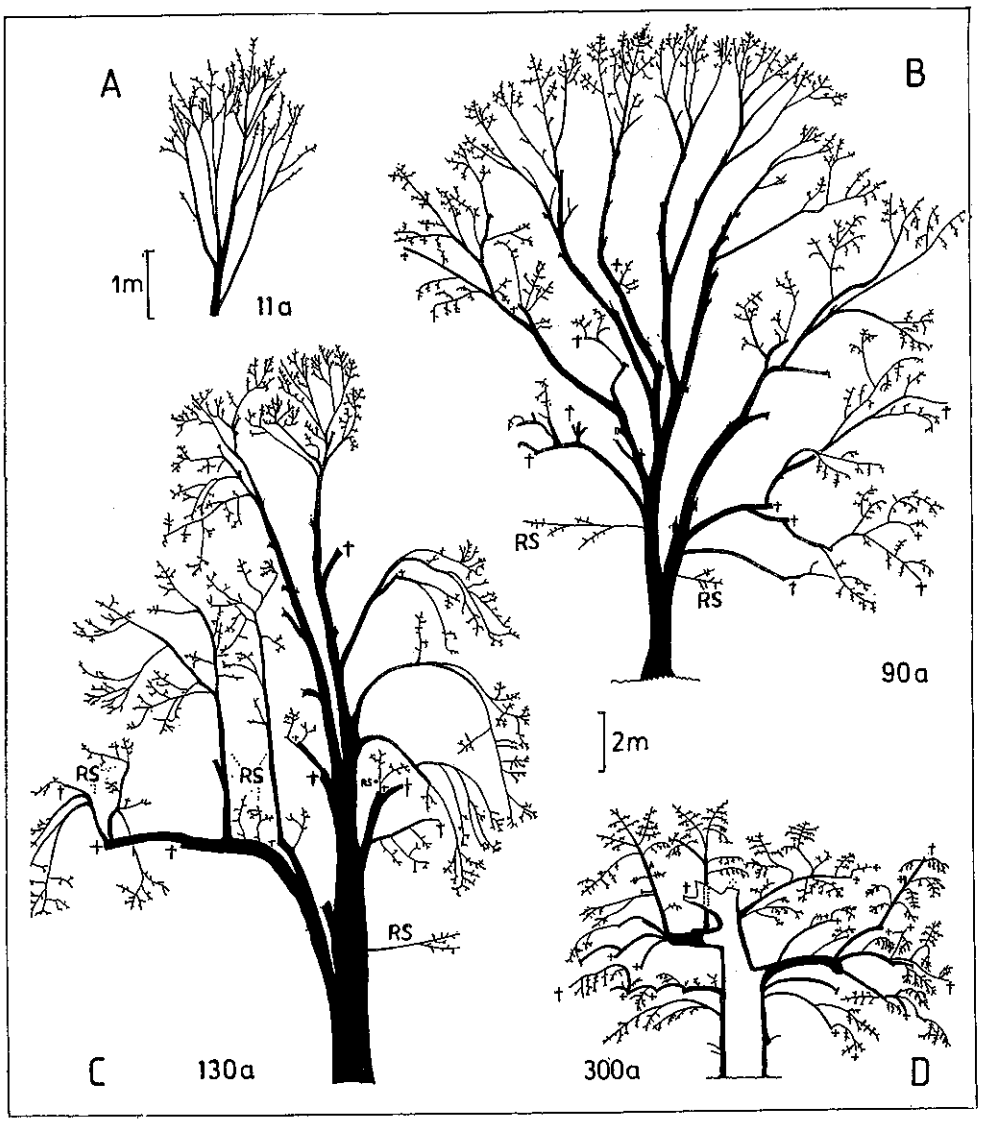


Fig. A -D: the habit of the lime during its developmental phases (details from the poster), B-D at the same degree, RS = reiteration, further explanation see text

# New aspects of pattern analysis of branching systems including its variation by forest dieback shown in maple and birch

Peter GLEIßNER

Institute of Botany, Dep. Plant Morphology, RWTH Aachen, Worringer Weg, D-52056 Aachen

Apart from the viewpoint of modular tree construction an additional way of understanding the branch system of trees is suggested: They are built up of metameric units which lie on top of each other in a centrifugal direction. Basic characteristics of axis morphology are closely linked with each of the following axis increments:
- the rhythmic change in leaf morphogenesis (between foliar leaf and bud scale)
- the rhythm in the length of the internodes
- the shoot extension mode (the position of the most extended lateral shoots per unit)
- the fixed position of inflorescences

In accordance with HALLÉ et al. (1978) this is the unit of extension ($U_E$). It is shown by way of maple (*Acer pseudoplatanus L.*) and birch (*Betula pendula ROTH.*) that growth habit, the framework as well as fine-twigged peripheral layers, and its changes during life time can be characterized by the metamorphosis of the $U_E$ in time and space (i.e. the change of interaction of related parameters).

The maple axis system (Fig. 1) is built up by a sympodial way of shoot connection (= succession of terminal axes and lateral innovation axes (renewals), the latter here are caused by terminal inflorescence). During the vegetative phase (Fig. 1a) the $U_E$ consists of a terminal bud and lateral subacrotonic shoots (i.e. the extension mode is almost distal). In the later adult stage (b1 and b2) a switch takes place from a $U_E$ state similar to the vegetative phase and a $U_E$ state with terminal flowering, acrotonic renewals and decreased length. During later stages of adolescence (c1 and c2) the $U_E$ becomes shorter and shorter. The program of lateral shoot extension is also reduced. At phase a the total of $U_E$s produces a monoaxial tree consisting of the primary stem and orthotropic frame branches which compete. The growth habit quite suddenly becomes polyaxial during adult stage (b,c). The axis system consists of 2-4-year modules with decreasing length depending on the age of the tree.

The $U_E$ of the birch shows interaction of two different times of unfolding shoots. The sylleptic mode produces lateral shoots in the middle part of the $U_E$ (mesotonic), the cataleptic one produces distal shoots (acrotonic) and female inflorescences at base (Fig. 2 a, during early adult stage). Later on, the terminal bud will regularly convert to a male inflorescence followed by a sympodial renewal axis (Fig. 2 b). This is the maximum program of the $U_E$, which will usually be shortened in non-orthotropic shoots. At plagiotropic orientation (c) the cataleptic parts are established (the sylleptic one is reduced). On overhanging shoots only the base section with female inflorescences is established. All other shoots except these flowers end in a male inflorescence. Although the birch belongs to the group with continuously growing shoots, its axis system is articulated in a regular way. This is because the lateral shoots are produced rhythmically by the acrotonic and mesotonic extension mode.

We suggest that different developmental aspects such as vegetative and reproductive phases and the sylleptic and cataleptic programs be integrated into the description of the tree construction as a whole. In this way it is easier to recognize the different internal programs innate to the genetic model of a tree species. After all, the 'Gestalt' of the tree is definitely varied by external environmental factors.

Non-pathological diseases vary the branching pattern in the peripheral layers of the crown: the shortening of the abscission time of twigs, the breakdown of lateral axis differentiation, the reduction of the the length of $U_E$ and the lack of lamma shoots.

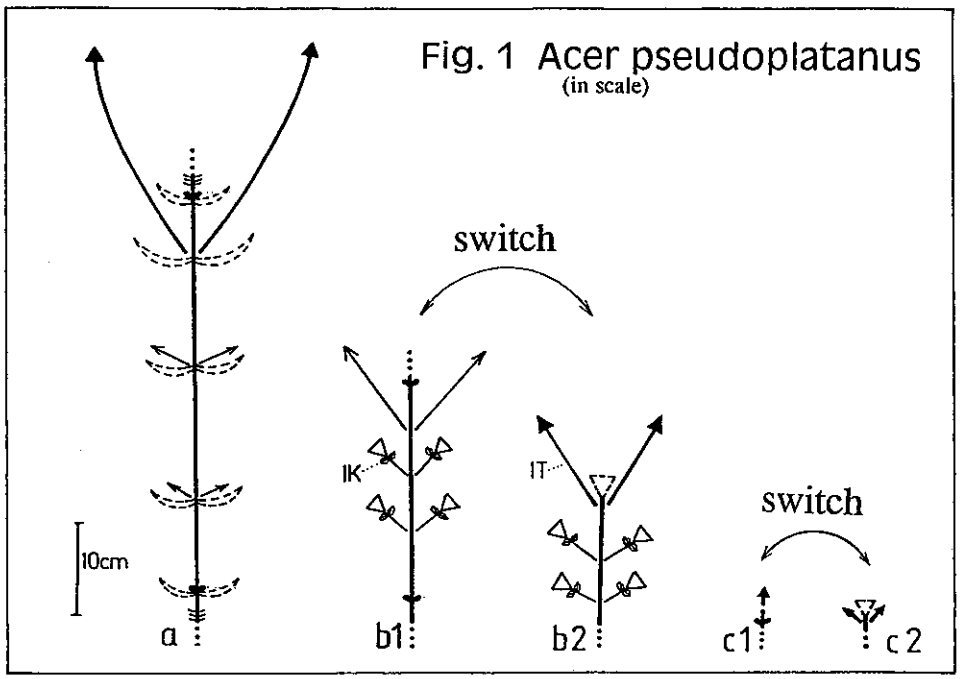


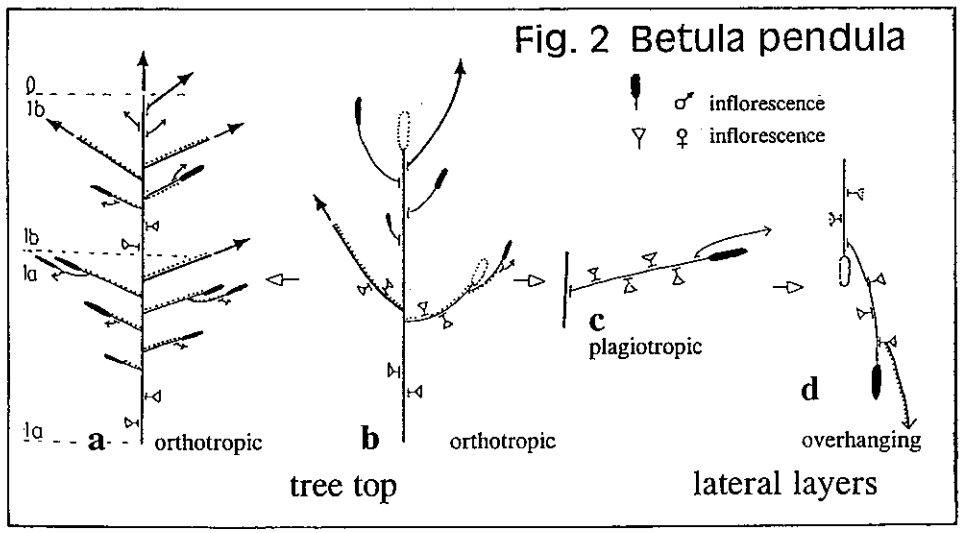


HALLÉ, F./OLDEMAN, R.A.A./TOMLINSON, P.B. 1978: Tropical trees and forests. An architectural analysis. Berlin

# Biomechanical response of reed bamboo along the length of the culm and across the culm wall thickness

**R. GNANAHARAN**
**Kerala Forest Research Institute**
**Peechi 680 653**
**INDIA**

Bamboos are the fastest growing plants. They are a unique group of grasses which can be used for a variety of purposes. Unlike a tree, bamboos do not acquire more girth as they grow. The new sprouts emerge with full diameter. New culms reach full height in 3 to 4 months.

Reed-like bamboos or reed bamboos (*Ochlandra* spp) generally have thin culm wall and long internodes. *O.travancorica* (Bedd.) Benth. ex Gamble is the most common and commercially important reed bamboo which occurs in the evergreen and semi-evergreen forests of southern India. Culms of *O.trvancorica* are tender during the first year and they become mature in the second year. Even though the culms can reach 7 to 10 m in height, the usable length is only 3 to 4 m.

Eight mature culms were collected from the natural forests. Usable lengths with six internodes were cut and removed. The internode legths were measured. One ring of about 20 mm length was removed from the middle of each internode of five culms. Culm diameter, culm wall thickness, moisture content and density were determined from these rings. The basal, middle and top portions of the remaining three culms were split into slats of 12 to 15 mm width. Slivers of about 0.7 mm thickness were obtained from these slats across the wall thickness. These slivers were dried to about 12% moisture content and they were tested for tensile strength along the grain.

As diameter decreases from base to top from 28.3 mm to 19.4 mm, wall thickness reduces from 5.9 mm to 2.5 mm (Table 1). Reduction in wall thickness is very steep. An interesting feature of this reed bamboo is that, even though the top portion is thinner, it is denser. This is because of the arrangement and frequency of vascular bundles. The top internode had a density (625 kg/m$^3$) which is nearly 35% higher than the density of the basal internode (463 kg/m$^3$). Also, it can be seen from Table 1 that moisture content of green culm decreases from base to top.

As can be seen in Figure 1, tensile stress increases along the length of the culm. This clearly shows that density and strength are positively correlated. As density increases, strength also increases along the culm length. Figure 2 shows the radial variation of tensile strength from the periphery to the inner wall across the wall thickness. Slivers from outer periphery, with higher density, have higher strengths compared to slivers from the inner wall.

The biomechanical response of reed bamboo varies from base to top of the culm as well as from outer periphery to inner wall. If reed bamboo is used in round form or in split form or in the form of slivers, the strength will vary accordingly. It is quite important to know this difference so that the right portion of the culm is used for the right purpose.

**Table 1. Basic data on the culms of *Ochlandra* travancorica**

| Property | Internode | | | | | |
|---|---|---|---|---|---|---|
| | 1 | 2 | 3 | 4 | 5 | 6 |
| Internode length (mm) | 535.0 | 584.0 | 627.0 | 677.0 | 690.0 | 668.0 |
| diameter (mm) | 28.3 | 27.7 | 26.3 | 24.6 | 22.6 | 19.4 |
| wall thickness (mm) | 5.9 | 5.6 | 4.2 | 3.4 | 3.1 | 2.5 |
| density (kg/m$^3$) | 463.0 | 487.0 | 528.0 | 546.0 | 587.0 | 625.0 |
| moisturecontent (%) | 115.9 | 118.4 | 92.1 | 76.7 | 75.6 | 35.0 |

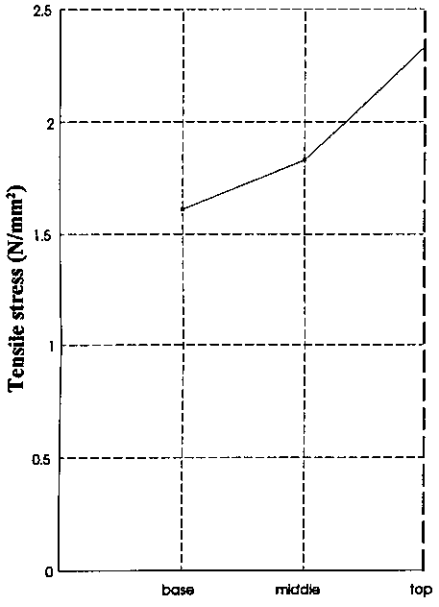


**Figure 1**

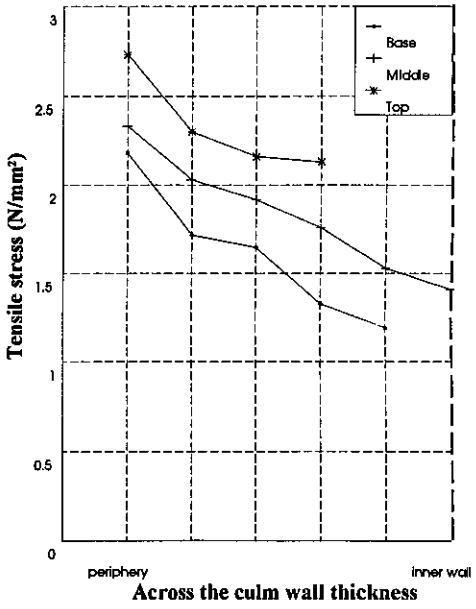


**Figure 2**

# Coloration macroscopique du bois de tension chez le Peuplier

Valérie GRZESKOWIAK, François SASSUS
LMGC/ bois, CP 081, Université Montpellier II, Place E. Bataillon, 34095 Montpellier cedex 5, France.

Le bois de tension est un bois aux caractéristiques mécaniques et anatomiques différentes du bois dit "normal". Ce bois ne se trouve que chez les angiospermes. Il est généralement formé dans un secteur angulaire d'une section transversale de tige et pendant certaines phases de croissance seulement. Il est alors le moteur, pendant la fin de sa différenciation, d'une réorientation active (mouvement de flexion) de la tige (Fournier *et al.* 1994, Chanson 1993). Dans de nombreuses espèces, le bois de tension se distingue par la présence de fibres gélatineuses. Ces fibres ont une couche interne "G" constituée en majorité de cellulose cristalline. Chez le Peuplier, la couche G remplace la paroi S3. Le bois de tension forme des bandes tangentielles situées essentiellement dans le bois initial.

La mise au point d'une coloration macroscopique permettant la mise en évidence du bois de tension a rarement fait l'objet d'études systématiques. L'idée est de tester des colorants de la cellulose connus pour la préparation des coupes microscopiques (Jensen, 1962).

Le but est de donner une image de la répartition du bois de tension sans faire de coupes anatomiques. Cette cartographie permet de retracer l'histoire des réorientations de l'axe, ainsi que les profils de contraintes internes dans le bois à l'âge de l'exploitation (en utilisant en plus un modèle mécanique du cumul de ces précontraintes et la donnée des déformations de maturation dans le bois de tension). Ces observations sont à la base des travaux menés au LMGC sur la biomécanique de l'arbre qui visent à étudier les relations entre la qualité du bois et l'histoire du développement morphologique de l'arbre. Les problèmes de qualité dûs à la formation de bois de tension (fentes d'abattage induites par les forts gradients de précontraintes, tuilage et voilement des sciages et placages pendant le séchage, liés aux hétérogénéités de retraits) sont tout particulièrement étudiés.

Matériel:

- le colorant utilisé est le chloro-iodure de zinc (ou réactif de Herzberg).Sa réactivité est basée sur la composition chimique particulière de la couche G.
- matériel végétal : peuplier clone I 214

Méthodes :

- prélèvement sur un billon de deux rondelles successives d'un centimètre d'épaisseur
- badigeonnage avec le réactif sur la face inférieur de la première rondelle (Photo 1)
- coupe et coloration microscopique (safranine - bleu astra) sur la face supérieur de la seconde rondelle pour validation (Photo 2)

Résultat :

- Les zones de bois de tension sont colorées en mauve. Le chlorure de zinc attaque les liaisons hydrogène situées entre les chaînes de cellulose. L'iode (qui est responsable de la coloration) pourra alors s'accumuler entre les chaînes. Le bois normal est coloré en jaune. La coloration est fugace (une dizaine de minutes) et peut être renouvelée plusieurs fois
- Les coupes microscopiques nous confirment que l'iode a bien coloré les zones de bois de tension.

Utilisation et perspectives :

- La méthode a été appliquée par F. Sassus (1994, cf Poster dans ce même volume).

- Cette coloration ne sera applicable à d'autres espèces que si elles possèdent des fibres G caractérisées. Les bois devront être clairs afin de faire ressortir le contraste de couleur.

- Lors des essais de coloration , nous avons pu observer des nuances de teinte (rose au mauve). Peut-on attribuer ces différences de couleur à des variations de propriétés physiques (densité) ou chimiques ? Ces variations sont-elles corrélées aux variations de déformations de maturation ? Peut-on alors détecter différentes "intensités" de bois de tension ? Des études complémentaires sont en cours.

Bibliographie :

Chanson B., 1993 : Déformations de maturation : hétérogénéités angulaires en fonction du plan d'organisation des arbres. *Acta Bot. Gallica,* **140** (4), 395-401.

Fournier M., Chanson B., Thibaut B., Guitard D., 1994 : Mesure des déformations résiduelles de croissance à la surface des arbres. Observations sur différentes espèces. *Ann. Sci. For.* **51** (2)

Jensen W.A., 1962: *Botanical histochemistry.* U. California Berkeley. W. Freeman & Co. San Francisco.

Sassus F., 1994 : Contraintes de croissance et morphologie chez un clone de Peuplier. *DEA en Sciences du Bois. ENGREF Nancy (France).*

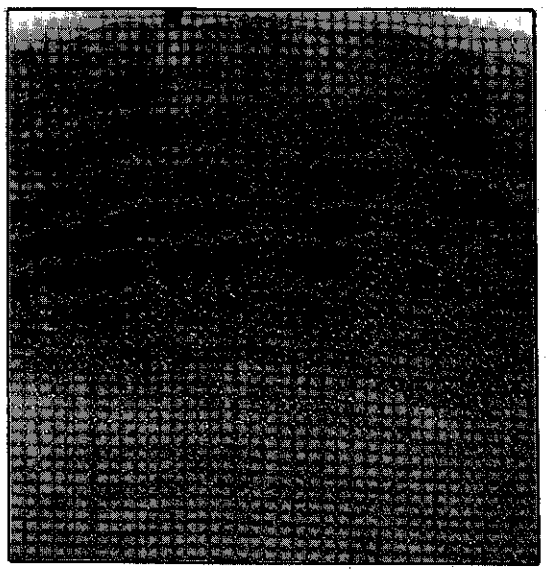

Photo 1: Coloration macroscopique
au chloro-iodure de zinc (bt = bois de tension)

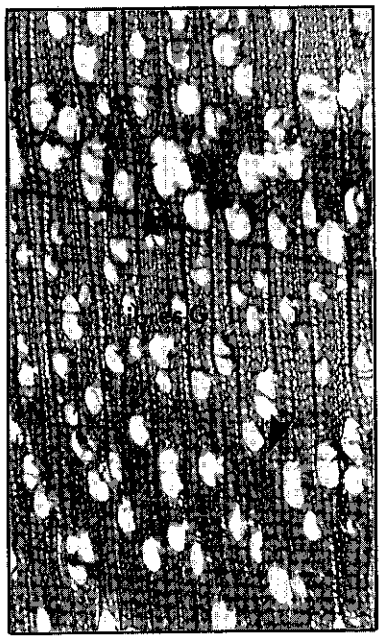

Photo 2: Coloration microscopique
Safranine-bleu Astra

# Computerized Tomography- A Non Destructive Method for Evaluating the Mechanical Properties and Strength of Trees

Adolf Habermehl and Hans-Werner Ridder

Medical Physics in the Center of Radiology
Philipps-University, Bahnhofstr. 7, 35033 Marburg/Lahn, Germany

## INTRODUCTION

Computerized tomography is the only non-destructive method in arborology yielding detailled density pattern of the trunk. It allows the quantitative determination of the locally varying absorption coefficients for penetrating radiation within a thin layer of the trunk and gives in the tomogram an image of the layer showing not only rot, hollows and other defects and the thickness of the wall at every point of the circumference but also the distribution of water in the stem so providing data which may be used for calculating and evaluating the mechanical properties and strength and the stability of the tree.

## EQUIPMENT

Different portable systems have been developed and built for computerized tomography of trees. All are using radionuclides as sources of radiation.

The MCT-3 is based an the translations-rotation-method. A base ring and a bearing ring can be divided into two separate parts to be put around the tree to be examined. They carry the source and three radiation detectors. Stepping motors perform the translational and rotational movements. The system is controlled by micro-computer. It can examine trees with a diameter up to 72 cm and has adjustable legs to perform measurements up to 2 m of altitude.

The MCT-F has a similar mechanical construction, but is based on the fan-beam method and has 30 detectors. (Fig. 1) It has an inner diameter of 100 cm and a stronger source to measure larger trees.

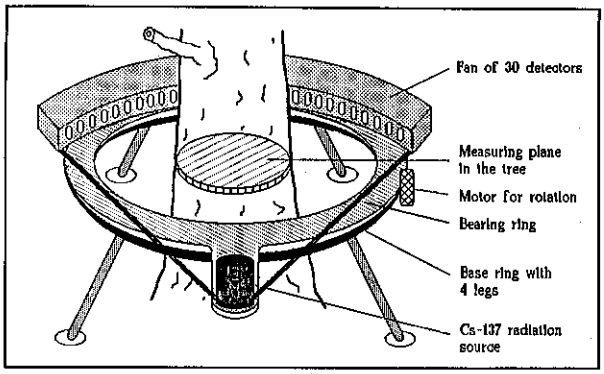


Fig. 1: Diagram of the MCT-F

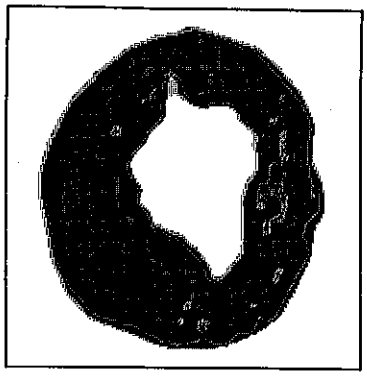

Fig. 2: Tomogram of a chestnut

APPLICATIONS

Trees in parks and besides streets have been investigated to get informations for evaluating strength, stability and preservation states. Location and extent of wounds and interior butt rot of different tree species could be determined as well as the thickness of the wall along the circumference (Fig. 2). Tomograms of silver lime trees, for example, revealed the trunk structure consisting of several smaller trunks, the state of welding, areas of higher moisture content and frost damages. The extent of welding of frost damages could be detected as well as interior roots within the hollow stems of lime-trees.

In forestry sciences decay, checks, heartwood formation, moisture content and, in general, the locally varying density within the stem could be studied. The method was applied for the detection of butt rot and its spreading within the stem in horizontal and vertical direction, for determining sapwood areas in spruce stems in dependence of fertilization, and for evaluating development and treatment of tree wounds, and the damaging by resin tapping. In all cases the suitability of the method was revealed, especially due to its possibility of examining living trees unlimitedly, at any time periods and without damaging the tree.

LITERATURE

Habermehl, A. u. Ridder, H.-W. (1992/1993): I: Methodik der Computer-Tomographie zur zerstörungsfreien Untersuchung des Holzkörpers von stehenden Bäumen; II: Anwendungen: Forstbotanische Untersuchungen; III: Anwendungen: Untersuchungen an Allee- und Parkbäumen; Holz als Roh- und Werkstoff I: 50: 465-474; II: 51: 1-6; III: 51: 101-106; - Habermehl, A. and Ridder, H.-W. (1994) : Computerized Tomographic Investigations of Street and Park Trees. Arboricult. Journ. (to be published).

# Défilement du tronc chez le chêne sessile; Test de différents modèles et influence de l'architecture.

HATSCH Elvire; RITTIE Daniel; DHOTE Jean-François.

Laboratoire de Recherches en Sciences Forestières-
Unité de Dynamique de Systèmes Forestiers- ENGREF, 14 rue Girardet
54042 Nancy Cedex. FRANCE.

Nous avons décrit la géométrie de l'aubier et des accroissements ligneux dans des tiges de chênes sessiles (*Quercus petraea* (Matt.) Liebl.), en fonction de la hauteur.

Ce travail a été effectué sur 18 arbres jeunes (stades gaulis et perchis), de morphologies différentes, et se poursuit sur 100 arbres arrivés à maturité, issus de futaie et de taillis sous futaie.

Nous avons testé la validité de deux modèles reliant la formation du houppier et le développement de la tige : la loi de Pressler (1865 cité par Larson 1963) et le "pipe-model" de Shinozaki *et al* (1964), utilisés sur des résineux. La loi de Pressler décrit l'accroissement en surface qui, à un niveau donné est proportionnel à la biomasse foliaire présente au dessus, donc reste constante sous la base de la couronne. Le "pipe-model" est utilisé pour expliquer la répartition de l'aubier le long de la tige: la surface d'aubier est proportionnelle à la surface foliaire située au dessus.

Cette étude montre que les lois testées ne permettent pas de décrire clairement la géométrie interne des tiges de chênes sessiles, qui apparaît plus complexe que chez les résineux.

Nous avons regardé ensuite la validité de deux modèles de défilement fondés sur une adaptation mécanique ("Optimal Stem Mechanical design") : optimisation vis à vis des risques de casse au vent (Metgzer, cité par Larson,1963) ou optimisation de la hauteur maximale atteignable (MacMahon et Kronauer, 1976). Ces théories modélisent le tronc (net de branches) par une poutre à section circulaire variable. Le premier modèle suppose que les efforts de compression ou de tension longitudinales, subis de haut en bas par la tige sous l'effet d'une force perpendiculaire (vent horizontal), sont répartis uniformément dans le bois (constant stress design); sous l'hypothèse d'un bois homogène, le modèle prévoit que le diamètre au cube ($d^3$) de la tige augmente linéairement de bas en haut. Le second modèle suppose que pour un volume de bois constant, le défilement (allométrique) maximise la hauteur critique au delà de laquelle la poutre "flambe". Ceci permet à l'arbre d'atteindre une hauteur importante en limitant les risques d'effondrement. Sous l'hypothèse d'un bois homogène, ce modèle prévoit que $d^{2/3}$ augmente linéairement de bas en haut.

Comme énoncé par les auteurs précédents, aucune des deux règles ne s'applique à la zone basale de l'arbre qui correspond à l'empattement, de même qu'à l'intérieur de la couronne. Sur nos chênes, les régressions donnent de meilleurs résultats pour le second modèle en $d^{2/3}$ ($r^2$ toujours supérieur et répartition des résidus sans biais).

Enfin, nos résultats montrent que l'insertion des branches crée des irrégularités dans le défilement du tronc. La ramification influe sur la distribution des surfaces des cernes et de l'aubier mais cela dépend de l'état de vigueur des branches; toutes les branches ne participent pas à l'élaboration du tronc. Au delà des modèles précédents, la compréhension de l'acquisition de la forme de la tige passe par l'étude de l'influence des critères architecturaux (position des branches, fourche), de l'âge et de la taille de la couronne.

Références bibliographiques :

Larson P.R., 1963. Stem form develoment of forest trees. *For. Sci. Monogr.* **5** : 1-42.

Mac Mahon T.A., Kronauer R.E., 1976. Tree structures : deducing the principle of mechanical design. *J. Theor. Biol.* **59** : 443-466.

Shinozaki K., Yoda K., Hozumi K., Kira T., 1964. A quantitative analysis of plant form - The pipe model theory. I. Basic analysis. *Japanese Journal of Ecology.* **14** (3) : 97-104.

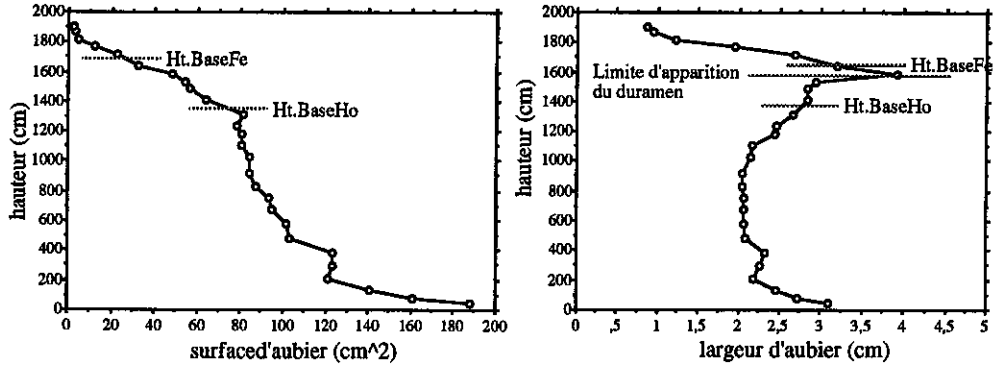


Fig.1 Largeur d'aubier et surface d'aubier correspondante en fonction de la hauteur : arbre dominant de 59 ans.
Ht.BaseHo: hauteur de la base du houppier; Ht.BaseFe: hauteur de la base des feuilles.

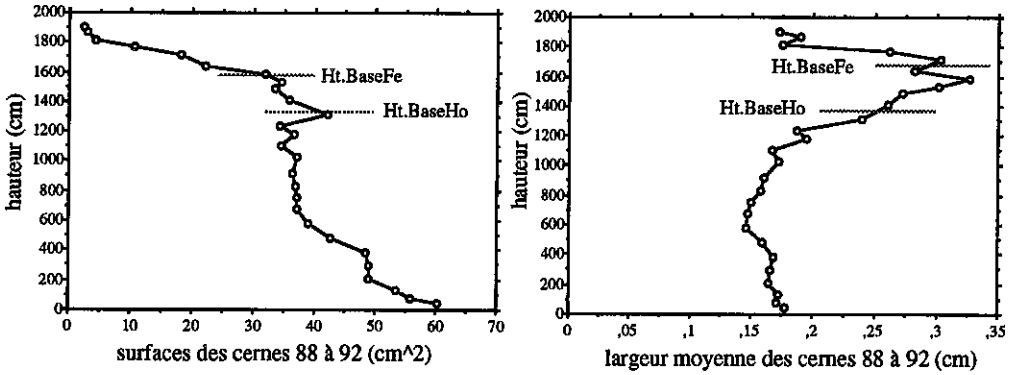


Fig.2:Evolution de la surface des cernes de 1988 à 1992: surfaces cumulées sur cinq ans et les largeurs des cernes: moyenne sur cinq ans, 1988-1992 en fonction de la hauteur : arbre dominant de 59 ans.
Ht.BaseHo, Ht.BaseFe: hauteur de la base du houppier et du feuillage.

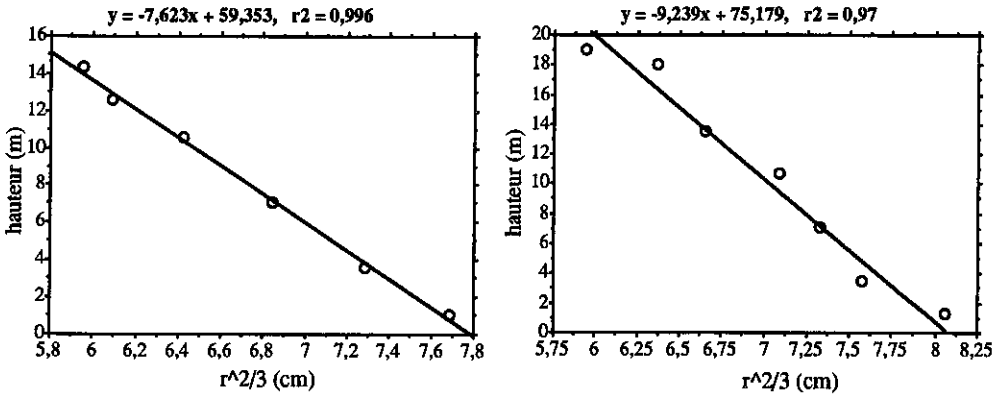


Fig.3: Régression effectuées avec le rayon moyen mesuré sur des rondelles à différentes hauteur le long de la tige nette de branche, chez deux arbres de futaie. On utilise le rayon à la puissance 2/3 (r2/3).

# Tissue stresses, their origin and biomechanical significance

Z. Hejnowicz and A. Sievers
Botanisches Institut, Universität Bonn, Venusbergweg 22,
D-53115 Bonn, Germany

Tissue stresses, longitudinal and transverse, were determined for the hypocotyl of sunflower using Poisson's ratios and data from measurements of: (i) changes in the length and width of the epidermal tissue (DT) which occur upon peeling from the hypocotyl and the forces necessary to restretch the isolated tissue to its original length in situ; (ii) the external compressive force and (iii) the external osmotic pressure required to prevent the extension of isolated ground tissue (GT) immersed in water or mannitol solutions. These three independent measurements gave a simular magnitude of the longitudinal forces (tensile in the DT, compressive in the GT), being 0.37 N in the apical region. More than 80% of the tensile force is concentrated in the epidermis, resulting in longitudinal stresses which are > 3 times higher than that due directly to turgor pressure there. Transverse tissue stresses - circumferencial in the DT and radial in the GT - were calculated from the longitudinal forces, so the study provides a complete, three-dimensional picture of the tissue stresses in the hypocotyl (Fig. 1).

A simple model, based on (i) symplastic turgor-induced extensions of tissues which differ in moduli of elasticity, and (ii) static equilibrium, predicts the occurrence of longitudinal tissue stresses in stem-like organs. The model was applied to the hypocotyl of sunflower. Tissue composite moduli of elasticity in the longitudinal direction for uniaxial and multiaxial stresses in the DT and the GT of the hypocotyl, which are necessary to calculate the longitudinal forces involved in the tissue stresses in the hypocotyl have been determined. In the DT, the moduli are strongly dependent on applied uniaxial stress due to stress-hardening. Thanks to the tensile stress, the DT acts mechanically in an intact hypocotyl having a hardened modulus. The force obtained from the model fits well that measured. The model obeys the condition of the minimum of strain energy in the organ. It follows that the tissue stresses may arise in the turgor-derived mechanism described by the model without differential growth of the tissues, as hitherto assumed, though a differential growth may modify the tissue stresses. As to biomechanical significance the following aspects are considered. (i) The tissue stresses represent an analogue of prestresses in engeneering constructions. To study this point, the stresses in the sunflower hypocotyl were released by treatment with auxin to cause differential growth counteracting the tissue stresses. The stability of the hypocotyl was strongly reduced. (ii) The tissue stresses in a growing organ allow to exceed the yield threshold of the tissue which has the highest modulus of elasticity; a longitudinal tensile stress in addition to that imposed by turgor on

the DT in sunflower hypocotyl is necessary to exceed its yield threshold. (iii) A considerable elastic energy is accumulated in the organ with tissue stresses. In a vertically growing stem this energy is distributed symmetrically around the stem axis. In a gravireacting stem this symmetry is broken and a bending moment appears. We studied this aspect using stems of *Reynoutria*. In this plant, in normal vertical position, the epidermis and the collenchyma are in tension and the GT is under compression. The longitudinal forces are considerable: 0.24 N per 1 mm of circumference, or 5 N for the stem of 6 mm in diameter. In a horizontally positioned stem the first expression of gravistimulation is lowering of the tension in the lower side by a wall loosening process: The collenchyma creeps on this side and a bending moment appears, tending to bend the stem upward. On the lower side, the tensile force in the collenchyma decreases to 30 % of the original one after 1 h of gravistimulation. When a horizontally positioned stem is restrained by binding to stiff rods the elastic energy is partly released from the tissue stresses but remains accumulated in the restraints. When the restraints are removed the stem rapidly bends.

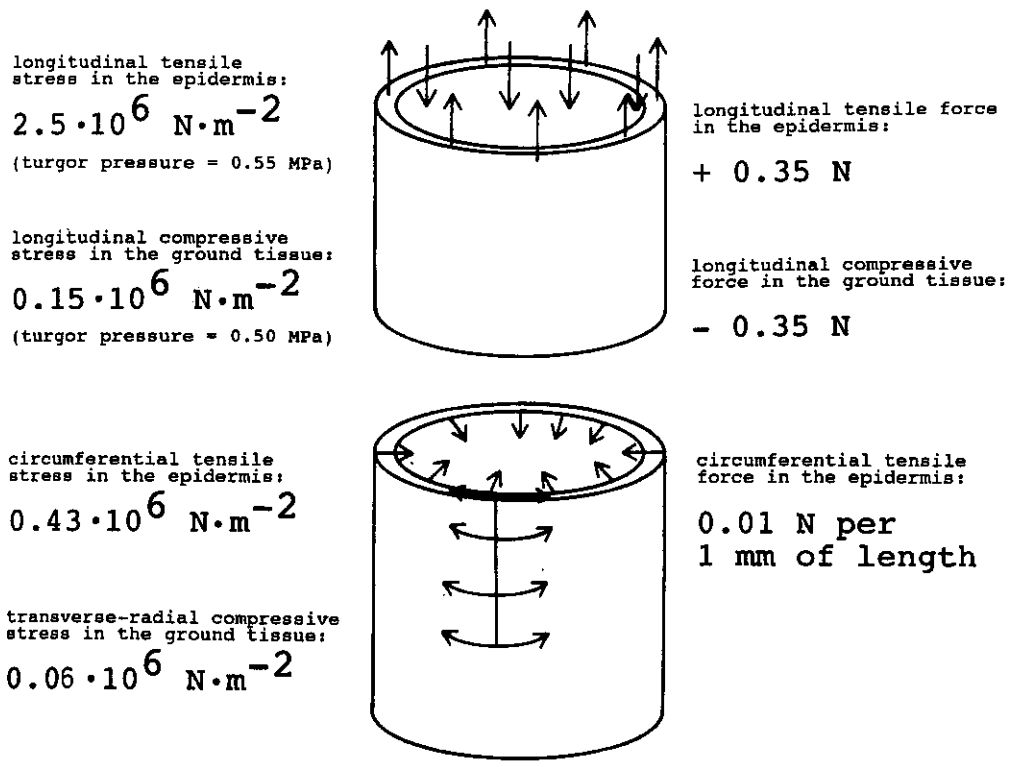


Fig. 1 The forces involved in tissue stresses and stresses themselves in the apical region of the hypocotyl of *Helianthus annuus*

# THE MECHANICAL PROPERTIES OF TRANSGENIC PLANTS WITH MODIFIED LIGNIN.

David G. Hepworth

University of Reading Centre for Biomimetics, TOB1, Earley Gate, The University, Reading, RG6 2AT, UK.

The presence of lignin in plant cells has massive commercial consequences for processes such as the manufacture of paper. Here lignin has to be removed using chemical extraction methods which are both commercially expensive and environmentally unfriendly. Therefore it would be an advantage to grow plants with modified lignin. The problem is, how much modification can be carried out without greatly reducing the mechanical rigidity of the stem.

Tobacco plants have been produced by Zeneca with an antisense CAD gene blocking the conversion of phenolic aldehydes to phenolic alcohol's. The alcohol's are normally polymerised into lignin. In the antisense plants lignin is still produced but with a higher aldehyde content. When wood is stained with Schiffs reagent, antisense wood shows up dark red while control wood stains light pink. The wood of the antisense plants is much less stiff in tension than the wood of control plants . The mean Young's modulus for control plants is 2.58 GPa (sd, 0.08). The mean Young's modulus for antisense plants is 1.49 GPa (sd, 0.07). These values are for wood equilibrated at 100% relative humidity at 20°C. Drying wood out reduces the difference in stiffness between control and antisense wood. Sorption isotherms for control and antisense plants showed that

antisense wood contains more water (15 % more), which is free water. Extracting lignin components from the wood revealed that the lignin matrix in antisense plants is less cross linked than in control plants i.e. more material can be extracted using milder treatments. The conclusion from these results is that the antisense wood has a lower tensile stiffness due to lower cross linking in the lignin matrix .

The properties of antisense wood can be simulated in control wood by treating the wood with sodium hydroxide solution for a short time. This reduces the stiffness and increases the free water content of the wood.

Using image analysis of tissue sections I have plotted the thicknesses of cell walls with distance from the stem centroid and with height from the base of the stem and calculated the second moments of area of the different tissues in the stem at different heights. The results show that under green house conditions the antisense plants do not have increased wood cell wall thickness or increased second moment of area of woody tissue within the stem. Consequently the stems of antisense plants have a lower bending stiffness than the stems of control plants. Experiments are currently under way to grow antisense plants under conditions simulating wind stress to see whether this will induce them to compensate for the reduced stiffness of the wood.

References.

Fry, S. C. 1986. Cross-linking of matrix polymers in the growing cell walls of angiosperms. Plant Physiol. 37:165-186.

Halpin, C., Knight, M. E., Grima-Pettenati, J. Goffner, D. Boudet, A. and Schuch, W. 1991. Purification and characterization of cinnamyl alcohol dehydrogenase from tobacco stems. Plant Physiol. 98: 12-16.

Iiyama, K., Lam, T. B-T. and Stone, B. A. 1994. Covalent cross-links in the cell wall. Plant Physiol. 104: 315-320.

Monties, B. 1989. Lignins. In: Methods in plant biochemistry vol. 1 (Eds. P.M.Dey and J.R.Harborne). 113-157. Academic press.

# Turgor/Mechanical Property Relations in Potato Tuber Parenchyma

S. Hiller
Silsoe Research Institute, Wrest Park, Silsoe,
Bedford, MK45 4HS, England.

In many plant organs, especially those not reinforced with long fibres, the interaction of cell turgor pressure with cell walls is a major determinant of structural stiffness (1). Falk et al showed experimentally that tensile stiffness was linearly related to turgor pressure in potato parenchyma tissue (2), while Murase et al highlighted the strain-rate dependence of stiffness values measured in compression (3). More recent work by Lin and Pitt studied the mechanical behaviour of apple and potato parenchyma equilibrated in a range of mannitol solutions, examining tissue stiffness and failure modes as a function of cell turgor pressure and strain rate (4).

The experimental work reported below was a small-scale trial with the object of verifying some of the results of Lin and Pitt for potato, albeit of a different variety.

Experiments were carried out to determine the quasistatic mechanical behaviour of specimens of potato tuber parenchyma, cv 'Cara', after soaking in a range of buffered and unbuffered mannitol osmotica, from 0.0M in 0.1M steps to 0.8M. The soak time required for the tissue samples to reach weight/dimensional equilibrium in the various solutions was monitored. Consistency of solution concentration was checked using a sugar refractometer. Two replicates were equilibrated in each of the eight solution strengths, for buffered and unbuffered solutions.

After equilibration of all the samples, the first of each pair of replicates was compressed between flat platens at a constant deformation rate until tissue failure. The second sample of each pair was loaded and unloaded cyclically to successively higher nominal 10% strain increments until failure. Results were plotted in nominal and in true stress/strain formats. Mean turgor pressures for cells within tissue samples were inferred from a knowledge of weight/dimension change with solution molarity.

Compression test results clearly differentiated the samples soaked in 0.0M, 0.1M and 0.2M mannitol solutions, from those soaked in solutions of higher concentration. However, it was found that large differences in stress/strain behaviour occurred for relatively small changes in the inferred mean tissue turgor pressure. It is interesting to speculate on the possible causes of such behaviour.

**References**

(1) Atkins, A.G. The Basic Principles of Mechanical Failure in Biological Systems in Food Structure and Behaviour, chap. 8, publ. Academic Press Ltd.; 1987; (pp 149-176).

(2) Falk, S.; Hertz, C.H.; Virgin, H.I. On the relation between turgor pressure and tissue rigidity. 1. Experiments on resonance frequency and tissue rigidity. Physiologia Plantarum; 1958; 11 (pp 802-817).

(3) Murase, H.; Merva, G.E.; Segerlind, L.J. Variation of Young's modulus of potato as a function of water potential. Trans. ASAE; 1980; pp 794-800.

(4) Lin, T.-T.; Pitt, R.E. Rheology of apple and potato tissue as affected by cell turgor pressure. J. Texture Studies; 1986; 17 (pp 291-313).

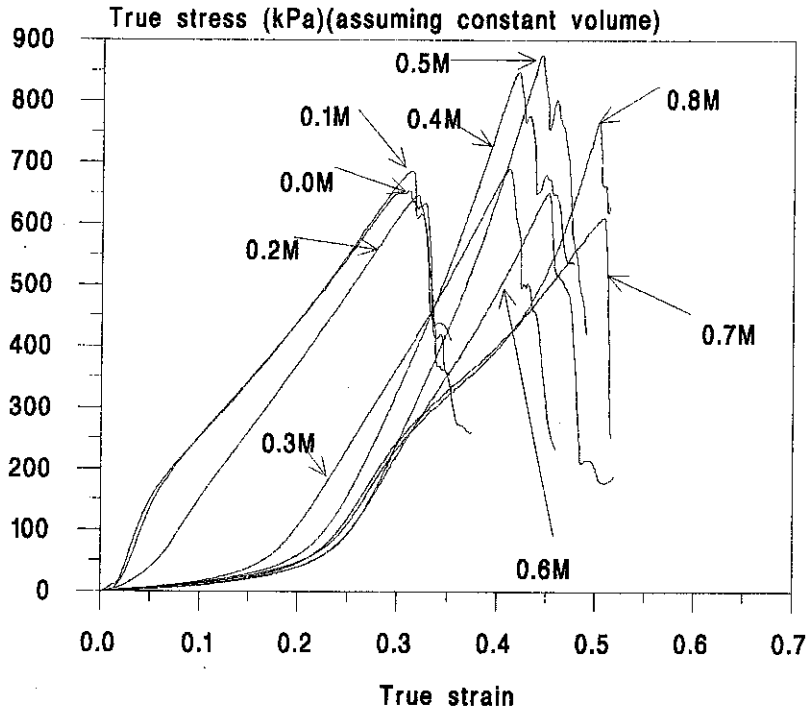


**Fig. 1 Compression behaviour of potato tuber tissue (cv 'Cara') after equilibration in a range of buffered mannitol solutions of differing concentration.**

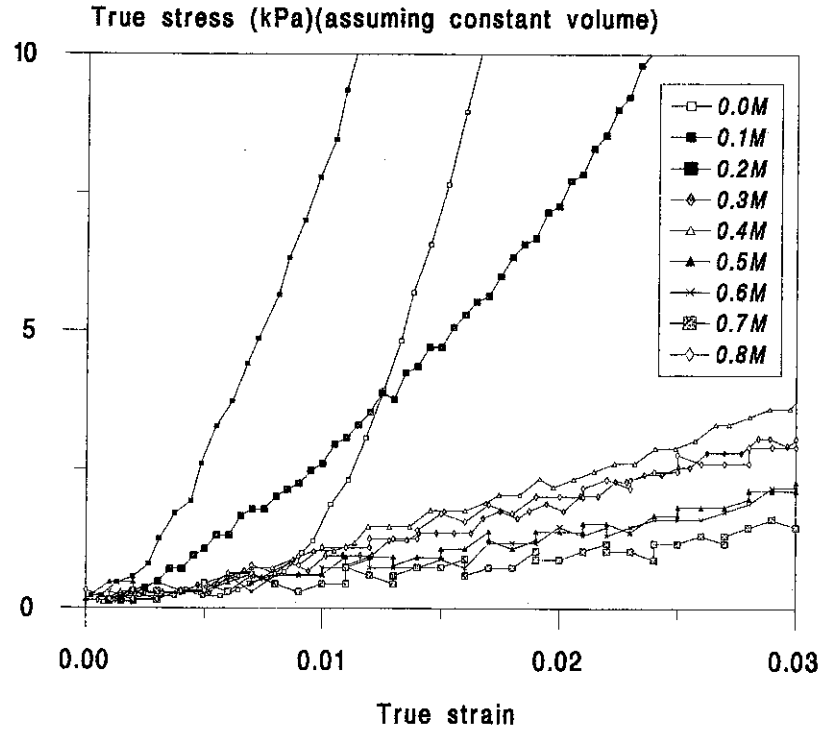


**Fig. 2 Detail of low-strain portion of above graph, showing clear differences in gradient of stress-strain curve between variously equilibrated samples, even at the start of deformation.**

# THE MECHANISM OF LEAF MOVEMENT IN BEAN *PHASEOLUS VULGARIS*

M.S. Irving[1], S. Ritter[2], D. Koller[2] and A.D. Tomos[1].

[1]: *School of Biological Sciences - UCNW Bangor, Gwynedd LL57 2UW, Wales UK. Tel - (0248) 351151 Fax - (0248) 370731*
[2]: *Institute of Life Sciences, The Hebrew University, Jerusalem 91904, Israel.*

The trifoliate leaves of bean (*Phaseolus vulgaris*) exhibit heliotropic responses which are mediated by changes in the volume and length of specialised motor cells in the cortex of the pulvinus. This can be readily studied in the laboratory using exposure to unilateral light [1].

The turgor pressure, osmotic pressure and individual solute concentrations of the vacuoles of cortical cells were determined in upper and lower sides of the pulvinus of *Phaseolus* at different leaf elevations. Single-cell sampling and analysis techniques were used [2,3,4].

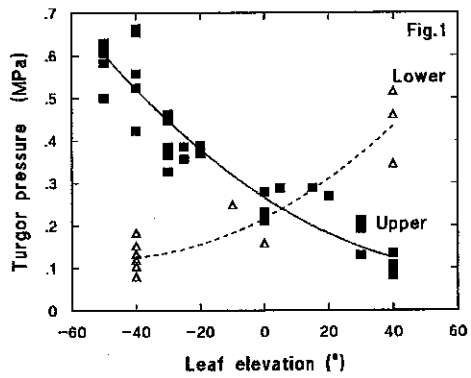


***Figure 1:*** *Turgor pressure in upper and lower cortical cells of the pulvinus at different leaf elevations.*

Results indicate that light-activated changes in leaf elevation are associated with, and presumably caused by, alterations in cell turgor pressure in the cortical region of the pulvinus (Figs 1and 2). As the leaf is elevated, turgor decreases on the upper side and increases on the lower side.

However, osmotic pressure and ion concentration ($K^+$, $Cl^-$, $Mg^{2+}$ and $Ca^{2+}$) did not show significant changes at different leaf elevations (Table 1). Clearly, changes in turgor pressure are not due to osmotic adjustment of the protoplast. We conclude therefore, that the light-activated turgor pressure changes are facilitated by apoplastic osmotic regulation. There is evidence that turgor regulation by the apoplast occurs in sugarbeet and wheat mesophyll [5], and in *Suaeda maritima* [6]. This behaviour is in sharp contrast, however, to

the phototropic responses of mustard seedlings where differential expansion is due to changes in cell wall mechanical properties [7].

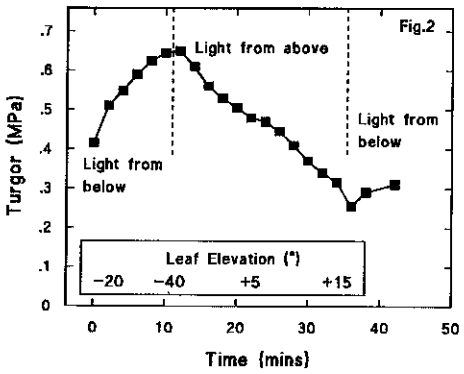


***Fig. 2:*** *Turgor changes in a single upper cortical cell in response to changes in light direction.*

| Pulvinus surface | Leaf elevation (°) | $K^+$ (mM) | $Cl^-$ (mM) | $Mg^{2+}$ (mM) | $Ca^{2+}$ (mM) | Osmotic pressure (mOsmol) |
|---|---|---|---|---|---|---|
| Upper | +35 | 71 ± 34 | 112 ± 82 | 139 ± 8 | 15 ± 2 | 391 ± 45 |
| Lower | " | 60 ± 20 | 116 ± 34 | 161 ± 13 | 18 ± 17 | 427 ± 33 |
| Upper | -5 | 109 ± 36 | 74 ± 15 | 140 ± 34 | 14 ± 14 | 388 ± 19 |
| Lower | " | 83 ± 31 | 161 ± 38 | 161 ± 29 | 9 ± 10 | 436 ± 60 |
| Upper | -50 | 115 ± 22 | 94 ± 15 | 97 ± 4 | 16 ± 9 | 373 ± 78 |
| Lower | " | 77 ± 51 | 173 ± 22 | 183 ± 60 | 5 ± 6 | 436 ± 100 |

***Table 1.*** *Inorganic solutes and osmotic pressure in upper and lower cortical cells of the pulvinus (mean of 3 plants ± SD).*

1. D. Koller and S. Ritter, (1994). *Plant, Cell and Environ.* (in press).
2. M. Malone *et al.*, (1989). *Plant, Cell and Environ.*, **12**, 919-926.
3. A.D. Tomos *et al.*, (1994). *In*: Plant Cell Biology- A practical approach. N. Harris, K.J. Oparka (Eds.), JRL Press (in press).
4. W. Fricke *et al.*, (1994). *Planta* (in press).
5. A.D. Tomos *et al.*, (1992). *In*: Carbon Partitioning. C.J. Pollock, J.F. Farrar and A.J. Gordon (Eds.), Bios, pp 71-89
6. N.J.W. Clipson *et al.*, (1985). *Planta*, **165**, 392-396.
7. T.C.G. Rich and A.D. Tomos, (1988). *J. Exp. Bot.*, **39**, 291-299.

# ANALYSIS OF THE MECHANICAL RESPONSE OF CELLULAR TURGID PLANT TISSUE

G. Jeronimidis and J.H. Liu
Centre for Biomimetics, TOB 1, Earley Gate
University of Reading, Reading RG6 2AT, UK.

This paper present results on the analysis and modelling of the deformation mechanics of turgid, multicellular plant tissue. The effect of cell geometry, dimensions and internal pressure levels has been related to applied average external loads, resulting global deformations of the tissues and to the cell wall stresses which arise from the combination of internal pressure from turgidity and from applied external forces. The aim of this work is to develop a quantitative model for the prediction of cell wall fracture and tissue damage.

The cellular structure of soft plant tissue (parenchyma cells) has been modelled as a regular array of closed hexagonal cells. The cell geometry can be changed by changing the length of the sides and the angle between them, with cubic and regular hexagonal arrays as two limit cases. The distribution of cell wall material in the model is controlled by its partitioning between edges (struts) and faces (plates). The cells are filled with an incompressible liquid. External loads, tensile or compressive, are applied to two opposite edges (Figure 1) and the deformation of the various elements is calculated; in the model, elements whose orientation is not parallel with the load direction experience both bending and stretching whereas the elements parallel to the load direction are subjected only to stretching or compression. This analysis follows the work of other researchers in this field [1-5]

The results of the full analysis can be summarised in a number of equations which describe the global average stress-strain behaviour of the tissue, the change of internal pressure due to applied external loads or deformation, and the magnitude of the cell wall stress. The parameters needed for the analysis are the average cell dimensions, the cell wall thickness, the elastic properties of the cell wall and the initial turgor pressure in the undeformed tissue.

Figures 2, 3 and 4 show some of the results obtained together with a comparison of stress-strain behaviour between experimental results (potato tisssue in compression) and analytical predictions (Fig.2). Finite Elements simulation techniques are also being developed to extend this work to irregular cell geometries and non-uniform cell size distributions.

References

[1] Pitt, R.E. (1982) Models for the rheology and statistical strength of uniformely stressed vegetative tissue. *Trans. ASAE,* 1776-1784.

[2] Gibson, L.J. and Ashby, M.F. (1988) *Cellular Solids-Structure and Properties,* Pergamon Press, Oxford.

[3] Jeronimidis, G. (1988) Structure and properties of liquid and solid foams. In *Food Strucure - its creation and evaluation,* Blanchard, J. M. V. and Mitchell, J. R. Eds., 59-74, Butterworths, London.

[4] Gao, Q., Pitt, R.E. and Ruina, A. (1990) A mechanics model of the compression of cells with finite initial contact area. *Biorheology,* **27,** 225-240.

[5] Gao, Q. and Pitt, R.E. (1991) Mechanics of parenchyma tissue based on cell orientation and microstructure. *Trans. ASAE,* **34,** 223-238.

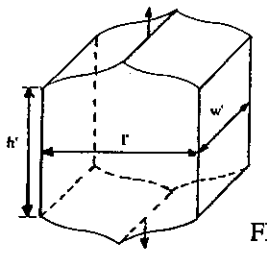


FIGURE 1

Deformed Cell Geometry

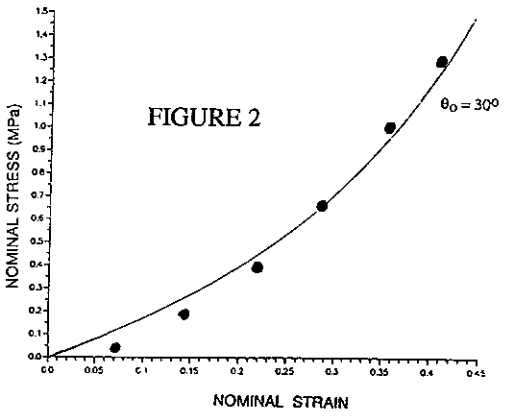


FIGURE 2

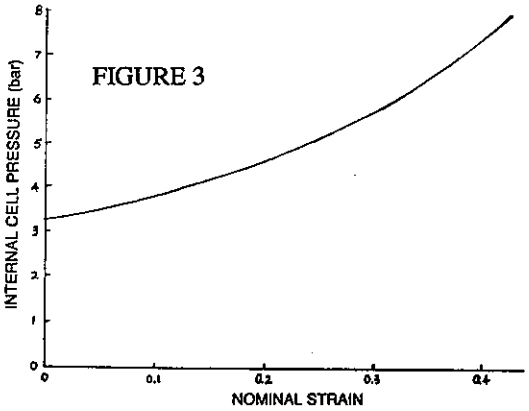


FIGURE 3

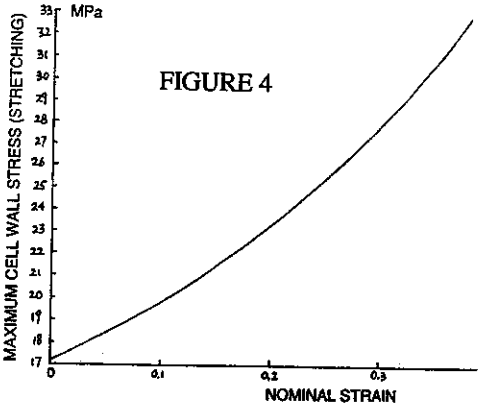


FIGURE 4

# MECHANICAL RESPONSE OF PLANT TISSUE TO IMPOSED COMPRESSIVE DEFORMATIONS

G. Jeronimidis and B. M. Stühlen
Centre for Biomimetics, TOB 1, Earley Gate
University of Reading, Reading RG6 2AT, UK.

Experiments carried out on cylindrical specimens extracted from potato and sugar beet have shown that when these tissues are subjected to a constant, uniform applied compressive deformation, the applied load decreases initially, reaches a minimum and then increases again [1]. The plant tissues appear to be able to react actively to the imposed deformation, after some time. The increase in load at constant deformation implies a tendency to expand.

Typical load-time curves, at two different temperatures, for fresh potato tissue (Cara variety) are shown in Figure 1. The applied deformation corresponding to the initial load of 1.25 N is of the order of 0.4 %, well below the value where irreversible damage occurs. The tests have been carried out in an Instron testing machine with the tissue samples fully immersed in liquid paraffin to prevent water loss.

The initial reduction in force is associated with "passive" stress-relaxation behaviour of the polymeric materials in the cell walls. The rate of relaxation is strongly temperature-dependent, which corresponds to what is observed during the first few hours of testing. The increase in load which occurs after several hours is believed to be associated with some physiological response of the tissue, probably related to metabolic rates. The time of initiation of this "active" response, its rate and magnitude depend on test temperature, storage temperature before testing and, possibly, on light conditions. Figure 2 shows the difference in response between tissues stored before testing at 6° C and 24° C. The low temperature appears to inhibit the active response. This type of "active" response has been observed also in sugar beet and may well be very general for plant tissues with parenchyma cells under turgor pressure.

The effects of time, temperature, initial deformation levels, etc. will be presented in more detail, together with modelling aspects.

The mechanism associated with the type of observed response is not yet known. It is reasonable to speculate that one possible explanation is that the cells "sense" the applied load or deformation and react by changing the osmotic potential of the cell content, increasing turgidity as a response to the external stimulus [2-4]

References

[1] Purkayastha, S. and Peleg, M. (1986) Comparison between projected mechanical equilibrium conditions of selected food materials in stress-relaxation and creep. *J. Text. Studies,* **17**, 433-444.

[2] De Baerdemacker, J. G. (1976) Determination of the viscoelastic properties of apple flesh. *Trans. ASAE.*

[3] Finney, E.E., Hall, C.W. and Mase, G.E. (1964) Theory of Linear Viscoelasticity applied to potato. *J. Agric. Eng. Res.* **9** (4), 307-312.

[4] Cosgrove, D.J. and Van Volkenburgh, E. (1984) Stress relaxation of cell walls and yield threshold of growth. *Planta,* **162**, 46-54.

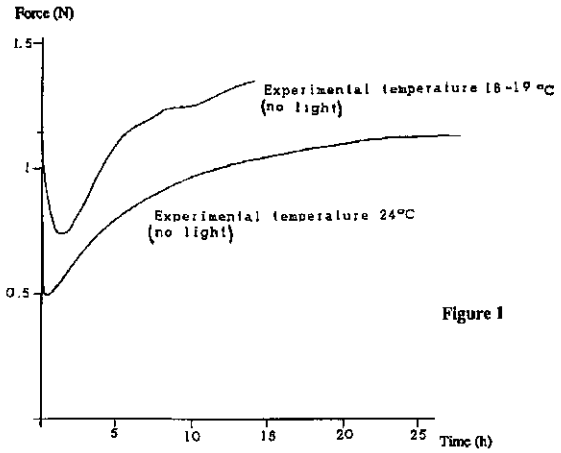


**Figure 1**

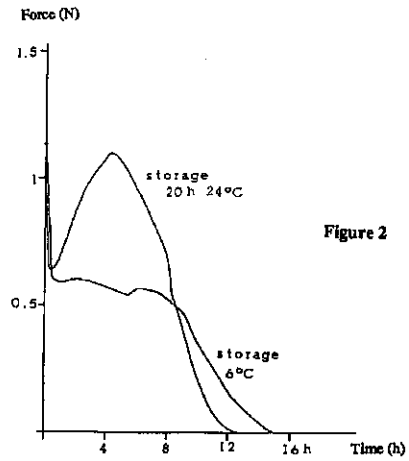


**Figure 2**

**Plant Biomechanics Conference - Montpellier, 5-9 September, 1994**

# IMAGING OF CELLULAR DEFORMATIONS FOR PLANT BIOMECHANICS

G. Jeronimidis and S.H.P. Tolkien
Centre for Biomimetics, TOB1, Earley Gate
Reading University, Reading RG6 2AT

The mechanical testing of plant structures requires accurate measurements of deformations. This is relatively straightforward in the case of average global strains of the tissues (leaves, roots, stems, branches, etc.) but becomes increasingly more difficult as the dimensions of the structural elements to be measured decreases. In many instances, for example, it is desirable to measure local deformations at the cellular level as well as global ones. Image Analysis combined with optical, electron or X-ray microscopy, provides a powerful technique for this kind of work. Image Analysis (IA) is principally used to acquire numerical data from photomicrographs or direct images of the sample. It can be employed to store and process, with relative speed and accuracy, a wide variety of tissue and cellular parameters such as counts, linear dimensions, volume fractions, shapes, orientation and local strain fields in deformed plant materials.

The poster will illustrate the use of Image Analysis applied to the direct measurement of cellular deformations within plant tissues subjected to tensile or compressive loading and to the identification of local micromechanisms of failure (cell wall rupture, cell wall buckling, etc.) associated with damage initiation. The primary information (image) has been obtained from a variety of sources: confocal microscopy, low-vacuum scanning electron microscopy and X-ray microscopy. This last technique, developed and refined at Unilever Research, Colworth, UK, consists in taking a "soft" X-ray picture of the tissue at various stages of deformation, exploiting optical principles to get sufficient magnification. The network of interconnected cell walls can be resolved with sufficient accuracy on a photograph to enable Image Analysis to process the information.

Examples of potato and sugar beet tissues before and after deformation will be presented, together with quantitative measurements of local strain fields at the cellular level, comparisons between global and local deformations and events related to damage initiation.

N-SEM micrographs of Potato tissue, variety Cara; 1-3 under tension, 2 under compression.

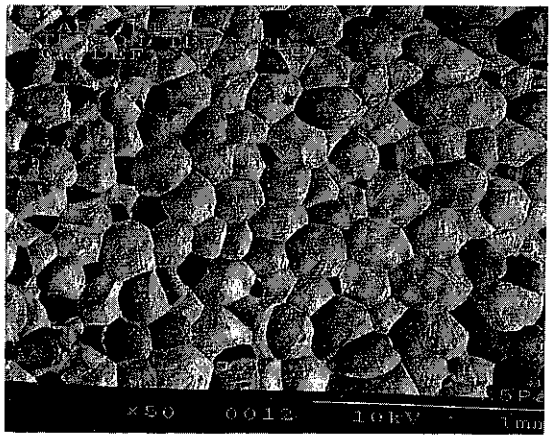


1) 0 % strain

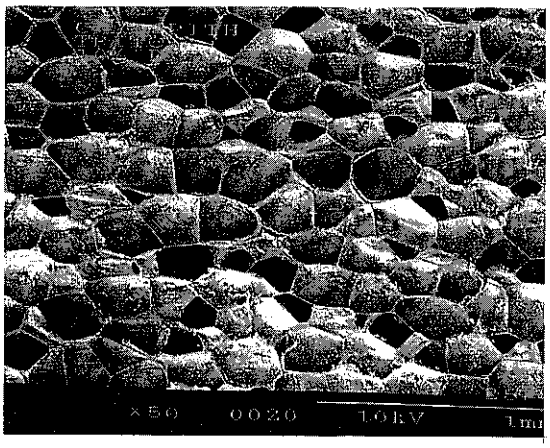


2) 10 % strain

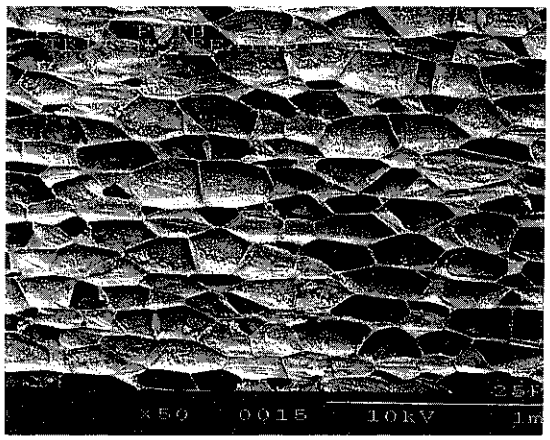


3) 20 % strain

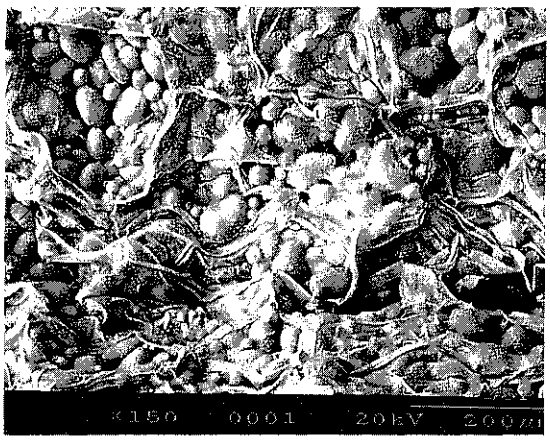


4) compression damage

Bradbury S (1979). *Microscopical Image Analysis: problems and approaches.* Journal of Microscopy, **115**(2), 137-150.

Dziezac J D (1988). *Microscopy and Image Analysis for R&D.* Food Technology, 110-124.

Ford TW, S.A., Cotton RA (1991). *Soft X-ray contact microscopy of biological materials.* Electron Microscopy Review., **4**, 269-292.

Gunasekaran S, P.M., Shove GC (1985). *Optical Methods for Nondestructive quality evaluation of Agricultural and Biological materials.* Journal of Agricultural and Engineering Research, **32**, 209-241.

# GROWTH RESPONSES TO MECHANICAL STIMULATION IN SOME HERBACEOUS PLANTS

**J.L. Julien, N. Boyer, M.O. Desbiez and J.C. Mauget***

*Unité Associée Bioclimatologie-PIAF (INRA-Université Blaise Pascal), 4 rue Ledru, F-63038 Clermont-Ferrand Cedex 01.*
** Unité Associée Bioclimatologie-PIAF (INRA-Université Blaise Pascal), INRA, Centre de Clermont-Fd-Theix, Domaine de Crouelle, F-63039 Clermont-Ferrand Cedex 02.*

Different mechanical stimulations such as pricking, rubbing or bending induce growth responses in herbaceous plants consisting in a reduction of elongation and an increase in radial expansion (Boyer *et al.*, 1979 ; Desbiez *et al.* 1981, Jaffe 1998)[1].
These modifications are considered as a possible mechanism for improved protection against further mechanical perturbation in artificial or natural conditions.
The mechanisms leading to the growth responses have been widely described in *Bidens pilosa* and in *Bryonia dioica* and are now being studied in *Lycopersicon esculentum.*
The main following results have been obtained :
- In *B. pilosa*, cotyledonary pricks induced a growth inhibition in reference to the length of the cells (Table 1). No modification of growth in reference to the width of the cells were observed 24 hours after the mechanical stimulation. After cotyledonary pricks, the mitotic percentage was reduced by 72% compared to the control plants (Pichon *et al.*, 1993)[2].
- In *B. dioica*, the lignin content of both untreated and rubbed internodes increased steadily during the 96 h following rubbing but was always higher in the rubbed ones (Figure 1). Twenty four and 48 h after rubbing, the number of lignifying xylem vessels was markedly increased (Figure 2). Phenylalanine-ammonia-lyase activity of rubbed internodes was already higher than in control plants 6 h after the mechanical stimulation and increased up to a peak at 48 h (Figure 3).
- The inhibition of the hypocotyl elongation has also been found in young plantlets of tomato in response to cotyledonary pricks. On another hand, in older plants, a rubbing treatment applied to the petiole of the second leaf induced an inhibition of the elongation of the above internodes and an increase in their diameter (Figure 4).

These data indicate that herbaceous plants respond to mechanical stimulations by reducing their elongation and increasing their radial expansion. These modifications are related to cell wall rigidification as a result of accelerated lignification. Nevertheless, several questions are raised :
- Is it possible to characterize the mechanical stimulation in physical term?
- Is there a proportional relationship between the growth response and the intensity of the mechanical stimulation?
- Do the observed modifications really lead to an increased mechanical resistance of the stimulated plants?

---

[1]**Boyer N., Gaspar T. and Lamond M. (1979).** Modifications des isoperoxydases et de l'allongement des entre-noeuds de Bryone à la suite d'irritations mécaniques. Z Pflanzenphysiol, 93, 459-470.
**Desbiez M.O., Boyer N. and Gaspar T. (1981).** Hypocotyl growth and peroxidase of Bidens pilosus L. Effects of cotyledonary prickings and lithium pretreatment. Plant Physiol., 68, 41-43.
**Jaffe M.J. (1988).** Wind and other mechanical effects in the development and behaviour of plants, with special emphasis on the role of hormone. Encycl. Plant Physiol., 11, 444-483.
[2]**Pichon O., Bonnin B., Gendraud M. and Desbiez M.O. (1993).** Ionic and cellular responses to traumatisms in Bidens pilosa : Effect of light quality. Plant Physiol. Biochem., 31, 175-180.

| | Mitotic percentage | Length of cells (µm) | Width of cells (µm) |
|---|---|---|---|
| Control plants | 1.8 ± 0.7 | 148 ± 5.1 | 18.4 ± 0.2 |
| Pricked plants | 0.5 ± 0.1 | 98 ± 2.5 | 18.4 ± 0.6 |
| Δ (%) | -72.2 | -33.8 | 0 |

**Table 1.** Variations of hypocotyl cell size and mitotic activity after cotyledonary pricks. Δ, percentage of variation between control and pricked plants [(control-pricked/control) x 100]. Measurements were performed at a distance of 0.2 mm under the cotyledonary node (for mitotic percentage) and at 2 mm under the cotyledonary node (for cell size). Values ± SE.

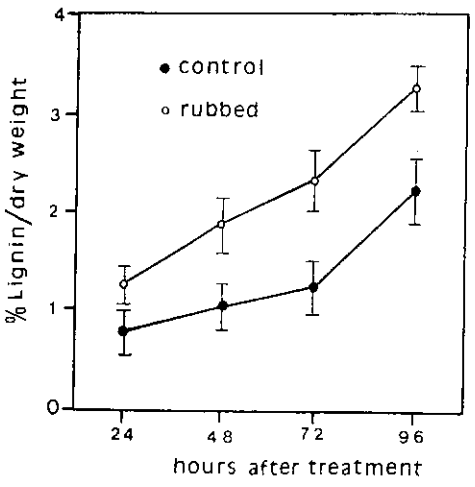


**Figure 1.** Lignin content of control and rubbed *Bryonia dioica* internodes at different times after treatment.

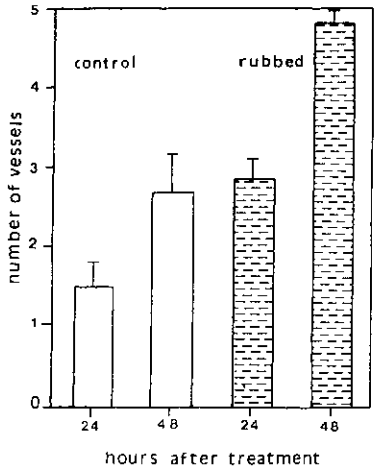


**Figure 2.** Number of lignifying vessels per vascular bundle in control and rubbed *Bryonia dioica* internodes 24 h and 48 h after rubbing.

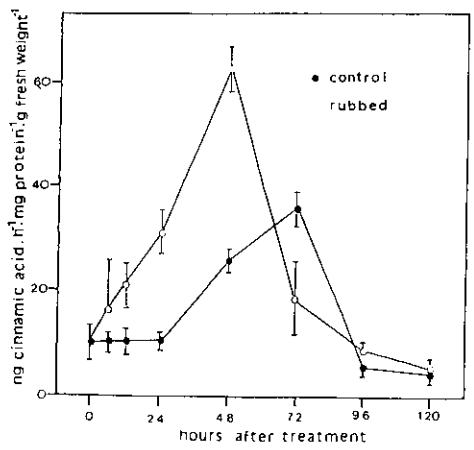


**Figure 3.** Time course of PAL activity in control and rubbed *Bryonia dioica* internodes.

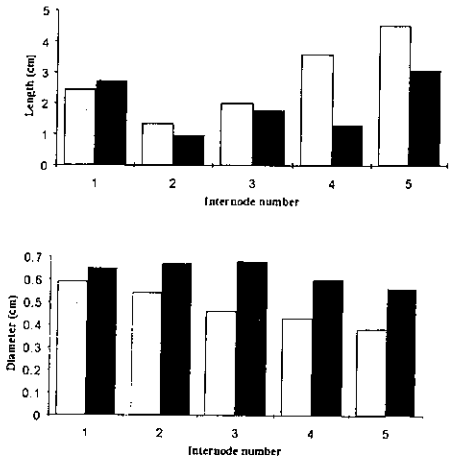


**Figure 4.** Effects of rubbing the petiole of the second leaf of a tomato plant. **A**. Internode length in control □ and treated plants ■. **B**. Internode diameter in control □ and treated plants ■.

# EVALUATING TRANVERSE STRAINS IN GREEN WOOD.

Delphine JULLIEN,
Laboratoire de Mécanique et génie Civil, URA 1214 du CNRS
Université Montpellier 2, F 34095 MONTPELLIER CEDEX 5

During tree growth, wood appears by successive layers around the trunk (secondary growth). This formation mode leads to stress field introduction, consisting in longitudinal and transverse stresses. The longitudinal stress role is well known (tree bearing and orientation) and strain evaluating methods (Fournier) exist. Concerning transverse stresses, things are less mastered: they are revealed by heart checks, especially during steaming. We can note a peripherical tangential compression, which protects the tree in the sense that it contributes to close and heal cracks, but also contributes to brittle heart phenomenon. But there is still no simple way to evaluate the corresponding strains. This paper suggests one.

The study started because of the industrial problems caused by the heart checks apparition and their developpement during steaming. For this reason, the method is also applied to measure strains due to steaming operation.

## Material and method.

The studied samples are 8 or 16 mm thick wood disks, sawn from green trunks. Longitudinal release measurements have been made previously on the standing chesnut trees. The cutting operation consists in sawing off a thin angular sector from the periphery to the heart, and the steaming operation in heating the disk in 80°C temperature water in a bain-marie during half an hour.

The length-measuring device was made of a system of pins hammered in the disk and a modified displacement transducer measuring the distance between the pins. It allows to evaluate the lips end relative displacement due to cutting and steaming (fig.1). In some cases, numerous judiciously chosen displacements were also evaluated (fig.2), they verified measurement coherence.

## Results and discussion.

It appears that the lips end displacement divided by the remaining circonferency (fig.1) gives a good transverse strain estimate, obtained by a quick and simple way.

The graph (fig.3) shows only weak correlation between transverse and longitudinal strains. This result is not surprising because longitudinal strains reflect only the peripherical stress field, unlike the transverse ones that give a global value of the stress field integrating all the tree history locked in the whole section.

To gain better understanding of the experimental method, a numerical simulation using a finite element method (fig.4) was performed. First an initial residual stress field corresponding to the tree state prior to felling is simulated, through the successive addition of the stress field due to the deposition and maturation of new layers. Second, the cutting operation described above is simulated too.

## Conclusion.

To establish a better parallel between experimentations and simulations, tree growth eccentricity as well as wood material anisotropy will be taken into account.

Steaming is also an interesting aspect to develop since it allows to reach locked strains. Because steaming softens lignin and gives it back the rheological properties it had at the beginning of the lignification during wood formation, we can imagine that phenomenons observed at high temperature may be linked to wood formation in some way.

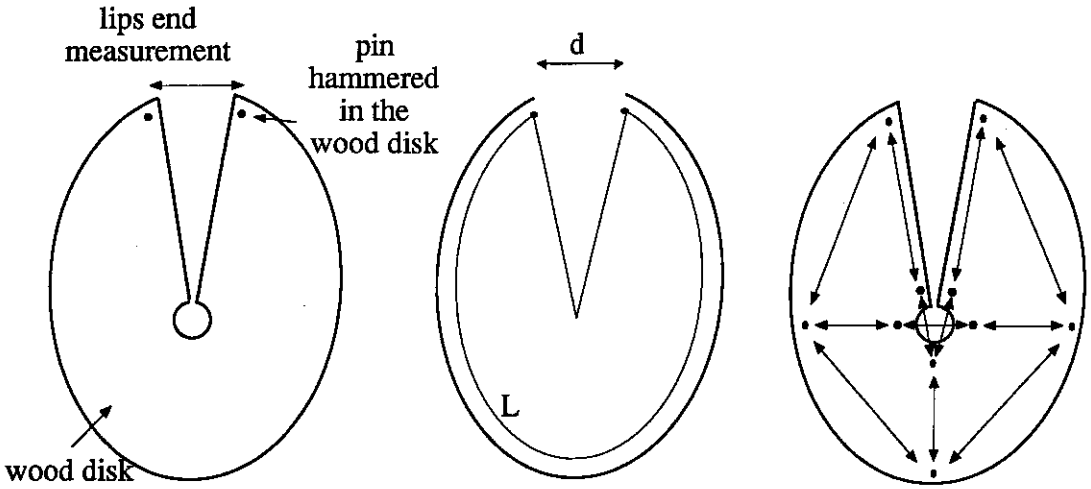


Δd the lips end relative displacement
L the remaining circonferency
L/Δd the tranverse strain

fig. 1: method of global transverse strain evaluation

fig. 2 : verification of coherence

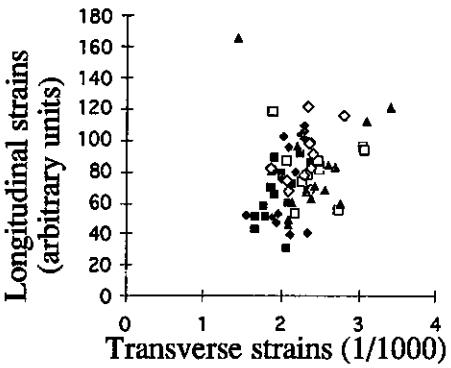


fig. 3 : longitudinal-transverse strains relation

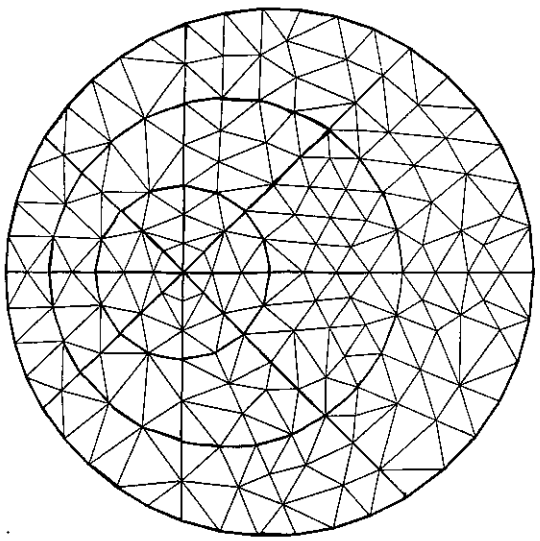

fig. 4: Finite element simulation of maturation-induced strains

# Biomimicking of Plant Stems

G.N. Karam and L.J. Gibson
Department of Civil and Environmental Engineering
Massachusetts Institute of Technology
Cambridge, MA 02139
USA

Abstract

Plant stems resist both axial load (due to their own weight) and bending moments (due to the wind). Failure is typically by local buckling of the compressive face. Microscopic investigation reveals that many plant stems are made up of an almost solid cylindrical shell lined with an inner layer of foam-like parenchyma cells (a " core-rind" structure). This foam core may totally or partially fill the shell.

Recently, we have analyzed the elastic buckling of a cylindrical shell with a compliant core under both uniaxial load and bending moment. The analysis showed that the foam core stabilizes the shell against local compression buckling due to axial load or bending moment. It also serves to prevent Brazier ovalization of the section under bending. The stresses due to shell buckling were found to decay to negligible values at a core depth equal to a multiple of the buckling wavelength. Removal of the core material beyond that given depth does not affect the buckling stress of the shell. The results of a parametric study indicates that for a given mass and diameter, a cylindrical shell with a foam core of sufficient depth for stress decay has a higher buckling load or moment than an equivalent hollow shell (Fig 1). The analysis has been confirmed by tests on silicone rubber shells with and without foam cores.

The microstructure of a number of plant stem cross sections was investigated. The shell radius, thickness and density and the core depth and density were measured. The parenchymatous core was modeled as an isotropic foam neglecting turgor pressure. The application of the results of the previous analysis to plant stems revealed their "core-rind" structure to be well described by the theoretical predictions based on the minimum depth for stress decay. The analysis also suggests that due to their microstructure, the plant stems can eliminate totally Brazier ovalization and can achieve improvements in their mechanical efficiency of a factor of up to 2 in local buckling resistance. The mechanical efficiency of other natural materials with a similar structure, such as porcupine quills and hedgehog spines, is also described. The effect of neglecting turgor pressure on the mechanical efficiency of plant stems is explained and the relationship

between mechanical and physiological function is investigated to explain differences in mechanical efficiency among different natural strucutres.

The role of these simple mechanical efficiency models in understanding plant and animal evolution and their potential application to the selection of agricultural varieties with improved resistance to lodging is discussed.

Finally, we conclude by suggesting that the mechanical efficiency of engineering cylindrical shell structures (eg. aircraft fuselages, offshore oil platforms) may be improved by biomimicking the core-rind structure of plant stems.

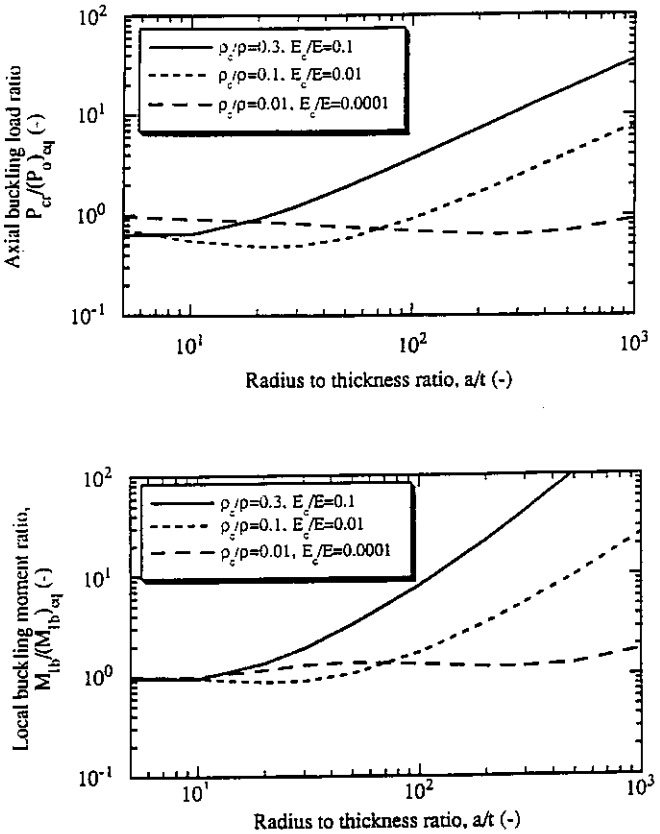


Fig. 1 .The ratio of (a) the uniaxial compressive buckling load and (b) the local buckling bending moment of a cylindrical shell with a foam core to that of an equivalent shell (of equal radius and mass) without a foam core. The foam core improves performance in uniaxial compression at higher core densities and shell radius to thickness values. The core improves the local buckling resistance in bending at all core densities and a/t values.

# BENDING PATTERN OF GRASSES WITH DIFFERING CONSTRUCTION

A.B. Kesel, W. Nachtigall, A. Wisser
Universität des Saarlandes, Fb.13.4 Zoologie, D-66041 Saarbrücken

Grasses (*Poaceae*) as slim self-supporting constructions are frequently exposed to the pressures of strong winds. These induced a load which is composed of statical as well as dynamical parts. The latter will be compensated by turn aside, which reduces the bending moments in the blade and enables it to tolerate high wind loads (Rasdorsky 1937, Vogel 1981). Nevertheless the statical wind load induces a high flexion which must be compensated by the arrangement and distribution of building materials (parenchyma, sclerenchyma) as well as stiffening structures (nodes).

Using a laminar wind tunnel, the bending patterns under continual loading of three species of grass (*Lolium perenne, Molinia coerulea, Echinochloa crus-galli*) are compared. Morphological and histo-morphological studies (cross-section analysis) allows the division into distinct types of construction. By observing the nodes, first morphological studies show two principle types: A) The nodes are distributed evenly throughout the stem (*Lolium p., Echinochloa c.*). B) The nodes are concentrated at the base of the blade, the stem is represented by the last internodes (*Molinia c.*).

The histo-morphological analysis show a peripheral arrangement of the sclerenchyma, which improves the flexural stiffness of the blade (Speck 1991, Speck and Vogellehner 1992). The arrangement of supporting elements (parenchyma, sclerenchyma) in the blade cross-section depends on the grass species and enables one to divide grasses into three main patterns of arrangement (Nachtigall et al. 1988) (Fig). In addition the observations show a species dependend distribution of the percentage parts of sclerenchyma and parenchyma, this distribution is changing along the blade length (decreasing: *Lolium p.* and *Molinia c.*; increasing: *Echinochlod c.*) (Tab).

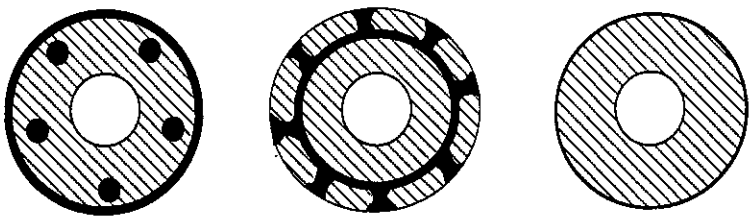

Type I Type II Type III

Fig: A) Type I: Outer sclerenchyma ring (*Lolium p.*); B) Type II: Inner sclerenchyma ring with sclerenchyma rods leading to the epidermis (*Molinia c.*); C) Type III: Outer sclerenchyma ring and thinner inner ring (*Echinochloa c.*) (shadowed: parenchyma; black: sclerenchyma).

Tab: Percentage parts of the stabilization materials in the three species of grass and the length dependend changing of the sclerenchyma part.

| species | Lolium p. | Molinia c. | Echinochloa c. |
|---|---|---|---|
| lenght [m] | 0,55 | 0,61 | 0,95 |
| blade lenght [m] | 0,39 | 0,48 | 0,82 |
| parechnchyma [%] | 63,5 | 57,5 | 85,3 |
| sklerenchyma [%] | 34,5 | 42,5 | 14,7 |
| sclerenchyma changes [%] | -37 | -8 | 30 |

In order to quantify the contribution of individual structure stabilizating elements, models of grasses under continual loading were made using the Finite Element Methode (ANSYS). The important arrangement of nodes (Gappoev 1991) and, in first calculations, the material distribution in the stem were also taken into consideration. The FE-Models aims to understand the contribution of the individual elements to stability as well as their combined influence.

From the arrangement of the structural elements together with surface interia moments and elasticity modules, one understands the bending resistance and thus the bending behaviour of the different grass constructions.

References:

Gappoev M. 1991. Untersuchung zur Form und Faserstruktur von Gras- und Halmpflanzen unter Berücksichtung der Kräfteverteilung in den Knoten. Mitteilungen des SFB 230, Heft 6, Stuttgart.

Nachtigall W., Wisser C.M., Wisser A. 1988. Natürliche Konstruktionen - Mitteilungen des SFB 230, Teil I.

Rasdorsky W. 1937. Über die Baumechanik der Pflanzen. Biologia generalis, Internationales Archiv für die allgemeinen Fragen zur Lebensforschung XII: 359 - 398.

Speck T. 1991. Biophysikalische Methoden in der Paläobotanik: Möglichkeiten - Problematik. Ber.Naturf.Gesa. Freiburg i. Br. 79: 99 - 131.

Speck T., Vogellehner D. 1992. Fossile Bäume, Spreizklimmer und Lianen. Versuch einer biomechanischen Analyse der Stammstruktur. Cour. Forsch.-Inst. Senkenber. 147: 31 - 53.

Vogel S. 1981. Life in moving fluid. Boston.

# FRACTURE PROPERTIES OF AN ANISOTROPIC BIOLOGICAL CELLULAR MATERIAL - APPLE FLESH

## Abstract

**Ali A Khan**
Centre for Biomimetics, University of Reading, Reading , Berkshire, U.K.

The texture of apple flesh is important in assessing its eating qualities. The texture is in turn related to the structure of the parenchyma. The parenchyma cells of the fruit are predominantly arranged in radial quasi-columnar form with long radially arranged spaces in between. This anisotropy has a marked effect in the fracture properties such that it is much easier to drive the crack between the cell columns (radially) than to drive it across them (tangentially). The fracture tests used were simple crack-opening tests on geometrically cut specimens, e.g. notched tensile and wedge penetration tests. The latter is particularly useful for specimens which are small and awkwardly shaped and cannot be easily prepared for tensile testing. This directional difference in the mechanical properties was also detected by a taste panel. The radial spaces ease the passage of cracks travelling along them, and act as crack stoppers for cracks travelling at right angles to them. The spaces along with the radially elongated cells also allow the tissue to deform much more in the tangential orientation giving the structure greater ductility and making the parenchyma tougher in that orientation. It is possible to increase this effect by controlled damage to the material such as slow freezing which causes the intercellular spaces to expand increasing the crack stopping mechanisms and increasing the ductility, therefore increasing the fracture toughness. Toughness first increases, then decreases with increasing damage. This effect can be mimicked with brittle paper: fracture toughness of tracing paper initially increases if holes are punched randomly in it.

Biruta KRESLING
Bionics & Experimental Design
170, rue Saint-Charles
F-75015 PARIS France
Tel. (1) 40 60 96 06
Fax. (1) 45 58 38 75

Biruta KRESLING

**Plant "Design" : Mechanical Simulations of Growth Patterns and Bionics** (*)

A plant, capable of reacting to its real physical environment (i.e. to the internal and external forces acting on its structures), adapts its forms during growth, continually achieving a quasi-stable state. The resulting patterns reveal a complex process of feedback between growth and form.

These growth patterns may be mechanically simulated, and some of their principles transfered to industrial design.

The design of leaf venation may be interpreted as patterns made by processes of folding and unfolding , and the regular design of stems as patterns mady by buckling, i.e. by failure of cylinders or prisms under excessive axial load. Such interpretations help to compare the mechanical behavior of natural and of technical structures and offer some surprising and even paradoxical aspects.

With students in Experimental Design (**) kinetic structures were elaborated that may simulate either leaf development or growth patterns on cylindrical elements in plants (trees, grasses, cacti, wood tracheids). These kinetic structures are based on the engineering principles of astronautical "solar sails", wich are foldable (K. MIURA), and of "plate-structures", which are stable (T.. WESTER). Both may be made with thin walls or with low cost materials.

In order to create a convincing simulation it is essential that a natural structure be regarded not as one that attains a technically ideal state, but on the contrary, one of "constant failure" (buckling, bistability, deformation under stress). Real, dramatical failure during budding or under excessive mechanical constraints also reveal principles of design in plants.

For a better understanding of the particular "logic" of plant design, some bionic industrial products (i.e. based on mechanical principles of natural structures) are presented, such as: sandwich panels, composite materials, foldable, flexible or stiff/stable tubular structures (R. LE RICOLAIS, G. JERONIMIDIS and J.E. GORDON, B. KRESLING and students in industrial design).

(*) Presentation supported by the MUSEUM NATIONAL D'HISTOIRE NATURELLE, Paris (Association pour la Promotion de la Binonique)

(**) Valenciennes (ISD and SUPINFOCOM at the Chamber of Industry and Commerce), Compiègne (UTC, University of Technology), Paris (ESDI Design School)

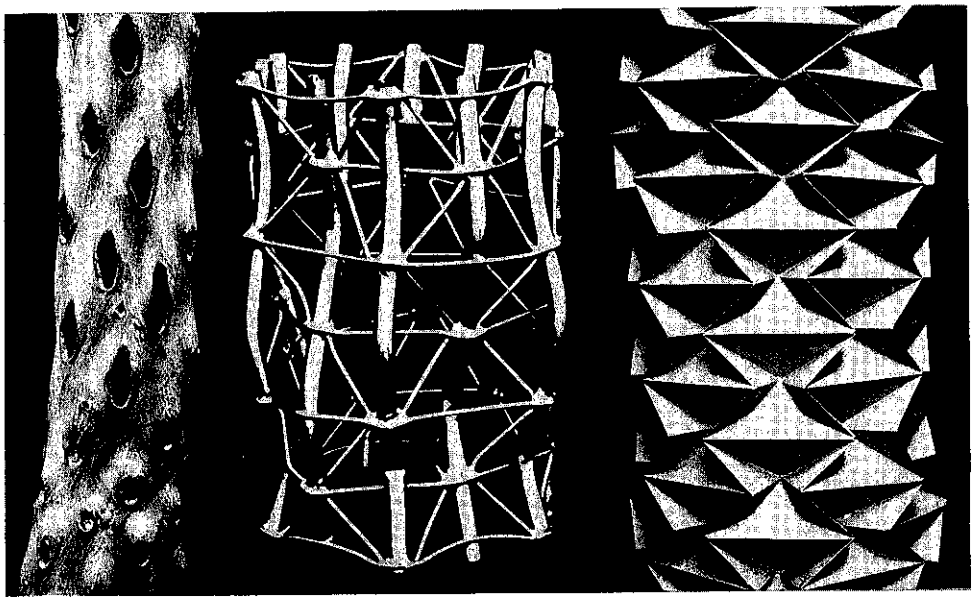

(a) (b) (c)

Figs.(a) Stem of an Opuntia-cactus with leaves removed. The pattern may be interpreted as the buckling of a cylinder. (b) 'Automorphic tube', experimental structure designed by the french engineer Robert LE RICOLAIS (about 1960). The 'harmonic' buckling is due to strong axial compression. (c) Folded structure obtained from a single sheet, designed by Nathalie MAILLARD, student in Experimental Design at SUPINFOCOM, Valenciennes (1991). For complete stabilization, the cylinder is combined with an interior tube presenting axial folds.

References:

R.C. CHAPLIN, J.E. GORDON, G. JERONIMIDIS (1983): *Composite Material,* U.S. Patent 4,409,274

B. KRESLING (1992 a): *La Bionique - Nouveaux Concepts pour le Design,* in Design Recherche Revue, **1**, 51-68, A Jour (Ed.), Paris

B. KRESLING (1992 b): *Folded Structures in Nature - Lessons in Design,* in: SFB 230 - *Natürliche Konstruktionen,* **7**, Proc. of the Internat. Symp. of the Sonderforschungsbereich 230, Universität Stuttgart, oct. 1-4 1991, Part **2,** 155-161

B. KRESLING (1993): *Folds,* in: *Bionics, Nature as a Model,* Pro Futura (Ed.) München, 13-33

R. LE RICOLAIS (1935): *Les tôles composées et leurs applications aux constructions légères,* in: Bull. Ing. Civils de France (mai - juin 1935), 410-431

K. MIURA (1989): *Folding a Plane - Scenes from Nature, Technology and Art*; in: G. DARVAS, D. NAGY (Ed.): *Symmetry of Structure,* Interdisc. Symp. Budapest, Hungary; Aug. 13-19, 1989, 391-394

W. NACHTIGALL, B. KRESLING (1992): *Bauformen der Natur - Teil I: Technische Biologie und Bionik von Knoten-Stabtragwerken,* in: Naturwissenschaften **79**, 193-201; *Bauformen der Natur - Teil II: Technische Biologie und Bionik von Platten-und Falt-Konstruktionen,* in: Naturwissenschaften **79**, 251-259, Springer, Heidelberg

# MEASUREMENT OF DEFORMATION USING IMAGE ANALYSIS

Rhizlane LAHBABI, Patrick PERRE and Alcir BRANDAO
Laboratoire de Recherches en Sciences Forestières
ENGREF - 14 rue Girardet, 54042 NANCY Cedex
FRANCE

In order to specify the mechanical behaviour of solid materials, it is necessary to measure deformation. Classicaly, strain was measured using electrical strain gages, mechanical extensometers and Moiré method. The techniques are limited by instrumentation, sample geometry, fragility of some particular materials and instrument size.

In this work, an automatic method to quantify deformation directly from image analysis was developed. Under the hypothesis of small deformation when materials are subjected to compressive, tensile and/ or shear stress, a computer code allows to determine the strain field which separates two images (fig.1). The code was written in the principle of simplex method to minimize a function which depends on the gray level of both images.

The advantage of this technique is that the measurement is made without contacting. By applying the method on wood, it is possible to have the microscopic deformations (fig.2), and to find out the mechanical behaviour and shrinkage for each of anatomical elements.

This technique can also be used to study the mechanical behaviour of standing trees under load. In this connection, the deformation parameters will change: only have the curvature and displacement to be found (fig.3). This method also permits to characterize the mecanical properties of some elements of tree structure, or to follow the shape evolution of trees resulting from natural growth.

Key words: deformation, image analysis, simplex method, gray level, non contact.

References

Chao, Y.J. and Sutton, M.A. Measurement of strains in paper tensile specimen using computer vision and digital image correlation-Part 1: Data acquisition and image analysis system. Tappi 71.3 : 173-175 (1988).

Chao, Y.J. and Sutton, M.A. Measurement of strains in paper tensile specimen using computer vision and digital image correlation-Part 2: Tensile specimen. Tappi 71.4 : 153-156 (1988).

Choi, D., Thorpe, J.L. and Hanna, R.B. Image analysis to measure strain in wood and paper. Wood Sci. Technol. 25 : 251-262 (1991).

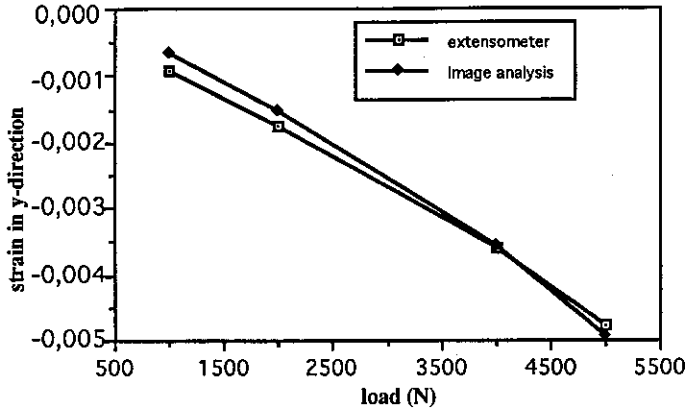


Fig.1 - Compressive test of oak: agreement between image analysis method and extensometer measurement.

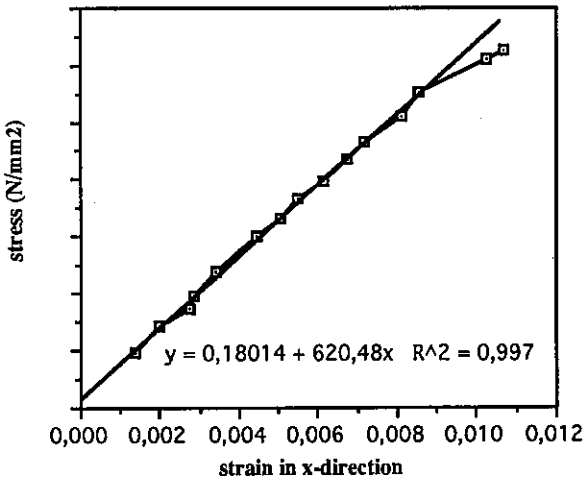


Fig.2 - Microscopic deformation under traction test for spruce

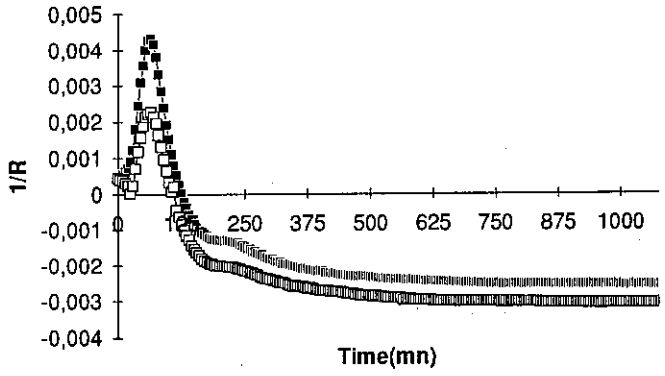


Fig.3 - Non symmetric drying experiment of beech : curvature radius (R) measured by image analysis

# SUMMARY OF VEGETABLE TRANSPLANT RESPONSE TO MECHANICAL CONDITIONING VIA BRUSHING

Joyce G. Latimer, Department of Horticulture, University of Georgia, Georgia Station, Griffin, GA 30223-1797 U.S.A.

By exploiting the effects of mechanical perturbation on plants, we can enhance plant habit, strength and structure under controlled environments. Since daminozide (Alar) is no longer registered for use on food crop plants in U.S.A., height control of greenhouse-grown vegetable transplants has been limited to restriction of water, nutrients, or both. Mechanical conditioning is the deliberate use of mechanical stress to provide an alternative means of height control of greenhouse-grown plants with the potential to produce a higher quality transplant (1). Brushing for regulation of plant growth and condition has been successful for a variety of vegetable crop species. In order to implement brushing in a commercial setting, we must identify the appropriate developmental stage for initiation of a brushing treatment and determine the responsiveness of various vegetable crop cultivars to brushing.

A brushing apparatus was designed for uniform application of the treatment across cultivars (2). Each vegetable species constituted a separate experiment using a split-plot design with three replications. The treatment was applied by brushing the upper one-third of seedlings with a wooden pole for about 1.5 min (80 or 40 strokes across a flat of plants) twice daily for one to three weeks depending on crop time. At the conclusion of treatment, all plants were rated for damage and six plants per subplot were harvested for measurement of stem length and shoot dry weight.

Solanaceous crops. Brushing initiated at the cotyledonary stage resulted in the shortest 'Sunny' tomato (Lycopersicon esculentum) transplants, with stem lengths 43% less than control, but treatment initiated at the first, second or third true-leaf stage also reduced stem length. All brushing treatments resulted in a 20% reduction in shoot dry weight. Damage was insignificant and plant appearance was excellent. Brushing initiated at the cotyledonary stage also resulted in the shortest pepper (Capsicum annuum) transplants, but over 40% of 'Marengo' plants and 90% of 'Jupiter' plants exhibited some damage from the treatment. Brushing initiated at the first or second true-leaf stage showed less reduction in stem growth but plant damage was still excessive. Brushing 'Pingtung Long' eggplant (Solanum melongena) seedlings at the cotyledonary, first, or second true-leaf stage resulted in good height control, stem lengths about 30% less than that of control, and moderate reductions in shoot dry weight.

Cucurbitaceous crops. Brushing of the cucurbit seedlings was initiated only at the cotyledonary stage. Brushing reduced stem elongation of 'Suyo Long' and 'Sweet Success' cucumber (Cucumis sativus) transplants 30% and 27%, respectively, and improved the plant appearance. Squash (Cucurbita pepo) was slightly less responsive to brushing: stem elongation of 'Dixie', 'All Seasons', and 'Cream of the Crop' was reduced 17%, 14%, and 25%, respectively. However, across squash cultivars, brushing reduced petiole length 43% and petiole dry weight 49%, without affecting leaf dry weight. Watermelon (Citrullus lanatus) cultivars vary in response to brushing, from no growth reduction for 'Sweet Favorite' to reductions of 45% in stem length and 24% in leaf area for 'Crimson Sweet'. Stem growth of 'Sugar Baby' watermelon was reduced 20% by brushing and plant appearance was improved.

Cruciferous crops. Broccoli and cabbage (Brassica oleracea) also show cultivar-specific responses to brushing, with two of five cultivars in each group exhibiting reductions in stem length after treatment. However, broccoli and cabbage seedlings were damaged by brushing, particularly when treatment was initiated at the second or third true-leaf stages. Stem length was generally reduced only 10 to 15% and some cultivars such as 'Conquest' exhibited excessive damage.

Brushing shows good potential as a non-chemical method of controlling the growth of some greenhouse-grown vegetable transplants, resulting in improved plant strength and appearance. Tomato and eggplant appear to be very responsive to the treatment, regardless of when brushing is initiated. Cucumber, watermelon and squash are responsive to brushing initiated at the cotyledonary stage, exhibiting moderate height control and very little leaf damage. In contrast, broccoli and cabbage did not respond well to brushing; exhibiting very little height control, but extensive damage on some cultivars, especially when treatment is initiated at later developmental stages. Brushing was least successful on pepper, which incurred moderate to extensive leaf damage depending on the experiment. In addition, Perhaps brushing is more injurious to plants with brittle leaves, such as pepper or cabbage. The application of other types of mechanical conditioning, such as shaking, vibration, or a static counterforce, may be less injurious to these more delicate transplants.

Literature Cited

1. Latimer, J.G. 1991. Mechanical conditioning for control of growth and quality of vegetable transplants. HortScience 26:1456-1461.

2. Baden, S.A. and J.G. Latimer. 1992. An effective system for brushing vegetable transplants for height control. HortTechnology 2:412-414.

# Mise au point d'un dispositif de mesure non destructif de la fermeté des fruits et des légumes . Essais sur tomate.

**P. Lesage, M.-F. Destain**

Mécanique agricole, Faculté des Sciences Agronomiques de Gembloux
2 Passage des Déportés, 5030 Gembloux (Belgique).

## Introduction

Les consommateurs sont de plus en plus sensibles à la *qualité* des fruits et légumes dont ils se nourrissent. Cette notion de qualité apparaît de prime abord comme subjective. En fait, elle peut être mise en évidence à l'aide de divers tests chimiques (mesure de la matière sèche, des sucres, des acides, ...) ou physiques qui, le plus souvent, sont *destructifs*. Notre recherche s'apparente aux tests physiques et présente une méthode permettant de déterminer de façon *non destructive la fermeté* d'un fruit.

## Principe de la méthode

La fermeté est la résistance offerte par le fruit ou le légume à la pénétration d'une tige. Habituellement, elle est mesurée de façon destructive à l'aide d'appareils du type Effigi ou Instron. Dans notre cas, la fermeté est mesurée en appliquant une force $F_1$ au fruit, à l'aide d'une tige qui se déplace de façon à provoquer une *déformation élastique* de la peau, selon la relation:

$$F_1 = \Delta x_{fr} \times K_{fr} \qquad (1)$$

avec:

$\Delta x_{fr}$ = déplacement de la tige dans le fruit (mm);

$K_{fr}$ = raideur ou fermeté du fruit (N/mm).

La Figure 1 montre le principe du dispositif d'essai. La force $F_1$ provient du ressort à spirales AB, travaillant en traction et engendrant une force de rappel $F_2$. L'équilibre de la bascule répond à la relation générale suivante:

$$F_1 \times 70 = F_2 \times 30 \qquad (2)$$

A partir de (1) et (2), on calcule la raideur du fruit selon:

$$\Delta x_r \times K_r \times 30 = \Delta x_{fr} \times K_{fr} \times 70 \qquad (3)$$

avec:

$\Delta x_r$ = déplacement relatif mesuré des extrémités A et B du ressort (mm)

$K_r$ = raideur du ressort, mesurée au préalable (N/mm).

La méthode s'applique aux fruits ou aux légumes dont la fermeté de l'épiderme est inférieure ou égale à celle de la chair. L'essai est non destructif pour autant que le déplacement de l'extrémité de la tige de pénétration reste très faible. C'est là que réside la caractéristique principale du

dispositif d'essai: il est nécessaire d'obtenir une grande précision à la fois dans la réalisation du montage expérimental et dans la mesure des déplacements.

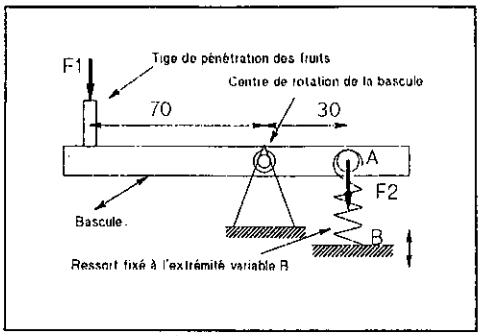


*Fig. 1. Schéma de principe du dispositif de mesure de la fermeté*
*$F_1$ = force exercée par le fruit;*
*$F_2$ = force de rappel du ressort.*

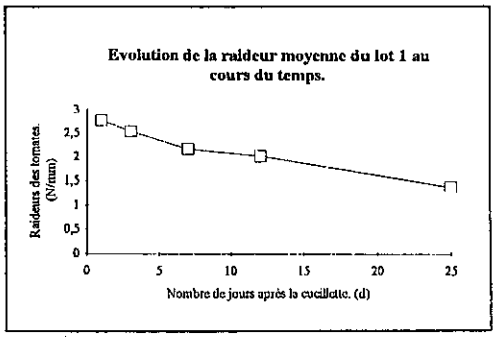


*Fig. 2. Evolution de la fermeté des tomates au cours du temps.*

## Essais sur tomates

Les essais ont été réalisés en imposant un déplacement maximum de la tige de pénétration dans le fruit égal à 1,5 mm. Dans cette gamme de mesures, le fruit n'est pas altéré et il existe une relation linéaire entre la force appliquée et la déformation de l'épiderme: la fermeté est donc constante.
Les tomates sont conservées à 4°C et les mesures sont répétées dans le temps, pendant une durée de 25 jours, ce qui permet d'observer l'évolution de leur fermeté. La Figure 2 montre les résultats obtenus pour un lot constitué de 30 tomates.
Bien que les tomates testées soient considérées par l'horticulteur comme "identiques", le coefficient de variabilité (C.V.) de leur fermeté atteint 17 %.
La tomate n'est pas un fruit homogène, les mesures présentent un C.V. de 12 % selon que la mesure est effectuée sur une paroi carpellaire ou non.
Le résultat des mesures est faiblement affecté, quel que soit l'opérateur (C.V. de 7 %).
La comparaison des résultats obtenus en utilisant des méthodes de référence (INSTRON et EFFIGI), avec des tiges de 3 mm de diamètre, a permis de mettre en évidence des relations très hautement significatives et significatives, du point de vue statistique.

## Conclusions

- Sur tomate, tant que la profondeur de la tige reste inférieure à 1,5 mm, la déformation de l'épiderme reste élastique et il existe donc une relation linéaire force-déplacement qui permet de déterminer la raideur du fruit ou sa fermeté;
- Le test de mesure de fermeté proposé est non destructif;
- Le dispositif permet de mesurer l'évolution de la fermeté de tomates cueillies à un moment donné et stockées en chambre froide;
- L'intérêt majeur du test provient du fait que les mesures qu'il fournit sont corrélées avec celles issues des méthodes de référence habituellement utilisées sans être destructives.

# APPAREIL DE MESURE DE LA RESISTANCE AU CASSAGE DE SCIONS D'ARBRES

J. LICHOU, A. AUDUBERT, M. EDIN
Ctifl
Centre de Balandran
B.P. 32
30127 BELLEGARDE
France

J.M. BROQUAIRE
SICA CENTREX
66440 TORREILLES
France

Le Ctifl et la SICA Centrex ont réalisé un prototype d'appareil destiné à mesurer la résistance à la rupture du point de greffe d'arbres fruitiers en vue d'avoir une appréciation précoce du niveau de compatibilité.

L'appareil permet de mesurer la force nécessaire au cassage avec une jauge de contrainte à lecture digitale. Un réglet permet de lire la longueur du déplacement pour fournir une information sur la flexibilité de l'union.

Des mesures seront effectuées en 1994 pour valider les données recueillies avec les notations réalisées sur vergers.

Cet appareil devrait pouvoir être utilisé pour des mesures de solidité et de fléxibilité du bois d'autres espèces d'arbres.

Selon la fiabilité des résultats et l'intérêt manifesté par les utilisateurs potentiels, une motorisation et une mémorisation automatique des données pourront être envisagées.

# The Sporangium as a Biomechanical Device.

**Philip M. Lintilhac**
**The University of Vermont**
**Burlington VT, 05405,USA.**

A central problem in plant developmental biology involves the differentiation of reproductive tissues. In contrast to animal development where the sexually competent germ line is differentiated and set aside early in embryology, in plants the sexual cells are produced from undifferentiated somatic cells which are genetically and phenotypically indistinguishable from any other undifferentiated cell. This means that genetic programming cannot be invoked as a first cause of reproductive differentiation. What biological mechanisms qualify as triggers of reproductive differentiation in plants?

In this paper I put forward the hypothesis that the sporangium, in all of its varied forms, is a stress mechanical device whose function is to shape and direct the mechanical forces produced by cell and organ growth, and that the differentiation of reproductive tissues is triggered by the unique stress mechanical conditions found at its center.

The multicellular sporangium is an ubiquitous plant structure. It is the characteristic reproductive structure for all plants from the bryophytes to the flowering plants where we find that the sporangium manifests itself in the integumented structure of the nucellus, which is the megasporangium, and in the anther sac which is the microsporangium.

Reproductive differentiation and development is initiated at a very early stage within the immature sporangium. In many cases a single cell is selected within a mass of identical cells. This means that some effector of great precision is able to reliably identify a single cell within a clonal mass and transmit a triggering signal to it alone.

Physically the sporangium is a container, usually roughly spherical or club-shaped, supported on a stalk of some sort. It usually comprises 1 or more concentric layers of cells which make up the sporangial wall, and an internal space or loculus within which differentiate reproductive structures such as spores, sperm cells, egg cells, or multicellular reproductive structures such as pollen grains, or the embryo sac. (Sinnott, 1960)

Developmental events within the sporangium lead inevitably to the production of reproductive cells, either by specialized mitoses as in the case of gametogenesis in the ferns, or more commonly by meioses which lead to the production of micro- and mega-spores in the higher plants. In the flowering plants meiosis within the mega- and micro-sporangia (the nucellus and the anther sac respectively) leads to the production of the embryo-sac and egg apparatus on the one hand and pollen grains on the other. These represent the full expression of the female and male gametophytes and result in the production of the egg and sperm cells respectively.

Traditional explanations for the differentiation of the reproductive cells invoke the establishment of steep chemical gradients which select centrally located cells for differentiation. However, the extreme precision necessary to locate single cells, and the temperature sensitivity of diffusion-based systems argue against gradient triggering mechanisms.

An alternative mechanism which relies only on the shape of the sporangium, and on locked-in stresses accumulated from cell enlargement growth, would seem to provide the necessary spatial precision, and freedom from environmental interference.

According to this hypothesis the outer layers of the sporangium accumulate compressive growth stresses due to successive anticlinal divisions and lateral expansion of the cells, however the free standing nature of the sporangium necessitates that it satisfies the conditions of an equilibrium structure, and that the circumferential compressive stresses present in the sporangial wall are balanced by tensile stresses distributed across the interior of the sporangium. (Lintilhac 1984)

In this way a cell or group of cells located at the center of the sporangium can be subject to unique mechanical conditions simply by virtue of their location and the build up of nat-

ural growth stresses within the structure. This would provide a temperature-independent, gradient free, and potentially high precision mechanism for the initial induction of reproductive differentiation.

The conditions which must be met for this mechanism to work are as follows: First, the sporangial head must be free-standing at the time of triggering, so that stresses generated in the sporangial wall equilibrate within the sporangium itself rather than being dissipated into surrounding structures which are touching it. Second, the mechanical coupling of the sporangial wall cells to the interior of the sporangium must be sufficient to effectively transmit tensile stresses to the cells at the center of the sporangium. Third, the constraints upon the shape of the sporangium are such that it must be roughly spherical or club shaped/cylindrical at the time of sporocyte differentiation so that the tensile forces secondarily induced in the central sporogenous region can be adequately focussed.

Evidence to support this hypothesis is at present restricted to a search for counter-examples reported in the literature. A survey of embryological and reproductive literature reveals no examples of cells of the outer sporangial wall differentiating into sporogenous cells. Secondly, in every case where the earliest stages of reproductive differentiation are adequately illustrated, it can be seen that the immature sporangium, however rudimentary, is a convex structure untouched by overlying tissues. Thirdly, sporangia are always club-shaped or nearly spherical during the initial stages of reproductive differentiation, and thus fulfill the requirements for a free-standing structure capable of focussing isotropic stresses on a central group of cells.

This interpretation of the sporangium as a stress-mechanical device solves the problem of reproductive differentiation in plants, and at the same time provides an unifying hypothesis which explains the homologies between sporangial structures from throughout the plant kingdom.

Examples of stress-mechanical controls during plant development are increasingly evident in the literature (Romberger, Hejnowicz, Hill 1993), (Lyndon 1990). What I propose here is that mechanical inputs into the developmental process offer the advantages of spatial precision and instantaneous action, and capitalize on the extensive apoplastic coupling of somatic cells. In this way mechanical effectors can meet the demands of developmental signalling in situations where hormonal signals cannot.

## LITERATURE CITED

Lintilhac, P. M. 1984. Positional controls in meristem development: A caveat and an alternative. In Positional controls in plant development, Eds P. W. Barlow and D. J. Carr, 83-105. Cambridge University Press.

Lyndon, R. F. 1990. Plant development: The cellular basis. London: Unwin Hyman.

Romberger, J. A., Z. Hejnowicz, and J. F. Hill. 1993. Plant structure: Function and development. Springer-Verlag.

Sinnott, Edmund W. 1960. Plant Morphogenesis. New York: McGraw-Hill.

# Continuous bending moment measurements from gravitropically responding roots.

**Philip M. Lintilhac, Sari Galanes and John Outwater**
**The University of Vermont,**
**Burlington, VT 05405 USA**

Gravitropically stimulated corn roots growing in a humid environment respond to their horizontal orientation by growing downward. We have developed an experimental system for following the response by continuously monitoring the self-generated bending moments.

New instrumentation makes it possible to measure growth parameters previously inaccessible to measurement.

We place the roots between two horizontal teflon surfaces which act to restrain downward bending. The forces generated in the vertical direction are measured continuously with a Vitrodyne V-200 mechanical testing frame, acting in displacement controlled mode to prevent bending of the root. The self-generated load is measured as a restoring force necessary to maintain constant displacement between the two teflon surfaces as the bending root tries to force them apart.

Initial characterization of the system shows a pH dependence of the response, as well as a characteristic lengthening of the presentation time under high Calcium conditions, and a depression of the bending moment output when the roots are flooded with $10^{-3}$ M EGTA. Decapping also eliminates all bending force production by the root.

Other measurements made possible by this system include axial growth rate measurements under continuous controlled tip load, indicating the sensitivity of overall root growth rates to tip impedance.

These measurements may afford a more realistic means of following the gravitropic bending response since they more accurately mimic the conditions existing in soil where the root is acting against a resistance (Goss, Russell 1980), (Goss 1977), (Feldman 1984). Using these methods we hope to build a more realistic biomechanical model of root performance.

## LITERATURE CITED

Feldman, Lewis J. 1984. Regulation of root development. Ann. Rev. Plant Physiol. 35:223-42.

Goss, M. J. 1977. Effects of mechanical impedance on root growth in barley. Jnl. Exp. Bot. 28:96-111.

Goss, M. J., and R. Scott Russell. 1980. Effects of mechanical impedance on root growth in barley, (Hordeum vulgare L.). Jnl. Exp. Bot. 31:577-88.

# Changes in wall architecture during plant cell growth and differentiation

Maureen C. McCann and Keith Roberts

Department of Cell Biology, John Innes Institute, Colney Lane, Norwich NR4 7UH, UK.

The macroscopic properties of fruits, vegetables, cereal crops, and plant-derived materials of industrial importance such as wood, paper and cotton, derive from the properties of plant cells and their surrounding walls (1). The biomechanical properties of each tissue within a plant are functions of the tissue anatomy (that is, cell shape, size, and packing), the adhesion between neighbouring cells, and the thickness and material composition of the cell walls. Cell walls form an apoplastic continuum in which the cells are compartmentalised constraining cell size and shape. Cell-cell adhesion depends upon the architecture of the regions of interface between walls from neighbouring cells, the middle lamella and cell corners. For example, mesophyll cells have reduced cell-cell adhesion to generate air-spaces. Even very minor changes in sugar composition, such as the absence of fucose, can have profound consequences for the tensile strength of cell walls (2). However, very little is known about the basic architecture of cell walls, and the changes in that architecture that occur during growth and differentiation, features that underpin the mechanical and rheological properties of whole tissues and plants (3, 4).

Our use of many methodologies has demonstrated that the apoplastic continuum is a mosaic of different architectures with major architectural differences between species, between tissues, and between domains within a single wall. In addition to conventional electron microscopy techniques, sugar analysis, FT-Raman spectroscopy and NMR spectroscopy, we have applied several novel methodologies which are suitable for analysis at the single cell wall level, including cryopreservation techniques for electron microscopy (5), the generation of probes to particular cell wall epitopes (6), and Fourier Transform Infrared microspectroscopy (7). The fast-freeze, deep-etch, rotary-shadowed replica technique allows us to visualise cell wall architecture at high resolution, as close to the in vivo state as possible, and with preservation of the three-dimensional spatial relationships of polymers. Images obtained by this method allowed us to propose a model of cell wall architecture for one chemically simple system, onion parenchyma cells (4), based on two inter-penetrating and coextensive networks, a load-bearing cellulose/xyloglucan network and a pectic network that, whilst not load-bearing, may nevertheless control the access and activity of enzymes that act on the cellulose/xyloglucan network by limiting wall porosity. Fourier Transform Infrared (FTIR) microspectroscopy permits us to detect the presence of some specific chemical bonds within the wall, and, in combination with polarisers, to detect their orientation. FTIR spectra constitute species-specific and tissue-specific fingerprints of cell walls, reflecting even subtle differences in composition. By generating a large spectral database, we hope eventually to use statistical analysis packages to correlate specific spectral features with particular cell wall properties such as tensile strength, and to establish predictive models.

Bearing in mind the spatial diversity of architectures, which may then confer differential mechanical properties on different organs of the plant, and within those organs on different parts of the wall, we have chosen to look at changes in wall architecture in suspension-cultured cells, since these are relatively homogeneous and easily manipulated in culture. We have mapped changes in composition and architecture of matrix polymers in carrot (8) and tobacco (9) suspension cultures during cell elongation, and Zinnia mesophyll cells during differentiation to tracheary elements at the single cell wall level. We observe changes in both the cellulose/xyloglucan network and the pectic network. In elongating cells, orientation of matrix polymers in addition to cellulose microfibrils

transverse to the long axis of the cell occurs. The original pectic network may be replaced by a more highly esterified network with altered rheological properties. Some constraints operate; wall thickness and microfibril spacing are maintained. In differentiating cells, new varieties of cell wall polymer are produced in a developmentally-regulated manner. Our observations lead us to propose some tentative models for the molecular rearrangements that occur within these walls during growth and differentiation. The biomechanical properties of plant tissues will depend on both the geography and history of the component cells and their walls.

1. McCann, M.C. and Roberts, K. (1993) Plant cell walls: murals and mosaics. Agro-Industry Hi-Tech, in press.
2. Reiter, W.D., Chapple, C.C.S., Somerville, C.R. (1993). Altered growth and cell-walls in a fucose-deficient mutant of Arabidopsis. Science 261, 1032-1035.
3. Carpita, N.C. and Gibeaut, D.M. (1993) Structural models of primary cell walls in flowering plants: consistency of molecular structure with the physical properties of the walls during growth. The Plant Journal 3, 1-30.
4. McCann, M.C. and Roberts, K. (1991) Architecture of the primary cell wall. In The Cytoskeletal basis of plant growth and form (ed. C.W. Lloyd), pp 109-129. Academic Press, London.
5. McCann, M.C., Wells, B. and Roberts, K. (1990) Direct visualisation of cross-links in the primary plant cell wall. J. Cell Sci. 96, 323-334.
6. McCann, M.C., Wells, B. and Roberts, K. (1992) Complexity in the spatial localisation and length distribution of plant cell-wall matrix polysaccharides. J. Microscopy 166, 123-136.
7. McCann, M.C., Hammouri, M.K., Wilson, R.H., Belton, P.S. and Roberts, K. (1992) Fourier Transform Infra-Red microspectroscopy is a new way to look at plant cell walls. Plant Physiology 100, 1940-1947.
8. McCann, M.C., Stacey, N.J., Wilson, R.H. and Roberts, K. (1993) Orientation of macromolecules in the walls of elongating carrot cells. J. Cell Sci. 106, 1347-1356.
9. McCann, M.C., Shi, J., Roberts, K. and Carpita, N.C. (1994) Changes in pectin structure and localisation during the growth of unadapted and NaCl-adapted tobacco cells. The Plant Journal, in press.

## Cellular basis of tissue strength in carrots

**A McGarry**
**Horticulture Research International**
**Wellesbourne**
**Warwick CV35 9EF**
**UK**

Carrots (*Daucus carota*) are subject to two major forms of damage, splitting (longitudinal cracking) and (transverse) breakage. Whilst breakage is largely a man-made problem caused by deficiencies in handling procedures, splitting can occur without human intervention. It must, therefore, be a consequence of carrot growth and development.

Some earlier work at HRI demonstrated that carrots split by cell wall breakage, even when cell packing appears to be structurally unsound. For instance, in the cultivar Tamino groups of cells are aligned with their walls in the same longitudinal plane. Despite this fracture is intracellular. As a result, the toughness of carrot tissue must be largely determined by cell wall strength.

Whilst splitting has been the subject of several empirical studies, the literature contains few clues to the causes of splitting or the basis of tissue strength in carrots. However, since variety trials indicate that certain cultivars consistently produce large numbers of split roots there would appear to be a genetic influence. Work on other horticultural products has shown that susceptibility to damage increases with turgor pressure. For these reasons work at Wellesbourne has concentrated on examining the cellular basis of tissue strength in carrots as affected by water status, genotype and agronomy.

Recent work has shown that,

(i) the fracture toughness (as measured using a crack-opening test) of phloem parenchyma tissue is negatively correlated with turgor,

(ii) tissue strength (as measured using a tensile test) is virtually independent of turgor but related to tissue apoplast volume (a measure of cell wall volume fraction),

(iii) carrot tissue is notch-sensitive. The introduction of a notch weakens a test piece out of proportion with the amount of material removed by notching. As turgor increases, carrot tissue becomes more notch-sensitive as the notch tip becomes more defined and more effective as a stress concentrator,

(iv) altering the timing of irrigation (but not the total amount) can produce carrots with different mechanical properties. Heavy irrigation during the period 56 - 90 d after drilling not only produces a large number of growth split roots (*ca.* 20%), but tougher tissue. This increase in toughness cannot be fully explained by differences in root water status.

## Problèmes mécaniques inhérents au mouvement révolutif d'exploration des tiges volubiles

**B. Millet, B. Bonnet et P.M. Badot**
Laboratoire de Sciences végétales, Université de Franche-Comté, Place Leclerc, 25030 Besançon Cedex (France)

Les plantes grimpantes sont connues pour leur aptitude à enrouler leur tige autour d'un tuteur (ex. : le haricot à rame) et à s'élever ainsi à plusieurs mètres au-dessus du sol. Ce mouvement d'enroulement est précédé pàr un mouvement d'un autre type le mouvement révolutif d'exploration au cours duquel l'extrémité de la tige décrit plusieurs cercles avant de rencontrer un support.

Les observations effectuées sur un nombre imposant d'espèces, ont conduit à dégager quelques règles concernant les caractéristiques du mouvement révolutif d'exploration : l'extrémité des tiges volubiles manifeste une courbure allant jusqu'à 90 degrés avec la partie proximale, le sens du mouvement est fixé génétiquement (la tige du Houblon tourne dans le sens des aiguilles d'une montre, celle du Haricot en sens inverse), la trajectoire est inclinée par rapport à l'horizontale, le mouvement est associé à l'élongation de la tige.

Des mesures à intervalles de temps rapprochés (5 ou 10 minutes) pendant plusieurs heures permettent de reconstituer la trajectoire décrite par l'extrémité de la tige au cours de sa croissance (fig. 1), de calculer la période du mouvement, son amplitude, sa vitesse et de suivre les variations de la hauteur du bourgeon terminal au cours d'une révolution (fig. 2).

Les éléments d'information rassemblés sont utiles pour tenter de construire une hypothèse explicative. Le fait que la durée de la période soit dépendante de la température, par exemple, est à prendre en considération. Concernant la mécanique du mouvement elle-même, trois questions se posent :

1/ Pourquoi la période du mouvement est-elle plus courte lorsque la portion libre de la tige est immobilisée à 20 cm du sommet que lorsqu'elle est longue de 10 cm ?

2/ La base de la tige peut être considérée comme étant fixe. Si on assimile la tige à un cylindre allongé de faible diamètre immobilisé par sa base, la partie apicale ne peut tourner que si des déformations apparaissent au niveau de la zone courbée. Comment expliquer mécaniquement la rotation de la tige sans torsion ? Au cours d'une révolution en effet, la même cellule se dilate et se contracte alternativement sous l'influence des variations de pression de turgescence dont elle est l'objet. Le phénomène se répète pendant le temps durant lequel cette cellule se trouve dans la zone de courbure, c'est-à-dire pendant une dizaine de révolutions

3/ Le mouvement révolutif d'une tige ne peut pas être assimilé à un mouvement circulaire uniforme car la vitesse de déplacement passe par un maximum et un minimum au cours d'une révolution. C'est lorsque la tige est sur le point de culminer que sa vitesse est la plus grande et lorsqu'elle se trouve à sa position la plus basse que la vitesse est la plus lente.

Les problèmes mécaniques se compliquent lorsqu'on s'adresse aux vrilles ou au mouvement d'enroulement des tiges autour du tuteur. Quoi qu'il en soit, les réponses apportées à ces questions par les mécaniciens seront intéressantes à prendre en considération pour comprendre les processus physiologiques à l'échelle cellulaire.

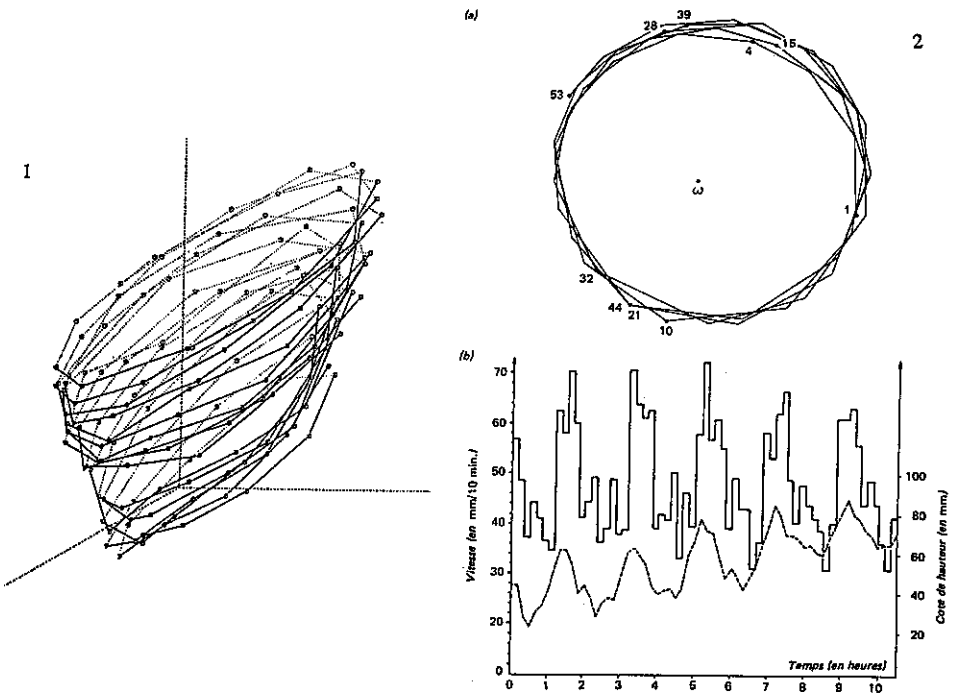


Fig. 1. Extrémité d'une tige de Haricot grimpant. 1. Partie linéaire horizontale. 2. Zone de courbure. 3. Partie linéaire verticale.

Fig. 2. Mouvement révolutif de la tige de Haricot. a) Projection sur un plan horizontal de la trajectoire décrite par l'extrémité d'une tige de Haricot. Le point ω correspond à la projection sur le plan du point d'immobilisation de la tige. Les nombres de 1 à 53 permettent de suivre la trajectoire. Les points successifs sont portés toutes les 10 min. b) En pointillés, les variations au cours du temps de la distance de l'extrémité de la tige par rapport au plan horizontal passant par le point d'immobilisation (cote de hauteur). En trait plein, les variations correspondantes de la vitesse de déplacement de l'apex, exprimées en mm/10 min (Millet et coll., 1984).

## Biomechanics and the evolution of plant form

Volker Mosbrugger, Tübingen

Due to numerous morphological studies of fossil and Recent plants, the evolution of plant forms from unicellular to multicellular algae and finally to the various land plants is relatively well knwon. With respect to growth forms and structure, all algae remain comparatively simple whereas land plants developed a variety of highly complex plant forms. The earliest land plants from the Upper Silurian to Early Devonian (about 420 to 380 million years ago) consist either of simple flat-lying leaf-like structures or of dichotomously branched and naked upright axes (Fig. 1). At least the larger upright axes of more than a few millimeters in height have a cuticle, stomata and a central protostelar vascular bundle. From these simple early land plants more complex plant forms evolved: branching patterns became increasingly irregular and the vascular bundles more complex (Fig. 2); cambial growth and leaves with successively more intricate venation patterns developed. By the Carboniferous (about 350 to 300 Million years ago), land plants attained the basic structural complexity and life forms of modern land plants such as herbs, shrubs, trees, and lianas.

Four stages in the evolution of plant forms are analyzed using a biomechanical approach (including fluid dynamics): 1. evolution of morphologically complex algae; 2. evolution of growth forms and branching patterns in early land plants (cf. Fig. 1); 3. evolution of complex stelar types (cf. Fig. 2); 4. evolution of leaves and leaf venation patterns. The analysis of these examples indicates that size is the crucial driving force of the evolutionary sequence. For land plants an increase in size may be advantageous for various reasons (i.e. competition and light interception, reproduction, dispersal, etc.). It, however, also entails a number of difficulties because the surface to volume ratio (and hence photosynthesis and transpiration), stability and transport requirements for water and nutrients are size dependent. The evolution of more complex plant forms can therefore be understood in terms of an optimization process in which plants tend to develop an "optimum compromise" in which stability, a high photosynthetic surface and an internal water balance is maintained despite an increase in size.

At least parts of the morphological and anatomical changes of this evolutionary sequence resemble a self-organization process governed by the size increase. This is particularly evident in the evolution of the vascular system of shoot axes. For instance, FE-simulations of the water transport efficiency of various primitive bundle types indicate that an increasing axis diameter requires a more peripheral arrangement of the vascular system thus also leading to a higher second moment of area of the xylem. Obviously, this marks the beginning of a functional shift in in the evolution of the xylem: although the vascular system evolved as a water transport device, it then became a compromise structure providing water transport and bending stiffness.

All the examples discussed illustrate that plant biomechanics is essential if a causal understanding of plant evolution is to be achieved.

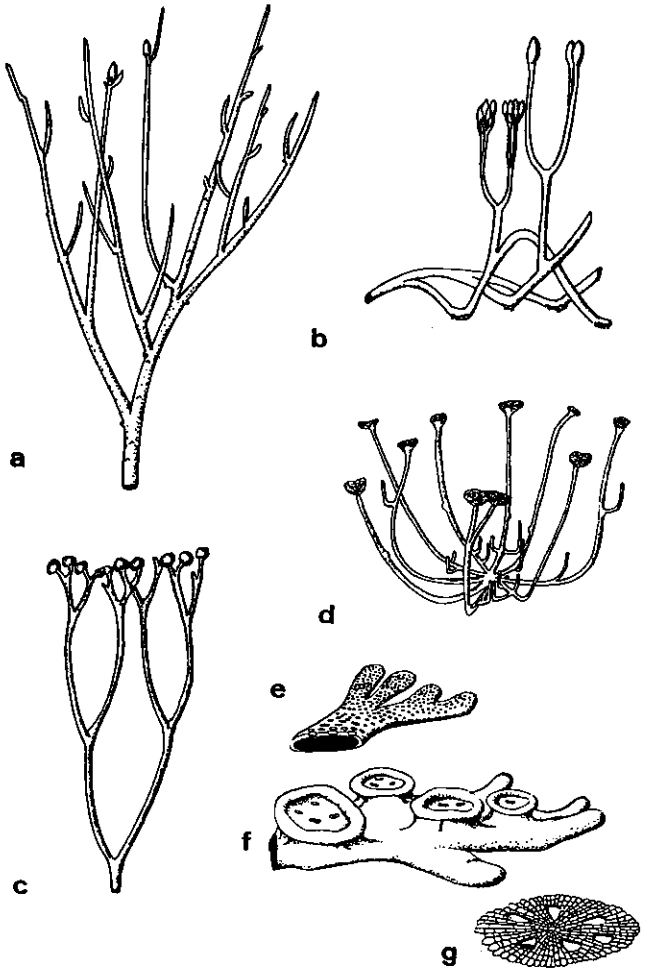


Fig. 1: Growth habits of some early land plants (adapted from various authors). a. Rhynia b. Aglaophyton c. Cooksonia d. Sciadophyton e. Spongiophyton f. Protosalvinia g. Parka

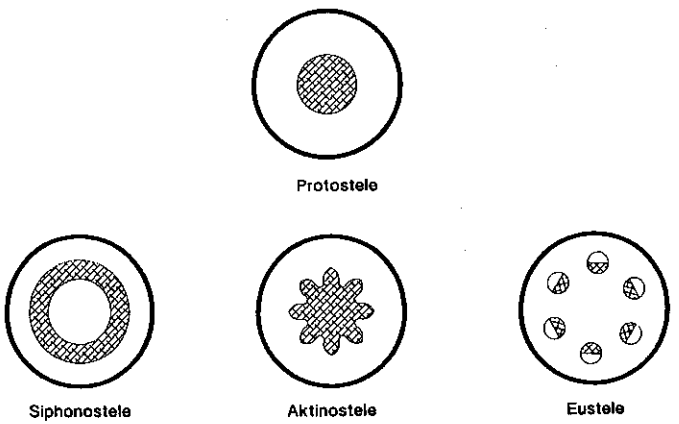


Fig. 2: Some basic stele types realized in tracheophytes

# The effect of gibberellin on weeping of growing branches of the Japanese cherry, *Prunus spachiana*

Teruko Nakamura[1], Maki Saotome[1], Tamiko Yamazaki[1], Kei'ichi Baba[2], Takao Itoh[2] and Toshitaka Yokoyama[3]

[1] Laboratory of Plant Physiology, Faculty of Science, Japan Women's University, Bunkyo–ku, Tokyo 112, Japan

[2] Wood Research Institute , Kyoto University, Uji, Kyoto 611, Japan

[3] Tama Forest Science Garden, Forestry and Forest Products Research Institute, Hachioji–shi, Tokyo 193, Japan

There have been very few studies of the weeping of growing shoots in woody plants. So, we have investigated the weeping using current–year branches of grafts of the Japanese cherry, a weeping type of *Prunus spachiana* and obtained the following results. 1, Current–year branches first elongate upward then gradually bend to elongate downward. The weeping growth may not be differential growth. 2, Gibberellin ($GA_3$) applied to apical buds 4 times weekly promoted the upward elongation of the branches and inhibited their bending. Namely $GA_3$ changed the orientation of branches during their growth. 3, The results on xylem thickening, vessel density and cellulose microfibril angle may suggest that the tension wood appears to be formed at the basal part of the branches treated with $GA_3$. In control branches, no tension wood was formed. 4, $GA_4$ did not show any effect on the orientation of the branches. 5, The similar effects of $GA_3$ were obtained using *Prunus persica* of

weeping type. 6, These results suggest that the weeping habit may be caused by the lack of mechanical rigidity due to the failure of a hormonal–control system relating to gibberellin.


Photographs showing the effects of $GA_3$ and $GA_4$ in the current year branch of *Prunus spachiana* of weeping type (1–4) and the branch of upright type (5) which is shown to be compaired with the result shown in weeping type.

GA treatment was done 4 times every week. Photograph was taken 7 days after the last treatment.

1: Control, 2: 10 µg/plant $GA_3$, 3: 10 µg/plant $GA_4$, 4: 100 µg/plant $GA_4$,

Arrow: vertical direction, Bar: 50 mm

# Internal stresses due to growth and differentiation in Norway Spruce - measurements and results

Magnus Nilsson, Department of Structural Engineering,
Lund University, P.O. Box 118, S-221 00 Lund, Sweden

## Introduction

In a research project, established in 1993, the presence, distribution and extent of the internal stresses in Swedish softwood are to be determined. A rather comprehensive programme will be carried out, including measurements of internal strains, variation of the modulus of elasticity in green timber and different parameters significant influence on the internal stresses. To achieve this, methods for measuring the internal strains in longitudinal, radial and tangential directions are developed. The first face of the investigation deals with the internal stresses in full grown Norway spruce (*Picea Abeis*) from different types of site quality.

## Method

Based on methods presented by Jacobs (Bulletin Commonwealth Forestry Bureau, 1945) and Post et. al. (Wood Science and Technology 14, 1980), a method is developed to measure the internal strains in logs. In longitudinal direction the distance between well-defined points is measured, with a resolution of 10 µm, before and after cutting the log in strips with a cross-section of 50x50 $mm^2$ and a length of 1000 mm. The cutting is done using a frame saw, thereby achieving a fast processing in order to maintain the green condition. The MOE is determined immediately after cutting, using a simplified bending test, which is related to more careful investigations done in the laboratory. In tangential and radial direction are the internal strains measured in the same manner, but here using smaller strips of 50x50x30 $mm^3$.

## Measurements

In three different sites, located within the same area, with site quality varying from poor to fairly good, sample areas of about 2.500 $m^2$ are selected. The history of the sites is quite known. In these areas are height, diameter breast height and type of crown determined for each tree, as well as their position. The trees are classified, and 13 trees are selected from each site representing different quality classes. After felling, these trees are investigated more carefully, parameters like type of bark, distribution and form of knots and occurrence of defects are determined.

The marking of cross-cutting is done so that three logs, each of a length of three meter, are cut from root-, middle- and top-log. In these logs internal strain and MOE in compression respectively tension are determined in longitudinal, radial and tangential direction. Measurements are also done in order to determine quite a few wood properties, i.e. density, moisture content, magnitude of growth rings, length and width of fibres and micro-fibril angle.

Logs not used in the determination of parameters described above, are processed to sawn timber and kiln dried using common techniques. The timber that is produced from these logs is stress graded and classified according to Swedish standards, and the defects are measured.

The expected results from the investigation, can be related to three levels. The influence on the presence, distribution and extent of the internal stresses related to the site quality, the type of tree in a site and finally within the tree itself are to be determined. By searching correlation between parameters describing the site, the tree respectively the wood and the internal stresses, the influence of such parameters on the internal stresses can be determined.

# Biomechanical Control of Elongation Growth by Phytohormones and Osmotic Stress

**Hisashi Okamoto and Akane Okamoto**

Graduate School of Integrated Science, Yokohama City University
22-2, Seto, Kanazawa-ku, Yokohama, 236 Japan

Elongation growth of plant cell or stem in a steady state can be described by the Lockhart's simultaneous equations:

$$v = ( 1/V) ( dV / dt) = \Phi ( P - Y ) \quad (1)$$

$$v = ( 1/V) ( dV / dt) = L ( \Delta\pi - P ) \quad (2)$$

Eq. (1) is the mechanical equation of empirical nature representing the cell wall yielding, where $V$ is the volume, $\Phi$ is the extensibility of the cell wall, $P$ is the turgor and $Y$ is the yield threshold of the wall. Eq. (2) is the (irreversible) thermodynamic equation of water uptake, where $L$ is the relative hydraulic conductivity of the plasmalemma and $\Delta\pi$ is the osmotic pressure difference across cell membrane.

From the biomechanical point of view, it is quite pertinent for the understanding of the mechanism of growth control to analyze the effects of phytohormones or osmotic stress on the elongation growth in terms of the changes in the biophysical parameters involved in both equations, although it is not easy to determine all of them simultaneously. Since the work done by Green and Cummins (1974), Cleland (1977) and Cosgrove (1985), it has generally been believed that auxin (IAA) increase $\Phi$ to elevate v, but has no effect on $Y$. It is well established that $P$ is kept constant during growth promotion by IAA (Nakahori et al. 1991).

However, by means of the pressure jump methods, both positive (Okamoto et al. 1989) and negative (Okamoto et al. 1990), in combination with the continuous pressure probe measurement (Nakahori et al. 1991), it has been discovered that *Y in vivo* is decreased largely by the action of IAA (by 40-100 kPa), or more with the adaptation to osmotic stress.

It is quite clear now why the regulatory change in $Y$ in higher plants due to hormonal action had not been discovered until rapid pressure jump method was invented recently. Applying a small jump in xylem pressure (10 kPa x 2 min), turgor $P$ lifts up by $\Delta P$ owing to the increase of water influx. According to the eq. (1), the steady growth rate will increase from $v_1$ to $v_2$.

Thus we can estimate wall extensibility and effective turgor as follows:

$$\Phi = ( v_2 - v_1 ) / \Delta P, \qquad P - Y = v_1 / \Phi$$

The classic methods, osmotic equilibrium (Green & Cummis 1974, Cleland 1977) or stress relaxation (Cosgrove 1985), used too big changes in turgor (more than 50-100 kPa) and /or required too long time (1-3 h) to obtain a single $Y$ value. Regulatory mechanism to keep the growth rate constant was activated under such circumstances and Y had been decreased by and by to a minimum value, say 0.3 MPa (Cosgrove 1985) or so, until the determination was over.

In order to investigate whether the yield threshold still exists in an *in vitro* system, we prepared glycerinated hollow cylinder (GHC) from cowpea hypocotyl. An extensometer has been developed to enable perfusion of experimental solution through the hollow and infusion of the solution into the tissue without abrasion of the cuticle layer on the organ surface. Stress-strain experiments clearly showed the existence of the pH-dependent yield threshold ($y$) in this *in vitro* system too. Acidification of the perfusion solution, from pH 6.2 to pH 4.0, caused the reversible decrease of $y$ by 55 g/ GHC, which coincides with the decrease of $Y$ *in vivo* by ca.

70 kPa (56 g/segment) due to IAA action (Fig. 1 (a)). These results strongly support the " acid growth theory" since it has already been established in cowpea that the proton pumps are activated by IAA *in vivo* prior to growth promotion (reviewed in Katou & Okamoto 1992), and the apoplast in the elongation zone of intact hypocotyl is acidified to pH 4 under natural condition (Katou & Okamoto 1970).

Heat treatment of the GHC completely inhibits the decrease of $y$ with acidification (Fig. 1 (b)). Increase of $\phi$ (*in vitro*) by acidification is not completely inhibited until being treated with a higher temperature. These discoveries suggest the participation of certain functional proteins (enzymes?) that reduces the activation energy of net splitting of weak bonds between cellulose microfiblils and hemicellulose bridges (corresponding to $y$), and that of sliding of the hemicellulose tethers along cellulose microfiblils (corresponding to $\phi$).

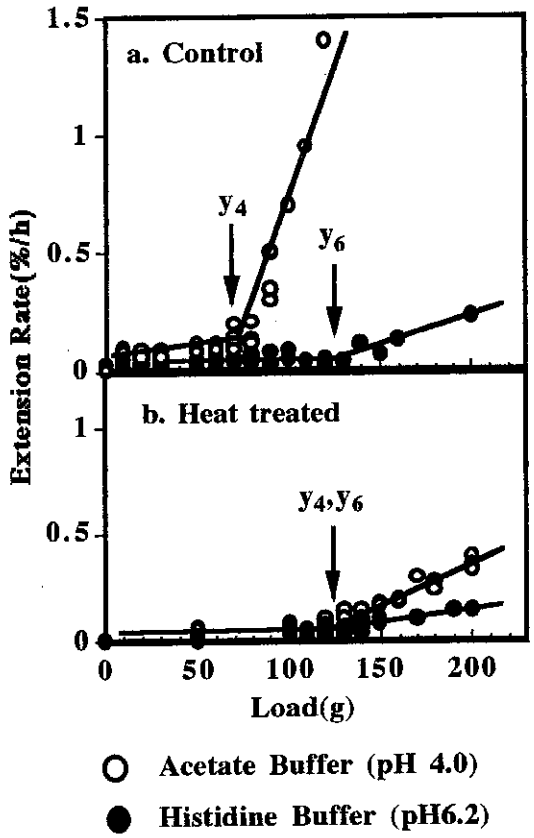


**Fig. 1**

**The results of the stress-strain experiments *in vitro***

The stress-strain relationship can be exactly simulated by Lockhart mechanical equation with pH-dependent yield threshold (y).

The glycerinated hollow cylinders, 15 mm in length, were prepared from cowpea hypocotyl segements excised from the elongation zone. They were stocked in 50 % glycerol aqeuous solution for 3 weeks under -15°C. The extension rates were determined under various tensions during 10 - 30 min after changing the load. The reaction pH was controlled by perfusion of buffer solution of the 10 mM acetate(pH 4) or 10 mM histidine (pH 6) through the hollow. The heat treatment was 90°C x 1 min in 50 % glycerol solution.

**References**

Katou, K. & Okamoto, H. (1992) Intern. Rev. Cytol. 142 (263-304).
Nakahori, K. et al. (1991) Plant Cell Physiol. 32 (121-129).
Okamoto, H. et al. (1990) ibid. 31 (783-788).
Okamoto, H. et al. (1989) ibid. 30 (979-985).
Cosgrove, D. (1985) Plant Physiol. 78 (347-356).
Cleland, R. (1977) Symp. Soc. Exp. Biol. 31 (101-115).
Green, P. B. & Cummins, W. R. (1974) Plant Physiol. 54 (863-869).
Katou, K. & Okamoto, H. (1970) Plant Cell Physiol. 11 (385-402).

# How to determine the Biomechanical Growth Parameters *in vivo* and *in vitro*?------A Theoretical and Technical note.

**Akane Okamoto, Kiyoshi Katou* and Hisashi Okamoto**

Graduate School of Integrated Science, Yokohama City University
22-2, Seto, Kanazawa-ku, Yokohama, 236 Japan and *Graduate School of Human and Information Science, Nagoya University, Furo-cho 1, Chikusa-ku, Nagoya, 460-01 Japan

## I. Lockhart's Simultaneous Growth Equations and Katou's Diagram

The steady growth rate of plant cell or organ is described by Lockhart simultaneous equations:

$$v = ( 1/V) ( dV / dt) = \Phi ( P - Y ) \quad (1)$$
$$v = ( 1/V) ( dV / dt) = L ( \Delta\pi - P ) \quad (2)$$

v, relative growth rate; V, the volume; $\Phi$, the wall extensibility ; P, intracellular hydrostatic pressure; Y, yield threshold; L, relative hydraulic conductance; $\Delta\pi$, osmotic pressure differennce across membrane. Eq(1) is a mechanical equation of the cell wall yielding and Eq. (2) is the thermodynamic equation of water uptake. Both process must occur simultaneously.

In this equation, P seems to play a contradictory role: it behaves as if it were a promoter of growth in Eq. (1) since it is a driving force of cell wall yielding, and as if it were an inhibitor of growth in Eq. (2) since it is an opponent against water uptake.

This contradiction was theoretically solved by Katou (1986) as illustrated in Fig. 1. We call the crossing point of the two lines which represent Eq. (1) and (2) " operational point" of the growth mechanism whose position is determined by two parameters (P, v).

## II. Determination of the Cell Wall Extensibility ($\Phi$) and the Yield Threshold of Cell Wall (Y) *in vivo* by pressure Jump Methods.

As shown by a bold triangle in Fig. 1, we can lift up turgor by $\Delta P$ by applying a jump in the xylem pressure ($P^X$) of a stem segment by means of the xylem perfusion system (Okamoto et al. 1989), since water influx from the xylem vessel is enhanced. After about 30 s, the transient elastic extension is relaxed. The steady growth rate increases from $v_1$ to $v_2$. Then we can determine the wall extensibility as follows:

$$\Phi = ( v_2 - v_1 ) / \Delta P$$

Simultaneously, we can determine the effective turgor:

$$P - Y = v_1 / \Phi$$

An example of the positive pressure jump is shown in Fig. 2.

In order to determine more precisely the yield threshold Y, negative pressure jump method was devised (Okamoto et al. 1990) in combination with the determination of P by a pressure probe (Nakahori et al. 1991). Instead of a positive pressure, short pulses (2 min) of negative pressure are applied to the xylem vessel until the growth is halted. A typical example is shown

in Fig. 3, where the $P^x$ axis can be converted to P axis irrelevantly whether IAA is perfused or not, scince it was proved that IAA does not change P during growth promotion (Nakahori et al. 1991). IAA definitely decreases Y by 80 kPa and accelarates elongation of cowpea hypocotyl segment ( Fig. 3 and Nakahori et al. 1991).

## III. Detemination of the wall extensibility (Φ) and the Yield Threshold Tension (y) *in vitro*: Glycerinated Hollow Cylinder System

Glycerinated hollow cylinders are prepared by boring the elongation region of cowpea hypocotyl with a stainless steel cylinders of sharp edge. They are immersed in 50 % glycerol aqueous solution at -15 C for 2-3 weeks. Abrasion of the cuticle layer on the epidermal surface is not necessary since any experimental solution can be perfused through the hollow in an extensometer of novel design. The stress-strain experiment is reported in another paper (p. -p. ) and elsewhere (Okamoto & Okamoto 1994).

**Fig. 1**

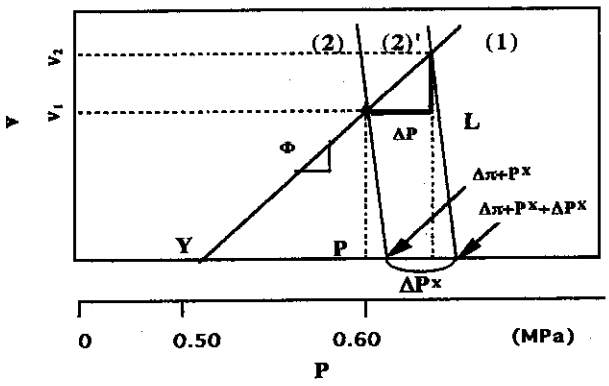


**Fig. 2**

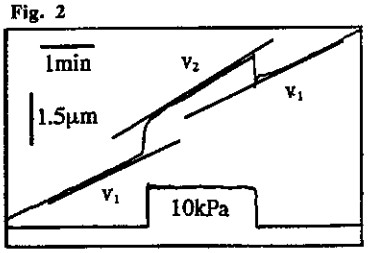


**Fig. 3** 930611

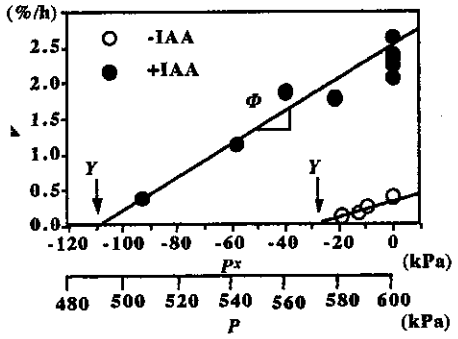


**References**
Katou, K. & Furumoto, H.(1986) Protoplasma 133, (174-185)
Nakahori, K., Katou, K., & Okamoto, H. (1991) Plant Cell Physiol. 32 (121-129)
Okamoto, H., Liu, Q., Nakahori, K. and Katou, K.(1989) ibid. 30 (979-985)
Okamoto, H., Miwa, C., Masuda, T., Nakahori, K. & Katou, K. (1990) ibid. 31 (783-788)
Okamoto, H. & Okamoto, A.(1994) Plant Cell Environ. (in Press)

## A Physical Behavior of Tree During Secondary Growth

– Diurnal change of tangential strain of sapling –

T.Okuyama, M.Yoshida, H.Yamamoto and T.Sakai
School of Agricultural Sciences
Nagoya University, Nagoya, 464–01 Japan

Diurnal change of inner bark strain which was induced by turgor pressure in the phloem was measured according to the strain gage method (Fig.1). Used materials were 3–year–age saplings of kuromatsu ( *Pinus thunbergii* Parl. ) and sugi ( *Cryptomeria japonica* D.Don ).

Strain gage printed on a plastic film with water proof cover was used with one active gage and three wires connection method. Arranging two or three measuring positions on the stem of each sapling, removing carefully the outer bark, strain gage with 4 mm in the length was pasted on the tangential direction of the surface of the inner bark. The strain gage was put over with vaseline and aluminum foil to protect from direct illumination and shrinkage. Strain change was also measured on the surface of an Invar rod to cancel the temperature drift of strain measurement devices. Strain output became stable within half hours after putting the strain gage and the strain drift by temperature was less than ±5μ strain / °C. Then the total measuring error during the experiment was estimated less than ±20μ strain including divers factors after the correction of temperature effect.

Measurement was carried out in the following three conditions.

1. In a room condition without any climate controls.
2. In a phytotron with natural sunlight, constant conditions at the temperature of 25°C and 60% of humidity.
3. In a growth cabinet at the temperature of 20°C, 90% of humidity and light control.

The results are as follows.

1. Strain change in the tangential direction of phloem is about ten times as large as that of xylem. Then the strain change comes from the change of turgor pressure in the phloem cells.
2. The minimum tangential strain, the maximum shrinkage, appears at about 14 o'clock in the natural climate condition, the strain increases (expands) gradually from afternoon to night, then reaches the maximum value at just before daybreak. The decrease in the strain (shrinkage) occurs sensitive to the light illumination. However the rate of decrease in the strain is faster than the increase after putting out the illumination, then a clear hysteresis can be seen in the periodic change of strain.

The strain change shows cyclic ups and downs corresponding to the sunlight period. It follows faithfully to the various lightening periods even under the light controlling condition (Fig.2).

3. A phase difference could not be observed between tangential strains in the various height in a sapling. This result predicts that the water in the phloem cells comes from the xylem according to the pressure difference between xylem and phloem cells.
4. The minimum strain during lighting period recovers rapidly to the maximum strain soon after the topping. The strain recovery according to topping shows faster movement than that at putting out the light (Fig.3,4).
5. The maximum shrinkage is in proportion to the logarithm of intensity of illumination. The amount of turgor pressure estimated from the change of the tangential strain was 10–50 KPa.

The tangential strain on the surface of inner bark gives a diametral change induced by turgor pressure change with enough accuracy. This method can be used for discussion on the role of water stress in the secondary growth of tree.

Fig.1 Scheme of strain measurement

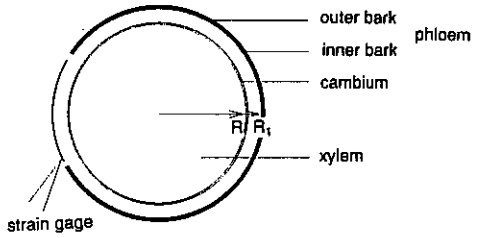


$P = \varepsilon_T E_T ( R_1/R - 1 )$

P: Internal pressure

$\varepsilon_T$: Tangential strain

$E_T$: Young's modulus in T-direction of phloem

Fig.2 The course of the strain of a sapling

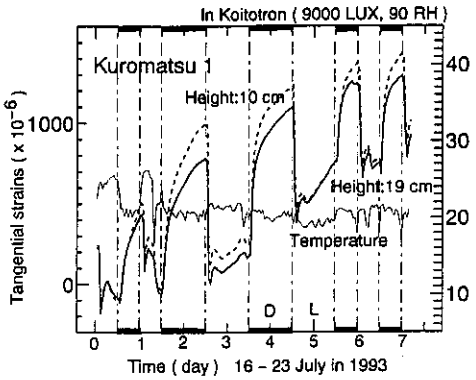


D: darkening period, L: lightening period

Fig.3 The effect of topping on the strain

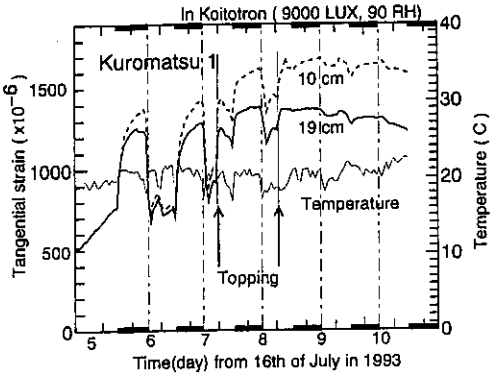


Fig.4 Course of strain after three kinds of treatment

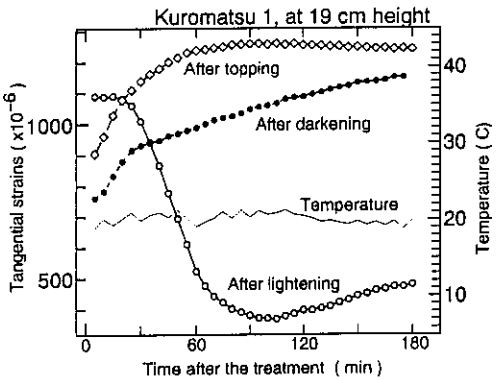


Lightening: 17:00, July 20,
Darkening: 17:00, July 21,
Topping: 10:00, July 23 in 1993.

# Plant and Fungal Cell Growth: Governing Equations for Cell Wall Extension and Water Transport

**Joseph K. E. Ortega**

Professor of Mechanical Engineering and
Director of the Bioengineering Laboratory
Department of Mechanical Engineering
University of Colorado at Denver
Campus Box 112, P.O. Box 173364
Denver, Colorado 80217-3364, USA

## Summary

Plant and fungal cell growth (enlargement) is a result of many complex biochemical and metabolic events in combination with physical processes. During the past decade, progress has been made in the development of "governing equations" that describe the relevant physical processes in terms of biophysical and biomechanical parameters. The magnitude and behavior of these parameters are controlled by biochemical and metabolic events.

Historically, governing equations play a key role in the evolution of a science from a descriptive, or qualitative, state to a quantitative state. It is well known that governing equations are fundamental to the physical sciences. For example, the field of electricity and magnetism would be severely diminished without Maxwell's Equations, and the fields of fluid mechanics and convective heat transfer would be reduced to an empirical science without Navier-Stokes Equations. Physical scientists and engineers have come to rely on the use of governing equations to determine the magnitude and behavior of a "parameter of interest" when several other parameters change simultaneously.

This communication will review recent progress made toward the goal of establishing governing equations for the two interrelated and simultaneous physical processes that are involved in plant and fungal cell growth; the rate of cell wall extension and the net rate of water uptake. The Augmented Growth Equations (1, 2, 3, 4; see References) provide the foundation for governing equations. The first Augmented Growth Equation describes the rate of cell wall extension and may be formulated to account for both irreversible (plastic) and reversible (elastic) extension. This equation relates the relative rate of change in volume of the cell wall chamber, $v_c$, to the sum of the relative rate of irreversible (plastic) extension and the relative rate of reversible (elastic) extension (1, 2, 3, 4):

[1] $$v_c = (dV_c/dt)/V_c = \phi (P - Y) + (dP/dt)/\varepsilon ,$$

where $V_c$ is the volume of the cell wall chamber, $t$ is the time, $\phi$ is the relative irreversible wall extensibility, $P$ is the turgor pressure (the pressure difference between the cell interior and the external medium), $Y$ is the yield threshold (a magnitude of turgor pressure which must be exceeded before plastic wall extension occurs) and $\varepsilon$ is the volumetric elastic modulus. The term, $\phi (P - Y)$, represents the relative rate of plastic, or permanent, wall extension. The term, $(dP/dt)/\varepsilon$, represents the relative rate of elastic wall extension.

The second Augmented Growth Equation is a mathematical statement describing the net rate of water uptake, and may be obtained from the well-established physical principle, the conservation of water mass (2, 3, 4):

[2] $$v_w = (dV_w/dt)/V_w = L(\sigma\Delta\pi - P) - T ,$$

where $v_w$ is the relative rate of change in volume of the cell contents (mostly water), $V_w$ is the volume of the cell contents, $L$ is the relative hydraulic conductance of the cell membrane, $\sigma$ is the solute reflection coefficient of the cell membrane, $\Delta\pi$ is the difference in osmotic pressure between the cell sap and the external medium, and $T$ is the relative transpiration rate. The term, $L(\sigma\Delta\pi - P)$, represents the rate of water uptake, and the term, $T$, represents the relative rate at which water is lost from the cell by transpiration. This term, $T$, is zero for cells that are not exposed to the external environment, and thus do not transpire. It should be noted that the volume of the cell contents must equal to the volume of the cell wall chamber, $V_w = V_c$, and that the respective relative rates of change in volume must also be equal, $v_w = v_c$.

Importantly these Augmented Growth Equations, equations 1 and 2, have demonstrated utility in understanding and predicting the growth rate behavior and water transport behavior of higher and lower plant cells, and fungal cells. Furthermore, these equations have proven useful in determining the magnitude and behavior of the inclusive parameters.

Because the turgor pressure, $P$, is a biophysical parameter that is present in three of the four terms of the Augmented Growth Equations, the pressure probe (which directly measures the turgor pressure of single cells) has proven to be an important tool in determining the magnitude and behavior of the biophysical and biomechanical parameters in equations 1 and 2. It is important to note that governing equations for nearly all pressure probe methods can be obtained directly from the Augmented Growth Equations in their present form or by examining them in limiting cases.

In this communication, recent pressure probe methods (and the associated governing equations) that have been developed to determine the magnitude and behavior of relevant biophysical and biomechanical parameters are reviewed, discussed, and evaluated. Some of the pressure probe methods reviewed are: (a) *in vivo* creep and *in vivo* stress relaxation methods to determine the relative irreversible wall extensibility, $\phi$, and the yield threshold, $Y$, of growing cells; (b) pressure pulse-up method to determine the volumetric elastic modulus, $\varepsilon$, of non-growing cells; (c) pressure clamp and pressure relaxation methods to determine the cell membrane hydraulic conductivity, $L_p$; and (d) pressure clamp and pressure relaxation methods to determine the relative transpiration rate, $T$, of single cells. Also discussed are some new pressure probe methods currently being developed in our laboratory, but not yet published: (e) pressure pulse-up method to determine the volumetric elastic modulus, $\varepsilon$, of growing single plant and fungal cells; (f) *in vivo* pressure relaxation - transpiration method to determine the average volumetric elastic modulus, $\varepsilon$, of the cells in plant tissue.

## References

1. Ortega, J.K.E. (1985) Augmented growth equation for cell wall expansion. *Plant Physiol.* **79**: 318-320.

2. Ortega, J.K.E. (1990) Governing equations for plant cell growth. *Physiol. Plant.* **79**: 116-121.

3. Ortega, J.K.E. (1993) Pressure probe methods to measure transpiration in single cells. *In:* Water deficits: Plant responses from cell to community (eds. J.A.C. Smith & H. Griffiths). BIOS Scientific Publishers Limited, Oxford, UK: 73-86.

4. Ortega, J.K.E., Keanini, R.G. and Manica, K.J. (1988) Pressure probe technique to study transpiration in *Phycomyces* sporangiophores. *Plant Physiol.* **87**: 11-14.

# ESTIMATION OF GENE ACTION GOVERNING THE MORPHOLOGICAL ATTRIBUTES IN *Eucalyptus* SPECIES

M.PARAMATHMA and C.SURENDRAN
Forest College and Research Institute
Tamil Nadu Agricultural University
Mettupalayam - 641 301
INDIA

## SUMMARY

Six species of *Eucalyptus* viz., *E. alba* Reomw-ex., B., *E. camaldulensis* Dehnh., *E. microtheca*, E.Muell, *E. tereticornis* Sm., *E. polycarpa* F. Muell and *E. torelliana* F. Muell., were subjected to a complete diallel mating. The experiment was carried out at the Forest College and Research Institute, Mettupalayam (11°19'N, 76°56' E, 300m a msl., Rainfall 830 mm; pH 7.1) during 1989-92. The direct as well as reciprocal crosses involving the two species viz., *E. polycarpa* and *E. torelliana* between themselves or with other species failed to set seeds. An evaluation of the other four parents and 12 hybrids for nature of gene action governing the morphological attributes indicated that characters like height, collar diameter, leaf number and leaf breadth were found to

be free from non-allelic interaction. For characters like internode length, leaf length, suitability index and volume index, non-allelic interaction was observed.

For the characters viz., leaf length and leaf breadth, where predominance of additive genes was observed, recurrent selection may be the appropriate strategy for accumulating favourable genes. The magnitude of dominant genes was high for most of the other characters investigated indicating the promise of heterosis breeding for these traits.

Symmetrical distribution of positive and negative genes was inferred. The gene distribution among the parents was observed to be unequal with greater frequencies of dominant alleles for most characters. Considering economic attributes, the number of genes that control the characters was one for collar diameter and leaf length, two for height, internode lendth and volume index and three for suitability index and leaf breadth. In general, the narrow sense heritability was high for growth attributes like height and collar diameter.

# Effects of gravity and microgravity on root growth and statocyte polarity

**Gérald PERBAL and Dominique DRISS-ECOLE**

Laboratoire CEMV, Bât. N2, case courrier 150, Université Pierre et Marie Curie, 4 place Jussieu, F - 75252 Paris Cedex 05

Gravitropism, growth of plant organs either towards (roots) or away from gravity (shoots) has been intensively studied in the last decade.

When a root is subjected to a change in orientation in the gravitational field, its extremity bends in order to reorient itself with respect to gravity. The signal of curvature comes from the cap (which is located in the root tip) and is transmitted to the zone of curvature. Bending occurs because of a differential growth in the upper and lower halves of the roots. It is due to an increase of cell growth in the upper part of the distal meristem and a decrease of cell growth in the lower part of the proximal region of the cell elongation zone.

The perception of gravity takes place in special cells (statocytes) which contain voluminous amyloplastes (statoliths). It is generally accepted that these amyloplasts play the role of gravisensors. Their density is greater than that of the surrounding cytoplasm and these organelles therefore sediment in the statocytes. These cells show a strict polarity: their nucleus is attached to the plasma membrane and in contact with it at the proximal cell pole, whereas the endoplasmic reticulum is located along the distal wall beneath the amyloplasts.

In microgravity (in space) this polarity is changed: the nucleus is slightly displaced and separated from the plasma membrane. The endoplasmic reticulum expands toward the cell center. The amyloplasts are not distributed at random but the majority of these organelles is mainly situated near the nucleus at the proximal pole of the cell. It has been proven that actin filaments attach the nucleus to the cell periphery since cytochalasin B (which perturbs the polymerisation of actin) provokes the sedimentation of the nucleus in the statocytes of roots grown on the ground.

The actin network is thus subjected to tensions on the ground and relaxed in microgravity. Both configurations of cytoskeleton could lead to different physiological activities of the statocytes.

On the ground, when a root is subjected for several hours to a gravistimulus, its extremity bends but it never overshoots the direction of gravity. On the contrary, when a root is stimulated for 1h on a centrifuge in space and placed in microgravity, its extremity overshoots the direction of the acceleration which is responsible for the bending of the root. Gravitropic reaction is thus regulated by gravity.

Space research represent a unique opportunity to understand better the action of gravity on plants.

# WOOD MOISTURE CONTENT MEASUREMENT BY X-RAY EXPOSURE METHOD

Patrick PERRE De-Ku SHANG
ENGREF/14, rue GIRARDET, F-54042 NANCY CEDEX, FRANCE

## ABSTRACT

Although quite a number of papers can be found up to now in dealing with the subject of the measurement of wood density by using the X-ray exposure methods, direct scanning or radiographic photography, the following two aspects, which are very important from both theoretical and engineering application points of view, have not yet been properly handled. One is that the elementary analyses or the experimental measurement on the mass attenuation coefficients were not specified in regard to spectrum energy distridutions [1]. In this connection, the ambiguities in the specification of the coefficients and in turn for the results among studies arise when only one of the two parameters, namely wave length and applied voltage, of defining the energy spectrum of X-ray is given. The other is that the relationships between the relative intensity and the sample thickness as well the wood moisture content [2], which are the critical factors for the design and the selection of X-ray apparatus, were not sufficiently examined. In addition, the knowledge of the measurement of wood moisture content by using the direct X-ray scanning method is also almost unavaible now.

In the study, the direct X-ray scanning method of measuring wood moisture content was at first investigated theoretically with respect to the relationship between the mass attenuation coefficients of wood (beech, *Fagus Sylvatica*) and the maximum spectrum energy of X-ray (Table 1). Secondly, the dependence of the relative intensity on the sample thickness and on the wood moisture content was analysed (Fig.1 and Fig.2). The main advantage of the method is on-site nondestructive measuring of wood moisture content in the processes such as drying, impregnation and unsteady mass diffusion. Specifically for the application in the area of biomechanics, the method can also be used for understanding the water pathway within wood, for example, the water around the knots and the relation between the stress distribution and the local moisture content of wood.

Key words: mass attenuation coefficient, maximum spectrum energy, moisture content, relative intensity, sample thickness, X-ray exposure

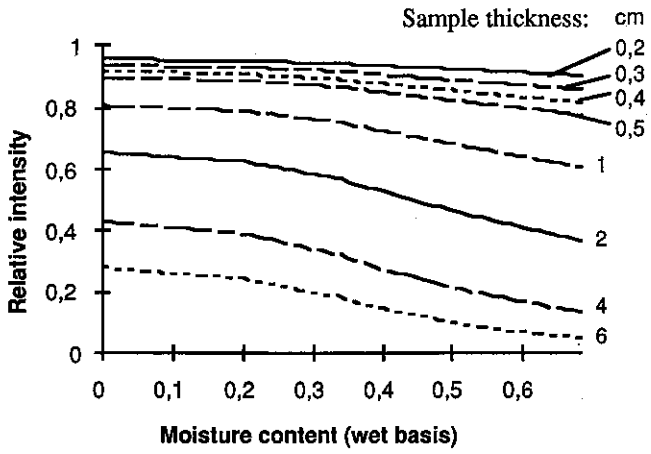


Fig.1 Relative intensity versus wood moisture content for different samples thickness at the maximum spectrum energy of X-ray for the applied voltage 50 kV

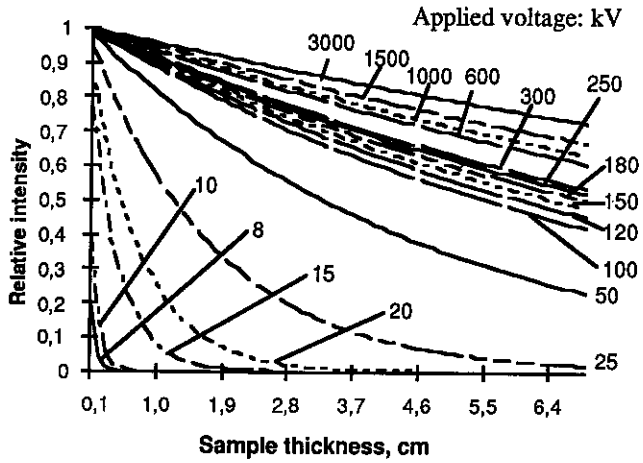


Fig.2 Relative intensity versus sample thickness of wood for different applied voltage at the maximum spectrum energy

Table 1 The mass attenuation coefficients of wood (beech) and water at the maximum spectrum energy of X-ray and the displacement

| $\lambda$(wave length, Å | $V$(applied voltage, kV | Photon energy, keV | $M_a$ (wood), cm²/g | $M_a$ ($H_2O$), cm²/g | $M_a$(wood)/ $M_a$($H_2O$), cm²/g | Displacement ($\lambda_{max} \cdot V$), Å·V |
|---|---|---|---|---|---|---|
| 9,870 | 2 | 1,22 | 1661,920 | 2255,770 | 73,67 | 19400 |
| 6,390 | 3 | 1,83 | 304,500 | 422,740 | 72,03 | 18060 |
| 3,930 | 5 | 3,04 | 119,710 | 167,850 | 71,32 | 18700 |
| 2,290 | 8 | 4,87 | 23,640 | 32,330 | 73,14 | 18560 |
| 1,930 | 10 | 6,08 | 14,070 | 19,330 | 72,78 | 19200 |
| 1,235 | 15 | 9,13 | 3,870 | 5,110 | 73,82 | 17850 |
| 1,000 | 20 | 12,17 | 2,100 | 2,830 | 74,21 | 18800 |
| 0,710 | 25 | 15,21 | 0,868 | 1,132 | 76,67 | 18500 |
| 0,417 | 50 | 30,42 | 0,317 | 0,374 | 84,68 | 19000 |
| 0,195 | 100 | 60,83 | 0,191 | 0,204 | 93,63 | 19500 |
| 0,161 | 120 | 73,00 | 0,174 | 0,187 | 93,15 | 19320 |
| 0,120 | 150 | 91,25 | 0,162 | 0,172 | 94,09 | 18150 |
| 0,098 | 180 | 109,50 | 0,151 | 0,159 | 95,01 | 18000 |
| 0,072 | 250 | 152,08 | 0,143 | 0,150 | 95,77 | 18000 |
| 0,064 | 300 | 182,50 | 0,137 | 0,143 | 95,86 | 19200 |
| 0,030 | 600 | 365,00 | 0,109 | 0,121 | 90,10 | 18000 |
| 0,024 | 1000 | 608,33 | 0,100 | 0,117 | 85,50 | 24000 |
| 0,010 | 1500 | 912,50 | 0,088 | 0,108 | 81,50 | 15000 |
| 0,005 | 3000 | 1825,00 | 0,070 | 0,099 | 70,70 | 15000 |

## REFERENCES

[1]. Weast, R.C. and Selby, S.M.(editors), 1968. Handbook of Chemistry And Physics, 48th Edition, The Chemical Rubber Co. Publisher, Ohio.

[2]. Olson, J.R., 1981. Prodiction of Mass Attenuation Coefficients of Wood, Wood Sciences, 14(2):86-90.

# BIOMECHANICS OF GRASSES

## - Functional-morphological studies using finite element method -

U. Philippi, A.B. Kesel, W. Nachtigall
Universität des Saarlandes, Fb 13.4 Zoologie, D-66041 Saarbrücken

Grasses are slim high constructions. Depending upon their surrounding environment, they must possess certain characteristics in order to withstand the pressures of selection. The self-supporting construction "grass" must take into account a variety of different pressures and combination of pressures according to the physical boundary conditions (environment) (e.g. Schwendener 1874). Disregarding the dynamic aspects for the time being, the bending stability leads to four biomechanic loading models:

MODEL I: No wind, loading along the blade axis results exclusively from the weight of the head (Fig. 1).

In nature, this type of loading is rarely found in a blade of grass. The head is usually eccentric.

MODEL II: No wind, loading due to the weight of head is eccentric (Fig. 2).

However, the two problems mentioned can be solved analytically only if the blade of grasses is taken to be constant or at least constant in sections. Furthermore, only concentrated single forces and not widespread attacking forces are assumed. This single force, the weight force of the head, may not exceed at certain critical value $F_c$ otherwise the blade will snap over.

Normally, the blade will not only be influenced by the weight of its head, but also by the wind load $F_W$.

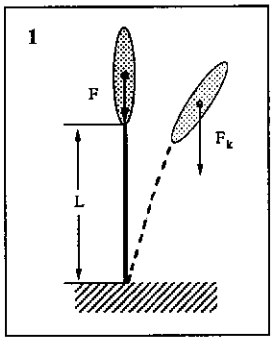


Fig 1: MODEL I

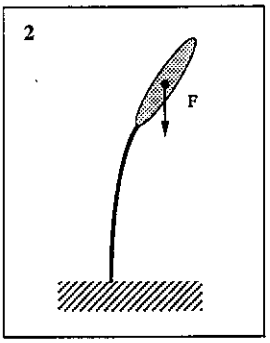


Fig 2: MODEL II

MODEL III: Blade under wind and head loading (Fig. 3).

Wheras the snaping force caused by the head froms the main loading component with a low wind force, the bending strain on the blade increases with increasing wind force. This bending strain is dependent directly upon the wind, since blade deformation is depend upon the attacking load.

MODEL IV: Blade under strong to maximal wind load (Fig. 4).

The greater the wind load, the more the blade will evade it. At maximum wind loading, the blade stalk is attacked mainly by tangential forces. Strong bending forces occur only at the base.

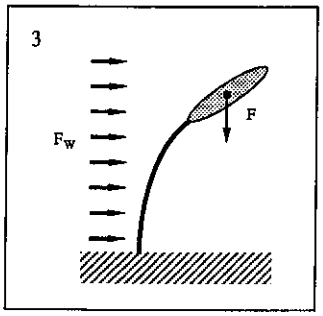


Fig 3: MODEL III

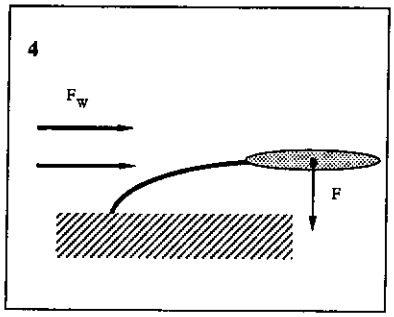


Fig 4: MODEL IV

Both these cases are non-lineare problems. If one wishes to avoid non-linear calculations, one must use iterative methods. Once adequate models have been built, the holding behavior of grasses under the types of loading described can be analysed using the Finite Element-Method (Niklas 1977). This method enables one to take into consideration the distribution and arrangement of tissues gained from histological and morphological studies.

Because of the biomechanical importance of the nodes (Niklas 1989, Gappoev 1991) the various distribution were taken into consideration when calculating MODEL III and leads in two construction typs: A) even distribution along the stem B) concetrates at the base of blade. The blades (L: 0.55 m) were fixed at the base and loaded with line load which is equvalent to a wind speed of 8 m $s^{-1}$.

The two construction types show little deviation with regard to their deflection in the x- or y-direction (3 % resp. 6 %). Due to the greater stiffness created by the distribution of nodes along the entire blade, the bending moments are increased approximately 3.5 times in this type of construction, and the axial forces and tensions are reduced by 50 % compared to type B. The latter does not appear to have any advantages despite its more complicated construction. First calculation on MODEL IV however suggest a greater degree of security.

From these analysis, one gains valuable indications of eventual restrictions or peculiarities regarding habitat, propagation etc of grasses which result from their construction.

References:

Gappoev M. 1991. Untersuchung zur Form und Faserstruktur von Gras- und Halmpflanzen unter Berücksichtigung der Kräfteverteilung in den Knoten. Mitteilungen des SFB 230, Heft 6, Stuttgart.

Niklas K.J. 1977. Applications of Finite Element Analyses to problems in plant morphology. Ann. Bot. 41: 133.

Niklas K.J. 1989. Nodal septa and the rigidity of aerial shoots of *Equisetum hyemale*. Amer. J. Bot. 76 (4): 521.

Schwendener S. 1874. Das mechanische Prinzip im anantomischen Bau der Monocotylen mit vergleichenden Ausblicken auf die übrigen Pflanzenklassen. Engelmann, Leipzig.

# THE BIOPHYSICS OF ROOT GROWTH

**Jeremy Pritchard and Deri Tomos**

*School of Biological Sciences, UCNW, Bangor, Gwynedd LL57 2UW, Wales, UK. Tel- (0248) 370731*

**Growth, turgor pressure and temperature**: Roots increase in length as a result of the expansion of single cells in the root apex. Changes in turgor pressure and\or the properties of the cell wall might be expected to affect cell expansion. This is described by the equation;

$$r = \phi (P - Y) \qquad \textit{equation 1}$$

where r = growth rate, P = turgor pressure. $\phi$ and Y are the wall extensibility and the yield threshold respectively and are physical properties of the cell wall. The relationship described in equation 1 can be demonstrated experimentally (Fig 1).

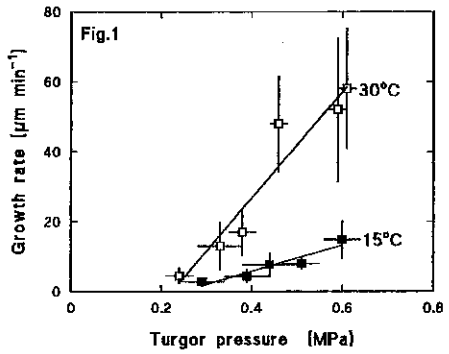


***Figure 1:*** *Turgor pressure of the growing zone vs growth rate of hydroponically grown maize roots. The reduced slope of the relationship at 15°C indicates a reduction in $\phi$.*

As turgor pressure of the growing zone, measured with the pressure probe (1), is lowered by incubation in different mannitol solutions, root extension rate is also reduced. In maize roots growth ceased at around 0.2 MPa at 30°C. This pressure is the yield threshold of equation 1. The slope of the line is the wall extensibility ($\phi$). In common with other organs, roots grow slower at lower temperatures. This reduction in growth is not due to a change in yield threshold or turgor pressure but is caused by a reduction in wall extensibility (Fig.1).

**Development, osmotic stress and cell wall properties:** The growing zone consists of columns of many expanding cells, which can respond in different ways during development and in response to changes in the environment. The growth rate along the root apex has a characteristic bell shaped distribution (Fig.2a).

This variation in growth must also be due to changes in cell wall properties since the turgor pressure (the driving force for expansion) along the same region is constant (Fig.2b).

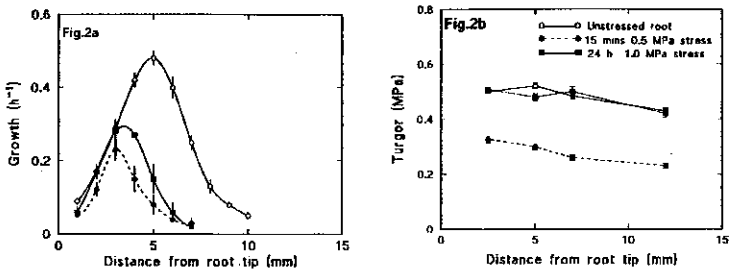


***Figure 2:*** *Profiles of growth rate (2a) and turgor pressure (2b) along the apical 12 mm of maize roots under different osmotic stresses. Changes in growth rate despite a relatively constant turgor indicates changes in cell wall properties.*

The relationship between turgor pressure, growth rate and wall properties is a dynamic one. If turgor pressure is reduced along the growing region, 15 minutes later growth rate is reduced in the region 7-10 mm but remains unchanged 0-3 mm from the root tip (Fig.2a). Since turgor pressure is reduced but growth rate remains unchanged the cell walls must have become looser. If roots experience a prolonged (24h) osmotic stress turgor pressure recovers along the whole growing zone. In contrast growth rate remains low in the proximal region but is the same as unstressed roots nearer the tip. Cell wall properties are therefore tighter in the proximal region but are unchanged in the root apex.

**Soil and root growth**: Roots grown in soil of high density have a reduced growth rate in comparison to those in loose soil. This reduction in growth is accompanied by a reduction in mature cell length. Evidence (obtained using tensiometric methods) suggests that this is due to a tightening of the cell wall (a decrease in $\phi$ or an increase in Y).

**Summary:** Thus root growth is the result of the interaction of turgor pressure and wall properties leading to alteration in growth rate by a variety of different environmental stresses. The changes in cell wall properties have their basis in changes in the cell wall biochemistry. It is becoming apparent that enzymes which catalyse the formation and breakage of cross linkages between wall components may be responsible for some of the effects mentioned above. These include wall peroxidases (2) and xyloglucan endotransglycosylase (3). Further characterisation of the effect of the environment on root cell biophysics and the correlation of this with changes in biochemistry will lead to a deeper understanding of growth processes in roots.

**References**

1) Hüsken D *et al* (1978) *Plant Physiol.* **61** 158-63.
2) Pritchard J & Tomos A D (1993). In "*Water deficits*" eds. JAC Smith & H Griffiths, Bios, Oxford pp.53-71.
3) Pritchard *et al* (1993) *J.Exp.Bot.* **44** 1281-1289.

**Underground Plant Movement by Contractile Roots. An Experimental Approach to the Functionality of Channel Formation**

N. Pütz, G. Hüning, Botanisches Institut der R.W.T.H. Aachen, D-52056 Aachen

Contractile roots develop a pulling force to overcome soil resistance (Pütz 1992). This pulling force produces underground movement of the plant body, e.g. a bulb, corm or rhizome. The distance moved by the plant is in most cases only a few centimetres (e.g. Nothoscordum inodorum, Alliaceae, Pütz 1993). However, some species show a movement of 20 cm and above in the course of a single vegetation period (Oxalis pes-caprae, Pütz 1994).

Plants are helped to move by the channel effect. The contractile root increases in diameter and forms a channel in the soil through which the plant body can move without soil resistance. The channel effect in contractile roots varies from species to species. A few species show no channel effect (e.g. Sauromatum guttatum, Pütz 1992), while others show a 100% channel (Oxalis pes-caprae, Pütz 1994, Triteleia hyacinthina, Pütz 1992). In most cases, the channel effect varies between 10 to 40% (Pütz 1992a).

Thus, energetically considered, there are two forces working together when a plant body moves in the soil:

(1) a **pulling force** for overcoming soil resistance
(2) a **pushing force** for displacing soil to form a channel.

Using a new modeling technique we were able to simulate the underground movement of a bulb. We measured the pulling force necessary to move different distances in relation to various channel effects. A second new method proved useful in calculating the pushing force necessary to form different soil channels.

Conclusions about the energetics involved can be drawn from comparing these different forces. It can generally be demonstrated that a channel effect favourably influences underground plant movement. However, differences in effect can be shown. A channel of 10 or 40% is optimal if the distance to be moved is relatively low (20-30 mm). However, the formation of a 100% channel effect seems to be advantageous if the distance traveled reaches 50 mm or higher.

These energetic conclusions correspond very closely to field observations. The channel effect in bulbous plants showing underground movement of 10-30 mm is normally small (Pütz

1992a). However, in every species where greater movement is found, a 100 % channel effect seems always present (Pütz 1992, 1994)

Literature:

PÜTZ, N., 1992: Measurement of the pulling force of a single contractile root. - Can. J. Bot. 70, 1433-1439.
- - 1992a: Das Verhältnis von Bewegung und Wurzelkraft bei Monokotylen. - Beitr. Biol. Pfl. 67, 173-191.
- - 1993: Underground plant movement. I. The bulb of Nothoscordum inodorum. - Bot. Acta 106, 338-343.
- - 1994: Underground Plant Movement. II. Vegetative Spreading of Oxalis pes-caprae.- Plant. Sys. Evol. (in press).

**Water transport in vessel elements with helical thickenings**

A. Roth

Institut und Museum für Geologie und Paläontologie

Sigwartstr. 10, D-72076 Tübingen, Germany

The water-conducting tissue of a vascular plant, the xylem, provides a low-resistance pathway for water transport. The high water permeability of the xylem is achieved by programmed cell death of its elements. Longitudinal water flow occurs in the resulting void spaces. Vessel elements show thickened and lignified cell walls which are required in order to withstand the mechanical forces due to the negative pressure gradient occurring during transpiration.

The structure of the inner sides of vessel elements is dependent on the development of the secondary wall. The first vessel elements to be differentiated show annular or helical arrangement of the secondary wall due to local deposition of wall material. These are followed by reticulate elements. Finally, vessel elements with pitted walls develop in the metaxylem. At this stage in the ontogenetic sequence, the secondary wall covers almost the entire area of the primary wall. Helical sculptures on the inner surface are, however, not only a feature of the protoxylem as spiral thickenings may also be present in elements of the secondary xylem. The frequency of their occurrence in secondary wood tends to be a function of climatic factors, as was reported by Baas & Schweingruber (1987). A satisfactory functional interpretation of helical thickenings in secondary wood is, however, still lacking (Baas 1986). As was shown experimentally by Jeje & Zimmermann (1979), certain geometric parameters of helical thickenings and their arrangement influence the friction drag acting on water as it passes through a vessel. Thus, the structure of helically sculptured inner surfaces of vessels contribute to the water transport properties of xylem. They speculated that the observed effects can be explained by a limited "slip flow" occurring between the rings.

In the present study, the water flow through vessels with various patterns of helical thickenings was investigated using a fluid mechanical approach suitable for simulating the flow in a single capillary with a sculptured inner surface. For this purpose, a commercial CFD (Computational Fluid Dynamics) - programme (FIDAP) based on the Navier-Stokes-equations which are solved using the Finite Element Method (FEM) was used. The programme readily allows for the construction of arbitrarily complex wall structures. This approach was successfully used by Schulte & Castle (1993), who investigated the hydrodynamic effect of scalariform perforation plates.

Examples of the results are shown in Figs. 1 and 2. Figure 1 represents the FE-grid of an axisymmetrical structure (longitudinal axis of rotation at the left) with a radius of 25 $\mu$m and with helical thickenings (width of rings: 23 $\mu$m, height of rings: 10 $\mu$m and distance between rings: 10 $\mu$m). The lumen of the vessel is divided by the FE-grid, whereas the helical thickenings are represented by the white rectangles. The pressure gradient occurring along the helical zone amounts to about 90% of the gradient which is present when the gaps between rings are completely filled with wall material. The pressure gradient can be increasingly reduced by changing such parameters as the distance between the rings as well as their width. As is shown by Fig. 2 (a magnification of a region between two adjacent

wall protrusions), the decreased pressure gradient is due to the presence of a "recirculation zone" between the rings. In this manner, a "limited" slip flow at the interhelical zones is generated.

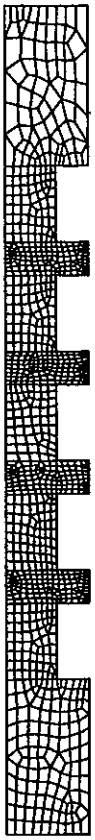

Figure 1: The FE-grid.

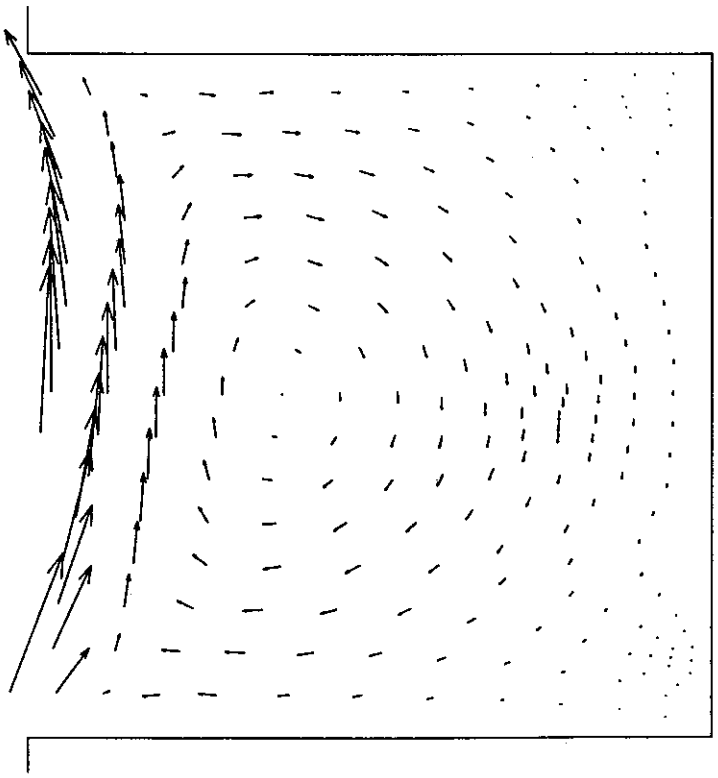

Figure 2: Fluid movement between two adjacent rings.

The results demonstrate the effects of internal sculpturing of vessels on water flow. It may be speculated that helical thickenings in vessels represent an interaction of mechanical and hydrodynamical requirements, thus reflecting an optimization process.

**References:**

Baas, P. 1986 Ecological patterns in xylem anatomy. In: On the economy of plant form and function. (ed.: T.J. Gvinish):327-352

Baas, P. & Schweingruber, F.H. 1987 Ecological trends in the wood anatomy of trees, shrubs and climbers from Europe. IAWA Bull. n.s. 8:245-274

Jeje, A.A. & Zimmermann, M.H. 1979 Resistance to water flow in xylem vessels. J. exp. Bot. 30(117):817-827

Schulte, P.J. & Castle, A.L. 1993 Water flow through vessel perforation plates - a fluid mechanical approach. J. Exp. Bot. 44(264):1135-1142

# Morphogénèse et fermeté de la pomme

A.-C. Roudot*, C.J. Studman**, F. Duprat***

* Ecole Supérieure de Microbiologie et Sécurité Alimentaire
Technopôle Brest-Iroise
29280 Plouzané

** Massey University
Department of Agricultural Engineering
Palmerston North
Nouvelle Zélande

***Institut National de la Recherche Agronomique
Laboratoire de Méthodes Physiques d'Etude
Domaine St Paul
BP 91
84143 Montfavet cedex

Lors des études expérimentales de la fermeté des pommes, on trouve une grande variabilité de ce paramètre, que les mesures soient faites sur la périphérie du fruit ou réparties sur une tranche (1). L'origine de cette hétérogénéité est encore peu claire, on invoque divers paramètres agronomiques, climatiques, ou autres, mais aucune certitude n'est acquise dans ce domaine à l'heure actuelle.

La simulation numérique est un moyen efficace de tester les divers paramètres supposés intervenir dans cette hétérogénéité. La méthode utilisée dans ce travail consiste à appliquer des procédés de simulation de croissance sur des modèles préalablement définis par modélisation histologique. Cette modélisation est une méthode de caractérisation physique des milieux cellulaires qui tient compte de l'hétérogénéité de distribution et de dimension des cellules au sein d'un tissu. Son intérêt majeur réside dans sa facilité à représenter des structures cellulaires complexes sans nécessité de simplification outrancière au niveau de la géométrie (2).

Dans cette simulation, le processus de croissance est essentiellement géométrique, seules quelques rares conditions mécaniques ont été utilisées. Le modèle présenté est bidimensionnel, les quelques différences apparaissant dans sa comparaison avec des essais tridimensionnels, ne justifiant pas les contraintes de temps de calcul et de taille mémoire nécessitées par un traitement 3D.

On suppose que dans un premier temps, la division cellulaire sera le phénomène prépondérant et que la croissance ne prendra toute son ampleur que dans un second temps après que les divisions soient achevées. Les cellules en croissance sont considérées comme des sphères en contact les unes avec les autres. La contrainte mécanique de chaque cellule (que nous assimilerons à sa fermeté) augmentera dans deux cas:

- lorsqu'elle entrera en contact avec une autre cellule voisine. Dans ce cas leurs contraintes mutuelles augmentera selon la loi de Hertz. Ceci peut se produire lorsqu'une cellule

voit son volume croître et nécessite un espace vital plus important qu'auparavant, et lorsque suite à une croissance, des cellules voisines sont obligées de se réarranger localement, et donc de se déplacer les unes par rapport aux autres, pour laisser un espace libre suffisant afin que la croissance s'effectue convenablement.

- du fait de la présence de la peau du fruit. Celle-ci exerce un effort qui s'oppose à la croissance globale de la pomme, et a donc pour effet de créer une pression externe qui est supposée d'autant plus forte que le fruit est gros.

La croissance est anisotrope du fait de la différence de rigidité mécanique entre l'axe principal du fruit et un rayon perpendiculaire. Cet effet est modélisé en renforçant la contrainte externe due à la peau lorsque l'on se rapproche de l'axe principal.

Les résultats des diverses simulations effectuées montrent que globalement le fruit a une forme proche de la réalité, mais surtout que les contraintes (ou les fermetés) peuvent varier dans une gamme allant du simple au triple. Globalement la fermeté maximale se situe dans la zone interne, elle diminue ensuite en s'éloignant du coeur du fruit pour augmenter légèrement au niveau de la peau. Enfin, ces simulations montrent une hétérogénéité de distribution des fermetés, certaines zones pouvant être plus fermes que d'autres bien que situées plus à l'extérieur du fruit. La totalité de ces observations effectuées en simulation correspond aux résultats obtenus lors de manipulations réelles.

Il semble donc qu'une part importante, voire largement prépondérante, de l'hétérogénéité de distribution de la fermeté dans la pomme soit liée au processus de croissance, et puisse être rattachée à des considérations géométriques de remplissage d'un volume par des sphères en croissance.

1- F. Duprat, F. Roudot, M. Grotte-Nicolas, A.-C. Roudot, 1991
De l'hétérogénéité des fruits
*Sciences des Aliments*, 11, 613-626

2- C. Wenian, F. Duprat, A.-C. Roudot, 1991
Evaluation de l'importance de la géométrie du tissu cellulaire dans les déformations observées sur les pommes après une compression ou un choc
*Sciences des Aliments*, 11, 105-116

# Fossil plants: biomechanics as an aid to interpreting growth form and habit

Nick P. Rowe[1] and Thomas Speck[2]

[1]Université de Montpellier II, Institut des Sciences de l'Evolution, Laboratoire de Paléobotanique et Evolution des Végétaux, F-34095 Montpellier, France.

[2]Botanischer Garten der Albert-Ludwigs-Universität, Schänzlestr. 1, D-79104 Freiburg, Germany.

Reconstructions of the size and growth form of fossil plants have important implications on the evolutionary processes and ecological mechanisms occurring in plant ecosystems. However, a major problem in determining the overall size, habit and ecology of extinct plants originates from the consistently disarticulated nature of the fossils.

Experimental findings of extant plants demonstrate that self-supporting and non-self-supporting plants (eg. lianas and semi-self-supporting plants) differ significantly in their bending mechanical properties such as Young's modulus and flexural stiffness and in the variation of these properties during ontogeny (Speck 1991). All tested extant self-supporting woody plants show an increase in Young's modulus during ontogeny. In all tested lianas the Young's modulus decreases during ontogeny to 15%-25% of the values found in the youngest ontogenetic stage. Changes in stem mechanics during ontogeny are correlated with shifts in anatomy and contributions of stem tissues towards the cross sectional area and axial second moment of area (Speck 1991, 1994).

In the two extant semi-self-supporting plants experimentally studied up to now, a more or less constant Young's modulus during all ontogenetic stages is found. These plants show neither a marked increase (self-supporting) nor decrease (non self-supporting) in the Young's modulus from young to older ontogenetic stages.

These differences observed in Young's modulus and flexural stiffness of living plants have been employed to distinguish self-supporting and non self-supporting habits among long extinct fossil plants. Different ontogenetic stages of anatomically preserved stems are arranged according to their ontogenetic sequence. For each level, the geometric distribution of tissues: pith, wood, sclerenchyma etc. is measured and installed into a model describing the distribution of tissue types for each stage. Analytically derived formulae describing the tissue distribution are used to determine the contribution of each tissue type to cross-sectional area and axial second moment of area of the stem. Each tissue type is correlated as closely as possible in terms of wall thickness, cell shape, ornamentation and pitting with extant plant tissues for which the Young's modulus has been experimentally determined. By considering the fossil plant stems as composite materials, the flexural stiffness and Young's modulus of the entire plant stem and the contribution of each stem tissue to flexural stiffness can be calculated. As in modern plants the variation of these parameters is assessed over differing ontogenetic stages and the habit of the fossil plant is inferred. Our studies focus on growth forms among early seed plants that showed

a rapid radiation and morphological differentiation during the Lower Carboniferous. Biomechanical analyses of *Calamopitys* and *Lyginopteris oldhamia* stems suggest that both were semi-self supporting (Speck & Vogellehner 1992, Rowe et al. 1993, Speck 1994). Semi-self-supporting plants may have either a scrambling growth mode or a habit as social plants living in dense stands, characterized by individuals providing mutual support from densely interacting fronds or branches. The mechanical parameters of semi-self-supporting early seed plants rely mostly on hypodermal support and not on secondary wood.

The mechanical parameters of these semi-self-supporting taxa are compared with results for *Pitus dayi* in which a hypoderm is not developed and in which a periderm is rapidly established. A rapid shift in mechanical support occurs from one dominated by support from the leaf traces, wood and parenchymatous cortex to one dominated by wood and periderm. The appearance of a truly self-supporting habit among seed plants and its significance in the evolution of plant communities is discussed with reference to recent biomechanical studies of Palaeozoic self-supporting and non-self-supporting seed plants and to late Devonian progymnosperms.

Rowe, N. P., Speck, T. & Galtier, J. (1993) Biomechanical analysis of a Palaeozoic gymnosperm stem. Proc. R. Soc. Lond. B, **352**: 19-28.

Speck, T. (1991) Changes of the bending mechanics of lianas and self-supporting taxa during ontogeny. Proc. II. Int. Symp. Sonderforschungsber. 230, part I. Mitt. SFB 230, **6**: 89-95.

Speck, T. (1994) A biomechanical method to distinguish between self-supporting and non self-supporting plants. Rev. Palaeobot. Palynol. (in press).

Speck, T. & Vogellehner, D. (1992) Fossile Bäume, Spreizklimmer und Lianen. Versuch einer biomechanischen Analyse der Stammstruktur. Cour. Forsch.-Inst. Senckenberg, **147**: 31-53.

# An ultrastructural study of the qualitative distribution of lignin in a developing internode of maïze

**Katia RUEL and Jean-Paul JOSELEAU**

***Centre de Recherches sur les Macromolécules Végétales (CERMAV-CNRS)***
***B.P. 53 X 38041 Grenoble-cedex, France.***

The description of the ultrastructural organization of polysaccharides and lignin in the plant cell wall is of great importance for the understanding of the role of these macromolecules in the cell wall cohesion. In particular, lignin distribution is of great importance in this domain.

In Gramineae, lignin has a great complexity because it is made of three different monomers which give rise to three types of lignin : p-Hydroxyphenyl (H), Guaiacyl (G) and Syringyl (S). The relative distribution of the three types of lignin has been determined in a developing internode of maïze by means of immunocytochemical markers. To that effect antibodies were prepared against the three types of lignin.

The results showed differences in the overall lignification of the different tissues and variations in the intensity of the labelling by the different markers as a function of maturation.

The most characteristic result was that all the different types of lignin seem to be evenly distributed throughout the secondary wall, without preferential localization of a given type.

Another interesting observation was the different reactivity of the middle lamella versus the secondary walls. This variation in reactivity may correspond to differences in the respective content of condensed lignin in these parts of the plant cell walls.

# STANDING TREE QUALITY ASSESSMENTS USING ULTRASOUND

J.L. Sandoz[1)], P. Lorin[2)]

Trees are organic vegetal materials forming an important link in the carbon turn-over cycle. In the forest, they are associated together in the eco-system. In the cities, they act singly in ecological and decorative functions.

Quality assessments of standing trees may be considered to have two separate targets: biological internal quality related to the wood degradability and elastic quality of the heartwood regarding the industrial valuation of the wood products.

Biological internal quality of standing trees can be non-destructively evaluated using ultrasound. The speed of a low frequency wave propagated on the radial axis of the tree is measured. Compared to a referential speed for each species, deviation of the speed is considered to be indicative of degraded wood. Diameter and seasoning effects must be taken into account for better accuracy of the diagnostics.

Elastic quality of the wood contained in the tree can be evaluated by ultrasound. In this application, speed of sound is measured on the longitudinal axis in the sapwood area. Dispersion of the results in terms of speed is the basic information allowing a first step in grading the internal wood material.

1) Professor J.L. Sandoz
EPFL-IBOIS, GCH2-Ecublens, CH-1015 Lausanne
Tel. (+41-21) 693 39 30, Fax (+41-21) 693 23 94

2) Ing. P. Lorin, scient. assistant
EPFL-IBOIS, GCH2-Ecublens, CH-1015 Lausanne
Tel. (+41-21) 693 39 30, Fax (+41-21) 693 23 94

# Contraintes de Croissance et Morphologie chez un clone de Peuplier (I214)

François SASSUS, Rémi THOMAS, Valérie GRZESKOWIAK,
Bernard CHANSON, Mériem FOURNIER, Bernard THIBAUT

Université Montpellier II - LMGC-Bois - CP081 - Place E. Bataillon, 34095 Montpellier Cedex 5 (FRANCE).
tél. (33) 6714 3431, 3483, 3433, 4739 - fax (33) 6754 4852

L'élaboration du champ de contraintes est influencé par des facteurs morphogénétiques :

1.l'inclinaison de l'arbre (Polge, Ferrand, Saurat&Guéneau, Nicholson),
2.le phénomène de réorientation (Fournier, a),
3.le phototropisme (Kubler),
4.le plan d'organisation de l'arbre (Chanson).

Le but de l'étude est d'approfondir les relations entre la morphologie de l'arbre et le champ de contraintes de croissance à l'intérieur.

Cinq peupliers, en âge d'exploitation, ont été choisi pour leurs particularités : un arbre de lisière, un arbre droit et incliné avec une fourche équilibré, un arbre courbe et incliné avec une fourche basse et importante, un arbre droit vertical et élancé, un arbre avec une courbure importante. Les arbres sont écorcés sur 6 m. Des mesures de déformations de maturation (Fournier, b) sont réalisées avec un capteur extensométrique après libération des contraintes (méthode du "trou unique"). Elles sont effectuées sur une couronnes de 8 points (fig 1) à des hauteurs à priori stratégiques (aux départs d'axes réorientés, aux points de courbure importante, etc.).

Nous avons ensuite abattu les arbres pour prélever des billons aux endroits des mesures. Le bois de tension est détecté sur les rondelles entières en utilisant un colorant macroscopique (chloro iodure de zinc), après avoir vérifier sa spécificité sur une "rondelle test".

On peut voir les résultats suivants sur les profils de déformations de maturation :

- l'arbre de lisière est "tiré" vers la lumière, les pics de tension se situent de manière inhabituelle sur la face inférieure de l'arbre (fig 2). Le phototropisme du Peuplier est marqué et influence la mise en place des contraintes de croissance ;
- l'importance de l'inclinaison, l'arbre vertical a un profil plat avec des valeurs faibles, alors que les arbres penchés ont un maximum fort sur la face supérieure (sauf arbre de lisière);
- la courbure est le siège de valeurs fortes (fig 3), les contraintes de croissance permettent à l'arbre de garder (au maximum) une direction de croissance verticale.

Grâce aux données récoltées, nous chercherons d'abord à estimer la mesure à partir de la coloration (en affectant un poids aux zones de fibres G). Ensuite à étudier la variation de la mesure sur de faibles écarts de hauteur. Et enfin, à réaliser les cartographies de bois de tension, qui nous permettront de relier l'apparition du bois de réaction au différents phénomènes morphogénétiques.

## Bibiographie

CHANSON B., 1992 - Hétérogénéités angulaires des déformations de maturation : interprétation basée sur le concept de plan d'organisation des arbres - Acta bot. Gallica, 1993, **140**(4), 395-401.

FERRAND J.C., 1981 - Recherches des solutions pratiques à apporter aux problèmes posés par les contraintes de croissance des arbres forestiers - Thèse INPL.

FOURNIER M.(a), 1989 - Déformations de Maturation, Contraintes "de Croissance" dans l'arbre sur pied, réorientation et stabilité des tiges - publication ASMA - LMGC bois, USTL, Montpellier.

FOURNIER M., 1991 - Mécanique de l'arbre sur pied : modélisation d'une structure en croissance soumise à des chargements permanents et évolutifs. 2.analyse tridimensionnelle des contraintes de maturation, cas du feuillu standard.

NICHOLSON J.E., HILLIS W.E., DITCHBURNE N. - 1975 -Some tree growth wood property relashionships of eucalyptus. Canadian journal of Forest Research **5**(3) 424-432;

POLGE H., 1981 - Influence of the thinning regime on growth stresses in beech. Annales des Sciences Forestières **38** (4) 407-423.

SAURAT J. & GUÉNEAU P., 1976 - Contraintes de croissance dans le Hêtre. Wood Science and Technology **10**(2) 111-123.

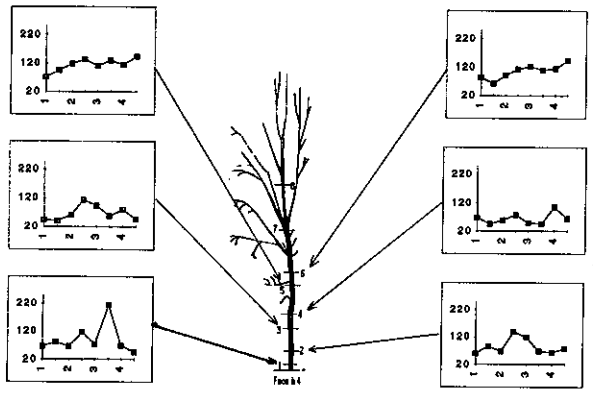

Figure 2

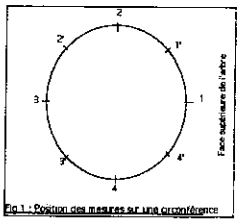

Fig 1 : Position des mesures sur une circonférence

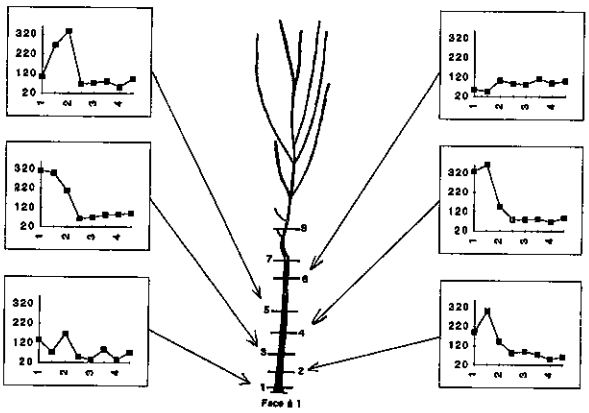

Figure 3

# Studies on the wood degrading basidiomycete *Inonotus hispidus*; an assessment of the different impact on the physical properties of partially decayed ash and London plane wood

F.W.M.R. Schwarze[1], D. Lonsdale[2], C. Mattheck[3] and S. Fink[1]

[1]Albert-Ludwigs-Universität Freiburg, Insitut für Forstbotanik und Baumphysiologie, Bertoldstr. 17, 79098 Freiburg i.Br., Germany. [2]Forest Authority Research Station, Alice Holt Lodge, Farnham, Wrecclesham, Surrey, GU10 4LH GB. [3]Institut für Materialforschung, Kernforschungszentrum Karlsruhe GmbH, Postfach 3640, 76021 Karlsruhe, Germany.

## Abstract

The wood degradation pattern of *Inonotus hispidus* was studied on naturally and artifically infected ash (*Fraxinus excelsior*) and London plane (*Platanus x hispanica*) wood. For *in vitro* studies wood samples from the two hosts were used, these being 18 $cm^3$ blocks.

After both six and twelve weeks incubation, the highest weight losses and moisture contents were recorded on London plane wood. Cell wall degradation of *I. hispidus* in ash and London plane wood is predominantly reminiscent of that described by Courtois (1963) for soft-rot fungi (ascomycetes and fungi imperfecti) of the form-group 11. Cell wall degradation resulted in chains of minute biconical cavaties, joined by proboscis hyphae, following the orientation of the cellulose microfibrillar axis. Penetration hyphae of *I. hispidus* tend to branch repeatedly in the wood cell wall and hyphal alignment with the cellulose microfibrillar axis in the $S_1$ and $S_2$ layer of fibre and fibre tracheid cell walls is often consistent. Once single cavaties merge the degradation pattern caused by *I. hispidus* results in the appearance of sphaerical tunnels arranged in a steep helix within the $S_2$ layer and in a shallow helix within the $S_1$ layer. Due to the different alignment of the cellulose microfibrillar axis within the two layers tunnels frequently overlap each other when observed in longitudinal sections.

At an early stage of decay in ash *I. hispidus* was found to exhibit a preferential attack of the xylem rays and early wood vessels, whereas in London plane the xylem rays and vessels remained intact even at a very advanced stage of decay. The two different wood degradation patterns caused and described by *I. hispidus* on ash and London plane and the resulting impact on the strength and stability of partially decayed wood provides a reasonable explanation for the tendency that infected branches and stems of ash are far more likely to fail than those of London plane.

# Mechanical aspects of new SEM observations on the fibril/matrix structure of the S2 layer of softwood tracheids

Jürgen Sell, Swiss Federal Laboratories for Materials Testing and Research (EMPA), Wood Department, CH-8600 Dübendorf

## 1. Introduction

The relevant literature on the ultrastructure of wood describes its cell wall as an arrangement of lamellae with different thicknesses and different portions of their main chemical compounds (cellulose, hemicellulose, and lignin). The helical orientation of the cellulosic fibrils or their inclination to the longitudinal cell axis, respectively, is also different for the distinct layers of the secondary wall: the thin S1 (adjacent to the compound middle lamellae, MCL), the thick S2, and the thin S3 (adjacent to the cell lumen) [e.g. Core et al. 1979; Coté 1967; Fengel, Wegener 1989; Liese 1970].
With respect to its obvious importance for the mechanical functions of wood, the ultrastructure of the thick S2 is especially interesting. This structure has been described not always consistently. However, several authors postulate a S2 model consisting of thin concentric and helical lamellae with little, but slightly different inclinations (5° to 30°) to the cell axis [Braun 1992; Liese 1970; Ruel et al. 1978], fig. 1.
In the course of high-resolution SEM studies on transverse-fracture surfaces of tension-loaded samples of softwood (Picea abies, Abies alba, Pinus sylvestris, and others) significant indications have been found that the S2 structure exhibits a sandwich-like assembly of the fibrils with the following characteristics [Sell, Zimmermann 1993], fig. 2.

- The fibrils of the S2 are agglomerated radially to the cell axis: The tangential thickness of these agglomerations is 100 to 1000 nm. Radially, they often extend from the S1 to the S3.
- The bonds between the distinguishable S2 fibrils (diameters between 20 and 100 nm) are stronger in the radial then in the tangential direction (related to the cell axis). Also the adhesion to the adjacent layers S1 and S3 seems to be stronger then the tangential bond within the S2.

A modified model of the entire cell wall of softwood has been proposed [Sell, Zimmermann 1993], fig. 3. The radial arrangement of the structure elements of the S2 has meanwhile been confirmed by the light microscope [Sell 1994], fig. 4.

## 2. Mechanical aspects of the sandwich-like structure of the cell wall

The proposed radial fibril assembly within the S2 or, in other words, fibril agglomerations perpendicular to the "cross-banding faces" S1 and S3 would obviously be beneficial to the mechanical properties of the entire tree. The bending stiffness and thus the buckling resistance of such a sandwich-like cell wall under longitudinal compressive load might be markedly higher then with a cell wall consisting of concentric lamellae. Therefore, the bending stiffness of the whole stem would be improved when loaded by wind pressure or by forces of gravity. This is particularly important for wood with moisture contents (MC) close to or above the fiber saturation point where the strength of wood is significantly reduced. This is the case for the compression zone of a living tree under bending load which lies in the outer sapwood where the MC by far exceeds the saturation point. By the following model test (carried out by K. Timmermann), we tried to illustrate the functional advantage of such a cell wall structure.

## 3. Bending stiffness of two wall models

*Material and methods:* Bending test of 270 mm long rods, cross section 12x14 $mm^2$, consisting of glued beech veneers (1 mm thick). Two types (6 replicas each) of the arrangement of the veneers of the 12 mm thick core layer: "standing" veneers (directed parallel to the bending load) and "lying" veneers (perpendicular to the bending load), see fig. 5. The first type is supposed to represent the new S2 model and the latter the former model. The face layers representing the S1 and S3 are identical for both types with a slope of grain perpendicular to that of the middle layer. The veneers were glued using a PVAC-dispersion glue of rather little moisture resistance similar to the "glue" between the S2 fibrils. Conditions of the standardised bending test: (1) application of the load at a temperature of 23°C and an equilibrium wood

MC of 12%, (2) loading at a temperature of 50°C and 12% MC, (3) loading after 24 hours water-submersion of the samples at a temperature of 23°C and a wood MC between about 50 and 65%.

The *results* are summarised in fig. 5. As to be expected, there is no significant difference of the stiffness of the two sample types tested at normal temperature under dry conditions when the bond of the PVAC glue is not reduced. However, when an increased temperature and particularly a high wood MC reduces the glue bond markedly, the bending stiffness of the sample with "standing" veneers in the middle layer is only reduced by approx. 25 or 50%, respectively. Contrary to that, the bending stiffness of the samples with "lying" veneers is reduced by approx. 75 to 100%, respectively. The results may illustrate the beneficial role of "standing" structure elements of the S2 layer to the stiffness of the wood cell wall.

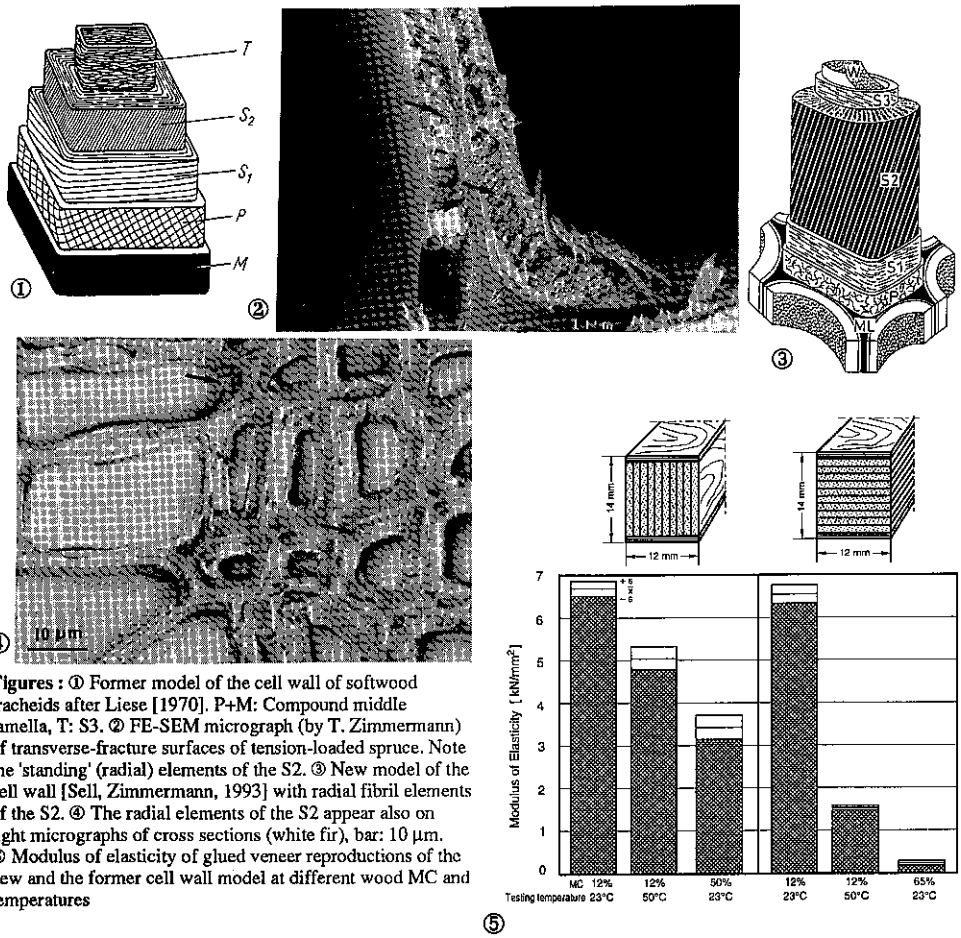


**Figures :** ① Former model of the cell wall of softwood tracheids after Liese [1970]. P+M: Compound middle lamella, T: S3. ② FE-SEM micrograph (by T. Zimmermann) of transverse-fracture surfaces of tension-loaded spruce. Note the 'standing' (radial) elements of the S2. ③ New model of the cell wall [Sell, Zimmermann, 1993] with radial fibril elements of the S2. ④ The radial elements of the S2 appear also on light micrographs of cross sections (white fir), bar: 10 µm. ⑤ Modulus of elasticity of glued veneer reproductions of the new and the former cell wall model at different wood MC and temperatures

**Literature**

Braun, H.J. 1992. Bau und Leben der Bäume (3. Aufl.) Verlag Rombach Freiburg

Core, H.A., Coté, W.A., Day, A.C. 1979. Wood structure and identification. Syracuse Univ. Press, New York

Coté, W.A. 1967. Wood ultrastructure - An atlas of electron micrographs. Univ. of Washington Press, Seattle

Fengel, D., Wegener, G. 1989. Wood-Chemistry, ultrastructure, reactions. (2. Aufl.). De Gruyter-Verlag Berlin, New York

Liese, W. 1970. Elektronenmikroskopie des Holzes. In: H. Freund (ed.). Handbuch der Mikroskopie in der Technik. Bd. V, Teil 1: Mikroskopie des Rohholzes und der Rinden. Umschau Verlag, Frankfurt a.M.

Ruel, K., Barnoud, F., Goring, D.A.I. 1978. Lamellation in the S2 layer of softwood tracheids as demonstated by scanning transmission electron microscopy. Wood Sci. Technol. 12: 287-291

Sell, J. 1994. Confirmation of a sandwich-like model of the cell wall of softwoods by light microscope. Holz Roh-Werkstoff 57: in press

Sell, J., Zimmermann, T. 1993. Das Gefüge der Zellwandschicht S2 — Untersuchungen mit dem FE-SEM an Querbruchflächen von Fichten- und Tannenholz. Forsch. u. Arbeitsber. EMPA.- Dept. Holz, Nr. 115/28

# DIFFERENCES IN PHOTOTROPIC SENSITIVITY, STEM STRAIGHTNESS AND COMPRESSION WOOD FORMATION IN *Pinus pinaster* Ait., *Pinus canariensis* Sweet. AND *Pinus nigra* Arn. SEEDLINGS

SIERRA DE GRADO, ROSARIO (*); ALÍA MIRANDA, RICARDO

*Dpto. Sistemas Forestales, C.I.T.-I.N.I.A. Ctra. de La Coruña km 7. 28040 Madrid (Spain).*
(*) Present address: *Dpto. Producción Vegetal y Ciencia Forestal. E.T.S.I. Agraria. Universidad de Lleida. Rovira Roure, 177.- 25006 Lleida (Spain).*

*Pinus pinaster* Ait., *P. nigra* Arn. and *P. canariensis* Sweet. seedlings were exposed to two treatments: 1.- fixed lateral light, and 2.- alternate lateral light (monthly rotation of light incidence angle 180°). After two years of treatment in *Pinus pinaster* and *P. nigra* seedlings, and one year in *P. canariensis*, compression wood development was analyzed.

Diagrams of stems and the respective compression wood formed at several levels of the stem are presented (fig.1), showing great differences in the stem form found in the three studied species. Combinations of phototropic sensitivity, elongation rate and righting ability by formation of compression wood allow to offer an explanation to the found differences.

The vertical and straight stems exhibited by *Pinus canariensis* seedlings in comparison with the other two species, was acompained to the limited presence of compression wood in their sections. It suggests that the form of *P. canariensis* stems were not the result of an efficient reorientation mechanism, via compression wood formation, but the consequence of weak phototropic sensitivity.

The growth rate of *Pinus nigra* seedlings was very low during the experiment, which has determined its evolution over the other involved factors.

*Pinus pinaster* seems to be the more sensitive of the three species to the lateral incidence of the light. Its sensitivity and its great elongation rate originate severe deformations in the stems, which are not compensated by compression wood formation.

FIGURE 1. Diagrams of stems and compression wood formed at several levels of the stem.

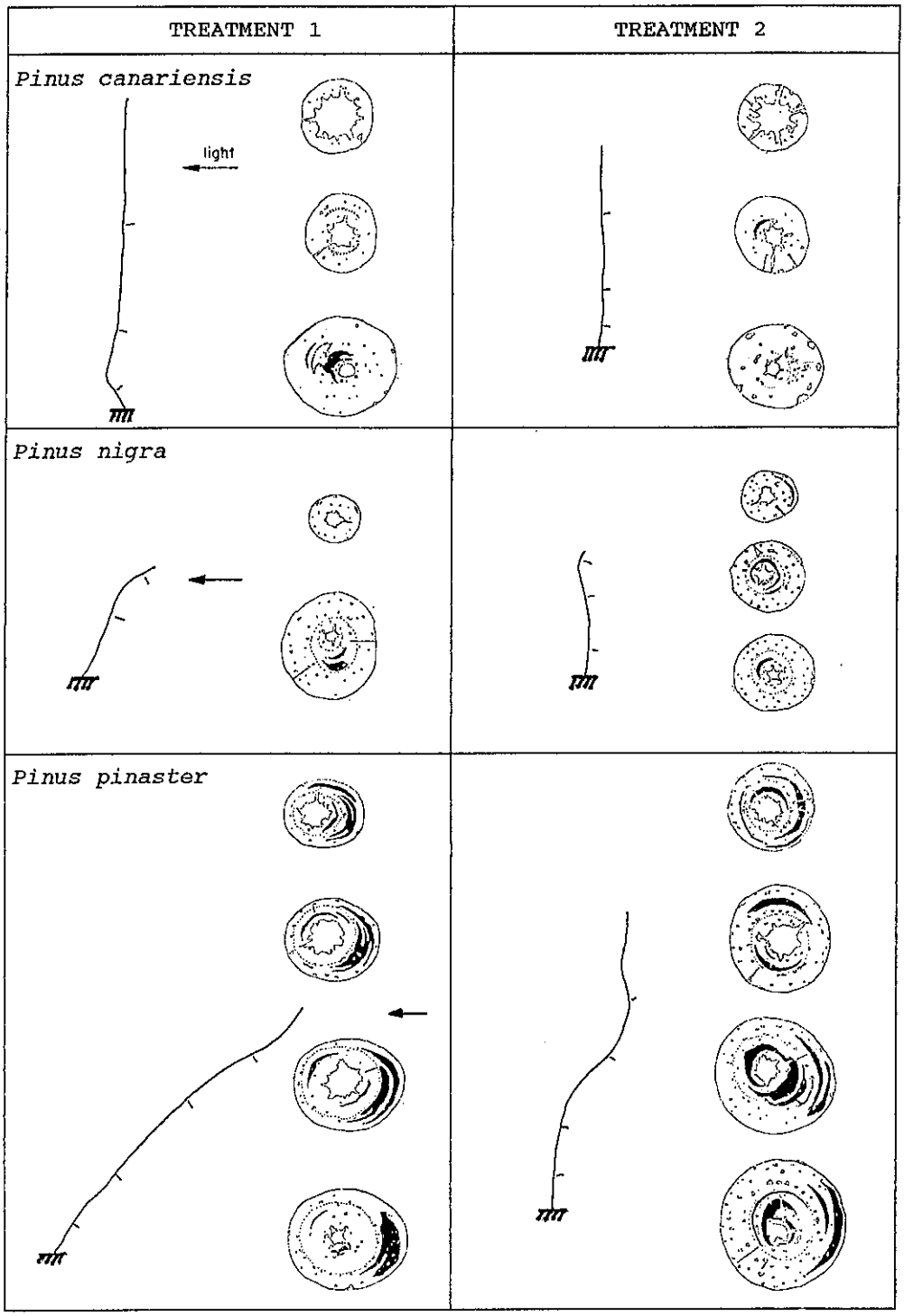

# KINEMATICS OF TWINING GROWTH AND MECHANICS OF THE TWINING HABIT

*W.K. Silk*
University of California at Davis, U.S.A.

Analysis of growth of twining vines gives a geometrical twist to problems in botano-mechanics. Twining stems wind around a vertical pole to make a corkscrew-shaped form, a helical tube of tissue. The plant apex has an undulating growth trajectory, while behind the apex older tissue expands and is displaced rather smoothly through the steady form. The stem can be modelled as a tube surrounding a generative helix $\alpha(s)$, where s is arc length along $\alpha$. Points in the stem can be given in terms of $\alpha$, the Frenet vectors, and some natural coordinates. If growth velocity along $\alpha(s)$ is known, then a form of strain rate tensor can be used to find elongation rates of line elements through the cross-section. The continuum-mechanical analysis shows a growth rate maximum on the bottom surface of a stem which is twining clockwise and rotating counterclockwise as it elongates.

The geometry of the growth analysis also serves for mechanics of the twining habit. I hypothesize that contact forces are important in maintaining the form of the vine. An axial force within the stem should be balanced by a normal load distributed along the line of contact between stem and supporting pole. Two empirical studies verified the importance of the putative normal load. Firstly, vine geometry was measured on and off the supporting pole. When removed from the pole, the helical coil forms a coil of smaller radius, smaller wavelength, and larger torsion. Next, forces were estimated from observations of the pressure exerted by a stem twining around a water-filled balloon. The twining stem was observed to put itself into tension and to use a helical geometry to generate contact forces which are large relative to the stem weight. Most recently, the time course of development of the normal load has been determined with an electronic device, based on a thin beam load cell, which gives continuous, in situ measurement of contact loads.

## REFERENCES

**Silk, W.K. 1989** - Growth Rate Patterns which Maintain a Helical Tissue Tube. *J. Theor. Biol.*, 138 : 311-327.

**Silk, W.K. and Haidar, S.A. 1986** - Growth of the stem of *Pharbitis nil* : analysis of longitudinal and radial components. *Physiol. Veg.*, 24 : 109-16.

**Silk, W.K. and Hubbard, M. 1991** - Axial forces and normal distributed loads in twining stems of morning glory. *J. of Biomechanics*, 24 : 599-606.

# A MECHANISTIC STUDY OF SEEDLINGS EMERGENCE FROM UNDER SUPERFICIAL OBSTACLES.

Nicole SOUTY and Colette RODE

*INRA, Unité de Science du Sol, Centre de Recherches d'Avignon, BP 91, F 84143 Montfavet Cedex France.*

In laboratory the emergence of seedlings was studied in relation to soil crusting and heavy obstacles independent of the underlying layer. Relationships were established between the physical and mechanical characteristics of these different obstacles and the growth force of the seedling measured previously, which made it possible to develop a predictive model of the percentage and kinetics of emergence.

If there was a crust at the surface of the seedbed, a mechanical model of rupture (bending and fracture of the crust) was assumed. It was very important to make homogeneous, continuous crusts and to repeat the same experimental conditions when measuring the resistance of the crusts and determining the experimental percentage of seedling emergence.

The crust resistances were measured with a penetrometer; the growth strengths of the seedlings (same age and issuing from calibrated seeds of same mass) and the amount of time necessary for the seedling to exert a known force, were determined by using the steel beam method adjusted in the laboratory.

The calculated probability of emergence was estimated from statistical distribution of seedling forces by using the mechanical model of rupture. There was a good agreement between this calculated curve and the observed emergence in the range of resistance of crusts from 0 to 0,8N for the sugar beet and from 0 to 3N for the maize for example. A 0.2N crust resistance allowed 100% of maize emergence and only 50% of sugar beet emergence.

The experimental maximum emergence percentages through different crusts were reached after the amount of time previously measured (with the steel beam method) increased by the amount of time necessary for the seedling to break through the crust, about 40 hours.

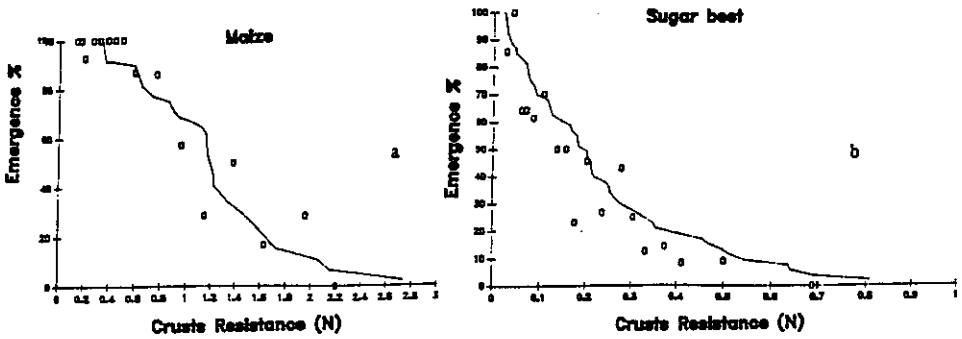


*Comparison of experimental emergence (o) with theoretical emergence (–) if bending hypothesis: a) maize, b) sugar beet.*

If clods were on the surface of the seedbed, two processes could be involved in emergence: the seedling lifted the clod or it grew under the clod to escape.

The first process was independent of the surface aera; it appeared that the seedlings were able to lift obstacles the weight of which was greater than the growth force because the growing aerial part could change its shape and or move under the obstacle. To obtain the moment of the clod weight equal to the moment of the seedling force, the probability of heaving was determined after about 6 hours by using the statistical distribution of the forces developed during this period. The percentage of heaving was lower than 50 per cent when the weight of the obstacle was greater than 0.1N.

The resulting emergence percentage (heaving and escape) was greatly reduced when the seedling encountered an obstacle with a diameter greater than 3 cm.

## Mechanical Stability of Hollow Trees

Hanns-Christof Spatz
Institut für Biologie III
Schänzlestr. 1, D-79104 Freiburg i.Br.

A theoretical description for the bending stability of hollow plant stems, originally developed to describe local buckling in cereals (Spatz et al.,1990; Spatz et al., 1993) was extended to calculate the critical bending moments for a hollow elm tree as a function of the wall thickness, more exactly of the thickness of the remaining unaffected wood. Using data for "healthy" wood (Wessolly, personal communication), our computations show that buckling, as apparent from an ovalisation of the cross-section occurs to an appreciable extent only for a ratio of wall thickness/radius below 0.05 (Spatz, 1994).

Therefore, the resistance to bending moments as excerted by wind forces can for all practical cases be computed with conventional mechanics: The critical bending moment is obtained from the critical compression and the bending stiffness, i.e. the product of the second moment of area of the ring shaped cross-section and Young's modulus of elasticity in longitudinal direction. At a ratio of wall thickness/radius of 0.3 the stability is reduced to 75 % of that for a corresponding full stem, and is gradually decreased with further reduction of the wall thickness.

The mechanical properties of wood can change in various ways upon infection with different fungi (Wilcox, 1978; Schwarze, 1994). Before the stability of such trees can be assessed on the basis of theoretical considerations alone, research has to provide a much larger data base. Particularly, Young's moduli in all three directions of space and the critical compression for wood infected with fungi to various degrees need to be known.

**References:**

Spatz, H.-CH., Speck, T., and Vogellehner, D.: "Contributions to the Biomechanics of Plants. II. Stability Against Local Buckling in Hollow Plant Stems". Botanica Acta 103 (1990), 123-130.

Spatz, H.-CH., Boomgaarden, Ch., and Speck, Th.: "Contribution to the Biomechanics of Plants. III. Experimental and Theoretical Studies of Local Buckling". Botanica Acta 106 (1993), 254-264.

Spatz, H.-CH.: "Ein Kommentar zur mechanischen Stabilität hohler Bäume". Das Gartenamt, in press (1994).

Schwarze, F.W.M.R., and Fink, S.: "Möglichkeiten und Grenzen von Diagnosemethoden unter besonderer Berücksichtigung des Holzzersetzungsmusters". Neue Landschaft (1994), in press.

Wilcox, W. Wayne: "Review of Literature on the Effects of Early Stages of Decay on Wood Strength". Wood and Fiber 9 (1978), 252-257.

**Effect of branching on the internal distribution of strength within a root system.**

A. Stokes & C. Mattheck

Institut für Materialforschung II
Kernforschungszentrum Karlsruhe,
Postfach 3640
76021 Karlsruhe
Germany

One of the most consistent responses of trees subjected to mechanical loading is the laying down of wood in areas of highest stress. The increase in new wood then increases the rigidity of those areas, thus reducing the stress to which they were first subjected. Hence, when applied to the whole of a tree, the tree will experience the same maximum stress all over its surface, resulting in a tree with a constant surface stress. This "constant stress hypothesis" (Metzger 1893, Mattheck 1991) would help explain the cause of localised growth in trees, such as the swelling around branch joints and buttress roots. As most trees must resist uprooting by the wind, roots must transmit bending and compression forces into the ground. If the radial growth of roots under the most stress, such as the lateral root bases, is increased, these forces will be transmitted into the soil much more smoothly. Without such an increase in woody growth, the roots might experience much larger bending forces and possibly fail under loading. As the stress decreases away from the root bases and the roots bifurcate, rigidity may also be reduced.

In order to assess how the internal distribution of strength differs within a woody root, wood samples were taken from the first and second order roots of mature beech (*Fagus silvatica*) and ash (*Fraxinus excelsior*). The beech trees examined were growing on strongly sloped ground in the Palatinian forest, whilst the ash were on flat ground in a seasonally waterlogged area of the Rhine valley (both sites in south west Germany). The samples were collected by drilling 5 mm diameter cylindrical cores through the root, at regular intervals along its length. The strength of each fresh sample was quantified by measuring the bending moment at 12 mm intervals along the length of the core, using a newly developed, pocket-size, wood-testing device (Fractometer II) (Mattheck *et al.* 1994). Using Fractometer II, it is possible to determine the lateral strength in the radial direction and also the "crushing" strength parallel to the fibre direction of the wood.

The highest values for lateral bending and crushing strength were found in the buttress roots of both beech and ash and reduced with decreasing root cross-sectional area (CSA) away from the stem. Regression coefficients of $\log_{strength}$ vs. $\log_{csa}$ can be used to determine differences in strength between compression roots (uphill) and tension roots (downhill) in beech. It is considered how the internal strength distribution within both beech and ash roots is related to branching and whether woody growth alters in response to the local loading environment, thus reducing stress within the root.

## References

Mattheck C. 1991, Trees - The mechanical design. Springer Verlag, Heidelberg, New York.

Mattheck C., Bethge K. & Zipse A. 1994, Das Fractometer. Submitted to Allgemeine Forstzeitschrift.

Metzger C. 1893, Der Wind als massgebender Faktor für das Wachstum der Baüme. Mündener Forst Hefte, Berlin, 3:35-86.

# INCREASE IN LEAF YIELD BY DWARF SHOOTS IN DENSE-PLANTED MULBERRY FIELD

Masaki Tateno

Faculty of Agriculture, Tokyo University of Agriculture and Technology, Fuchu, Tokyo 183, Japan

Present address: c/o Professor F. S. Chapin III, Department of Integrative Biology, University of California at Berkeley, Berkeley, CA 94720, U.S.A.

A shoot of mulberry tree consists of a perpendicular stem for mechanical support and leaves for assimilation. The leaves are used as feed for silkworm. Tateno and Bae (1990) defined the lodging safety factor, an indicator of mechanical stability of the shoot, as the ratio of the critical lodging load to the leaf fresh weight observed. The mulberry trees developmentally control the value of the lodging safety factor in response to the environmental condition (Tateno, 1991).

Our mechanical model based on Euler's buckling formula predicted following three: 1) When the lodging safety factor and shoot dry weight is constant, proportion of shoot dry matter partitioned into leaves increases as shoot length decreases (Fig. 1A and 1B). 2) When shoot length and shoot dry weight are constant, proportion of shoot dry matter partitioned into leaves increases as the lodging safety factor decreases (Fig. 1A). 3) When the lodging safety factor and shoot length are constant, proportion of shoot dry matter partitioned into leaves increases as shoot dry weight increases (Fig. 1B). If net shoot production per unit area remains unchanged, these increases in leaf percentage in individual shoots lead to increase in leaf production per unit area.

To examine the effect of dwarf shoots on the leaf yield per unit area, densely planted mulberry field was treated with 4000 ppm solution of succinic acid 2,2-dimethylhydrazide (SADH). SADH is a growth retardant and does not change the lodging safety factor of mulberry shoots (Tateno and Bae, 1990). We used two-year-old graftings of *Morus alba* cv Minamisakari. The shoot density was 16 per square m.

Figure 2 shows the productive structure of the untreated and SADH-treated shoots at the end of experimental period. The mean shoot length and net shoot production in the untreated plots were 1.66 m and 683 g per square m, respectively. The shoot length in the SADH-treated plots decreased by 18.7%, whereas the net shoot production was not significantly different from that in the untreated plots. In the SADH-treated plots, the trees remarkably increased the percentage of shoot dry matter partitioned into leaves. As a result, the leaf yield per unit area in the treated plots increased by 23.0%. Although this value did not precisely consist with the value predicted by the model, 29.6%, these results suggest that, in the case of dense planting, the dwarf shoots are effective for increasing the leaf yield per unit area.

References
Tateno, M. & Bae, K. (1990) Plant Physiology 92: 12–16.
Tateno, M. (1991) Physiologia Plantarum 81: 239–243.

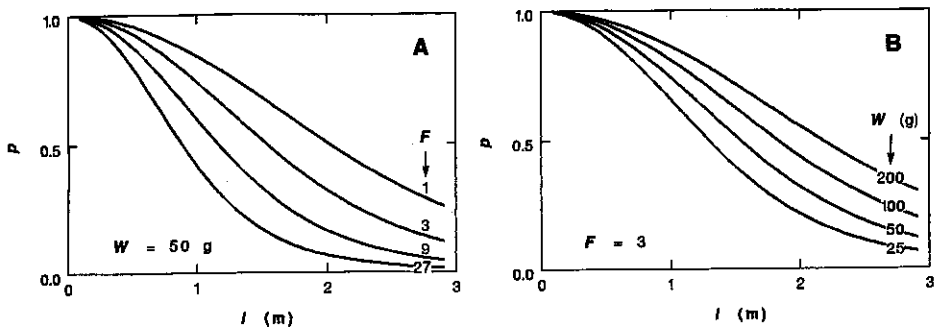


Fig. 1. A) The predicted relationship between proportion of shoot dry matter partitioned into leaves ($p$) and shoot length ($l$) assuming that the shoot dry weight ($W$) is 50.0 g. B) The predicted relationship between $p$ and $l$ on the assumption that the lodging safety factor ($F$) is 3.0.

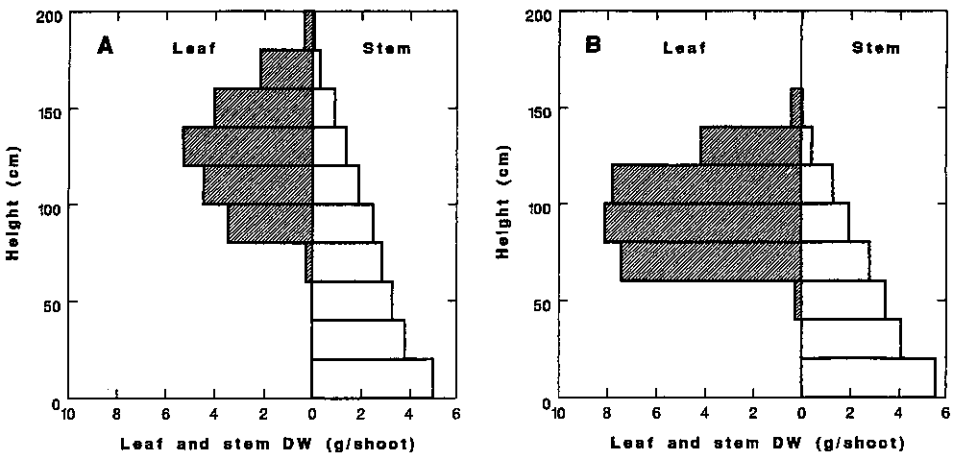


Fig. 2. A) Productive structure of the untreated shoots. B) Productive structure of the SADH-treated shoots. Mean of 24 shoots.

# THE EFFECT OF WIND OR GRAVITY ON WOOD FORMATION (XYLOGENESIS)

Frank W. Telewski
Assistant Professor and Curator of the W.J. Beal Botanical Garden
Department of Botany and Plant Pathology
Michigan State University
East Lansing, MI 48824 USA

Trees experience complex loading patterns involving tension, compression, torque, shear and bending, induced by a number of external mechanical stresses including wind, precipitation loading, and displacement with respect to the gravitational vector. The most obvious developmental response is the formation of reaction wood, known as tension wood in dicotyledonous woody angiosperms and compression wood in conifers.

The existence of compression wood in conifers has been recognized for over one hundred years. Its structure, function and formation have been the subject of numerous studies since the latter half of the 19$^{th}$ century. Numerous reviews of past research and interpretations of the collective data have been produced, most recent is the comprehensive review presented by Timell (1986,a,b,c).

Compression wood forms typically, but not exclusively, on the lower sides of branches, and leaning or crooked stems of conifers. It is characterized as being composed of tracheids which are rounded in transverse section, are shorter in length, with highly lignified secondary cell walls containing spiral cell wall checks. There is also an increase in the angle of the cellulose microfibrals within the secondary cell walls of compression wood tracheids. Compression wood is usually denser and darker than normal wood with larger rays (Timell 1986a). The axial rate of cell enlargement of compression wood is greater than in normal or opposite wood. The increased elongation of the differentiating cells creates a compressive forces resulting in the righting of the stem (Timell 1986a,b,c).

Historically, wind-induced developmental responses in the tree stem have been mixed with studies on reaction wood formation and the gravitropic response (Timell 1986b,c). Under field conditions, trees exposed to strong winds tend to lean and contain reaction wood in the displaced main axis. It was not clear if the wind-induced movement of the stem induced compression wood formation in conifers or if the formation of compression wood in wind stressed conifers was the result of their displacement with regard to the gravational vector. Wind sway is a dynamic movement of the stem creating an alternating compressive and tensile force within a vertical or displaced stem. The force of gravity, on the other hand, creates a static load on the stem with an internal compressive force on the lower side and an internal tensional force on the upper side of a displaced stem.

Telewski (1989) reported flexure stimulates wood formation and the wood shares characteristics similar to both normal and compression wood. From the perspective of design principles for biological structural systems, the structure of both compression wood and flexure wood must share some structural similarities. Purely tensile elements resist tensile forces only, whereas bending and compression elements also resist tension and shear (Wainwright et al. 1976). Compression elements need to be shorter and larger in external diameter, increasing the second moment of cross-sectional area (I), in order to withstand compression (Wainwright et al. 1976). Compression wood tracheids are consistent with this

requirement. Trees experience a complexity of loading patterns under windy conditions, including compression, tension, torque, shear and bending. Therefore, flexure wood should, and does, have some characteristics of compression elements. There is also an increase in the flexural stiffness (EI) of flexed stems. The increase is due to a significant increase in radial growth, increasing the second moment of area (I) in the direction of flexure. However, there is a decrease in the elastic modulus (E) in response to flexure. The increased I and decreased E creates a stem which is overall stiffer and more resistant to bending, but is capable of absorbing more energy as deformation of materials, a result of the lower E of the stem.

Tension wood is characterized by the presence of gelatinous fibers. These fibers have a lower lignin and higher cellulose content compared to normal fibers and create a tensional force within the stem. Very little data exists concerning the developmental anatomy of flexure wood in angiosperms and how it compares with tension wood anatomy and development. Neel & Harris (1971) observed a reduction in vessel element length and diameter in shaken *Liquidamber styraciflua* as compared to the vessel elements of untreated trees. Holbrook & Putz (1989) reported increased density (g $cm^{-3}$) and radial growth in non-constrained (free swaying) *Liquidambar styraciflua*. As in the conifer response, this translates into a greater mass and volume of xylem produced per $cm^2$ of cambial surface area in response to flexure.

Based on the principles for biological structural systems, the tensional elements of tension wood may not be effective components within the flexure wood of woody angiosperms. A detailed comparison between tension wood and wind or flexure stimulated xylogenesis is the focus of current research.

Holbrook, N.M. & Putz, F.E. (1989). American Journal of Botany **76**, 1740-1749.
Neel, P.L. & Harris, R.W. (1971). Science **173**, 58-59.
Telewski, F.W. (1989). Tree Physiology **5**, 113-122.
Timell, T.E. (1986a). *Compression Wood In Gymnosperms, Volume I.* Springer Verlag, Berlin.
___ (1986b). *Compression Wood In Gymnosperms, Volume II.* Springer Verlag, Berlin.
___ (1986c). *Compression Wood In Gymnosperms, Volume III.* Springer Verlag, Berlin.
Wainwright, S.A., Biggs, W.D., Currey, J.D. and Gosline, J.M. (1976). *Mechanical Design in Organisms.* Princeton University, Princeton.

# Mechanical Control of Root Growth

M. Teschner, C. Mattheck
Kernforschungszentrum Karlsruhe GmbH
Institut für Materialforschung II
Postfach 3640, 76021 Karlsruhe
Federal Republic of Germany

The present paper investigates tree-root morphologies with regard to the introduction of wind loads into the soil. From the mechanical point of view the tree can be compared to a sailing ship, this means that stem, branches, roots and their joints are designed in such a way that notch stresses and waste of material are avoided. Tree roots are biological soil anchorages which fulfil the mechanical rule of biological load carriers. This is achieved by growth into a state of constant stress on the surface (**constant stress axiom**). The roots care for a very good anchorage of the tree in the soil with a minimum of material. Because the root-soil plate is a compound structure (root-reinforced soil) the material properties of the soil are very important. An additional difficulty is that the shear strength of the soil depends on the normal pressure on the shear lines. This is characterized by Mohr-Coulomb's law. The basic idea of this law is that the friction (shear strength) between the shear lines within the soil increases with increasing normal pressure. Therefore, there are normally more roots for soil reinforcement on the windward side where the soil is lifted than on the lee-side where it is compressed. This is the simplest example which results from Mohr-Coulomb's law. At the Karlsruhe Nuclear Research Centre the so-called SKO method was modified to predict root morphologies of trees for different loading and boundary conditions. The predictions are based on the assumption that the optimum root design (in pure mechanical sense !) is a design which guarantees an even distribution of shear stresses along the roots. This approach gives good qualitative agreement with the root formation observed in nature for cases considered here. It is clear that this mechanical optimum can be disturbed drastically by biological growth regulators as for example hydrotropism. The use of the optimization method SKO (adapted for soil problems) in the design process for technical soil anchors (foundations) leads to a increase in the loading capacity under the demand of a lightweight design.

# Examples

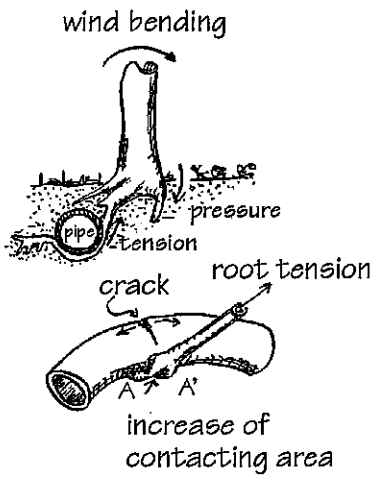


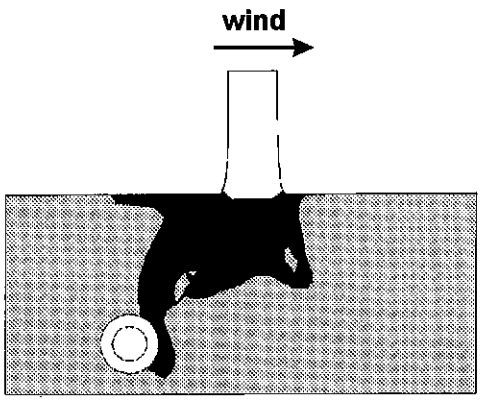


FEM: M. Lumpp, J. Schäfer

Real tendril formation and SKO prediction (pipeline on the windward side)

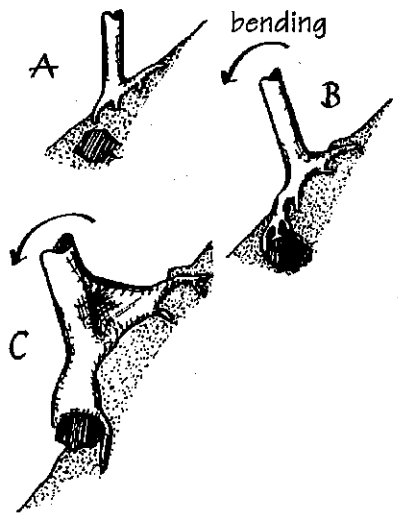


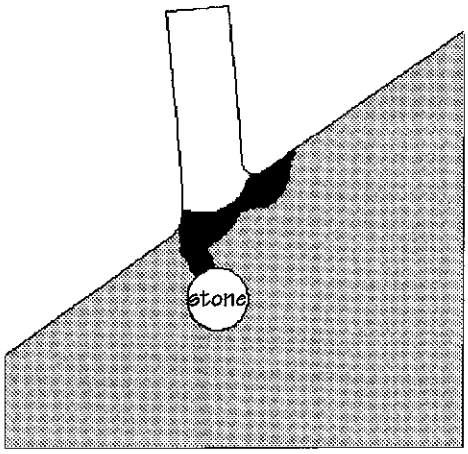


Interaction between tree roots and stones

# Measurement of transverse growth stresses in wooden disks

Rémi THOMAS , Meriem FOURNIER, Jean-Louis KERGUÈME , Bernard THIBAUT
Université Montpellier II - L.M.G.C. Bois - CP081 - Place E. Bataillon - 34095 Montpellier Cedex 5 - FRANCE
tél : (33) 6714 3483, 4739, 3431 - fax : (33) 6754 4852

Wood in standing trees is pre-stressed. These stresses originate in a physico-chemical transformation of wood at the end of its differentiation (cellular maturation). These maturation stresses (often called growth stresses) are useful for trees (they allow bending movements of reorientation or stabilization and reduce the initiation and propagation of shakes in the cambial zone). But they cause troubles during wood processing (heart shakes during felling, deformations and bad quality of sawn wood). The researches leaded in the LMGC of Montpellier aim at modelling these stresses, relating their variations to wood structure and tree growth.

The objective of our work is to validate the mechanical models. To study the stress field along the radius, an destructive experiment based on successive cuts seems necessary. This is a complement to the usual measurements of peripheral strains (Baillères 1994). Among the existing methods (Archer 1986), we have chosen to adapt the Sachs'one (1927).
This method is based on the measurements, at the periphery of a log, of the longitudinal and tangential strains induced by the drilling of successive holes (concentric and centred). These strains as interpreted as the result of the releasing of i) radial stresses of the hole surface and ii) longitudinal stresses on the transverse area supressed. This interpretation have been calculated first by Sachs (for isotropic metals), then by Doi & Kataoka 1967 (on an homogeneous circular cylindrical anisotropic log) and Sasaki & al 1981 (radially unhomogeneous cylindar).

First, we have chosen to implement the experiment on disks (rather than logs). Thus, only the transverse stresses can be valued. The Sachs'calculations have been modified to account for plane stresses, in a very thin, cylindrical orthotropic homogeneous disk. The tangential strain $\varepsilon_\theta$ at the disk surface is :

$$\gamma^2 = \frac{K_{22}}{K_{11}}$$

$$\varepsilon_\theta = (AR_f^{\gamma-1} + BR_f^{-\gamma-1}).\sigma_{rr}^{\circ}(R) \text{ with } A = \frac{K_{11}\gamma - K_{12}}{K_{11}\gamma + K_{12}} Rf^{-2\gamma}$$

$$B = \frac{K_{11}\gamma - K_{12}}{(-K_{11}\gamma + K_{12})^2 R^{\gamma-1} Rf^{-2\gamma} - (K_{11}\gamma + K_{12})^2 R^{-\gamma-1}}$$

where $K_{11} = C_{11} - C_{13}^2 / C_{33}$ ; $K_{22} = C_{22} - C_{23}^2 / C_{33}$ et $K_{12} = K_{21} = C_{12} - C_{13}C_{23} / C_{33}$
($C_{ij}$ : elastic compliances, $R_f$ : disk radius, R : radius of the drilled hole, $\sigma_{rr}^{\circ}(R)$ : radial stress released by drilling).
The diameter variation $\Delta\phi$ also allows to estimate $\sigma_{rr}^{\circ}(R)$ since $\Delta\phi/\phi = \varepsilon_\theta$.
The compliances $C_{ij}$ will be calculated from the specific density of wood using Guitard's models for air-dried wood corrected for green wood (Fournier 1989). Simulations have been done, assuming that $\sigma_{rr}^{\circ}(R) = -\hat{\sigma}_\theta \text{Log}^{R}/_{R_f}$ (Kübler's model).

Experimentally, the disk (≈1cm thick) is prepared with a bandsaw (and a special truck) and put on a hard and smooth bearer (disk of teflon) in order to minimise the risk of adherence. Then, it is necessary to clamp the disk (two opposite tightening points of are sufficient) against cutting forces. Lastly, contrary to what is usually done, the cutting and feeding speeds Vc and Vf are taken very low (Vc≈6,5m/mn ; Vf≈0,01mm/tooth) to avoid vibrations. Moreover, four extensometers (using electric strain gages, H.B.M. type DD1) are nailed (using compasses points) tangentially around the disk , two displacement sensors (Mitutoyo 543) allows to measure the variations of diameter.diamétralement opposés. For each drilled hole, measurements are done after tightening, after drilling, and after loosening.

Figure 1 shows the experimental apparatus and figure 2 an example of results obtained on a disk of poplar I-214. Observed results are slightly lower than theoritical calculations, which can be explained by a partial recovery of locked-in strains during disk conservation.

This experimental device is now operational to evaluate transversal stresses in disks. The aim is to use it to study the variability of these stresses in different species, for different histories of growth, and relate the results to longitudinal strains measured at the stem surface in the standing trees. It will be also used to study the relaxation of stresses with time, temperature, etc. Improvements are planned in the theoretical calculations to take into account asymmetries often observed (eccentricity of the pith, circumferential heterogeneities). Lastly, we will try to develop the same experiment on logs (that will allow also the measurements of longitudinal strains).

## References

Archer R. (1986) "Growth stresses and strains in trees".Springer Series in Wood Science. Ed. E. Timell,Springer Verlag

Baillères H. (1994) "Précontraintes de croissance et propriétés mécanophysiques de clones d'*Eucalyptus* (Pointe Noire - Congo) : hétérogénéités, corrélations et interprétations histologiques" Thèse de l'Université de Bordeaux 1

Fournier M. (1989) "Mécanique de l'arbre sur pied : maturation, poids propre, contraintes climatiques dans la tige standard." Thèse de l'INPl, Nancy

Kubler H. (1959a) "Stuies on growth stresses in trees. 1. The origin of growth stresses and the stresses in transverse direction." Holz als Roh und Werkstoff 17(1) 1-9. In German

Sachs G. (1927) Zeitschrift für Metalkunde 19 352-357.

Sasaki Y., Okuyama T. & Kikata Y. (1981) "Determination of the Residual Stress in a Cylinder of Inhomogeneous Anisotropic Material I & II"- Mokuzai Gakkaishi vol.27 n°4 : 270-282

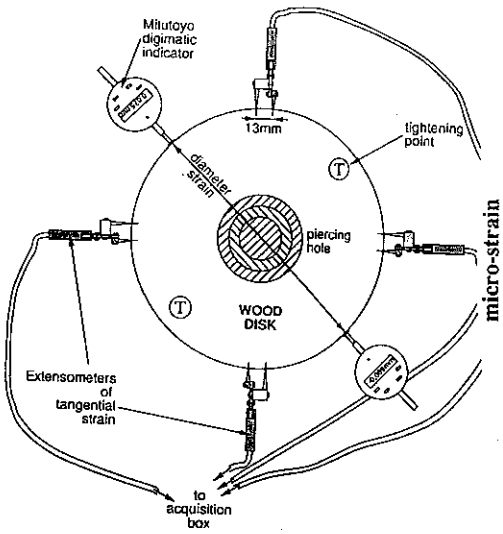


fig 1 : **Pratical Application**

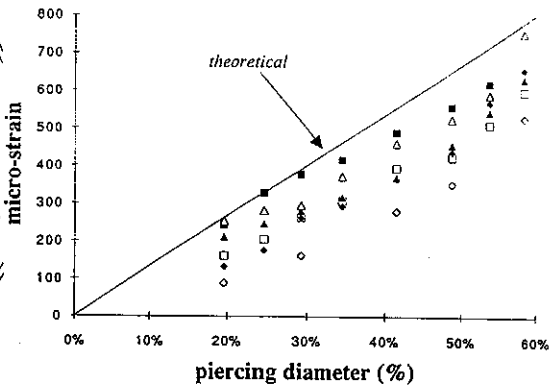


fig 2 : **Experimente Results**

# WATER RELATIONS OF ROOT GROWTH OF *PINUS PINASTER* AT SINGLE-CELL LEVEL

Marie-Béatrice Triboulot[1], Jeremy Pritchard[2] and Deri Tomos[2]

[1] : *INRA, Laboratoire Sol et Nutrition, Route d'Amance, 54280 CHAMPENOUX. Tel : 83-39-40-41, Fax : 83-39-40-69.*
[2] : *School of Biological Sciences, UCNW Bangor, Gwynedd LL57 2UW, Wales, UK. Tel : (0)248-351151, Fax : (0)248-370731.*

The ability to maintain root growth in a drying soil is considered an adaptation to drought. A continuation of root growth allows an exploitation of a larger volume of soil. Root growth is the consequence of the elongation of the cells produced by the meristem situated in the tip of the root. When water is not limiting the control of the expansion of cells can be summarized by this equation (1) :

$$r = \phi\ (P\text{-}Y)$$

where r = expansion rate, $\phi$ = cell wall extensibility, Y = yield threshold and P = turgor pressure. $\phi$ and Y are the rheological cell wall properties. The cell turgor is dependant of the cell sap osmotic pressure ($\pi_i$). Bulk measurments of P and $\pi_i$ will obscure a cell-to-cell heterogeneity within a root. The cell pressure probe and the picoliter osmometer (2) have been used to study the water relations of the root of seedlings of maritime pine, *Pinus pinaster*, at the single-cell level in well watered conditions and at two levels of osmotic stress.

P and $\pi$ were measured in the first root of 2-week old pines grown in hydroponics. The local growth rate of the root tip was determined from the cell length profile along the root apex (3). Figure 1 shows that the elongation zone expands over the first 8 mm.

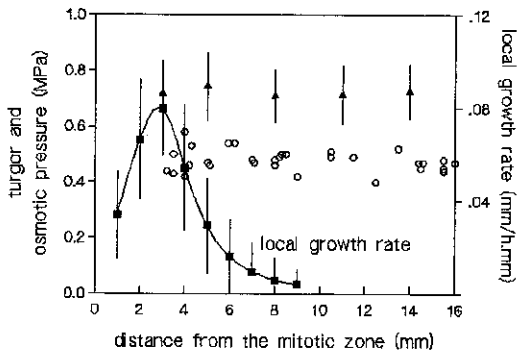


*Fig. 1 : Local growth rate, turgor (○) and osmotic pressure (▲) along the root apex. Turgor : single cell measurements. Osmotic pressure : samples pooling 2-3 cells, means ± s.d., n = 4. Local growth rate : means ± s.d., n = 9.*

Despite the large changes in growth the turgor pressure was constant at about 0.5 MPa along the apical 16 mm. According to the equation the constant turgor along the growing zone implies a modification of the rheological properties. The walls must loosen in the apical part of the expanding zone (as r increases) and tighten in the distal part (as r decreases). The osmotic pressure of the vacuole sap was also constant over the apical region but higher than was P, by about 0.7 MPa. So the water potential of the cell was -0.2 MPa but the root bathing medium water potential was only -0.05 MPa. The presence of solutes in the apoplast may provide an explanation for the lower water potential than these of the nutient solution.

Two levels of osmotic stress have been applied by adding polyethylenglygol (M = 3500 g/mol) to the nutrient solution. After a 3-day adaptation period the seedlings showed a stable growth rate.

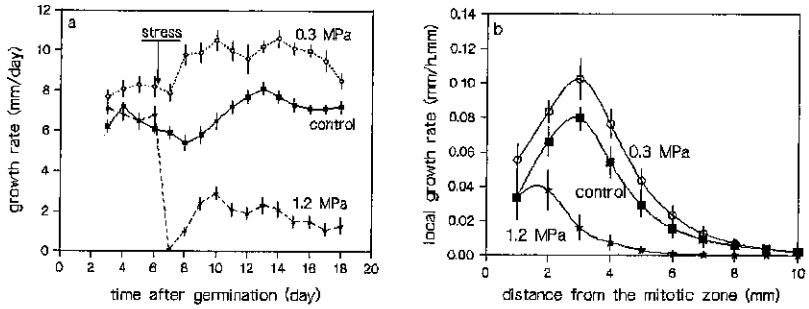


*Fig. 2 : (a) Growth rate of the first root for the control and the two osmotically stressed treatments. Means ± s.e., n = 24. (b) Local growth rate along the root apex for the three treatments. Means ± s.d., n = 6.*

Surprisingly a moderate osmotic stress (0.3 MPa) increased the root growth rate whereas a more severe stress (1.2 MPa) decreased it (fig. 2a). The local growth rate for the three treatments is given in figure 2b. The moderate osmotic stress induced an increase of the local growth rate all over the growing zone but the strong one decreased it and shortened the elongation zone. This might imply that the growth rate increase was governed by a different mechanism than the decrease. This hypothesis is being tested by measuring P and $\pi$ of individual cells along the expanding zone as the root grows under both moderate and severe stresses.

*References :*
*(1) : Lockhart J.A. (1965), J. Theoret. Biol. 8 264-275.*
*(2) : Tomos et al. (1994), in Plant cell biology - A practical approach. (eds. N. Harris and K.J. Oparka) IRL Press, Oxford (in press).*
*(3) : Silk et al. (1989), Plant Physiol. 90 708-713.*

# Influence of Global Shape and Internal Structure of the Tomato on the Reliability of Firmness Estimation by the Acoustic Impulse Response Technique

*Xavier Vandewalle,*
*Jan Langenakens,*
*Josse De Baerdemaeker,*
*Department of Agricultural Engineering, Katholieke Universiteit Leuven*
*Kardinaal Mercierlaan 92, 3001 Heverlee, Belgium*

The firmness of a tomato is becoming one of the main characteristics on which it is classified in different classes of quality. Recently a non-destructive acoustic response technique, based on resonance frequencies, has been under development. The measurements are conducted by monitoring the response of the tomato which is excited by impact. The response is captured by a small microphone. This method allows to monitor the firmness evolution of tomatoes during storage or on the plant to estimate the optimal time of harvesting. The technique has application possibilities to be implemented in sorting lines for grading or to be used as an objective tool to check the initial quality of the fruit at the auctions. So far, little is known about the sensitivity of the method to non-regular fruit shapes and to internal structure.

Tomatoes of different sizes, shapes and maturity stages were tested with the experimental modal analysis technique. Modal analysis is a technique applied in vibration analysis to describe the dynamic behaviour of mechanical structures. The modal analysis theory shows that this dynamic behaviour depends on the modal parameters such as the resonance frequencies of the system, damping factors and mode shapes (deformation shapes at the resonance frequencies). The modal parameters are estimated through frequency response function (FRF) measurements. An FRF is the ratio between the output (acceleration) and the corresponding input (force) as a function of the frequency. For describing the system dynamics at least the measurements of the FRF between the response location and the force positions of interest are necessary. The second step, modal parameter estimation, fits an analytical expression to the measurements, describing the FRF's in terms of the modal parameters. The resulting modal model is useful in further analysis as vibration trouble shooting, sensitivity analysis and others. In the modal analysis here the tomatoes are excited with a small impact hammer instrumented with a force cell and the response is measured with a small accelerometer which was attached to the tomato surface. Measurements and analysis were performed with LMS CADA-X software on HP 715 workstation combined with a DIFA-SCADAS II data acquisition system.

Analysis results show that the resonance frequencies can be accurately measured by a microphone. Secondly, the first mode shape, which is most conveniently used to estimate the firmness, is an 'oblate-prolate' shape (Figure 1). This mode shape has the largest deformations at the equator of the tomato. This fact implies that the best positions for measuring and impacting are located on the equator and 180° from each other. Taking these considerations into account, no significant difference between spherical and non-

spherical tomatoes was found.
The influence of internal compartment structures on the resonance frequencies was also studied. No meaningful differences could be found between frequencies, measured on locations of juicy parts as on flesh or wall constructions. While maturing, tomatoes get more soft. This effect can be monitored by the acoustic impulse response technique. The resonance frequency of all the mode shapes decreases gradually.

The modal analysis was an important step in setting up the testing procedure for the evaluation of the tomato firmness on the basis of its resonance frequency. Using the acoustic impulse response technique, this can be very easily used in practice to estimate tomato quality. The results of the research presented here show the method not to be sensitive to the global shape and internal structure of the tomato.

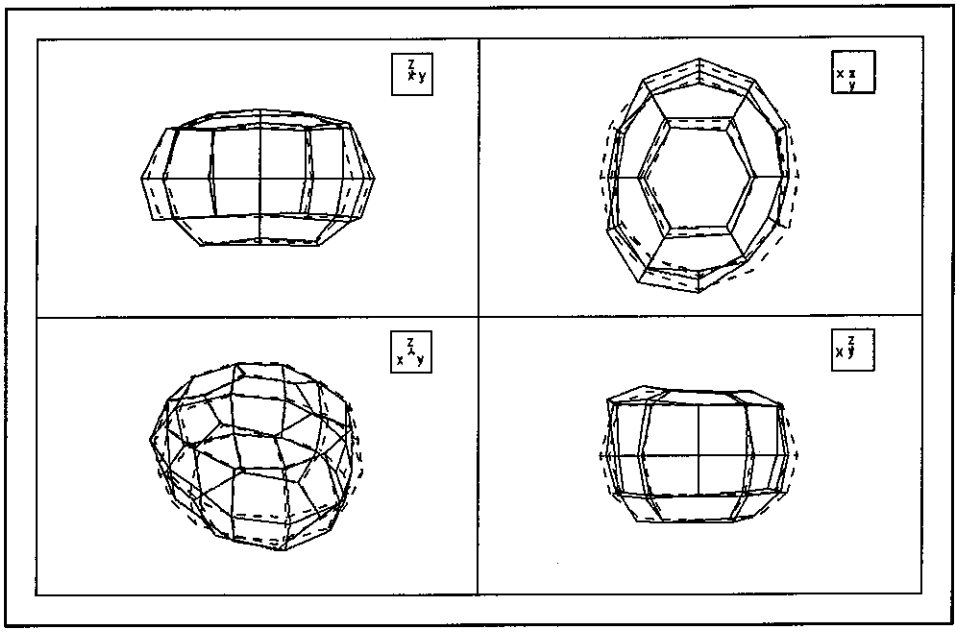

**Figure 1: First mode shape of a non-spherical tomato (±260 Hz)**

# Biomechanical properties of *Cyclamen persicum* MILL. flower stalks

Julia Vocke und Thomas Speck

Botanic Garden of the Albert-Ludwigs-University
Schänzlestr. 1, D-79104 Freiburg, Germany

Four cultivars of *Cyclamen persicum* with - in fully bloomed condition - different length and diameter of flower stalks have been investigated with regard to their biomechanical properties. In order to test, if the biomechanical properties change in the course of the ontogeny, flower stalks of each cultivar, in different developmental stages were experimentally studied. For characterization of the biomechanical properties, the following parameters have been determined quantitatively: 1.) tapering mode of the flower stalks, 2.) specific gravity of the flower stalks, 3.) flexural stiffness and Young's modulus of the flower stalks, 4.) weight of the flower bud respectively the flower.

**1.) Tapering mode of the flower stalks:** the vertical part of the flower stalks - i.e. the flower stalk section between the short, bent, in direction to the bulb conically tapering basic part and the short, apical section bent in form of a hook where the flower is attached - can best be discribed as a rotation paraboloid of 2. order (tapering mode: n = 0.5) for all cultivars and all ontogenetic stages (see figures).

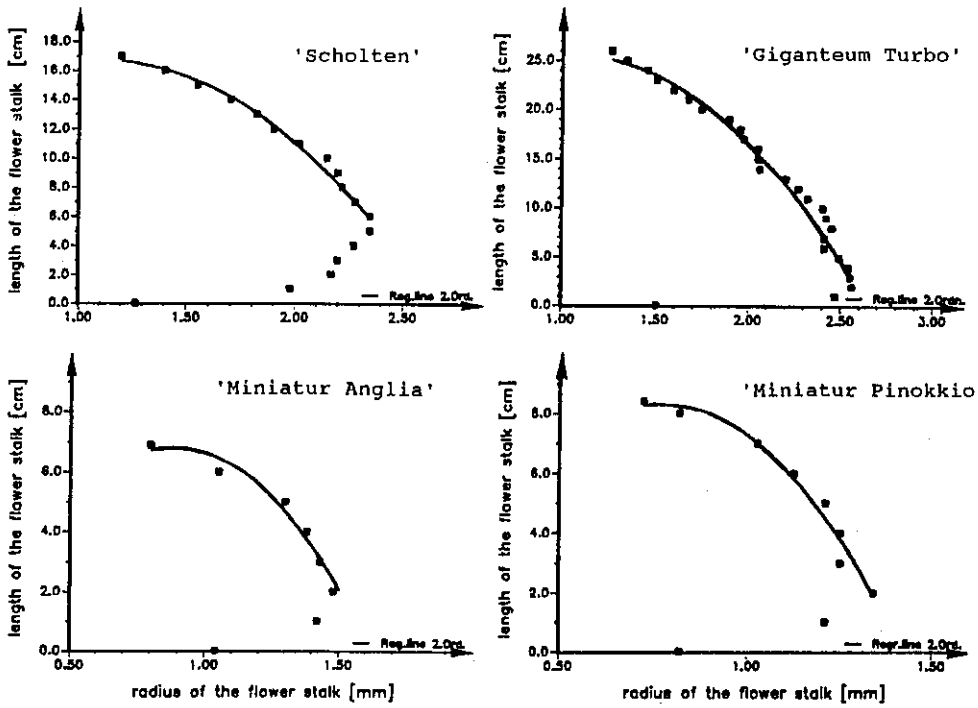


**2.) Specific gravity of the flower stalks:** the specific gravity of freshly gathered flower stalks does not differ significantly between the different ontogenetic stages neither of a single cultivar nor if combined for all four tested *Cyclamen persicum* cultivars (see table 1 & 2; average specific gravity of all tested flower stalks: $\gamma = 10.0 \pm 0.9$ [kNm$^{-3}$], n = 65).

**3.) Young's modulus of the flower stalks:** The Young's modulus (E) of the straight part of the flower stalks have been measured by 3-point-bending with discret increase of the bending weight forces. Young's modulus had been determined for different ontogenetic stages of freshly gathered flower stalks of the four tested *Cyclamen persicum* cultivars, grown in water saturated soil (water potential of the stalks: -0.15 [MPa] < $\psi$ < -0.47 [MPa], mean value $\psi$ = -0.33 $\pm$ 0.01 [MPa]). The Young's moduli greatly vary within the different tested cultivars as well as within the different ontogenetic stages (11 [$MNm^{-2}$] < E < 120 [$MNm^{-2}$]). Statistical tests show, that only flower stalks of the oldest studied ontogenetic stage - i.e. flower stalks with fully bloomed flowers - differ significantly from the other ontogenetic stages, having significantly higher Young's moduli as flower stalks of younger ontogenetic stages (see table 1). This is due to the increasing amount of collenchymatous respectively thick-walled parenchymatous cells in the stalks periphery found in the oldest ontogenetic stage.
**4.) Weight of flower bud respectively the flower:** The weight of the flower bud respectively the flower increases more or less continously from the early bud phase until the stage of fully bloomed flowers in the four investigated cultivars of *Cyclamen persicum* (the weight of the flower reaches during ontogeny about three- to fourfold its initial value).

These parameters allow to calculate the safety factor (s) of the flower stalks against failure by global buckling. These safety factors can be calculated as a quotient of the critical buckling length and the real length of the investigated stalk. The safety factor (s) means, that a stalk could be s-times longer until it would fail by global buckling due to the load produced by the weight of the stalk itself which is continiously distributed along its length and by the apical weight of the flower. All investigated *Cyclamen persicum* cultivars showed a decrease of the safety factors during the ontogeny of the flower stalks. The safety factors decrease from average s = 2.9 in the youngest studied ontogenetic stages to s = 1.8 in the oldest testet ontogenetic stages, i.e. of flower stalks with fully bloomed flowers. This finding may be correlated with the mode of seed dispersal in *Cyclamen*. The safety factors will be experimentally checked by loading the flower stalks with additional loads.

Table 1: Mean values of all tested cultivars (n = number of measurements)

| | specific gravity [$kNm^{-3}$] | Young's modulus [$MNm^{-2}$] |
|---|---|---|
| Ontogenetic stage 1 | 9.8 $\pm$ 0.8 (n = 12) | 34.5 $\pm$ 13.5 (n = 13) |
| Ontogenetic stage 2 | 10.1 $\pm$ 1.1 (n = 13) | 37.4 $\pm$ 16.1 (n = 12) |
| Ontogenetic stage 3 | 10.0 $\pm$ 0.9 (n = 14) | 40.5 $\pm$ 19.3 (n = 17) |
| Ontogenetic stage 4 | 10.1 $\pm$ 0,9 (n = 26) | 70.0 $\pm$ 23.2 (n = 20) |

Table 2: Mean values of the specific gravity of all ontogenetic stages

| | |
|---|---|
| 'Giganteum Turbo' | 10.6 $\pm$ 0.5 $kNm^{-3}$ (n = 11) |
| 'Scholten' | 10.2 $\pm$ 0.9 $kNm^{-3}$ (n = 20) |
| 'Miniatur Anglia' | 9.8 $\pm$ 0.8 $kNm^{-3}$ (n = 21) |
| 'Miniatur Pinokkio' | 9.7 $\pm$ 1.2 $kNm^{-3}$ (n = 13) |

**Literature:**

Dierks, K., Hafner, L., Tietge, H.-W. & Wenderling, R. (1986): Zum Tragverhalten des Alpenveilchens. - Symposium on Cellular Mechanics, Konzepte SFB 230, Heft **18**: 25-29.
Niklas, K.J. (1992): Plant biomechanics. University of Chicago Press, Chicago.
-.- (1994): The allometry of safety-factors for plant height. - Am. J. Bot., **81**: 345-351.

# THE MECHANICAL EFFICIENCY OF BAMBOO AND PALM

U.G.K. Wegst, H.R. Shercliff and M.F. Ashby
University of Cambridge, Department of Engineering,
Trumpington Street, Cambridge, CB2 1PZ, U.K.

It is well known that the natural materials bamboo and palm have a good specific stiffness in bending, and also resist buckling under their own weight. These properties are exploited in engineering design using bamboo. Microscopical examinations have been conducted to reveal the key features of the structure of bamboo and palm from an engineering standpoint. These show that: (i) both materials are composites of two components, i.e. bamboo and palm are fibre composites in which the fibres are aligned with the longitudinal axis of the culm or petiole respectively; (ii) the materials have a density and modulus gradient across the section, (iii) the composite material is disposed in an overall shape, such as a hollow tube (e.g. bamboo), or a tube with a low density core and a dense, stiff wall (e.g. palm) (Figures 1& 2).

The structural efficiency of bamboo, palm and other light, stiff natural materials may be evaluated using the Cambridge Materials Selector (CMS) software package, which is based on *material property charts*. These show, for example, Young's modulus $E$ against density $\rho$, as in Figure 3. Engineering performance is captured by an appropriate *merit index*, a combination of material properties which need to be maximised to maximise performance (e.g. the lightest beam of a given stiffness is the one with the maximum value of $E^{1/2}/\rho$). Figure 3 shows the line $E^{1/2}/\rho$ = constant, for bamboo: materials above the line give better performance in bending than bamboo; those below (including many common engineering materials) are less effective.

Further bending efficiency is obtained by disposing the material in an overall shape such as a tube. This may be described by a *shape factor*, which measures the gain obtained in flexural rigidity (at constant mass) by shaping the material, relative to a solid cylinder. The radial gradient in modulus in palm and bamboo gives a small additional shape factor of, at most, 1.5 (Gibson *et al.*, 1994). Figure 4 tabulates shape factors for structural natural and engineering materials, with the modified merit index for bending $(\Phi E)^{1/2}/\rho$ including shape. Bamboo in its natural tubular state still performs very well in bending compared to the much thinner tubes which can be made with engineering materials.

This approach allows conclusions to be drawn on the structural optimisation found in natural materials, how these may be exploited in engineering design and how the underlying principles may be employed in the development of new materials.

**References**

1. M.F. Ashby (1992), *Materials Selection in Mechanical Design*, Pergamon Press, Oxford.
2. M.F. Ashby, L.J. Gibson, U.G.K. Wegst and R. Olive (1994), The mechanical properties of natural materials I: Material property charts, to appear in *Proc. Roy. Soc. A.*
3. L.J. Gibson, M.F. Ashby, G.N. Karam, U.G.K. Wegst and H.R. Shercliff (1994), The mechanical properties of natural materials II: Microstructures for mechanical efficiency, to appear in *Proc. Roy. Soc. A.*

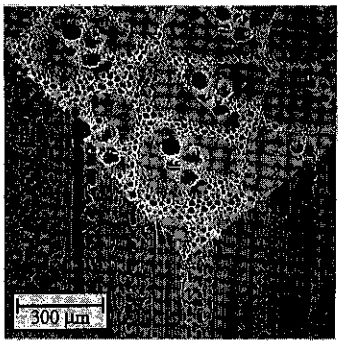


**Figure 1**: Micrograph of a cross-section of bamboo culm wall.

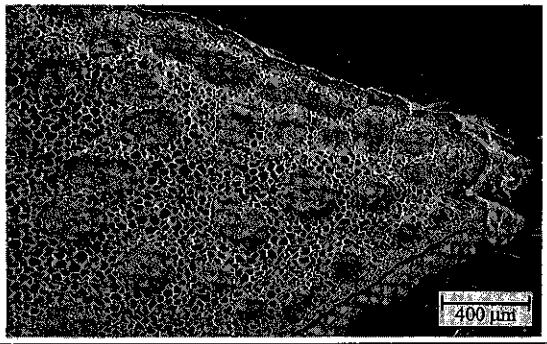


**Figure 2**: Micrograph of a cross-section of a palm petiole (Chamaerops humillis).

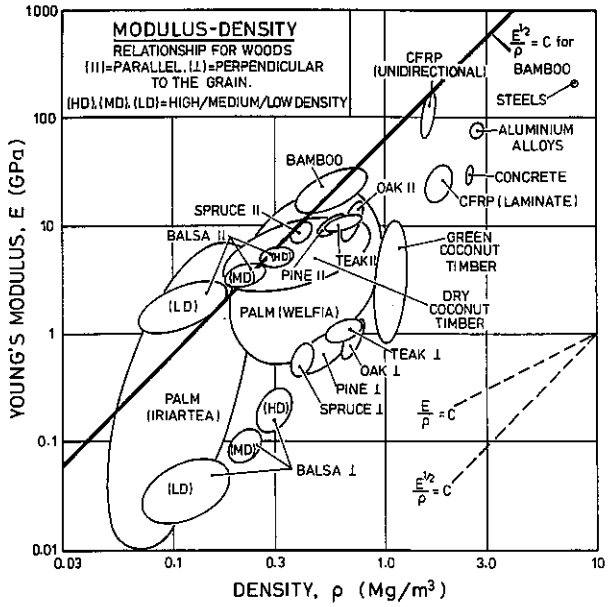


**Figure 3**: The Young's modulus $E$ - density $\rho$ chart for natural and engineering materials.

| MATERIAL | $E$ | $\rho$ | Shape factor | $E^{1/2}/\rho$ | $(\Phi E)^{1/2}/\rho$ |
|---|---|---|---|---|---|
| | GPa | Mg/m³ | $\Phi$ | $GPa^{1/2}/(Mg/m^3)$ | $GPa^{1/2}/(Mg/m^3)$ |
| Balsa (MD) | 4.0 | 0.2 | 4.0 | 10.0 | 20.0 |
| Oak | 11.5 | 0.7 | 4.0 | 4.8 | 9.7 |
| Pine | 11.0 | 0.5 | 4.0 | 6.3 | 12.5 |
| Bamboo | 22.5 | 0.75 | 7.5 | 6.3 | 17.3 |
| CFRP unidirectional | 160.0 | 1.5 | 15.0 | 8.4 | 32.7 |
| CFRP laminate | 45.0 | 1.5 | 12.0 | 4.5 | 15.5 |
| Aluminium alloys | 75.0 | 2.8 | 40.0 | 3.1 | 19.6 |
| Steels | 210.0 | 7.9 | 40.0 | 1.8 | 11.6 |

**Figure 4**: Shape factors and merit indices for bending for natural and engineering materials.

# Two methods to measure the strengh and stability of trees

Dr. Ing. Lothar Wessolly
Institut für BaumDiagnose
Gerokstaffel 1
D - 70184 Stuttgart
Allemagne

Trees are an indispensible part of town planning. However, They compete continously with others using the same site. As a result, a tree can suffer a variety of injuries which transform it into an unsuspected danger. Internal rotting in the part above ground or in the roots may have reduced itsstability to such an extent that the tree could break or uproot. The sudden exposure of a tree which was previously sheltered may lead to excessive loads which can turn into a hazard.

Within the framework of a research project carried out at the University of Stuttgart, methods began to be developed in 1986 to determine the stability of trees without destroying them. This non - destructive process was an important aim since any investigation involving destruction leads to subsequent damage and reduces stability still further. In engineering, it is standard practice to carry out an individual structural analysis of the object in question. The loads, the loaded structure and the materials involved are analysed as one unit.

In the statics of trees, we distinguish two basic types of failure: uprooting and breaking. In the former case, the roots are levered out of the ground, in the latter case, the tree above ground breaks under excessive bending pressure.

Neither of these two types of failure can be predicted theoretically. The missing values have to be ascertained for each individual tree. In order to investigate the anchoring, the **stability,** the **inclino - method** was developed in practical experiments. Following the determination of the size of the crown and the analysis of the prospective loading during hurricane winds by means of computer graphics, the tree is subjected to a wind-equivalent load using a rope winch or similar method. This load is measured. Simultaneously, the resulting inclination is measured between the bases of the main roots with an **inclinometer.** Measurements taken on more than 1000 trees situated in towns an parks have revealed a tilding behaviour, described in a **generalised tilt curve**. The tild mechanics of trees has thus become clear for the first time. In the case of normal soils, the force can be increased to an inclination of only about 2,5 - 3 degrees. In then remains constant, falling again for higher inclinations in dependence of the quality of the anchoring. A knowledge of this generalised tilt curve allows the prediction of the expected tilt load in the case of destruction-free inclinations below 0,5 degrees. With a comparison of the loading analysed for hurricane conditions, the stability of a tree can be stated explicitly without digging up the roots. No other method of analysing the stability than that using the difference in inclinations is as yet known.

The analysis of fracture limits also uses methods from experimental mechanics and is based on the following: during bending, the wood fibres are loaded in cross-section depending on their position. The further they are towards the centre of the trunk, the less significant they are for the statics. Thus, the wood fibre subject to the highest loading is always directly beneath the bark. The loading is evident in the strain. We have now discovered that the bark undergoes this strain process without resistance. this means that, if two needles are fixed vertically at a distance in the bark, their relative displacement under a bending load can be

measured. This measurement is thus also carried out without destruction of the tree and allows the investigation of any number of areas on it. We have mentioned the special strain measurement device, the **elastometer**. For this investigation, the crown of the tree is subjected to forces. The elastometer is moved vertically over an area of suspected rotting until the weakest point has been found, this being the point with the greatest strain value. A comparison of the wind-equivalent load and the load for hurricane conditions yields the strain in the case of hurricane. We now compare whether or not this strain exceeds the limit value for the specific type of wood in a hurricane. The limit value is defined as the point at which a load increase causes plastic deformation in the compression zone. A subsequent failure is determined by secondary processes and is not directly connected with this primary failure. The limit values for green wood in the case of short-term loading, as in a storm, are recorded in the "Stuttgart Strength Catalogue". With the elasto-method, the fracture point and fracture limit value can be determined in a closed system integrally and without causing damage. The validity of this procedure has been proven in numerous experiments.

Moreover, growth stresses in trees an the response of trees in storms can also be measured with the **elastometer.** Long-term observations of damage caused by fungus are naturally also possible on a living tree.

As a reinforcement of the load analysis, storm-load investigations of trees are beeing carried out with the aforementioned mobile measuring devices in northern Corsica. The measurements are taken with respect to time: how high is the maximum loading of a tree during a particular hurricane period ? In this way, it is unnecessary to analyse each movement of the tree and each storm eddy. The drag coefficient of trees in hurricane conditions is between cw = 0,1 and 0,35.

Both the elasto- and the inclino-method - wich can be applied simultaneously - represent well-tested techniques which have considerably extended the possibilities for tree diagnosis in a safety context and opened new areas of research.

**Towards an understanding of the mechanical behaviour of cereal crops**

Ethel M. White

Department of Agriculture for Northern Ireland, Plant Testing Station, Crossnacreevy, Castlereagh, Belfast BT6 9SH

Crops of the temperate cereals - wheat, barley and oats - are somewhat artificial because they are monocultures of genetically identical plants. They are also managed 'to the limit' in Western Europe where growers' objectives have been, until recently, to produce maximum yields by maximising the quantity of N fertiliser applied and using plant growth regulators to reduce lodging. This has put a strain on both breeders and agronomists in their endeavours to improve productivity and at the same time to minimise problems associated with damage due to lodging. Whilst their efforts have been successful in that very high yielding crops can be grown without problems associated with straw damage, we have still some way to go in our understanding of the phenomenon of lodging.

In this paper, the structure of the cereal plant will be examined from a mechanical perspective and the characteristics contributing to the plant's mechanical behaviour will be identified. The influence of agronomic factors on these characteristics will be discussed, using results from experiments conducted on winter wheat and winter barley in Northern Ireland.

The type of damage described as lodging will be considered in relation to 'synoptic' mechanical behaviour of the crop. Lodging is generally considered to be a catastrophic event resulting from failure somewhere in the shoot/root/soil system. The various theories about the mode of failure will be discussed and alternatives presented and explored.

Finally, the nature of crop management will be taken into account in a consideration of strategies which can be developed to limit and control damage due to lodging.

# THE EFFECT OF MOISTURE CONTENT ON THE MECHANICAL PROPERTIES OF A SEED SHELL

*Lisa WILLIAMSON and Peter LUCAS*

Department of Anatomy, University of Hong Kong
Li Shu Fan Building, 5 Sassoon Road, HONG KONG

A seed contains the embryo - a potential member of the next generation of a species - and its food store. The latter is an attraction for seed predators. Most seeds are heavily protected from predation by chemical or mechanical means. Many seeds, though not normally those species from tropical rainforests, can survive a considerable reduction in their moisture content and reduce their metabolic activity to a very low (dormant) level.

The mechanical properties of the seed shells of the African mongongo nut, *Schinziophyton rauteneii* (Euphorbiaceae), were measured by compressive C-ring tests while they were avi-dry and also after soaking in distilled water. Young's modulus was about 5 GPa and fracture strength was 45-50 MPa, for both conditions. However, fracture toughness was affected significantly by moisture content. The critical stress intensity factor (Kic) of air-dry specimens was 27% greater and the work of fracture (R) 69% greater than those of wet specimens. This difference corresponded well with microscopic observations of the complexity of the fracture surface. Viewed either by scanning electron microscopy or confocal microscopy, cracks in wet shell deviated neatly around individual fibres while cracks in air-dry shells either crossed individual fibres or ran obliquely across the outer layers of the secondary cell wall leaving a feathered appearance. It is proposed that the increase in toughness of shells which would be obtained from air-drying may help protect embryonic seed tissues from predation by larger animals (e.g. vertebrates such as rodents) after abcission from the parent plant. These seeds can then lie on the ground or in the soil as a "seed bank".

In the effect on toughness that we have demonstrated were to be general, then the outer protective layer of such seeds, nearly always a thick-walleddead tissue -a "pallisade" fence-like tissue if not truly fibrous, would act more efficiently after air-dryin. This would be expected to reduce the rate of seed loss to predators, particularly from those predators large enough for crack propagation between cells to be a factor. These would include many mammals, typically rodents which specialise on dry fruits, but also peccaries and some human groups. The effectiveness of the fruit pod (a dry type of pericarp which protects orthodox seeds in, for example, legumes) may also be enhanced by drying. Some seed predators, particularly primates like new and old world monkeys and also apes, tend to eat unripe seeds. The need to attack the seed while the toughness of the seed coat or shell is still low may play some part in this decison. Germination of a seed follows a period of water uptake. An increase in water content would decrease the toughness of protective tissues. However, this reduction in toughness is probably necessary if germination is dependent on turgor pressure to open the shell. Mechanical protection is obviously ruled out at this stage.

Many thanks to Charles R. Peters for providing mongongo nuts that he collected. This study was supported by grants CRCG 337/031/0015 from the University of Hong Kong and RGC HKU324/93M from the Research Grants Council of Hong Kong.

# Axial alteration of stem and leaf sheaths stiffness in cereal plants as revealed using an ultrasonic method

Jacek Żebrowski

*Plant Breeding and Acclimatization Institute*
*Radzików, POB 1019, PL-00-950 Warsaw, Poland*

Stems tapered accropetally, the presence of leaf sheaths enforcing lower parts of internodes and peripheral location of sclerenchyma on cross-section are the most striking features of cereal plant shoots related to their mechanical function as beam structures. Material properties of the shoots have been determined as averaged over whole length of the internodes and the leaf sheaths (Hozyo and Oda, 1965; Niklas, 1990). The present study investigates the alteration of stiffness within particular internodes and leaf sheaths in four species of cereals at two stages of their development.

## MATERIALS AND METHODS

Plants of rye, triticale, wheat and barley were harvested at heading and milk maturity. The stiffness was examined in c. 3 cm long sections of internodes and separated leaf sheaths by means of a through-transmission ultrasonic method based on propagating the longitudinal waves of the frequency of 100 kHz in axial direction of the specimens. The specific dynamic modulus of elasticity calculated as the squared ultrasound velocity was a measure of the stiffness. The ultrasonic measurements were performed using a concrete tester (model CT1, UNIPAN, Poland) interfaced with a computer.

## RESULTS

The measurements of the ultrasound velocity revealed considerable alteration of the stiffness within particular internodes and leaf sheaths that follows pattern similar for all tested species of cereals. Much more pronounced heterogeneity in the material properties within the internodes was observed at heading (Fig. 1), when the stems still elongate, in comparison to that at the stage of milk maturity (Fig. 2), when the development of all tissues was completed. Local reduction in the stiffness from values ranging from 2 to 8 MPa $m^3$ $kg^{-1}$ typical for mature sections to values much below 0.1 MPa $m^3$ $kg^{-1}$ in elongating zones made the stems at heading structures instable even under their own weight. The leaf sheaths, which protect the elongating zones and reinforce the shoots exhibited the stiffness increasing basipetally, in the direction of increasing flexibility of the internodes (Fig. 1). In fully developed stems at milk maturity the stiffness was distributed rather uniformly along whole its length with local maxima occurring at mid parts of the internodes. Relatively taller plants of rye and triticale exhibited higher values and more pronounced alteration of the stiffness within both the internodes and the leaf sheaths in comparison to wheat and barley. The local variations of the stiffness were found to coincide, generally, with the alterations of the second moment of inertia.

The present studies indicate that the vertical alteration in the material properties results not only from the intercalar pattern of the shoot growth but also has some functional significance with respect to the mechanics of cereal plants.

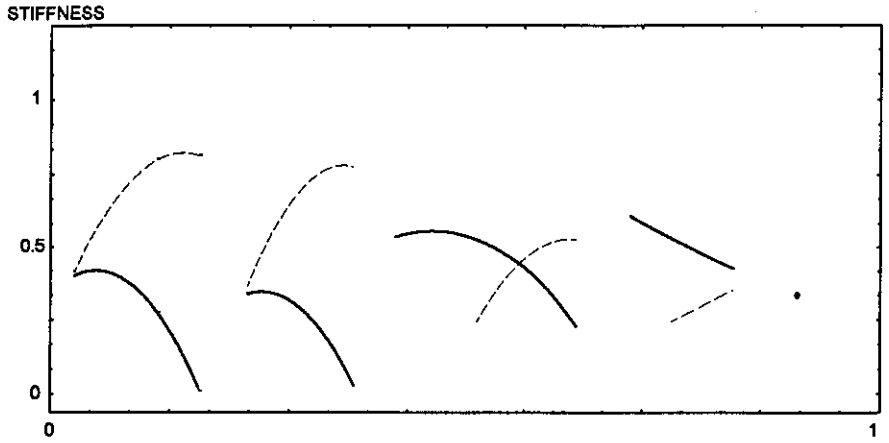


Fig. 1. Schematic presentation of a typical pattern of stiffness alteration in stem (solid line) and leaf sheaths (dashed line) along shoot axis in cereal plants at heading. The stiffness, determined using an ultrasound velocity method, is given in relative values.

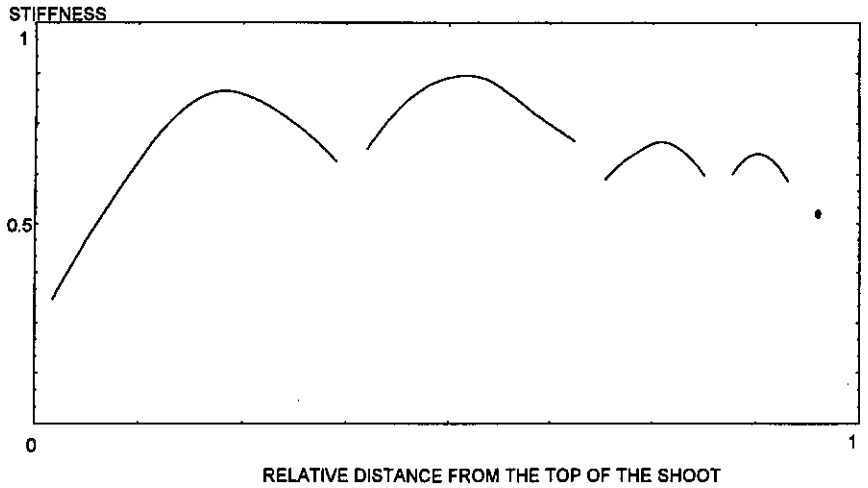


Fig. 2. Schematic presentation of a typical pattern of stem stiffness alteration along shoot axis in cereal plants at the stage of milk maturity. The stiffness, determined by means of the ultrasound velocity measurements, is given in relative values.

## REFERENCES

Hozyo Y., Oda K. (1965) Jap. J. Crop Sci. 33: 263-267
Niklas K.J. (1990) Ann. Bot. 19: 962-966

# Déformations du fût et fibre torse chez l'épicéa (*Picea abies Karst.*)

Dr. Ernst Zürcher
Prof.Dr. Ladislav J. Kucera
Matthias Brunner

Ecole Polytechnique Fédérale de Zürich, Département de Recherche sur les Forêts et le Bois, Chaire des Sciences du Bois, ETH-Zentrum, CH-8092 Zürich.

**Résumé**

Les déformations du fût, provoquées par une irrégularité des cernes d'accroissement, ainsi que la fibre torse (forte déviation des éléments du xylème par rapport à l'axe de la tige) provoquent une importante diminution de la qualité et de la valeur du bois. Ces anomalies de croissance sont notamment à l'origine d'un comportement au séchage irrégulier (gauchissement) et d'une réduction de la résistance à la flexion.

Ces particularités de la formation du bois ont connu récemment un regain d'intérêt, notamment en relation avec la thèse selon laquelle elles représenteraient sous cette forme un phénomène nouveau, à tendance croissante au courant de la dernière décennie.

Par l'étude de l'anatomie et de la morphologie d'un groupe d'arbres particulièrement atteints, ce travail cherche d'une part à distinguer clairement chacune de ces deux particularités de croissance. D'autre part, il détermine à partir de quelle année on peut respectivement les observer, en essayant d'établir la relation avec des interventions sylvicoles notifiées depuis l'année 1926.

Il en ressort les résultats principaux suivants:

- la densité des rayons médullaires, leur hauteur, le diamètre des canaux résinifères et leur enveloppe épithéliale varient selon qu'ils soient mesurés dans des cernes annuels réguliers (normaux) ou irréguliers (provoquant des déformations du fût),
- dans les zones de fût excentriques, la proportion de bois de réaction est supérieure sur le grand rayon, intermédiaire sur le rayon nord et minimale sur le petit rayon,
- l'excentricité est orientée selon l'axe sud-ouest (petit rayon) - nord-est (grand rayon),
- le degré de déformation du fût (cannelures) décroît rapidement de bas en haut dans les deux premiers mètres,
- chez les arbres de la strate dominante (à fortes déformations), les cernes irréguliers apparaissent presque simultanément durant les années 1964-1967,
- à partir de cette époque et surtout dans les dernières années (périphérie), les parties de cernes hypertrophiées sont placées sur les cernes successifs selon un mouvement centrifuge en sens généralement inverse de la rotation des aiguilles de montre - ce phénomène est décrit pour la première fois ici, et se place probablement sous le principe de la spiralité régissant les végétaux dans différents niveaux de structure,

- la déviation des fibres à la surface du fût par rapport à l'axe est maximale sur les faces est et nord,
- la fibre torse orientée vers la gauche est trois fois plus fréquente que celle orientée vers la droite,
- la fente de rondelles selon les quatre directions cardinales confirme la formation de fibre torse orientée systématiquement à gauche dès les premières années, et ceci indépendamment de l'apparition ultérieure de cernes irréguliers,
- sur les grands rayons des rondelles excentriques, la part de fibre torse orientée à droite est supérieure à celle observée sur les petits rayons,
- la déviation des fibres par rapport à l'axe est donc un phénomène distinct et indépendant de déformations apparaissant sur la surface du fût.

# Biomécanique des végétaux
# *Plant biomechanics*

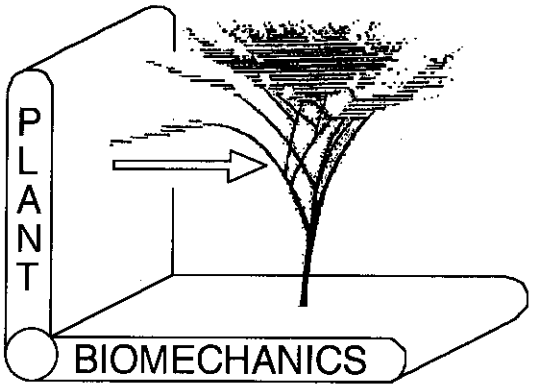


**EXPOSES INVITES - *INVITED TALKS***

Colloque interdisciplinaire
du Comité national de la recherche scientifique
Montpellier (France) du 5 au 9 Septembre 1994

**Volume 2, Number 2** **June 1994**

Special Issue:
Plant Biomechanics Congress

BIMIEL 2(2) 77–192 (1994)
ISSN 1059-0153

# Biomimetics

**PLENUM PRESS • New York and London**

# BIOMIMETICS

*Biomimetics* is an international interdisciplinary forum for the publication of original papers in areas at the intersection of biology and engineering. The journal publishes research papers and short notes (2000 words or less) on: mechanical and chemical analysis of structural biological materials leading to an understanding of their performance; development and production of materials based on direct copying of nature; analysis of the mechanical performance of materials produced using biotechnological processes; novel applications of biomimetic materials; improvements in the design of current organisms based on mechanical analysis of their structure; and analysis of the optimization criteria used in natural materials and structures. *Biomimetics* also publishes letters to the editor (published at the editor's discretion), book reviews, and announcements of relevant meetings.



---


*Biomimetics* is published quarterly by Plenum Publishing Corporation, 233 Spring Street, New York, N.Y. 10013. *Biomimetics* is abstracted or indexed in Alerts (Series), Aluminium Industry Abstracts, Applied Mechanics Reviews, Chemical Abstracts, Current Contents, Engineered Materials Abstracts, Metals Abstracts, and Physics Abstracts.




Advertising inquiries should be addressed to Advertising Sales, Plenum Publishing Corporation, 233 Spring Street, New York, N.Y. 10013—telephone (212) 620-8495 and fax (212) 647-1898.

Subscription inquiries and subscription orders should be addressed to the publisher at Subscription Department, Plenum Publishing Corporation, 233 Spring Street, New York, N.Y. 10013 or faxed to the Subscription Department at its number (212) 807-1047. Subscription rates:

Volume 2, 1994 (4 issues) $125.00 (outside the U.S., $145.00). Price for individual subscribers certifying that the journal is for their personal use, $50.00 (outside the U.S., $60.00).

Postmaster: Send address changes to *Biomimetics*, Plenum Publishing Corporation, 233 Spring Street, New York, N.Y. 10013.

Printed in the USA.

# Biomimetics

**Volume 2, Number 2** **June 1994**


## CONTENTS

### Special Issue: Plant Biomechanics Congress

### Montpellier, France, September 5–9, 1994

*Biomimetics, Vol. 2, No. 2, 1994*

# Biomechanics in Botany: A General Introduction[1]

**Julian F. V. Vincent**[2]

*Plants are ideal subjects for biomechanics, often better than animals. At our current levels of understanding there are several problems which seem ready to be solved. These are the energetics of cell shape, wound repair and growth, the structural parameters of turgor systems, the energetics of lignification, plant form and evolution, plants as foods, designing for fracture, plants as a renewable resource for structural materials, and biomimicry of the structures and mechanisms of plants. A checklist is provided, covering these and related topics.*

**KEY WORDS:** plants; growth; cellular mechanics; turgor; cell shape; lignification.

## INTRODUCTION

Plants are a far more convenient subject for the study of biological engineering than are animals. They are more simply constructed, have fewer cell types, do not move around nearly so much, are easier to maintain under experimental conditions, and do not require a license for their experimentation. At the same time we can learn general principles from them such as mechanical sensing and response at the cellular level, the pros and cons of hierarchical construction, and the nature of mechanical optimization in biology.

The mechanisms used to reach the shapes of plants (morphogenesis) and the mechanical properties and possibilities of those shapes (biomechanics) form the bulk of the subject matter of this conference. In addition, the mechanical properties and design of plants are important in food science, agriculture, horticulture, etc., and can suggest ideas for technology (Velcro is a well-known example). I highlight some problems in plant biomechanics which I see as

[1] This is the published version of a paper presented at the Plant Biomechanics Congress, Montpellier, France, September 5-9, 1994.

[2] Centre for Biomimetics, The University, Reading RG6 2AT, United Kingdom.



1059-0153/94/0600-0077$07.00/0 

interesting. One of the purposes of a conference like this must be for people to assess each other's lists of imperatives and modify them accordingly. A collection of attributes and ideas which can be used as a checklist and framework for the conference appears in Fig. 1.

## CELLS

D'Arcy Thompson (1917) showed that the shapes of many cells could be mimicked by soap films. In some ways this was a disservice, since some think that the shape of cells is defined by the same balance of forces which shapes soap bubbles. That the shapes are similar is true not only of isolated cells but of cells surrounded by others (Marvin, 1939). However, it is also true that the soap film, being fluid, cannot support shear. Therefore the curves which a soap film, and many plant cell walls, displays are those in which there is no shear. This will necessarily be energetically cheaper to construct and therefore the shape of choice. It should therefore be possible to make some predictions: In an environment where energy is scarce, the shapes of cells will be simple. As the availability of energy increases, cells will take on more complex shapes, which will help them access energy more effectively but which themselves will require more energy for maintenance. The optimization is obvious; the experiments require some estimate to be made of the energy requirements of assuming shapes which are varying distances from a shear-free shape and the increased efficiency of those shapes.

The subcellular morphology of plants is well documented, but the mechanical significance is still under debate. Of the cellular components, microtubules are probably the stiffest materials and so are the most obvious candidates for the maintenance of shape. Anisotropy in their arrangement can lead to specific shapes, and changes in their arrangement can lead to changes in shape. This has been observed as part of the process of wound healing (Hush *et al.*, 1990; Hush and Overall, 1991). But how does the cell sense wounding of the tissue within which it sits? The biochemist would immediately talk of chemicals released from cells; the engineer would think about detection of nonuniform strain fields. Events at the apical meristem such as determination of leaf primordia have been associated with nonuniform strain distribution in the cell walls, due either to natural causes or to specific lesions caused by laser. The implication must be that the biochemistry, if it does not lead (which I think is unlikely), must follow the distribution of strain (Steucek *et al.*, 1992) modulated by turgor pressure and the anisotropic orientation of cellulose fibrils in the cell wall (Green, 1991). The strain is probably sensed by changes in membrane permeability—a specific pathway opens up in the cell membrane. Certainly animal cells can respond to changes in shape by changing their synthetic pathways (B. Thorp, personal communication) and do so in a remarkably short time. In Reading we

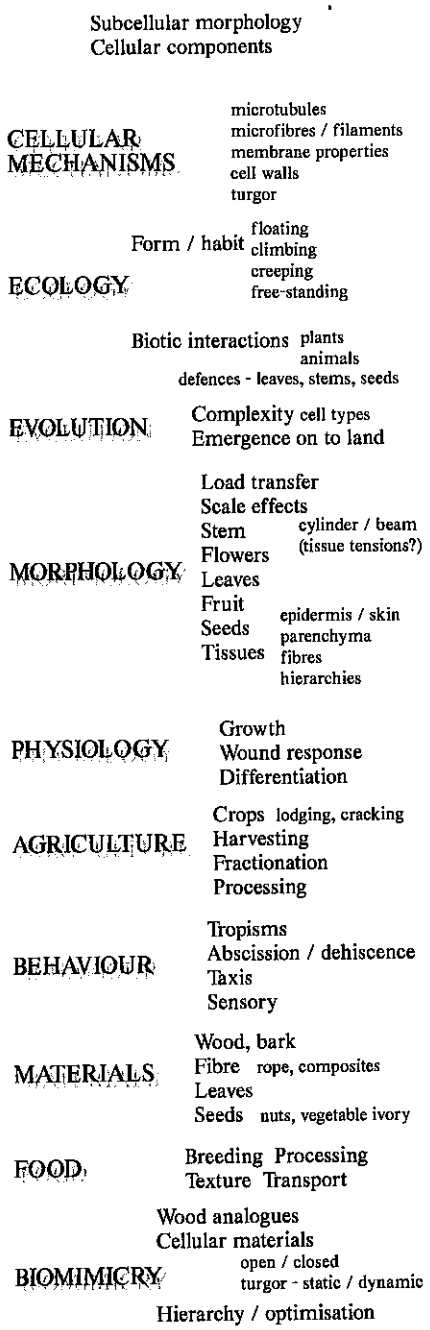


**Fig. 1.** A collection of attributes and ideas that can be used as a checklist and framework for the conference.

have found that potato cells can respond very quickly to applied stress. No doubt experienced experimental botanists know of many more examples.

## TISSUES

At the tissue level we are concerned with assemblages of cells which may or may not have an internal pressure above ambient. The mechanics of nonturgor systems are probably moderately well understood (Gibson and Ashby, 1988) but turgor systems continue to present problems (Jeronimidis, this conference) since the response of the turgid cell to external stress depends on its surroundings. A nice example of this is given in the anisotropy of apple flesh, where radial compression (perpendicular to the columnar arrangement of the parenchyma cells) leads to failure in a band across the specimen, while compression in the orthogonal direction leads to shear failure (Khan, 1988). The difference in response is due to the space each cell has available in which to deform. The mechanical properties of leaves and stems have been modeled as a simple sandwich or column of foam with a continuous membrane (epidermis) on the outside (Gibson *et al.*, 1988). This approach is of only limited success since it gives the foam bulk properties which are not derived from the properties of the individual cells (size, wall thickness) and does not take account of turgor. The problems were also sidestepped by Vincent and Jeronimidis (1991), who, trying to model the flowering stem of the dandelion, *Taraxacum officinale*, found they could not cope with the turgor system as an assemblage of cells, but could use the analogy of a metal expanding as it is heated. The gradient in the amount of cell wall material across the stem (1:20, with the largest amount externally) makes the stem equivalent to a bimetallic strip structure which can be solved mathematically.

## STRUCTURES AND STEMS

For many years the perceived wisdom as to the state of stress in an herbaceous stem has been, broadly, that the inner tissues are held in compression and the outer ones in tension. For instance, Strasburger *et al.* (1903) say that "the rigidity of parenchymatous tissue although to a large extent dependent upon the tension arising from the turgidity of its individual cells, it nevertheless considerably enhanced by the opposing pressure between the inner and outer tissue systems. . .The tension thus arising from the mutual resistance of different tissue systems acts upon the various plant organs like the turgidity of the single cells, and keeps them firm and rigid." The confusion here is due to inadequate distinction between material and structure. It is certainly true that the way in which the cells are packed into the herbaceous stem leads to mutual constraint, which can be released only when the structure of the stem is destroyed, but the

fact that a strip of stem will curl when the constituent cells are turgid is most readily explained by pointing out that the walls of the inner cells are much thinner and therefore will extend farther under the same or similar internal turgor pressure. Thus the inner cells find themselves on the outside of the curl. That this is due simply to the interaction of turgor and the cell walls is shown by strips in which the cells are plasmolysed and have no positive turgor. These strips are straight, showing that under these conditions the strain in the cell walls is constant across the stem (in fact under these conditions the epidermal layer is wrinkled, again suggesting that the cell walls are contracting when turgor is lost). Thus in the intact turgid stem, the cell walls are all at the same state of strain but obviously, therefore, not at the same state of stress since they are of different thicknesses. Therefore a turgor-stiffened system exists in some sort of mechanical equilibrium. If the constraints of the structure are changed (e.g., by cutting it in half and destroying the continuity of the epidermis), then the stresses and strains will be redistributed within the structure and it will assume a new equilibrium shape. Clearly turgor systems are far from understood; we need much more clear thinking if we are to bridge the gap between physiology and mechanical properties.

The decision by the plant to shift from turgor to lignification as the main mechanism for support must involve a number of factors. Although all plants above about 30 cm high seem to have some lignification in the stem, they do not necessarily increase in stiffness. A number of student projects at Reading have shown that in the umbellifers of the genus *Heracleum*, whose stems are made of a number of similar internodes, it is impossible to tell simply by measuring the stiffness of the stem whether the main support is lignification or turgor. Despite the fact that in the one lignified herb which we have analyzed so far (*Nicotiana*) the ring of lignified tissue clearly dominates the stiffening effects of the various tissues, the extra stiffness which lignification gives to woody cells is not required for structural stiffness of the stem. The thought arises that the plant is minimizing the total energy used to maintain its shape. If the plant is to last for a shorter time, low-level expenditure of energy on maintaining turgor is cheaper; if it is to last for a longer time, then it might be worth a short burst at a comparatively high energy level to lignify, and then reduce the energy necessary to maintain turgor in those tissues. Is this what happens?

## EVOLUTION

The morphology of the stems of fossil plants can be used to predict their mechanical properties (Speck *et al.*, 1990). Using the flowering stem of *Taraxacum* as the modern type, Vincent and Jeronimidis (1991) assessed the likelihood that *Rhynia gwynn-vaughni* was truly a land plant. In section, the gradients of cell size and cell wall thickness between the center and the periphery

of the stem are much less pronounced and much more variable in *Rhynia*, which has cell walls which are slightly thicker in the outer layers of cells (3 $\mu$m) than the inner (1 $\mu$m), but suffers by having a distinct zone (the inner cortex) made of one or more layers of large cells just beneath the outer layer (Edwards, 1986). The calculated distribution of stem stress shows that the maximum stem stresses ascribable to turgor are less than in *Taraxacum*. In *Rhynia* the prestress in the center of the stem is much higher than in *Taraxacum*, which seems rather a bad design since prestress in this position can contribute so little to bending stiffness. Rough calculation shows that the prestress in the dandelion stem is just about sufficient to resist side loads due to wind. With its lower prestress *Rhynia* could not support anything at the tip of its axis which was likely to generate drag forces. It is tempting to suggest that *Rhynia* was actually partly submerged, like many plants found today growing at the edge of lakes and ponds. It is unlikely that they grew totally or continually partially submerged since they have stomata along the entire length of the stem (Kidston and Lang, 1917). However, they are always found densely packed in the chert with their stems laid parallel as if they were growing in clumps. So they might have needed to grow in dense stands simply to make up for the shortcomings in the design of their stem. Since there are so many specimens of *Rhynia* in such good preservation, it would be very interesting to look for evidence of modes of failure of the axis.

## PLANTS AND ANIMALS

The mechanical properties of plants as food are of importance for the animals which feed on plants (Vincent, 1991). The mechanical design of grass has been shown to dictate the way in which animals feed on it (Vincent, 1982, 1983; Wright, 1992) and the ease with which they can extract the nutrients (Lees, 1984; Lees *et al.*, 1981, 1982). This reduces to problems in fracture mechanics at all levels of morphology, ultimately at the cellular level. Very little is known about the mechanical interaction of teeth with plants, and whether it is better for plant cells to resist being broken open by being tough and strong (which is expensive in terms of dry matter in the cell walls) (Choong *et al.*, 1992) or to break open in a brittle ("crisp") manner and hope that the path of the fracture will not branch, thus opening the minimum number of cells and restricting the availability of nutrient to the animal (Vincent and Sibbing, 1991). There is some indication that plants make themselves tough specifically to avoid being eaten (Lucas *et al.*, 1991; Lucas and Corlett, 1991; Wright, 1992).

## DIRECTED FRACTURE

The fracture mechanics of abcission and dehiscence have not been investigated, although a moderate amount is known about the morphology and physiology. There is a fruitful area of work here, which would yield much benefit.

Dehiscence in fruits is, mechanically, of two kinds. The capsule may simply split open to expose the seeds or it may dehisce explosively to broadcast the seeds. In the former the expectation is that the line of dehiscence will be a line of weakness. In the seed pod of rape the middle lamella is dissolved along the joint between the valves and the central diaphragm which supports the seeds. It remains joined in a few places so that a sharp knock will rupture it and send the seeds flying. The energies and forces involved in this mechanism are unknown.

The mechanics of explosive dehiscence have been investigated in the soybean (Weeks *et al.*, 1975). The strength of the dehiscence layer and the force available from the pod were measured by pulling the pod open and then forcing the pod valves together. The force needed to close the pod was assumed to be that available for dehiscence and is directly related to the thickness of the pod (i.e., the elastic prestrain is probably constant and independent of thickness). The force increases greatly as the pod dries out, showing that as the stiffness of the pod wall increases with reduced water content, a constant prestrain results in higher prestress. The strength of the dehiscence layer increases as the water content falls and then becomes more or less constant but very variable, which is typical of brittle fracture, which can be very sensitive to cracks and imperfections. If one wanted to breed a pod which would not dehisce before harvesting, it might be easier to select for a thinner pod wall for a given size of pod, rather than a stronger dehiscence layer (Weeks *et al.*, 1975).

## PLANT MATERIALS

The use of plants as "renewable" sources of materials is gaining political and financial credibility as the concepts of ecology and "Spaceship World" finally filter through to the politicians. The most credible additions to current materials are fibers (from flax, hemp, and such traditional sources as *Urtica*), which will find uses in fiberboard, cementitious and phenolic resin composites, and paper, replacing current wood sources (though this will take up to 50 years, even if the benefits are immediately apparent). Eucalypts are the current best source of quality paper fiber, and there is work in progress to reduce the lignification of these trees transgenically, thus reducing both energy requirements and pollution. If plant fibers are going to be more widely used in materials, then it is important not only to characterize them properly but to persuade those who use them to use the tools of materials science to analyze the properties of the materials into which the fibers are incorporated. For instance, the current units used to describe the mechanical properties of paper are a mess, mixing forces with weights per unit area. They are little better than quality control tests and of little or no use in forecasting the results of specific changes in the components

of the material. Perhaps we should think of some way of ensuring that the industrial and agricultural aspects of plant mechanics are properly researched.

## BIOMIMICRY

If plants are such successful machines, why should we not learn from them? Relieved of the limitations of processing at ambient temperatures, using readily available materials, using the weakest of bonds compatible with the necessary stiffness and strength, we should be able to do better than nature. The trick is understanding the mechanisms and materials which we are trying to copy. A successful fiberglass material based on the fracture toughening mechanism of wood is 50 times tougher, weight for weight, than any other man-made material (Gordon and Jeronimidis, 1980). Cellular materials offer significant material efficiencies, and the possibilities of turgor-driven systems have not yet been explored. The blueprints exist in nature for a variety of hydraulic control and actuation systems and for an infinite variety of buildings and structures. As always, the trick is discovering which parts of nature's design to steal and which bits to leave alone until we are clever enough to understand them.

## REFERENCES

Choong, M. F., Lucas, P. W., Ong, J. S. Y., Pereira, B., Tan, H. T. W., and Turner, I. M. (1992). Leaf fracture toughness and sclerophylly, their correlations and ecological implications. *New Phytol.*, **121**:597–610.

Edwards, D. S. (1986). *Aglaophyton major*, a non-vascular land-plant from the Devonian Rhynie chert. *Bot. J. Linn. Soc.* **93**:173–204.

Gibson, L. J., and Ashby, M. F. (1988). *Cellular Solids, Structure and Properties*, Pergamon, Oxford.

Gordon, J. E. and Jeronimidis, G. (1980). Composites with high work of fracture. *Phil. Trans. R. Soc. Lond. A* **294**:545–550.

Green, P. B. (1991). Morphogenesis. In Steward, F. C., and Bidwell, R. G. S. (eds.), *Plant Physiology, a Treatise, Vol. X. Growth and Development*, Academic Press, New York, pp. 1–64.

Hush, J. M., and Overall, R. L. (1991). Electrical and mechanical fields orient cortical microtubules in higher plant tissues. *Cell Biol. Int. Rep.* **15**:551–560.

Hush, J. M., Hawes, C. R., and Overall, R. L. (1990). Interphase microtubule re-orientation predicts a new cell polarity in wounded pea roots. *J. Cell. Sci.* **96**:47–61.

Jaffe, M. J., Telewski, F. W., and Cooke, P. W. (1984). Thigmomorphogenesis: On the mechanical properties of mechanically perturbed bean plants. *Physiol. Plant.* **62**:73–78.

Khan, A. A. (1988). *Mechanical and Fracture Properties of Fruit and Vegetables*, Ph.D. thesis, University of Reading, Reading.

Kidston, R., and Lang, W. H. (1917). On Old Red Sandstone plants showing structure, from the Rhynie chert bed, Aberdeenshire. I. *Rhynia gwynne-vaughni* Kidston and Lang. *Trans. R. Soc. Edinb.* **51**:761–784.

Lees, G. L. (1984). Cuticle and cell wall thickness: Relation to mechanical strength of whole leaves and isolated cells from some forage legumes. *Crop Sci.* **24**:1077–1081.

Lees, G. L., Howarth, R. E., Goplen, B. P., and Fesser, A. C. (1981). Mechanical disruption of leaf tissues and cells in some bloat-causing and bloat-safe forage legumes. *Crop Sci.* **21**:444–448.

Lees, F. L., Howarth, R. E., and Goplen, B. P. (1982). Morphological characteristics of leaves from some forage legumes: Relation to digestion and mechanical strength. *Can. J. Bot.* **60:**2126–2132.

Lucas, P. W., and Corlett, R. T. (1991). Quantitative aspects of the relationship between dentitions and diets. In Vincent, J. F. V., and Lillford, P. J. (eds). *Feeding and the Texture of Food*, Soc. Exp. Biol. Semin. Ser. 44, Cambridge University Press, Cambridge.

Lucas, P. W., Choong, M. F., Tan, H. T. W., Turner, I. M., and Berrick, A. J. (1991). The fracture toughness of the leaf of the dicotyledon *Calophyllum inophyllum* L (Guttiferae). *Phil. Trans. R. Soc. Lond. B* **334:**95–106.

Marvin, J. W. (1939). The shape of compressed lead shot and its relation to cell shape. *Am. J. Bot.* **26:**280–287.

Speck, T., Spatz, H. C., and Vogellehner, D. (1990). Contributions to the biomechanics of plants. I. Stabilities of plant stems with strengthening elements of different cross-sections against weight and wind forces. *Bot. Acta* **103:**111–122.

Steucek, G. L., Selker, J. L., and Reif, W. E. (1992). Architecture of the plant shoot apex. *Natural Structures*, Proc. SFB230, Stuttgart, pp. 151–157.

Strasburger, E., Noll, F., Schenck, H., and Schimper, A. F. W. (1903). *A Text-book of Botany* (translated from the German by H. C. Porter, revised by W. H. Lang), Macmillan, London, pp. 166–167.

Thompson, d'A. W. (1917). *On Growth and Form*, Cambridge University Press, Cambridge.

Vincent, J. F. V. (1982). The mechanical design of grass. *J. Mater. Sci.* **17:**856–860.

Vincent, J. F. V. (1983). The influence of water content on the stiffness and fracture properties of grass leaves. *Grass For. Sci.* **38:**107–114.

Vincent, J. F. V. (1991). Plants as food. In Vincent, J. F. V., and Lillford, P. J. (eds)., *Feeding and the Texture of Food*, Soc. Exp. Biol. Semin. Ser. 44, Cambridge University Press, Cambridge.

Vincent, J. F. V., and Jeronimidis, G. (1991). The mechanical design of fossil plants. In Rayner, J. M. V., and Wootton, R. (eds.), *Biomechanics in Evolution*, Soc. Exp. Biol. Semin. Ser. 36, Cambridge University Press, Cambridge.

Vincent, J. F. V., and Sibbing, F. N. (1991). How the grass carp (*Ctenopharyngodon idella*) chooses and chews its good—Some clues. *J. Zool.* **226:**435–444.

Weeks, S. A., Wolford, J. C., and Kleis, R. W. (1975). A tensile testing method for determining the tendency of soybean pods to dehisce. *Trans. A.S.A.E.* **18:**471–474.

Wright, W. (1992). *The Fracture Properties of Grasses and Their Relevance to Feeding in Herbivores*, Ph.D. thesis, University of Reading, Reading.

*Biomimetics, Vol. 2, No. 2, 1994*

# On the Research History of Plant Biomechanics[1]

**Werner Nachtigall**[2]

*The research history of plant biomechanics between the period of first analyses and the late thirties of this century is elucidated. Special consideration is given to early ideas, Schwendener and contemporaries, and Rasdorsky and contemporaries. Aspects of bodies of equal resistance, the role of turgescent tissues, stem mechanics and stiffness, dimensional problems, mechanics of "plant buildings," modulus of elasticity, flexibility, and finally, the plant as a compromise construction are discussed. Examples are illustrated by original drawings from the authors cited.*

**KEY WORDS:** plant biomechanics; biomechanics; history of botany; research history.

## INTRODUCTION

Investigation of the plant as a biomechanical construction began spectacularly: Simon Schwendener's treatise on *Das mechanische Prinzip im anatomischen Bau der Monocotyledonen* (The Mechanical Principles of the Anatomy of Monocotyledons) (Fig. 1) appeared in 1874. This was the beginning of a new field of research and one it was to influence for the next 25 years. Diverse approaches and notes had been made long before Schwendener, but they were sporadic and unsystematic. He was followed by Rasdorsky, with a fundamental and widespread handling of this subject between 1911 and 1937. Various other morphological and mechanical approaches were made during this period, but they stand more or less apart. The question of automatic regulation under mechanical loading in growing plants was soon taken up.

[1] This is the published version of a paper presented at the Plant Biomechanics Congress, Montpellier, France, September 5-9, 1994.

[2] Department of Zoology, Division of Technical Biology and Bionics, University of Saarland, 66041 Saarbrücken, Federal Republic of Germany.



1059-0153/94/0600-0087$07.00/0 

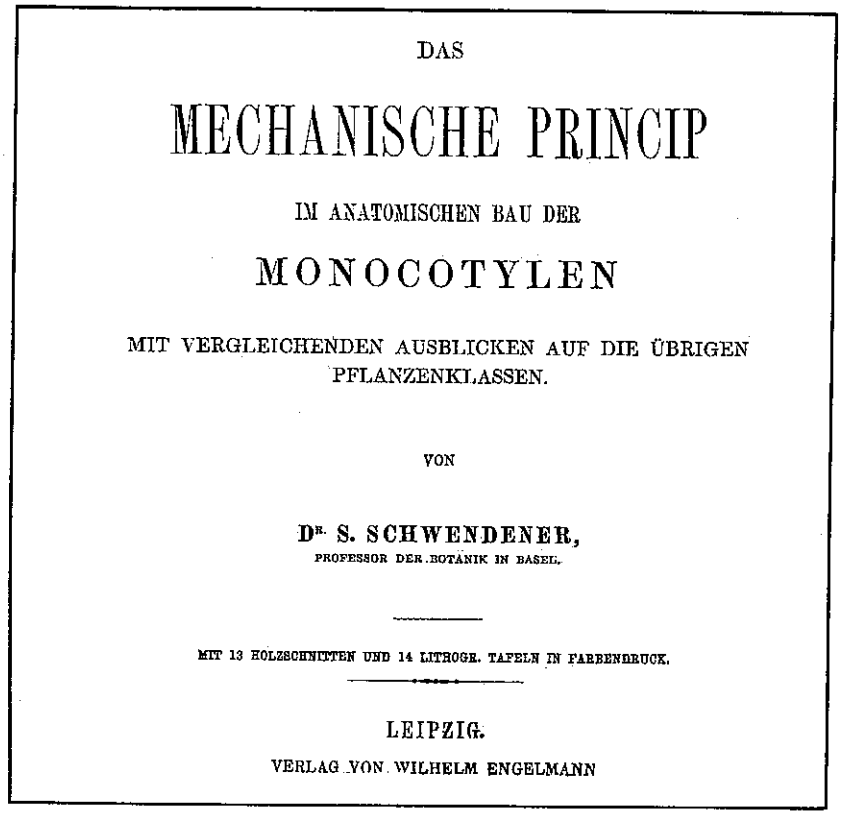

DAS

MECHANISCHE PRINCIP

IM ANATOMISCHEN BAU DER

MONOCOTYLEN

MIT VERGLEICHENDEN AUSBLICKEN AUF DIE ÜBRIGEN PFLANZENKLASSEN.

VON

Dr. S. SCHWENDENER,
PROFESSOR DER BOTANIK IN BASEL.

MIT 13 HOLZSCHNITTEN UND 14 LITHOGR. TAFELN IN FARBENDRUCK.

LEIPZIG.
VERLAG VON WILHELM ENGELMANN

**Fig. 1.** Title page from Schwendener's 1874 treatise.

I divide this historical compilation into three sections: (1) Early Ideas, (2) Schwendener and Contemporaries, and (3) Rasdorsky and Contemporaries. Quotations are used to enhance descriptions wherever they seemed appropriate, and for the purpose of continuity some modern concepts have been added to the classical approaches. The period under consideration here begins with the first approaches and continues into the first three decades of this century.

## EARLY IDEAS

### "Plant Skeletons" and Similitude Mechanics

Galilei [1638 (1890)] used the grass stalk to illustrate his ideas on increased bending resistance due to peripheral accumulation of material. He formulated the first ideas on similitude mechanics, comparing a small oak to a large one.

The physicist Hooke (creator of Hooke's law) advised the botanist Grew (1682) in his book on the anatomy of plants. In this case the stiff hollow cylinder with peripheral supporting cords was correctly recognized as an important aspect of a plant's lightweight structure, as opposed to the flexible roots, which have centrally massed stiffening elements. Contemporary quotations, for example, from van Marum (1773) and Senebier (1800), show that these principally correct ideas on construction mechanics were already widespread. In the eighteenth century a discussion began on whether the supporting structures of plants were comparable to the skeletons of animals. Du Monceau (1758) assumed that there is a functional similarity between the wood structure of a tree and the skeleton of an animal. Bonnet (1782) even placed herbaceous plants with respect to their static conception analogous to insects, because both possess external reinforcement. Humboldt (1794), on the other hand, contested that plants possess anything "which may be similar to bones." Although he hindered the correct line of pursuit due to his scientific authority, the idea of a plant possessing a kind of skeleton gradually asserted itself.

## The Role of Turgescence

It is remarkable that, already during these early stages, not just the special strengthening tissues were said to have a skeletal character. In fact, present-day discussions on the significance of internal pressure and the seemingly novel concept "Der Pneu-Bauprinzip des Lebens" [The Pneu—Life's Principle of Construction (Otto, 1978)] just take up the classical ideas again. Halfway through the nineteenth century the significance of turgor as global stiffening in plants was already generally accepted. Thus, according to Sachs (1868), the rigidity or flexibility of a plant is determined by the "global result of the co-ordination between the variable growth in cell walls, their flexibility and elasticity and the turgor." This statement—though using other words—is more or less identical in meaning to the modern definition of a pneu: a flexible membrane enclosing a substance standing under internal pressure.

The combination of turgescent and hard reinforcing materials was recognized more than 100 years ago. So that Schwendener (1874) noted "daß die parenchymatischen Gewebe den Widerstand bedeutend erhöhen" (that parenchyma tissue greatly increases the resistance) during bending in a plant stem attached horizontally at one end and loaded at the other (Fig. 2). He also noted that the sclerenchyma fibers had to be kept apart. This was accomplished by "pressure pads" of highly pneumatic parenchyma lying in between them: ". . . so leuchtet ein, daß dieselben i m Z u s t a n d d e r T u r e s z e n z (spaced out by Schwendener himself!) einen bedeutenden Widerstand gegen Druck darbieten. . ." (thus it is obvious that they, with their condition of turgidity, offer an important resistance to pressure. . .; see Studies on Bodies with Equal Resistance and the Role of Turgescent Tissue, below).

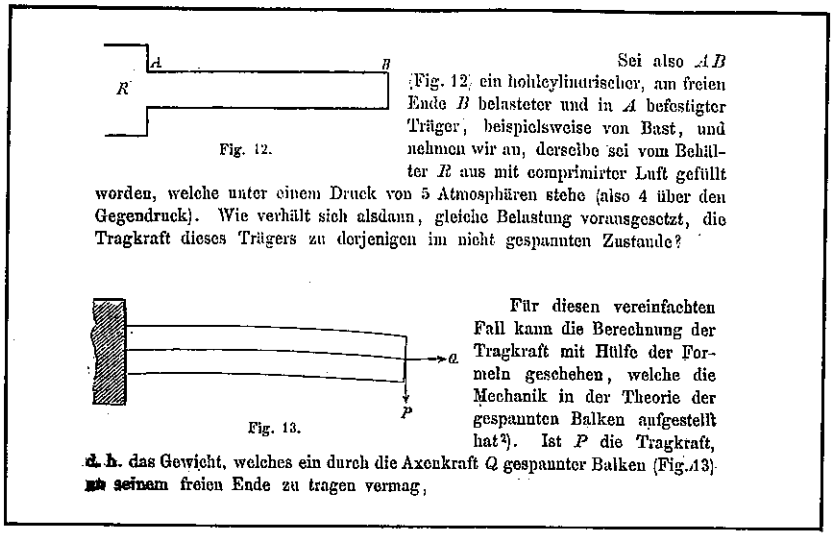


**Fig. 2.** Schwendener's (1874) deliberation on the effect of hydraulic stiffening. Top: Unloaded hollow cylinder, filled with compressed air. Bottom: Same as *A*, with load *P*(*Q* hydraulic axial force).

## SCHWENDENER AND CONTEMPORARIES

During the second half of the nineteenth century, the idea that the hollow cylindrical structure of a plant stem or stalk is a principle of lightweight construction, constituting material saving, finally asserted itself. Biologists schooled in physics and even physicists themselves were becoming increasingly interested in the construction of plants. Preliminary ideas on the building of strengthening tissues as a possible reactions to mechanical influences were beginning to form. The philosopher and engineer Spencer (1863/1864) assumed that the "mechanical stress itself" caused the formation of "strong bonds" with which plants "can resist the stresses" (quoted by Rasdorsky 1937). Culmann (1866), the founder of graphical statics, used this very successful method of applying the architecture of bone (the stress trajectories of the femur head) on plants, but apparently he interpreted the growth rings falsely. It was left to Schwendener (1874), a biologist strongly interested in constructional statics, to carry out a comprehensive study (a completely new departure at that time) of "the mechanical principle of anatomical construction" in plants and to raise it to the rank of an independent botanical discipline. Apart from his classical 1874 paper, Schwendener published several papers on plant biomechanics, for example, on elasticity (1878), reinforced plant parts (1882); and microbotany (1887).

## Schwendener's World of Mechanical Concepts

In 1874 Schwendener, stimulated by the use of steel girders in building bridges, published a comprehensive study of statically important structures, in particular, in stalks and blades, but also in leaves and roots of monocotyledons (Fig. 3), and compared them to the mechanical principles of construction in dicotyledons, mosses, ferns, lycopods, and horsetails. First he described "specific mechanical cells" and reported on determining the cross-sectional areas as well as flexibility tests to measure the "load-carrying capacity" (weight per unit cross-sectional area at the breaking limit) and the modulus of elasticity of the inner bark fiber. Xylem, parenchyma, and collenchyma are generally ignored. He assumed (erroneously) that the fibrous strips were I-beams (Fig. 4). [Just how strongly this principle influenced ideas at that time has been shown by studies to demonstrate such I-beams even in lichens (Zukal, 1895) and mosses (Istvanffi, 1896).] However, he interpreted correctly the influence of tensile and compressive stress. He recognized the importance of peripheral accumulation and fusion into rings of the mechanical elements, but also the danger of buckling with too much peripheral emphasis, i.e., a supporting cylinder with too thin walls. He suggested a wall thickness of one-seventh to one-eighth of the diameter as optimal.

## Characterization of Monocotyledons

The blades or stems of monocotyledons were grouped by Schwendener (1874) according to the position and degree of fusion of the fibrous elements. He created no fewer than seven systems with a total of 20 characteristics such as simple rings of fibrous ribbing in *Arum maculatum*, hollow fibrous cylinders with vascular bundles leaning against them as in most Poaceae, etc. Today these allocations, illustrated with extremely schematicized lithographs (creating an impression of suggestive simplification), appear excessively and ineffectively differentiated. If this had to be done again today, one would probably select only four or five clearly defined basic types.

## Studies on Bodies with Equal Resistance and the Role of Turgescent Tissues

Stems (and leaves) are often known as bodies of equal resistance, for which model constructions are presented. This idea and, also, the idea that trees are beams of equal resistance have not been proved experimentally or definitely confirmed (Detlefsen 1884a). Furthermore, this was criticized by Meschayeff (1882) after the studies *Über die Anpassungen zum Aufrechterhalten der*

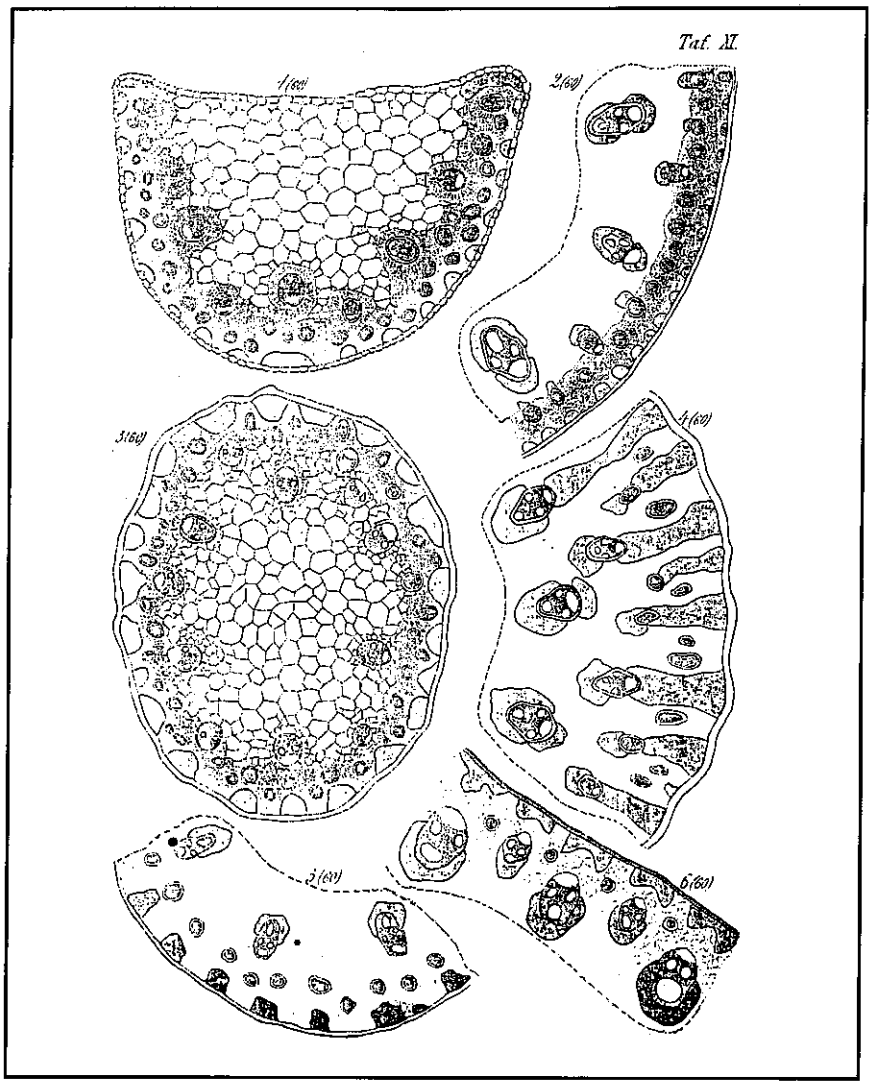


**Fig. 3.** Schwendener's (1874) plate XI, showing cross sections of a *Fimbristylis spadeacea* (1) leaf and of the stalk of *Cyperus eregius* (2), *Fimbristylis spadicea* (3), *Cyperus conglomeratus* (4), *Hypolytrum argenteum* (5), and *Cyperus* sp. (6).

*Pflanzen* (On the Adaptations of Plants to Stay Upright). One hundred years later, it appears that Schwendener's ideas have been confirmed by recent data (e.g., Silk *et al.*, 1982).

Another approach aspect is whether the turgescence of nonsclerenchyma-

Zur Beurtheilung dieses Typus in mechanischer Hinsicht mag die approximative Berechnung eines bestimmten Falles, wie er in Fig. 5 dargestellt ist, als Grundlage dienen. Die Figur ist schematisch gehalten, entspricht aber ungefähr den bei *Scirpus caespitosus* vorkommenden Dimensionsverhältnissen.

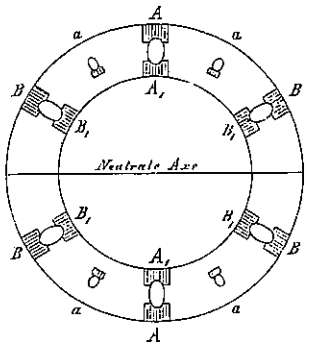

Fig. 5.

Wir denken uns auch hier wieder den Durchmesser des peripherischen Kreises auf 1000 Centim. vergrössert; die Wanddicke $AA$, sei 0,17 oder ungefähr $^1/_6$ des ganzen Durchmessers. Für die speziellen Daten genügt folgendes Verfahren. Die Querschnittsfläche der Bastbündel, die übrigens nachträglich durch einfache Division reducirt werden kann, lässt sich mittelst directer Messung am Objecte selbst oder an genauen Abbildungen ungefähr bestimmen; der Abstand derselben resp. ihrer Schwerpunkte von der neutralen Axe wird dagegen am besten auf der schematischen Figur (hinreichend gross ausgeführt) mit dem Zirkel gemessen. Nachstehend das Ergebniss der Messung und das davon abgeleitete Maass der Biegungsmomente; die Querschnittsflächen sind mit $F$, die Abstände von der neutralen Axe mit $D$, die Maasse der Biegungsmomente mit $W$ bezeichnet. Die Epidermis wurde wegen ihrer beträchtlichen Widerstandsfähigkeit mit in Rechnung gebracht.

| | | | | | | | |
|---|---|---|---|---|---|---|---|
| 1) | Die Epidermis, 1 Ctm. dick; | $F$ = | 3140 □Ctm.; | — | | $W$ = | 392 Million. |
| 2) | Die zwei Bastbündel $AA$ | $F$ = | 9000 - | $D$ = | 470; | $W$ = | 1988 - |
| 3) | Die zwei Bastbündel $A, A,$ | $F$ = | 9000 - | $D$ = | 350; | $W$ = | 1102 - |
| 4) | Die 4 Bündel $BBBB$ | $F$ = | 18000 - | $D$ = | 240; | $W$ = | 1036 - |
| 5) | Die 4 Bündel $B, B, B, B,$ | $F$ = | 18000 - | $D$ = | 180; | $W$ = | 583 - |
| 6) | Die 4 kleinen Bündel $aaaa$ | $F$ = | 4000 - | $D$ = | 330; | $W$ = | 436 - |
| | | | 61140 □Ctm. | | | | 5537 Million. |

**Fig. 4.** Schwendener's (1874) calculations of "Maasse der Biegemomente."

tous tissues (parenchyma, etc.), other than keeping the sclerenchyma fibers apart, plays a measurable part in the bending stiffness of the "whole organ," i.e., the blade of grass (cf. Fig. 3). Comparing the measured downward bending $B_{bl}$ of pieces of blade (which were attached to a rod at one end and bent by their own weight) to the downward bending $B_{scl}$ calculated for a "pure sclerenchymatous system" with the same cross-sectional area, the same second moment of area, and the known modulus of elasticity, a proportionality constant $F$ is obtained; $B_{bl} = F \cdot B_{scl}$. Parenchyma has a positive share in the bending stiffness of a blade at $F < 1$, and the smaller $F$ is compared to 1, the greater the share. Values between 0.94 in *Juncus* and 0.34 in *Molinia coerulea* were obtained, but there were also inexplicable values of $F > 1$, so that Schwendener was unable to solve the question definitely.

Schwendener had already published many of his ideas in 21 essays before his classical treatise (1874), summarizing them again in various later works. Holtermann (1909) issued *Schwendener's Vorlesungen über mechanische Probleme der Botanik* (Schwendener's Lectures on the Mechanical Problems in Botany) (Fig. 5). In 1919 his achievements were summarized by Haberlandt, the famous author of *Physiologische Pflanzenanatomie* (six issues between 1884 and 1924) in a "Gedächtnisrede auf Simon Schwendener" (Commemorative Speech on Simon Schwendener). Schwendener died in 1919 at the age of 91; his final resignation should be taken note of by all laboratory-fixed biologists: ". . .er hatte kein Interesse, kein Vernügung mehr an einer neuen Beobachtung" (. . .he was no longer interested in, had no more fun in making new observations) and thus "blieben auch die wissenschaftlichen Anregungen aus, die dem Biologen nur im steten innigen Verkehr mit der unergründlich mannigfaltigen Natur zuströmen" (the scientific stimulus, which flows to the biologist only from a regular and intimate contact with nature in its unfathomable diversity, was not present any more).

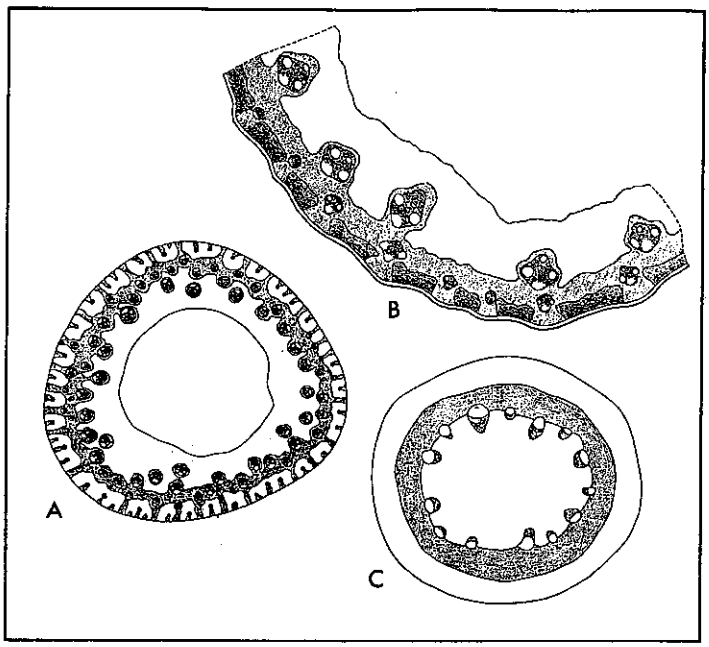


**Fig. 5.** Holtermann's (1909) copies of some of Schwendener's tables as a basis for statical considerations. Cross sections. (A) *Cladium mariscus*; (B) *Molinia coerulea* (detail); (C) *Armeria elongata*. "Mechanical tissues," dark area.

## Stem Mechanics and Stiffness

Detlefsen (1994a), a high-school teacher in Wismar, was first to criticize profoundly Schwendener's ideas. His work "Über die Biegungselastizität von Pflanzenteilen" (On the Bending Elasticity of Parts of Plants) appeared in two parts and is one of the most important publications within this field to have been made during the nineteenth century. Beginning with a clear definition of the modulus of elasticity and with reference to earlier works (e.g., from Wertheim and Chevandier, 1846), he then discussed the correlation between this modulus and the water content. The tensile tests made by the Schwendener school were rejected as methodically deficient. He then continued with the geometrical distortion of a clearly defined "free of stress, homogeneous, and isotropic straight body," stating that the neutral axis joining the centers of gravity of all cross-sectional areas does not necessarily coincide with the geometrical median line, which gives rise to the relation $r = \Theta E M^{-1}$ ($r$ = bending radius, $\Theta$ = second moment of area, $E$ = modulus of elasticity, $M$ = bending moment). Therefore, $M_1 : M_2 = (\Theta E)_1 : (\Theta E)_2$ is valid for two bodies of differing rigidity but the same curvature, so that one may use the product $\Theta E$ to characterize the rigidity of a body.

For the first time in botanical literature Detlefsen (1884a) clearly proved that rigidity changes with changes in geometry and absolute size: $d_2^4 = 2$ is valid for a solid rod with a cross section of $d_2$ and rigidity twice that of a rod with a cross section of $d_1 = 1$ cm and of the same material. Thus the diameter $d_2$ is $\sqrt[4]{2}$ cm = 1.189 cm. The same rigidity is found in a hollow rod with a wall thickness of 0.095 cm and an internal diameter of 1.189 cm, weighing only 0.414 times as much, etc.

Long before Rasdorsky approached the bending spring concept (1930), Detlefsen (1884) went a step further than Schwendener with the idea of bending elasticity as a constructional goal: "It only requires a little thought to realise that the mechanical efficiency of elastic parts of plants more frequently results from the fact that with less important rigidity they are capable of withstanding considerable bending without damage, rather than preventing any bending from the start due to the type and arrangement of the materials they are made of." These aspects were enhanced by the author with his own calculations (Fig. 6) and measuring techniques and, also, with regard to the different water contents. He concluded his paper with two graphs which show the (nonlinear) decrease in the bending moment (during bending without remaining distortion) of *Helianthus tuberosus* and *Urtica dioica* from the base to the tip. Thus the stiffness and concentration of material (defined as dry weight) gradually decrease from the bottom towards the top, which is more or less equivalent to theoretical, round substitutes with the same stiffness (Fig. 7).

Zimmermann (1884), an admirer of Schwendener, attacked Detlefsen's

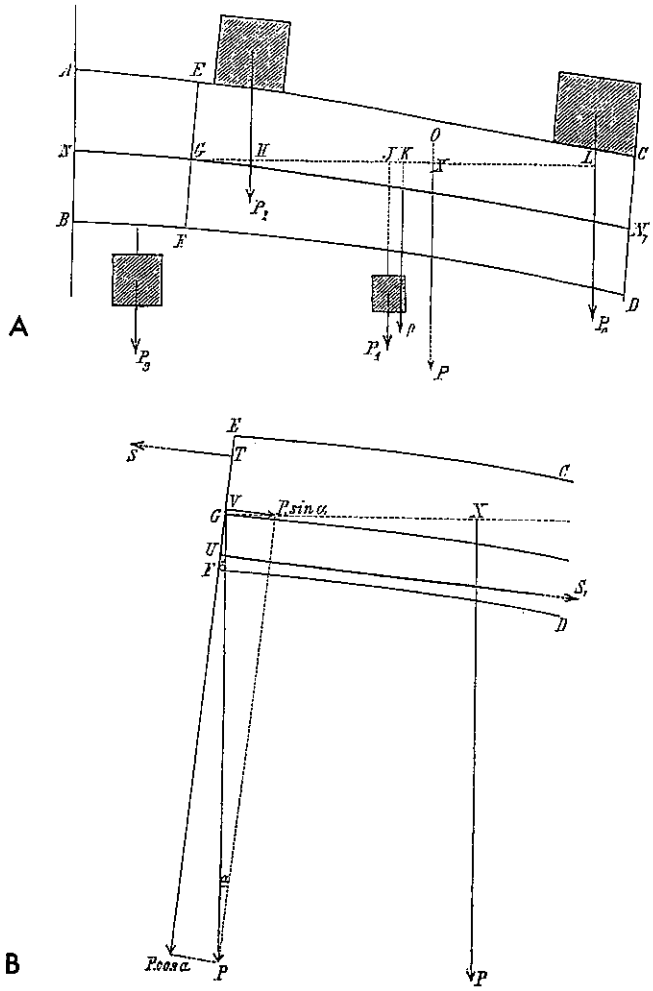


**Fig. 6.** Detlefsen's (1884a) demonstration of beam theory.

hypotheses angrily and without reason. Detlefsen (1884b) responded to this briefly, but then, unfortunately, he decided to break off his research ("Following this communication, I do not believe that any one will request me to continue with my studies").

## RASDORSKY AND CONTEMPORARIES

The Russian botanist Wladimir Rasdorsky, writing frequently in German and French, published a series of papers between 1911 and 1937 on the statics of plants, which in principle are still valid today. They deal with questions on

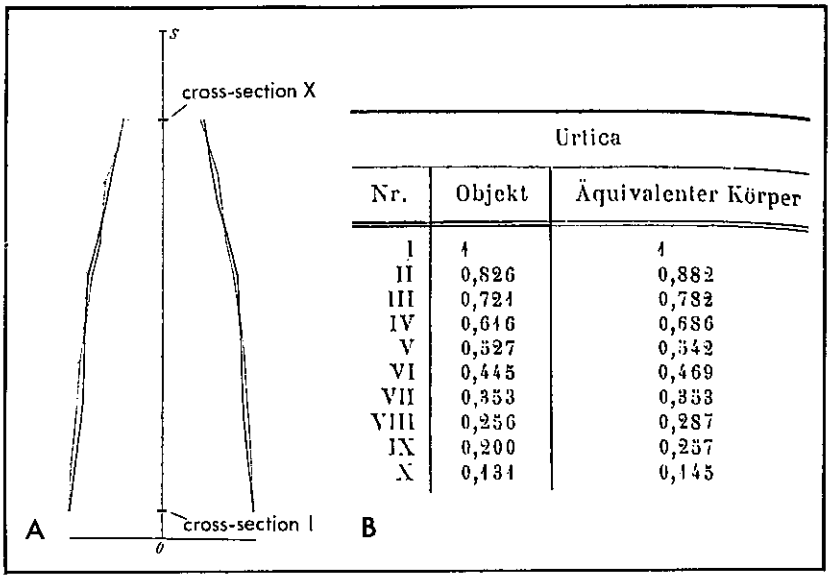


Urtica

| Nr. | Objekt | Äquivalenter Körper |
|---|---|---|
| I | 1 | 1 |
| II | 0,826 | 0,882 |
| III | 0,721 | 0,782 |
| IV | 0,616 | 0,686 |
| V | 0,527 | 0,542 |
| VI | 0,445 | 0,469 |
| VII | 0,353 | 0,353 |
| VIII | 0,256 | 0,287 |
| IX | 0,200 | 0,257 |
| X | 0,131 | 0,145 |

**Fig. 7.** Detlefsen's (1884a) measurements of the cross section of an *Urtica dioica* stem and calculation of the cross section of an equivalent body of rotation. (A) graphs (thin line, object; thick line, equivalent body); (B) table.

research history, for example, the mechanical construction of plants, (1928, 1929), dimensional proportions of blades and stalks, spring-like flexural characteristics (1930), and plant reaction to mechanical loading (1937).

## Dimensional Problems

In the nineteenth century, Sachs (1868), for example, stated that the absolute size of a plant, as far as its organization and construction are concerned, cannot be a matter of indifference to it. However, when comparing plant constructions and high buildings, the laws of similarity were overlooked, even in the twentieth century (Welzien 1926). An unreasonable superiority is given to a plant when one thinks that "the technical achievements of the plant's body are unique of their kind and highly perfected" (Fitting, cited by Strasburger, 1923). "The lightest wrought iron post seems clumsy in comparison to the slim soaring cane of the bamboo" (Schwendener, 1874). "Even the Eiffel tower is clumsy and wide compared to most plant construction" said Francé (1919), who introduced the ideas of technical biology to a larger public with his book *Die technischen Leistungen der Pflanze* (Fig. 8). Comparisons of the slenderness ratio $\lambda = h/d$ ($h$, height; $d$, mean diameter) are made with the inadmissible proportion $h_1:d_1 = h_2:d_2$. On the other hand, Rasdorsky (1928) recalls the

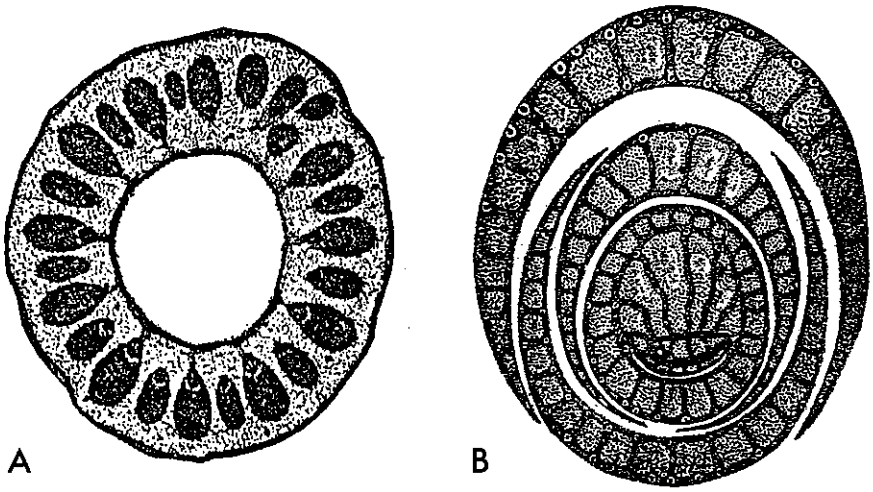


**Fig. 8.** Francé's (1919) simplified illustrations to the "statics and mechanics of plants." (A) Cross section through a grass stalk. (B) Application of I-beams in the mechanical system of plant; cross section of a rush stalk.

Barba-Kick law on proportional resistance (Kick, 1885), an empirical formula mathematically substantiated, within the limits of elasticity, by Steiner (1884; quoted by Kick, 1885). This law means, among other things, that tower-like bodies of different absolute height can be geometrically similar only when the forces change proportionally to the square of the longitudinal dimensions. However, the body's own weight is already proportional to the cube of its length. It follows that, alone as safety against buckling under self-loading, $d^2 \sim l^3$ and $d \sim l^{3/2} \sim l\sqrt{l}$, and Greenhill (1881) has shown, in continuation of Euler's theories, that self-loading in pines is already relevant for buckling.

Higher plants (and of course technical) constructions must therefore show a lower slenderness ratio, in other words, become more clumsy. Later, this was introduced into the popular literature by Welzien (1927) (Fig. 9). It confirms the actual $\lambda$ values: *Secale cereale* ($h$ = 2 m), 500; *Bambusa* sp. (25 m), 100; *Abies nobilis* (70 m), 37.5; *Eucalyptus amygdalina* (128 m), 28; and *Sequoia gigantea* (92 and 100 m), 12.5 and 8.3. This correlation had been formulated by Galilei (1638) by comparing two different-sized oaks: ". . .una quercia degunto braccia alta non potrebbe sostenere i suoi rami sparsi alla similitudine di una di mediocre grandezza."

## Mechanics of "Plant Buildings"

Rasdorsky (1911, 1928, 1929), who refuted much of Schwendener's theories on H-beams (Fig. 10), came to the conclusion, after hearing lectures on reinforced concrete engineering between 1906 and 1907, that a plant should be

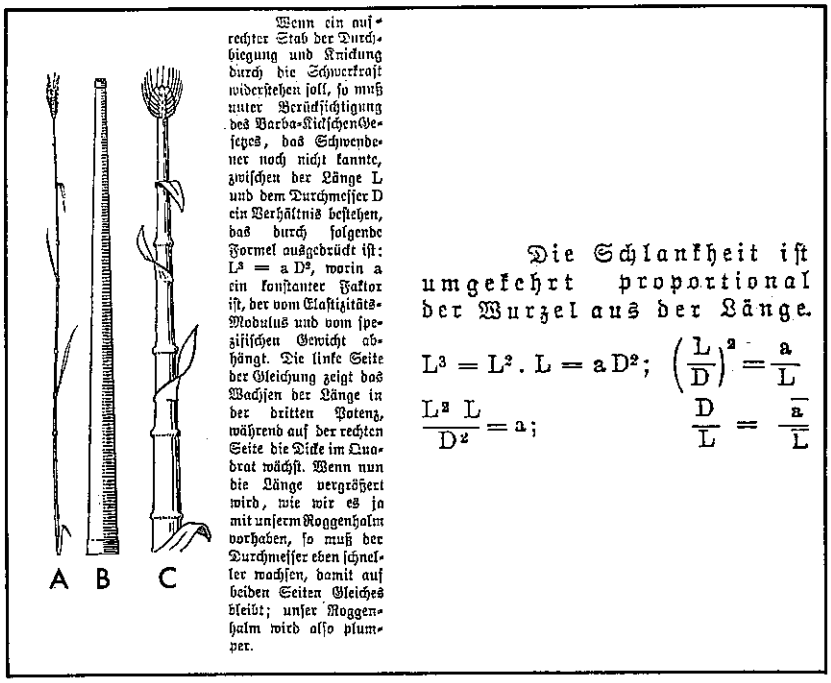


**Fig. 9.** Welzien's (1928) explanation of the degree of slenderness, leading back to Rasdorsky. (A) Hypothetical rye stalk, 140 m high, which is statically impossible (B) Halsbrücker Esse (Freiberg, Saxonia), 140 m high. (C) Hypothetical rye stalk, 140 m high, which does not contradict the laws of statics.

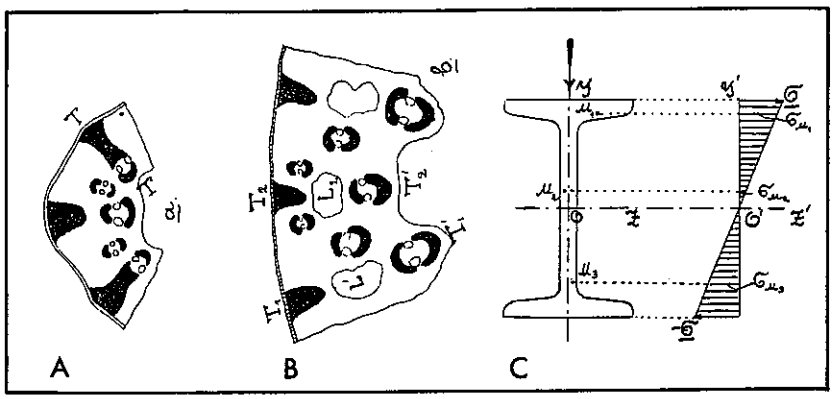


**Fig. 10.** Rasdorsky's (1928) drawings of "so-called I-beams" (A, B) and a "real I-beam" (C). (A, B) "Schwendeners I-beams" $T$-$T$, $T_1$-$T_1$, and $T_2$-$T_2$ in *Juncus glaucus*. (C) Normal tensions in a real I-beam with loading at one end (arrow). Above zero line, tension zone; below zero line, compression zone.

taken as a composite construction in which the sclerotic strands and parenchyma correspond to the metal reinforcement and concrete matrix, respectively (Fig. 11). This is the right road to reaching an understanding and clearly demonstrates the important heuristic role of analogy in research, which Helmcke (1972) later demanded most emphatically for biotechnical work: "Accordingly, there is a large degree of analogy in the principles of construction in technical composite construction and plant organisms. . ." (Rasdorsky, 1929). This idea was presented for the first time by Rasdorsky in 1911 in a section on "the mechanical characteristics of tissues not belonging to those specifically classified as mechanical tissues." Later, other authors will express the same views. During a discussion on leaves, for example, Giesenhagen (1912) observed that their "strengthening tissues formed a grille like the metal gridding of a reinforced concrete floor."

Bach and Baumann (1924) compared the arrangement of tensile fibers in bamboo with "a fortification of the external layer which is most heavily used during bending (similar to reinforced concrete)," and Bower (1930) wrote with reference to reinforced concrete: "Ordinary herbaceous plants are constructed on the same principle. The sclerotic strands correspond to the metal straps, the surrounding parenchyma with its turgescent cells corresponds mechanically to the concrete."

Just what are they, these characteristic and, at the time, so novel peculiarities of the composite building material concrete, "which are basically very simple" (Probst, 1931)?

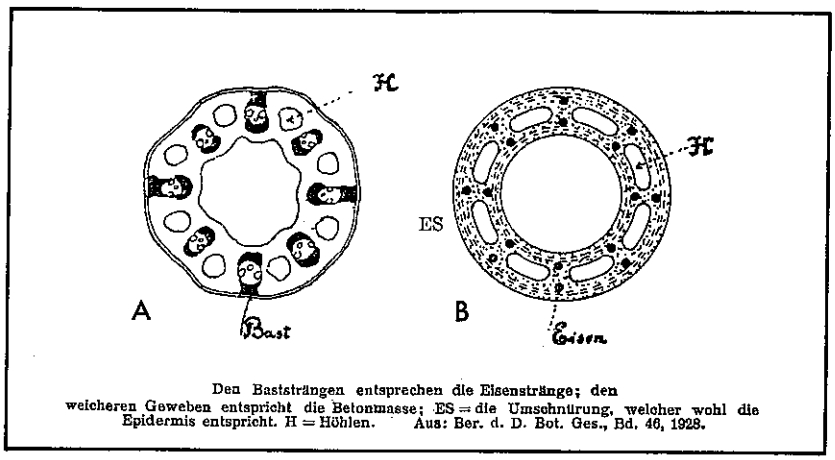


**Fig. 11.** Rasdorsky's (1928) comparison of the cross sections of a plant and a technical building. (A) *Trichophorum germanicum*, taken from Haberland (1884). (B) Factory stack in Elysabethport.

*Each* elemental area of *each* tissue—besides sclerenchyma, if necessary collenchyma, parenchyma, epidermis, bark—delivers its share, derived from its Young modulus and its distance from the neutral axis, toward bending stiffness. Schwendener's terms "mechanical" and "not mechanical" tissues are not very suitable for the constructional mechanics of a plant's body. "Reinforcement" and "ground mass" or "matrix" would be better terms (Fig. 12). "Even if the weaker tissues. . .as a result of the lower E-values of their cell wall materials, incur less stress and their constructionally active cross-sectional parts are relatively small (due to thin walls), their total contribution. . .is not in the least insignificant; because the entire ground mass is extensive. . ." (Rasdorsky, 1929).

## Modulus of Elasticity

Tensile tests with biological materials to determine the strain $\epsilon = e/l$ ($e$ = additional length under stress, $l$ = starting length) and the modulus of elasticity $E = \sigma/\epsilon$ ($\sigma$ = stress = $F/A$; $F$ = tensile force, A = cross-sectional area before loading) were carried out at a very early date. Wertheim and Chevandier (1846) studied the effects of four states of drying on wood from 15 types of trees. Moduli of elasticity between 12,900 N mm$^{-2}$ (pine) and at least 29,700 N

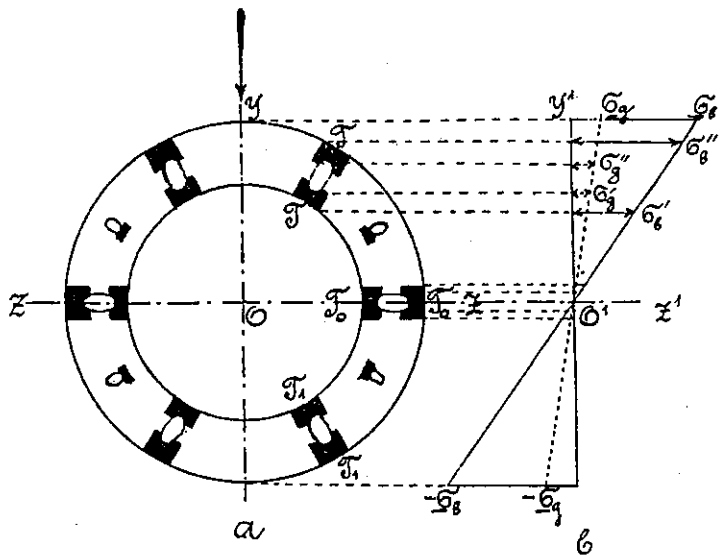

**Fig. 12.** Rasdorsky's (1928) view of a composite beam cross section analogue to Schwendener's cross section of *Scirpus caespitosus*. $T$–$T$ and $T_1$–$T_1$, Schwendener's "I-beams"; stress distribution for "ground mass" (parenchyma, $\sigma_g$) and for "reinforcement" (sclerenchyma, $\sigma_b$).

$mm^{-2}$ (fir) are obtained "for the cell walls alone" after conversion for a moisture content of 23%. A modern comparative value for average conifers amounts to 10,000 N $mm^{-2}$. Three methods were used to make these early measurements, which appear quite reliable, in contrast to some later measurements. In longitudinal, radial, and tangential cuts, the tensile forces leading to a lengthening in *Abies pectinata* behave as 1:0.085:0.031.

## Flexibility

The confusion created by unclear definitions is demonstrated by the discussion on the bending ability of plants at the beginning of the twentieth century. The terms bending and flexibility, bending ability and bending strength, flexural stiffness and bending elasticity, etc., are all muddled and their use is not standardized.

Thus the botanist Schwendener (1874) was accused by Rasdorsky of using his "stereom" as a means of obtaining greater stiffness, i.e., he believed that a plant is well constructed if it bends only slightly or not at all. (Schwendener did not actually maintain this view, but his analogous comparison to earlier railway bridges suggests it. "A maximum sagging of 1/1800–1/5700 of the space is permitted in such bridges; the horizontal extensions caused by storm winds are of the same order.") For comparison, before the First World War, a maximum sagging of 1/2000 to 1/5000 was permitted in fractions of the span of girders in reinforced concrete bridges (Pederij, 1912; Patton, 1915, quoted by Rasdorsky, 1934). On the other hand, Schwendener (1874) wrote, "How conspicuously do the blades of grass play of the air, how lightly do the branches swing on a tree, and how much life seizes the forest when the storm blows through its mighty tops." In his book *A Botanical Journey to the Tropics* (1893), Haberlandt vividly described how far the palms bent over in stormy winds and how they changed their shape in doing so. Detlefsen (1884) complained vehemently about the confusion of terms: "One frequently finds e.g. the expression "bending stiffness" when "flexural elasticity" is meant, a fact which does not simplify comprehension." He went further: "If someone feels the need to express himself vaguely, then he should indicate this with his choice of words, because one writes for people who wish to understand and not for those who admire just what they cannot really understand."

Technicians alone used a clear technical terminology, even when they were analyzing biological materials. Thus Baumann (1913) studied the elasticity and stiffness of bamboo, acacia, ash, and hickory and tested wooden pipes for torsional stiffness, bending strength, and compressive strength. For bending tests, bamboo, for example, was run on two-sided bearings at a distance of 25 times its diameter and loaded centrally. A modulus of elasticity of about 20,000 $Nm^{-2}$, a bending stiffness of about 800 $Nm^{-2}$, and breakage resulting from bending moments of about 1500 N m were obtained.

Many modern debaters should also take note of the lesson taught by this short historical resumee: Whole libraries have been written for nothing, because scientific analyses were made without standardizing the definitions.

## The Plant as a Compromise Construction

Rasdorsky (1930) clearly defined a compromise construction as follows:

> When stressed by static (bending and buckling) factors stiff materials should be located near the periphery. The feather-like bending in the wind (or from the impact of raindrops) however, is best provided for by a concentration of this material near the neutral plane or the longitudinal axis of the organ. Due to the composite building nature of plant organs, which dictates a distribution of reinforcement over the total cross section, the two tendencies (centrifugal and centripetal) are set certain limits.

Thus a series of constructional peculiarities, which Schwendener (1884) was unable to bring into accordance with his peripheral pipe systems as "not very rational reinforcing systems," become easily understood.

Haberlandt (1884), still under Schwendener's influence, spoke of beams and tensile fibers in palm leaves and from "irrational constructional peculiarities"—i.e., systems which apparently cannot be understood as "beams or girders"; Schutze (1905) discovered peripheral I-beams in the reinforcement of tropical tree ferns (Fig. 13A). Tschirch (1882) saw an internal and external system of struts (Fig. 13B) in the "long, very thin, but stiff leaves of *Kingia australis.*" However, an objective observation shows (Fig. 13) neither I-beams nor "peripheral tendencies" but, rather, an equal distribution of the supporting tissues over the entire cross section (Rasdorsky, 1930).

## Bending Elasticity as a "Constructional Goal"

Compared to a completely stiff stalk, a grass stalk bending in the wind reduces drag and bending moment, thus reducing the danger of breaking. With materials of suitable elasticity and a favorable arrangement of supporting structures, even bending in more complex three-dimensional configurations such as in bushes and trees may constitute the elements of an optimized automatic mechanism, inducing a reduction in area, drag, and moments under wind loading. This again assumes that plants "are able to withstand substantial bending without damage," by means of which "the pressure of the wind on the plant organs above the soil is considerably reduced: thus reducing the area exposed to the wind" (Detlefsen, 1884a). In fact, under high wind speeds $v$, the coefficient of drag $c_D$ and the loaded area $A$ can be reduced by such automatism and, at the same time, the perpendicular distance $a$ from the "basal turning point," so that with $D = c_w A \frac{1}{2} \rho v^2$ ($\rho$ air density) the drag, $D$, and with $B = a \cdot D$ the bending moment, $B$ are reduced compared to $D$ and $B$ without such automatisms (Fig. 14).

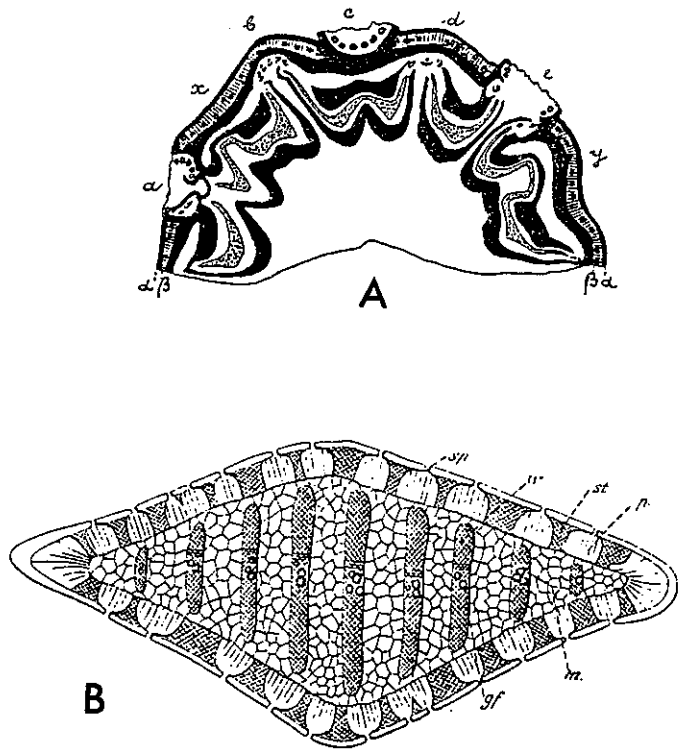


**Fig. 13.** Rasdorsky's copies of figures from the Schwendener school to demonstrate lack of I-beams (A) and tendency to peripheral aggregation of static material (B). (A) Cross section of a tree fern stem (*Dicksonia karsteniana*). White, parenchyma; black, "sclerenchyma"; dotted, main vascular bundles; a–e, nodes and internodes, $\alpha$, outer layer; $\beta$, fibrillar cell layer with air roots. (B) Schematic cross section of a *Kingia australis* leaf. gf, vascular bundle; m, mark; p, st, w, "I-beams"; sp, stomata. (A) From Schütze (1928); (B) from Tschirch (1881).

These possibilities were soon recognized: Rasdorsky (1937) saw, in very slender grasses, "even among hollow tube constructions, a high degree of passive withdrawal (due to extensive bending) from the influence of the wind." It has also long been known that, by means of elastic evasion, sedentary seaweeds are geared, in a very extreme manner, fully automatic to more or less pure tensile loading (Oltmanns, 1923). Such aspects have been taken up again in the last decades by the American Zoologist Vogel (1981) and his co-workers. They have shown that a passive automatic adjustment is present not only in algae and trees, but also in sedentary animals such as sea anemones and corals.

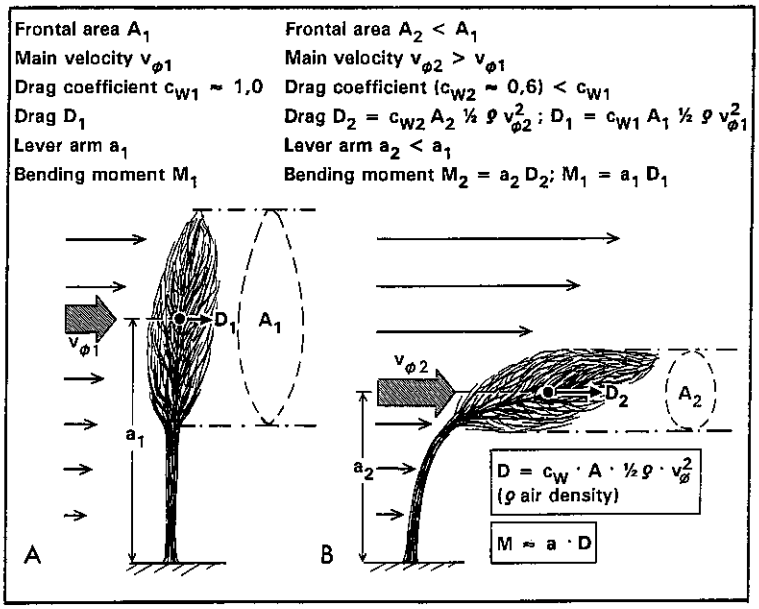


**Fig. 14.** Aerodynamic and bending characteristics of a tree. (A) Light wind; (B) very strong wind. See text.

## CONCLUSION

"Plant biomechanics" as a scientific discipline certainly goes as far back as Schwendener (1874), who was the first to combine botanical research with technical points of view on a broad, comparative scale. But, as nearly always in "one-man research projects," he was not free of autosuggestion, basing his point of view on an assumed overall existence of "I-beams," so that his scientific building was easily brought to near-collapse by showing that, very often, his I-beams were present only when seen through his eyes.

On the other hand, in Rasdorsky's work on plant statics a wealth of results can be found not only on statics and dynamics, but also on loading, which are, for the first time, biologically and technically satisfying and many of which are still valid today. However, Rasdorsky did not receive only recognition and agreement. Compared to other authors, Schwarz (1930) strangely underrates the Rasdorsky results in a "critical compilation" (how easy it is to veil performance and disguise priorities with tricks in formulation!), thus forcing Rasdorsky (1930) to reply in greater detail and more convincingly. Unlike any other author, Rasdorsky (1911–1937) has summarized, clearly formulated, and studied experimentally so many aspects of plant statics that it is certainly he who has created the essential fundamentals for a modern view of the "construction mechanics

of plants." However, one cannot imagine Rasdorsky without Schwendener's courageous beginnings.

## ACKNOWLEDGMENTS

This work was carried out at the Wissenschaftkolleg in Berlin as a preliminary study for plant biomechanics project B2/SFB 230 of the DFG. A short paper on the aspects presented here has already been published (Nachtigall, 1986a). Furthermore, part of the research history of another aspect of this complex, the (once again) much discussed principle of hydraulic formation in a pneu, has been also published (Nachtigall 1986b). A very detailed treatise on the history of plant biomechanics, containing a full bibliography, is in preparation for publication in the near future in a BIONA report (Fischer, Stuttgart).

I wish to thank Ms. Winifred Pattullo for executing the difficult task of translating the original German quotations into English and for the translation of this article in general.

## REFERENCES

Bach, C., and Baumann, R. (1924). *Elastizität und Festigkeit*, 9 Aufl., Berlin.
Baumann, R. (1913). Mitteilung über Forschungsarbeiten auf dem Gebiete des Ingenierwesens etc. **131**:41–70.
Bonnet, Ch. (1782). *Contemplation de la nature*, Nouv. ed., Hamburg.
Bower, F. O. (1930). *Size and Form in Plants*, Macmillan, London.
Culmann, R. E. (1866). *Die graphische Statik*, Meyer und Zeller, Zürich.
Detlefsen, E. (1884a). Über die Biegeelastizität der Pflanzen. *Arb. Bot. Inst. Würzburg* **3**:144–187, 408–425.
Detlefsen, E. (1884b). *Bot. Centralbl.* **19**:316–319.
du Monceau, D. (1785). *La Physique des Arbres, etc. I*, Paris.
Francé, R. H. (1919). *Die technische Leistungen der Pflanzen*, Veit & Co., Leipzig.
Galilei, G. [1638 (1890)]. *Discorsi e dimonstrazioni matematichi, intorno a due nouvo scienze*, Leida.
Galilei, G. (1898). *Edizione nazionale VIII*, p. 43.
Giesenhagen, K. (1912). *Handwörterbuch der Naturwissenschaften*, Fischer, Jena, Vol. 2, pp. 1–35.
Greenhill, A. G. (1881). Determination of the greatest height consistent with stability that a vertical pole or mast can be made, and of the greatest height to which a tree of green proportions can grow. *Proc. Cam. Phil. Soc.*, **4**:65–73.
Grew, N. (1682). *The Anatomy of Plants etc.*, 2nd ed., Book IV, London, pp. 145–160.
Haberlandt, G. (1884). *Physiologische Pflanzenanatomie* (1 Aufl.), Engelmann, Leipzig (2 Aufl., 1896; 3 Aufl., 1904; 4 Aufl., 1909; 5 Aufl., 1917; 6 Aufl., 1924).
Haberlandt, G. (1893). *Eine botanische Tropenreise*, 1 Aufl., Engelmann, Leipzig.
Helmcke, G. (1972). Cited by Otto (1976), p. 16.
Holtermann, C. (1909). *Schwendener's Vorlesungen über mechanische Probleme der Botanik*, gehalten an der Universität Berlin, Engelmann, Leipzig.
Humboldt, A. v. (1794). *Aphorismen aus der chemischen Physiologie der Pflanzen*, Leipzig.
Istwanffi, G. v. (1896). *Jb. Wiss. Bot.* **29**:394–402.
Kick, F. (1885). *Das Gesetz der proportionalen Widerstände*, Leipzig.
Meschayeff, v. (1882). *Bull. Soc. Nat. Moscou*, No. 4.

Nachtigall, W. (1986a). Pflanzenbiomechanik. Eine forschungsgeschichtliche Studie als Basis für weiterführende Ansätze. In Nachtigall, W., Wisser, Chr.-M., and Wisser, A. (eds.), *Pflanzenbiomechanik (Schwerpunkt Gräser) Konzept SFB 230*, Heft 24, Stuttgart, pp. 21–66.
Nachtigall, W. (1986b). Der Pneu-Begriff in der Botanik des 19 und beginnenden 20. Jahrhunderts. Eine wissenschaftliche Analyse des hydraulischen Formhaltungs- und Formbildungskonzepts. *Jb 1985/86 Wissenschaftskolleg*, Berlin, pp. 313–327.
Oltmanns, J. (1923). *Morphologie und Biologie der Algen*, 2 Bd., 2 Aufl., Jena.
Otto, F. (1976). Zum Kolloquium. In Burkhardt, B. (Hrsg.), *Pneus in Natur und Technik*, Mitt. d. Inst. f. leichte Flächentragwerke (IL), Univ. Stuttgart, vol. 9, pp. 11–19.
Otto, F. (1978). Der Pneu–Bauprinzip des Lebens. *Bild d. Wissenschaft* **10:**124–135.
Patton, E. O. (1915). *Eiserne Brücken, 1 Bd., Eiserne Balkenträger*, 2 Aufl., Kijew, (Russian).
Pederij (1912). *Handbuch der Eisenbetonbrücken*, Petersburg (Russian).
Probst, E. (1931). *VDI-Nachrichten* **11:**No. 21.
Rasdorsky, W. (1911). *Bull. Soc. Nat. Moscou Sect. Biol.* **4:**351–405.
Rasdorsky, W. (1928). Über das baumechanische Modell der Pflanzen. *Ber. d. Deutsch. Bot. Ges.* **46:**48–104.
Rasdorsky, W. (1929). Über die Baumechanik der Pflanzen (Teil I bis III). Biologia generalis. *Int. Arch. Allgemein. Fragen Lebensforsch.* **5:**63–94.
Rasdorsky, W. (1930). Die Lehre von den Biegungsfedern im Dienste der Pflanzenmechanik. *Ber. Deutsch. Bot Ges.* **48:**253–275.
Rasdorsky, W. (1937). Biologia generalis. *Int. Arch. Allgemein. Fragen Lebensforsch.* **XII:**359–398.
Sachs, J. (1868). *Lehrbuch der Botanik* (1 Aufl.), Engelmann, Leipzig (2 Aufl., 1870; 3 Aufl., 1873; 4 Aufl., 1874).
Schütze, M. (1905). *Zur physiologischen Anatomie einiger tropischer Farne, besonders der Baumfarne*, Berlin.
Schwendener, S. (1874). *Das mechanische Prinzip im anatomischen Bau der Monocotylen mit vergleichenden Ausblicken auf die übrigen Pflanzenklassen*, Engelmann, Leipzig.
Schwendener, S. (1878). *Jahresheft Vereins Vaterländ. Nat. Württemberg* **34:**76–81.
Schwendener, S. (1882). *Die Schutzscheiden und ihre Verstärkungen*, Abh. K. Akad. Wiss., Berlin.
Schwendener, S. (1887). *Über Richtungen und Ziele der mikroskopisch-botanischen Forschung*, Berlin.
Schwarz, W. (1930). *Beih. z. Bot. Centralbl. I Abt.* **46:**306–338.
Senebier, J. (1800). *Physiologie vegetale etc. I–V*, Geneva.
Silk, W. K., Wang, L. L., and Cleland, R. E. (1982). Mechanical properties of the rice panicle. *Plant Physiol.* **70:**46–464.
Spencer, H. (1863/1864). *The Principles of Biology*.
Strassburger (1923). *Lehrbuch der Botanik für Hochschulen*, 15 Aufl., Jena.
Tschirch, (1882). Beiträge zur Anatomie und dem Einrollmechanismus einiger Grasblätter. *Jb. Wiss. Bot.* **13:**544–568.
van Marum, M. (1737). Cited by Rasdorsky (1937) and Senebier (1800), Vol. V, p. 182.
Vogel, S. (1981). *Life in Moving Fluids*, Willard Grant Press, Boston, MA.
Welzien, R. (1926). *Kosmos* 44–47.
Wertheim, and Chevandier (1846). *Poggendorfs Annalen*, Ergänz.-Bd. II, p. 481.
Zimmermann, A. (1884). *Jb. Wiss. Bot.* **12:**542–577.
Zukal, H. (1895). *Sitzungsber. Akad. Wiss. Wien* **104:**1377–1395.

*Biomimetics, Vol. 2, No. 2, 1994*

# Bending Stability of Plant Stems: Ontogenetical, Ecological, and Phylogenetical Aspects[1]

**Thomas Speck**[2]

*Bending mechanical properties, their variation during ontogeny, and the underlying ontogenetic shifts in stem anatomy have been studied for plants of different growth habits. The results found for self-supporting trees and shrubs* (Syringa vulgaris, Alnus glutinosa *and* A. viridis) *are significantly different from the findings in non-self-supporting woody lianas* (Aristolochia macrophylla, A. cymbifera, A. gigantea, Fallopia aubertii, *and* Clematis vitalba). *In self-supporting woody plants the Young's modulus increases during ontogeny. In non-self-supporting lianas the Young's modulus decreases during ontogeny. These changes in stem mechanics are caused by changes in stem anatomy. In all self-supporting plants the contribution of the secondary wood to the axial second moment of area increases during ontogeny, whereas in lianas the contribution of the peripheral stiffening tissues decreases. In* C. recta, *a semi-self-supporting species, the Young's modulus is constant during ontogeny. In this plant in all ontogenetic stages a more or less constant contribution of all stem tissues toward the axial second moment of area is found. These findings in extant plants make it possible also to infer the growth habit of fossil plants with permineralized stem remains, by recalculating the mechanical properties of the stems.*

**KEY WORDS:** biomechanics; plant stems; self-supporting plants; semi-self-supporting plants; lianas; fossil plants.

## INTRODUCTION

Growth habit is a striking feature of plants and is often taken as an intuitive way for classifying plants in different "habit groups," as, for example, trees,

[1]This is the published version of a paper presented at the Plant Biomechanics Congress, Montpellier, France, September 5-9, 1994.

[2]Botanic Garden of the Albert-Ludwigs-University, Schänzlestr. 1, D-79104 Freiburg, Germany.



1059-0153/94/0600-0109$07.00/0 

bushes/shrubs, vines/lianas, herbs, and grasses. This classification is not phylogenetic, but this sometimes intuitive classification combines plants with similar architectural features and also often similar mechanical properties. A tree usually has an upright main trunk with lateral branches (acrotonic growth) and is a tall self-supporting woody plant. A bush, also a self-supporting woody plant, has several more or less equal-sized equivalent stems (basitonic growth) and is typically smaller than a tree. Vines are herbaceous or woody non-self-supporting climbing plants that need an external support to which they are fixed by various means. Woody vines are generally referred to as lianas (Putz and Mooney, 1991). In reality there is a continuum of forms from lianas to trees and it is often difficult to make a clear distinction between self-supporting and non-self-supporting plants by morphological and anatomical methods.

Size and growth habit are related to many properties of plants, important for their fitness and for an understanding of aut- and synecology and for the recognition of selective forces acting on plants. Because size and growth habit of plants are governed by mechanical constraints, quantitative studies in biomechanics and functional anatomy of plants with different growth habits assist the interpretation of the ecological significance of stem structure and help to analyze the selective forces acting on plants (Speck *et al.*, 1993, Brüchert *et al.*, 1994). By applying these studies to different ontogenetic stages, variations in biomechanical properties and the underlying changes in stem anatomy can be correlated and compared in self-supporting and non-self-supporting plants (Speck, 1991, 1994). I also summarize a method that allows a (semi-)quantitative distinction between extinct self-supporting and non-self-supporting plants (Speck *et al.*, 1990, 1994; Speck, 1994; Speck and Vogellehner, 1992; Rowe *et al.*, 1993).

## MATERIALS AND METHODS

Plant stems were tested in conventional two-point, three-point, or four-point bending (cf. Bodig and Jayne, 1988; Nachtigall *et al.*, 1988; Vincent, 1990, 1992; Speck, 1991) and in tension. By bending plant stems at different lengths, suitable span-to-radius ratios were determined such that shear forces could be ignored (cf. Kollmann and Côté, 1968; Bodig and Jayne, 1982). Bending forces ($F$) were increased discretely and the maximum deflection ($x_{max}$) was measured after 60 s. In each bending experiment 6 to 12 discrete force increments were applied. For a force increment from the Hookean part of the force–deflection curve, a regression line can be calculated. The slope of the regression line ($b$) allows calculation of the flexural stiffness ($EI$).

$$x_{max} = b \cdot F, \qquad E \cdot I = g/b$$

where $g$ (units of $m^3$) is a factor that takes into consideration the geometry of the different bending rigs.

By calculating the mean axial second moment of area ($I$) of the basal, middle, and apical parts of the tested stem segment, the Young's modulus of the bent stem can be calculated ($E = EI/I$). The allowable variation of the radius along the tested stem length was $<5\%$.

To check the results of the bending experiments, the Young's moduli were determined in tension. For a given species, the Young's moduli measured in tension or bending show the same variations during ontogeny.

Flexural stiffness and Young's modulus may be plotted against the axial second moment of area, which is correlated with the ontogenetic stage of the stems (Figs. 1 and 2).

To discern the different growth habits in the plots of flexural stiffness against the axial second moment of area, the mean value of the Young's moduli of plant stems belonging to the youngest ontogenetic stage ($E_{OS1}$) was used as a slope to calculate a straight line, which I call the neutral line (NL = $E_{OS1} \cdot I$). If the stem diameter increased during ontogeny by a proportinate growth of all stem tissues—that is, if the contribution of the different tissues toward the axial second moment of area were constant during ontogeny—the Young's modulus of the plant stems would also be constant during ontogeny and the data for flexural stiffness would fall on the neutral line. This assumes that the Young's moduli of the different stem tissues are constant for all tested ontogenetic stages. This assumption is acceptable and can be used as a first-order approximation for mature tissues in woody plants, as present in the tested plant stems.

For an analysis of the ontogenetic variations in stem anatomy underlying the observed changes in mechanical properties during ontogeny, a model of a transverse section of the stem is constructed which allows the calculation of the cross-sectional area and the axial second moment of area of the entire cross section and of the various stem tissues (Speck *et al.*, 1990; Rowe *et al.*, 1993). The geometrical parameters for calculation of cross-sectional area and axial second moment of area were measured on transverse sections of fresh material (stained with phloroglucinol/hydrochloric acid). The accuracy of this method has been tested in some transverse sections by using a digitizer pad describing the cross-sectional area and axial second moment of area of the different stem tissues. The results of this lengthy method differ only slightly from the values calculated using the models. Data for fossil plants came from thin sections and acetate peels of permineralized stems; furthermore, photographs from publications were used.

## BENDING MECHANICS AND FUNCTIONAL ANATOMY OF EXTANT PLANTS

### Self-Supporting Trees and Shrubs

More than 250 stems of three woody self-supporting plants [*Syringa vulgaris* L., *Alnus viridis* (Chaix) DC., *Alnus glutinosa* (L.) Gaertn.] were tested in bending experiments. The age of the stems ranges from 1 to 15 years.

The data of flexural stiffness for older ontogenetic stages are clearly above the neutral line (Fig. 1A). This increase in "bending effectivity" during ontogeny is also reflected in the variation of the Young's modulus. In small to medium-sized stems (1 to 3–4 years old) the Young's moduli increase steeply with the axial second moment of area (Fig. 2A). In bigger stems, of self-supporting plants 4–5 to 15 years old, the Young's moduli become more or less constant, varying randomly with large variation (Fig. 2A).

The increase in the Young's modulus during ontogeny is correlated with an increase in wood (Fig. 3). In *Syringa vulgaris*, for example, the contribution of wood to the axial second moment of area increases from 17% in the youngest, 1-year-old axes to 51% in the oldest ontogenetic stage tested (i.e., in 6- to 10-year-old stems). At the same time the contribution of the cortex (including outer bark and phloem) diminishes: in *S. vulgaris* from 75% in the youngest, 1-year-old axes to 49%, and the share of pith decreases from 8% to <0.5% (Table I).

The changes in contribution of the different stem tissues to the cross-sectional area and axial second moment of area occur mainly in stems 1 to 3–4 years old. In these ontogenetic stages the contribution of wood to the axial second moment of area increases rapidly. In older ontogenetic stages the increase in the share of wood to the axial second moment of area is drastically reduced. This means that the contribution of tissues to the axial second moment of area becomes more or less constant for the older ontogenetic stages within the age range tested (i.e., in 5- to 15-year-old stems). This explains why the Young's moduli increase rapidly in woody stems 1 to 3–4 years old. But then in older ontogenetic stages, which have a more or less constant contribution of tissues to the axial second moment of area, the increase in the Young's modulus also slows down extremely, to become more or less constant for 5- to 15-year-old stems.

The kind of variations of bending mechanical properties in bigger stems is possibly different in shrub-like and in tree-like species. In shrub-like species, e.g., *S. vulgaris* and *Alnus viridis*, the Young's moduli become more or less constant for stems older than 4–5 years. In the tree-like *A. glutinosa*, on the other hand, the Young's moduli show a slow increase with increasing stem diameter also in bigger stems. Some first results of bending tests in upright main stems with diameters between 30 and 40 cm yielded Young's moduli between 5.1 and 7.6 $GNm^{-2}$ [for the bending equipment used see Wessolly (1989, 1991, 1993) and Sinn and Wessolly (1989)]. The mean Young's modulus for stems of this size range is 6.6 $GNm^{-2}$, about 2.4 times larger than that found in 5- to 10-year-old stems with diameters between 1.3 and 2.2 cm ($E_{mean}$, 2.8 $GNm^{-2}$; $E_{min}$, 1.7 $GNm^{-2}$; $E_{max}$, 4.4 $GNm^{-2}$; see Fig. 7). The underlying anatomical reason may be that in trees, as in shrubs, the increase in the relative contribution of wood to the axial second moment of area slows down after a phase of rapid

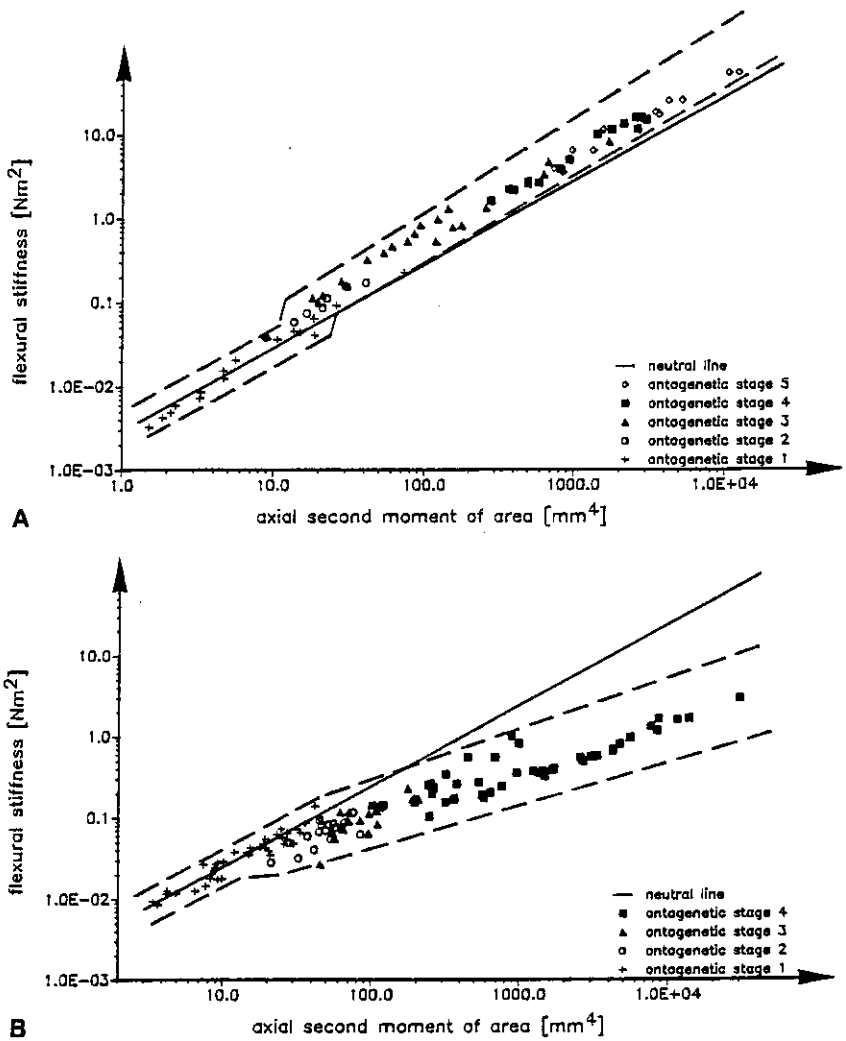


**Fig. 1.** The flexural stiffness of the plant stems plotted against the axial second moment of area (double logarithmic plot). The neutral line (NL) is calculated from the mean value of the Young's modulus of the youngest ontogenetic stage (OS1; marked by crosses); NL = $E_{OS1} \cdot I$. The ontogenetic stages (OS1 to OS5 for *Syringa vulgaris* and OS1 to OS4 for *Aristolochia macrophylla*) are defined morphologically according to the structure of the bark (Speck, 1991) and correspond to the age of the stems given by the number of annual rings (NAR). (A) In self-supporting woody plants data for older ontogenetic stages are clearly above the NL, as shown here for *S. vulgaris*. OS1, NAR = 1 (youngest annual shoots, $E_{OS1}$ = 2.85 GNm$^{-2}$); OS2, NAR = 1 (older annual shoots); OS3 NAR = 2 to 3; OS4, NAR = 4 to 5; OS5, NAR = 6 to 10. (B) In woody lianas data for older ontogenetic stages are below the NL, which is shown here for *A. macrophylla*. OS1, NAR = 1 ($E_{OS1}$ = 2.47 GNm$^{-2}$); OS2, NAR = 2; OS3, NAR = 3 to 5; OS4, NAR = 6 to 18. (C) In the semi-self-supporting taxon *Clematis recta* the data are scattered around the NL for all tested ontogenetic stages ($E_{youngest\text{-}OS}$ = 3.89 GNm$^{-2}$).

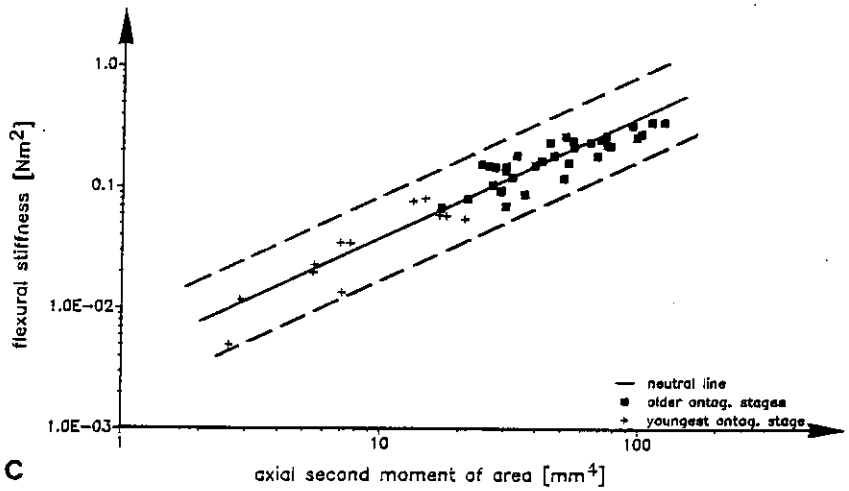


**Fig. 1.** Continued.

rise in young ontogenetic stages, but that in trees also in older ontogenetic stages a slow increase in the relative contribution of wood with increasing stem diameter occurs (e.g., in *A. glutinosa*, from 66% in 5- to 10-year-old stems to about 75% in stems 30 to 40 cm in diameter). In shrubs, on the other hand, the relative contribution of tissues to the axial second moment of area remains nearly constant in older ontogenetic stages, perhaps as a consequence of the shrub's restricted ability to develop stems with large diameters.

In addition to changes in the anatomical structure of the stems during ontogeny, (small) variations of the Young's modulus of the different stem tissues during ontogeny are also possible. Other changeable factors include, for example, chemical modifications of cell walls during the formation of heartwood or the functioning of wood as water storage tissue, so altering its mechanical properties. The larger share of late wood sometimes produced in older ontogenetic stages can also change the mechanical properties of the wood cylinder as a whole. These variations seem not to alter the observed overall trend of bending mechanical properties during ontogeny in woody plants. In nonwoody plants the variations of mechanical properties of tissues during ontogeny may be much more distinct, e.g., caused by lignification of the walls of parenchymatous cells (Niklas, 1990, 1992, 1993).

## Non-Self-Supporting Lianas

More than 400 stems of five woody lianas [*Aristolochia macrophylla* Lam., *A. cymbifera* Mart. & Zucc., *A. gigantea* Hook. (=*A. grandiflora* Arruda), *Clematis vitalba* L., *Fallopia aubertii* (L. Henry) Holub] were tested in bending and tension. The age of the stems ranged from 1 to 29 years.

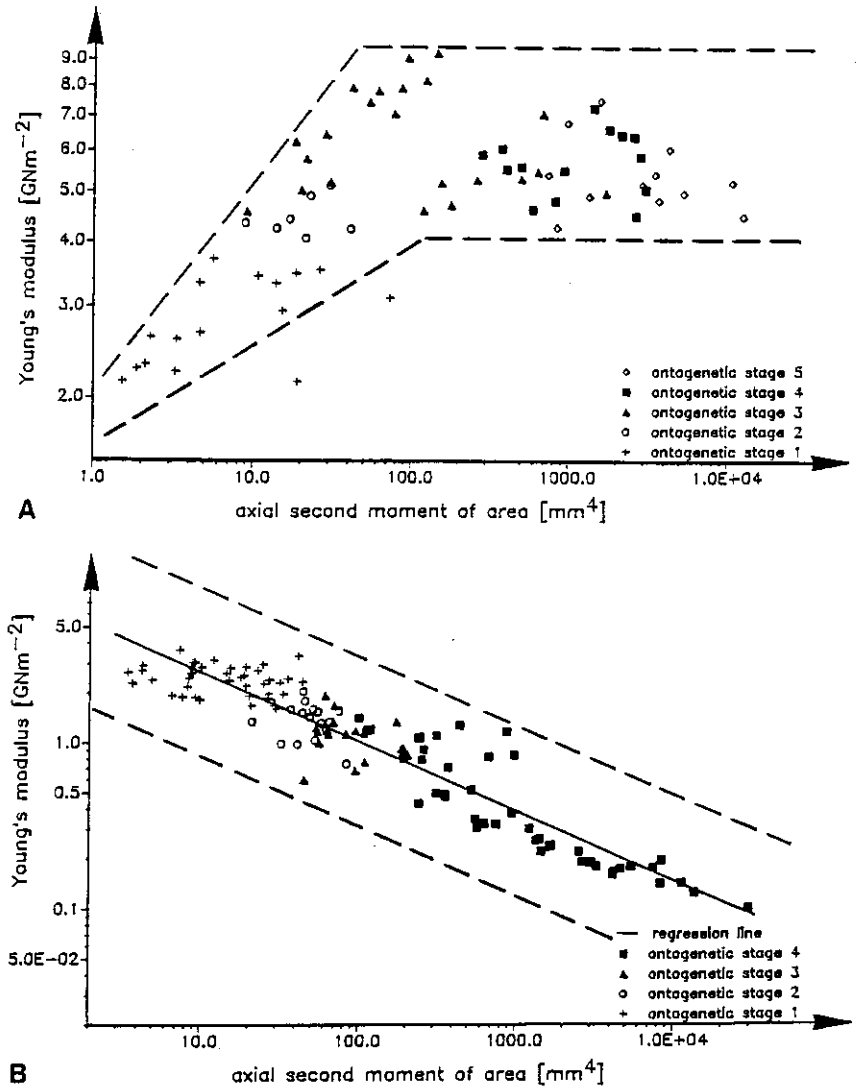


**Fig. 2.** The Young's modulus of the plant stems plotted against the axial second moment of area (double logarithmic plot). The meaning of ontogenetic stages is the same as in Fig. 1. (A) In self-supporting woody plants the Young's moduli increase rapidly during early ontogenetic stages (OS1 to OS3). In older ontogenetic stages (OS4 and OS5) the Young's moduli change very slowly and become more or less constant, at least in shrub-like self-supporting plants, as shown here for *Syringa vulgaris*. (B) In woody lianas, as in *Aristolochia macrophylla*, the Young's moduli decrease with increasing axial second moment of area. The regression line is given by $y = 10^{3.85} \cdot x^{-0.42}$; the correlation coefficient is $-0.939$. (C) In the semi-self-supporting plant *Clematis recta* the Young's moduli are constant during ontogeny but vary randomly over a large range.

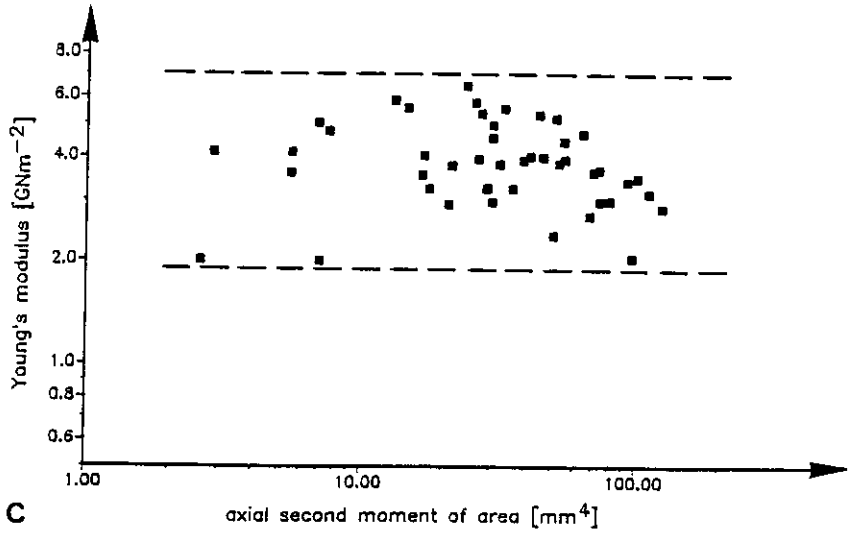


**Fig. 2.** Continued.

The flexural stiffness of older ontogenetic stages is clearly below the neutral line (Fig. 1B), showing that "bending effectivity" decreases drastically during ontogeny. In all five woody lianas, the Young's moduli of stems in the youngest ontogenetic stages are relatively high, after which the Young's moduli decrease during ontogeny to about 25 to 15% of their initial values.

The changes in the mechanical properties during ontogeny are correlated with changes in the amount and cross-sectional shape of the different stem tissues (Fig. 4). The decrease in the Young's modulus during ontogeny is correlated with an increasing fragmentation of the peripheral ring(s) of strengthening tissue which is/are entire in young ontogenetic stages. It is also correlated with a considerable decrease in the contribution of these stiffening tissue(s) to the axial second moment of area. In *A. macrophylla* (Table II), the contribution of the peripheral collenchymatous and sclerenchymatous tissues to the axial second moment of area decreases during ontogeny from 17 to 2% (collenchyma) and from 25 to 2% (sclerenchyma). On the other hand, the contribution to the axial second moment of area of compliant tissues such as parenchymatous cortex and outer bark increases during ontogeny. The contribution of the xylem, which is relatively compliant with large vessels and huge wood rays, also increases significantly (in *A. macrophylla*, from 8 to 29%).

In *A. macrophylla* the secondary phloem is, apart from the assimilate conducting elements, entirely parenchymatous (Figs. 4B and C). In *C. vitalba* and *F. aubertii*, on the contrary, in each annual growth phase in the secondary

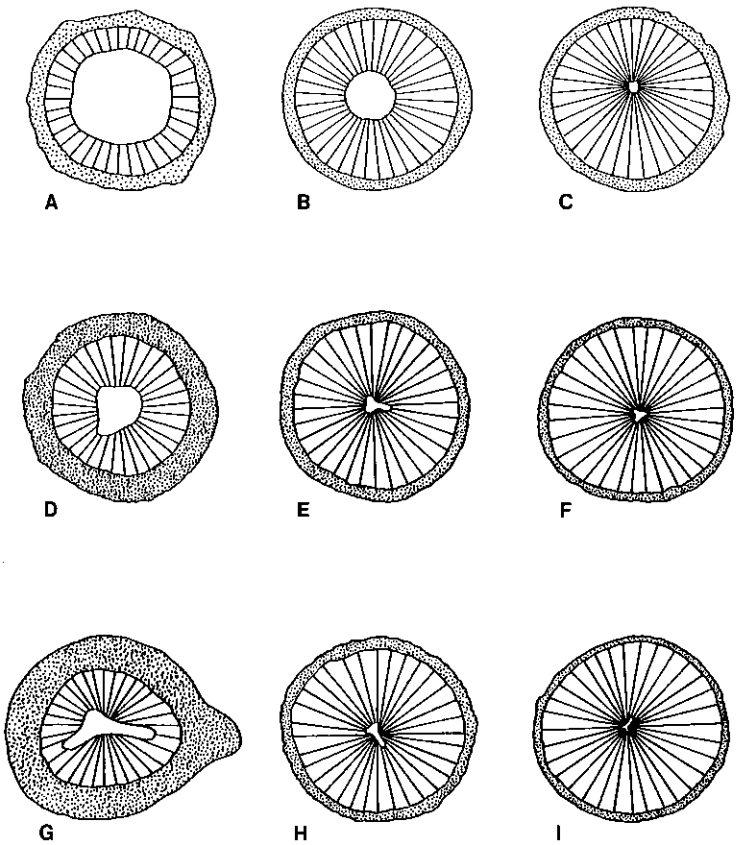


**Fig. 3.** Variations in stem anatomy in self-supporting shrubs and trees. The drawings represent transverse sections of different ages; all transverse sections are enlarged to the same size. The original diameter for each transverse section is given in parentheses. Tissues from the center outward: white, pith; hatched, wood; stippled, cortex (including phloem, epidermis, and bark). (A–C) *Syringa vulgaris*: (A) 1-year-old stem (4.0 mm); (B) 3-year-old stem (12.4 mm); (C) 18-year-old stem (38.5 mm). (D–F) *Alnus glutinosa* (stump shoots): (D) 1-year-old stem (4.0 mm); (E) 4-year-old stem (22.1 mm); (F) 8-year-old stem (37.0 mm). (G–I) *A. viridis* (from the Black Forest): (G) 1-year-old stem (2.9 mm, without "wing"); (H) 4-year-old stem (15.0 mm); (I) 12-year-old stem (25.5 mm).

phloem, sclerenchymatous segments are formed (Figs. 4E, F, H, and I). However, these segments are isolated and never fuse to a closed sclerenchymatous ring as in young stems.

In older *C. vitalba* the bark loosens from the stems in strips (Figs. 4E and F). The flexural stiffness for older ontogenetic stages is also below the neutral line and the Young's modulus decreases to 16% of its initial value (Fig. 5). A

**Table I.** *Syringa vulgaris:* Variation of the Percentage Contribution of Different Stem Tissues to the Axial Second Moment of Area During Ontogeny (Mean ± SD)[a]

| | NAR: 1 (youngest annual shoots), $n = 20$ | NAR: 1 (older annual shoots), $n = 12$ | NAR: 2, $n = 8$ | NAR: 3, $n = 12$ | NAR: 4–5, $n = 14$ | NAR: 6–10, $n = 25$ |
|---|---|---|---|---|---|---|
| Cortex | 74.6 ± 6.1 | 63.7 ± 3.0 | 62.0 ± 7.4 | 53.4 ± 6.8 | 50.5 ± 4.1 | 49.2 ± 3.9 |
| Wood | 17.3 ± 6.6 | 29.3 ± 4.1 | 34.1 ± 9.8 | 45.4 ± 6.9 | 49.0 ± 4.0 | 50.6 ± 4.0 |
| Pith | 8.1 ± 2.5 | 7.0 ± 2.7 | 3.9 ± 3.1 | 1.2 ± 0.5 | 0.5 ± 0.3 | 0.2 ± 0.3 |

[a] $n$, number of analyzed stems; NAR, number of annual rings.

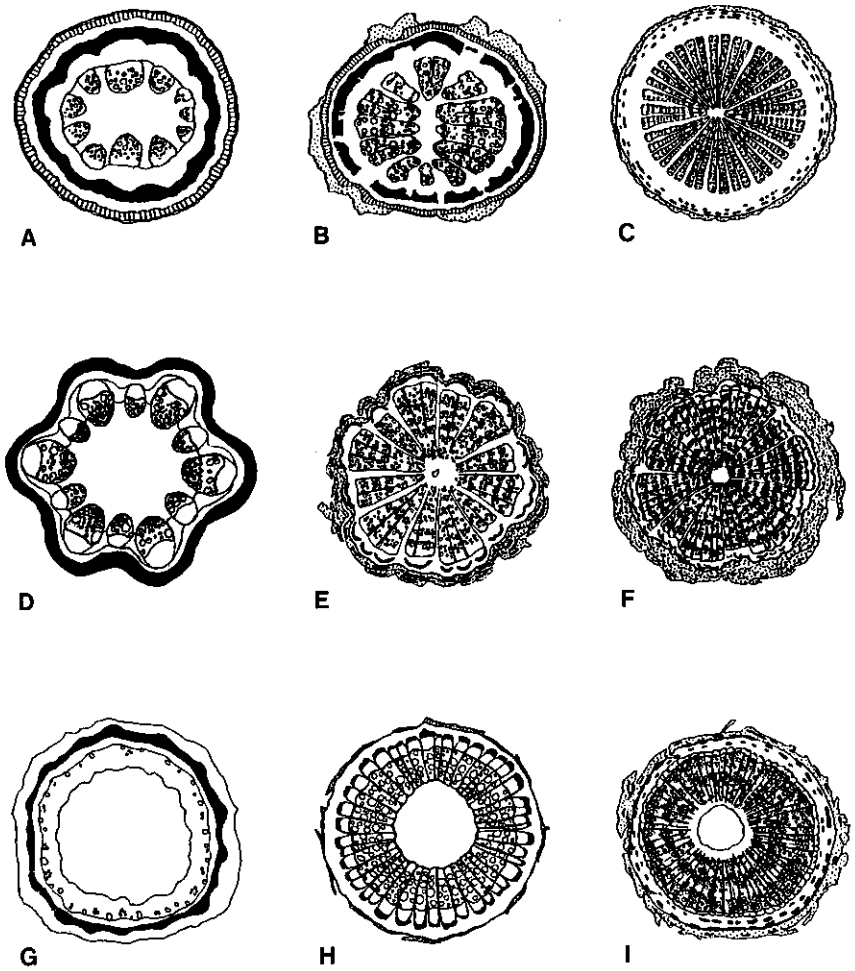


**Fig. 4.** Variations in stem anatomy in woody lianas. The drawings represent transverse sections of different ages; all transverse sections are enlarged to the same size. The original diameter for each transverse section is given in parentheses. Tissue types from the center outward: central white area, pith; wood consisting of vessels and tracheids (wedge-shaped area; the vessels are drawn as small circles) and ray parenchyma (white areas between the wedges); white area, parenchymatous cortex and phloem; black area, sclerenchymatous tissue; hatched area, collenchymatous tissue; stippled area, bark; outermost line, epidermis. (A–C) *Aristolochia macrophylla*—this species comprises an entirely parenchymatous secondary phloem: (A) 1-year-old stem (4.8 mm); (B) 4-year-old stem (6.6 mm); (C) 14-year-old stem (29.1 mm). In the other two liana species, *Clematis vitalba* and *Fallopia aubertii*, sclerenchymatous segments are built in the secondary phloem each year. (D–F) *C. vitalba*—in this species in older ontogenetic stages (E and F) the bark loosens from the stems in strips: (D) 1-year-old stem (4.4 mm, mean diameter of the star-shaped transverse section); (E) 6-year-old stem (13.4 mm); (F) 7-year-old stem (24.6 mm). (G–I) *F. aubertii*: (G) young 1-year-old stem (4.3 mm); (H) older 1-year old stem (6.6 mm); (I) 3-year-old stem (11.3 mm).

**Table II.** *Aristolochia macrophylla:* Variation of the Contribution of the Different Stem Tissues to the Axial Second Moment of Area During Ontogeny (Mean ± SD)[a]

| | NAR: 1 ($n$ = 7) | NAR: 2 ($n$ = 7) | NAR: 3-4 ($n$ = 7) | NAR: 5-7 ($n$ = 9) | NAR: 8-18 ($n$ = 4) |
|---|---|---|---|---|---|
| Bark | 5.5 ± 0.4 | 17.6 ± 12.2 | 20.8 ± 16.3 | 26.9 ± 3.3 | 18.8 ± 9.2 |
| Paren. cortex | 42.5 ± 4.5 | 40.9 ± 2.4 | 39.1 ± 6.4 | 46.5 ± 2.6 | 48.6 ± 7.9 |
| Collenchyma | 17.0 ± 1.9 | 13.4 ± 5.1 | 10.6 ± 4.0 | 3.5 ± 0.6 | 1.9 ± 0.9 |
| Sclerenchyma | 24.6 ± 4.0 | 17.0 ± 5.2 | 12.6 ± 3.2 | 4.6 ± 0.3 | 2.1 ± 1.6 |
| Wood | 8.2 ± 0.7 | 10.8 ± 0.4 | 16.6 ± 4.0 | 18.4 ± 2.0 | 28.6 ± 3.8 |
| Pith | 2.2 ± 1.6 | 0.4 ± 0.2 | 0.3 ± 0.3 | 0.05 ± 0.04 | 0.01 ± 0.01 |

[a] $n$, number of analyzed stems; NAR, number of annual rings.

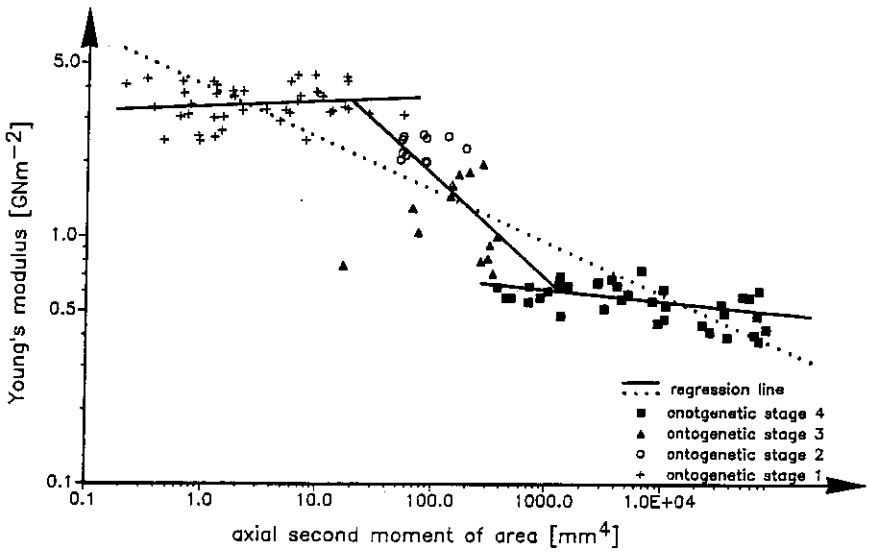


**Fig. 5.** *Clematis vitalba*: the Young's modulus of the plant stems plotted against the axial second moment of area (double logarithmic plot).

difference from the other lianas is the markedly two-phasic behavior stiffness and Young's modulus. The dotted line in Fig. 5 is a regression over all ontogenetic stages, whereas the three solid lines represent separate regressions for the two phases and the transition zone. These regressions fit the test data much better than the regression line for a continuous decrease in the Young's modulus. The first phase, given by ontogenetic stage 1, is characterized by a high Young's modulus of about 3.45 GNm$^{-2}$, which is nearly constant within this stage. The second phase, represented by ontogenetic stage 4, has a low Young's modulus

of about 0.55 $GNm^{-2}$, showing only a small decrease. The transition zone (ontogenetic stages 2 and 3) is characterized by a rapid decrease (about 84%) in the Young's modulus. This may be because as the bark loosens, parts of the stiffening sclerenchymatous cortex tissues sluff off (Figs. 4E and F). The loose bark contributes to the calculated axial second moment of area of the stem, but its contribution to the flexural stiffness is only small, because of its loose contact with the rest of the stem. This further reduces the Young's modulus of the stems, in addition to the anatomical changes found in the other lianas. A rapid increase in the amount of loose bark is found especially in ontogenetic stages 2 and 3, where the rapid decrease in the Young's modulus occurs.

### Semi-Self-Supporting Plants

Semi-self-supporting plants, which are perhaps best named with the German term "Spreizklimmer", have a growth form that can be described as neither truly self-supporting nor truly lianescent (Schenck, 1912). Plants with this growth habit can live in a more or less liana-like manner with the support of the surrounding vegetation. Furthermore, this life-form also enables growth in dense monotypic stands, where the plants provide mutual support (e.g., *Equisetum giganteum*). For both growth habits, a close interconnection with each other or with the surrounding vegetation is a prerequisite. This interconnection can be achieved by means of fronds or branches. The two growth modes of the semi-self-supporting habit can also be found in the bracken, *Pteridium aquilinum*. In the liana-like growth habit the fronds of *P. aquilinum* can grow up to 6 or 7 m in length (personal observation). In the "normal" self-supporting growth mode—often in dense monotypic stands—the length of fronds is restricted to about 2.5 m.

The mechanical properties of semi-self-supporting plants have been experimentally tested only in the perennial *C. recta*. This plant normally grows with upright axes, but the stems bend in a curved manner if they exceed a given length. It may, however, also grow in a more or less scrambling manner with support from the surrounding vegetation. Stems of the nonscrambling growth habit of *C. recta* show more or less constant Young's moduli during ontogeny, with a large variation, between 2.0 and 6.4 $GNm^{-2}$ (Fig. 2C). This huge variation may be because the degree of self-support in the tested stems differs, and the ontogenetic phase from which a given stem has been supported by the surrounding vegetation is different for different stems.

In this taxon there exists neither an increase in the bending effectivity during ontogeny, as found in true self-supporting plants, nor a decrease, as found in lianas. Stems of *C. recta* can be interpreted as being "neutral" during ontogeny as far as the bending mechanical properties are concerned.[3]

[3] *C. recta* has hollow stems. Values of the axial second moment of area and Young's modulus relate to the massive part of the stem, not to the entire stem with the medullary cavity.

This is because there is a proportionate increase in all stem tissues during ontogeny, entailing a more or less constant contribution of all stem tissues to the axial second moment of area. The nearly constant tissue distribution is brought about because the enlargement of the basal internodes is accompanied by the formation of additional entire vascular bundles (Fig. 6). All vascular bundles have a more or less constant tissue composition.

## DISCUSSION

The flexural stiffness and Young's modulus in lianas and in self-supporting plants change in a nearly opposite manner during ontogeny, because of the different selective forces acting on them. The loads caused by wind increase with height. Therefore it is an important selective advantage for self-supporting plants not only to enlarge the volume of the stabilizing tissues in the basal stem parts by secondary growth, but also to optimize the distribution of these tissues with regard to the mechanical properties in bending. This causes an increase in the Young's modulus of the stem as a whole during ontogeny.

For non-self-supporting plants, it is a selective advantage to be relatively stiff when young, until the stems have found a support. In older plants, if the lianas are already attached to their support, it is a selective advantage to be relatively flexible, so that the stems can shed the bending forces to a certain degree.

In some species of liana showing typical bending properties in the young

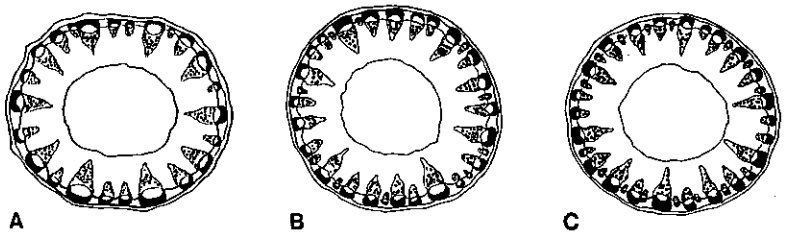


**Fig. 6.** Variations in stem anatomy in the semi-self-supporting plant *Clematis recta*. The drawings represent transverse sections of different internodes of one plant specimen, i.e., of stem segments of different ontogenetic ages. All transverse sections are enlarged to the same size. The original diameter for each transverse section is given in parentheses. Tissue types from the center outward: central white area, pith cavity; vascular bundles arranged as an eustele in the parenchymatous cortex tissue—each bundle comprises xylem (wedge-shaped inner area; the vessels are drawn as small circles), cambium, assimilate conducting phloem (white area), and sclerenchymatous bundle sheath (black area); outermost line of the transverse section, epidermis. Internodes are counted from the stem base upward. (A) Internode 6 (5.2 mm); number of vascular bundles, 24. (B) Internode 3 (6.6 mm); number of vascular bundles, 34. (C) Internode 2 (6.8 mm); number of vascular bundles, 39.

and middle-aged stages, the very basal, old stem parts seem to become more or less self-supporting. This seems to be true for *Wisteria sinensis*. Other lianas, such as many tropical forest lianas, start from a (short) upright stem and become lianescent in a second developmental stage (Putz, 1984, 1985; Caballé, 1986, 1993; Putz and Holbrook, 1991).

This mechanical behavior, also found in other self-supporting woody plants and lianas or lianescent plant parts, seems to be typical for plants of these growth habits. Putz and Holbrook (1991) found, in tropical lianas and tree saplings 2–5 cm in stem diameter (from Luquillo Mountains, Puerto Rico), Young's moduli that are very similar to ours. They reported a mean Young's modulus of $0.61 \pm 0.44$ GNm$^{-2}$ for 12 liana species (ranging from 0.15 to 1.7 GNm$^{-2}$), which is very close to the values found in similar-sized stems of the lianas we have tested (*A. macrophylla*, $E_{OS4} = 0.50$ GNm$^{-2}$; *C. vitalba*, $E_{OS4} = 0.56$ GNm$^{-2}$; *F. aubertii*, $E_{OS4} = 0.73$ GNm$^{-2}$). The data for the five tree saplings are, with $E = 4.7 \pm 3.8$ GNm$^{-2}$ (range of data, 1.7 to 12.0 GNm$^{-2}$), comparable to the values we measured in similar-sized stems of self-supporting woody plants (*S. vulgaris*, $E_{OS4/OS5} = 5.5$ GNm$^{-2}$; *Alnus glutinosa*, $E_{OS5} = 2.7$ GNm$^{-2}$; *A. viridis*, $E_{OS5} = 3.3$ GNm$^{-2}$). Gartner (1991a, b) found, in comparing the mechanical properties of shrub-like and vine-like specimens of *Toxicodendron diversifolium* (T. & G.) Greene, data similar to those of Speck (1991) and the present work. The Young's moduli for different stem diameters of the supported (vine-like) specimens fit very well with the pattern I found (Gartner, 1991a, Figs. 4 and 5). The Young's moduli of the unsupported (shrub-like) specimens resemble more the pattern I found for semi-self-supporting plants than the pattern found in self-supporting plants (cf. Cannell and Morgan, 1987; Cannell *et al.*, 1988). For that reason *T. diversifolium* could perhaps best be compared with the "Spreizklimmer" *Rosa canina* agg. L., a plant for which a liana-like and a shrub-like semi-self-supporting to self-supporting growth mode exists (cf. Haux, 1993).

The results for *C. recta* show that at least this semi-self-supporting plant can be characterized as being neither truly lianescent nor truly self-supporting. However, the question of whether the biomechanically "neutral behavior" is a feature typical of the semi-self-supporting growth habit cannot be answered before other (woody) semi-self-supporting plants have been tested. Recent studies on *R. canina* agg. corroborate these findings for young ontogenetic stages of woody stems from the shrub-like growth mode of this semi-self-supporting plant (cf. Haux, 1994).

These results prove that in extant plants form (growth habit), structure (stem anatomy), and function (mechanical properties) can be correlated in an unequivocal manner. The experimental findings in extant plants have been used to derive a method that allows a semiquantitative distinction between extinct self-supporting an extinct non-self-supporting plants (i.e., lianas and semi-self-

supporting plants). As methods and results for various fossil plants are described in detail elsewhere (Speck *et al.*, 1990, 1992; Speck and Vogellehner, 1992; Rowe *et al.*, 1993; Speck, 1994; Speck and Rowe 1994), I summarize only some main results.

It is sometimes very problematic to determine size and growth habit in fossil plants, because of (a) the often disarticulated nature of plant fossils and (b) the fact that the mechanical properties of fossil plant material cannot be tested experimentally. Mathematical models of the tissue distribution in the fossil stems make it possible to calculate the axial second moment of area of the various stem tissues and of the entire stem. The Young's moduli of the different fossil tissue types can be estimated quantitatively by recalculation from the most similar extant tissue type for which experimental mechanical data are known. If fossil plant stems are considered as composite structures, the flexural stiffness and Young's modulus of the fossil plant stem can be calculated. Thus, the changes in the bending properties during ontogeny can also be studied in fossil plants and their growth habit can be inferred.

The method was tested by applying it to *Diaphorodendron vascular* (Binney) DiMichele, for which a reliable reconstruction exists (DiMichele, 1981). *D. vascular* is a tree, 8 to 15 m tall, with unbranched main trunk and lateral branches. The calculated mechanical data are entirely consistent with experimental data from extant woody plants (Speck, 1994; Speck *et al.*, 1994). The flexural stiffness for older ontogenetic stages is clearly above the neutral line (Fig. 7A) and the Young's modulus increases during ontogeny to more than 3.5-fold its initial value (Fig. 8A). The results corroborate that this method can be used to identify growth habits in fossil plants with secondary growth.

Calculations for exceptionally well-preserved young stems of *Pitus dayi* Gordon prove that, independent of the tissue type inferred for the cortex/periderm, for which the actual tissue type cannot undoubtedly be determined, the mechanical data are consistent with a self-supporting growth mode (Figs. 7B and 8A) (Speck and Rowe, 1994). The biomechanical analysis of stems of two other pteridosperms, for which either the growth habit was controversially discussed [*Lyginopteris oldhamia* (Binney) Potonie] or a lianescent to self-supporting growth habit was assumed more intuitively for reasons of stem size and anatomy (*Calamopitys* sp.), helps to clear up the actual growth habit of these taxa. The mechanical data calculated for *L. oldhamia* make it very probable that this taxon was a non-self-supporting plant (data on flexural stiffness for older ontogenetic stages below the neutral line in Fig. 7C; decrease in the Young's modulus during ontogeny, Fig. 8B). The calculated Young's moduli of *L. oldhamia* are relatively high compared with the Young's moduli found in extant lianas and decrease to only about 60% of their initial value, so it is probable that *L. oldhamia* was a semi-self-supporting plant rather than a pure liana (Speck, 1994; Speck *et al.*, 1994). Data calculated for a thin stem of *Calamopitys* sp.

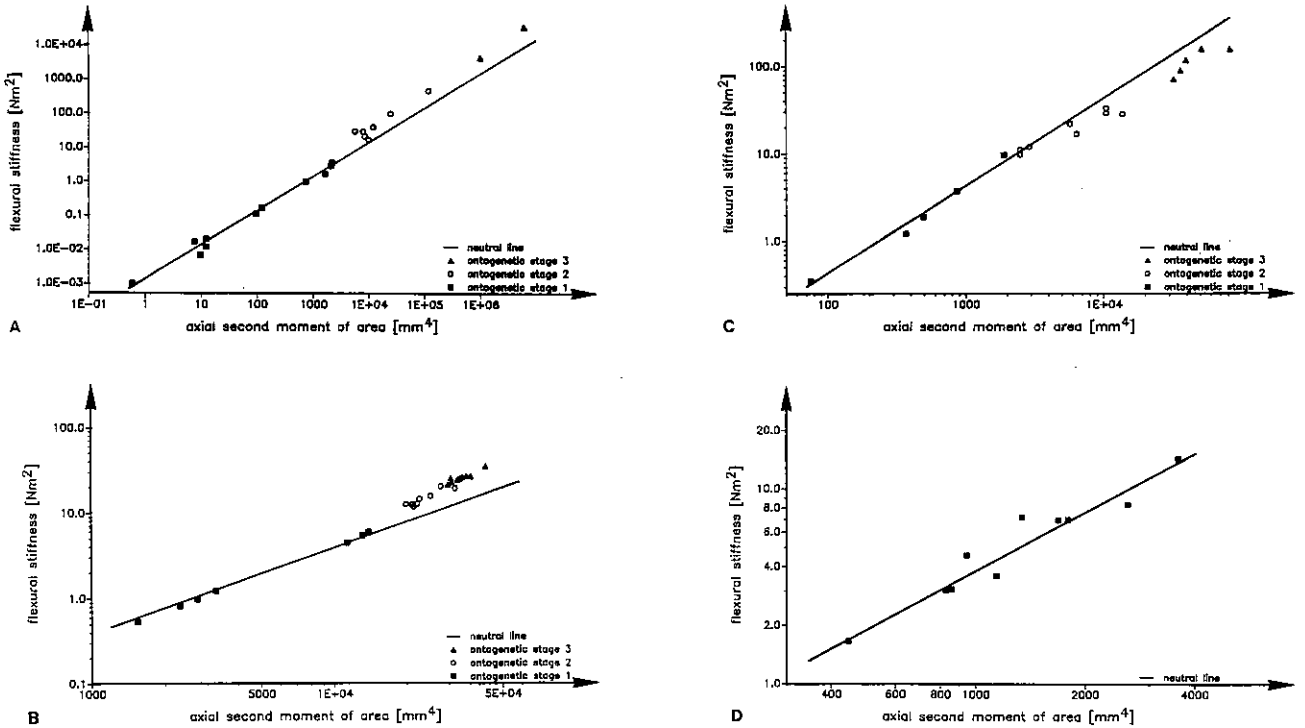


**Fig. 7.** The calculated flexural stiffness of fossil plant stems plotted against the axial second moment of area (double logarithmic plot). The neutral line (NL) is calculated from the mean value of the Young's modulus of the youngest ontogenetic stage (OS1; marked by filled squares); NL = $E_{OS1} \cdot I$. The ontogenetic stages (OS1 to OS3 for *Diaphorodendron vasculare*, *Lyginopteris oldhamia* and *Pitus dayi*) are defined according to anatomical shifts in stem anatomy (Speck, 1994; Speck and Rowe, 1994). In *Calamopitys* sp. no ontogenetic stages can be defined, as over the length of the studied stem fragment, there is no marked change in the percentage tissue contribution (Rowe *et al.*, 1993). (A) *D. vasculare*, $E_{OS1}$ = 1.35 GNm$^{-2}$; (B) *P. dayi* (calculated under the assumption that cortex tissues are bark-like), $E_{OS1}$ = 0.38 GNm$^{-2}$). For these two fossil plants the flexural stiffness data for older ontogenetic stages are clearly above the NL, consistent with the assumed self-supporting habit of these taxa. (C) *L. oldhamia*, $E_{OS1}$ = 4.26 GNm$^{-2}$. Data for older ontogenetic stages are below the NL, making it very probable that *L. oldhamia* is a non-self-supporting plant. (D) *Calamopitys* sp., $E_{youngest\text{-}OS}$ = 3.79 GNm$^{-2}$. The flexural stiffness data are clustered around the NL, i.e., showing an arrangement similar to that found in living semi-self-supporting plants. [A and C from Speck (1994); B from Speck and Rowe (1994); D from Rowe *et al.* (1993).]

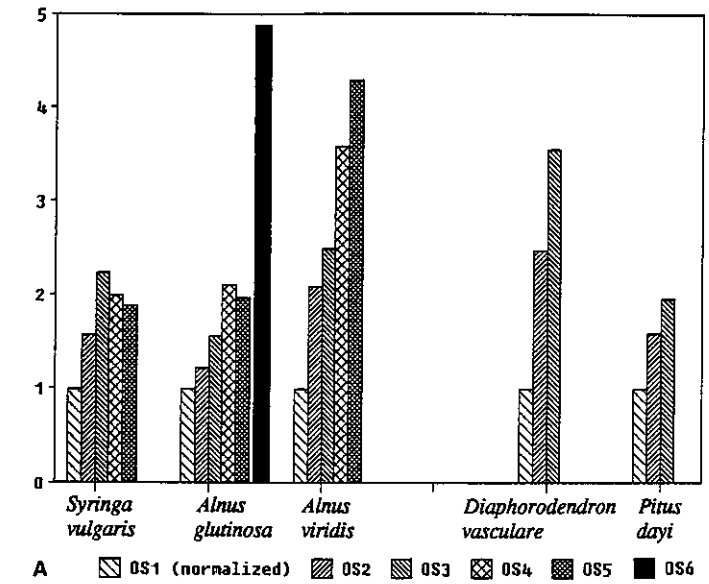


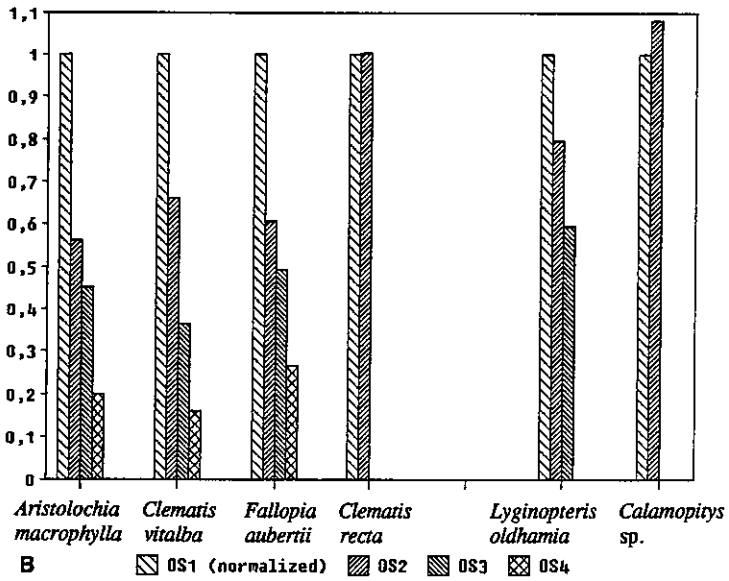


**Fig. 8.** Variations of the normalized Young's modulus during ontogeny in self-supporting and non-self-supporting plants. The mean Young's modulus of the youngest ontogenetic stage tested is normalized to 1.0. (A) In all extant and fossil self-supporting taxa a marked increase in the Young's modulus occurs. The black column [*Alnus glutinosa* (OS6)] represents data for stems 30 to 40 cm in diameter. (B) In all non-self-supporting taxa the Young's modulus either decreases during ontogeny (in plants with a lianescent growth mode) or remains more or less constant during the entire ontogeny (in semi-self-supporting plants).

are consistent with an interpretation, at least for a *Calamopitys* stem of this size, of a semi-self-supporting plant (Rowe *et al.*, 1993, Speck *et al.*, 1994). As in the extant semi-self-supporting *Clematis recta*, the data for flexural stiffness are scattered around the neutral line (Fig. 7D) and the Young's moduli remain more or less constant during ontogeny.

These few examples of fossil plants show that comparative investigations of the mechanics of lianas and self-supporting and semi-self-supporting plants not only yield a better understanding of some features of living plants, but also yield results important for a better understanding of the structure and function of fossil plants. In living plants, for example, the methods allow quantitative conclusions concerning the influence of changes of stem anatomy during ontogeny on the mechanical properties. In fossil plants comparatively reliable conclusions about whether a given taxon was a self-supporting plant or a liana or a semi-self-supporting plant are possible. This is of interest not only for reconstruction of fossil plants but also for questions concerning autecology and synecology of the fossil taxa.

## ACKNOWLEDGMENTS

I am grateful for stimulating discussions with Drs. A. Bogenrieder, N. P. Rowe, H.-Ch. Spatz, and D. Vogellehner. I thank N. P. Rowe and H.-Ch. Spatz for critical reading of the manuscript and Dipl-Biol. B. Heneka for preparing some of the drawings.

## REFERENCES

Bodig, J.; and Jayne, B. A. (1982). *Mechanics of Wood and Wood Composites*, Van Nostrand Reinhold, New York, Cincinnati, Toronto, London, Melbourne.

Brüchert, F., Bogenrieder, A., and Speck, T. (1994). Anatomischer und biomechanischer Vergleich der Sproßachsen von *Alnus viridis* (Chaix.) DC. aus dem Schwarzwald und den Lechtaler Alpen mit Stockausschlägen von *Alnus glutinosa* (L.) Gaertn. aus dem Schwarzwald im Hinblick auf die Standortsökologie beider Arten. *Ber. Naturf. Ges. Freiburg i. Br.* **81** (in press).

Caballé, G. (1986). *Sur la biologie des lianes ligneuses en forêt gabonaise*, Thèse de Doctorat d'Etat en Sciences, Université de Montpellier 2 Sciences et Techniques du Languedoc.

Caballé, G. (1993). Liana structure, function and selection: A comparative study of xylem cylinders of tropical rainforest species in Africa and America. *Bot. J. Linn. Soc.* **113**:41–60.

Cannell, M. G. R., and Morgan, J. (1987). Young's modulus of sections of living branches and tree trunks. *Tree Physiol.* **3**:355–364.

Cannell, M. G. R., Morgan, J., and Murrey, M. B. (1988). Diameters and dry weights of tree shoots: Effects of Young's modulus, taper, deflection and angle. *Tree Physiol.* **4**:219–231.

Carlquist, S. (1991). Anatomy of vine and liana stems: a review and synthesis. In Putz, F. E., and Mooney, H. A. (eds.), *The Biology of Vines*, Cambridge University Press, Cambridge, pp. 53–71.

DiMichele, W. A. (1981). Arborescent lycopods of Pennsylvanian age coals: *Lepidodendron*, with description of new species. *Palaeontographica* **175**:85–125.

Gartner, B. L. (1991a). Structural stability and architecture of vines vs. shrubs of Poison Oak, *Toxicodendron diversilobum*. *Ecology* **72**:2005–2015.

Gartner, B. L. (1991b). Is the climbing habit of poison oak ecotypic? *Funct. Ecol.* **5:** 696–704.
Haux, M. (1993). *Veränderungen der Anatomie und der biomechanischen Eigenschaften im Laufe der Ontogenese bei Sproßachsen der Gattung Rosa L.*, Staatsexamensarbeit (manuscript).
Kollmann, F. P., and Côté, W. A. (1968): *Principles of Wood Science and Technology. I. Solid Wood*, Springer, Berlin, Heidelberg.
Nachtigall, W., Wisser, C.-M., and Wisser, A. (1988). Ein erster Einblick in biomechanische Konstruktionsprinzipien von Gräsern. *Natürliche Konstruktionen, Mitteilungen des SFB 230* **1:**59–66.
Niklas, K. J. (1990). Biomechanics of *Psilotum nudum* and some early paleozoic vascular sporophytes. *Am. J. Bot.* **77:**590–606.
Niklas, K. J. (1992). *Plant Biomechanics*, University of Chicago Press, Chicago.
Niklas, K. J. (1993). Influence of tissue density-specific mechanical properties on the scaling of plant height. *Ann. Bot.* **73:**173–179.
Putz, F. E. (1984). How trees avoid and shed lianas. *Biotropica* **16:**9–23.
Putz, F. E. (1985). Woody vines and forest management in Malaysia. *Commonwealth Forest Rev.* **64:**369–365.
Putz, F. E., and Holbrook, N. M. (1991). Biomechanical studies in vines. In Putz, F. E., and Mooney, H. A. (eds.), *The Biology of Vines*, Cambridge University Press, Cambridge, pp. 73–97.
Putz, F. E., and Mooney, H. A. (eds.) (1991). *The Biology of Vines*, Cambridge University Press, Cambridge.
Rowe, N. P., Speck, T., and Galtier, J. (1993). Biomechanical analysis of a Palaeozoic gymnosperm stem. *Proc. R. Soc. Lond. B* **252:**19–28.
Schenck, H. (1912). Lianen. In *Handbuch der Naturwissenschaften, 6. Band*, Fischer, Jena, pp. 176–185.
Sinn, G., and Wessolly, L. (1989). Messungen an Bäumen: Ermittlung der Sicherheiten gegen Kippen oder Bruch. *Das Gartenamt* **38**(7):422–430, **38**(8):483–489.
Speck, T. (1991). Changes of the bending-mechanics of lianas and self-supporting taxa during ontogeny. *Proc. II. Int. Symp. SFB 230, Mitteilungen des SFB 230* **6:**89–95.
Speck, T. (1994). A biomechanical method to distinguish between self-supporting and non self-supporting fossil plants. In Chaloner, W. (ed.), *Fossil Plants as Palaeoenvironmental Indicators, Rev. Pal., Pal.* **81:** 65–82.
Speck, T., and Rowe, N. P. (1994). Biomechanical analysis of *Pitus dayi*: Early seed plant vegetative morphology and its implications on growth habit (submitted for publication).
Speck, T., and Vogellehner, D. (1992). Fossile Bäume, Spreizklimmer and Lianen. Versuch einer biomechanischen Analyse der Stammstruktur. *Cour. Forsch.-Inst. Senckenberg* **147:**31–53.
Speck, T., Spatz, H.-C., and Vogellehner, D. (1990). Contribution to the biomechanics of plants. I. Stabilities of plant stems with strengthening elements of different cross-sections against weight and wind forces. *Bot. Acta* **103:**111–122.
Speck, T., Brüchert, F., and Bogenrieder, A. (1993). A biomechanical and ecological comparison of *Alnus glutinosa* with *Alnus viridis*-clans from the Alps and the Black Forest. *J. Exp. Bot.* **44** (Suppl.):50.
Speck, T., Rowe, N., and Vogellehner, D. (1994). Growth habits in plants and their correlation with stem's functional anatomy and biomechanics. II. Fossil plants with secondary growth. *Architecture, structure, mécanique de l'arbre, 6ième Séminaire Interne, Montpellier 1994* (in press).
Vincent, J. F. V. (1990). *Structural Biomaterials*, 2nd ed., Princeton University Press, Princeton, NJ.
Vincent, J. F. V. (1992). *Biomechanics—Materials: A Practical Approach*, IRL Press at Oxford University Press, Oxford.
Wessolly, L. (1989). Zwei neue zerstörungsfreie Meßmethoden für Baumuntersuchungen zur Erhaltung der Verkehrssicherheit. *Garten und Landschaft* **89**(9):60–62.
Wessolly, L. (1991). Verfahren zur Bestimmung der Stand- und Bruchsicherheit von Bäumen. *Holz als Roh- Werkstoff* **49:**99–104.
Wessolly, L. (1993). Stand- und Bruchsicherheit von Bäumen. Leistungsfähigkeit und Grenzen der Zugversuche. *Das Gartenamt* **42:**486–491.

*Biomimetics, Vol. 2, No. 2, 1994*

# The Biomechanics of Root Anchorage[1]

**A. R. Ennos[2]**

*The mechanics of anchorage has only recently started to be studied, by combining theoretical analysis derived from materials science and foundations technology with experimental investigations in which plants are pulled out of the ground or pushed over. Analysis shows that the mechanical role of roots is restricted to basal regions, the strengthening of which imposes an anchorage cost. Root system morphology is correlated with aboveground morphology: procumbent and climbing plants have fibrous root systems, while upright ones have tap or plate root systems. Experimental studies of anchorage have shown two mechanisms of failure in different plants, which may be related to their pattern of development: In trees and dicots windward roots are pulled out of the ground, while the leeward roots of monocots are pushed farther* into *it. Despite the recent interest, many aspects of root biomechanics have been largely ignored. Further research in these areas could have both scientific and practical benefits, to help reduce the incidence of lodging in crops and windthrow in trees.*

**KEY WORDS:** roots; biomechanics; anchorage; soil.

## INTRODUCTION

Textbooks of botany usually list three functions of roots: to anchor the plant in the ground, to absorb water and nutrients, and to act as a site for food storage. Subsequent discussion, however, usually concentrates on absorption, and apart from brief mentions of the prop roots of maize and mangroves, the mechanical function of roots is ignored. Until recently root anchorage has also been ignored by researchers, partly because it seems intuitively obvious that uprooting of a

[1]This is the published version of a paper presented at the Plant Biomechanics Congress, Montpellier, France, September 5-9, 1994.

[2]School of Biological Sciences, Manchester University, Oxford Road, Manchester M13 9PL, England.



1059-0153/94/0600-0129$07.00/0 

plant will be resisted by the friction between the roots and the soil; research on such an apparently obvious mechanism has therefore seemed unnecessary. Since roots are underground, they are also both easier to ignore and much more difficult to study than the aboveground parts of plants. Finally, *all* mechanical aspects of plant design have been neglected over the past hundred years. After the excellent mechanical studies of German botanists such as Schwendener, Sachs, Pfeffer, and Metger, much of whose work is summarized by Haberlandt (1914), attention moved to the fields of physiology and biochemistry. Indeed, such has been the swing away from the mechanical sciences in botany that the recent renaissance in plant biomechanics has been inspired largely by zoologists and engineers (Wainwright *et al.*, 1976; Gordon, 1978; Vogel, 1989).

Whatever its cause, the lack of attention and thought has led botanists to hold several misconceptions about root anchorage, which are only now being corrected. Since root systems have very large surface areas for adequate absorption [Dittmer's (1937) rye plants had surface areas of over 200 $m^2$], it has been assumed that they are heavily overdesigned for their anchorage function and that the absorption function alone influences root system architecture. Without clear mechanical models of anchorage it has also been assumed that roots are always loaded in tension. Many experimental studies of lodging in cereal crops have therefore involved tensile tests on the roots (Neenan and Spencer-Smith, 1975) and measurements of the force required to pull individual roots or complete root systems out of the soil (Donovan *et al.*, 1982).

To correct these misconceptions, both theoretical and experimental studies have been performed to investigate the mechanisms by which forces are transmitted from the roots to the soil. At last we are beginning to understand how roots anchor plants and can suggest how and why the anchorage of crop plants (Pinthus, 1973) and forestry trees may be improved.

## THEORETICAL STUDIES

The process of pulling roots from the soil is analogous to the extraction of fibers from a composite material or pulling up foundation piles and can be analyzed in the same way (Ennos, 1989). Because roots are less stiff than the soil in which they are embedded, the top of the root will stretch and shear past the soil if it is pulled up. The soil will fail in shear but, because of its plastic nature, will continue to resist the displacement. Tension will therefore gradually be transmitted from the root to the soil. The greater the upward force applied to the root, the greater the area of soil which will fail and the farther down in the soil the root will be stretched.

The system may fail in one of two ways. If the root is relatively short and strong, the root will be pulled out of the ground, the force required being proportional to its surface area. In contrast, a long, narrow root will break at

the top before lower regions are stretched. In practice unstrengthened roots more than a few millimeters in length will break, before being pulled out, and at very low forces (Ennos, 1990).

## Design for Resisting Uprooting

These considerations have profound implications for the mechanical design of root systems. To improve the anchorage performance of a root it must be not only lengthened but also strengthened, especially at its base, to withstand tensile forces. The radicles of sunflower seedlings have just such a strengthened basal region, which is not only increased in thickness by secondary thickening, but also densely covered with root hairs, which improve the bond between the root and the soil (Ennos, 1989). These adaptations allow this region to withstand upward forces of over 0.6 N. Similar strengthening of the stele toward the base is also found in the seminal roots of wheat (Ennos, 1991a), which must anchor the seedling against uprooting, and indeed in most other plant species.

The production of strengthening material, which will not improve absorption, represents a real cost of anchorage. This cost can be minimized by strengthening only the basal regions of the roots which have to resist the largest forces, and by having many narrow roots radiating from the base of the stem rather than a single thick one (Fig. 1A). Since many thin roots have a larger surface area than a single root of the same cross-sectional area, they will transfer tension more rapidly to the soil and need not be strengthened so far down their length (Ennos, 1993a). However, if there are too many roots, the soil may fail in tension, and the roots and surrounding soil may be pulled intact from the ground at a low force. An optimal anchorage system should therefore contain an intermediate number of 10–100 roots (Ennos, 1993a).

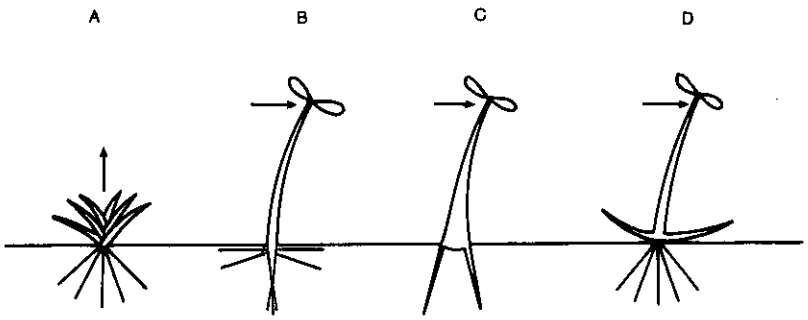


**Fig. 1.** Alternative types of anchorage system. A rope-like system (A) efficiently anchors a plant against uprooting, but to resist horizontal forces, rigid elements are also required. Plants may develop a tap root system (B), a system using rigid lateral roots emerging from an expanded stem base (C), or a lateral rosette of stalks (D) to lean against the ground.

Procumbent and climbing plants do indeed have root systems of the form that this model of anchorage predicts. Grasses and sedges have many fibrous roots emerging from the base of the shoot system, while dicots have root axes which branch rapidly near the base (Ennos and Fitter, 1992). However, in all these plants only the basal regions appear to be adapted for anchorage and are usually adequate to resist uprooting forces which exceed the tensile strength of the stem. The large numbers of fine, distal roots are unstrengthened and must have a role purely in absorption.

### Design for Resisting Overturning

Most tall, stiff-stemmed plants are much more likely to be blown sideways by the wind or to be pulled over by their own weight than to be pulled upward. Such plants must therefore have an anchorage system which resists being rotated in the soil, one that, unlike those of climbing plants, contains at least one rigid element. One solution is to produce a stiff "tap root" by secondary thickening of the main root axis (Fig. 1B), to resist toppling directly, like the point of a stake (Ennos and Fitter, 1992; Ennos, 1993a), and to act as the insertion for lateral roots, which can act like guy ropes to stabilize the plant further. A second solution would be to attach relatively stiff roots to the perimeter of a broad stem base (Fig. 1C); the resistances of these roots to bending and to axial motion through the soil should both help stabilize the plant (Ennos, 1991b). A third alternative is for the stem of the plant to support itself by leaning on stiff side shoots while a fibrous root system keeps the base of the stem in the soil (Fig. 1D).

The actual system a plant uses depends on many factors, including its ancestry, ecology, and size. Tap roots are used by the majority of herbaceous dicots and young trees. However, older trees tend to have a more complex plate system (Coutts, 1983; 1986), probably because, with their thick trunks, a tap root system would use too much material (Ennos, 1993a). Many trees actually extend the trunk outward by means of buttresses (Mattheck, 1991; Ennos, 1993b) and anchor the trunk with widely spaced sinker roots. Such a system is also used by the broad-stemmed Himalayan balsam *Impatiens glandulifera* (Ennos *et al.*, 1993a) and by monocots such as wheat and maize, which, being incapable of secondary thickening, cannot produce a tap root. A rosette of stalks is common only in weeds of bare ground, since these stalks would otherwise be shaded out. The stems of these plants are used to hold up flower stalks for better pollination of flowers and distribution of seed.

## EXPERIMENTAL STUDIES OF ANCHORAGE

Despite the success of theoretical studies in explaining the variation in root system morphology between plants of different growth forms, experimental studies of anchorage are also needed to determine exactly how failure occurs. The

first competent experimental study was carried out by Coutts (1983, 1986), who investigated the mechanical resistance of Sitka spruce trees to being overturned by the wind. He developed a practical approach to the study of anchorage which has been used in all subsequent studies.

Most importantly, Coutts emphasized the need actually to observe what is going on underground and developed two methods to do this: He cut vertical trenches in the soil alongside the trunk of his trees to expose a "cross section" of the root system, the morphology of which could be examined and the movements of which could be observed as the tree was being pulled over parallel to the trench. He also inserted microphones into the ground to record when the roots and soil were breaking.

Coutts also monitored the force required to pull his trees over *throughout* the process of uprooting and was able to relate the record of force to the movements and failure of roots and soil which he had observed directly. This allowed him to suggest several components of anchorage. The relative importance of each component could then be determined by carrying out consecutive pulls between which particular components of anchorage were destroyed. Typical experimental procedures involved cutting of roots or trenching around the root system.

Finally, Coutts emphasized the importance of measuring the mechanical strength of both the roots and the soil, as these will influence both the mode of failure and the force required.

To date, published experimental studies of anchorage have been carried out on only five species of mature plants: Sitka spruce (Coutts, 1983, 1986), sunflowers *Helianthus annuus* (Ennos *et al.*, 1993a), Himalayan balsam *Impatiens glandulifera* (Ennos *et al.*, 1993a), wheat *Triticum aestivum* (Ennos, 1991b; Crook and Ennos, 1993), and maize *Zea mays* (Ennos *et al.*, 1993b). Already, however, a pattern is emerging of the manner in which different plant types fail. In trees and dicots, movement of the root system is centered on the *leeward* side of the stem or trunk (Fig. 2A), and the windward roots tend to snap or be pulled out of the soil. Anchorage resistance can be split into several components: the resistance of windward roots to pullout and the soil to tensile failure, the bending resistance of the leeward hinge, and the weight of the root-soil plate or ball. The latter tends to be most important in trees, probably because of scale effects (Ennos, 1993a). In contrast, movement of the root systems of the monocots is centered on the *windward* side of the stem (Fig. 2B) and the cone of roots is pushed down *into* the soil. In these plants the components of anchorage result from the bending resistance of the stiff, basal roots and from the resistance of *compression* of the soil beneath the root cone.

Quite why there are these differences in behavior is unclear. They may occur because the roots of the monocots diverge at a lower angle. They would therefore resist upward forces more strongly but, with their narrower base, be

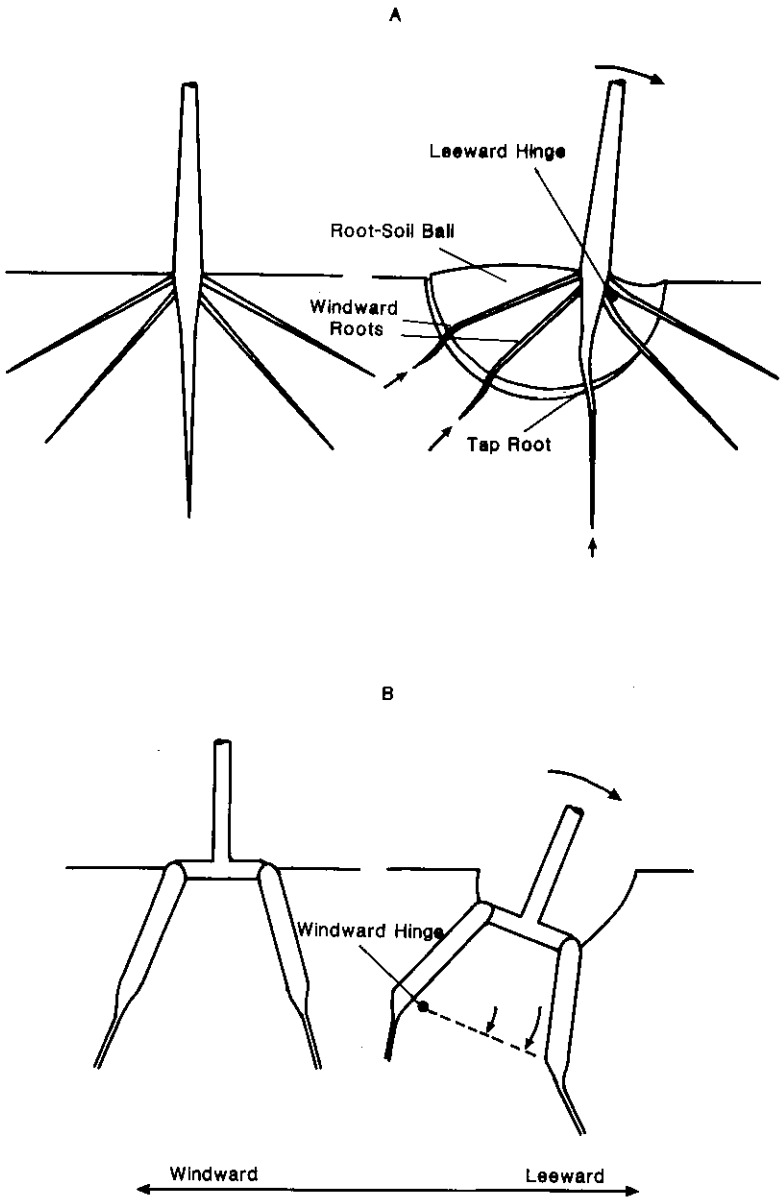


**Fig. 2.** The contrasting mechanisms of anchorage failure in (A) the sunflower *Helianthus annuus*, a dicot, and (B) winter wheat *Triticum aestivum*, a monocot. In the sunflower, rotation occurs around the leeward side of the stem and windward roots are levered out of the soil. In wheat, rotation occurs around the *windward* side of the stem and leeward roots are pushed *into* the soil.

pushed down in the soil more easily. The difference in anatomy of dicots and monocots might also have this effect; the roots of dicots and trees are usually solid rods of lignified tissue (though *Impatiens* is an exception). In contrast, monocot roots are stiffened in bending by an external ring of lignified material (Haberlandt, 1914), which results in a rather brittle structure. The lack of secondary thickening in monocots certainly constrains the form of their root systems since they must continually produce ever thicker adventitious roots to provide adequate anchorage as they develop.

## UNSOLVED PROBLEMS

Despite the attention in recent years, work has only scratched the surface of this complex topic. There are many aspects of anchorage that have never been tackled, some of which may be indeed be insoluble because of the great complexity and intraspecific variability of root system form. First, much basic work needs to be performed on the resistance of simple roots, branched roots, and collections of roots to motion through soil. Model tests would undoubtedly give useful information in this area. More studies also need to be carried out on the tensile root systems of climbing and prostrate plants.

The effect of soil strength and texture on anchorage have so far been largely ignored. It has been found that, as expected, failure occurs more distally and at lower forces when the strength of soil is reduced by wetting, but the effect of altering soil texture is more difficult to assess. Comparative studies need to be carried out on models and real plants in sandy and clay soils.

The pattern of development of anchorage systems is also an area which has been little studied. Undoubtedly, the root system becomes stronger throughout the life of a plant to counter the larger forces to which it is subjected, but the exact pattern of development may be critical to its ability to stand up. So far only one study has been carried out in this area, on the development of the anchorage systems of wheat (Crook *et al.*, 1994). It was found that the anchorage system developed its strength slightly in advance of the shoot system, providing a firm foundation for the later growth of the shoot. It is essential to repeat this study on other, wild species.

Little attention has also been paid to the effect of environmental conditions on root growth and anchorage strength. Only two studies have been carried out specifically on the effect of mechanical stimulation on root growth. Gartner (1994) found that shaking the *stems* of tomato plants caused an increased thickening of the base of the tap roots, a response which would have increased the anchorage strength. Working on young Sitka spruce trees subjected to a unidirectional wind, Stokes *et al.*, (1994) found that windward roots exhibited a greater degree of branching, which might improve their effect in preventing windthrow in the direction of the prevailing wind. Many more studies are needed

in this area. It should prove possible to stimulate individual roots of plants grown in nutrient culture or to measure the stresses to which individual roots are subjected with strain gauges. Such an approach is already being taken to examine the development of the buttress and I-shaped roots of trees (Ennos, 1994).

Finally, it is known that soil conditions profoundly affect the *primary* growth of roots (see Russell, 1977), but the effect on their *secondary* growth, which will influence anchorage strength, is unknown. Studies in this area are important since they will allow us to determine whether lodging of crop plants may be reduced by altering the management of the soil in which they are growing.

## REFERENCES


Coutts, M. P. (1983). Root architecture and tree stability. *Plant Soil* **71**:171–188.

Coutts, M. P. (1986). Components of tree stability in Sitka spruce on peaty gley soil. *Forestry* **59**:173–197.

Crook, M. J., and Ennos, A. R. (1993). The mechanics of root lodging in winter wheat *Triticum aestivum* L. *J. Exp. Bot.* **44**:1219–1224.

Crook, M. J., Ennos, A. R., and Sellers, E. (1994). Mechanical development of two winter wheat cultivars. *J. Exp. Bot.* (in press).

Dittmer, H. J. (1937). A quantitative study of the roots and root hairs of a winter rye plant (*Secale cereale*). *Am. J. Bot.* **24**:417–420.

Donovan, L. J., Jui, P., Kloek, M., and Nicholls, C. F. (1982). An improved method of measuring root strength in corn (*Zea mays* L.). *Can. J. Plant Sci.* **62**:223–227.

Ennos, A. R. (1989). The mechanics of anchorage in seedlings of sunflowers *Helianthus annuus*. *New Phytol.* **113**:185–192.

Ennos, A. R. (1990). The anchorage of leek seedlings: The effect of root length and soil strength. *Ann. Bot.* **65**:409–416.

Ennos, A. R. (1991a). The mechanics of anchorage in wheat *Triticum aestivum*. L. I. The anchorage of wheat seedlings. *J. Exp. Bot.* **42**:1601–1606.

Ennos, A. R. (1991b). The mechanics of anchorage in wheat *Triticum aestivum* L. II. Anchorage of mature wheat against lodging. *J. Exp. Bot.* **42**:1607–1613.

Ennos, A. R. (1993a). The scaling of root anchorage. *J. Theor. Biol.* **161**:61–75.

Ennos, A. R. (1993b). The function and formation of buttresses. *Trends Ecol. Evol.* **8**:350–351.

Ennos, A. R. (1994). Development of buttresses in rainforest trees: The influence of mechanical stress. In Coutts, M. P., and Grace, J. (eds.), *Wind and Wind-Related Damage to Trees*, IUFRO Conference (in press).

Ennos, A. R., and Fitter, A. H. (1992). Comparative functional morphology of the anchorage systems of annual dicots. *Funct. Ecol.* **6**:71–78.

Ennos, A. R., Crook, M. J., and Grimshaw, C. (1993a). A comparative study of the anchorage systems of himalayan balsam *Impatiens glandulifera* and mature sunflower. *Helianthus annuus*. *J. Exp. Bot.* **44**:133–146.

Ennos, A. R., Crook, M. J., and Grimshaw C. (1993b). The anchorage mechanics of maize *Zea mays*. *J. Exp. Bot.* **44**:147–153.

Gartner, B. L. (1994). Root biomechanics and whole-plant allocation patterns: Responses of tomato to simulated wind. *J. Exp. Bot.* (in press).

Gordon, J. E. (1978). *Structures or Why Things Don't Fall Down*, Penguin Books, London.

Haberlandt, G. (1914). *Physiological Plant Anatomy*, Macmillan, London.

Jeronimidis, G. (1980). Wood, one of mature's challenging composites. In Vincent, J. F. V., and Currey, J. D. (eds.), *The Mechanical Properties of Biological Materials*, S.E.B. Symposium 34, Cambridge University Press, pp. 169–182.

Neenan, M., and Spencer-Smith, J. L. (1975). An analysis of the problem of lodging with particular reference to wheat and barley. *J. Agr. Sci.* **85**:495–507.

Pinthus, M. J. (1967). Spread of the root system as an indicator for evaluating lodging resistance of wheat. *Crop Sci.* **7**:107–110.

Russell, R. S. (1977). *Plant Root Systems: Their Function and Interaction with the Soil*, McGraw-Hill, London.

Stokes, A., Fitter, A. H., and Coutts, M. P. (1994). Responses of young trees to wind: Effects on root growth. In Coutts, M. P., and Grace, J. (eds.), *Wind and Wind-Related Damage to Trees*, IUFRO Conference (in press).

Vogel, S. (1989). Drag and reconfiguration of broad leaves in high winds. *J. Exp. Bot.* **40**:941–949.

Wainwright, S. A., Biggs, W. D., Currey, J. D., and Gosline, J. M. (1976). *Mechanical Design in Organisms*, Wiley, New York.

*Biomimetics, Vol. 2, No. 2, 1994*

# Wind Damage to Forests[1]

**B. A. Gardiner[2] and C. P. Quine[2]**

*This paper provides a brief summary of research on understanding the mechanics of forest wind damage and the development of predictive and preventative management strategies. It concentrates on work carried out in Great Britain and the experience of British foresters. The first part of the paper details the mechanics of wind damage, how turning moments are produced by the wind and how the tree resists. It also discusses the ways in which trees can fail either by stem breakage or complete overturning. The paper then describes the specific tree and environmental factors that influence the stability of trees and how these are modified by management practices. Finally, an attempt is made to show how it is possible to quantify the probability of wind damage to forests and to develop a national wind risk system.*

**KEY WORDS:** wind damage; forest; trees; biomechanics.

## BACKGROUND

This paper discusses research, particularly in Britain, carried out in order to predict and prevent forest damage and illustrates the ways in which biomechanics can help our understanding.

Severe storms such as that on 31 January 1953, which caused substantial damage to forests in Northeast Scotland (Quine, 1989), alerted British foresters to the difficulties of growing exotic conifer plantations in the exposed uplands. The wind climate of these areas is severe and the soils are also generally waterlogged during the winter. Research into site limitations included tree pulling experiments in which mature trees of different size and species, growing on a

[1] This is the published version of a paper presented at the Plant Biomechanics Congress, Montpellier, France, September 5-9, 1994.

[2] Forestry Commission, Northern Research Station, Roslin, Midlothian EH25 9SY, Scotland.



1059-0153/94/0600-0139$07.00/0 

variety of soils, were winched over and the maximum turning moments required to uproot them recorded. The physical details of the tree were also measured including stem weight, diameter, height, root weight, root depth, and root spread (Fraser and Gardiner, 1967). Over 1000 trees were pulled and the subsequent database provides an essential underpinning to much of our current work.

The results from the tree pulling work were combined with estimates of the national wind climate obtained using tatter flags (Miller *et al.*, 1987) to create a "windthrow hazard classification" (Miller, 1985). This classification combines scores for forest location, elevation, topographic shelter, and soil type to derive an estimate of the height at which trees are likely to begin blowing over and how fast this damage will progress. The system has been widely adopted in Great Britain as a management and investment tool but it is an empirical model which cannot be easily adapted to different situations. It is now being replaced by a physically based model derived from an understanding of the mechanical behavior of trees and the nature of airflow in complex terrain. The availability of this type of model will allow forest managers to make contingency plans and select appropriate preventative techniques.

## MECHANICS OF WIND DAMAGE

Wind damage occurs when the overturning moment due to wind pressure on the canopy can no longer be resisted by the tree and some part of the tree fails. Failure may result in two ways. If the critical stress of the wood is exceeded, wood fibers begin to break or buckle, leading to stem or branch breakage. Alternatively, if the soil/root interface is unable to provide a resistive moment sufficient to counteract the overturning moment, the tree is uprooted and windthrow occurs. Figure 1 illustrates the different components we need to consider when discussing tree mechanics.

The overturning moment (or torque) applied to the tree by the wind is the product of the wind force and the distance between the point at which the force acts and the root hinge about which the tree turns. The total bending moment at the base of the tree is the sum of the force of the wind at each height in the canopy multiplied by that height. For simplicity the force on plantation trees can be regarded as acting at a single point within the canopy (center of pressure in Fig. 1) close to the zero-plane displacement height ($d$) which is between 70 and 80% of tree height (Gardiner, 1994). Generally, the force on an object due to the wind increases as the square of the windspeed, but because trees are flexible and the canopy streamlines, the wind force on trees increases almost linearly with windspeed (Gardiner *et al.*, 1994). As the tree is bent an additional turning moment develops due to the overhanging mass of the canopy and stem, the magnitude of which is the product of the displaced weight and its horizontal displacement from the root hinge point (see Fig. 1). This additional turning

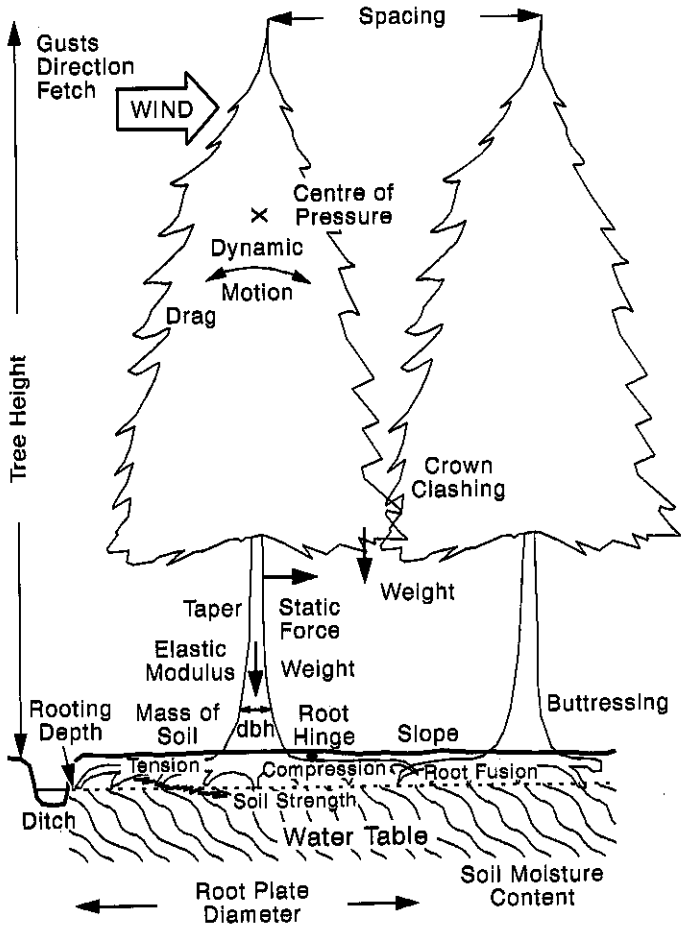


**Fig. 1.** Components of tree mechanics (after Bell *et al.*, 1991).

moment can be considerable, providing up to 30% of the total overturning moment. If the canopy is wet or covered in snow, the self-weight moment may exceed that due to the wind.

Stem or branch breakage occurs when the wood fibers are no longer able to withstand the compressive or tensile forces exerted on them by the overturning moment. Once a few fibers break or buckle the stress increases (due to reduction in cross-sectional area), additional fibers break, and a catastrophic failure occurs. On other occasions bending leads to stresses normal to the stem surface, causing delamination and rupturing of the wood. This is regarded as a common cause of stem breakage close to the ground following root buttress delamination (Mat-

theck and Bethge, 1990). Different species have different failure modes. Pines are vulnerable to breakage in the crowns at a branch whorl, particularly if they are fast growing at wide spacings, while spruces tend to break in the lowest third of the stem. The shape of the stem determines where the stress is greatest, although there is increasing evidence that trees grow in a manner designed to keep surface stresses as even as possible throughout the stem and roots (Mattheck, 1991). This adaptive growth helps to explain the details of tree shape including stem taper, buttressing, and root morphology. Trees that grow in situations exposed to the wind will be more tapered and invest a greater proportion of their available biomass in root development than those in sheltered situations. This may explain the observed stability of trees at the edge of forests during major storms. The exact biochemical mechanism by which trees modify their growth in response to applied stresses is not completely understood but appears to involve the release of ethylene in those cells that are most highly stressed (Telewski, 1994).

Windthrow occurs when the soil and root system can no longer provide a large enough resistive moment to counteract the turning moment due to the wind. The strength of the tree anchorage depends on the mechanical properties of the roots and soil and on the size and architecture of the root system. Four components of anchorage have been identified (Coutts, 1986). When the tree is displaced by the wind the weight of the roots and adhering soil helps to stop the tree from falling over. The soil underneath and around the root plate has to be physically broken and this contributes a further resistance. The tensile strength of the roots on the windward side of the tree is a third component of the resistive force and the resistance of the roots and soil to bending in the hinge zone provides a fourth component. For small displacements the soil strength is the greatest contributor to the resistive moment but further displacement breaks the soil and fine roots (illustrated by a crack in Fig. 1) and tension in the major roots and soil/root weight becomes more important. The soil/root system is subject to fatiguing by continuous motion and the force required to pull over a tree is reduced by repeated cyclic loading (O'Sullivan and Ritchie, 1993). This suggests that trees may become more vulnerable with successive winter storms, although the magnitude of increase in vulnerability and the ability of the system to recover during subsequent growing seasons require investigation. Although the soil/root system provides the major resistance to overturning, a further contribution is provided by crown contact with neighboring trees, and this can be particularly important in trees grown close together (see Fig. 1).

The resistive moment can be obtained from tree pulling experiments and an estimate then made of the forces required to blow trees over. However, the estimated forces appear to suggest that mean wind speeds of over 50 m $s^{-1}$ are necessary for windthrow when, typically, trees begin to blow down at just over 20 m $s^{-1}$. The reasons for this discrepancy are the gusty nature of the wind and

the dynamical behavior of the trees themselves. Trees subjected to wind loading can be regarded as forced damped harmonic oscillators (Gardiner, 1992) and their motion described by the standard equations for such first-order systems (Thompson, 1988). Coherent gusts of wind which form over the canopy intermittently load the tree, causing them to oscillate about their rest position for a few seconds until damping reduces the motion. The sudden impact and higher windspeed during gust passage result in much higher turning moments than those due to the mean wind. Experiments in the field and the wind tunnel have shown that the extreme forces on trees are 8–10 times higher than the mean forces (Gardiner *et al.*, 1994). Resonance at the tree's natural frequency does not appear to be a contributory factor (Gardiner, 1994), although as the windspeed increases gusts become more frequent (Paw U *et al.*, 1992) and they could begin to get in phase with tree motion.

An excellent review of tree mechanics is provided by Wood (1994).

## FACTORS INFLUENCING TREE STABILITY

Stability is a measure of a tree's vulnerability to wind damage. There are two groups of factors that influence tree stability: those that affect the strength of the overturning moment due to the wind and those that affect the resistive moment that the roots can provide.

Any change to canopy or stem shape or to the aerodynamic roughness ($z_0$) of the canopy will change the overturning moment experienced by the tree. Planting density, uniformity of growth, respacing, thinning, and cutting rides or roads all affect the tree shape. Practices which result in a sudden opening of the canopy will increase the loading on the tree and the magnitude of this increase is an extremely strong function of gap size (Stacey *et al.*, 1994). Therefore, trees exposed following thinning or the cutting of a new edge will be more vulnerable than before. However, adaptive growth will lead to recovery in response to the higher wind loading of the exposed position. The duration of this recovery relative to the frequency of damaging winds will be important (Quine, 1994). If root development is not restricted and the canopy can reform, the trees will eventually become as stable as those in an unthinned stand.

Edges, whether adapted to the wind or newly created by clear felling of a neighboring stand, are potential sites for windthrow. Experiments in the wind tunnel (Gardiner *et al.*, 1994) and in the field (Mattheson, 1992) have shown a beneficial effect of shaping the edge to create a more gradual change. This may be carried out by topping edge trees, planting slower-growing species such as broad-leaves along the edge, or having a gradual increase in tree planting density into the stand. Initial planting density or respacing does not appear to affect tree stability provided that root development is not restricted. Even though wind loading increases as the tree spacing is increased (Gardiner *et al.*, 1994), the

tree can compensate for this by enlarging the root system. This compensating growth in the roots may not be possible where the soil is particularly waterlogged or there is furrow plowing, and consequently in these situations stability will be reduced. Wider spacing does increase the stem diameter and taper, which increases the stem strength, and so wider-spaced trees have less chance of stem breakage.

The resistive moment will be reduced by factors which restrict root development. This is particularly true if the growth of the windward roots is affected because of their importance for stability. Plow furrows, drains (see Fig. 1), and damage from vehicles used for extraction can all prevent root spread or cause the roots to branch close to the base of the tree. Similarly, damage to leeward roots will reduce the distance to the root hinge, which reduces the mechanical advantage. Root system asymmetry due to poor planting practice will have similar effects. Root depth is a function of the soil type (for example ironpans restrict root penetration) and the depth of the winter water table. The strength of the soil/root attachment and the soil itself are also strong functions of soil wetness. Ponding, spring lines, or blocked drains can crucially reduce soil strength. Very often the beginning of windthrow is associated with particularly wet areas in the forest and subsequently spreads from that point.

A fuller review of these issues is provided by Coutts *et al.* (1994).

## ASSESSING THE RISK OF DAMAGE

Understanding the mechanics of wind damage allows the vulnerability of a particular tree to be calculated, where vulnerability is defined as the mean windspeed at which the tree will break or be uprooted. Assessing the risk of wind damage involves calculating the probability of this windspeed occurring at that particular site and requires a knowledge of the national wind climate (Quine, 1994), and the modification by topography and surface roughness.

Britain has a severe wind climate compared to the rest of Europe. Strong winds typically result from the passage of Atlantic depressions and only very rarely originate from thunderstorms, tornados, or squalls. Approximately 150 depressions affect Britain every year, crossing from west to east, but they vary in track (and hence area affected) and in intensity (and hence windspeeds experienced). Circulation around a depression is counterclockwise, and the strongest winds are commonly found to the west and south of the center of the low pressure. Most depressions track to the north and west of Britain, and their cumulative influence is responsible for the tendency to stronger winds in northern and western Britain. However, the variability in track can, albeit infrequently, bring strong winds to any part of the country; The general pattern of damage will then bear little relationship to the predictions of a generalized model. The storm of October 1987 is a good example of this variability (Quine, 1989).

Individual lowland forests were extensively damaged, while upland forests, classed as higher risk, remained undamaged. The stochastic nature of storm occurrence means that the level of damage may vary significantly from year to year; a succession of quiet winters can be followed by a sequence of damaging storms. The occurrence of a particularly severe storm in one year does not modify the chance of the same intensity of storm occurring in the following year. Thus, return periods, which are often quoted to illustrate the rarity of storms, represent the long-term average interval between exceedance of specified windspeeds, and not a prescribed cycle.

At the forest scale (kms × kms) the wind climate may vary rapidly, depending on the elevation, local shelter, and presence of surrounding forest. Calculating windspeed variation in complex forested terrain is a difficult task and two approaches have been taken. The first approach is to use computer airflow models in which the equations of fluid flow over digitized topography and surface roughness are calculated (Inglis *et al.*, 1994). The second approach is to use geographic predictors such as elevation, angle to the skyline, slope, aspect, and distance from the coast to calculate the variation in windiness (Hannah *et al.*, 1994). Both approaches have advantages and disadvantages. Airflow models are based on sounder physical principles than geographic predictors and do not require calibration for a particular area. However, the linearized models used to date are unable to deal with flow separation in the lee of hills and valleys even in relatively gentle terrain (slopes $< 10°$). Comparison between field measurement and model prediction shows that the models are conservative, underestimating the speed-up on hills and the speed reduction in their lee. The geographic predictor method is more accurate than airflow models for a particular area, but unfortunately correlations developed in one area may not be applicable elsewhere, and so their general use is less straightforward.

## THE FUTURE

The elements of a new predictive method for assessing the risk of wind damage to British forests are now in place. A detailed understanding of the mechanical behavior of plantation trees along with the data available in the tree-pulling database can be used to calculate the windspeed at which damage may be expected for a particular tree. Such a calculation will be possible for the common plantation species and soil types and will take into account cultivation treatment, management practices, and spacing. The natural variability of trees will be accounted for by calculating the spread in vulnerability of the whole stand. The probability of damaging winds occurring at the precise location of the forest stand will then be calculated using a combination of wind climate information and airflow model or geographic predictor methods to account for local topographic detail. The new risk model will be developed over the next

few years and will replace the existing "windthrow hazard classification." It will be a geographic information system (GIS)-based model so that the necessary forest and soil inventory information, already available to the forester, can be combined with topographic data to produce wind damage probability maps. Furthermore, the interactive nature of the system will allow the consequences of any management operation to be assessed ahead of time.

## REFERENCES


Bell, H. J., Dawson, A. R., Baker, C. J., and Wright, C. J. (1991). Tree stability. In Hodge, S. J. (ed.), *Research for Practical Arboriculture*, HMSO, London.

Coutts, M. P. (1986). Components of tree stability in Sitka spruce on peaty gley soil. *Forestry* **50**:173–197.

Coutts, M. P., Gardiner, B. A., Pyatt, D. G. and Quine, C. P. (1994). *Forests and Wind: Management to Minimise Damage*, Forestry Commission Bulletin, HMSO, London (in press).

Fraser, A. I., and Gardiner, J. B. H. (1967). *Rooting and Stability of Sitka Spruce*, Forestry Commission Bulletin 40, HMSO, London.

Gardiner, B. A. (1992). Mathematical modelling of the static and dynamic characteristics of plantation trees. In Franke, J., and Roeder, A. (eds.), *Mathematical Modelling of Forest Ecosystems*, Sauerländer's Verlag, Frankfurt am Main, pp. 40–61.

Gardiner, B. A. (1994). Wind-tree interactions. In Coutts, M. P., and Grace, J. (eds.), *Wind and Wind Related Damage to Trees*, Cambridge University Press, Cambridge.

Gardiner, B. A., Stacey, G. R., Belcher, R. E., and Wood, C. J. (1994). Field and wind-tunnel assessment of the implications of respacing and thinning on tree stability (submitted for publication).

Hannah, P., Palutikof, J. P., and Quine, C. P. (1994). Predicting windspeeds for forest areas in complex terrain. In Coutts, M. P. and Grace, J. (eds.), *Wind and Wind Related Damage to Trees*, Cambridge University Press, Cambridge.

Inglis, D. W. F., Choularton, T. W., Stromberg, I. M. F., Gardiner, B. A., and Hill, M. (1994). Testing of a linear airflow model for flow over complex terrain and subject to structured, stable stratification. In Coutts, M. P. and Grace, J. (eds.), *Wind and Wind Related Damage to Trees*, Cambridge University Press, Cambridge.

Mattheck, C. (1991). *Trees: The Mechanical Design*, Springer-Verlag, Berlin.

Mattheck, C., and Bethge, K. (1990). Wind breakage of trees initiated by root delamination. *Trees* **4**:225–227.

Mattheson, P. (1992). *Stabilising Effect from Pruning and Topping in Newly Exposed Edges of Old and Middle-aged Norway Spruce*, Internal Report, Forskningscentret for Skov & Landskab. Vejle, Denmark (Danish).

Miller, K. F. (1985). *Windthrow Hazard Classification*, Forestry Commission Leaflet 85, HMSO, London.

Miller, K. F., Quine, C. P., and Hunt, J. (1987). The assessment of wind exposure for forestry in upland Britain. *Forestry* **60**:179–192.

O'Sullivan, M. F., and Ritchie, R. M. (1993). Tree stability in relation to cyclic loading. *Forestry* **66**:69–82.

Paw, U. K. T., Brunet, Y., Collineau, S., Shaw, R. H., Maitani, T., Qui, J., and Hipps, L. (1992). On coherent structures in turbulence above and within agricultural plant canopies. *Agr. For. Meteorol.* **61**:55–68.

Quine, C. P. (1989). Description of the storm and comparison with other storms. In Grayson, A. J. (ed.), *The 1987 Storm: Impact and Responses*, Forestry Commission Bulletin 87, HMSO, London.

Quine, C. P. (1994). Assessing the risk of wind damage to forests: Practice and pitfalls. In Coutts, M. P., and Grace, J. (eds.), *Wind and Wind Related Damage to Trees*, Cambridge University Press, Cambridge.

Stacey, G. R., Belcher, R. E., Wood, C. J., and Gardiner, B. A. (1994). Wind and wind forces in a model spruce forest. *Boundary-Layer Meteorol.* (in press).

Telewski, F. W. (1994). Wind induced physiological and development response in trees. In Coutts, M. P., and Grace, J. (eds.), *Wind and Wind Related Damage to Trees*, Cambridge University Press, Cambridge.

Thompson, W. T. (1988). *Theory of Vibration with Applications*, Allen and Unwin, London.

Wood, C. J. (1994). Understanding wind forces on trees. In Coutts, M. P., and Grace, J. (eds.), *Wind and Wind Related Damage to Trees*, Cambridge University Press, Cambridge.

*Biomimetics, Vol. 2, No. 2, 1994*

# Local Buckling and Other Modes of Failure in Hollow Plant Stems[1]

**H.-Ch. Spatz[2] and T. Speck[3]**

*Hollow structures such as the stalks of cereals have the advantage that stiffness against bending can be achieved at a relatively low biological cost. However, such structures are endangered by local buckling. An equilibrium approach led to a theoretical description of the process of ovalization for nonisotropic material as found in plants. In particular, the computations allow discussion of three primary causes of failure: (i) failure of the material due to compressive strains in the longitudinal direction, (ii) failure of the material due to strains in the tangential direction, and (iii) failure due to a buckling collapse of the structure. They also show how nodal thickenings stabilize hollow structures. A new experimental device allows observation of the bending behavior of hollow plant stems up to the point of failure of the material or the structuring. Fitting the data with the help of the theory yields a Young's modulus in the transverse direction, which in stalks is difficult to measure directly. A comparison of data for different cereals points to a contribution of the parenchyma to the resistance against local buckling.*

**KEY WORDS:** local buckling; nodes; maximal bending moments; testing device; theoretical description.

## INTRODUCTION

Under compressive forces, but especially under bending loads, thin-walled hollow structures, like some hollow plant stems, are in danger of failing by local

[1]This is the published version of a paper presented at the Plant Biomechanics Congress, Montpellier, France, September 5-9, 1994.

[2]Institut für Biologie III, Universität Freiburg i.Br., Schänzlestraße 1, D-79104 Freiburg i.Br., Germany.

[3]Botanischer Garten, Universität Freiburg i.Br., Schänzlestraße 1, D-79104 Freiburg i.Br., Germany.



1059-0153/94/0600-0149$07.00/0 

buckling (Timoshenko and Gere, 1961; Wainwright *et al.*, 1976; Romberger *et al.*, 1993; Niklas, 1992). Theoretical approaches describing the phenomenon of local buckling are rare and confined mainly to local buckling under axial compressive stress (cf. Wainwright *et al.*; 1976). In engineering sciences most approaches apply only to very thin-walled cylindrical shells of isotropic material (cf. Brazier, 1927; Reissner, 1959; Seide and Weingarten, 1961; Axelrad, 1965; Stephens *et al.*, 1974).

Niklas (1992) gives an excellent account of the problems arising if formulas from engineering sciences derived for hollow tubes built of isotropic material are transferred to highly anisotropic plant materials. Niklas and co-workers also contributed some of the few experimental studies on local buckling processes in hollow plant organs. Niklas (1989) studied local buckling in the horsetail (*Equisetum hyemale*) and found that in this plant, local buckling occurs mostly in the mechanically weak (meristematic) basal zone of internodes near the nodes. The transverse nodal diaphragms contribute only 2% to the stem's total weight but can increase the modulus of the stem by 17–32% (see also Niklas, 1992). Niklas and O'Rourke (1987) examined the influence of water potential on the mechanical properties of hollow leaves of *Allium shoenoprasnum*, taking into account the ovalization of the originally ring-shaped cross sections during bending. They also stress the potential stabilizing influence of turgescent pith parenchyma, which can nearly eliminate the danger of local buckling in core-rind structures because of a high stability against compression (Niklas, 1991, 1992; see also Ennos, 1993). Foley (1983) and Lu *et al.* (1987) mention, in their studies of the mechanical properties of corn stalks (*Zea mays*), the danger of failing by local buckling in old corn stalks with (partly) decayed central parenchyma. In this developmental stage the corn stalks no longer represent solid stems, as in younger developmental stages, but are essentially slender thin-walled tubes. Vincent (1983) and Vincent and Jeronimidis (1991) investigated the functional anatomy and the mechanical properties of the herbaceous hollow flower stems of the dandelion (*Taraxacum officinale*) and point to the importance of prestressing in the periphery also of hollow herbaceous stems. They further discuss the problem of local buckling of cells exposed to compression on the outermost leeward side of the bent stem.

Mosbrugger (1990) discusses constructural constraints in fossil trees with (naturally) hollow stems and, especially, the shortcomings in terms of branching frequency and branching angle. Mattheck and co-workers (1992, 1993; Mattheck, 1992) refer mainly, in their studies on hollow plant organs, to trees in which a central cavity respectively a central part of disintegrated, mechanically ineffective wood results from fungus infection. They discuss the problem of safety margins for hollow trees in terms of the ratio of wall thickness to radius and stress the point that different modes of failure may cause local buckling of a hollow structure (Mattheck and Breloer, 1993). Biomechanics and safety mar-

gins of hollow trees have also been studied by Wessolly and co-workers (Herbig *et al.*, 1988; Wessolly, 1988, 1991, 1993; see also Sinn, 1993, 1994; Rinn, 1994).

The theoretical approach developed in Freiburg allows calculation of critical bending moments for hollow cylinders of nonisotropic material, taking into consideration different modes of primary failure. Our studies focus mainly on biomechanics, especially local buckling processes, as related to the anatomy of grass stalks, but the method can be used to describe the local buckling phenomenon in every kind of hollow tube, as, for example, hollow trees (Spatz, 1994).

## THEORETICAL CONSIDERATIONS

### Equilibrium Approach

As outlined previously (Spatz *et al.*, 1993), buckling of hollow tubes or plant stems under bending loads (Fig. 1) can be described by an equilibrium approach (Fig. 2). The considerations are summarized in this contribution. A more detailed account is given elsewhere (Spatz and Speck, 1994). In essence, the gain in energy upon releasing strain in the longitudinal direction is equal to the loss in energy upon deforming the ring-shaped cross section to an elliptical ring. Using energies (scalars) greatly simplifies the problem in comparison to approaches using forces or moments (vectors), which would render the problem intractable even on large computers.

Upon bending under wind loads (cf. Wainwright *et al.*, 1976; Speck *et al.*, 1990) longitudinal tensile strains develop on the windward side and compressive strains on the leeward side of a plant stem. In hollow structures the walls will tend to move toward the "neutral plane," thus releasing part of the strain (Fig. 1). In our experimental setup care is taken to minimize the bending moment at either end of the plant stem, where it is mounted (see below). The bending line (Fig. 3) for this type of loading can best be described by a third-order spline function. For a constant second moment of area, this function minimizes the strain energy (Böhm and Gose, 1977). For large degrees of ovalization of the cross section, a fourth-order spline function is an even better approximation (Spatz and Speck, 1994). The spline function is used to describe the neutral plane, but also the bending line for the compression and for the tension side, at any degree of ovalization. Using the definitions in Fig. 3 the lengths can be calculated numerically. Knowing the Young's modulus of elasticity in the longitudinal direction $\xi_{long}$, the strain energies can be calculated for any degree of bending and ovalization.

Spatz *et al.* (1993) have shown that the energies for deforming a circular ring to an elliptical ring can be calculated considering the degree of shearing of the structure. Both radial and tangential shear strains develop upon ovalization.

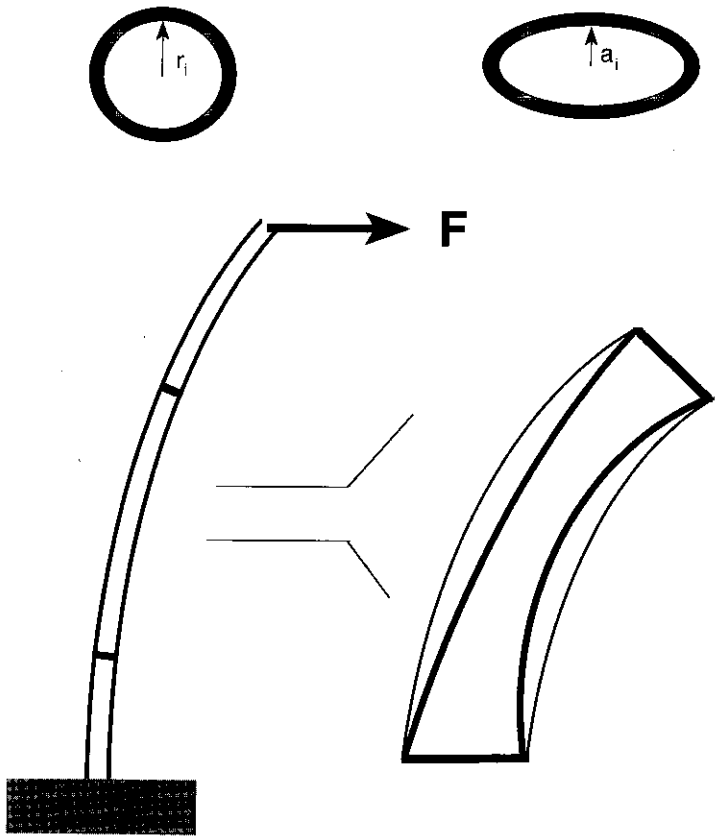


**Fig. 1.** Schematic representation of a hollow plant stem with nodes. A wind force $F$ causes a bending moment. This induces stresses in the longitudinal direction. Upon ovalization of the cross section the longitudinal strains are partially relaxed.

If the Young's moduli in the radial and tangential directions are known, the strain energies can be calculated by averaging over the entire ring and in a second step over the entire length of the hollow stem.

The process of buckling is simulated by carrying a given hollow tube through a series of discrete steps of increasing bending until failure either of the material or of the structure is observed (Fig. 4). The degree of bending can be described by the curvature in the vertex (Fig. 3). To obtain the degree of buckling, the bending line of the compression side is changed in small steps to $\Delta s + \Delta\Delta s$, until the sum of all mechanical energies reaches a minimum or

$$dE_{\text{long}} + dE_{\text{deform}} = 0 \tag{1}$$

Correspondingly the equilibrium is determined for the tension side. Unless the

## Equilibrium conditions

$$0 = dE_{long} \quad \text{[Strains in longitudinal direction]}$$

$$+ dE_{shear} \quad \text{[Shear strains in radial direction and in tangential direction]}$$

$$+ dE_{trans} \quad \text{[Change in circumference]}$$

$$+ dE_{bend} \quad \text{[additional bending of the walls]}$$

---

$$dE_{long} = -\pi * \xi_{long} * \Delta l / l * r * w * dl$$

$$dE_{shear} = \pi * M * S(a) * l * r * w * dS(a)$$

$$M = M(\xi_{radial}, \xi_{tangential}, r, w)$$

$$dE_{trans} = 0{,}135 * \xi_{tangential} * \Delta u / u * l * w * du$$

$$dE_{bend} = \pm 3.4 * \xi_{long} * r * w^3 / l^3 * \Delta s * ds$$

l = length of bending line ; r = radius ; w = wall thickness;
a = small axis of the ellipse ; S(a) = shear strain;
u = outer circumference ; Δs = displacement

**Fig. 2.** The states which a hollow tube undergoes upon bending can be described as equilibrium between energies gained in relaxing longitudinal strains and energies necessary to deform a ring. The first two terms of the equilibrium conditions are dominating (compare Spatz *et al.*, 1993).

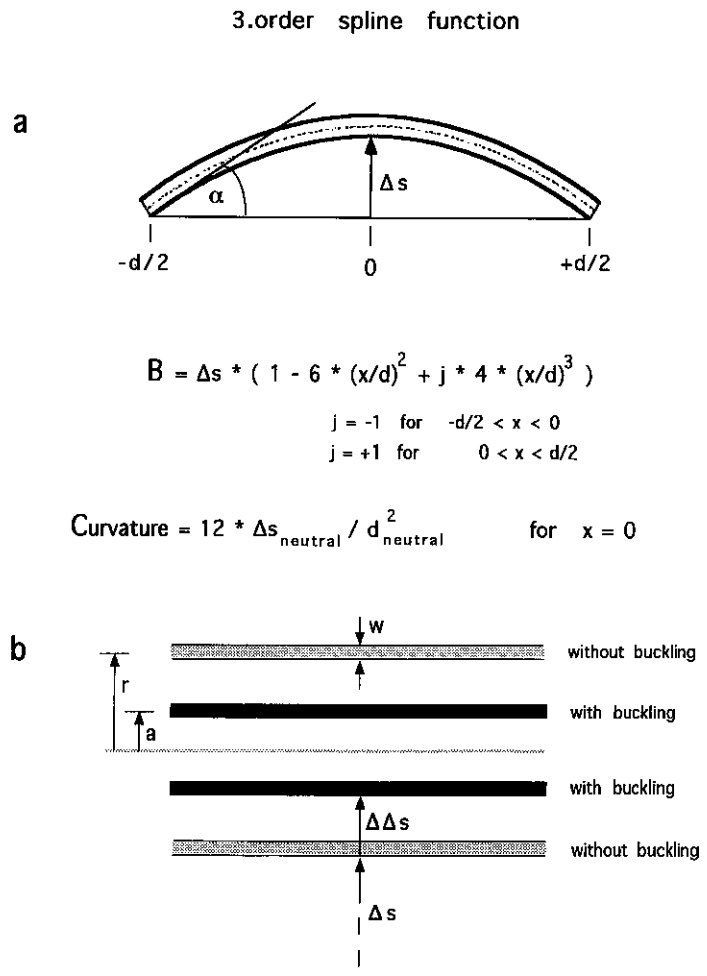


**Fig. 3.** (a) The bending line on the compression side can be represented by a third-order spline function. $B(d, \Delta s)$ is the bending line without buckling. Ovalization is described by increasing the displacement to $\Delta s + \Delta\Delta s$ in small steps, leaving $d$ and $\Delta s$ constant. On the extension side buckling is described by decreasing the displacement in small steps. Strains in the longitudinal direction can be calculated by numerical calculation of the length of the bending line for both compression and the extension side. The curvature in the vertex is obtained as the second derivative of an equivalent bending line for the "neutral axis" $B(d_{\text{neutral}}, \Delta s_{\text{neutral}})$. The bending line depicted in this drawing corresponds to the experimental arrangement. (b) An enlarged segment at the vertex showing the definitions of the parameters used. The wall thickness $w$ stands for the thickness of the ring of sclerenchyma.

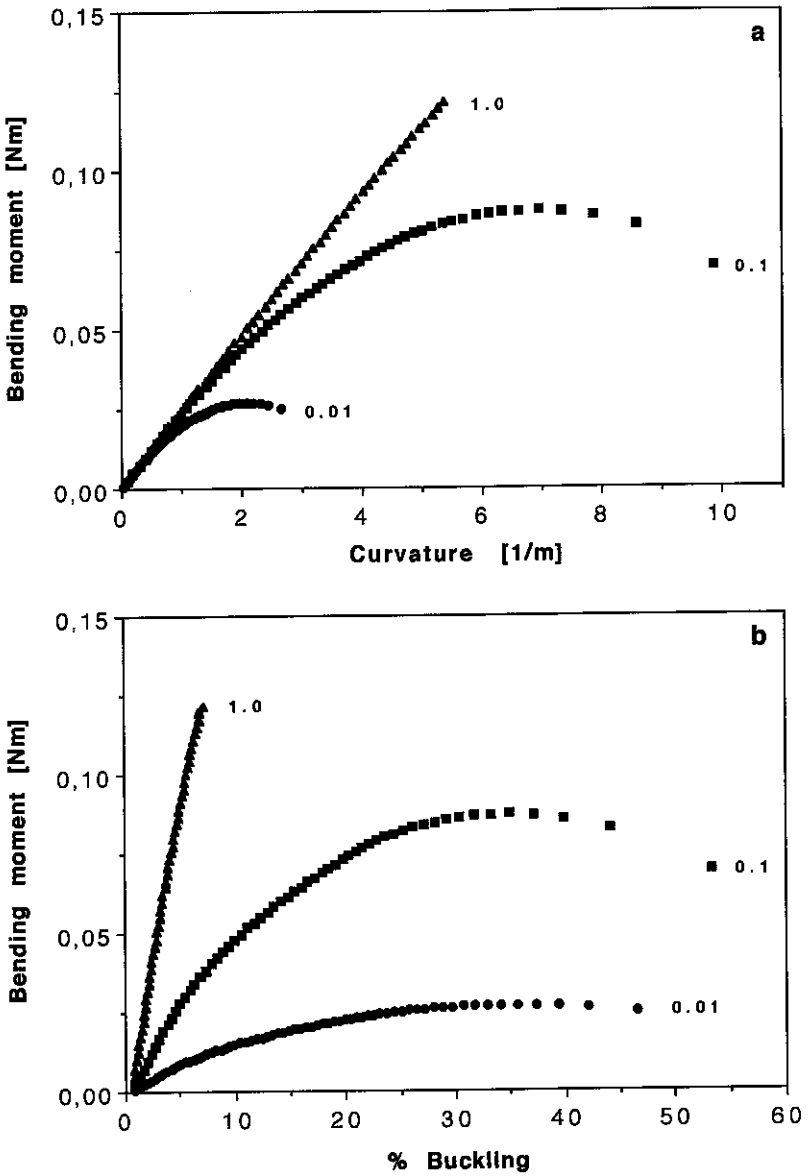


**Fig. 4.** The relation among bending moment, curvature, and degree of ovalization for a hollow tube of length $l = 20$ cm, radius $r = 0.2$ cm, and wall thickness $w = 0.01$ cm. The Young's modulus in the longitudinal direction is chosen as $\xi_{long} = 10$ GN/m$^2$. For all computations shown here the Young's moduli in the radial and tangential directions are considered equal: $\xi_{radial} = \xi_{tangential} \equiv \xi_{trans}$. The numbers in the graphs indicate the ratio of $\xi_{trans}/\xi_{long}$. To account also for high degrees of buckling, a fourth-order spline function has been used (Spatz and Speck, 1994). For small degrees of buckling this is equivalent to the third-order spline function introduced in Fig. 3. The relations between bending moment and curvature are almost perfect parabolic functions.

ratio of length/radius becomes lower than 30:1, the calculations lead to symmetrical results such that the cross section can be regarded as an ellipse. Knowing $\Delta\Delta s$ gives the small axes of the elliptical ring at equilibrium. This determines the axial second moment of area $I$,

$$I = (\pi/4) \cdot \{[a + (w/2)]^3 \cdot [b + (w/2)] - [a - (w/2)]^3 \cdot [b - (w/2)]\} \quad (2)$$

where $a$ is the small axis and $b$ the long axis of the ellipse and $w$ is the wall thickness. The bending moment is related to the curvature in the vertex by the basic equation

$$M = \text{curvature} \cdot I \cdot \xi_{\text{long}} \quad (3)$$

where $M$ is the bending moment at the vertex. $\xi_{\text{long}}$ is the Young's modulus in longitudinal directions.

At equilibrium the degree of buckling is defined as

$$\% \text{ buckling} = 100 \cdot (r - a)/[r - (w/2)] \quad (4)$$

where $r$ is the radius of the plant stem or tube before buckling (Fig. 3). The particular form is chosen, such that 100% buckling is reached, when the distal and the proximal wall touch each other, that is, if the structure is fully collapsed.

Figure 4 shows the relations among bending moment, curvature, and degree of buckling for a thin hollow tube. The mechanical behavior depends strongly on the Young's modulus in the radial ($\xi_{\text{radial}}$) and tangential ($\xi_{\text{tangential}}$) directions. Here we assume $\xi_{\text{radial}} = \xi_{\text{tangential}}$ and define it as $\xi_{\text{trans}}$.

## Modes of Failure

Two modes of failure are apparent in Fig. 4. At $\xi_{\text{trans}}/\xi_{\text{long}} = 1$ an almost-linear relationship between bending moment and curvature is observed. The hollow plant stem or tube ovalizes only a little, but upon bending the material reaches a critical compressive strain, chosen here as 1% (Fig. 5a). At $\xi_{\text{trans}}/\xi_{\text{long}} = 0.1$ the tube can be carried to higher curvatures, since ovalization reduces strains in longitudinal direction. But upon further bending the axial second moment of area is reduced to such an extent that the structure reaches the point of mechanical instability and ultimately buckling collapse. For $\xi_{\text{trans}}/\xi_{\text{long}} = 0.01$ mechanical instability is reached at low degrees of curvature.

Two quantities can be defined: the maximal bending moment and the critical curvature. The latter is defined as the curvature leading to critical compression of the material or the curvature reached before the structure collapses. (Since both experiment and calculation use discrete steps, this definition is less arbitrary than it may appear.)

A third type of failure, longitudinal splitting (Fig. 5b), is observed particularly for thick walled tubes of stiff material. Spatz *et al.* (1993) have calculated

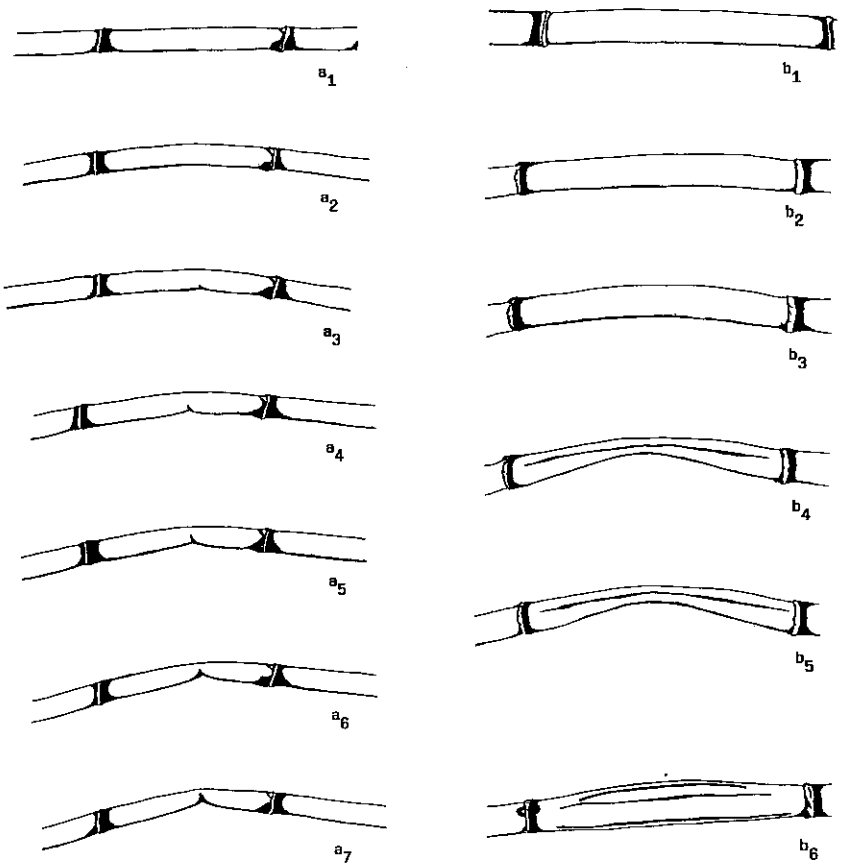


**Fig. 5.** Closeup views of two *Arundo donax* internodes during the process of bending, demonstrating two modes of failure. (a) An internode originating from the apical third of a 3.5-m-long stem (length of the internode $l = 8.6$ cm, mean radius $r = 0.66$ cm, mean wall thickness $w = 0.18$). Staining with phloroglucinol/hydrochloric acid reveals moderate lignification of the internodal wall. As shown in the series of drawings, local buckling starts, at relatively little ovalization, with a small indentation slightly right of the vertex on the compression side ($a_3$). The dent increases ($a_5$–$a_6$), inducing the buckling collapse of the internode ($a_7$). Primary cause of the buckling collapse is failure of the material due to exceeding the critical compressive strain. The ovalization of the hollow stem was relatively small. (b) Failure of a thicker internode of *Arundo donax* from the basal quarter of the same stem (length of the internode $l = 16.6$ cm, mean radius $r = 1.02$ cm, mean wall thickness $w = 0.35$ cm). In this internode the entire wall reveals extremely high lignification. This stiff, thick-walled internode fails by longitudinal splitting at small degrees of ovalization ($b_4$–$b_5$). Longitudinal splits occur first at the narrow vertex of the ellipse. As a consequence of the splintering of the hollow stem into two shells of semicircular cross section, longitudinal splits occur also in these shells, mainly at the shallow vertex of the deformation ellipse. This is shown in $b_6$, where the buckled internode is shown from above.

the strains in the radial and in the tangential directions which develop if a circular ring is deformed to an elliptical ring. The tangential strains reach their maximum at the point where the long axis meets the ellipse. Figure 6 shows the tangential strain as a function of the wall thickness and various degrees of ovalization. A reasonable estimate for the critical tangential strain in cereals is 2%.

Figure 7 presents the results of the computations for tubes with varying ratios of length/radius and material of different $\xi_{trans}/\xi_{long}$. Longitudinal splitting can reduce the maximum bending moment. In thin-walled tubes, however, such as the hollow stems of cereals, the maximum bending moment is usually reached before the tangential strains are larger than 2%. More salient is the limitation on the degree of curvature (Fig. 7b).

Short stout tubes are more stable than long slender tubes. This is due to the fact that for a ratio of length/radius below 30:1, buckling is no longer symmetrical. It occurs to a much lesser degree on the tension (windward) side than on the compression (leeward) side (Fig. 7c). In this case the cross section resembles a "doughnut" shape rather than an ellipse. At ratios of length/radius between 30:1 and 200:1 the maximal bending moment is nearly constant. At higher ratios we observe the counterintuitive result that for material with $\xi_{trans}/\xi_{long} = 0.1$, the maximal bending moment increases again. For ratios of length/radius $>1000$ this is observed even for tubes from a material with $\xi_{trans}/\xi_{long}$

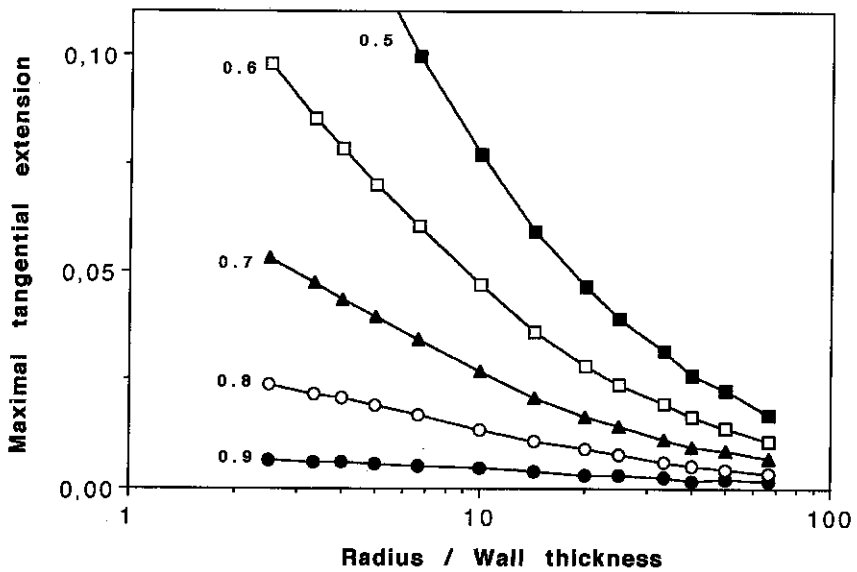


**Fig. 6.** Maximal strains in the tangential direction as a function of the ratio of radius/wall thickness for different degrees of deformation of a circular cross section. The numbers in the graph indicate the degree of ovalization *a*/*r*.

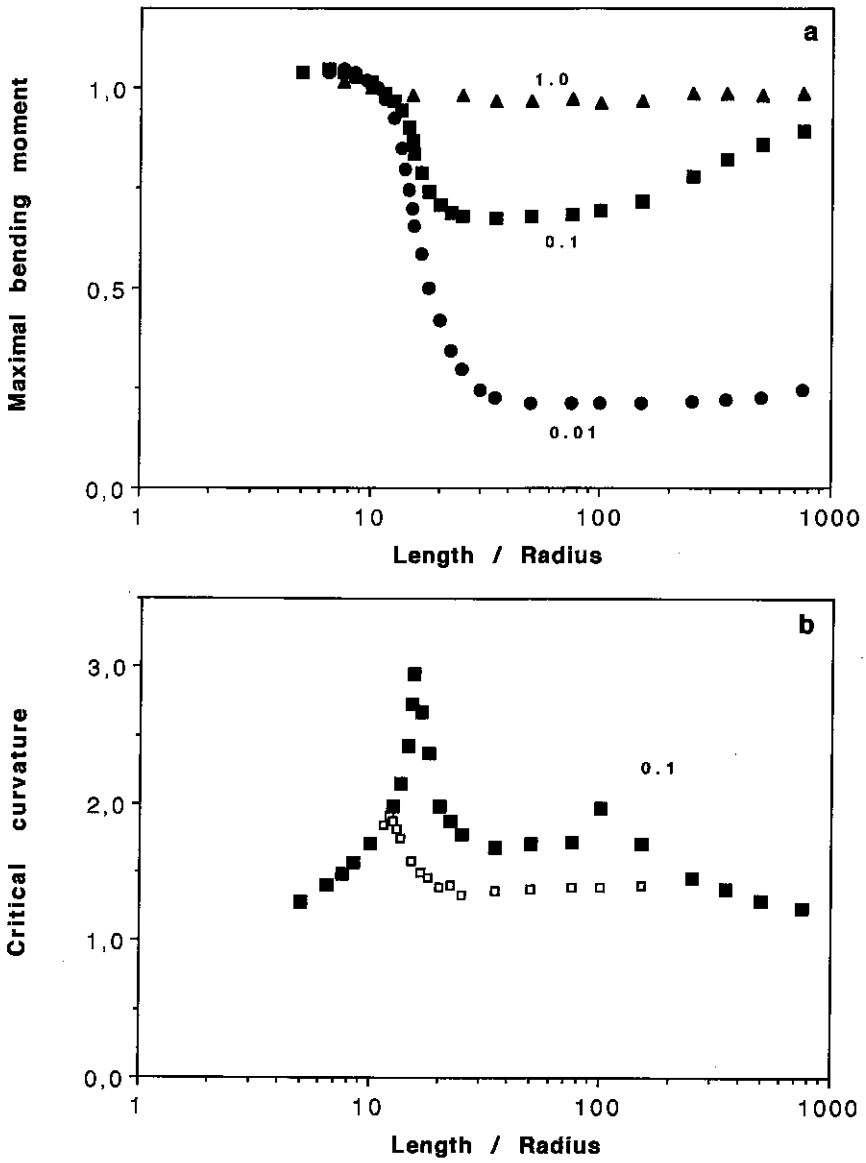


**Fig. 7.** Maximal bending moment, critical curvature, and buckling as a function of the ratio length/radius for a hollow tube of radius $r = 0.2$ cm and wall thickness 0.01 cm. The numbers in the graphs indicate the ratio $\xi_{trans}/\xi_{long}$. The data are normalized with the maximal bending moment and critical curvature of a tube which does not buckle ($\xi_{trans} \gg \xi_{long}$). The filled symbols indicate data for which the criterion for failure was either 1% longitudinal compressive strain or a buckling collapse, which in (c) is symbolized by 100% buckling. The open symbols in (b) indicate data where the additional failure criterion of 2% strain in the tangential direction led to termination of the calculation. For the thin-walled tubes considered, this had little effect on the values for maximal bending moments. (c) In short tubes the degree of buckling is less on the extension side (■) than on the compression side (●).

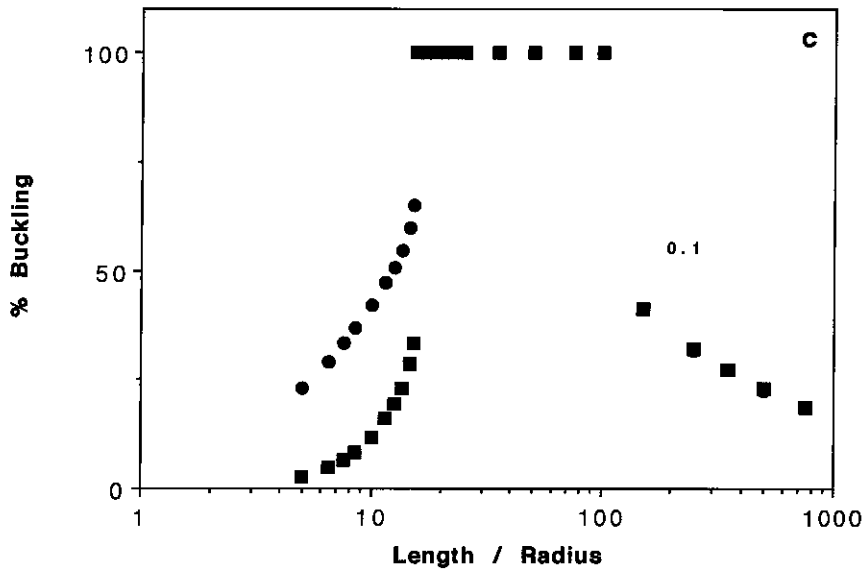


Fig. 7. Continued.

= 0.01. As discussed later the increase is a consequence of the assumption that the bending line on the compression side follows a smooth spline function. For this the relative gain of strain energy in the longitudinal direction decreases with increasing length, such that the equilibrium is reached at lower degrees of ovalization.

Optimal construction has to compromise between high flexural stiffness and elusion of dangerous degrees of buckling. This becomes apparent if structures with equal cross-sectional areas but different ratios of radius/wall thickness are considered (Fig. 8). Upon increasing the radius at the expense of the wall thickness, the maximal bending moment increases. Ultimately, however, ovalization will reduce the mechanical stability again. The ratio of radius/wall thickness, at which the optimum is found, depends on the Young's modulus in the transverse direction.

## The Mechanical Impact of Nodal Thickenings

The approach used allows one to subdivide the length of the hollow tube into segments. No ovalization may occur at the ends of each segment. This is equivalent to introducing nodes into the structure.

Figure 9 shows the maximal bending moments, the critical curvature, and the degree of ovalization for a hollow plant stem of constant length as a function of the length of the segments, i.e., the distance of nodes. The data closely

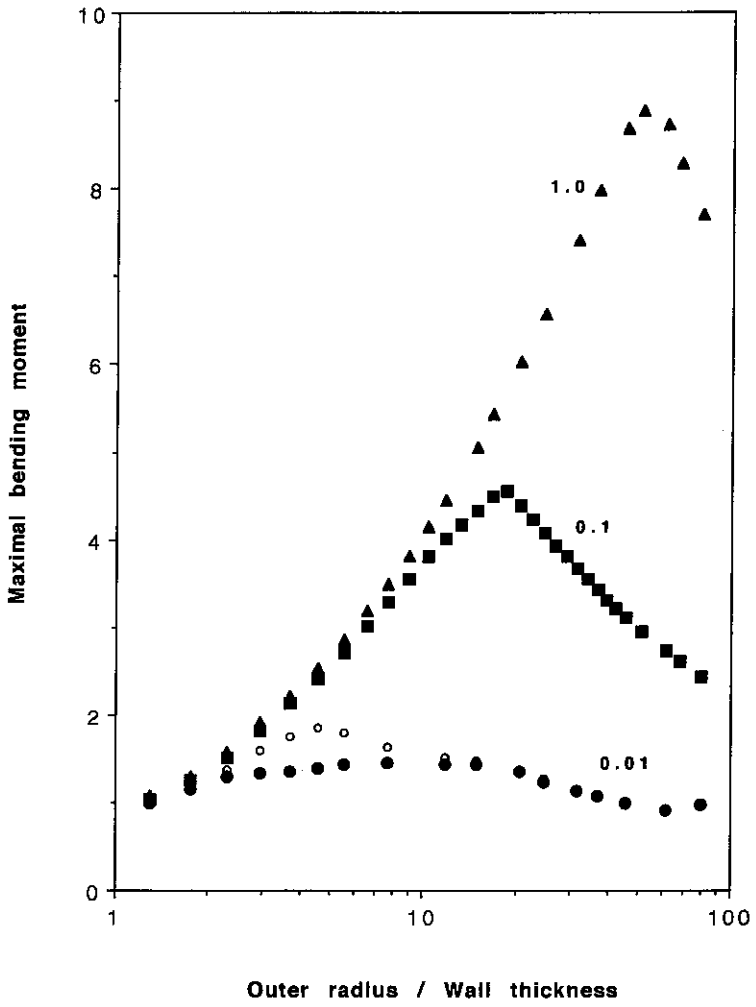


**Fig. 8.** The maximal bending moment for a hollow tube of length 20 cm and cross-sectional area of $\pi \cdot 0.4$ mm$^2$ as a function of the ratio of outer radius/wall thickness. The numbers in the graph indicate $\xi_{trans}/\xi_{long}$. The data are normalized to the maximal bending moment of a full cylinder of equal cross-sectional area. The criterion for failure is 1% strain in compression, 2% tangential strain, or failure of the structure. Disregard of failure due to tangential strain leads, in a few cases, to higher maximal bending moments. This is indicated by open symbols.

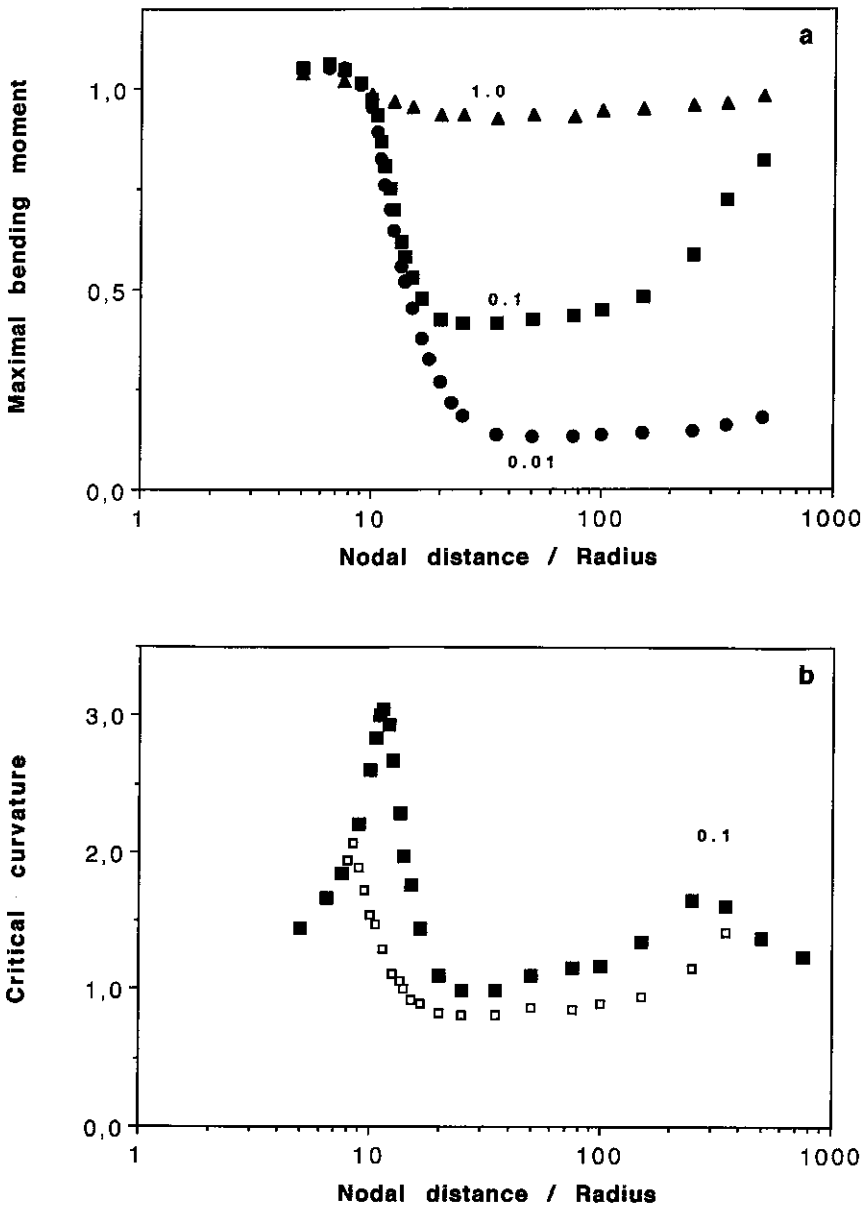


Fig. 9. Maximal bending moment, critical curvature, and buckling as a function of the ratio of nodal distance/radius for a tube with length $l = 2$ m, radius $r = 0.2$ cm, and wall thickness $w = 0.01$ cm. Since the bending line is symmetrical, this corresponds to a length of the stalk of grass of 1 m, disregarding tapering. The data are normalized and plotted as in Fig. 7. (c) Buckling on the extension side (■) is less than on the compression side (●) if nodes are located at short distances.

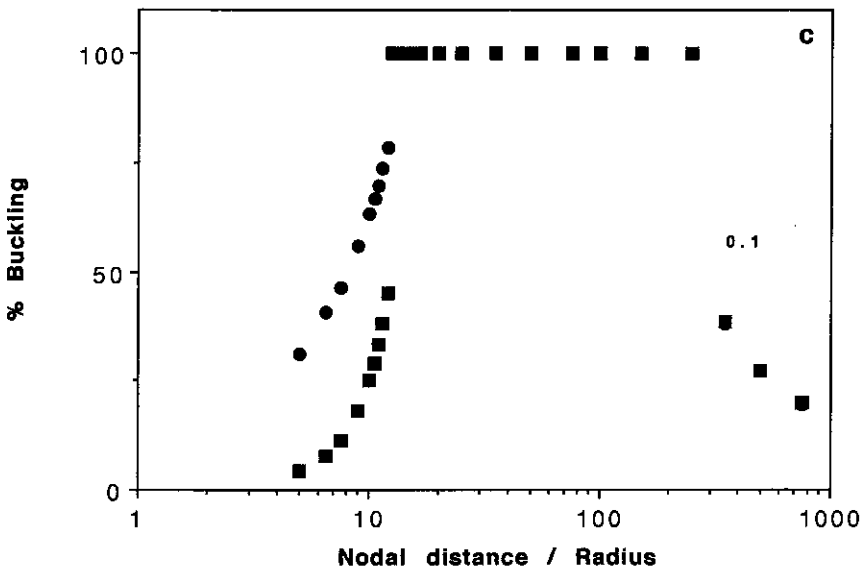


**Fig. 9.** Continued.

resemble those shown in Fig. 7. Again, we observe the counterintuitive increase in the maximal bending moment for a ratio of nodal distance/radius above 200. Most significant is the increase in the maximal bending moment with decreasing nodal distances. As seen in Fig. 9 this results from the fact, discussed before, that the degree of buckling is quite different for the compression side and the tension side.

Stabilization of the structure by nodal thickenings can be effective only for rather thin-walled tubes. Figure 10 shows the maximal bending moments for structures with equal cross-sectional areas as a function of the ratio of radius/wall thickness and different distances of the nodes. If nodes are placed at relatively short distances, the degree of stabilization can become quite remarkable.

## RESULTS

An automated measuring instrument was developed to observe the bending behavior of hollow plant stems up to the point of failure of the material or the structure (Spatz *et al.*, 1993; Spatz and Speck, 1994). A major difficulty in applying forces or bending moments to biological material is damage at the point of attachment. To avoid this problem we constructed a device consisting of a rail and two wagons which can be pulled together by a motor-operated ratchet via a string and pulleys. The wagons carry the mounts for tubes or plant

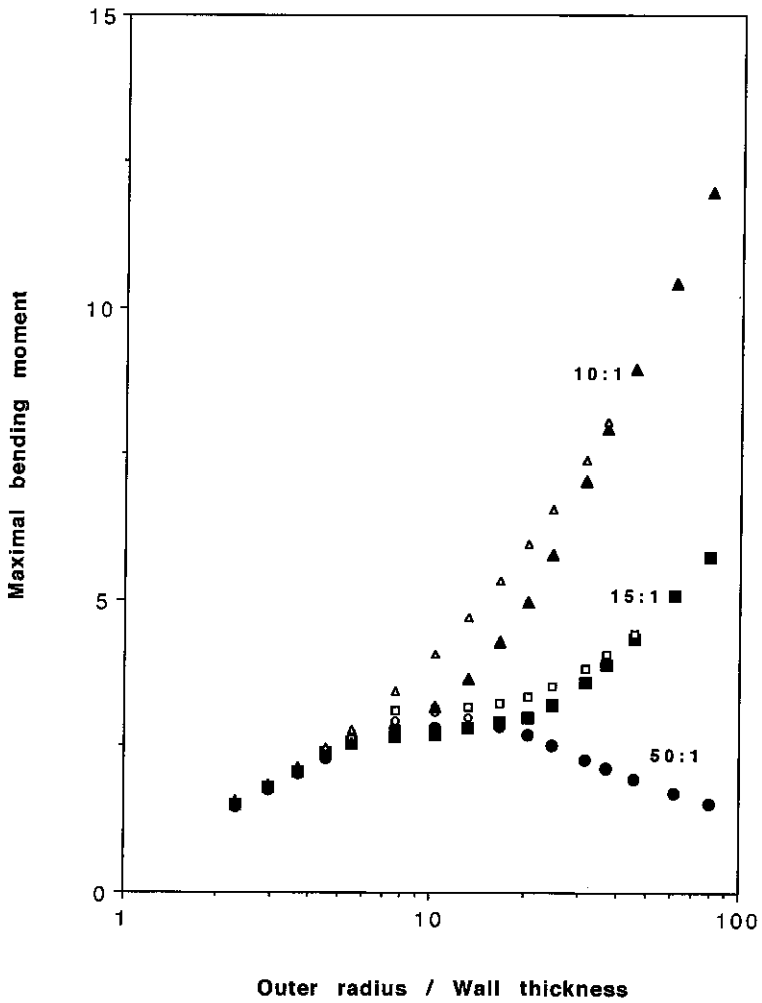


**Fig. 10.** The maximal bending moment for a hollow tube of length 2 m and cross-sectional area $\pi \cdot 0.4$ mm$^2$ as a function of the ratio of outer radius/wall thickness. The ratio of the Young's moduli $\xi_{trans}/\xi_{long} = 0.1$. The numbers in the graph indicate the ratio of nodal distance/radius. The failure criterion is the same as for Fig. 8. Also, the data are normalized and plotted in the same way as for Fig. 8.

stems. The mounts can rotate freely around a horizontal axis, such that bending moments directly at the mounts are avoided. The forces to pull the two wagons together, and thereby bend the object like an arrow, are measured with a force transducer. The position of the two wagons is measured by two displacement detectors. To obtain the height of the vertex, a CCD camera recorder was

mounted on a motor-operated stand, equipped with a displacement detector. A computer program was developed to operate the motor such that the camera was automatically adjusted to the height of the vertex of the bending object. The data force, distance of the two wagons, and height of the vertex were collected every 2 s. From these, the bending moment and the curvature in the vertex were calculated.

Figure 11 shows a corresponding plot for an internodium of *Secale cereale* ssp. *cereale*. The relation between bending moment and curvature is clearly nonlinear. This can be due to two reasons:

(i) a decrease in the second moment of area due to ovalization of the cross section and

(ii) a reduction of the Young's modulus in the longitudinal direction due to exceeding the limits of elastic behavior of the material.

To distinguish between these possibilities, the data were fitted with the help of

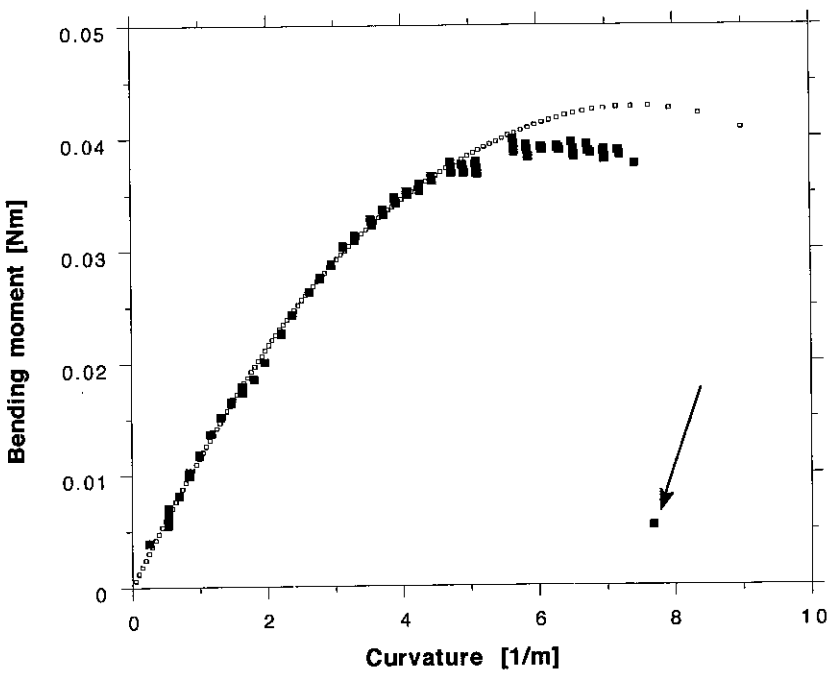


**Fig. 11.** The relation between bending moment and curvature as obtained experimentally (filled symbols) for a segment of a stalk of *Secale cereale* ssp. *cereale* of length $l = 30.7$ cm, radius $r = 0.15$ cm, and wall thickness of the sclerenchyma $w = 0.010$ cm. The arrow indicates the point of mechanical failure. The data were fitted up to a curvature of 4.5 $m^{-1}$ with the help of the theoretical approach (open symbols). From this, the Young's modulus in the longitudinal direction was obtained as $\xi_{long} = 11.3$ GN/m$^2$ and $\xi_{trans}/\xi_{long}$ as 0.031.

the theory outlined before. Up to a curvature of 4.5 $m^{-1}$ the fit represents the data quite well, indicating that up to this point ovalization of the cross section accounts for the nonlinearity. If the plant stem is bent further, the bending moments are consistently lower than predicted by the theory, indicating that the material is carried beyond the limits of Hooke's law until it finally fails in compression.

In *Triticum durum* var. *aegyptiacum* the range of non-Hookean behavior is extended to exceptionally high degrees of curvature (Fig. 12) before failure occurs. This correlates with a very large proportion of parenchymatic tissue (Fig. 13d).

To obtain the Young's moduli we take advantage of the fact that the data from the theoretical description can be represented by a second-order polynomial. Knowing the geometrical parameter of the sclerenchyma, it is possible to obtain the Young's modulus in the longitudinal direction from the linear term

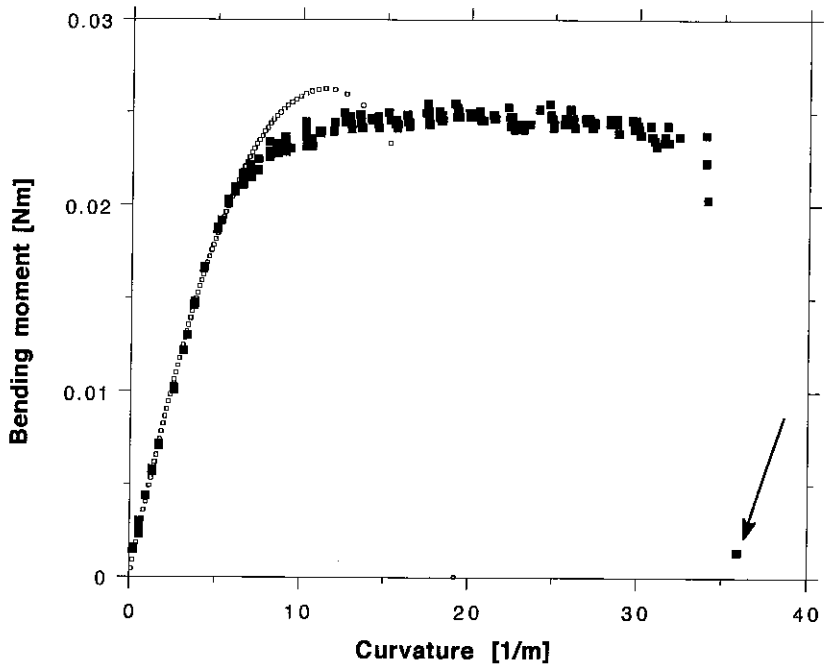


**Fig. 12.** The relation between moment and curvature for a segment of *Triticum durum* var. *aegyptiacum* of length $l$ = 16.4 cm, radius $r$ = 0.12 cm, wall thickness of the sclerenchyma $w$ = 0.0055 cm. The data are plotted as in Fig. 11. The simulation with the help of the theoretical approach can represent the experimental data only up to a curvature of 6 $m^{-1}$. Further increase in curvature at almost-constant bending moments before mechanical failure (arrow) can be attributed to nonelastic behavior of the material.

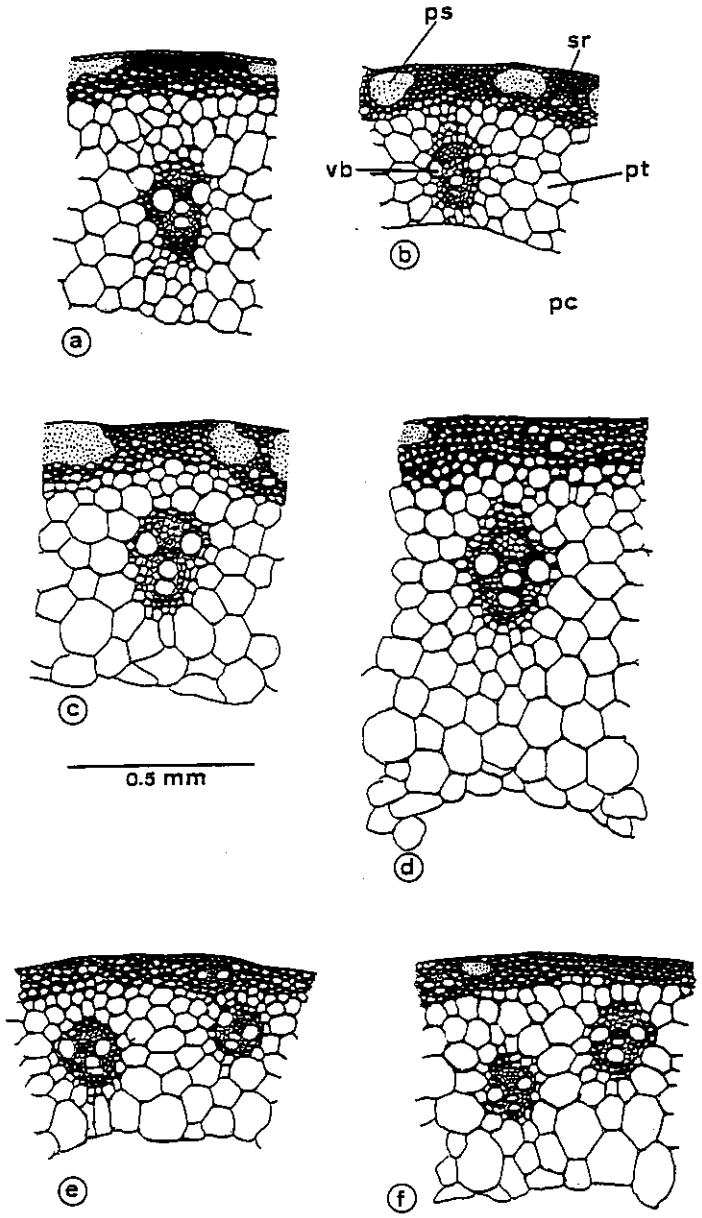


**Fig. 13.** Cross sections showing parts of the stalk walls of the six cereals studied: (a) *Secale cereale* spp. *afghanicum*, (b) *Secale cereale* ssp. *cereale*, (c) *Triticum aestivum* var. *lutescens*, (d) *Triticum durum* var. *aegyptiacum*, (e) *Triticum monococcum* var. *vulgare*, and (f) *Triticum spelta* var. *coeruleum*. sr, sclerenchyma ring (including epidermis and sometimes also vascular bundles); in some taxa in the outer parts of the sclerenchyma ring areas of photosynthetic tissue are found (ps), pt, parenchymatous tissue; vb, vascular bundles; pc, pith cavity.

of the fit for the data and to extract the Young's modulus in the transverse direction from the quadratic term.

Table I lists these constants together with the maximal bending moment and the critical curvature for internodal segments of some cereal taxa. Although the mechanical characteristics are not linearly related to the geometrical parameter, presenting averages is not inappropriate since the variations in the geometry are quite small.

The Young's moduli in the longitudinal direction vary only twofold between the varieties investigated. The variation within species is mainly of biological origin. In particular, the ontogenetic state influences the Young's modulus in longitudinal direction. While the ratio of the Young's moduli $\xi_{trans}/\xi_{long}$ is between 0.05 and 0.08 for the majority of the taxa, *Triticum spelta* var. *coeruleum* marks an exception.

## DISCUSSION

Hollow plant stems are found in several plant families, for instance, Apiaceae, Poaceae, and Equisetaceae. Such structures realize a high bending stiffness at a relatively low biological cost, but they are endangered by local buckling (Brazier, 1927), particularly under bending loads. In some of the taxa the stem is subdivided into hollow internodes and nodes with a high degree of nodal thickening. These reduce the danger of buckling (Gappoev, 1992; Niklas, 1989, 1992). Hollow structures can be endangered by bending moments exerted by side branches or large leaves. This is presumably the reason why side branches usually include only very small angles to the main stem (Mosbrugger, 1990). Where the angle is nearly 90°, as in the large leaves of *Heracleum mantegazzianum*, the nodal thickenings are collar-like and quite massive.

Previous work (Spatz *et al.*, 1990, 1993) showed that the bending behavior of hollow tubes could be described by considering the equilibrium between strain energies in longitudinal direction and deformation energies acting in radial and in tangential direction. Here the numerical values of Young's moduli in radial and in tangential direction are assumed to be equal. This assumption has little significance for the calculation of the maximal bending moment, but it influences the strains developing in the tangential direction upon ovalization and, therefore, the limitations imposed by the danger of longitudinal splitting.

The computations show that the stability of hollow structures against buckling is greatly enhanced by nodal thickenings provided that the ratio of nodal distance/radius is below 30:1. In this range buckling is asymmetrical. The cross section has a "doughnut"-like rather than an elliptical shape. Strains are transferred from the compression side to the tension side, such that the strains on this side can become quite large. We have chosen a value of 2% extension as the failure criterion, compared to 1% in compression.

**Table I.** Geometrical and Mechanical Data for Internodia of Cereals (Mean ± SD)

| | *Secale cereale* ssp. *afghanicum* | *Secale cereale* ssp. *cereale* | *Triticum aestivum* var. *lutescens* | *Triticum durum* var. *aegyptiacum* | *Triticum monococcum* var. *vulgare* | *Triticum spelta* var. *coeruleum* |
|---|---|---|---|---|---|---|
| Length (cm) | 25.7 ± 2.2 | 29.9 ± 4.3 | 25.7 ± 2.5 | 20.9 ± 2.1 | 16.7 ± 4.1 | 23.1 ± 5.1 |
| Mean radius (cm) of sclerenchyma | 0.174 ± 0.018 | 0.173 ± 0.026 | 0.19 ± 0.01 | 0.130 ± 0.018 | 0.118 ± 0.011 | 0.155 ± 0.023 |
| Wall thickness (cm) of sclerenchyma | 0.0072 ± 0.00066 | 0.0092 ± 0.002 | 0.0118 ± 0.0019 | 0.0076 ± 0.0012 | 0.0077 ± 0.0020 | 0.0055 ± 0.0006 |
| Water content (%) | 67.9 ± 2.9 | 65.7 ± 3.2 | 69.7 ± 3.1 | 65.4 ± 3.2 | 68.6 ± 2.6 | 69.4 ± 2.3 |
| Maximal bending moment (nm) | 0.071 ± 0.005 | 0.045 ± 0.006 | 0.071 ± 0.020 | 0.037 ± 0.018 | 0.025 ± 0.005 | 0.034 ± 0.015 |
| Critical curvature (1/m) | 7.23 ± 0.8 | 5.19 ± 1.54 | 7.27 ± 1.65 | 25.9 ± 11.1 | 22.5 ± 8.35 | 9.07 ± 1.39 |
| Young's modulus $\xi_{long}$ (GN/m$^2$) | 22.3 ± 3.4 | 14.6 ± 3.9 | 10.7 ± 2.6 | 15.6 ± 4.6 | 12.9 ± 5.7 | 13.4 ± 4.0 |
| $\xi_{trans}/\xi_{long}$ | 0.08 ± 0.035 | 0.053 ± 0.049 | 0.054 ± 0.013 | 0.07 ± 0.03 | 0.071 ± 0.036 | 0.17 ± 0.06 |
| Number of measurements | 5 | 6 | 8 | 7 | 6 | 8 |

A counterintuitive result is shown in Figs. 7a and 9a. For very thin long tubes the maximal bending moments appear to increase again. This is the result of the assumption of a "smooth" spline function as the bending line on the compression side. A "wavy" bending line would lead to a higher degree of relaxation of strains. This supposition can be tested within the framework of the theoretical approach by introducing "virtual" nodes into the hollow structure. Figure 14 shows the computational results for such an interpretation. The introduction of "virtual" nodes leads to a nearly constant maximal bending moment. For a ratio of distance of virtual nodes/radius above 20:1, the values are lower than those observed without virtual nodes, indicating that wavy bending lines can destabilize the structure. It should be pointed out that we have not yet observed wavy bending lines in our experiments.

It is the aim of our work to understand the mechanical properties from the structural properties of the plant stem, in particular, the distribution of tissues in the cross section. In previous work we observed a correlation between the Young's modulus in the longitudinal direction and the compactness of the sclerenchyma (Spatz *et al.*, 1993). This observation is confirmed here. *Secale cer-*

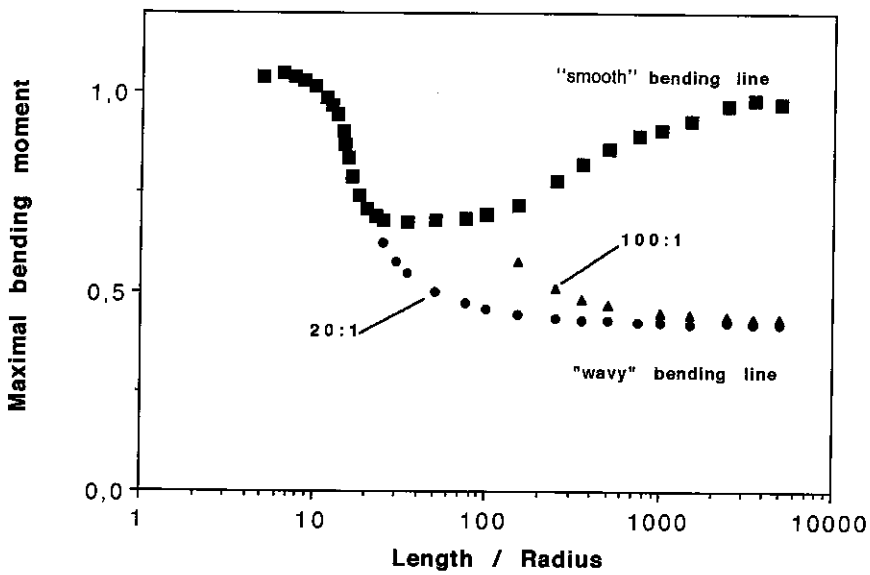


**Fig. 14.** The maximal bending moment as a function of the ratio length/radius calculated for a ratio of Young's moduli $\xi_{trans}/\xi_{long} = 0.1$. The assumption that the bending line on the compression side follows a "smooth" spline function leads to a counterintuitive result. A more reasonable assumption is a "wavy" bending line. In the framework of the theoretical approach this can be demonstrated by introducing "virtual" nodes into the structure. The numbers in the graph indicate the ratio of "nodal distance"/radius used in the computations. A ratio of 20:1 leads to a minimum of the mechanical stability. Wavy bending lines have not yet been observed.

*eale* ssp. *afghanicum*, with the most compact sclerenchyma (Fig. 13a), has the highest Young's modulus in the longitudinal direction, in contrast to *Triticum aestivum* var. *lutescens*, with the least compact sclerenchyma (Fig. 13c).

Spatz *et al.* (1993) suggested that the parenchymatous tissue can contribute to the stiffness in the transverse direction, thus stabilizing the structure against buckling. This supposition is confirmed here in two ways.

(i) The Young's modulus in the transverse direction as obtained from the fit of the nonlinearity of the bending moment–curvature relation implicitly contains the contributions of the parenchyma to the transverse stiffness. The apparent ratios of the Young's moduli $\xi_{trans}/\xi_{long}$ are found in the range of 1 : 20 to 1 : 12 with one exception, *Triticum spelta* var. *coeruleum*. If it is assumed that $\xi_{trans}/\xi_{long}$ for sclerenchyma alone is 1 : 20, as for bamboo (Niklas 1991), then an apparent value of 1 : 6 is a clear indication of a stabilizing influence of the parenchyma either through sclerenchymatized parenchyma (Spatz *et al.*, 1993) or through turgor pressure.

(ii) *Triticum durum* var. *aegyptiacum* tolerates exceptionally high degrees of curvature (Fig. 12). The portion of the parenchymatic tissue is very large (Fig. 13d). This prevents ovalization to more than 20%. Failure occurs after extensive plastic deformation of the material. High degrees of curvature are also found in *Triticum monococcum* var. *vulgare*. As in *Triticum durum* var. *aegyptiacum* this can be ascribed only partly to the small radii of the internodes tested. Again, a relatively large portion of parenchymatic tissue is characteristic (Fig. 13e), though not as large as in *Triticum durum* var. *aegyptiacum*. Correspondingly, the mechanical behavior is intermediate between that shown in Fig. 11 and that in Fig. 12.

Understanding the mechanical properties of hollow plant stems may help to reduce the enormous economic losses due to lodging of cereal. The base of empirical data, however, is still quite incomplete. Studies of the changes of the mechanical properties during ontogeny are missing. Also, the influence of the degree of hydration or the use of different fertilizers during growth needs to be investigated before generalizations of structure–function relations can be made in such a way as to develop guidelines for plant breeders.

## ACKNOWLEDGMENTS

We are grateful for stimulating discussions with Drs. C. Mattheck, W. Nachtigall, and L. Wessolly. B. Bambai carried out some of the experiments and B. Heneka prepared the drawings.

## REFERENCES


Axelrad, E. L. (1965). A more precise estimation of the upper critical bending load of a tube taking into account the geometrical nonlinearity. *Trans. (Iswestia) Acad. Sci. USSR. Sect. Mech. Mech. Eng.* **4**:133–139 (Russian).

Böhm, W., and Gose, G. (1977). *Einführung in die Methoden der Numerischen Mathematik*, Vieweg Verlag, Braunschweig.

Brazier, L. G. (1927). On the flexure of thin cylindrical shells and other "thin" sections. *Proc. Roy. Soc. Lond. Ser. A* **116**:104–114.

Ennos, A. R. (1993). The mechanics of the flower stem of the sedge *Carex acutiformis*. *Ann. Bot.* **72**:123–127.

Foley, D. C. (1983). Mechanical properties of *Zea mays* stems. *Iowa State J. Res.* **58**:235–246.

Gappoev, M. (1992). Statische Interpretation grasartiger Konstruktionen. *Natürliche Konstruktionen—Mitteilungen des SFB 230* **7**:73–77.

Herbig, A., Sinn, G., and Wessolly, L. (1988). Zur Standsicherheit von Bäumen im städtischen Bereich *Natürliche Konstruktionen. Leichtbau in Architektur und Natur. Mitteilungen des SFB 230* **1**:39–57.

Lu, R.-F., Bartsch, J. A., and Ruina, A. (1987). Structural stability of the corn stalk. *Am. Soc. Agr. Eng.* Paper No. 87-6066:1–16.

Mattheck, C. (1992). *Design in der Natur. Der Baum als Lehrmeister*, Rombach Verlag, Freiburg.

Mattheck, C., Gerhardt, H., and Breloer, H. (1992). VTA: Visual tree defect assessment based on computer simulation of adaptive growth. In Little, E. G. (ed.), *Experimental Mechanics*, Elsevier, Amsterdam.

Mattheck, C., Bethge, K., and Erb, D. (1993). Failure criteria for trees. *Arb. J.* **17**:201–209.

Mattheck, C., and Breloer, H. (1993). Der Baumbruch in Mechanik und Rechtsprechung. In *Handbuch der Schadenskunde von Bäumen*, SVK-Verlag, Erndtebrück.

Mosbrugger, V. (1990). The tree habit in land plants. *Lecture Notes in Earth Sciences 28*, Springer Verlag, Berlin.

Niklas, K. J. (1989). Nodal septa and the rigidity of aerial shoots of *Equisetum hyemale*. *Am. J. Bot.* **76**:521–531.

Niklas, K. J. (1991). Bending stiffness of cylindrical plant organs with a "core-rind" construction: evidence from *Juncus effusus* leaves. *Am. J. Bot.* **78**:561–568.

Niklas, K. J. (1992). *Plant Biomechanics*, University of Chicago Press, Chicago, London.

Niklas, K. J. (1993). Influence of tissue density-specific mechanical properties on the scaling of plant height. *Ann. Bot.* **72**:173–179.

Niklas, K. J., and O'Rourke, T. D. (1987). Flexural rigidity of chive and its response to water potential. *Am. J. Bot.* **74**:1033–1044.

Reissner, E. (1959). On finite bending of pressurized tubes. *Trans. ASME* **81**:386–392.

Rinn, F. (1994). Wie genau kann die Bruchsicherheit eines Baumes ermittelt werden? *Das Gartenamt* **43**:104–108.

Romberger, J. A., Hejnowicz, Z., and Hill, J. F. (1993). *Plant Structure: Function and Development. A Treatise on Anatomy and Vegetative Development, with Special Reference to Woody Plants*, Springer-Verlag, Heidelberg.

Sinn, G. (1993). Grundsätzliches zur Bruchsicherheit von Bäumen. Eine Argumentationshilfe in Schadensfällen. *Das Gartenamt* **42**:387–392.

Sinn, G. (1994). Bruchsicherheit von Bäumen und Restwandstärke geschlossener Stammquerschnitte. *Das Gartenamt* **43**:100–103.

Spatz, H.-Ch., Speck, T., and Vogellenhner, D. (1990). Contributions to the biomechanics of plants. II. Stability against local buckling in hollow plant stems. *Bot. Acta* **103**:123–130.

Spatz, H.-Ch., Boomgarden, Ch., and Speck, T. (1993). Contribution to the biomechanics of plants. III. Experimental and theoretical studies of local buckling. *Bot. Acta* **106**:193–276.

Spatz, H.-Ch. (1994). Ein Kommentar zur mechanischen Stabilität hohler Bäume. *Das Gartenamt* **43**: 92–95.

Spatz, H.-Ch., and Speck, T. (1994). Mechanische Eigenschaften von Hohlrohren am Beispiel von Gräsern. BIONA-reports (in press).

Speck, T., Spatz, H.-Ch., and Vogellehner, D. (1990). Contributions to the biomechanics of plants.

I. Stabilities of plant stems with strengthening elements of different cross-sections against weight and wind forces. *Bot. Acta* **103:**111–112.

Stephens, W. B., Starnes, J. H., Jr., and Almroth, B. O. (1974). Collapse of long cylindrical shells under combined bending and pressure loads. In *AIAA/ASME/SAE 15th Structures, Structural Dynamics and Materials Conference*, Las Vegas, pp. 1–8.

Timoshenko, S. P., and Gere, J. M. (1961). *Theory of Elastic Stability*, McGraw–Hill, New York.

Vincent, J. F. V. (1983). Biomechanics in schools. *School Sci. Rev.* **43:**648–663.

Vincent, J. F. V., and Jeronimidis, G. (1991). The mechanical design of fossil plants. In: Rayner, J. M. V., and Wootton, R. J. (eds.), *Biomechanics in Evolution*, Cambridge University Press, Cambridge, pp. 21–36.

Wainwright, S. A., Biggs, W. D., Currey, J. D., and Gosline, J. M. (1976). *Mechanical Design in Organisms*, Arnold, London.

Wessolly, L. (1988). Die natürliche Konstruktion Baum als intelligentes statisch-dynamisches System. *Natürliche Konstruktionen. Mitteilungen des SFB 230* **2:**203–212.

Wessolly, L. (1991). *Material- und Struktureigenschaften der Bäume*, Fortschreibung des Stuttgarter Festigkeitskatalogs, Stuttgart.

Wessolly, L. (1993). Stand- und Bruchsicherheit von Bäumen. Leistungsfähigkeit und Grenzen der Zugversuche. *Das Gartenamt* **42:**486–491.

*Biomimetics, Vol. 2, No. 2, 1994*

# Growth and Architecture of the Plant Cell Wall: Biomechanical Problems[1]

**Roger Prat[2,3], Michèle Mosiniak[2,4] and Jean-Claude Roland[2,4]**

*This paper deals with the dynamics of the cell wall during plant growth. The study focuses on the extension of mung bean seedlings. First, the parameters of growth were defined (duration, actual localization, polarity, time change of elongation rate, change of osmotic pressure, etc.). Then the specific mechanical properties of the primary cell wall were considered and compared in living and nonliving tissues. Rheology and deformation responses, plasticity, and creep were followed along the growth gradient and when the surface expansion had ceased. Different potential activators (low pH, hormones) were tested. The cell wall texture and its changes were then followed, step-by-step, at the ultrastructural level along the growth gradient; the expanding cell wall appears as a mesophase (liquid crystal-like) of cholesteric type. The helical construction is transient and dispersed when intense surface expansion occurs. Thus, the growing wall changes from order to a dramatic thinning and a complete randomization. Finally, the question of the primary wall dynamics is discussed and the risks of oversimplification when modeling the plastic cellulosic composite within living organs is emphasized.*

**KEY WORDS:** biological composite; cellulose; growth; mesophase; mung bean.

## INTRODUCTION

Obviously, the mechanical properties of plants depend mainly on the fact that each constitutive cell is surrounded by a more or less stiff and thick wall. In

[1]This is the published version of a paper presented at the Plant Biomechanics Congress, Montpellier, France, September 5-9, 1994.

[2]University Pierre & Marie Curie, Paris, France.

[3]Laboratoire d'enzymologie en milieu structuré, Institut Jacques Monod, tour 43, 2 Place Jussieu, 75 251, Paris cedex 05, France.

[4]Laboratorie de cytologie expérimentale et morphogenèse végétale, UPMC, bât. N2, 4 Place Jussieu 75 252, Paris cedex 05, France.



1059-0153/94/0600-0175$07.00/0 

higher plants, the cell wall is secreted and assembled outside the cytoplasm as a fibrous composite. It is made of ground components (pectic substances hemicelluloses, etc.), or matrix, in which a frame of microfibrils of cellulose is embedded and strengthens the system.

During growth, the cell wall is in a complex and rather paradoxical situation: It must be both resistant enough to behave as a supporting structure and plastic enough to allow often dramatic surface extension (i.e., an increase of several times the initial surface of the cell wall within a few hours). The cell wall surrounding the young and growing cell is called the primary wall. Its sheets are deposited first against the middle lamella. Growth remains possible because the cellulosic microfibrils keep a certain degree of freedom and can be individually displaced (by sliding and/or reorientation; the point remains moot) within a soft and highly hydrated matrix (the movement is no longer possible in the so-called secondary wall deposited later, after cessation of growth).

It was long considered that the primary wall architecture showed no defined order and was dispersed passively according to the laws of flows of viscous fluids. But with the development of ultrastructural data, the original assumption has been found to be false and it was soon shown that the formation of different textures must be ascribed, at least in part, to the creative power of the plasmalemma, which organizes the cell wall with regard to its future function (Frey-Wyssling and Mühlethaler, 1963). The nature of this morphogenesis and wall ordering is still discussed. Different mechanisms could cooperate at the wall–membrane interface. During recent years, the possibility that the primary wall is, at least in part, precisely and specifically self-assembled in this cell area has emerged. The cell wall could be a "mesophase" or a "mesomorphic phase" somewhat comparable to certain liquid crystals (for reviews see Roland *et al.*, 1992; Neville, 1993).

In this paper, we present different mechanical, physiological, and structural data which are integrated during the course of growth of the cell wall and must be taken into account when the living plant is considered.

## THE LOCALIZATION OF CELL GROWTH

In most plant organs, cell growth is localized in minute zones of young levels; it is distributed according to precise gradients which are time dependent (Prat, 1985; Silk, 1992). The most analyzed organs from this point of view were taken from young seedlings in the course of elongation: coleoptiles (maize, etc.), hypocotyls (mung bean, sunflower, etc.), and/or epicotyls (stem of pea, beans, etc.).

The distribution of growth in *Vigna radiata* (mung bean) is shown in Fig. 1. The expansion is highly polarized (= elongation; according to a major axis). The main growth occurs at the top of the organ (just below the apical hook).

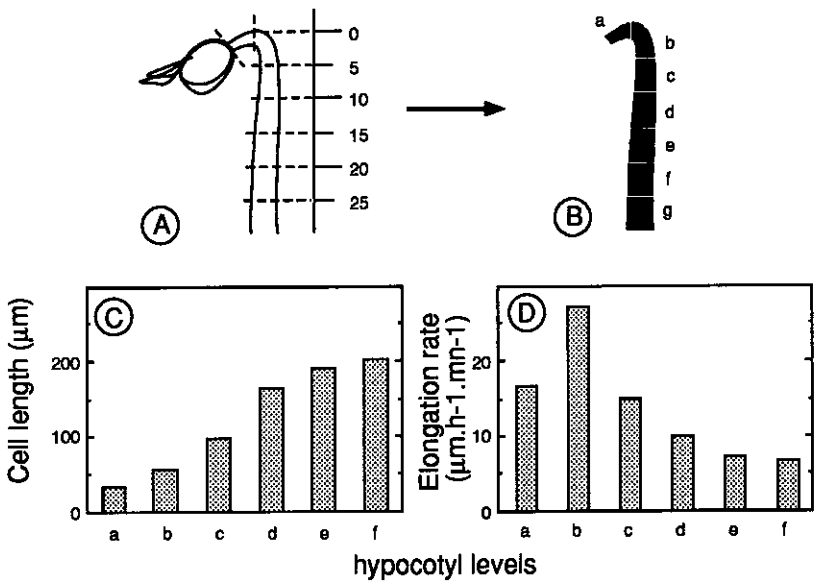


**Fig. 1.** Growth gradient of a 4-day-old hypocotyl of *Vigna radiata*: (A, B) hypocotyl cut in successive 5-mm-long segments; (C) epidermal cell length (mean value) measured for each segment; (D) rate of elongation of successive segments.

The lower and basal regions have lost any expression of cell elongation. The distribution and intensity of elongation of the organ along a growth gradient can be directly correlated with the changes in cell length and local modifications of plasticity.

During a relatively short time [1 or 2 days, depending on the environmental conditions (temperature, light, etc.)], the cells of the subapical zone are able to increase their length 10 times (Fig. 2) or more, before being driven toward lower zones, where their rate of expansion decreases and progressively tends to zero. The intense change in dimensions and size of cells implies both extension (loosening of the preestablished network) and synthesis (apposition and intussuception) of new components. It implies also an increase in the vacuolar volume and a maintenance of the osmotic pressure above a critical threshold by concentration of solutes. A rapid surface increase in the membranes (both of the plasmalemma and of the tonoplast) is also among immediate prerequisite conditions for extension.

Therefore, the regulation of the rate of growth and the arrest of the surface expansion can be due either to variations of pressure, to changes in the plastic properties of the wall itself, or to variations of physiological properties (e.g.,

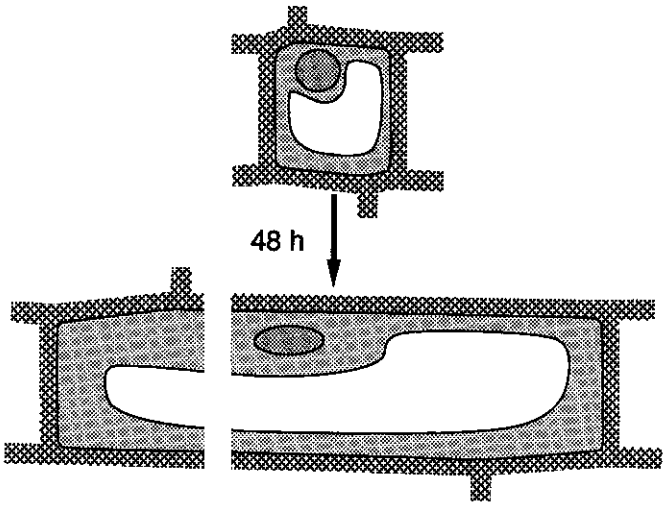


**Fig. 2.** Diagram of a plant cell before and after growth. The initial length of the cell is about 20 $\mu$m, and the final length about 200 $\mu$m.

increase in inhibitors, decrease in synthesis and endomembrane flows, change of hormone sensibility).

## THE DRIVING FORCE: TURGOR PRESSURE

Growth occurs only if the cell presents a turgor pressure high enough to ensure cell wall deformation. Turgor pressure of a cell depends on its own water potential and on the water potential of the environment (neighboring cells and external medium); it is relatively easy experimentally to modulate the relative turgor pressure by changing the osmotic pressure of the external medium (Prat *et al.*, 1977, Fig. 3).

For cells whose growth has ceased, variations of the external water potential produce reversible changes of volume (Fig. 3A), which are relevant to the elastic properties of the organ and therefore of the cell wall; if cells are young (Fig. 3B), identical variations more or less block growth. There is an external pressure which prevents any growth, indicating that a minimum turgor pressure is necessary (the "critical turgor pressure"). We can notice that when cells are transferred to a new suitable medium, their growth is restored, but the final size is lower than the final size of the controls (untreated by concentrated medium): That means that there is no "stored growth" (Cleland, 1981).

Kinetics show two components: (1) an elastic deformation comparable to the elasticity of older cells and (2) a plastic deformation (nonreversible) that appears only when the internal pressure is higher than a specific threshold.

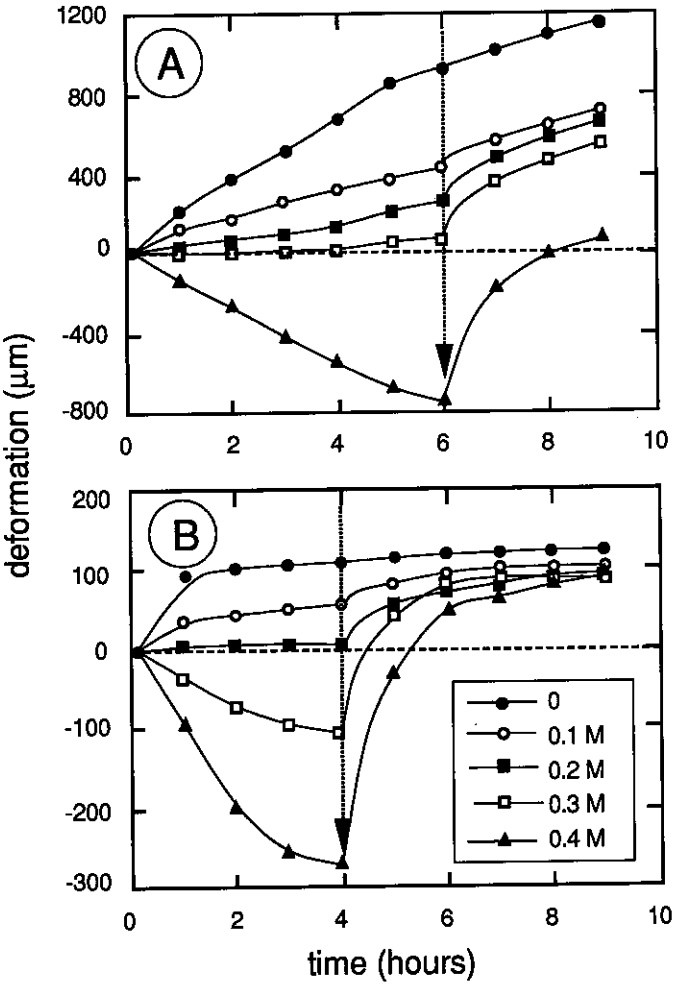


**Fig. 3.** Responses of segments excised from the elongating zone (A) and nonelongating zone (B) for different concentrations of mannitol; note that the *Y* scales in A and B are very different.

## CELL WALL EXPANSION: DISPERSION OF A CHOLESTERIC MESOPHASE

In the growth gradient, tissue differentiation is precocious (Fig. 4) and cell wall thickening begins early. The wall thickness is uneven in different cells: the maximum layering is present at cell corners (Fig. 5) and on certain outer cell facets. The elongating zone is already heterogeneous and complex from the

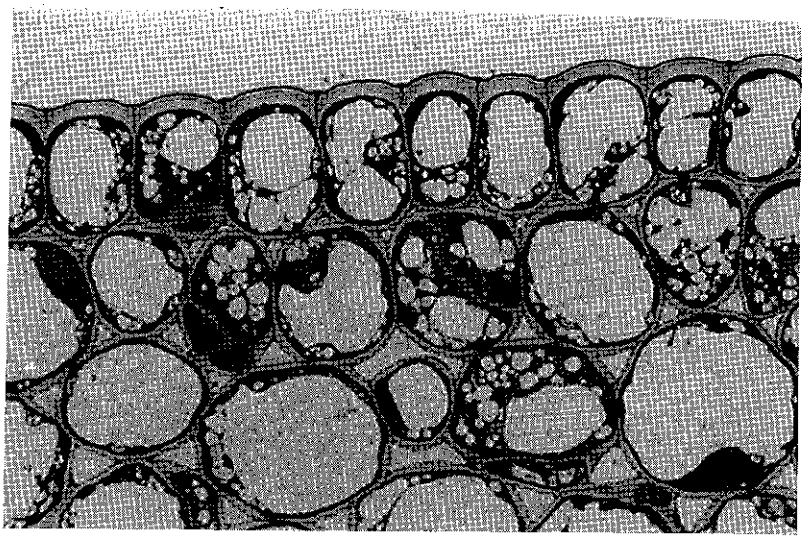

**Fig. 4.** Transverse section of mung bean hypocotyl in the growing zone; epidermis and parenchyma with primary cell wall. ×450.

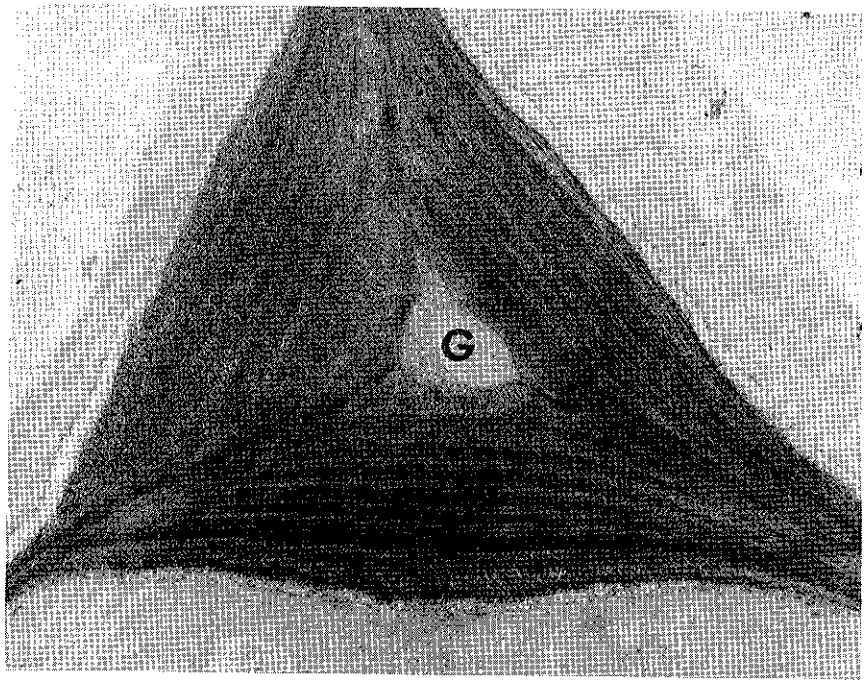


**Fig. 5.** Same level, parenchyma; view of a cell corner with local ("rib") layered thickenings of the cell wall. G, intercellular gas space. ×1200.

microstructural viewpoint. When the thickened parts of the growing cell wall are observed in ultrathin sections, the characteristic so-called arced layers are seen, especially in the youngest domains, i.e., in the upper levels and near the plasmalemma (Fig. 6).

It is now well-known that arced layering is frequent in microfibrous biological composites and is indicative of helicoidal architecture. It corresponds to a progressive rotation of the orientation of the successive cellulosic microfibrils which are secreted and deposited beyond the plasmalemma. The whole construction forms a twisted plywood (Fig. 7). The cell wall shows, for a while, a liquid crystal-like architecture (of the cholesteric or chiral nematic type). The

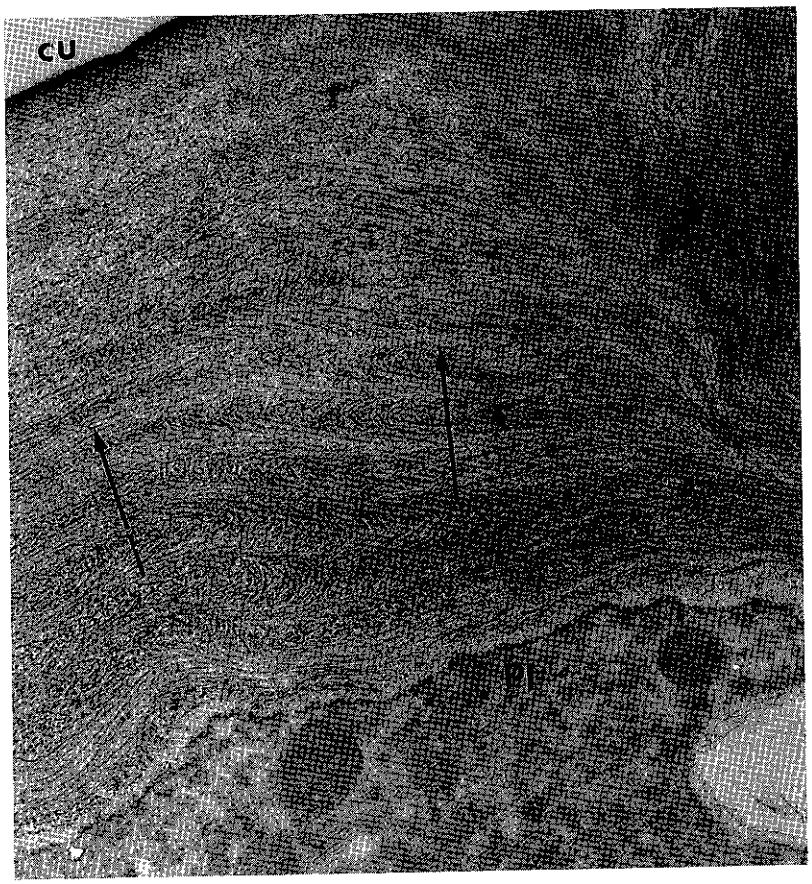


**Fig. 6.** Ultrastructural organization of the cell wall of epidermis in the course of growth; arced patterning near the plasmalemma (pl) and progressive dispersion in the former parts (arrows). cu, cuticle. ×20,000, reduced to 90% for reproduction.

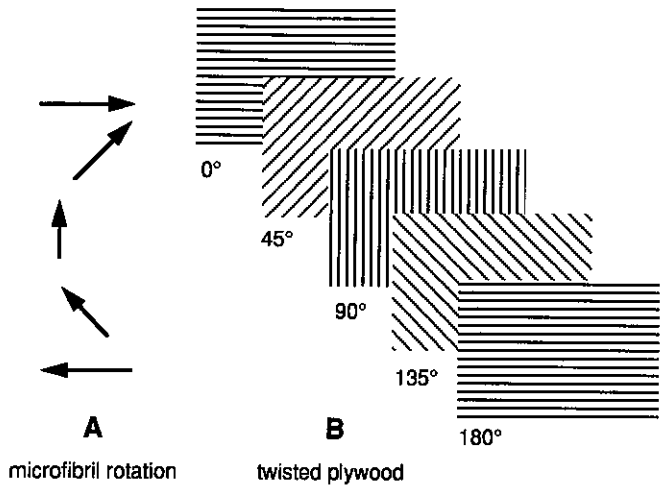


**Fig. 7.** Orientation of the cellulose microfibrils in a twisted plywood: (A) section for five successive positions; (B) face view.

construction of the helicoidal architecture—from a single arc to complete arced layering—is briefly summarized in Fig. 8. Neville (1993) gives a full explanation of this characteristic mesophase and its specific properties. Each layer of cellulosic microfibrils is oriented in parallel sheets; the direction of the microfibrils changes through a small angle from sheet to sheet (helicoidal geometry is thus somewhat comparable to the change in direction of the grain of a wooden spiral staircase).

The spatial disposition of the microfibrils is multidirectional; it is efficient and well adapted, owing to the longitudinal intramolecular arrangement of the cellulose [close array of $\beta$-(1,4) glucan chains], to resist tension. The primary wall composite combines multidirectional microfibrils of high stiffness with a matrix of lower stiffness. It is specially suited to resist shearing forces coming from all directions; fracture energy is absorbed and dissipated through the laminated composite. The propagation of fractures will be prevented or limited and buckling reduced. From the mechanical point of view, it must be emphasized that the skeletal microfibrils are strategically oriented so as best to be able to cope with various tensile stresses and strains operating upon them, both from an internal source (weight, etc.) and from environmental origin (wind, etc.).

Therefore, on one hand, the twisted architecture optimizes the distribution of forces and has the advantage to secure the best multidirectional strengthening supported by young and slender organs, and, on the other hand, the liquid crystal-like phase remains fluid enough and the molecules are internally mobile when forces are acting (in the present case, tension due to osmotic pressure).

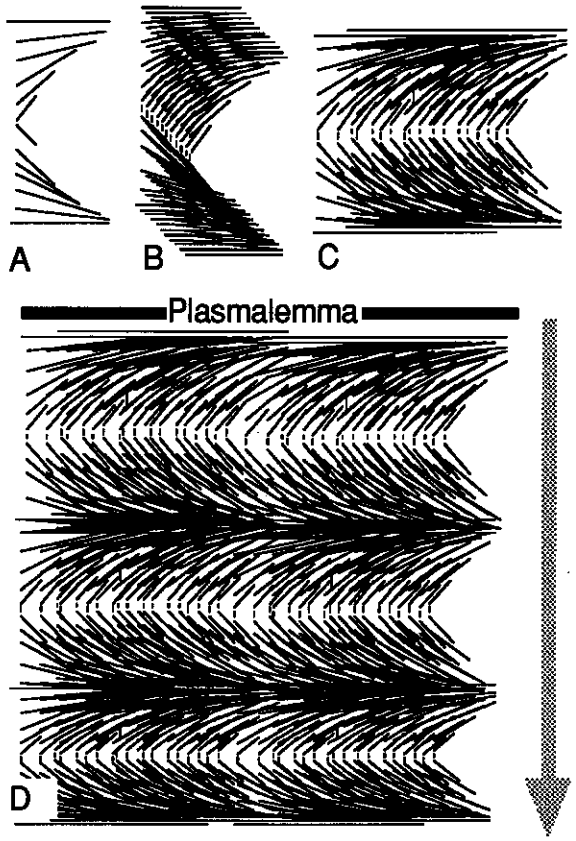


**Fig. 8.** Diagrammatic construction of the helicoidal pattern: (A) section of one arc with progressive rotation; (B) three-dimensional view of neighboring arcs; (C) nested arcs associated in a layer; (D) section of successive arcs assembled at the plasmalemma interface.

Submitted to shearing forces, the helicoids are stretched and a dramatic new molecular arrangement occurs. The primary cell wall construction is transient: When moving toward the base of the growth gradient and/or the outer part of the cell wall, the helicoidal texture changes and progressively vanishes. Identical gradients of destruction are seen on sections for different tissues (arrows, Fig.9A). In the older parts of the cell wall, the nested arcs become less clear and the layering disappears (Fig. 9B). In the course of growth, the cholesteric-like ordering is used and destroyed by the surface expansion (Fig. 9C). The cell wall becomes thinner, and when no more helical order is seen, growth ceases.

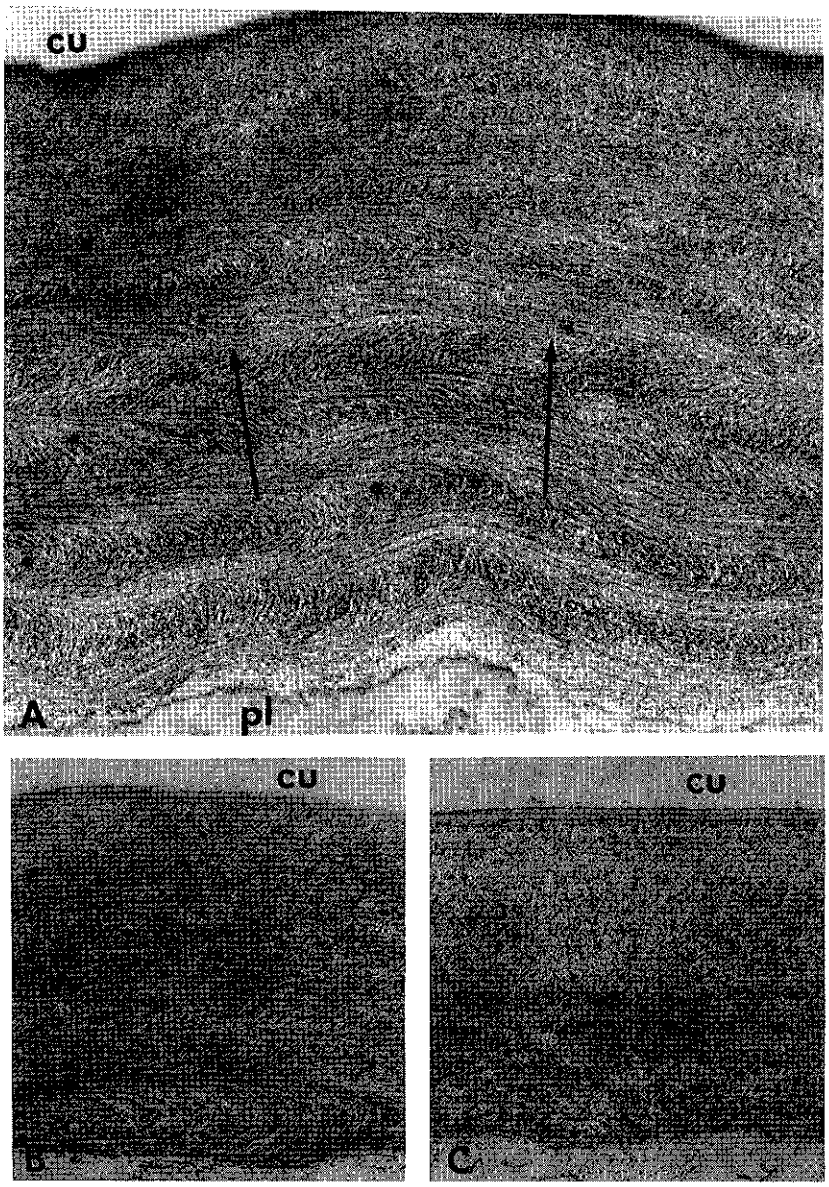


**Fig. 9.** Changes in epidermal cell wall ultrastructure along the growth gradient. (A) General view of the progressive change (arrows) from a helicoidal texture (recent) to a scattered texture (older and stretched). pl. plasmalemma; cu, cuticle. (B) The very end of the growth gradient (epidermis): thinning of the cell wall and dispersion of the last layer. (C) Complete dispersion after growth. (A, B) ×26,000 and (C) 32,000; reduced to 90% for reproduction.

## MECHANICAL PROPERTIES OF THE GROWING CELL WALL

It is usually difficult to study the mechanical properties of a growing cell wall of a living specimen. It is necessary to exclude cytoplasmic components to cancel out the action of the internal vacuolar pressure and use external tension as a substitute. Different procedures can be used to eliminate the cytoplasmic components and preserve cell wall microstructures. More often, the technique requires either hot methanol followed by the action of a pronase (Cleland, 1981), simple boiling in water, or freezing. According to the method used, the functional integrity of the cell wall microstructures is more or less preserved, especially the *in muro* proteins and enzymatic activities.

To study the rheological properties of biological materials, various methods can also be used (Prat and Paresys, 1987), for example, (1) measurement of the relaxation capacities of tissues under constant deformation [sequential stress/relaxation, developed mainly by the Japanese school (Yamamoto *et al.*, 1975)], (2) tension response of specimens under a cycle of tension/relaxation at a constant rate of deformation (Fig. 10) [improved by Cleland (1981, 1984)], and (3) simple measurement of deformation during a sequential tension/relaxation (Fig. 11). The latter, the easiest to perform, allows the distinction between an irreversible plastic (P) deformation and a reversible elastic (E) deformation, comparable to those observed in natural conditions for a living specimen (Fig. 3). In all cases, a decrease in the intrinsic wall plasticity is noticed when the cell walls are prepared from specimens whose growth has ceased (Fig. 10B).

From the deformation curves obtained under a constant load (Fig. 11A),

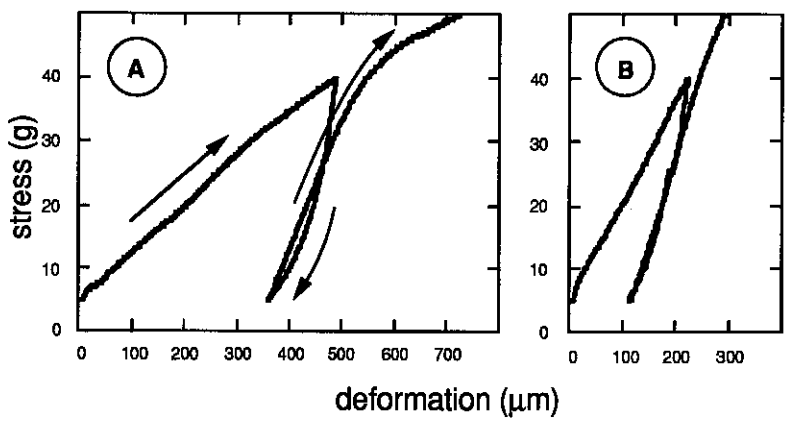


**Fig. 10.** Extensibility measurements at a constant rate of deformation of segments excised from the elongating zone (A) and nonelongating zone (B) of *Vigna radiata* hypocotyls. The segment is extended until a 40-g stress is reached, relaxed, then reextended until 50 g is reached. Arrows indicate the direction of the deformation.

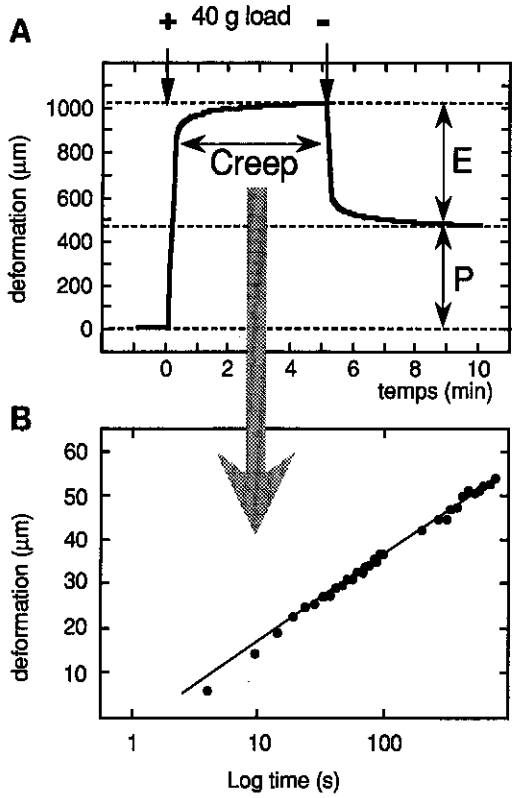


**Fig. 11.** Extensibility measurements under a constant load of a segment of the elongating zone of *Vigna radiata* hypocotyl. (A) Deformation after loading (+) then unloading (−). The force used is 40 g. P and E represent the plastic and elastic deformations. The creep represents the slow deformation under a constant load. (B) Creep plotted versus log time.

an immediate elasticity and a progressive plasticity can be distinguished. This low deformation, or creep, is the most comparable to the actual growth of a living specimen. However, its exponential shape (Fig. 11B) is significantly different from a growth curve obtained when the rate is steadily maintained.

An important part of the immediate elasticity is due not to the wall structures but to the alveolar (cellular) organization of plant tissues (Fig. 12) and has as a consequence, to produce reversible volume changes in relationship with external pressure changes. It seems that only the "low plasticity," or creep, can be correlated with the intrinsic properties of the cell wall structure.

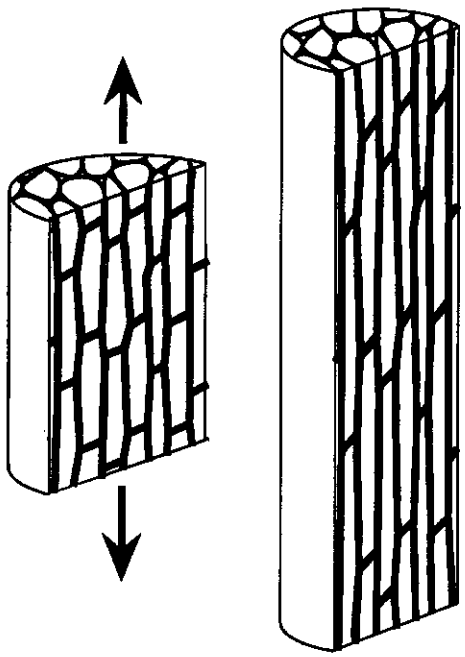

**Fig. 12.** Schematic behavior of a piece of tissue during longitudinal stress: A great part of the deformation is due to the elastic deformation of the cell wall network.

Among the main physiological factors regulating expansion, the mechanism of action of a growth hormone, auxin, is now the best known. It is generally considered that auxin has a first and short action via secretion of protons. This produces a lowering of pH within the wall compartment, which can be experimentally mimicked by the addition of an acid buffer to the incubating medium. Figure 13A shows the response of a living specimen: A pH of 5 highly and rapidly stimulates elongation. No significant response is noticed with a killed specimen under tension, at the same pH (Fig. 13B) (Rayle and Cleland, 1972; Prat, 1987). Only a lower pH (pH 3) produces a stimulation. The latter result is explained by a purely chemical process (ruptures of weak linkages), whereas the pH 5 stimulation requires the integrity of the cell structure and is probably of a physiological and biochemical nature. It is possible to check the point using, in the same experiment, specimens killed in different ways (Fig. 14). Specimens killed by methanol show no reaction for a moderately acid pH (pH 4.7); conversely, specimens simply frozen and thawed (in which the enzymatic activities are preserved) react rapidly.

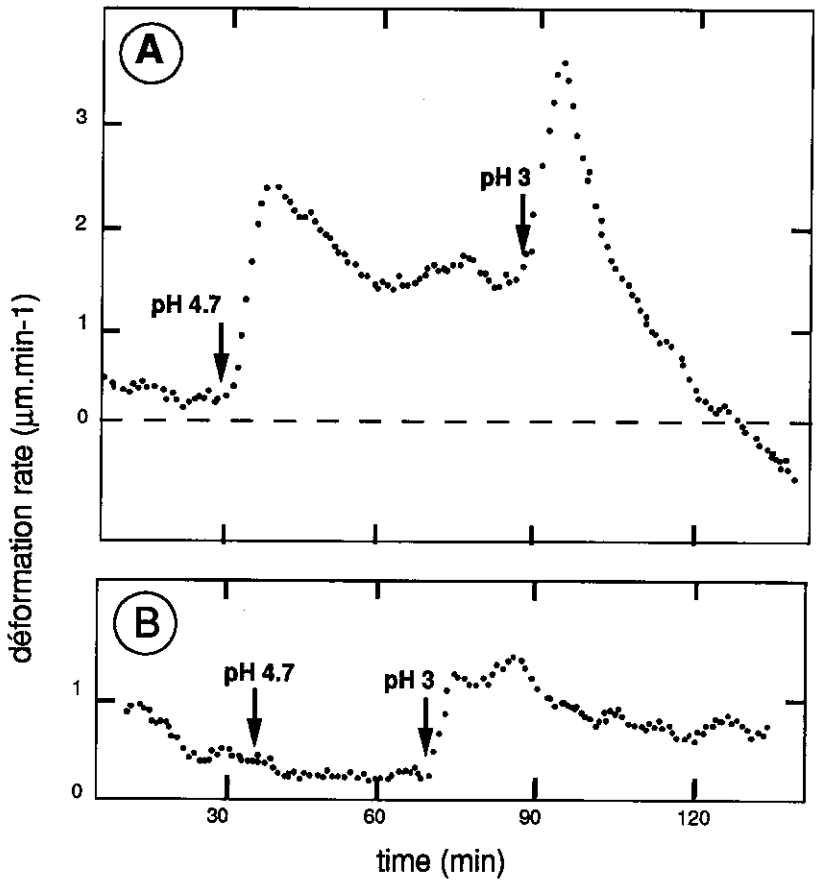


**Fig. 13.** Effect of low pH's on elongation of a living segment (A) and deformation under a constant load of a killed segment (B). The segments were excised from the elongating zone of *Vigna radiata* hypocotyls when cuticle was abraded with carborundum powder. In B, the segment was killed by boiling in methanol during 5 min. The segments were incubated with 5 m*M* phosphate buffer, pH 7.7. The medium was changed to phosphate buffer, pH 4.7 (first arrow), then to HCl solution, pH 3 (second arrow).

Numerous diagrams have been proposed for the supramolecular architecture of the growing wall. One of the last published (Carpita and Gibeaut, 1993), for example, shows with great accuracy the intermolecular relationship which allows the assembly of the network. It is now widely accepted that specific hemicelluloses (xyloglucans) play a major role in the cellulosic microfibril connection. Transglucosidases seem to be good candidates for the regulation of cell wall plasticity (Nishitani and Tominaga, 1991). Their optimum pH (acidic) agrees well with the role of low pH in growth stimulation. Numerous factors modulate

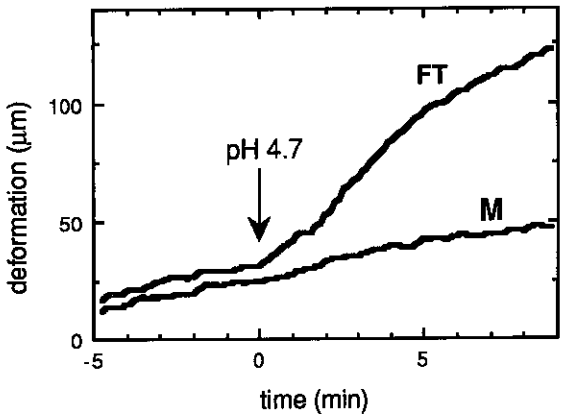


**Fig. 14.** Effect of preparation of killed segments on responses to low pH. The segments excised from the elongating zone were abraded with carborundum powder, then boiled for 5 min in methanol (M) or freeze-thawed (FT). The segments were incubated in 5 m*M* phosphate buffer, pH 7.7, then transferred (arrow) to phosphate buffer, pH 4.7.

the local intrawall pH, especially growth hormones, such as auxin, and specific wall enzymes, namely, pectinmethylesterases.

## CONCLUSION

The mechanical properties of the primary cell wall are the key features for the regulation of plant growth (Cosgrove, 1993). Knowledge of them is essential to understanding the successive events which interact in the course of the surface expansion (exponential increase, progressive decrease, and final cessation) of the cell wall. However, experimental measurement of these properties indicates only the immediate growth potentialities or, more precisely, the "immediate past wall extensibility" (Cleland, 1984) when the tissue was excised. The later properties will depend on the intrinsic potentialities of the wall but also on the actual regulating processes controlled by the cell biology: (a) synthesis and assembly of the wall components and (b) biochemical and enzymatic reactions interacting within the previously secreted components, which continuously change the positioned network.

It is nearly impossible to deduce the properties of one cell from the study of the whole specimen, for various reasons: (a) the cell number is very high (about $10^5$ cells in a 10 mm-long segment); (b) the size of associated cells in the course of growth is heterogeneous (diameter from 5 $\mu$m for procambial cells to 100 $\mu$m for pith cells); and (c) in a given cell, the wall is a sort of puzzle of microdomains, each with a different thickness, composition, and structure.

Experiment and structure are found to agree well with the so-specific behavior of the growing cell wall, associating dramatic surface expansion and supporting function. The cholesteric mesophase, owing to its short-lived multidirectional architecture, appears to be outstandingly important in controlling the mechanical efficiency of growing plant organs. However, numerous questions still need to be answered if we are to understand the detail of dispersion and randomization of the cellulosic network (Figs. 15 and 16). The risk of modeling is an oversimple explanation: The primary wall cannot be considered

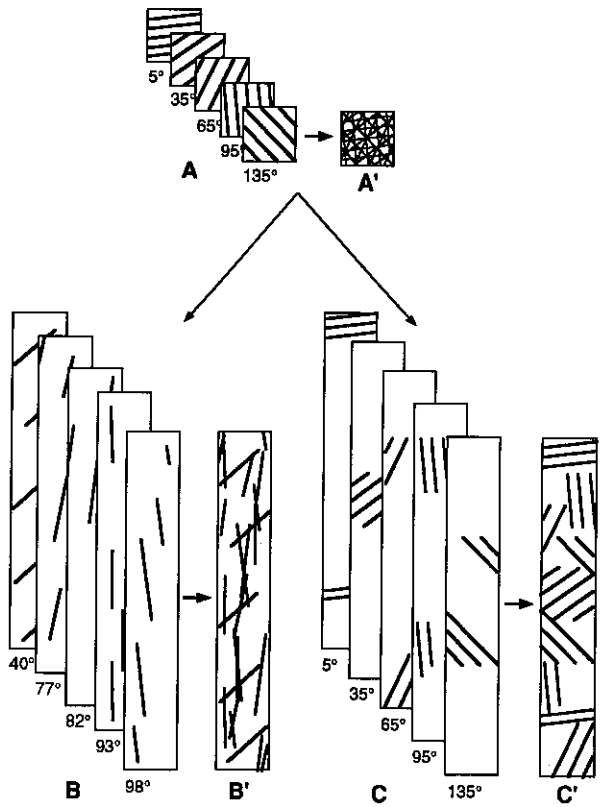


**Fig. 15.** Diagram of scattering and change in the cellulose microfibril density according to surface extension; two hypothesis concerning the behavior of the fibrils during growth process. (A) Fibril arrangements before growth in a three-dimensional model. (B, C) Fibril arrangements after growth (×5 in length): (B) first hypothesis—sliding and change of orientation of the fibrils according to expansion; (C) second hypothesis—microbeaks without sliding or reorientation. The orientation of the fibrils is indicated as degrees. (A', B', C') Superimposed views of A, B, and C layers.

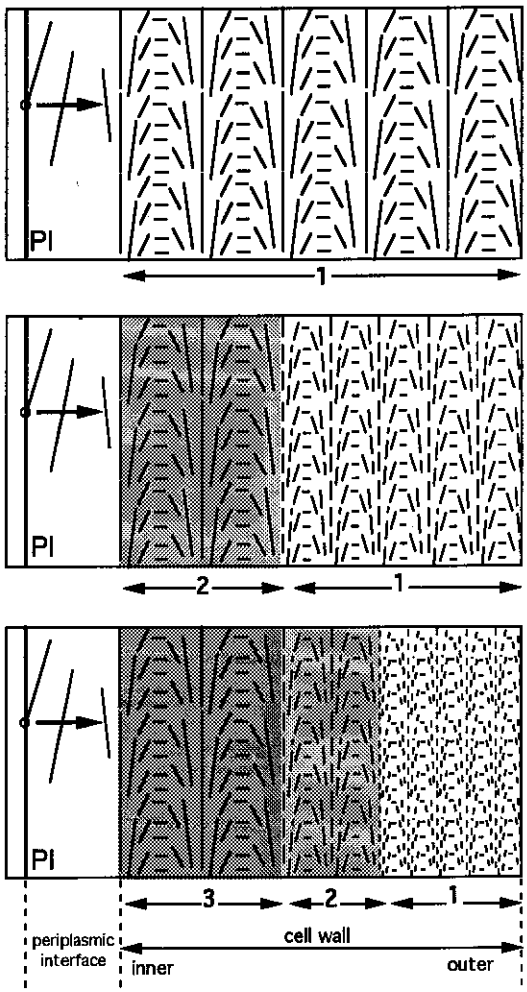


**Fig. 16.** Time change of the wall arced patterns during cell elongation. The fibrils of cellulose were synthesized by cellulose synthetase located in the plasmalemma (Pl). In the periplasmic interface, the fibrils were self-assembled in the inner layer of the cell wall. During the same time, the outer (former) layers of the cell wall were dispersed. An identical diagram is obtained according to the first or the second hypothesis described in the legend to Fig. 15.

as an ordinary composite material with physical preestablished properties; it is a specific biological compartment continuously renewed and locally modified.

## REFERENCES

Cleland, R. E. (1981). Wall Extensibility: Hormones and wall extension. In Tanner, W., and Loewus, F. A. (eds.), *Plant Carbohydrates. II. Extracellular Carbohydrates*, Springer Verlag, Berlin, pp. 255–269.

Cleland, R. E. (1984). The Instron technique as a measure of immediate-past wall extensibility. *Planta* **160:**514–520.

Cosgrove, D. J. (1993). How do plant cell walls extend? *Plant Physiol.* **102:**1–6.

Frey-Wyssling, A., and Mühlethaler, K. (1963). *Ultrastructural Plant Cytology*, Elsevier, Amsterdam.

Carpita, N. C., and Gibeaut, D. M. (1993). Structural models of primary cell walls in flowering plants: Consistency of molecular structure with the physical properties of the walls during growth. *Plant J.* **3:**1–30.

Neville, A. C. (1993). *Biology of Fibrous Composites. Development Beyond the Cell Membrane*, Cambridge University Press, Cambridge.

Nishitani, K., and Tominaga, R. (1991). In vitro molecular weight increase in xyloglucans by an apoplastic enzyme preparation from epicotyls of *Vigna angularis*. *Physiol, Plant.* **82:**490–497.

Prat, R. (1985). A comparative study of some methods for measuring cell growth potentials in *Vigna radiata* hypocotyls, *in situ* and after excision. *J. Exp. Bot.* **36:**1150–1158.

Prat, R. (1987). Interrelations between IAA- or $H^+$-induced cell elongation and cell wall extension in mung bean hypocotyl. *Plant Physiol. Biochem.* **25:**401–408.

Prat, R., and Paresys, G. (1987). Multiple use apparatus for cell wall extensibility and cell elongation studies. *Plant Physiol. Biochem.* **27:**955–962.

Prat, R., Vian, B., Reis, D., and Roland, J. C. (1977). Evolution of internal pressure, vacuolation and membrane flow, during cell growth in mung bean hypocotyl. *Biol. Cell.* **28:**269–280.

Rayle, D. L., and Cleland, R. E. (1972). The *in-vitro* acid-growth response: Relation to *in-vivo* growth responses and auxin action. *Planta* **104:**282–296.

Roland, J. D., Reis, D., and Vian, B. (1992). Liquid crystal order and turbulence in the planar twist of the growing plant cell wall. *Tissue Cell* **24:**335–345.

Silk, W. K. (1992). On the kinematics and dynamics of plant growth. In Karalis, T. K. (ed.), *Mechanics of Swelling*, Springer Verlag, Berlin Heidelberg, pp. 165–177.

Yamamoto, R., Kawamura, H., and Masuda, Y. (1975). Stress relaxation properties of the cell wall of growing intact plants. *Plant Cell Physiol.* **15:**1073–1082.

**Volume 2, Number 3** **September 1994**

Special Issue:
Plant Biomechanics Congress

BIMIEL 2(3) 193–282 (1994)
ISSN 1059-0153

# Biomimetics

PLENUM PRESS • New York and London

# Biomimetics

**Volume 2, Number 3** **September 1994**

## CONTENTS

**Special Issue: Plant Biomechanics Congress**
**Montpellier, France, September 5–9, 1994**

*Biomimetics, Vol. 2, No. 3, 1994*

# Morphogenesis and Training of Trees: Questions from Physiology to Biomechanics[1]

**Jacques Crabbé**[2]

*A review is presented with comments on the various effects on plants—particularly on trees—exerted by gravity, with or without other mechanical stress of different origin. Questions are raised about these phenomena, which would require collaboration with a biomechanical approach in order to improve the physiological understanding of the sequence of events from perception of the stimulus to growth response.*

**KEY WORDS:** trees; gravity stimulus; gravitropism; reaction wood; gravimorphism; plagiotropy.

Among the factors acting mechanically on self-sustaining, tall plants, such as trees, **gravity** is certainly the most prevalent and ubiquitous. While growing and ramifying, the tree constantly has to resist—through its growth processes—the constraints generated by the weight of its limbs. Other external factors (wind, rain, snow), of course, intervene, but mostly because they amplify the strain or change the direction of the resultant force. Incidentally a gust of wind may increase the lateral component force by bending a trunk or a branch—perfectly self-supporting at the start—and lead to its sudden buckling. Nevertheless, an analysis of the problems to bring together biomechanics and physiology must first consider the effects of gravity.

The different growth manifestations wherein a perception of gravity can be suspected are presented in Fig. 1 and its legend. These phenomena are essential to describe the architectural models of the trees (Troll, 1937; Rauh, 1939; Hallé *et al.*, 1978) and to understand the changes that they undergo in various circumstances. For example, many horticultural practices, such as staking of trunks,

[1]This is the published version of a paper presented at the Plant Biomechanics Congress, Montpellier, France, September 5-9, 1994.

[2]Faculté des Sciences agronomiques, Morphogenèse végétale appliquée, Avenue de la Faculté 2, B-5030 Gembloux, Belgium.



1059-0153/94/0900-0193$07.00/0 

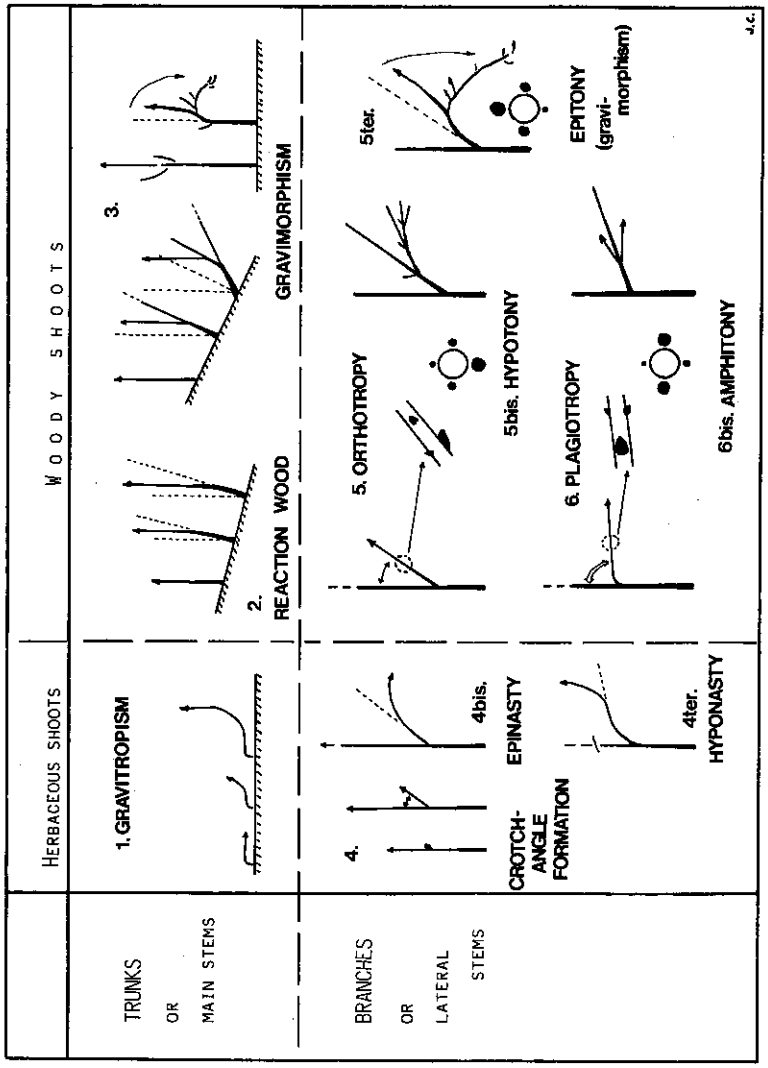
HERBACEOUS SHOOTS
WOODY SHOOTS
TRUNKS OR MAIN STEMS
BRANCHES OR LATERAL STEMS
1. GRAVITROPISM
2. REACTION WOOD
3. GRAVIMORPHISM
4.
4bis.
CROTCH-ANGLE FORMATION
EPINASTY
4ter.
HYPONASTY
5. ORTHOTROPY
5bis. HYPOTONY
5ter.
EPITONY (gravi-morphism)
6. PLAGIOTROPY
6bis. AMPHITONY

**Fig. 1. Diagrammatic representation of the various reactions of trunks and branches implying gravity perception. Trunks or main stems.** (1) *Gravitropism* is a primary growth reaction of herbaceous shoots, wherein the curvature results from an unequal distribution of growth factors (auxin), according to a still controversial theory (Firn and Digby, 1980; Wilkins, 1984). (2) *Reaction wood* contributes to putting the trunk upright again, when the tree is moderately or slowly tilted. The response occurs at the level of xylem differentiation (Wilson and Archer, 1977). (3) *Gravimorphism* consists of preferential outgrowth of upward-oriented lateral buds and happens in fast tilting (steep slope, river bank) or sharp bending (buckling through excess load, manual arching). This is discussed by Crabbé and Lakhoua (1978) and Crabbé (1987). **Branches or lateral stems**. (4) Young herbaceous shoots initially form a *crotch angle* due to intraangular pressure of tissues (Jankiewicz, 1964). Later they may curve upward—hyponasty (4ter), generally a gravitropic reaction—or downward—epinasty (4bis), often a prelude to plagiotropism. (5) *Orthotropy* is a nearly erect growth direction of an axis, except for the formerly established crotch angle. Its lateral buds or shoots sometimes show *hypotony* (5bis), a differential development favoring those at the lower side. The opposite reaction, *epitony* (5ter), appears in gravimorphism, i.e., when a branch is rapidly arched by hand or by its own weight. (6) *Plagiotropy* is a nearly horizontal growth direction of an axis, depending or not on a prevailing apical dominance. Often, lateral buds and shoots preferentially develop in a horizontal plane: *amphitony* (6bis). As far as the direction of growth is concerned, both orthotropy and plagiotropy require a balanced formation of reaction wood to maintain the direction (Fisher and Stevenson, 1981). Both also demand perception of gravity, only the translations of the stimulus in the proper response are different.

palisading, and bending of branches, disturb the plant's primary reactions to gravity and related factors.

From left to right, Fig. 1 shows an increasing gradient in complexity of the plant's response. In herbaceous shoots, the gravitropic reaction consists of a different rate of cell extension between the upper and the lower halves of the subapical growing zone of the organ. The current explanation, known as the Cholodny–Went hypothesis, requires a regulated asymmetrical distribution of growth factors, to a sufficient extent, through that zone: a situation which is thought doubtful in dicotyledonous shoots (Firn and Digby, 1980). In woody shoots anyway, such a direct growth curvature is no longer possible and different mechanisms are involved. As far as reaction wood formation is implied (upright bending of a trunk, maintenance of ortho- or plagiotropy in branches), the sequence of events from the perception of the gravity stimulus to the response may be short. On the other hand, when the reaction consists of differential bud formation and outgrowth, as in hypo- and epitony and gravimorphism, correlative influences between plant parts clearly play an essential role in its expression.

Our knowledge is still deficient and controversial about all of these phenomena. Superficial morphological descriptions and premature hormonal interpretations seem to be the main shortcomings. A correct approach would conform to the classical scheme used in the study of irritability phenomena and neglect none of its steps.

PERCEPTION of the stimulus (Where? How? Intensity?)
↓
TRANSDUCTION (Nature of the signal? Modes of production and transmission?)
↓
RECEPTION of the signal (Where? When? How is it translated?)
↓
RESPONSE (Where? When? How? Intensity?)

And somewhere a step of "memorization" or "fixation" would be inserted in the sequence, when a long time lapse occurs between perception and reaction, as demonstrated in gravimorphism (Crabbé and Lakhoua, 1978).

The level of **perception of the stimulus** is probably the one that needs a close collaboration between biomechanics and physiology. Most experimental approaches indicate the stem itself—and almost certainly living tissues within the stem—as the locus of perception. In woody shoots, the cambial zone and the ray parenchymas thus appear to be the possible candidates. It seems reasonable to point to the former, when reaction wood formation is the response, as this process is linked to xylem cell differentiation. But what about hypotony and gravimorphism, where differential bud formation and development are involved?

The very first questions to the biomechanician would consequently be: What are the strains appearing in normal and modified positions of the stem? and How do *both* candidates undergo these constraints? Further, according to the stiffness of the stem, its actual elongation and diameter growth, and the changes in the distribution of mass subsequent to growth, foliage development, and branching, how are these constraints modified by the mechanical stresses which may be added by spontaneous or artificial bending of the axis? In this respect, is the different response induced by slow or rapid tilting, i.e., reaction wood or gravimorphism, due only to a different intensity of the same stimuli or to a combination of gravity and flexion stresses, whose perceiving structures might be as different as their transduction and response mechanisms evidently are?

A correct and precise evaluation of the constraints and a precise identification of the affected anatomical structures represent the inescapable requirements for further progress in the physiology of these phenomena. First, the physiologist should be able properly to appreciate, in mechanical terms, the treatments that he is applying in his experiments. Further, on the basis of the strains laid upon possible sensor tissues, the next steps toward the response could be identified and described.

Finally, attention should be paid to the effects of staking or, generally speaking, of the suppression of tree swaying, perhaps the simplest of mechanical situations. Foresters (Larson, 1965) and horticulturists (Leiser *et al.*, 1972) have demonstrated that the absence of mechanical stress changes elongation and diameter growth and the shape of the trunk, and causes a significant decrease in flexion and buckling resistance (Barnola and Crabbé, 1993). It is thus evident that gravity and mechanical stress combined, however subtle their effects may be, are an essential but ill-recognized part of the plant's environment. They shape its architecture through many varied stimulus–response processes. Moreover, over many years, man has empirically learned to use them in order to tailor the plant to his needs. This would suffice to unite our skills to understand them better.

## REFERENCES

Barnola, P., and Crabbé, J. (1993). L'activité cambiale, composante active ou passive dans les réactions de croissance de l'arbre? *Acta Bot. Gallica* **140**(4):403–412.

Crabbé, J. (1987). *Aspects Particuliers de la Morphogenèse Caulinaire des Végétaux Ligneux et Introduction à Leur Étude Quantitative*, IRSIA, Bruxelles.

Crabbé, J., and Lakhoua, H. (1978). Arcure et gravimorphisme chez le pommier. Mise en évidence d'effets gravimorphiques sur bourgeons isolés. *Ann. Sci. Nat. Bot.* **19**(2):125–140.

Firn, R. D., and Digby, J. (1980). The establishment of tropic curvatures in plants. *Annu. Rev. Plant Physiol.* **31**:131–148.

Fisher, J. B., and Stevenson, J. W. (1981). Occurrence of reaction wood in branches of dicotyledons and its role in tree architecture. *Bot. Gaz.* **142**(1):82–95.

Hallé, F., Oldeman, R. A. A., and Tomlinson, B. P. (1978). *Tropical Trees and Forests. An Architectural Analysis*, Springer Verlag, Berlin.

Jankiewicz, L. S. (1964). Mechanism of the crotch angle formation in apple trees, I. *Acta Agrobot.* **15**:21–49.

Larson, P. R. (1965). Stem form of young *Larix* as influenced by wind and pruning. *Forest Sci.* **11**(4):412–424.

Leiser, A. T., Harris, R. W., Neel, P. L., Long, D., Stice, N. W., and Maire, R. G. (1972). Staking and pruning influence trunk development of young trees. *J. Am. Soc. Hort. Sci.* **97**(4):498–503.

Rauh, W. (1939). Ueber die Gesetzmässigkeit der Verzweigung und deren Bedeutung für die Wuchsformen der Pflanzen. *Mitt. Deutsch. Dendrol. Gesell.* **52**:81–111.

Troll, W. (1937). *Vergleichende Morphologie der höheren Pflanzen*, Bornträger, Berlin.

Wilkins, M. B. (1984). Gravitropism. In Wilkins, M. B. (ed.), *Advanced Plant Physiology*, Pitman, London, pp. 163–185.

Wilson, B. F., and Archer, R. R. (1977). Reaction wood: Induction and mechanical action. *Annu. Rev. Plant Physiol.* **28**:23–43.

*Biomimetics, Vol. 2, No. 3, 1994*

# Kinematics and Dynamics of Primary Growth[1]

**Wendy Kuhn Silk**[2]

*The spatial distribution of growth is reviewed in terms of growth trajectories and fields of displacement velocity and growth rate. A one-dimensional analysis has been suitable for many studies of roots, stems, and monocot leaves. To analyze growth in two dimensions, growth rate tensors and finite element methods have been used to show the direction and magnitude of the local growth rates. Natural coordinate systems have helped to analyze the growth of curved surfaces such as twining stems. A decade ago, thermodynamic considerations suggested the existence of a nonuniform water potential field in growing tissues. In recent years the water potential field for primary growth has been characterized by comparing the local growth rate to intracellular pressure and osmotic potential. For maize roots in solution culture, when growth is steady, the growth-sustaining influx of water appears to be driven by a radial gradient in osmotic potential.*

**KEY WORDS:** plant growth; kinematics; spatial patterns; water potential; root; *Zea mays*.

## INTRODUCTION: PLANT GROWTH AS FLUID FLOW

When seeds of broad-leaved plants germinate, the seedlings grow through the soil with a curved shape, a hook, which is thought to protect the apex from damage. After emergence from the soil, if the plant grows in dim light, the hook is maintained for many hours. As the seedling grows the hook can be said to migrate from the hypocotyl into the first and then the second internode. But from another perspective the shape of the hook can be seen to be steady, i.e., unchanging in time. The steady form is apparent in a moving reference frame

[1]This is the published version of a paper presented at the Plant Biomechanics Congress, Montpellier, France, September 5-9, 1994.

[2]Department of Land, Air, and Water Resources, Hoagland Hall, University of California, Davis, California 95616.



1059-0153/94/0900-0199$07.00/0 

attached to the plant apex: A plot of stem curvature vs distance from the plant apex does not change (Fig. 1). The steady form, however, is composed of changing elements. An epidermal hair appears to flow through the hook. Initially found near the shoot meristem, the hair will be observed later at the hook summit and then on the basal straight side of the hook. This observation tells us that the seedling hook is composed of a parade of tissue elements, each of which first curves and then straightens as it is displaced from the apical meristem during growth.

The situation of a form that is unchanging (or slowly changing) in time, and that is composed of elements that are experiencing rapid change, is reminiscent of fluid structures. And indeed, allusions to rivers, fountains, and the wakes of boats appear often in classical botanical literature. The seedling hook is a paradigm for primary growth in plants.

Another example is the root apex, which can be described in terms of regions of cell division, rapid cell expansion, and cell differentiation. These regions are formed by a procession of cellular tissue elements, which first grow slowly while producing new cell walls, then elongate rapidly and then differentiate. If one observes root development from an origin attached to the (moving) apex, tissue elements appear to flow through the standing pattern. In an analogous fashion, the shoot bears a succession of leaves of different developmental stages; during a plastochron (time to make a leaf), a leaf may grow to have the same size, shape, and biochemical composition as its distal neighbor as observed

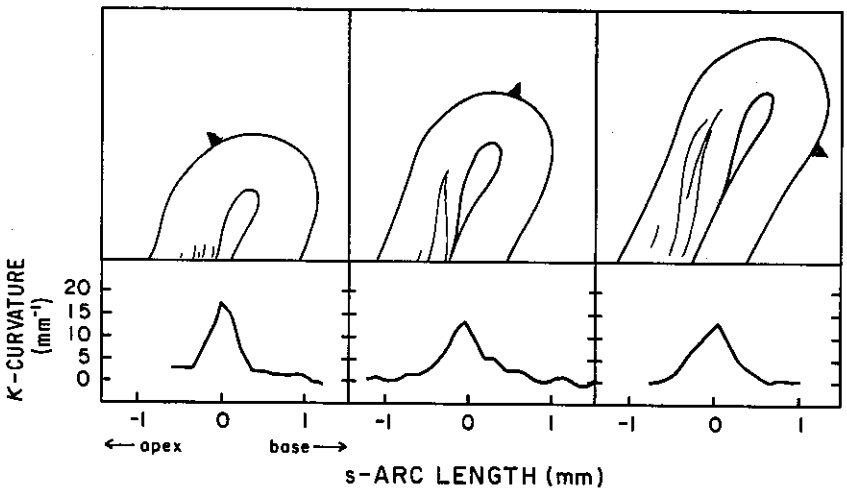


**Fig. 1.** Seedling hook, a steady structure composed of changing elements. The form (curvature distribution, bottom figures) is maintained over time, while constituent tissue elements first curve and then straighten as they are displaced from the seedling apex during growth. Thus a surface mark seems to flow through the hook. [From Silk (1984); reproduced with permission.]

at the beginning of the plastochron. Shoot form also is produced by a parade of changing tissue elements.

The analogy between primary growth and fluid flow suggests the use of concepts and numerical methods from fluid dynamics to solve problems in plant development. The distinction between Eulerian (spatial or site-specific) and Lagrangian (material or cell particle-specific) specifications of developmental variables is important for understanding plant development (Green, 1976; Silk and Erickson, 1979; Gandar, 1980). And evaluation of local, convective and material derivatives is necessary for calculating rates of change in growing tissue (Silk and Erickson, 1979; Gandar, 1980, 1983). An especially important application is the characterization of growth (volumetric expansion) itself.

## SPECIFICATION OF THE GROWTH FIELD IN ONE DIMENSION

Historically, botanists have observed that primary growth is confined to apical regions of roots and shoots. Marks placed near an apex move away from the soil surface and also separate from each other. Marks placed far from the apex do not separate from each other, although they are found progressively farther from the growing apex. One way of specifying growth is to plot the position of cellular particles, or applied marks, versus time (Fig. 2, top). The resulting "pathline" (Gandar, 1983) or "growth trajectory" (Silk and Wagner, 1980; Hejnowicz, 1984) is a material specification of growth, because a real or material particle is followed. If distance is measured from the apex, the slope of the growth trajectory increases monotonically from small values near the apex to a constant value at the base of the growth zone. To characterize the growth pattern, a family of curves can be obtained to show growth trajectories of particles at different initial positions.

Another useful way to describe growth is with a velocity field, $v(z)$ (Erickson and Sax, 1956). This is a spatial, or Eulerian, specification of growth because it involves the movements of many particles found instantaneously at different locations. The velocity field increases monotonically with position, because progressively more expanding tissue is found between the origin and the point of interest (Fig. 2, center). At the base of the growth zone, where expansion is no longer occurring, the growth velocity acquires a uniform value equal to the elongation rate of the organ. In the maize root, individual particles accelerate to a growth velocity (rate of displacement from the apex) of 3.1 mm $h^{-1}$. The velocity field can be calculated from short-term marking experiments. The velocity field is used in some important physiological applications, including calculation of biosynthesis rates and material derivatives in growing tissue (Silk and Erickson, 1979; Gandar, 1980).

For the physiologist, the most useful growth descriptor is probably the relative elemental growth (REG) rate (Erickson and Sax, 1956), which engineers

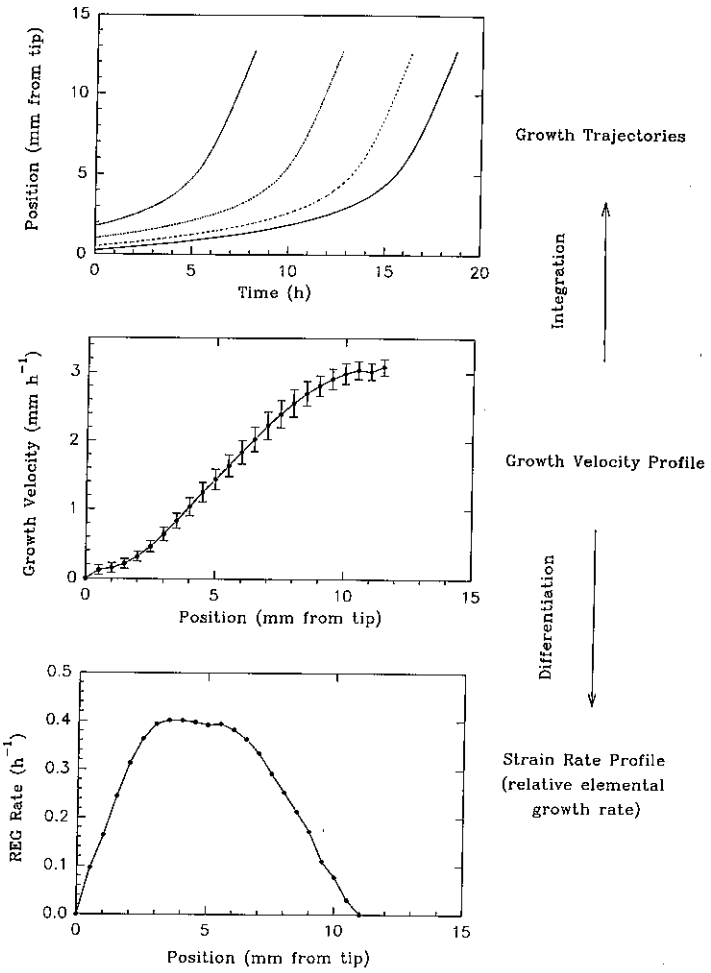


**Fig. 2.** Kinematics of growth of the primary root of *Zea mays*. These figures were obtained by computer-assisted analysis of time-lapse marking experiments. Top: Growth trajectories. The growth trajectory is a fate map and can be used with data on spatial distributions of developmental variables to find the time course of these variables. Middle: Growth velocity field. Growth velocity is used to calculate rates of change in expanding tissue. Bottom: Relative elemental growth rate. For the physiologist, this curve is the best way to localize growth.

call the growth strain rate. In one dimension, the REG rate, $r$ is the velocity gradient; mathematically, $r = \partial v/\partial z$. If care is taken to choose appropriate spatial and temporal scales, the REG rate field can be evaluated from measurement of the separation of applied marks (Erickson and Silk, 1980). This field

shows quantitatively the location and magnitude of growth within the organ. In the maize root, for example, growth can occur over a length of 11 mm (Fig. 2, bottom). The REG rate maximum, 0.42 $h^{-1}$, is found 4 mm from the apex. In contrast, a vine stem may have a smaller REG rate of 0.02 $h^{-1}$ distributed over a longer, 200-mm region to give a similar axis extension rate of 2 mm $h^{-1}$ (Silk and Haidar, 1986).

The effect of environmental variation on growth can be quantitatively described with the REG rate field. We know, for instance, that a decline in temperature causes a decrease in the growth rate almost uniformly throughout the growth zone of the maize root (Pahlavanian and Silk, 1988). In contrast, water stress does not affect the REG rate in the apical 3 mm of the maize root but causes elongation to cease in the basal half of the growth zone (Sharp *et al.*, 1988).

A one-dimensional analysis is also suitable for the growth of some gramineous leaves. In recent years, studies of monocot leaves have revealed growth patterns in important crop and pasture species and the effects of environmental and genetic variation on the spatial and temporal distribution of growth rate (Schnyder *et al.*, 1987; Schnyder and Nelson, 1989; Paolillo and Sorrels, 1992; Meiri *et al.*, 1992; Bernstein *et al.*, 1993).

## SPECIFICATION OF THE GROWTH FIELD IN TWO DIMENSIONS

### Strain Rate and Vorticity Tensors

Expansion patterns of many leaves and apices can be described with a two-dimensional analysis (Richards and Kavanagh, 1943; Erickson, 1966). The early leaf growth analyses have been shown to be closely related to strain rate tensors of classical fluid dynamics (Silk and Erickson, 1979). The magnitude and direction of growth can be quantified by growth rate tensors, and change in element orientation can be characterized by the vorticity vector. Both growth rate and vorticity are obtained from the velocity field in two dimensions. The growth rate tensor is visualized as the rate at which circles placed on the leaf are deforming into slightly larger ellipses. The length of the axis of the ellipse in a particular direction gives the relative growth rate in that direction; the maximum and minimum relative growth rates are represented by the major and minor axes of the ellipse. Relative area expansion is given by the difference in area between the ellipse and the circle. The vorticity is the rate of rotation (as radians per unit time) and can be considered a measure of the change of orientation experienced by the elements.

## Finite-Element Methods

In the past decade, finite-element computational methods have been developed to reveal the expansion pattern from "landmarks" or material points on the surface of the growing tissue. In analyzing growth of grape leaves, Wolf *et al.* (1986) identified vein intersections as material elements on the leaf surface. Cartesian coordinates for each element were digitized in a sequence of photographs of the growing leaf. Particle pathlines were plotted in two dimensions. Using the vein intersections as vertices, Wolf *et al.* also triangulated the leaf surface and used finite-element formulae to find the local area growth rates; the deformation of each element was completely specified. Their analysis considered some numerical problems that arise in the measurement of large deformations. In particular, the "relative growth rate," $k1 = \partial A/A\ \partial t$, becomes larger than the "exponential growth rate," $k2 = \partial \ln A/\partial t$, when $\partial A/A$ becomes larger than 0.1, i.e., when the element area increases by more than 10% during the observation period. Wolf *et al.* point out that in the literature the methods giving the "divergence of velocity" or "relative elemental growth rate" give numbers close in value to $k2$. However, trends in growth rate and effects of environmental variation are more easily detected with the more sensitive measure, $k1$.

Goodall and Green (1986) introduced several improvements for characterizing the REG rate tensor. They decomposed growth strains into components that yield canonical parameters to characterize the local growth pattern. Like Wolf *et al.*, they avoided Eulerian (site-specific) velocity fields and worked directly with elements bounded by identifiable landmarks. Their method is a regression technique and has the advantage of giving error estimates as well as best-fit values for directionality of the local expansion. The computation methods of Goodall and Green are proving powerful tools for studies of mechanics of morphogenesis. Used with nondestructive cellular imaging techniques involving SEM of casts of growing apices (Williams, 1991), the numerical methods gave quantitative descriptions of leaf formation (Tiwari and Green, 1991) and the morphogenesis of floral apices (Hernandez *et al.*, 1991). These kinematic analyses are also providing the foundation for analysis of the mechanics of apical morphogenesis (Selker *et al.*, 1992).

## Natural Coordinates

Hejnowicz and colleagues (e.g., Hejnowicz and Karczewski, 1993) have introduced two-dimensional analyses using natural coordinates. The periclines, lines formed by cell files in apices of roots and shoots, are hypothesized to correspond to the particle pathlines during growth. The periclines are also assumed to lie along the principal directions of growth. Hejnowicz and colleagues fit analytical functions to the periclines and use tensorial expressions to calculate the fields of velocity and growth rate. These studies have shown some interesting

properties of apical growth. For instance, as a consequence of minimizing shear during growth, the lines of equal displacement velocity prove to be orthogonal to the particle pathlines.

The analysis of twining growth was also facilitated by the use of a natural coordinate system (Silk, 1989). Twining plants have a growth rate pattern that maintains a corkscrew-shaped form. The twining stem was modeled as a tube surrounding a helix $\alpha$. Position vectors to points in the stem were given in terms of $\alpha$, the Frenet vectors, and the natural coordinates $s$ representing arc length along the helix; $\phi$, angular displacement from the unit normal; and $r$, distance along the radius of the tube (Fig. 3, top). Using growth velocities measured along the helix (Silk and Haidar, 1986), a form of the strain rate tensor was calculated for the curvilinear, nonorthogonal, natural coordinate system, and the elongation rates were found for line elements in the twining stem (Fig. 3, bottom). For stems such as *Pharbitis nil*, which twine clockwise and simultaneously twist counterclockwise about their stem axis, the growth rate maximum occurs on the bottom surface of the stem.

## DYNAMICS OF GROWTH

While the REG rate field, described above, provides the kinematic basis for growth analysis, an understanding of growth in biomechanical terms must also involve growth dynamics, i.e., the study of the forces and energies involved in producing the observed spatial and temporal expansion patterns. The plant cell is typically 85% water; and, to a first approximation, local volume increase is caused by a local water influx. The driving force for growth is thought to be the gradient in water potential, i.e., the gradient in the chemical potential energy of water in the tissue.

Empirically, the cell growth rate has been shown to depend on the extensibility of the wall and the difference between the turgor pressure and some yield stress of the wall. The mechanics of cell wall expansion is an extensively studied topic. Other contributors to this symposium are reviewing work on mechanical properties of cell walls, on the development of new analytical chemical techniques to understand the structure of the growing wall, and on recent mechanical models for tissue expansion. An understanding of the role of water potential is also important for growth dynamics. Here I review the theory and empirical measurements of growth-sustaining water potentials in multicellular tissues.

### Equation for Growth-Sustaining Water Potential

To find the relationship between REG rate and water potential, $\psi_i$, one must consider the growth velocity, $\underset{\sim}{u}$ of the moving tissue element as well as the flux $\underset{\sim}{j}$ (volumetric flow rate per unit cross-sectional area) of the water move-

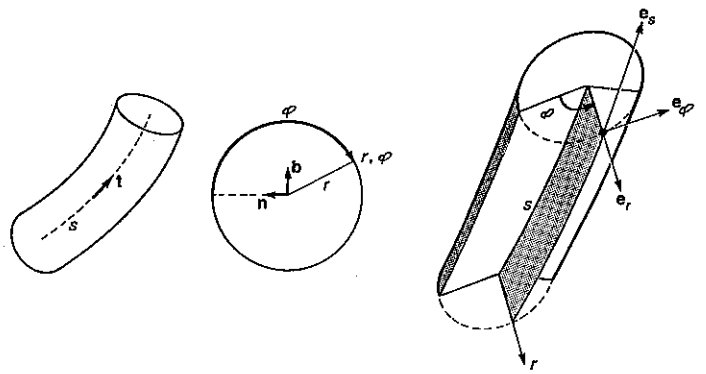


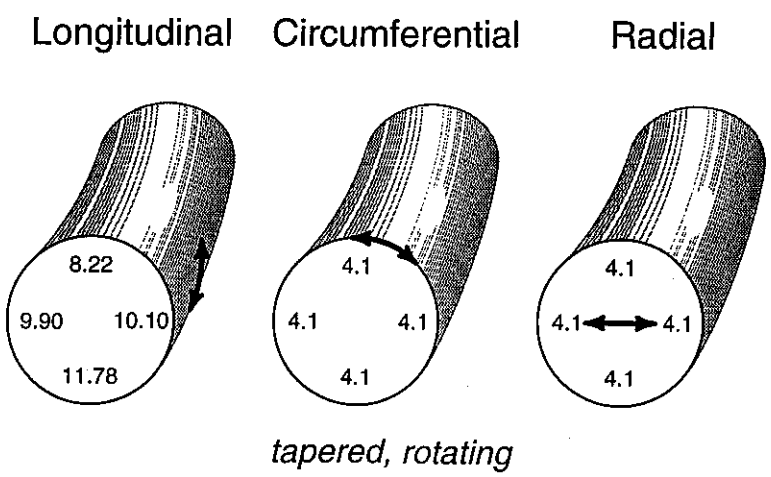


**Fig. 3.** Top: Natural coordinate system for twining growth. The curvilinear coordinate $s$ is distance along the central helix $\alpha$ (left). The Frenet vectors **t**, **n**, and **b** vary with $s$; and the coordinates $\phi$ and $r$ are defined in terms of the Frenet trihedron (middle). Surfaces can be visualized corresponding to constant values of the natural coordinates (right). [Redrawn from Silk (1989); with permission.] Bottom: Growth rate patterns that produce twining in a tapered stem that is twisting counterclockwise about **t**. The numbers give the elongation rates of lines, initially 0.5 mm, long drawn on the surface in a longitudinal (left) or circumferential (middle) directions or along the radius in the normal plane (right). Rates are microns per hour. The growth rate maximum occurs on the lower surface. [Drawings from Silk (1989); reproduced with permission.]

ment, for only water that is moving faster than the growing element will cross the element boundary to enlarge the cell (Silk and Wagner, 1980). In symbols,

$$\int_s (\underset{\sim}{j} - \underset{\sim}{u}) \cdot \underset{\sim}{n}\, dS = \int_s -(\underset{\approx}{K} \cdot \nabla\psi) \cdot \underset{\sim}{n}\, dS \tag{1}$$

Flux across surface = conductivity · driving force

where $\underset{\sim}{n}$ represents the unit normal to the surface, $S$, $\psi$ is the water potential, and $\underset{\approx}{K}$ is the hydraulic conductivity tensor. Then by the divergence theorem,

$$\int_v \nabla \cdot (\underset{\sim}{j} - \underset{\sim}{u})\, dV = \int_v \nabla \cdot (-\underset{\approx}{K} \cdot \nabla\psi)\, dV \tag{2}$$

Since water is largely incompressible,

$$\nabla \cdot \underset{\sim}{j} \approx O \tag{3}$$

And we find that the fundamental relationship between growth at a point and water potential at a point in an expanding continuum is given by

$$L = \nabla \cdot (\underset{\approx}{K} \cdot \nabla\psi) \tag{4}$$

where $L = (\nabla \cdot \underset{\sim}{u})$ is recognized as the REG rate.

### Simplified Versions of Eq. (4)

Some simplifying assumptions make Eq. (4) more tractable. For the maize root, one can assume that the tissue is cylindrical, with radius $r$, and growing only in the direction of its long axis. The distribution of $\psi$ is axially symmetric. The growth pattern is steady, so that the equation may be treated as a time-independent problem with coordinate origin at the root tip. It is recognized that the frame of reference is moving at constant velocity and that one is solving for spatial values of $\psi$. Conductivities in the radial ($K_r$) and longitudinal ($K_z$) directions are independent so that radial flow is not modified by longitudinal flow. The boundary condition is to assume that the root is not transpiring and is growing in pure water or saturated air, i.e., $\psi = 0$ in the nongrowing region and outside the root. If these assumptions are made, then Eq. (4) becomes

$$K_z \frac{\partial^2\psi}{\partial z^2} + K_r \frac{\partial}{\partial r}\left(r \frac{\partial\psi}{\partial r}\right) + \frac{\partial K_z}{\partial z} + \frac{\partial\psi}{\partial z} + \frac{\partial K_r}{\partial r}\frac{\partial\psi}{\partial r} = L(z) \tag{4A}$$

Equation (4A) implies that if the spatial distributions of REG rate and hydraulic conductivity are known, the growth-sustaining distributions of $\psi$ can, in theory, be calculated. As implied in the section on growth kinematics, the REG rate distribution has long been known (e.g., Erickson and Sax, 1956). Good empirical data on radial and longitudinal hydraulic conductivities are es-

sential for solution of Eq. (4) and evaluation of the growth-sustaining $\psi$ field. However, measurements of hydraulic conductivity in the growing regions of maize roots have taken longer to achieve.

## Estimates for Hydraulic Conductivity

A mathematically rigorous analysis of water transport in a growing root, properly accounting for tissue geometry, is lacking in the literature. Nevertheless, several different experimental and numerical approaches seem to be yielding estimates of the same order of magnitude for hydraulic conductivity through cortical cells. Radial transport of water through the nongrowing cortex of maize roots (30–70 mm from the tip) was measured by Ginzburg and Ginsburg (1970). Correcting their value of conductivity ($1.2 \times 10^{-7}$ m $MPa^{-1}$ $s^{-1}$) for the radial geometry of the root, one obtains $7.3 \times 10^{-11}$ $m^2$ $MPa^{-1}$ $s^{-1}$. This value is just a bit lower than the estimate of $1\text{–}5 \times 10^{-10}$ $m^2$ $MPa^{-1}$ $s^{-1}$ calculated by Bret-Harte and Silk (1994) assuming a modified Hagen–Poiseuille law with recent estimates for size and frequency of plasmodesmatal pores. From timing of turgor transients in growing regions of maize roots subjected to osmotic shock, Frensch and Hsiao (1994a) have calculated $1.3 \times 10^{-10}$ $m^2$ $MPa^{-1}$ $s^{-1}$. It is interesting that these estimates for hydraulic conductivity of maize root cortex, expressed per unit of cell length, have the same order of magnitude as the hydraulic conductivities reported for growing pea stem cortical cells (Cosgrove and Steudle, 1981) and *Kalanchoe* leaf mesophyll cells (Steudle *et al.*, 1980) from the timing of transient water influx or efflux induced by pressure perturbations.

## Solutions to the Simplified Water Potential Equation

It is instructive to consider two different sets of assumptions regarding hydraulic conductivity. Silk and Wagner (1980) assumed that longitudinal and radial conductivities are of a similar magnitude. The geometry of the maize root then determines that most of the growth-sustaining water flux is radial.

The growth-sustaining $\psi$ field, calculated from Eq. (4A) and assuming isotropic, uniform hydraulic conductivity of $1.3 \times 10^{-10}$ $m^2$ $MPa^{-1}$ $s^{-1}$ and the REG rate distribution of Erickson and Sax, is shown in Fig. 4A. The magnitude of $\psi$ increases with distance from the bounding water source and also parallels the strain rate to produce egg-shaped water potential shells. Individual tissue elements are displaced through the standing pattern and experience a decrease and then an increase in $\psi$ as they approach the nongrowing region. The solutions imply a small water potential differential, of the order of 0.04 MPa, sustains the maximum REG rate.

It is also interesting to consider the possibility that growth-sustaining water flux is longitudinal, with water flowing acropetally from the nongrowing region

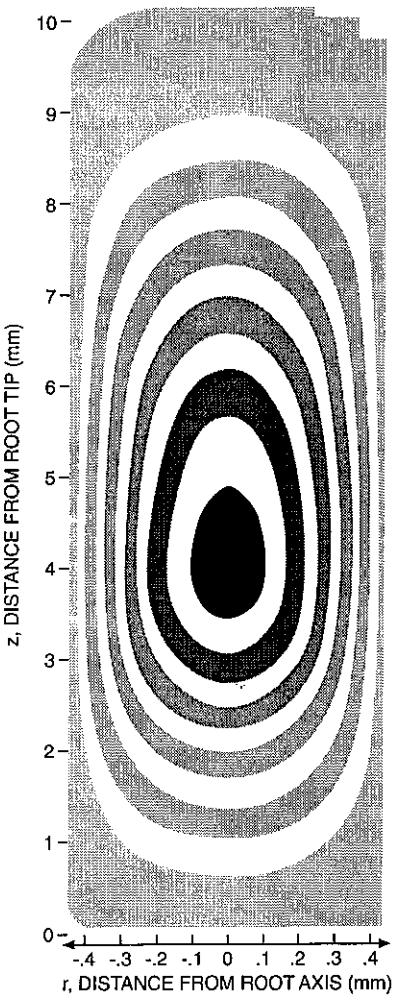


**Fig. 4A.** Contour map shows the distribution of $\psi$ in a longisection of the growth zone of the maize root. The root is presumed to be growing in pure water ($\psi = 0$) without transpiration. Hydraulic conductivity is assumed isotropic. The darkest region in the center has $-\psi = 4 \times 10^{-2}$ MPa, and water potentials become progressively less negative with distance from the root center and with decreasing growth rate. Current estimates for hydraulic activity are used with the solution (in terms of $K\psi$) shown by Silk and Wagner (1980).

of the root. This could happen if radial hydraulic conductivity is negligible. Then a one- dimensional version of Eq. (4) can be obtained by integration:

$$\int v\, dz = A + Bz - K_z\psi \tag{4B}$$

One can solve for $\psi$ by numerical integration of the empirically determined velocity field. The growth-sustaining $\psi$ field under these assumptions is shown in Fig. 4B. Water potential becomes less negative with distance from the apex. The solutions are not physically reasonable. Even if longitudinal flow were

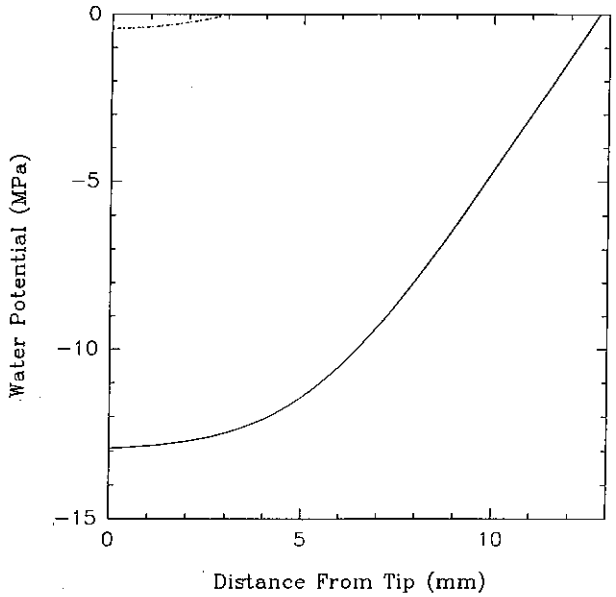


**Fig. 4B.** Growth-sustaining $\psi$ field under the assumption that water flux is longitudinal. The graph shows the growth-sustaining water potential if the longitudinal hydraulic conductivity is high, $5 \times 10^{-10}$ $m^2$ $MPa^{-1}$ $s^{-1}$, and the radial conducitivity is negligible. Water potential becomes less negative with distance from the apex. The solution is not physically reasonable, especially if flux is longitudinal throughout the growth zone (solid line), and even if flux is longitudinal only through the meristem (dashed line).

required only to sustain meristematic growth, the required differential water potential of −0.4 MPa is considerably greater than any observed pattern in the root tip. Thus growth-sustaining water flux must be mostly radial.

## Components of Growth-Sustaining $\psi$

Solutions of Eq. (4) displayed in Fig. 4A show the spatial pattern of growth-sustaining water potential in the maize root. For the physiologist the puzzle is then to find the components of water potential that are providing the driving force. According to conventional theory, the possible components are turgor pressure and osmotic potential.

In the past 5 years, improvements in technology—refinement of the pressure probe—have resolved spatial patterns of turgor pressure within growing regions. We now know the turgor pressure distribution within the growth zone of the maize root during steady growth (Spollen and Sharp, 1991; Rygol *et al.*, 1993; Pritchard and Tomos, this symposium) and in response to perturbations in water

potential (Frensch and Hsiao, 1994a, b). The turgor pressure distribution appears to be fairly uniform during steady growth, although slightly higher pressures can sometimes be detected in the root center and at the tip of the growth zone. Thus the distribution of turgor potential would not drive a growth-sustaining influx of water.

There is no evidence for a growth-sustaining longitudinal gradient in solute potential (Silk *et al.*, 1986; Sharp *et al.*, 1990). Thus the prime candidate for the growth-sustaining water potential gradient is a radial gradient in solute potential. In recent years, improvement in technology—use of the nanoliter osmometer—has also permitted measurement of this putative gradient. Rygol *et al.* (1993) recently showed that, at least in roots of transpiring plants, the osmotic potential decreases with distance from the root surface. Frensch and Hsiao (1994a) also interpret their pressure probe studies in support of this hypothesis. They find that when a root is immersed in a medium of low solute potential, the half-time for turgor reequilibration increases with distance from the root center. They believe that the restoration of turgor depends on solute transport into the cells, and the solute concentration increases fastest in the region closest to the phloem. These empirical studies are at least consistent with the hypothesis that a radial gradient in solute potential drives the growth-sustaining flux of water from the bathing medium into the root center.

Not all empirical evidence is consistent with the hypothesis described above. In a nontranspiring plant, 7 mm from the root tip, solute potential was found to be uniform across the root cortex (Rygol *et al.*, 1993). A likely explanation is that this region, especially in solution culture, was not growing rapidly. Or hydraulic conductivity may be at the high end of the estimated range, so that the growth-sustaining water potential is not empirically detectable. On the other hand, Nonami and Boyer (1993) found strong evidence for growth-sustaining solute gradients in the soybean hypocotyl. In this stem tissue, water is supplied from the xylem centripetally to the pith cells and centrifugally to the cortex. Using a nanoliter osmometer, Nonami and Boyer found that solute potential is least negative in the xylem and decreases in both directions from the water supply, as required by the theory. (The term "growth-sustaining water potential" used here is similar to the "growth-induced water potential" described by Boyer and colleagues. My choice of terminology is intended to beg the question of cause and effect.) The association of sucrose import with stem growth (Schmalstig and Cosgrove, 1990) is also consistent with an important role for solute potential in sustaining growth.

## CONCLUSION

More than a decade ago, theoretical studies predicted the shape of the field of water potential that sustains longitudinal growth (Molz and Boyer, 1978; Silk and Wagner, 1980). The tissue was considered to be a noncompartmented con-

tinuum in steady-state growth. The analyses considered the thermodynamic basis for growth and did not address the coupling to mechanical extensibility.

Measurement of the fields of turgor and solute potential in growing organs, at least for roots growing in aqueous solution, is now possible. Thus the water relations of root growth can empirically characterized with current technology, and a comprehensive theory seems achievable. Some mathematically rigorous analysis is needed to characterize rates of water transport in an appropriate geometry for the growing region. For the maize root in solution culture, growth-sustaining water flux appears to be mostly radial and driven by a radial gradient in solute potential.

## ACKNOWLEDGMENTS

The author's research is supported by Grant 92-37100-7625 from the United States Department of Agriculture.

## REFERENCES

Bernstein, N., Silk, W. K., and Läuchli, A. (1993). Growth and development of sorghum leaves under conditions of NaCl stress–spatial and temporal aspects of leaf growth inhibition. *Planta* **191**:433–439.

Bret-Harte, M. S., and Silk, W. K. (1994). Nonvascular, symplasmic diffusion of sucrose cannot supply the carbon demands of growth in the primary root tip of *Zea mays*. *Plant Physiol* **105**:19–33.

Cosgrove, D. J., and Steudle, E. (1981). Water relations of growing pea epicotyl segments. *Planta* **153**:343–350.

Erickson, R. O. (1966). Relative elemental rates and anisotropy of growth in area: A computer programme. *J. Exp. Bot.* **17**:390–403.

Erickson, R. O., and Sax, K. B. (1956). Elemental growth rate of the primary root of *Zea mays*. *Proc. Am. Phil. Soc.* **100**:487–498.

Erickson, R. O., and Silk, W. K. (1980). The kinematics of plant growth. *Sci. Am.* **242**:134–151.

Frensch, J., and Hsiao, T. C. (1994a). Transient responses of cell turgor and growth of maize roots as affected by changes in water potential. *Plant Physiol.* **104**:247–254.

Frensch, J., and Hsiao, T. C. (1994b). Rapid response of the yield threshold and turgor regulation during adjustment of root growth to water stress in *Zea mays* (submitted for publication).

Gandar, P. W. (1980). The analysis of growth and cell production in root apices. *Bot. Gaz.* **141**:131–138.

Gandar, P. W. (1983). Growth in root apices. I. The kinematic description of growth. *Bot. Gaz.* **144**:1–10.

Ginzburg, H., and Ginsburg, B. Z. (1970). Radial water and solute flows in roots of *Zea mays*. I. Water flow. *J. Exp. Bot.* **21**:580–592.

Goodall, C. R., and Green, P. B. (1986). Quantitative analysis of surface growth. *Bot. Gaz.* **147**:1–15.

Green, P. B. (1976). Growth and cell pattern formation on an axis. Critique of concepts, terminology and modes of study. *Bot. Gaz.* **137**:187–202.

Hejnowicz, Z. (1984). Trajectories of principal directions of growth, natural coordinate system in growing plant organ. *Acta. Soc. Bot. Polon.* **53**:29–42.

Hejnowicz, Z., and Karczewski, J. (1993). Modeling of meristematic growth of root apices in a natural coordinate system. *Am. J. Bot.* **80**:309–315.

Hernandez, L. F., Havelange, A., Bernier, G., and Green, P. B. (1991). Growth behavior of single

epidermal cells during flower formation-sequential scanning electron micrographs provide kinematic patterns for *Anagallis*. *Planta* **185**:139–147.

Meiri, A., Silk, W. K., and Laeuchli, A. (1992). Growth and deposition of inorganic nutrient elements in developing leaves of *Zea mays* L. *Plant Physiol.* **99**:972–978.

Molz, F. J., and Boyer, J. S. (1978). Growth induced water potentials in plant cells and tissues. *Plant Physiol.* **62**:423–429.

Nonami, H., and Boyer, J. (1993). Direct demonstration of a growth-induced water potential gradient. *Plant Physiol.* **102**:13–28.

Pahlavanian, A., and Silk, W. K. (1988). Effect of temperature on spatial and temporal aspects of growth in the primary maize root. *Plant Physiol.* **87**:529–532.

Paolillo, D. J., and Sorrels, M. E. (1992). The spatial distribution of growth in the extension zone of seedling wheat leaves. *Ann. Bot.* **70**:461–470.

Richards, O. W., and Kavanagh, A. J. (1943). The analysis of the relative growth gradients and changing form of growing organisms: Illustrated by the tobacco leaf. *Am. Nat.* **77**:385–399.

Rygol, J., Pritchard, J., Zhu, J. J., Tomos, A. D., *et al.* (1993). Transpiration induces radial turgor pressure gradients in wheat and maize roots. *Plant Physiol.* **103**:493–500.

Schmalstig, J. G., and Cosgrove, D. J. (1990). Coupling of solute transport and cell expansion in pea stems. *Plant Physiol.* **94**:1625–1633.

Schnyder, H., and Nelson, D. J. (1989). Growth rates and assimilate partitioning in the elongation zone of tall fescue leaf blades at high and low irradiance. *Plant Physiol.* **90**:1201–1206.

Schnyder, H., Nelson, D. J., and Coutts, J. H. (1987). Assessment of spatial distribution of growth in the elongation zone of grass leaf blades. *Plant Physiol.* **85**:290–293.

Selker, J. M. L., Steucek, G. L., and Green, P. B. (1992). Biophysical mechanisms for morphogenetic progressions at the shoot apex. *Dev. Biol.* **153**:29–43.

Sharp, R. E., Silk, W. K., and Hsiao, T. C. (1988). Growth of the maize primary root at low water potentials. I. Spatial distribution of expansive growth. *Plant Physiol.* **87**:50–57.

Sharp, R. E., Hsiao, T. C., and Silk, W. K. (1990). Growth of the maize primary root at low water potentials. II. Role of growth and deposition of hexose and potassium in osmotic adjustment. *Plant Physiol.* **93**:1337–1346.

Silk, W. K. (1984). Quantitative descriptions of development. *Annu. Rev. Plant Physiol.* **35**:479–518.

Silk, W. K. (1989). Growth rate patterns which maintain a helical tissue tube. *J. Theor. Biol.* **138**:311–327.

Silk, W. K., and Erickson, R. O. (1979). Kinematics of plant growth. *J. Theor. Biol.* **76**:481–501.

Silk, W. K., and Haidar, S. A. (1986). Growth of the stem of *Pharbitis nil*: Analysis of longitudinal and radial components. *Physiol. Veg.* **24**:109–116.

Silk, W. K., and Wagner, K. K. (1980). Growth sustaining water potential distributions in the primary corn root. *Plant Physiol.* **66**:859–863.

Silk, W. K., Hsiao, T. C., Diedenhofen, U., and Matson, C. (1986). Spatial distributions of potassium, solutes, and their deposition rates in the growth zone of the primary corn root. *Plant Physiol.* **82**:853–858.

Spollen, W. G., and Sharp, R. E. (1991). Spatial distribution of turgor and root growth at low water potentials. *Plant Physiol.* **96**:438–443.

Steudle, E., Smith, S. A. C., and Luttge, U. (1980). Water-relations parameters of individual mesophyll cells of the crassulacean acid metabolism plant *Kalanchoe daigremontiana*. *Plant Physiol.* **66**:1155–1163.

Tiwari, S. C., and Green, P. B. (1991). Shoot initiation on a graptopetalum leaf-sequential scanning electron microscopic analysis for epidermal division patterns and quantitation of surface growth (kinematics). *Can. J. Bot.* **69**:2302–2319.

Williams, M. H. (1991). A sequential study of cell divisions and expansion patterns on a single developing shoot apex of *vinca major*. *Ann. Bot.* **68**:541–546.

Wolf, S. D., Silk, W. K., and Plant, R. E. (1986). Quantitative patterns of leaf expansion: Comparison of normal and malformed leaf growth in *Vitis vinifera* cv. Ruby Red. *Am. J. Bot.* **73**:832–846.

*Biomimetics, Vol. 2, No. 3, 1994*

# Plant and Fungal Cell Growth: Governing Equations for Cell Wall Extension and Water Transport[1]

**Joseph K. E. Ortega[2]**

*A set of governing equations for plant and fungal cell growth (enlargement) is reviewed, whose foundation is the augmented growth equations. These equations describe two interrelated and simultaneous physical processes that are involved in enlargement of plant and fungal cells: cell wall extension and water uptake. Special emphasis is put on the systematic development of the many governing equations that are used as theoretical foundations for pressure probe methods. Some new equations are presented which may provide the theoretical foundation for new measurement methods and/or better analyses.*

**KEY WORDS:** augmented growth equations; governing equations; pressure probe; cell wall extension; water relations; plant cells; fungal cells.

## INTRODUCTION

Governing equations have played key roles in the evolution of physical sciences from a qualitative state to a quantitative state. They are fundamental to the physical sciences. Navier–Stokes equations in fluid mechanics and convective heat transfer and Maxwell's equations in electricity and magnetism, are but two examples of governing equations that have become the theoretical foundation of their respective field. Physical scientists, engineers, and, to some extent, biologists have come to rely on the use of governing equations to determine the

[1] This is the published version of a paper presented at the Plant Biomechanics Congress, Montpellier, France, September 5-9, 1994.

[2] Department of Mechanical Engineering, Bioengineering Laboratory, University of Colorado at Denver, Campus Box 112, P.O. Box 173364, Denver, Colorado 80217-3364.



1059-0153/94/0900-0215$07.00/0 

magnitude and behavior of a "parameter of interest" when *several* other parameters change *simultaneously*.

Growth is the result of biochemical and metabolic events in combination with physical processes. During the past decade, progress has been made in the development of governing equations that describe the relevant physical processes involved in plant and fungal cell enlargement, in terms of biophysical and biomechanical parameters. The magnitude and behavior of the biophysical and biomechanical parameters are controlled by relevant biological processes.

This paper attempts systematically to review governing equations relevant to plant and fungal cell enlargement. Emphasis is put on a systematic development of the governing equations used as theoretical foundations for "pressure probe" methods. This systematic approach might provide an effective method for investigators trained in related fields, and/or new investigators interested in using pressure probe methods, to review this topic. This paper does not attempt to provide a comprehensive review of all related work. Because the main objectives are to provide a systematic review of established governing equations for *in vivo* cell wall extension and water transport and to provide a systematic review of the theoretical foundations for common pressure probe methods, only selected references are provided, to give examples of applications and a deeper discussion of the method. A few new governing equations are derived and presented for the first time in this review. It is hoped that these new governing equations will provide theoretical foundations for new experimental methods and analyses.

## GOVERNING EQUATIONS

### The Augmented Growth Equations

The augmented growth equations (Ortega, 1985, 1990, 1993; Ortega *et al.*, 1988a) provide the foundation for a set of governing equations that describe plant and fungal cell enlargement. These equations are extensions of the previously established growth equations (Lockhart, 1965; Taiz, 1984).

The first augmented growth equation describes the rate of cell wall extension and may be formulated to account for both irreversible and reversible extension (Fig. 1). This equation relates the relative rate of change in volume of the cell wall chamber, $\nu_c$, to the sum of the relative rate of irreversible (plastic) extension and the relative rate of reversible (elastic) extension (Ortega, 1985):

$$\nu_c = (dV_c/dt)/V_c = \phi(P - Y) + (dP/dt)/\epsilon \qquad (1)$$

(relative rate of extension) = (plastic) + (elastic)

where $V_c$ is the volume of the cell wall chamber, $t$ is time, $\phi$ is the relative

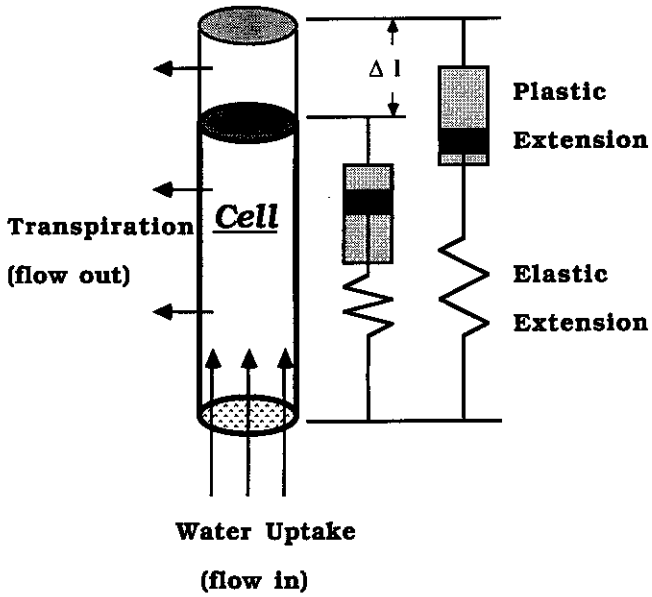


**Fig. 1.** A schematic illustration of the two simultaneous and interrelated physical processes that regulate the growth (enlargement) rate of plant and fungal cells: the rate of cell wall extension and the *net* rate of water uptake. The rate of wall extension is the sum of plastic (dashpot) and elastic (spring) extension rates. The net rate of water uptake is the difference between the rate of water uptake (flow in) and the rate of transpiration (flow out).

irreversible wall extensibility, $P$ is the turgor pressure (the pressure difference between the cell interior and the external medium), $Y$ is the yield threshold (a magnitude of turgor pressure which must be exceeded before plastic wall extension occurs), and $\epsilon$ is the volumetric elastic modulus. The term $\phi(P - Y)$ represents the relative rate of plastic, or permanent, wall extension. The term $(dP/dt)/\epsilon$ represents the relative rate of elastic, or reversible, wall extension.

The second augmented growth equation is a mathematical statement describing the *net* rate of water uptake (Fig. 1) and may be obtained from the conservation of mass (water mass) (Ortega *et al.*, 1988a):

$$\nu_w = (dV_w/dt)/V_w = L(\sigma\Delta\pi - P) - T \tag{2}$$

(*net* rate of water uptake) = (flow in) − (flow out)

where $\nu_w$ is the relative rate of change in volume of the cell contents (mostly water), $V_w$ is the volume of the cell contents, $L$ is the relative hydraulic conductance of the cell membrane ($L = L_pA/V_w$, where $L_p$ is the hydraulic conductivity of the cell membrane and $A$ is the area of the cell membrane), $\sigma$ is the

solute reflection coefficient of the cell membrane (whose value can range from zero to unity; in most cases it is unity), $\Delta\pi$ is the difference in osmotic pressure between the cell sap, $\pi_i$, and the external medium, $\pi_e$, and $T$ is the relative transpiration rate. The term $L(\sigma\Delta\pi - P)$ represents the relative rate of water uptake, and the term $T$ represents the relative rate at which water is lost from the cell by transpiration. This term $T$ is zero for cells that are not exposed to the external environment and, thus, do not transpire. It should be noted that the volume of the cell contents must equal the volume of the cell wall chamber, $V_w = V_c$, and that the respective relative rates of change in volume must also be equal, $\nu_w = \nu_c$. Therefore, for the remainder of this paper, there is no distinction between $V_w$ and $V_c$, or between $\nu_w$ and $\nu_c$; they are simply represented by $V$ and $\nu$, respectively. Finally, observe that Eqs. (1) and (2) are coupled by the turgor pressure, $P$, and by the relative rate of change in volume, $\nu$.

## Turgor Pressure Behavior

The governing equation describing the turgor pressure behavior can be obtained by combining Eqs. (1) and (2) with the elimination of $\nu$:

$$dP/dt + \epsilon\phi(P - Y) - \epsilon L(\sigma\Delta\pi - P) + \epsilon T = 0 \quad (3)$$

In the special case when the turgor pressure is constant (thus, $dP/dt = 0$) and the cell is not transpiring ($T = 0$), the following equation describing the turgor pressure is recovered: $P = (L\sigma\Delta\pi + \phi Y)/(L + \phi)$, which is the same equation derived by Lockhart (1965) for this same case.

## Pressure-Dependent Parameters

In the most general of cases, Eqs. (1), (2), and (3) are not *linear* differential equations, because the magnitude of some of the inclusive parameters is known to vary with the turgor pressure; $\epsilon$, $L$, and $\Delta\pi$ have all been shown to be functions of $P$. The functional relationship between $\epsilon$ and $P$, $\epsilon(P)$, may be described by the following equation (Ortega, 1990, 1993; Ortega *et al.*, 1988a):

$$\epsilon(P) = \epsilon_\infty - [(\epsilon_\infty - \epsilon_0) \exp(-kP)] \quad (4)$$

where $\epsilon = \epsilon_\infty$ when $P = P_\infty$ (for many cells, $P \approx P_\infty$, when $P > 0.5$ MPa), and $\epsilon = \epsilon_0$ when $P = 0$, and $k$ is a rate constant which is different for each species of cells.

Similarly, it has been reported that for some algal cells (Zimmermann and Steudle, 1974a, b) and higher plant cells (Steudle *et al.*, 1982), the hydraulic conductivity of the cell membrane, $L_p$, increases at low turgor pressure (also see review by Steudle, 1993). Therefore, for these cells, there exists a functional relationship between $L_p$ and $P$. Based on the published results of Zimmermann

and Steudle (1974a, b) and Steudle *et al.* (1982), the following relationship is derived to describe $L_p(P)$:

$$L_p(P) = (L_{po} - L_{p\infty}) \exp(-aP) + L_{p\infty} \quad (5)$$

where $L_p = L_{p\infty}$ when $P = P_\infty$, $L_p = L_{po}$ when $P = 0$, and $a$ is a rate constant which is different for each species of cells. The functional relationship for $L$ and $P$ is obtained from the equation $L(P) = L_p(P)(A/V)$.

The dependence of $\Delta\pi$ on $P$, $\Delta\pi(P)$, can be described by the following equation, where the expression for $\pi_i(P)$, first derived by Dainty (1976), is employed:

$$\Delta\pi(P) = \pi_i(P) - \pi_e = (\pi_o - \pi_e) - \pi_o[P/\epsilon(P)] \quad (6)$$

where $\pi_i = \pi_o$ when $P = 0$, and Eq. (4) describes $\epsilon(P)$.

It is not known whether the parameters $\phi$, $Y$, and $T$ are dependent on the turgor pressure [although for some cells, there is evidence which suggests that $Y$ is "adjustable" or "nonadjustable," depending on the magnitude of $P$ (Green *et al.*, 1971; Ortega *et al.*, 1989)]. More investigations are needed to determine whether $\phi$, $Y$, and $T$ are dependent on $P$.

Equations (1)–(6) represent a "set of governing equations" for plant and fungal cell growth (enlargement). Importantly, the augmented growth equations and the original growth equations (the foundations of this set of the governing equations) have demonstrated utility in understanding and predicting the growth rate behavior of higher and lower plant cells (see reviews by Cosgrove, 1986, 1993a, b; Ortega, 1990; Steudle, 1993, Taiz, 1984; Tomos *et al.*, 1989) and fungal cells (Money, 1990, 1992; Ortega, 1990, 1993; Ortega *et al.*, 1988a, b, 1989, 1991, 1992).

## PRESSURE PROBE METHODS

The augmented growth equations have also proven useful in determining the magnitude and behavior of the inclusive parameters. Because the turgor pressure, $P$, is present in three of the four terms of the augmented growth equations, the cell pressure probe [which directly measures the turgor pressure of single cells (see review by Steudle, 1993)] has proven to be an important tool in determining the magnitude and behavior of the biophysical and biomechanical parameters in Eqs. (1) and (2) (Cosgrove, 1985, 1986, 1987, 1993a, b; Cosgrove *et al.*, 1987; Hüsken *et al.*, 1978; Money, 1990, 1992; Okamoto *et al.*, 1989; Ortega, 1990, 1993; Ortega *et al.*, 1988a, b, 1989, 1991, 1992; Steudle, 1993; Steudle *et al.*, 1982; Tomos *et al.*, 1989; Wendler and Zimmermann, 1982; Zimmermann and Steudle, 1974a, b, 1978). The governing equations for nearly all pressure probe methods can be obtained directly from

the augmented growth equations in their present form or by examining them in limiting conditions.

## Determination of ε

A typical method for determining $\epsilon$ utilizes a turgor pressure pulse-down and pulse-up produced with the pressure probe (Fig. 2a). After the cell is impaled with the microcapillary tip of the pressure probe to measure the turgor pressure, cell sap is quickly withdrawn with the pressure probe to lower the turgor pressure, thus producing a step-down. Subsequently, a step-up of equal magnitude is produced by injecting the cell sap back into the cell, and if the time interval between the step-down and step-up is short, a pulse-down is produced. If the change in pressure, $\Delta P$, and the volume of the cell sap removed

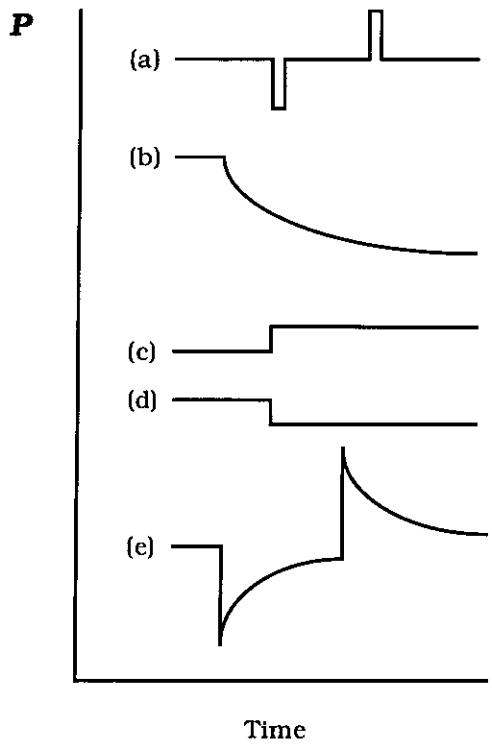


**Fig. 2.** Examples of some turgor pressure traces produced or observed in pressure probe methods: (a) pulse-down followed by pulse-up, (b) pressure relaxation from a constant pressure, (c) step-up, (d) step-down, and (e) step-down with subsequent relaxation, followed by a step-up with subsequent relaxation.

or injected, $\Delta V$, are measured, together with the initial volume of the cell, $V$, then $\epsilon$ can be calculated.

The governing equation that describes the "elastic" deformation of the cell wall chamber can be obtained from Eq. (1) for the special case when there is no plastic deformation, $\phi(P - Y) = 0$ (this would be the case for nongrowing cells):

$$v = (dV/dt)/V = (dP/dt)/\epsilon \tag{7}$$

Now multiplying Eq. (7) by $dt$, and solving for $\epsilon$, the following relationship is obtained (Philip, 1958):

$$\epsilon = V(dP/dV) \cong \Delta P/(\Delta V/V) \tag{8}$$

To determine $\epsilon$ for growing cells, it is important to account for the plastic extension related to growth; $\phi(P - Y)\Delta t$. The relevant governing equation used to determine $\epsilon$ for growing cells is Eq. (1); by simply solving for $\epsilon$, and substituting in "finite-difference" operators, the following equation is obtained (Ortega, 1985):

$$\epsilon = \Delta P/[(\Delta V/V) - \phi(P - Y)\Delta t] \tag{9}$$

Recently, a new method to determine the *average* value of $\epsilon$ for cells in plant tissue was introduced (Ortega, 1993). In this method, the transpiration rate of the tissue and turgor pressure decay (relaxation) of the cells (Fig. 2b) are measured after the water source is removed from the tissue. The governing equation can be obtained from Eq. (3) by accounting for the following conditions; the water source is removed, $L(\sigma\Delta\pi - P) = 0$, and the cells are not growing, $\phi(P - Y) = 0$. Equation (10) is obtained by solving the resulting equation for $\epsilon$ (Ortega, 1993):

$$\epsilon_{av} = (-dP/dt)_{av}/T \tag{10}$$

## Determination of $\varphi$ and $Y$

In Vivo *Stress Relaxation.* This method consists of measuring the pressure decay (relaxation) of cells (Fig. 2b) when the transpiration is suppressed and the water source is removed. The governing equation for the *in vivo* stress relaxation method can be obtained directly from Eq. (3) by accounting for the following conditions: water source is removed, $L(\sigma\Delta\pi - P) = 0$, and transpiration is suppressed, $T = 0$. Given these conditions, the following equation is obtained (Cosgrove, 1985; Ortega, 1985):

$$dP/dt + \epsilon\phi(P - Y) = 0 \tag{11}$$

When $\phi$, $\epsilon$, and $Y$ are assumed constant during the turgor pressure decay, this

differential equation can easily be solved to obtain the turgor pressure as a function of time, $P(t)$ (Cosgrove, 1985; Ortega, 1985):

$$P(t) = Y + (P_i - Y) \exp(-\epsilon\phi t) \tag{12}$$

where the initial condition $P = P_i$ at $t = 0$ is employed. It is apparent that at times greater than zero, the turgor pressure decays exponentially to a constant value, $Y$, with a time constant, $t_c = 1/\epsilon\phi$. Thus, if the magnitude of $\epsilon$ is known, theoretically $\phi$ and $Y$ can be obtained from the turgor pressure decay curve (Cosgrove, 1985, 1987; Ortega *et al.*, 1989). A problem implicit to the *in vivo* stress relaxation method is that the pressure decay can take a significantly long period of time to complete (typically longer than an hour), and it cannot always be assumed that the parameters, $\phi$ and $Y$, remain constant during this long period of time.

Sometimes the turgor pressure decay occurs over the range where $\epsilon$ varies with $P$. In these cases, the following integral should be evaluated with the appropriate limits to obtain $P(t)$:

$$\int [(P - Y)\epsilon(P)]^{-1} dP = -\int \phi \, dt \tag{13}$$

where Eq. (4) is substituted for $\epsilon(P)$.

In Vivo *Creep.* This method consists of producing a step-up in turgor pressure, $\Delta P$ (Fig. 2c) and measuring the growth rate before and after the step-up to determine the difference. The governing equation for the *in vivo* creep method can be obtained from Eq. (1) by considering the effects of a step-up in turgor pressure on the plastic extension rate (growth rate) of the cell wall; the elastic extension that occurs immediately after the step-up is neglected in the analysis (Green *et al.*, 1971; Okamoto *et al.*, 1989; Ortega *et al.*, 1989, 1991). The following equation is obtained when the total differential of modified Eq. (1) [(Lockhart, 1965) sometimes referred to as the "Lockhart equation," which is Eq. (1) without the elastic term] is taken and then solved for $\phi$ (it is assumed that $\phi$ and $Y$ remain constant for a short time interval before and after the $\Delta P$):

$$\phi = \Delta v/\Delta P = [v_{ave(after)} - v_{ave(before)}]/\Delta P \tag{14}$$

Once the magnitude of $\phi$ is determined, then the Lockhart equation may be used to solve for $Y$ using the obtained value of $\phi$ and the growth rate before $\Delta P$ (Ortega *et al.*, 1989, 1991):

$$Y = P - v/\phi \tag{15}$$

A more direct method can sometimes be used to determine $Y$. In theory, a turgor pressure step-down (Fig. 2d) whose magnitude is equal to or greater than the difference, $P - Y$, will stop growth. When this $\Delta P$ can be determined experimentally, it can be used to determine $Y$ with the equation $Y = P - \Delta P$ (Green *et al.*, 1971).

The *in vivo* creep method offers the important theoretical advantage (in comparison to the *in vivo* stress relaxation method) of not requiring $\epsilon$ in the analysis of the results. This eliminates both the need to measure $\epsilon$ for the determination of $\phi$ and the need to account for its dependence on $P$, if the pressure decay occurs in the range where $\epsilon$ varies with $P$.

## Determination of $L_p$

*Pressure Relaxation Method.* In this method, a rapid decrease in turgor pressure is produced with the pressure probe by withdrawing a small, fixed amount of cell sap in a short time (in less than a second) and recording the subsequent pressure relaxation (Fig. 2e). After the pressure relaxation is complete, the removed cell sap is injected back into the cell to produce a rapid increase in turgor pressure, and the pressure relaxation is again recorded. Typically, the half-times for the pressure relaxation curves are used to determine $L_p$.

The governing equation for the pressure relaxation method can be obtained from Eq. (3) for the following conditions: $T = 0$ (no transpiration), $\phi(P - Y) = 0$ (nongrowing cell) and $\epsilon$ = constant. The solution to the resulting differential equation (not shown here) is an exponential decay of turgor pressure with the time constant: $t_c = V/[AL_p(\epsilon + \sigma\pi_{io})]$, where $\pi_{io}$ is the equilibrium osmotic pressure of the cell sap. Typically, the $L_p$ is determined by measuring $\epsilon$, $\pi_{io}$, $V$, $A$, and the half-time of the exponential decay, $t_{1/2}$; in most cases, $\sigma$ can be assumed to be unity. The following equation is used to calculate $L_p$ (Hüsken *et al.*, 1978; Zimmermann and Steudle, 1978):

$$L_p = V \ln 2/[t_{1/2}A(\epsilon + \sigma\pi_{io})] \tag{16}$$

In the case of a growing cell, when $\phi$ = constant (but not zero), the relevant governing equation can be obtained from Eq. (3) by applying the conditions $T = 0$ (no transpiration) and $\epsilon$ = constant (Ortega, 1985). Using Eq. (6) to describe $\Delta\pi(P)$, the solution to the resulting differential equation (not shown here) will be an exponential decay of turgor pressure with the following time constant (Cosgrove, 1986): $t_c = 1/[L(\epsilon + \sigma\pi_o) + \epsilon\phi]$.

*Pressure Clamp Method.* This method makes use of the turgor pressure step-down and/or step-up produced by the pressure probe (Figs. 2d and c). Using the pressure probe, a decrease in turgor pressure is produced and maintained (clamped) by continuously withdrawing cell sap into the microcapillary of the pressure probe; subsequently, the cell sap can be injected back into the cell to produce a step-up in turgor pressure. The rate at which the cell sap is removed from the cell, or injected into the cell, decreases as a function of time after the initiation of the step-down or step-up, i.e., a "volume relaxation." The governing equation for this volume relaxation can be obtained from Eq. (2) by

imposing the condition that $T = 0$ and by multiplying the equation by $V$. In this equation, the osmotic pressure of the cell sap is a function of time, $\pi_i(t)$, and is approximated with the relationship $\pi_i(t) = \pi_{io}[1 - V(t)/V_o]$, where $V_o$ is the initial cell volume (Wendler and Zimmermann, 1982). The resulting differential equation can be solved for $V(t)$. The solution (Wendler and Zimmermann, 1982) is an exponential decay with a time constant $t_c = V_o/(AL_p\sigma\pi_{io})$. It is apparent that $L_p$ can be determined when $t_c$, $V_o$, $A$, and $\pi_{io}$ are measured; typically, $\sigma$ is assumed to be unity. Importantly, Wendler and Zimmermann (1982) further demonstrated that $L_p$ can be determined from the initial slope of the volume relaxation curve:

$$L_p = -s_v/(A\Delta P) \tag{17}$$

where $s_v$ is the magnitude of the initial slope. Thus, implicit in the pressure clamp method is the important advantage of being able to determine $L_p$ without knowing $V_o$, $\epsilon$, or $\pi_{io}$. On the other hand, unstirred layers adjacent to the cell membrane during the induced water flow can affect the accuracy of the results obtained with the pressure clamp method (Steudle, 1993).

## Determination of $T$

*Pressure Relaxation Method.* This method consists of removing the water source from nongrowing cell(s) and measuring the resulting decay in turgor pressure (Fig. 2b). The relative transpiration rate, and transpiration rate, can be calculated from the magnitude of the turgor pressure decay rate, provided that $\epsilon(P)$ is known, or measured independently. The relevant governing equation can be obtained from Eq. (3) by accounting for the following conditions: The water source is removed, $L(\sigma\Delta\pi - P) = 0$, and the cell is not growing, $\phi(P - Y) = 0$. The resulting equation can be solved for $T$ to obtain (Ortega, 1993; Ortega *et al.*, 1988a, 1992)

$$T = -(dP/dt)/\epsilon(P) \tag{18}$$

Since $\epsilon$ is a function of $P$, a series of governing equations can be obtained, each depending on the range in which the turgor pressure decay occurs (Ortega, 1993):

$$T = -(dP/dt)/\epsilon_\infty \qquad \{\text{high } P\} \tag{18a}$$

$$T = -(dP/dt)/(\epsilon_o + bP) \qquad \{\text{low } P\} \tag{18b}$$

$$T = -(dP/dt)/\{\epsilon_\infty - [(\epsilon_\infty - \epsilon_o)\exp(-kP)]\} \qquad \{\text{all } P\} \tag{18c}$$

where $\epsilon_\infty$, $\epsilon_o$, and $k$ have been defined previously, and $b$ is the slope of the $\epsilon$ versus $P$ curve at low $P$.

*Pressure Clamp Method.* This method consists of removing the water

source from a growing or nongrowing cell and clamping the turgor pressure at its equilibrium value (the value of $P$ that was measured before the water source is removed) by continuously injecting silicon oil into the cell vacuole. The transpiration rate, $[dV/dt]_T$, and relative transpiration rate, $T = [dV/dt]_T/V$, can be determined when the volumetric growth rate and the volumetric rate of oil injection are measured. The relevant governing equation can be obtained by multiplying Eq. (2) by $V$ and noting that, $Vv = [dV/dt]_g$ (volumetric growth rate), $VL(\sigma\Delta\pi - P) = [dV/dt]_i$ (volumetric rate of water uptake, which is equal to the volumetric rate of oil injection during the pressure clamp), and $VT = [dV/dt]_T$ (volumetric transpiration rate). The following equation is obtained by solving for the volumetric transpiration rate, $[dV/dt]_T$ (Ortega, 1993; Ortega *et al.*, 1992):

$$[dV/dt]_T = [dV/dt]_i - [dV/dt]_g \tag{19}$$

Two theoretical advantages of the pressure clamp method (in comparison with the pressure relaxation method) are that (i) it can be used to measure transpiration rates from growing cells, as well as nongrowing cells, and (ii) $\epsilon$ is not used in the analyses. Two experimental disadvantages of the pressure clamp method are that (i) injection of silicon oil into the cell is required, although it is envisioned that water or cell sap can be substituted for the oil in the microcapillary tip and injected into the cell instead of oil, and (ii) this method cannot be easily adapted to measure transpiration rates from tissue.

## DISCUSSION

Analogous to the many sets of governing equations in the physical sciences, Eqs. (1)–(6) can be interpreted as a set of governing equations for plant and fungal cell growth (enlargement). This is the first time that all of these equations have been reviewed together, although some previous papers have reviewed a smaller and more limited set of equations (Cosgrove, 1986, 1993b; Lockhart, 1965; Ortega, 1990; Taiz, 1984). It is envisioned that this set of governing equations will grow as more research is conducted in this area. However, it is doubtful that this set of governing equations will ever become a "deterministic" set of equations, because of the implicit dependence of the inclusive biomechanical and biophysical parameters on the many biological processes that control their magnitude and behavior. Still, similar to other sets of governing equations, this set of governing equations [Eqs. (1)–(6)] provides an important feature that other mathematical models (such as correlations between parameters) cannot, that is, that the magnitude and behavior of a dependent parameter (of interest to the investigator) can be determined when *several* other parameters vary *simultaneously*. This important property of governing equations can provide more qualitative and quantitative insights and more in-depth knowledge of integrated

effects of many biomechanical and biophysical parameters (biological processes) on each other.

It is apparent that this set of governing equations [Eqs. (1)–(6)] also demonstrates utility in developing new methods to measure and study many biomechanical and biophysical parameters. In this review, it is demonstrated that nearly all the governing equations for pressure probe methods can be systematically derived from the initial set of six governing equations. It is reasonable to anticipate that these governing equations will provide the theoretical foundation for new and better methods to measure many biomechanical and biophysical parameters. It should be emphasized that these new methods are not restricted to pressure probe methods but can employ other related instruments (such as the pressure bomb and psychrometer) and may inspire the invention of new instruments such as the "pressure block" (Cosgrove, 1987).

## ACKNOWLEDGMENTS

The author gratefully acknowledges support by U.S. National Science Foundation Grants DCB-8514902, DCB-8801717, and IBN-9103760.

## REFERENCES

Cosgrove, D. J. (1985). Cell wall yield properties of growing tissue: Evaluation by *in vivo* stress relaxation. *Plant Physiol.* **78**:347–356.

Cosgrove, D. J. (1986). Biophysical control of plant cell growth. *Annu. Rev. Plant Physiol.* **37**:377–405.

Cosgrove, D. J. (1987). Wall relaxation in growing stems: Comparison of four species and assessment of measurement techniques. *Planta* **171**:266–278.

Cosgrove, D. J. (1993a). Wall extensibility: Its nature, measurement and relationship to plant cell growth. *New Phytol.* **124**:1–23.

Cosgrove, D. J. (1993b). Water uptake by growing cells: An assessment of the controlling roles of wall relaxation, solute uptake, and hydraulic conductance. *Int. J. Plant Sci.* **154**:10–21.

Cosgrove, D. J., Ortega, J. K. E., and Shropshire, W., Jr. (1987). Pressure probe study of the water relations of *Phycomyces blakesleeanus* sporangiophores. *Biophys J.* **51**:413–423.

Green, P. B., Erickson, R. O., and Buggy, J. (1971). Metabolic and physical control of cell elongation rate: *In vivo* studies in *Nitella*. *Plant Physiol.* **47**:423–430.

Dainty, J. (1976). Water relations in plant cells. In Luettge, U., and Pitman, M. (eds.), *Encyclopedia of Plant Physiology* (NS), Springer-Verlag, Berlin, Vol. 2, pp. 12–35.

Hüsken, K., Steudle, E., and Zimmermann, U. (1978). Pressure probe technique for measuring water relations of cells in higher plants. *Plant Physiol.* **61**:158–163.

Lockhart, J. A. (1965). An analysis of irreversible plant cell elongation. *J. Theor. Biol.* **8**:264–275.

Money, N. P. (1990). Measurement of hyphal turgor. *Exp. Mycol.* **14**:416–425.

Money, N. P. (1992). Extension growth of the water mold *Achlya*: Interplay of turgor and wall strength. *Proc. Natl. Acad. Sci.* **89**:4245–4249.

Okamoto, H., Liu, Q., Nakahori, K., and Katou, K. (1989). A pressure-jump method as a new tool in growth physiology for monitoring physiological wall extensibility and effective turgor. *Plant Cell Physiol.* **30**:979–985.

Ortega, J. K. E. (1985). Augmented growth equation for cell wall expansion. *Plant Physiol.* **79**:318–320.

Ortega, J. K. E. (1990). Governing equations for plant cell growth. *Physiol. Plant.* **79:**116–121.
Ortega, J. K. E. (1993). Pressure probe methods to measure transpiration in single cells. In Smith, J. A. C., and Griffiths, H. (eds.), *Water Deficits: Plant Responses from Cell to Community*, BIOS Scientific, Oxford, pp. 73–86.
Ortega, J. K. E., Keanini, R. G., and Manica, K. J. (1988a). Pressure probe technique to study transpiration in *Phycomyces* sporangiophores. *Plant Physiol.* **87:**11–14.
Ortega, J. K. E., Manica, K. J., and Keanini, R. G. (1988b). *Phycomyces*: Turgor pressure behavior during the light and avoidance growth responses. *Photochem. Photobiol.* **48:**697–703.
Ortega, J. K. E., Zehr, E. G., and Keanini, R. G. (1989). In vivo creep and stress relaxation experiments to determine the wall extensibility and yield threshold for the sporangiophores of *Phycomyces*. *Biophys. J.* **56:**465–475.
Ortega, J. K. E., Smith, M. E., Erazo, A. J., Espinosa, M. A., Bell, S. A., and Zehr, E. G. (1991). A comparison of cell wall yielding properties for two developmental stages of *Phycomyces* sporangiophores: Determination by *in vivo* creep experiments. *Planta* **183:**613–619.
Ortega, J. K. E., Bell, S. A., and Erazo, A. J. (1992). Pressure clamp method to measure transpiration in growing single plant cells: Demonstration with sporangiophores of *Phycomyces*. *Plant Physiol.* **100:**1036–1041.
Philip, J. R. (1958). The osmotic cell, solute diffusibility, and the plant water economy. *Plant Physiol.* **33:**264–271.
Steudle, E. (1993). Pressure probe techniques: basic principles and application to studies of water and solute relations at the cell, tissue and organ level. In Smith, J. A. C., and Griffiths, H. (eds.), *Water Deficits: Plant Responses from Cell to Community*, BIOS Scientific, Oxford, pp. 73–86.
Steudle, E., Zimmermann, U., and Zillikens, J. (1982). Effect of cell turgor on hydraulic conductivity and elastic modulus of *Elodea* leaf cells. *Planta* **154:**371–380.
Taiz, L. (1984). Plant cell expansion: Regulation of cell wall mechanical properties. *Annu. Rev. Plant Physiol.* **35:**585–657.
Tomos, A. D., Malone, M., and Pritchard, J. (1989). The biophysics of differential growth. *Environ. Exp. Bot.* **29:**7–23.
Wendler, S., and Zimmermann, U. (1982). A new method for the determination of hydraulic conductivity and cell volume of plant cells by pressure clamp. *Plant Physiol.* **69:**998–1003.
Zimmermann, U., and Steudle, E. (1974a). Hydraulic conductivity and volumetric elastic modulus in giant algal cells: Pressure- and volume-dependence. In Zimmermann, U., and Dainty, J. (eds.), *Membrane Transport in Plants*, Springer-Verlag, New York, pp. 64–71.
Zimmermann, U., and Steudle, E. (1974b). The pressure-dependence of the hydraulic conductivity, the membrane resistance, and membrane potential during turgor pressure regulation in *Valonia utricularis*. *J. Membr. Biol.* **16:**331–352.
Zimmermann, U., and Steudle, E. (1978). Physical aspects of water relations of plant cells. *Adv. Bot. Res.* **6:**45–117.

*Biomimetics, Vol. 2, No. 3, 1994*

# Tree Biomechanics: Growth, Cumulative Prestresses, and Reorientations[1]

**Meriem Fournier,[2] Henri Bailleres,[3] and Bernard Chanson[4]**

*Three progressive steps are distinguished in the biomechanical study of tree growth and wood differentiation. For the first, tree mechanics, emphasis is put on the maturation prestress and on the surprising results of a time-differentiated analysis of radial growth. In particular, maximal bending stresses due to self-weight in leaning stems are usually not located in the peripheral youngest wood. The second step, biomechanical characterization, concerns a wide range of works. Here we present examples that deal with the relations between maturation strains and (i) tree architecture and morphology and (ii) histological and biochemical features of wood (microbiomechanics of wood). Finally, the state of the art concerning the biomechanical regulation of growth and differentiation is reviewed, through the examples of (i) the activation of radial growth to ensure a constant stress design at the stem periphery (Mattheck's model) and (ii) the righting movements of leaning stems due to asymmetric prestresses related to the differentiation of reaction wood.*

**KEY WORDS:** tree mechanics; wood; growth stresses; reaction wood; cambial growth.

## INTRODUCTION

Tree stems are tall and slender mechanical structures that support other aerial organs, withstand winds, and allow the plant to explore its environment. The design and movement of such structures are related to some morphological, histological, and physiological aspects of growth. Moreover, they ask basic

[1]This is the published version of a paper presented at the Plant Biomechanics Congress, Montpellier, France, September 5-9, 1994.

[2]École Nationale du Génie Rural, des Eaux et Forêts, 14 rue Girardet, 54042 Nancy Cedex, France.
[3]CIRAD Forêt, 45 bis Avenue de la Belle Gabrielle, 94 Nogent/Marne, France.
[4]Laboratoire de Rhéologie du Bois de Bordeaux, BP 10, 33610 Cestas Gazinet, France.



1059-0153/94/0900-0229$07.00/0 

biomechanical questions as some phenomena are explainable by a physical necessity while others involve regulation or adaptation of the living plant. Hence, our approach will be organized in three steps, that state progressively the interaction between mechanics and biology.

## THE THREE STEPS OF OUR BIOMECHANICAL APPROACH

Tree mechanics is based on the mechanics of solids. The inputs are supported loads, the outputs are fields of local variables such as displacements, strains (variations of form and movements), and stresses (local distributions of loads). Global characteristics of the structure such as safety factors (Tateno, 1991; Tateno and Bae, 1990), buckling loads (Greenhill, 1881; McMahon, 1975), and frequencies of sways (Milne, 1991; Fournier *et al.*, 1993) can also be included.

In addition to these inputs and outputs, a mechanical problem involves the geometry of the structure and the properties of materials: the critical stresses or strains that lead to failure and the local relation between stresses and strains, for example, the Young's modulus. The characterization of these properties requires the description of heterogeneities and anisotropies. Finally, note that a mechanical problem can be stated at different levels: The analyzed structure can be the whole tree (a truss of stems), the organ (a stem), the tissue (an elementary piece of wood), the isolated cell, or the cell wall.

Tree mechanics can be used to analyze the consequences of biological factors (genotype, environment, etc.) on the mechanical properties and response of the plant. This is biomechanical characterization. It aims a defining sets of data (inputs and parameters) for the mechanical problem, of typical biological situations, and can use data collected for other purposes (biometrics, tree architecture, wood quality).

Adaptations and physiological reactions of plants to their mechanical state are commonly observed; Stem taper seems to be optimized to withstand wind or gravitational forces (see, e.g., Greenhill, 1881; Schwendener, 1884; Metzger, 1893; Esser, 1946; Larson, 1963; McMahon, 1975; King and Loucks, 1978; Wilson and Archer, 1979; Dean and Long, 1986; West *et al.*, 1989; Bertram, 1989; Mattheck, 1991); moreover, stems react to mechanical stress and grow faster in height and slower in diameter when they are prevented from swaying (Larson, 1965; Quirk *et al.*, 1975; Quirk and Freeze, 1976a, b; Kellog and Steucek, 1977, 1980; Telewski and Jaffe, 1986a–c; Grace, 1977; Timell, 1987; Osawa, 1993); finally, reaction wood is a response to an abnormal orientation and allows secondary movements of the stem, often gravitropic (Wilson and Archer, 1979; Fisher and Wassmer-Stevenson, 1981; Timell, 1987; Archer, in press). A third step is thus to model these biological reactions or adaptations. Such models are based on a previously built mechanical model and postulate a

biological control of some outputs of this model. They are called "biomechanical models of regulation."

To apply these general principles to the biomechanical study of the tree growth, a mechanical model for stresses and strains in the woody cross section of a growing tree is developed. We emphasize growth and maturation prestresses. In addition, we develop examples of the variation of maturation strain related to the morphology and architecture of the tree and to anatomical and biochemical features of the wood. Other work concerns the bending mechanics of trees, stems, and branches submitted to external loads (wind and snow) and involves biomechanical characterization of parameters as moduli of elasticity or rupture (Cannell and Morgan, 1989; Langbour *et al.*, 1988; Nakatani *et al.*, 1984; Koizumi and Ueda 1986; Mamada *et al.*, 1984).

Finally, there are biomechanical models such as the regulation of cambial growth based on the constant stress hypothesis (Mattheck's model) and the regulation of lean by asymmetric maturation prestresses induced by the differentiation of reaction wood.

## THE MECHANICAL CONSEQUENCES OF RADIAL GROWTH

A mechanical model of the cross section of the woody stem loaded by external or internal forces can use classical tools for the mechanical analysis of cylinders, made of anisotropic elastic materials (Lekhnitskii, 1963; Maiti and Adams, 1968). The model can consider

(i) some heterogeneities, since further biomechanical characterization shows radial, longitudinal, and circumferential variation of wood properties (Zobel and van Buijtenen, 1989);

(ii) the possible discrepancy between the cylinder axes and the directions of anisotropy (the grain is sometimes wavy or helicoïdal and the tree rings not concentric);

(iii) noncircular cross sections; and

(iv) nonelastic materials.

Even though the material is anisotropic, beam theory gives a very good approximation of longitudinal stresses and strains (Fournier, 1989).

There is another specificity of tree mechanics that is rarely mentioned: The cross section grows while it is loaded. Usual mechanical analyses are not suitable for radially growing structures, which are loaded by continuously changing forces, while new tissues are differentiated progressively. Therefore, based on Eulerian formalism, an original mechanical analysis has been developed, taking into account relative kinetics of both loads and growth (Fournier, 1989; Fournier *et al.*, 1992). It generalizes the original idea of Martley (1928) and is achieved by two processes:

(1) an incremental problem between two times $t$ and $t + dt$, is stated as a classical problem since growth remains infinitesimal between these two instants;

(2) the mechanical state (i.e., the position of each material point and the stress field at a final time $t_f$ is calculated by superimposing the successive incremental solutions calculated from process 1).

For each material point, the superposition of stress and strain begins from the time it was differentiated. That allows for the assumption that a tissue cannot be loaded before it exists. In addition, the mechanical analysis requires data about the whole history of the structure, since the relative kinetics of growth and loads are necessary to solve the incremental problem.

Many numerical simulations both of stresses in a growing cross-section (Fournier, 1989; Fournier *et al.*, 1990, 1991a, b) and of successive forms of stems (Schaeffer, 1990; Castera and Morlier, 1991; Fournier and Moulia, 1994) have been performed. Great discrepancies can be shown between classical beam theory and the previous analysis, when both are applied to the modeling of the self-weight effects in a branch or a leaning tree cross section: At the level of the cross section, the distribution of bending and compressive stresses given by classic strength of materials varies linearly along the radius, from tensile value on the upper side to a compressive one on the lower side. The improved model predicts very low support stresses everywhere at the stem surface (Fournier *et al.*, 1991a) (Fig. 1). Actually, the very young peripheral wood supports only the last increment of weight added since it was differentiated (i.e., a very small load in most cases). Furthermore, the radial position of maximum stress depends not only on the present weight $P$ but also on the relative kinetics of both $P$ and radial growth.

At the level of the whole stem, the predicted deflections of a leaning stem are also different and cannot be qualified by a simple tip deflection in the most general case. The initial lean of the apical growth is defined by the stem architecture. At a given part of the stem, the lean increases with time as the stem becomes older and loaded. When considering the stem at a given age, this increase took longer in the older stem closer to the base. However, at each lapse of time, it was less important near the base which is closer to the fixed restraint. Therefore, the shape of the growing stem is an "S" form, due to the competitive effect of age and spatial position (toward the restraint) along the stem (Schaeffer, 1990). This shape can be computed from (i) the original orientation and kinetics of primary growth, (ii) the kinetics of loads, and (iii) the kinetics of secondary growth (Fig. 2). Small differences in radial growth can lead to great changes in form.

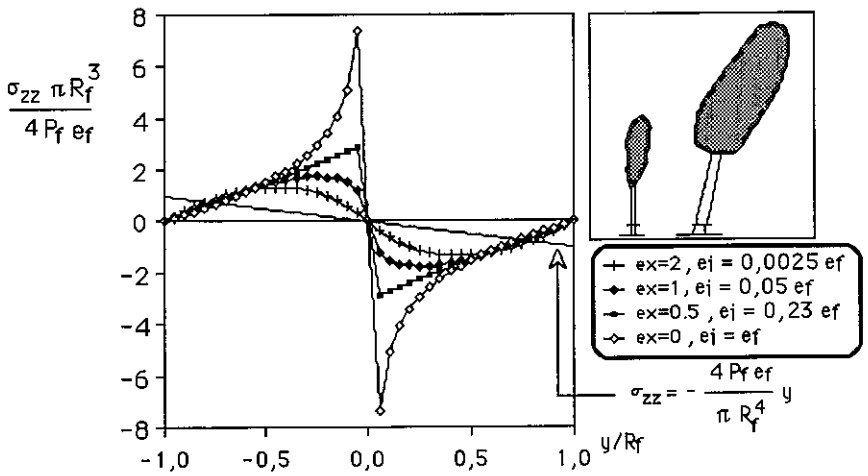


**Fig. 1.** Distribution of support longitudinal stresses on a leaning tree (from Fournier *et al.*, 1991a). The crown weight $P$ varies as $R^{2.5}$ ($R$ stem radius at the trunk base). The lever arm of the crown weight varies as $R^{ex}$. The higher the value of $ex$, the greater the variation of the lever arm since the beginning of growth. Stresses are compared to the "nongrowing" distribution of usual strength of materials, computed from the final weight $P_f$, the final lever arm $e_f$, and the final second moment of area $\pi R_f^4/4$.

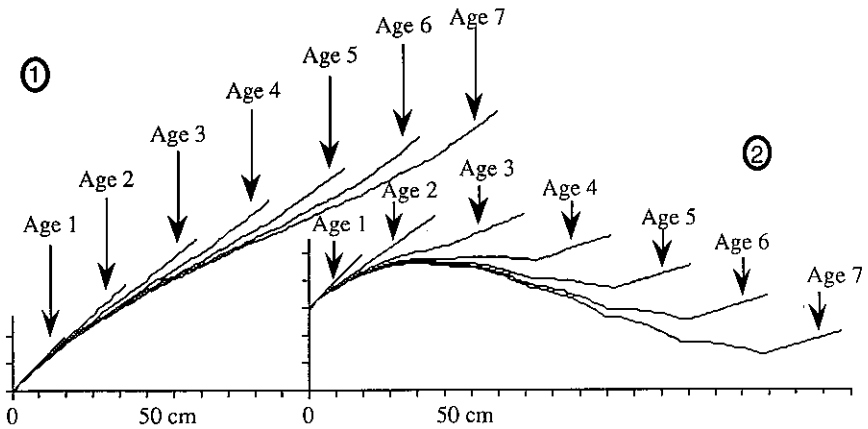


**Fig. 2.** Gravitationally strained form of a radially and longitudinally growing branch. Growth is divided into seven units of equal length (30 cm) and initial orientation (45°). A load of 200 g is supported at the beginning of the last two growth units. The Young's modulus and the specific gravity of the homogeneous material are 5000 MPa and 1 g/cm$^3$. The only difference between 1 and 2 is related to radial growth: for simulation 1, the increment of radius for each growth unit is 2 mm (everywhere and at any time); for simulation 2, this value is 1.5 mm for the three first increments and 2 mm thereafter.

## PRESTRESSES DUE TO WOOD DIFFERENTIATION— ASSOCIATED DEFORMATIONS IN THE GROWING STEM

Wood is internally prestressed in the living tree (Archer, 1986). Moreover, since material starts to be loaded after its formation, the high levels of stress observed in peripheral young wood must be explained by a phenomenon that occurs continuously just at the end of wood differentiation. Therefore, the origin of growth stress can be described by the following assumption: During radial growth, cells of the outermost layers, just after differentiation, have a tendency to strain. As the new cells are glued on the internal older wood, this tendency is impeded in longitudinal and tangential directions and the wood is prestressed. This assumption of macroscopic maturation strains can be related to underlying physical and chemical mechanisms at the scale of the cell wall; these mechanisms are still a matter of discussion and would be a swelling of the lignin matrix (Boyd, 1972) and a shrinkage of cellulose microfibrils (Bamber, 1987).

Stress and strain due to the maturation of a new peripheral layer can be calculated by an incremental problem, and stress at any final time is calculated by superimposition (Archer and Byrnes, 1974; Archer, 1986; Fournier *et al.*, 1991b) (Fig. 3).

Finally, the consequence of an angular (i.e., circumferential) asymmetry of maturation strains on the cross section is reorientation of the stem, since the side with the higher tensile stress pulls the other one (Fig. 4 and the Appendix). A mechanical model has been derived to compute, at each step of radial growth, the bending movements of a stem, from (i) the variation of the gravitational bending moment and (ii) the differentiation of heterogeneous wood (Fournier, 1989; Fournier *et al.*, 1991a, b, 1992). The model uses a superimposition of (i) a time-differentiated expression of classical equations of beams in pure bending (see the last paragraph and the simulations in Fig. 2) and (ii) the effect of asymmetric maturation strains (see the Appendix).

So far, we have considered the mechanical analysis of tree growth. Now we focus on specifically biomechanical questions.

## VARIATIONS OF MATURATION STRAINS RELATED TO TREE ARCHITECTURE

The hypothesis is the functional interpretation of circumferential peaks of longitudinal maturation strains related to stem reorientations. These strains have been estimated by the measurement of released strains at the stem surface (i.e., strains of a small piece of wood isolated from the stem by cutting grooves, drilling holes, etc.). Different metrologies are available (Archer, 1986). We usually used the single-hole method or Wap's method (Fournier *et al.*, 1994; Baillères, 1994).

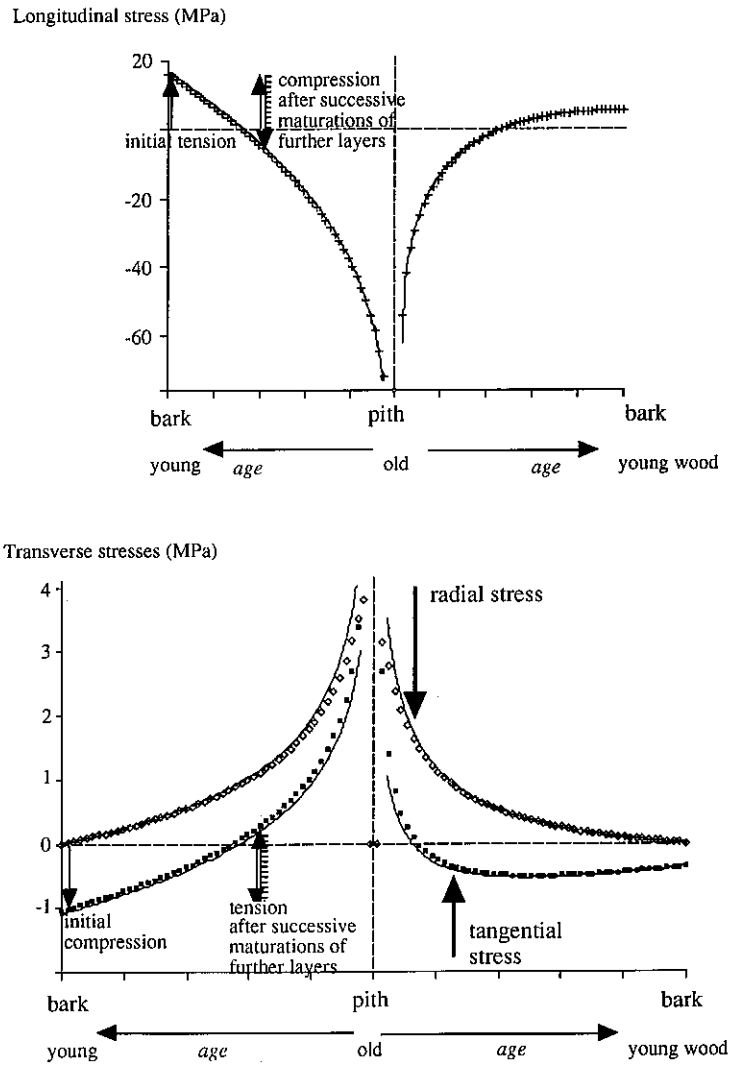


**Fig. 3.** Longitudinal and transverse maturation stresses in a standard stem (calculated from Fournier *et al.*, 1991b). Just after its differentiation, wood is under longitudinal tensile stress and compressive tangential stress. As it becomes older, the tangential stress becomes a tension, and the longitudinal stress a compression; the radial stress is a tension.

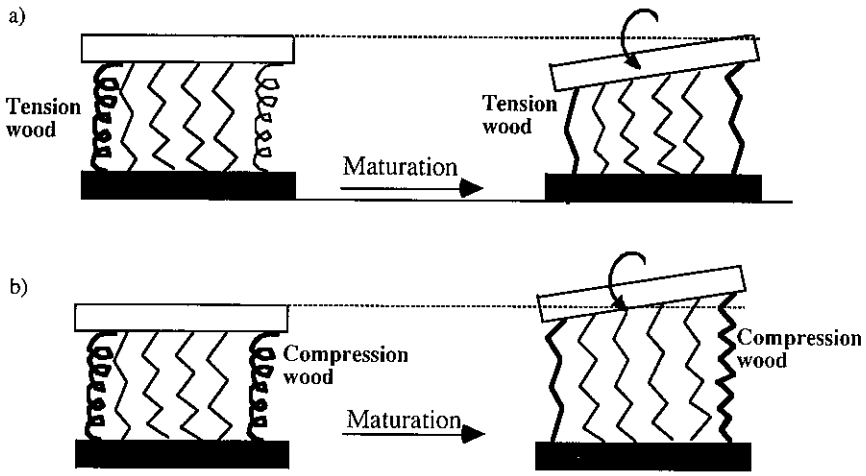


**Fig. 4.** Bending reorientation of tree stems due to the maturation of heterogeneous wood from one side to the other, usually related to the formation of reaction wood. (a) The case of angiosperms: The longitudinal maturation strain of tension wood is a higher shrinkage. (b) The case of gymnosperms: The longitudinal maturation strain of compression wood is dilatation.

Maturation strains usually vary along the circumference (formation of "peaks" of strains) with two typical patterns (Fig. 5) (Archer, 1986): (i) a peak of longitudinal shrinkage (i.e., the initial stress is a longitudinal tension) on angiosperm trees and (ii) a peak of longitudinal dilatation (i.e., the initial stress is a compression) on gymnosperm trees. These peaks can be large: The higher value can be eight times the lower. They are mostly associated with sections of reaction wood: compression wood in gymnosperms (Timell, 1987) and tension wood in angiosperms (Scurfield, 1973). Notice, however, that the dichotomy between angiosperms and gymnosperms may be not so contrasted since very low values of shrinkage have been measured in some angiosperms (Baillères *et al.*, 1994), and quite high values in gymnosperms. These peaks are not an anomaly but most stems have to differentiate reaction wood during specific periods of their life. For instance, in very homogeneous plantations of *Eucalyptus*, we find great longitudinal shrinkage on the upper side, although the trees were very slightly tilted (Fig. 6) (Baillères, 1994). This observation does not contradict the functional interpretation of peaks of strain: Verticality may be the consequence of efficient reorientation.

Peak strain usually corresponds to the lean of the stem (peak tensions are on the upper side and peak compressions are on the lower face) but not always, since other situations lead to reorientations: For example, most conifers are monopodial: The trunk is normally formed by a single meristem during the whole life of the tree (Edelin, 1989; Bell, 1991). However, the apical bud can

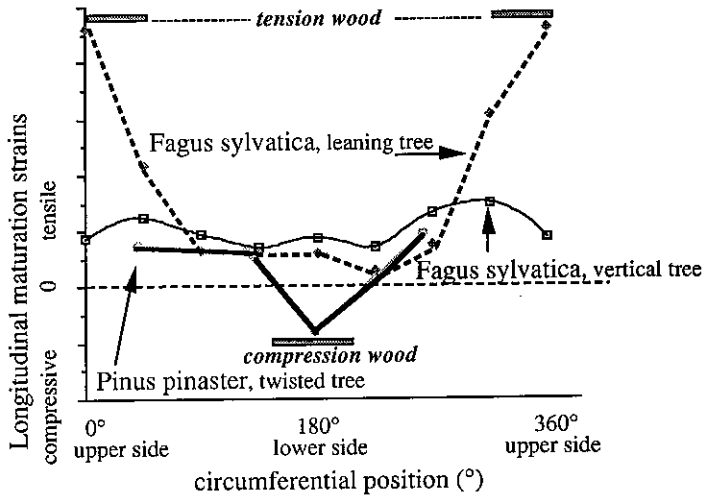


**Fig. 5.** Typical circumferential variations of longitudinal maturation strains at the stem periphery of two *Fagus sylvatica* (Chanson *et al.*, 1992) and one *Pinus pinaster* (Loup *et al.*, 1991). The measurements were made by the single-hole method (CIRAD's sensor): 100 $\mu$m corresponds approximately to a strain of 0.12%. (Baillères, 1994). In angiosperms, peaks of high tensile maturation strains (i.e., high longitudinal shrinkages) are related to the formation of tension wood. In gymnosperms, peaks of compressive strains (i.e., high longitudinal dilatation) are related to the formation of compression wood.

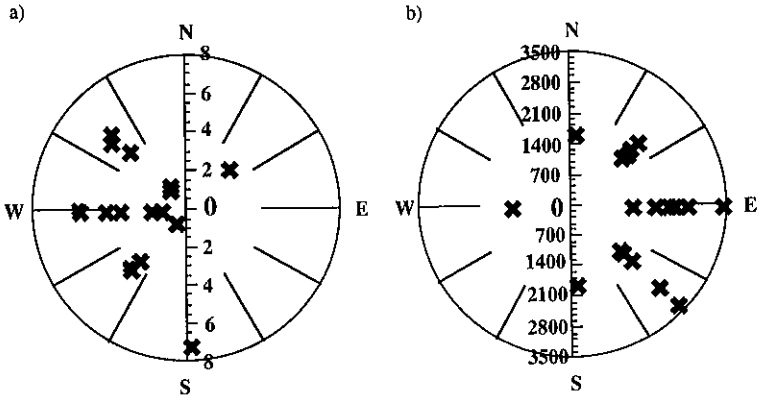


**Fig. 6.** Lean and peaks of maturation strains in *Eucalyptus* [clone 1-45; industrial plantations of Pointe-Noire, Congo, Africa (from Ballères, 1994)]. (a) Lean of the trunk (at breast height): values (%) and angular direction of the lower side (polar graphic). (b) Maximal maturation strain (from eight measurements) measured on the trunk circumference (at breast height): values (microstrains) and angular direction (polar graphic).

die accidentally. A branch then rights itself and becomes the new leader. This is linked to a reorientation that can require the formation of compression wood. We observed on a *Pinus pinaster* Ait. that the induced "flows" of compression wood can spread widely in space and time (Fig. 7a) (Loup *et al.*, 1991a, b). Other examples concern peak strains associated with the maintenance of verticality in trees that support an asymmetric crown. Radi (1992) found a great amount of compression wood in a *Pinus pinaster* Ait., almost vertical at the base but strongly tilted in the crown. We measured peak strains in an almost-vertical *Fagus sylvatica* L. that were not opposite to the direction of lean but to a great branch. These peaks disappeared above the branch (Fig. 7b) (Chanson *et al.*, 1992; Chanson, 1993).

A last observation is much more puzzling: Two opposite peaks (on the same circumference) have been measured on *Eperua falcata* Aubr. (French Guyana), *Sacoglottis gabonensis*, *Dichostemma* sp., *Alstonia* sp., (Cameroon), and *Castanea sativa* Mill (France, Italy) (Chanson, 1993; Fournier *et al.*, 1994). The functional explanation is not obvious, as the consequence for the tree is a tendency to split. Each side pulls the stem toward itself (Fig. 7c). Actually, these patterns of maturation strains have been observed on sympodial trees, where the stem is made of successive growth units from axillary buds (Bell, 1991), and thus, these double peaks can be interpreted as conflicting signals coming from the former and the new leader.

## RELATIONS BETWEEN MACROSCOPIC PROPERTIES OF WOOD AND HISTOLOGICAL FEATURES (MICROBIOMECHANICS)

The understanding of macroscopic mechanical properties of wood from the microstructure of the material at the scale of cells, cell walls, etc., (Barber and Meylan, 1964; Mark, 1967; Cave, 1968; Barrett, 1973; Archer, 1987a, b; Gibson and Ashby, 1988; Vieville, 1992) provides the mechanical basis for further biomechanical studies. The cell wall can be modeled as a composite made of a matrix of lignins, hemicelluloses, and amorphous cellulose, reinforced by long bundles of crystalline cellulosic fibrils. In the S2 layer—which represents the greatest part of the cell wall in fibers or tracheids—the fibrils are oriented helicoïdally and the angle between the fibrils and the cell axis (the "microfibril angle;" MFA) can vary from 0 to 50° among woods. Models derived from mechanics of composite materials emphasize the importance of the MFA, as well of other parameters such as the crystalline cellulose content or the mechanical properties of the matrix, to explain the variations of macroscopic properties of wood. Longitudinal shrinkage (longitudinal tensile stress) decreases when the MFA or the lignin content increases, and increases with the crystalline cellulose content; it becomes a dilatation (a compressive stress) for a high MFA or high lignin content (Yamamoto and Okuyama, 1988; Okuyama *et al.*, 1993).

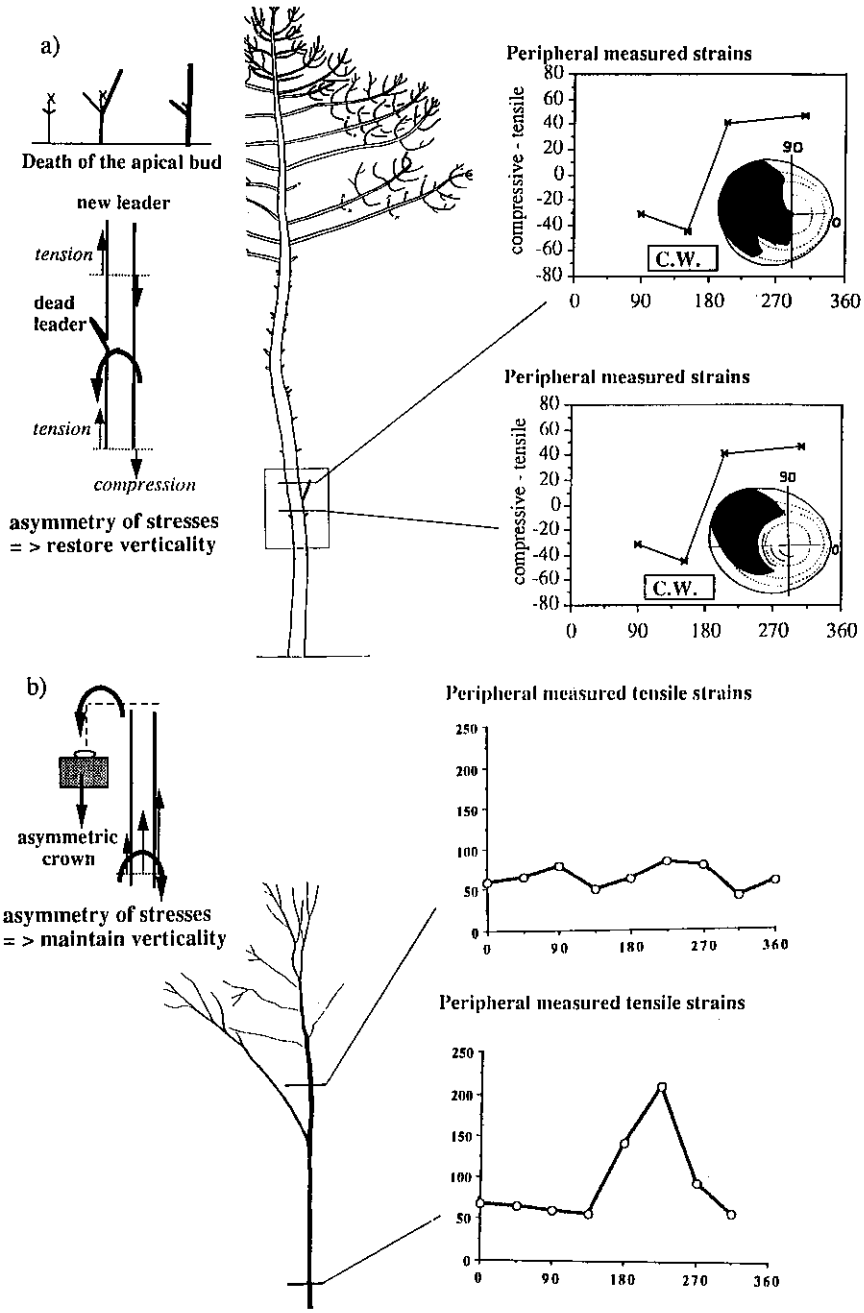


**Fig. 7.** Unusual peaks of maturation strains related to tree morphology. (a) Accidental death of the apex and traumatic reorientation in a *Pinus pinaster* Ait. (b) asymmetry of crown in a *Fagus sylvatica* L.; (c) double peak of tension in a *Saccoglottis gabonensis*. (From Loup *et al.*, 1991; Chanson, 1993; Fournier *et al.*, 1994.)

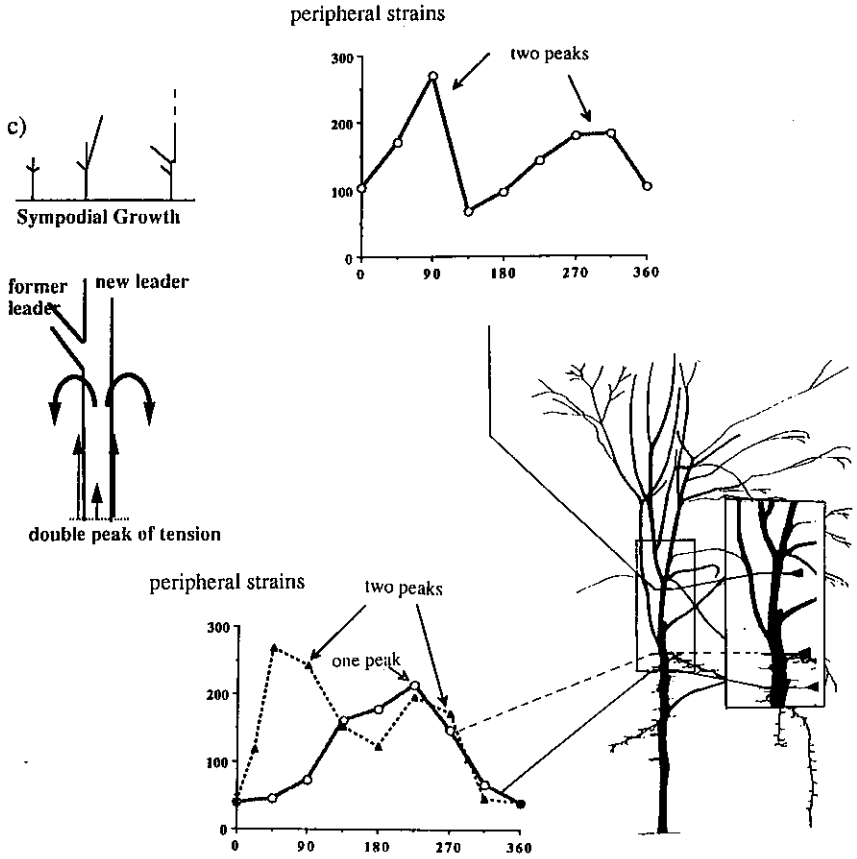


**Fig. 7.** Continued.

The biomechanical problem is then to establish the laws of variations of microstructural parameters within a sample of woods that characterize a biologically significant range of situations. The variations of structural variables usually show intricate interactions: For example, in conifers, the MFA increases with the lignin content since a higher MFA and lignin content is typical of compression wood or juvenile wood (Timell, 1987; Zobel and van Buijtenen, 1989).

A similar law has been observed in a *Eucalyptus* (clones planted in Congo, Africa) by Baillères (1994; Baillères *et al.*, 1994 (Fig. 8), correlated with variations in the longitudinal maturation shrinkage (Fig. 8). However, we cannot really validate the mechanical model since the effects of the variations of MFA and lignin content cannot be tested independently. Moreover, a very good cor-

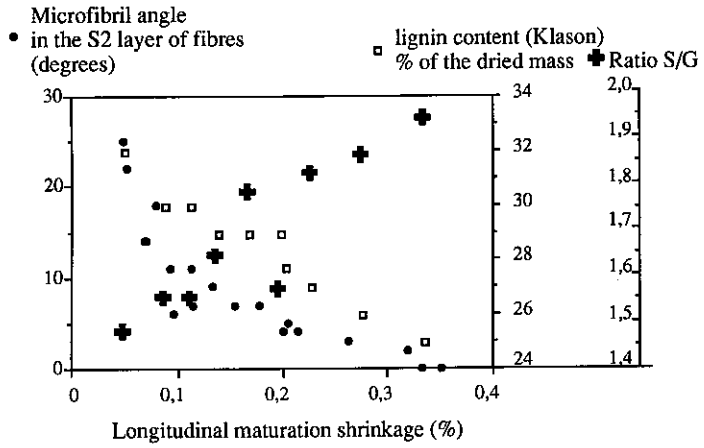


**Fig. 8.** Relations between longitudinal maturation and some histological features—the microfibril angle (MFA), lignin content, and monomeric composition—in clones of *Eucalyptus* (Congo, Africa). (From Baillères, 1994; Baillères *et al.*, 1994.)

relation between the longitudinal maturation strain and the monomeric composition of lignins (the ratio of syringil-to-gaiacyl units; S/G) has been found (Fig. 8). This correlation is difficult to explain from a mechanical model. It could be explained by variations of the mechanical properties of the lignin matrix due to monomeric composition (direct physical cause) but also by a more complicated correlation between the S/G ratio and the microfibril angle (or the lignin content) due to biological mechanisms related to the cambial activity and the secondary wall formation and lignification.

We now focus on biomechanical models of regulation. Two examples are studied: Mattheck's "constant stress" growth and the regulation of lean by the differentiation of heterogeneous wood.

## BIOMECHANICAL MODELS OF REGULATION

These models assume, in addition to the mechanical model, biological control of output (i.e., control of strained forms, supported stresses, safety factors, etc.).

Since trees seems to grow faster in diameter when they are loaded, cambial growth can be postulated to be proportional to the stress level at the stem periphery. From a mechanical model giving the distribution of stresses from the applied loads and the stem geometry, the more stressed zones are assumed to grow faster, and thus the distribution of growth along and around the stem is modeled. From this idea, Mattheck (1990a–d; Mattheck and Korseka, 1989;

Mattheck and Prinz, 1991; Mattheck, in press) developed a finite element method for computing shapes of trees or of parts of trees. It has been applied to study forks, branch joints, welds, stems near stakes and buttresses loaded by bending forces, wounds submitted to tensile surface stresses, and mechanical contacts at the tree surface (stones, other trees). The level of stress is characterized by the Von Mises stress, which is independent of the material direction, usually not used by engineers in highly anisotropic materials such as wood. However, in each case, the computed form is checked to be in good visual agreement with the natural form observed.

Another example comes from compression (resp. tension) wood on the lower (resp. upper) side of leaning trunks or branches of gymnosperms (resp. angiosperms), associated with high asymmetry of maturation strains, as shown in our previous biomechanical characterization. From our preliminary mechanical analysis (see the Appendix), we know that this asymmetry (represented by a parameter $\alpha_1$) allows the stem to bend upward and we can compute the successive forms of the growing leaning stem, loaded by gravitational forces and maturation prestresses, if the value of $\alpha_1$ is given at each step of growth. We can estimate $\alpha_1$, independently of the mechanical computation, by measurements of released strains or observations of histological features. But $\alpha_1$ can also be modeled assuming that the formation of reaction wood is locally related to the stem lean. When this lean overcomes a given value, reaction wood is differentiated to restore the stem verticality, and thus $\alpha_1$ becomes different from zero. The sign of $\alpha_1$ is given by the sign of the lean. Its intensity has been assumed from different laws: (i) a given value (based on the assumption of a unique "quality" of reaction wood), (ii) a value proportional to the lean, (iii) a value proportional to the velocity of the lean variation, and (iv) a combination of the last two factors.

We applied this model (under the simplest assumption, i) to the description of the reactions of a young maritime pine artificially tilted (Fournier and Chanson, 1994). The results (Fig. 9) show a good qualitative agreement with the experiment: First, the whole stem bends and compression wood is formed on the lower side. The base goes on bending up, while the top straightens itself by bending down forming compression wood on the upper side. However, in the model the overcorrection is activated when the stem passes the vertical, while in the experiment the top of the plant anticipates the curvature of the base and begins to bend down when the whole stem is still severely tilted. Moreover, the model underestimates the curvatures of the base and overestimates those of the top. Therefore, the necessity for a more complicated regulation law (iv) is demonstrated. The parameters that govern such a law remain to be determined.

Finally, the regulation has been based on the cambial perception of lean (graviperception). However, a perception of stresses or strains, or an apical perception diffused along the stem, could also be tested. We prefer the first one

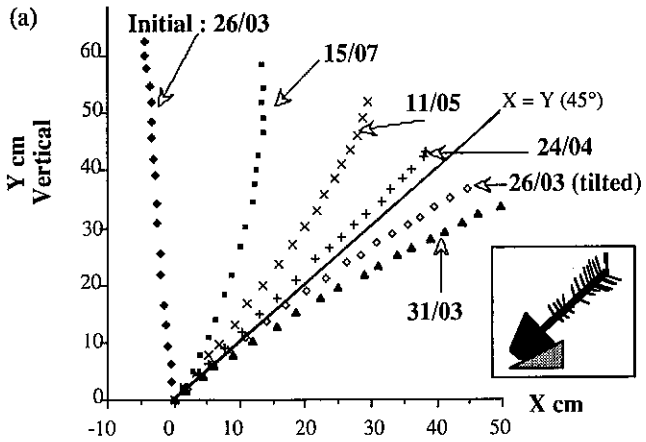


**Fig. 9.** Biomechanical regulation of lean on a *Pinus pinaster* Ait. artificially tilted. (a) Observed successive forms, from digitized photographs; (b) observed distributions of compression wood (C.W.) (drawn from microscopic observations) (c) simulation by the biomechanical model of both righting movements and formation of C.W. The asymmetry of maturation strains $\alpha_t$ is 0.25%; the mean radial growth and diameters were measured on the previous drawings, at five heights. Computations use 10 spatial elements and 10 temporal units of growth, and thus the See Loup *et al.* (1991) for more details about a and b.

since it fits most of the experiments that have been done on conifers [artificial leans, loops (Timell, 1987)]. For example, we observed that an artificially tilted but not stressed (sustained in a pipe) stem of maritime pine differentiates compression wood associated with a high asymmetry of maturation strains (Chanson and Fournier, unpublished).

## FUNCTIONAL INTERPRETATION OF BIOMECHANICAL MODELS OF REGULATION

A further problem is to ask whether the regulation leads to or restores a characteristic mechanical state. For example, Mattheck's model leads to a morphology where peaks of stress at the stem periphery are avoided since the faster growth in more loaded areas homogenizes the distribution of loads. As a consequence, the safety factor (i.e., the ratio between the critical stress at failure and the supported stress) is kept constant along and around the stem periphery. Such a mechanical state is called "constant stress design." Our model refers to an equilibrium lean, which we assumed to be vertical in our example, but it could be oblique or horizontal for branches (Sinott, 1952). Hence, the mechanism of regulation generally induces peculiar mechanical states.

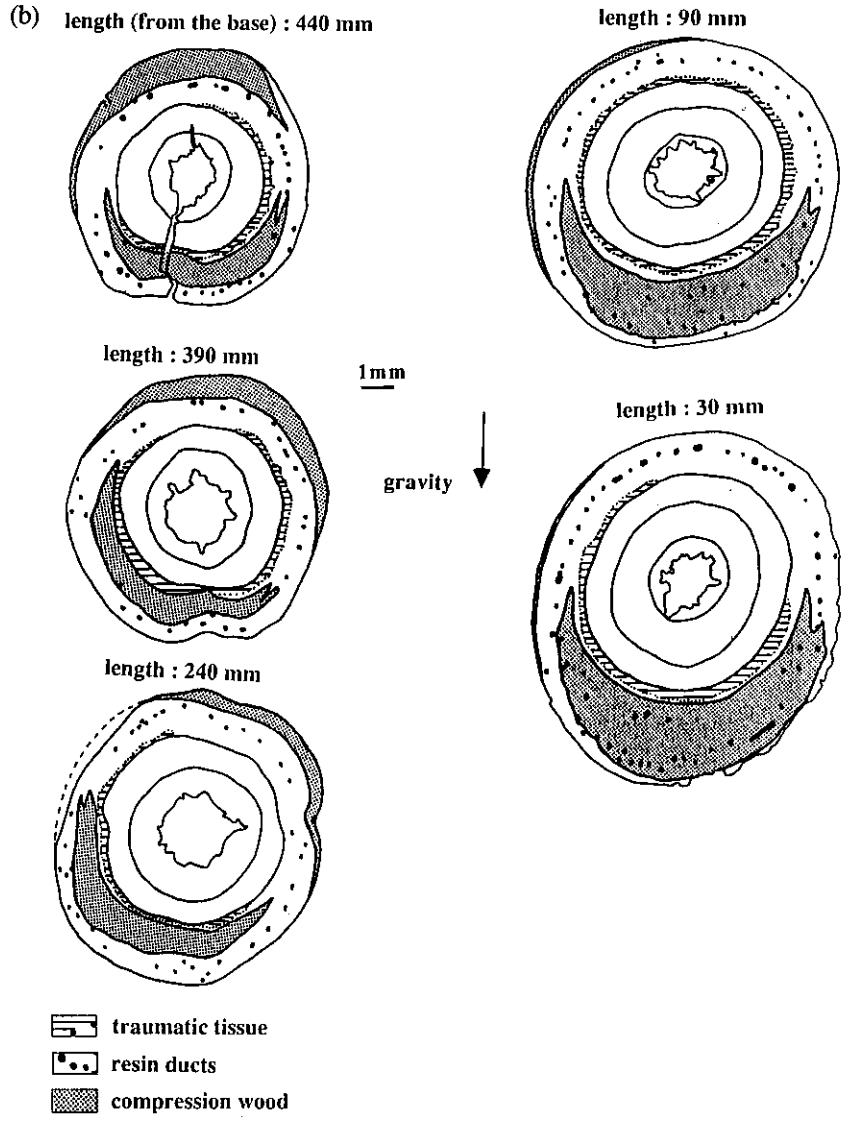


**Fig. 9.** Continued.

These mechanical states can be interpreted as "targets," which can be related to principles of economy or efficiency (optimal design). Constant stress design usually ensures the minimal quantity of material required, for a given level of this safety factor and a given load (Fleury, 1978). Actually, Mattheck

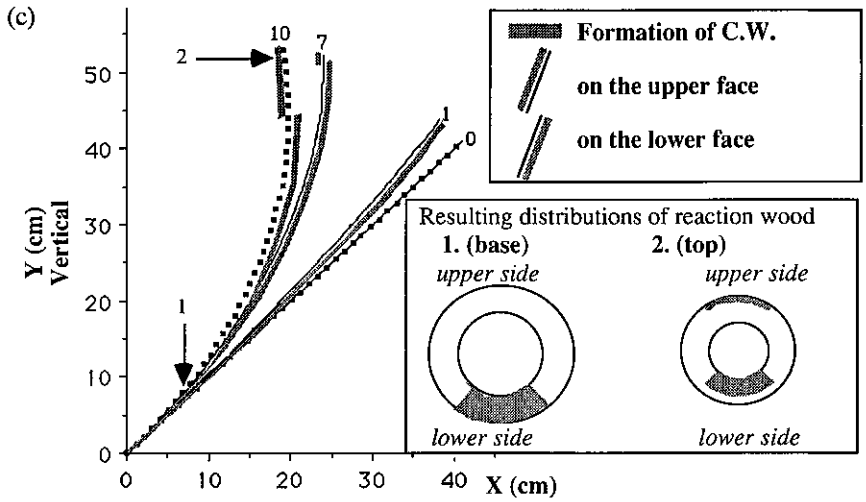


**Fig. 9.** Continued.

put the emphasis on the optimality of the computed morphologies toward this principle of both economy (minimal quantity of material) and efficiency (given level of safety factor). Concerning our second example, the vertical position of our model is also a mechanical advantage for a trunk since it minimizes the bending moments due to weights and the risks of torsional strains in the case of lateral winds.

However, optimality is a deep problem in biology. Its interpretation as a consequence of a neo-Darwinian process of adaptation is usually the matter of deep discussion (Maynard Smith, 1978; Givnish, 1986; Gould, 1986; Niklas, 1988). Therefore, the existence of a mechanical target cannot be proved by a simple principle of efficiency and economy and must be validated carefully.

## CONCLUSION

We have tried to organize and summarize the biomechanics of tree growth, mainly at the level of the organ (the stem). As these studies require the use of both mechanical and biological concepts and methods, three methodological steps have been carefully distinguished, from classical mechanical analysis (which includes, however, the surprising effects of radial growth) to the more original biomechanics of regulation. This last step is much more ambitious than the first approach, as it aims at predicting the geometry of the structure or the mechanical properties of materials (which are data and not results in the preliminary mechanical problems). However, the hypothesis of a biological control

must be assumed and validated. Up to now, biomechanical models of regulations are based on very simple hypotheses, while the biological control of growth and differentiation is obviously much more complex.

The biomechanics of tree growth and wood formation provides methods of analysis as well as practical results for forestry, wood technology, and arboriculture. The biomechanical analysis of the righting movements of an artificial stem, in relation to the formation of reaction wood, could be the basis of a test for breeding selection applied to the ligniculture of pines, poplars, eucalyptus, etc., where reaction wood due to a gravitropic response and associated great curvatures of trunks are supposed to be responsible for a lower quality of trees.

Finally, trees are interesting plants to perform biomechanical investigations, since wood has a tremendous memory, which allows one to read a *posteriori* the plant's reactions.

## APPENDIX: LONGITUDINAL PRESTRESSES AND ASSOCIATED BENDING MOVEMENTS

This Appendix develops the mechanical model of longitudinal strains and prestresses due to the cellular maturation of a new peripheral thin layer. This model allows calculation of the reorientation (curvature) of the stem due to asymmetry of maturation strains, taking into account the geometry (radius and thickness of the peripheral layer) of the stem.

Assuming that between $t$ and $t + dt$, a new layer of wood (thickness $dR$) has been added on the surface of the tree (radius $R$), and that stresses other than longitudinal are of negligible magnitude, unidirectional, very simple behavior laws can be written as

$$\partial\sigma_L^* = E(\epsilon_L - \alpha_L \Delta M) = E(\epsilon_L - \alpha_L) \qquad \text{in the new layer} \qquad (1)$$

$$\partial\sigma_L = E(\epsilon_L) \qquad \text{in the older wood} \qquad (2)$$

where $E$ is the longitudinal Young's modulus, $\alpha_L$ is the tendency of the new layer to shrink longitudinally during cellular maturation, and $\partial\sigma_L$ and $\epsilon_L$ are, respectively, the incremental stresses and strains in the stems between $t$ and $t + dt$.

Then assuming that the experimentally observed datum $\alpha_L$ varies with the angular position $\theta$ as

$$\alpha_L(\theta) = \alpha_0 + \alpha_1 \sin\theta \qquad (3)$$

and that the cross section remains plane so that $\epsilon_L$ varies linearly along the $y$ axis ($y = r \sin\theta$),

$$\epsilon_L(r, \theta) = \epsilon_0 + \epsilon_1 \frac{r}{R} \sin\theta \qquad (4)$$

behavior laws can be rewritten as

$$\partial\sigma_L^* = -E[(\alpha_0 - \epsilon_0) + (\alpha_1 - \epsilon_1)\sin\theta] \quad \text{in the new layer} \quad (r = R) \tag{5}$$

$$\partial\sigma_L = E\left(\epsilon_0 + \epsilon_1 \frac{r}{R}\sin\theta\right) \quad \text{in the older wood} \quad (r < R) \tag{6}$$

Thus, $\epsilon_1$ follows from the equilibrium of bending moments within the cross section:

$$\int_0^{2\pi}\int_0^R \partial\sigma_L r \sin\theta\, r\, dr\, d\theta + \int_0^{2\pi} \partial\sigma_L^* R \sin\theta (R\, dR\, d\theta) = 0 \tag{7}$$

so (by replacing $\partial\sigma_L$ and $\partial\sigma_L^*$ by their above-written expressions and after integrating)

$$\epsilon_1 = 4\frac{dR}{R}\alpha_1 \tag{8}$$

Note that $\epsilon_1 \ll \alpha_1$ (it could be shown as well that $\epsilon_0 \ll \alpha_0$) since $dR \ll R$. Therefore,

$$\partial\sigma_L^* = -E[\alpha_0 + \alpha_1 \sin\theta] = -E\alpha_L \tag{9}$$

Maturation strains are entirely impeded and converted into stresses in the new thin layer. The variation of curvature is finally,

$$\partial C = \frac{\epsilon_1}{R} = 4\frac{dR}{R^2}\alpha_1 \tag{10}$$

## REFERENCES


Archer, R. R. (1986). *Growth Stresses and Strains in Trees*, Springer Series in Wood Science, Timell, E. (ed.), Springer Verlag, New York.

Archer, R. R. (1987). On the origin of growth stresses in trees. 1. Micromechanics of the developing cambial cell wall. *Wood Sci. Tech.* **21**:139–154.

Archer, R. R. (1988). On the origin of growth stresses in trees. 2. Stresses generated in a tissue of developing cells. *Wood Sci. Tech.* **23**:311–322.

Archer, R. R., and Byrnes, F. E. (1974). On the distribution of tree growth stresses. 1. An anisotropic plane strain theory. *Wood Sci. Tech.* **8**: 184–196.

Baillères, H. (1994). *Précontraintes de Croissance et Propriétés Mécanophysiques de Clones d'Eucalyptus (Pointe Noire—Congo): Hétérogénéités, Correlations et Interprétations Histologiques*, Thèse de Doctorat, University of Bordeaux 1; Bordeaux.

Baillères, H., Chanson, B., Fournier, M., Tollier, M. T., and Monties, B. (1994). Structure composition chimique et retraits de maturation du bois chez des clones d'Eucalyptus. *Ann. Sci. Forest.* (in press).

Bamber, R. K. (1987). The origin of growth stresses: A rebuttal. *IAWA Bull.* **8**(1):80–84.
Barber, N. F., and Meylan, B. A. (1964). The anisotropic shrinkage of wood: A theoretical model. *Holzforschung* **18**:146–156.
Barrett, J. F. (1973). *Theoretical Models of Wood Shrinkage and Elasticity*, Ph.D. thesis, University of California, Berkeley.
Bell, A. (1991). *Plant Form. An Illustrated Guide to Flowering Plant Morphology*, Oxford University Press, Oxford.
Bertram, J. E. A. (1989). Size-dependent differential scaling in branches: The mechanical design of trees revisited. *Trees* **4**:241–253.
Boyd, J. D. (1972). Tree growth stresses. Evidence of an origin in differentiation and lignification. *Wood Sci. Tech.* **6**:251–262.
Cannell, M. G. R., and Morgan, J. (1989). Branch breakage under snow and ice loads. *Tree Physiol.* **5**:307–317.
Castera, P., and Morlier, V. (1991). Growth patterns and bending mechanics of branches. *Trees* **5**:232–238.
Cave, I. D. (1968). The anisotropic elasticity of the plant cell wall. *Wood Sci. Tech.* **2**:268–278.
Chanson, B. (1993). Déformation de maturation: Hétérogénéités angulaires en fonction du plan d'organisation des arbres. *Acta Bot. Gallica* **140**(4):395–401.
Chanson, B., Dhote, J. F., Fournier, M., and Loup, C. (1992). Dynamique des contraintes de croissance dans le bois de hêtre sur pied, en liaison avec la morphologie de l'arbre et l'expansion du houppier. *Rapport intermédiaire de la Convention ONF-INRA 12-90/03*, INRA, Nancy, France.
Dean T. J., and Long, J. N. (1986). Validity of constant-stress and elastic-instability principles of stem formation in *Pinus contorta* and *Trifolium pratense*. *Ann. Bot.* **58**:833–840.
Edelin, C. (1989). Données fondamentales d'Architecture des plantes. In Thibaut, B. (ed.), *Proceedings of the first Seminar "Architecture, structure, mécanique de l'Arbre,"* Montpellier, LMGC, University of Montpellier II, Montpellier.
Esser, M. H. M. (1946). Tree trunks and branches as optimum mechanical supports of the crown. I. The trunk. *Bull. Math. Biophys.* **8.**
Fisher, J., and Wassmer-Stevenson, J. (1981). Occurrence of reaction wood in branches of dicotyledons and its role in tree architecture. *Bot. Gaz.* **142**(1):82–95.
Fleury, C. (1978). *Le Dimensionnement Automatique des Structures Élastiques.*, Thèse Doct. Sc. Appl., Université de Liège, Belgium.
Fournier, M. (1989). *Mécanique de l'Arbre. Maturation, Poids Propre, Contraintes Climatiques dans la Tige Standard*, Thèse de Doctorat, Institut National Polytechnique de Lorraine, Nancy, France.
Fournier, M., and Chanson, B. (1994). Mécanique des structures évolutives et auto-adaptatives, le cas des arbres. 2. Modélisation biomécanique de la régulation de l'inclinaison d'un Pinus pinaster artificiellement incliné. In Thibaut, B. (ed.), *Proceedings of the Fifth Seminar "Architecture, Structure, Mécanique de l'Arbre,"* Montpellier, LMGC, University of Montpellier II, Montpellier.
Fournier, M., and Moulia, B. (1994). Mécanique des structures évolutives et auto-adaptatives, le cas des arbres. 1. Définitions biomécaniques. In Thibaut, B. (ed.) *Proceedings of the Fifth Seminar "Architecture, Structure Mécanique de l'Arbre,"* Montpellier, LMGC, University of Montpellier II, Montpellier.
Fournier, M., Bordonné, P. A., Guitard, D., and Okuyama T. (1990). Growth stress patterns in tree stems: A model assuming evolution with the tree age of maturation strains. *Wood Sci. Tech.* **24**:131–142.
Fournier, M., Chanson, B., Guitard, D., and Thibaut, B. (1991a). Mécanique de l'arbre sur pied: Modélisation d'une structure en croissance soumise à des chargements permanents et évolutifs. I. Analyse des contraintes de support. *Ann. Sci. Forest.* **48**:513–525.
Fournier, M., Chanson, B., Thibaut, B., and Guitard, D. (1991b). Mécanique de l'arbre sur pied: Modélisation d'une structure en croissance soumise à des chargements permanents et évolutifs. II. Analyse tridimensionnelle des contraintes de maturation—cas du feuillu standard. *Ann. Sci. Forest.* **48**:527–546.
Fournier, M., Moulia, B., Chanson, B., and Thibaut, B. (1992). Trees stems mechanics: A study

of loads and forms of a biological growing structure. In Motro, R. (ed.), *Proceedings of the 1° International Seminar on Structural Morphology*, LMGC, University of Montpellier II, France.

Fournier, M., Rogier, P., Costes, E., and Jaeger, M. (1993). Modélisation mécanique des vibrations propres d'un arbre soumis aux vents, fonction de sa morphologie. *Ann. Sci. Forest.* **50**:401–412.

Fournier, M. Chanson, B., Thibaut, B., and Guitard, D. (1994). Mesures des déformations résiduelles de croissance à la surface des arbres. Observations sur différentes espèces. *Ann. Sci. Forest.* **51**(2) (in press).

Gibson, L. J., and Ashby, M. F. (1988). *Cellular Solids. Structure & Properties*, Pergamon Press, London.

Givnish, T. J. (1986). In Givnish, T. J. (ed.), *On the Economy of Plant Form and Function*, Cambridge University Press, Cambridge.

Gould, S. J. (1986). Archetype and adaptation. *Nat. Hist.* **10/86**:16–27.

Grace, J. (1977). *Plant Response to Wind*, Academic Press, London,, New York, San Francisco.

Greenhill, A. G. (1881). Determination of the greatest height consistent with stability that a vertical pole or mast can be made, and of the greatest height to which a tree of given proportions can grow. *Proc. Phil. Soc.* **4**:65–73.

Kellog, R. M., and Steucek, G. L. (1977). Motion-induced growth effect in Douglas fir. *Can. J. Forest Res.* **7**:94–99.

Kellog, R. M., and Steucek, G. L. (1980). Mechanical stimulation and xylem production in Douglas fir. *Forest Sci.* **26**:643–651.

King, D., and Loucks, O. L. (1978). The theory of tree bole and branch form. *Radiat. Environ. Biophys.* **15**:141–165.

Koizumi, A., and Ueda, K. (1986). Estimation of the mechanical properties of standing tree by bending tests. I. Test method to measure the stiffness of a tree trunk. *Mokuzai Gakkaishi* **32**(9):669–676.

Langbour, P., Fournier, M., and Guitard, D. (1988). Etat mécanique d'un tronc d'arbre forestier: Rigidité à la flexion. *Actes du Colloque Scientifique Européen "Rhéologie du Bois,"* GS Rhéologie et Mécanique du Bois, LRBB, Cestas, France.

Larson, P. R., (1963). Stem form development of forest trees. *Forest Sci.* Monogr. 5.

Larson, P. R. (1965). Stem form of young *Larix* as influenced by wind and pruning. *Forest Sci.* **11**:413–424.

Lekhnitskii, S. G. (1963). *Theory of Elasticity of an Anisotropic Elastic Body*, Holden-Day, San Francisco.

Loup, C., Fournier, M., and Chanson, B. (1991a). Relations entre architecture, mécanique et anatomie de l'arbre: Cas d'un Pin maritime (*Pinus pinaster* Ait.). L'arbre, biologie et développement, *Naturalia monspelliensia* n° h.s., Ed. C. Edelin.

Loup, C., Fournier, M., Chanson, B., and Moulia, B. (1991b). Redressements, contraintes de croissance et bois de réaction dans le bois d'un jeune *Pinus pinaster* Ait. artificiellement incliné. In Thibaut, B. (ed.), *Proceedings of the Third Seminar "Architecture, Structure, Mécanique de l'Arbre,"* Montpellier, LMGC, University of Montpellier II, Montpellier.

McMahon, T. (1975). The mechanical design of trees. *Sci. Am.* **233**:92–102.

Maiti, M., and Adams, S. F. (1968). Isotropy at the center of a cylindrical wood pole. *Wood Sci. Tech.* **2**:44–45.

Mamada, S., Kawamura, Y., Yashiro, M., and Taniguchi, T. (1984). The strength of plantation Sugi trees. *Mokuzai Gakkaishi* **30**(7):530–537.

Mark, R. E., (1967). *Cell Wall Mechanics of Tracheids*, Yale University Press, New Haven, CT.

Martley, J. F. (1928). Theoretical calculation of the pressure distribution on the basal section of a tree. *Forestry* **2**(1):69–72.

Mattheck, C. (1990a). Engineering components grow like trees. *Mat.-wiss. Werkstofftech.* **21**:143–168.

Mattheck, C. (1990b). Design and growth rules for biological structures and their application to engineering. *Fatigue Frac. Eng. Mater. Struct.* **13**(5):535–550.

Mattheck, C. (1990c). Why they grow, how they grow: The mechanics of trees. *Arbor. J.* **14**:1–17.

Mattheck, C. (1990d). A new method of structural shape optimization based on biological growth. *Int. J. Fatigue* **12**(3):185–190.
Mattheck, C. (1991). *Trees: The Mechanical Design*, Springer-Verlag, Berlin.
Mattheck, C. (in press). *Biomimetics*.
Mattheck, C., and Korseka, G. (1989). Wound healing in a plane (*Platanus acerifolia* (Ait.) Willd.). An experimental proof of its mechanical simulation. *Arbor. J.* **13**:11–218.
Mattheck, C., and Prinz, M. (1991). Buttress roots: Why they grow and what they are good for. Internal Report. Karlsruhe Nuclear Research Centre.
Maynard Smith, J. (1978). Optimization theory in evolution. *Annu. Rev. Ecol. Syst.* **9**:31–56.
Metzger, K. (1893). Der Wind als massgebender Faktor für das Wachsthum der Baüme. *Mündener forstl.* **3**:35–86.
Milne, R. (1991). Dynamics of swaying of *Picea sitchensis*. *Tree Physiol.* **9**:383–399.
Nakatani, H., Kato, A., Taira, H., Lijima Y., and Sawada, M. (1984). Deflection and resistance performance of tree stems subjected to snowloads in Sugi stands. *Mokuzai Gakkaishi* **30**(11):886–893.
Niklas, K. J. (1988). Biophysical limitations on plant form and evolution. In Gottlieb, L. D., and Jain, S. K. (ed.), *Plant Evolutionary Biology*, Chapman and Hall, London, pp. 185–220.
Okuyama, T., Sugihama, K., Yamamoto, H., and Yoshida, M. (1993). Generation process of growth stresses in cell wall: Relation between longitudinal released strain and chemical composition. *Wood Sci. Tech.* **27**:257–262.
Osawa, A. (1993). Effects of mechanical stresses and photosynthetic production on stem form development of *Populus maximowiczii*. *Ann. Bot.* **71**:489–494.
Quirk, J. T., and Freeze, F. (1976a). Effect of mechanical stress on growth and anatomical structure of red pine (*Pinus resinosa* Ait.): Compression stress. *Can. J. Forest Res.* **6**:195–202.
Quirk, J. T., and Freeze, F. (1976b). Effect of mechanical stress on growth and anatomical structure of red pine (*Pinus resinosa* Ait.): Stem vibration. *Can. J. Forest Res.* **6**:375–381.
Quirk, J. T., Smith, D. M., and Freese, F. (1975). Effect of mechanical stress on growth and anatomical structure of red pine (*Pinus resinosa* Ait.): Torque stress. *Can. J. Forest Res.* **5**:691–699.
Radi, M. (1992). *Analyse Morphologique de l'Arbre en Vue de sa Modélisation Mécanique*, Thèse de Doctorat, University of Bordeaux 1, Bordeaux.
Schaeffer, B. (1990). Forme d'équilibre d'une branche d'arbre. *C. R. Acad. Sci. Paris* **311**(II): 37–43.
Schwendener, S. (1884). *Das mechanische Prinzip im anatomischen Bau des Monocotylen*, Wihelm Engelmann, Leipzig.
Scurfield, G. (1973). Reaction wood: Its structure and function. *Science* **179**:647–655.
Sinnott, E. W. (1952). Reaction wood and the regulation of tree form. *Am. J. Bot.* **39**:69–78.
Tateno, M. (1991). Increase in lodging safety factor of thigmomorphogenically dwarfed shoots of mulberry tree. *Physiol. Plant.* **81**:239–243.
Tateno, M., and Bae, K. (1990). Comparison of lodging safety factor of untreated and succinic acid 2,2-dimethylhydrazide-treated shoots of mulberry tree. *Plant Physiol.* **92**:12–16.
Telewski, F. W., and Jaffe, M. J. (1986a). Thigmomorphogenesis: Field and laboratory studies of *Abies fraseri* in response to wind or mechanical perturbation. *Physiol. Plant.* **66**:219–226.
Telewski, F. W., and Jaffe, M. J. (1986b). Thigmomorphogenesis: Anatomical, morphological and mechanical analysis of genetically different sibs of *Pinus taeda* in response to mechanical perturbation. *Physiol. Plant.* **66**:219–226.
Telewski, F. W., and Jaffe, M. J. (1986c). Thigmomorphogenesis: The role of ethylene in the response of *Pinus taeda* and *Abies fraseri* to mechanical perturbations. *Physiol. Plant.* **66**:227–233.
Timell, T. E. (1987). *Compression Wood in Conifers*, Springer Series in Wood Science; Springer Verlag, Berlin.
Vieville, P. (1992). *Influence des Paramètres Architecturaux sur les Caractéristiques Viscoélastiques du Bois à Ses Différentes Échelles d'Hétérogénéités*, Thèse de Doctorat, Institut National Polytechnique de Lorraine, Nancy, France.
West, P. W., Jackett, D. R., and Sykes, S. J. (1989). Stresses in, and the shape of, tree stems in forest monoculture. *J. Theor. Biol.* **140**:327–343.

Wilson, B. F., and Archer, R. R. (1979). Tree design: Some biological solutions to mechanical problems. *Bioscience* **29**(5).

Yamamoto, H., and Okuyama, T. (1988). Analysis of the generation process of growth stresses in cell walls. *Mokuzai Gakkaishi* **34**:788–793.

Zobel, B. J., and van Buijtenen, J. P. (1989). *Wood Variation. Its causes and control*, Springer Series in Wood Science, Springer-Verlag, Berlin.

*Biomimetics, Vol. 2, No. 3, 1994*

# Stem and Root Tree Architecture: Questions for Plant Biomechanics[1]

**C. Edelin[2] and C. Atger[2,3]**

*The analysis of the architecture and ontogenesis of trees reveals growth processes which bring into play the mechanical reaction of the organism. We present some of these processes concerning both shoot and root systems. The problems they entail might serve as study models for biomechanics.*

**KEY WORDS:** tree architecture; development; stems; roots.

## INTRODUCTION

Trees are branched organisms. Growing from a fixed point, the collar, they develop below and above the ground a system of axes which is grouped in three parts: the crown, the trunk, and the root system. The stability of the whole system, which can be huge, is devoted to support tissues which are variously located on axes, wood being functionally the most important of these tissues. The knowledge of wood properties is essential for understanding the mechanics of a tree and is the subject of numerous studies (Kollmann *et al.*, 1968). However, this knowledge is not enough to illustrate the way by which a plant organism supports itself. The development of wood, its location, and its structure are the tree's adaptative response to mechanical problems inherent in its architecture and vary with its immediate needs. This tissue has been selected during evolutionary processes because of its efficiency to solve problems, but it is an executor and not a cause. We will understand its role better when these mechanical problems are clearly exposed.

[1]This is the published version of a paper presented at the Plant Biomechanics Congress, Montpellier, France, September 5-9, 1994.

[2]Laboratoire de Botanique, CNRS URA 327, 163 rue Broussonet, 34000 Montpellier, France.
[3]To whom correspondence should be addressed.



1059-0153/94/0900-0253$07.00/0 

In studies on whole-tree mechanics, the plant is often considered as a simple geometrical shape quite far from the botanical reality. This reduction is justifiable for the needs of modeling, but we think that, far from being a difficulty, to take into account the real tree shape is, on the contrary, a sign of progress. By posing new problems, this approach can stimulate reflection, open new fields of research, or give some interesting information that leads to a better view of problems already in course of study. That is why, in this paper, we present real phenomena of tree mechanics which, to our knowledge, have not been already studied. First, we analyze some problems inherent in shoot and root systems; second, we try to replace them on a larger scale of reflection.

## VARIOUS MECHANICAL PROBLEMS ENCOUNTERED IN SHOOT SYSTEMS

### Growth and Straightening Up

Trunk or branches straightening up is a frequent phenomenon that has been little studied. It occurs frequently, without any trauma, during the ontogeny of numerous species and allows the tree to express its specific architecture. Two examples taken from tropical trees allow us to illustrate different ways of becoming erect.

#### *The Erection of Tree Trunks in Troll's Model*

Architectural models (Hallé *et al.*, 1978) are fundamental shapes which can be encountered in the plant kingdom. There are about 20 which account for all the known species. Architectural models are based on the analysis of some fundamental characters which establish the tree shape: pattern of branching, pattern of growth, growth direction of axes, and location of flowers. One of the most frequent is the Troll model. According to its definition, plants conforming to this model are built with plagiotropic axes only, growing in a horizontal direction. Such a direction, which concerns branches as well as the trunk, seems at first sight to be incompatible with arborescent status. However, some of the biggest trees in the plant kingdom conform to this model, such as *Koompasia malaccensis*, which, with its height of 70 m, dominates the forest in Malaya. To gain in height, trees conforming to the Troll model have developed various growth strategies, some of which involve mechanical problems. We study these processes on *Muntingia calabura*.

*Muntingia calabura* (Elaeocarpaceae) is a small tree from Central America, widespread in the tropics. It is usually named the cherry tree. The young individual (Fig. 1a) is composed of a monopodial first-order axis (A1), with distichous phyllotaxis: Leaves are placed on a horizontal plane, alternately at the

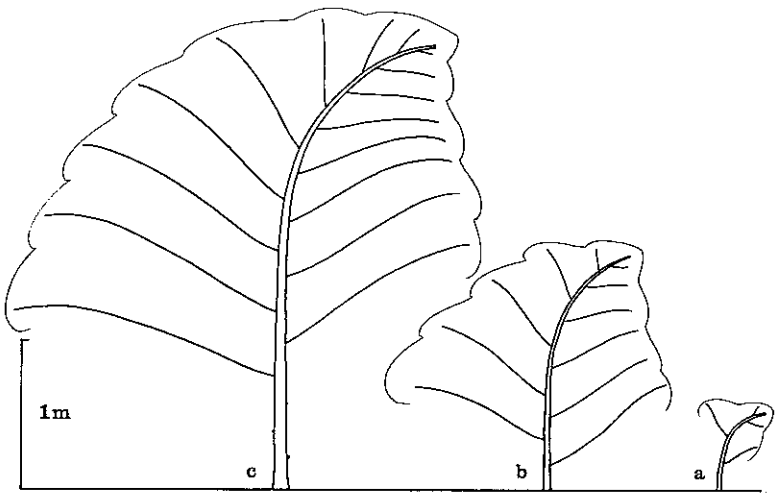


**Fig. 1.** Three stages in the development of *Muntingia calabura*.

right and the left side of the bearing axis. The base of this axis is vertical (orthotropic); its distal part is horizontal (plagiotropic). This growth direction is the result of the apical meristem activity. After germination, the apical meristem grows orthotropically a few centimeters. This way of growing allows the axis to emerge from the soil, then its direction changes and it becomes plagiotropic: It grows perpendicularly to the gravity gradient.

When the tree reaches 1 or 2 m in height (Fig. 1b), its trunk bears long branches alternately disposed to the left and the right side of the bearing axis. These branches are disposed in a horizontal plane. They are composed of three orders of axes, all disposed in the same horizontal plane. The trunk is vertical except for its distal part, which is horizontal and illustrates the plagiotropic behavior of its apical meristem.

The adult does not exceed 10 m in height (Fig. 1c). Its trunk bears long plagiotropic branches composed of five orders of axes, the most peripheral order bearing lateral flowers. The trunk is vertical to oblique for the first two-thirds of its length and then its apex is horizontal. During the later stage, the latter grows definitively plagiotropically. In this species, the development of an orthotropic trunk is a consequence of the main axis straightening up. This phenomenon occurs 10 cm behind the apex. It begins exactly in a zone where the leaves begin to fall as a consequence of cambial growth: It is a process linked to wood formation.

Many trees conforming to the Troll model show such a development. Secondary from the viewpoint of morphogenesis, this process is of great importance because it allows the tree to gain in height. It depends on the surrounding

conditions: When the tree grows in open light, growth stops quickly and the tree remains small. On the other hand, in a dense population, growth goes on for a long time: The trunk is vertical for the greater part of its length, and only its tip when located in the forest canopy is horizontal.

### *The Turning-Up of Branches*

Some trees conform to the same architecture all their life. Others change in growth patterns during their ontogenesis. In those trees that show metamorphosis (Edelin, 1990), one very important process that accompanies such a transformation is the progressive setting-up of branches when they become larger and larger and more and more branched, as can be seen, for example, in *Shorea leprosula*.

Young *S. leprosula* has an architecture conforming to Roux's model. A monopodial orthotropic trunk bears plagiotropic branches subtended by each leaf axil (Figs. 2a and b). These branches are made of two types of axis (Fig. 2c); the second-order axis (A2) is horizontal to oblique, with distichous phyllotaxis. It is branched in one plane. Its third-order laterals (A3) are also pla-

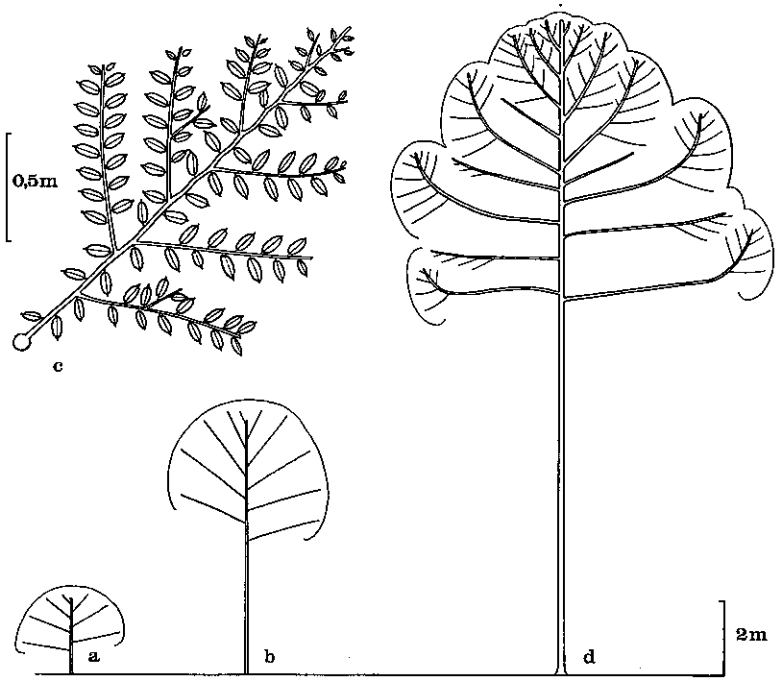


**Fig. 2.** (a, b, d) Three stages in the development of *Shorea leprosula*; (2c) view of a plagiotropic branch.

giotropic, with distichous phyllotaxis. They are short-lived and remain unbranched.

At the top of the trunk, the branching angle is more acute and branches are oblique. Nevertheless, they become nearly horizontal away from their apices. This event is not the consequence of simple drooping. The branching angle varies during the first stages of cambial growth of the trunk.

When the tree reaches 10 to 20 m in height (Fig. 2d), its architecture is different. Its crown is composed of three types of branches. The first is plagiotropic branches, with three orders of axis. They are quite short and similar to those already described. The second is orthotropic branches, which develop from the upper part of the trunk. They are vertical and their branching angle is acute and remains constant during the cambial growth of the trunk. Nevertheless, during their growth they subside later, so that, finally, their distal part becomes oblique. These branches have a spiral phyllotaxis and their branching is continuous and radial. They bear plagiotropic order 3 and 4 axes. The third type is architecturally intermediate between the first two. Their orientation and their organization change during their ontogenesis. At its basal part, the order 2 axis, A2, is plagiotropic; its branching angle is wide and its phyllotaxis is distichous. It bears twigs disposed on a horizontal plane. At its distal part, the order 2 axis is orthotropic and its growth direction vertical. Its phyllotaxis is spiral and its branching is continuous and radial. The connection zone between these two parts is short. The turning-up takes place on only a few internodes.

When these branches are disposed at the base of the crown, the connection zone between the orthotropic and plagiotropic parts is located near the end of the branches. When these branches are located in the middle of the crown, the change of orientation takes place earlier. In older trees these intermediate branches disappear: Mostly orthotropic branches occur, separated here and there by a few plagiotropic branches, which soon fall. The turning-up observed in *S. leprosula* is a process which accompanies axial growth. It differs from the situation described in Troll's model by the fact that it takes place in the growing end, and not behind it. It originates in apical meristem activity and is reinforced later by wood development.

## The Strengthening of Branches

The mechanical stability, or even the integrity, of the organism may be endangered by the development of certain formations inside the crown of trees. For example, an abnormally heavy load of fruits can cause a branch to break. As soon as there is a change in the mechanical balance of the crown, the tree generally reacts by reinforcing its existing structure. Provided that the reaction is quick and intense enough, it manages to compensate for the mechanical loss of balance which has begun to appear. This adaptive process occurs continually

in the life of the organism and even plays an essential part for certain species. We illustrate such a phenomenon with the example of the crown development of *Virola surinamensis* (Barthélémy *et al.*, 1991).

*Virola surinamensis* is a tree growing in the swamp forest of Amazonia. It can reach a height of 35 m and form a crown 25 m in diameter. The architecture of the young tree conforms to Massart's model: The trunk is an orthotropic monopodium which bears whorls of regularly spaced plagiotropic branches (Figs. 3a and b). Its structure changes completely on becoming an adult. At this stage we can observe small trees developing from resting buds located on the large plagiotropic branches growing on the upper part of the crown (Fig. 3c). They are easy to recognize in the crown, as the vertical orientation of their small trunk contrasts with the horizontal direction of its bearing branches. They develop quickly, and after a few years each one makes a heavy load for its bearing branch. The latter reacts by increasing its diameter in its basal part to maintain it in a horizontal position. On the other hand, the end part dies and degenerates gradually, so that eventually the branch seems to end in a small upright tree. When it has spread over the whole crown (Fig. 3d), this process gives the adult tree its very characteristic "candelabra" habit. The development of these small trees in the crown can cause the trunk to bend, though generally only slightly,

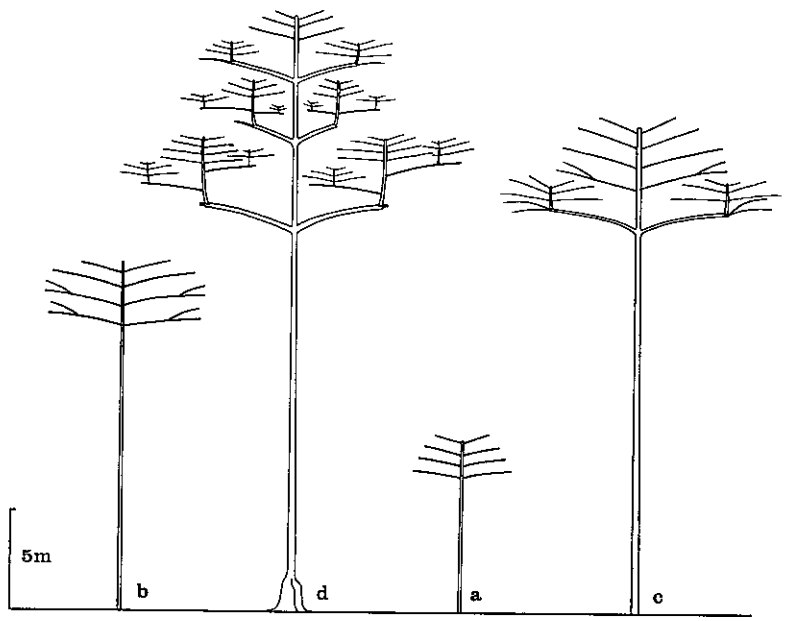


**Fig. 3.** (a, b) *Virola surinamensis*—young stages conforming to Massart's model; (c) development of small trees on some branches; (d) crown architecture of the adult tree.

as their pattern of appearance on each branch whorl allows for a symmetrical distribution of weight.

The shoot system of the tree must react against the tendency of its different parts to droop. Nevertheless, the examples we have analyzed show that wood production can also respond to other imperatives. It may be linked with the expression of ontogenetic processes—differentiation, metamorphosis, and reiterative patterns—which have nothing to do with support problems.

## VARIOUS MECHANICAL PROBLEMS ENCOUNTERED IN ROOT SYSTEMS

In subterranean systems, roots are also sensitive to gravity but they are included in the soil and they have no problem about support. They are under the influence of the shoot systems that they have to stabilize. This role needs several mechanical properties. Stabilization of the tree is based on the general shape of its root system. In outline it is a disk-like structure (Fig. 4) composed of big perennial roots which are superficially buried in the soil and radiate far from the collar (Atger *et al.*, 1994). This disk is sometimes strengthened with oblique roots (Raimbault, 1991). This group of roots prevents the tree from falling over. Furthermore, one or several tap roots anchor it. We have to notice that, contrary to what can be seen in the literature, the horizontal extent of roots can be much greater than the height of the trunks and the tap roots are generally much smaller. We study several variations of this organization.

### Tree Anchorage

There are several species in which stability and anchorage are provided by the tap root, for instance, *Anaxagorea dolichocarpa* (Fig. 5). This is a small tree from the swamp forest of the Guyanas. It does not exceed 15 m in height.

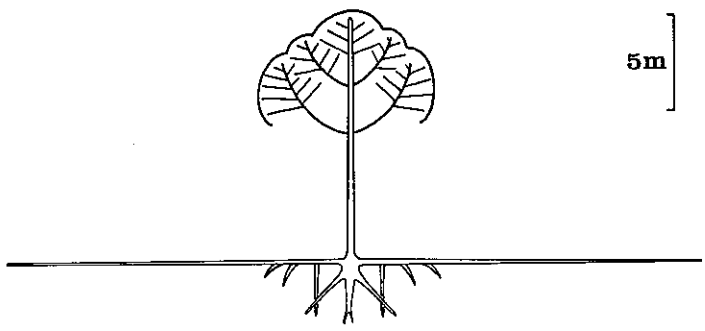


**Fig. 4.** General architecture of shoot and root system in trees.

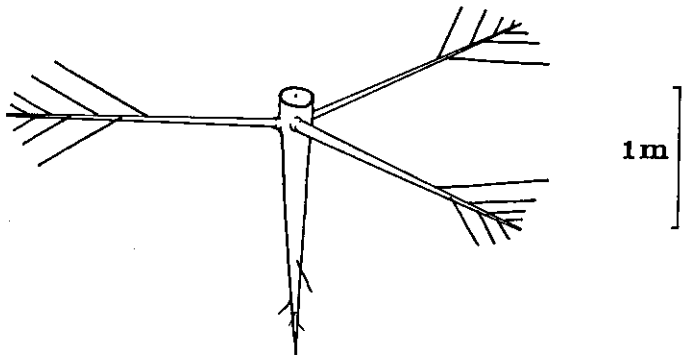


**Fig. 5.** *Anaxagorea dolichocarpa*: a view of the root system.

Its root system is composed of a straight tap root bearing, near the collar, a whorl of three or four sinuous perennial horizontal roots. Laterally, these horizontal roots bear two rows of thin roots which are short-lived and disappear quickly. The tap root is 1.5 to 2 m in length and 10 cm in diameter near the collar, whereas its perennial laterals are only 3 m in length and 3 cm in diameter near its base. During the disinterring of the root system, the cutting of these horizontal laterals does not result in the tree falling but only reduces its stability. In this species, the tap root represents the greater part of the mechanical support of the plant during its whole life.

In other species, such a situation can be observed only at the beginning of ontogenesis. With germination, the tap root develops more quickly than its laterals or the shoot; in the same way, its diameter increases more quickly than that of the lateral roots. The tap root is then the major part of the vegetative system of the seedling. For several years, it provides the stability of the young plant. Later this function is transferred to the horizontal roots which develop more than the tap root.

## Horizontal Stability

The greater part of tree stability is devoted to the horizontal system. Its organization, like a disk, is adapted to this need provided that it is well secured and rigid enough. Trees can respond to such a need by different properties such as root tension, cambial growth, and forking of roots.

### *Root Tension*

In several species of *Clusia* (Fig. 6), the seedling germinates in the crown of a host tree; more frequently, in a fork of its main branches. To reach the soil, it quickly develops a tap root, which goes down freely along the trunk. As

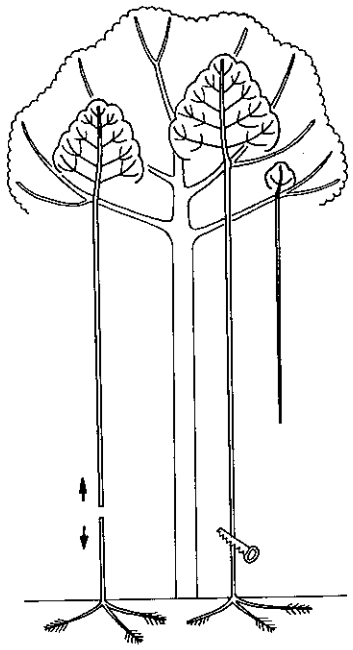

**Fig. 6.** Development of the root system of *Clusia* sp. and experimental demonstration of tension in tap roots.

its distal part touches the soil, it branches and several horizontal roots begin to form. At the same time, the tap root begins to be in tension. If one cuts it at the height of a man, one can indeed observe that its two ending parts separate and cannot be joined again without forcing them together. This retraction of tap root tissues is the consequence of the anchorage of its end part. When such a phenomenon occurs on horizontal laterals, as can be observed in several other species such as *Cecropia obtusa* and *Ficus* spp, it is the whole root disk which goes under tension and braces the tree.

### *Formation of the Forks*

The pattern of branching in horizontal perennial roots leads to the formation of forks, which play a direct part in tree stability. *C. obtusa* shows such a pattern of branching (Fig. 7). Its root system is composed of a tap root 60 cm in length bearing, near the collar, a whorl of horizontal perennial roots. The basal part of these roots forms several successive forks composed of three members: two horizontal ones and a third vertical one, which branches from the lower face of the fork and penetrates deeply into the soil. At the end of these perennial horizontal roots, some forks can be found, but they are quite different. They are

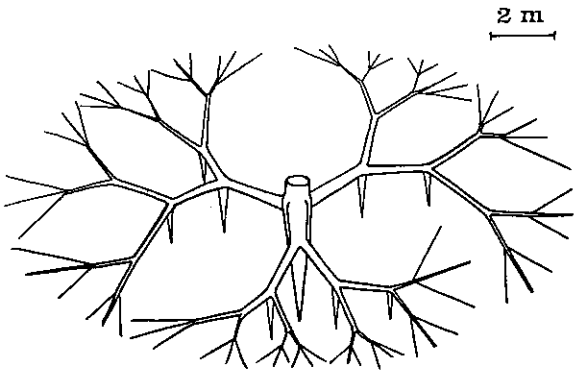


**Fig. 7.** Horizontal stability of the *Cecropia obtusa* root system: development of forks and supplementary tap roots on the perennial horizontal roots.

composed of three horizontal members: the perennial root and two of its shedding laterals, which are subopposed. These two patterns of branching allow the root system to radiate widely on soil surface and are the basis of the spreading of the root system. Furthermore, these three branched forks act as anchorage points which prevent any slipping of roots during an eventual tilting of the trunk.

### *Cambial Growth*

The large diameter of the perennial roots—about several dozens of centimeters—is one of the most important properties which contributes to the rigidity of the root disk and to the stability of the tree. But many structures increase this rigidity, such as root grafts, butresses, and adventitious roots.

*Root Grafts.* The root system of the plane tree (*Platanus hybrida*, Platanaceae) is composed of a whorl of perennial horizontal roots branching in one or two forks near the collar (Fig. 8a). Some additional roots appear on that structure later (Fig. 8b). During their growth these additional roots intertwine and come into contact one with another; their cambium goes into fusion (Fig. 8c). Gradually, they develop as a net of grafted roots which, with cambial growth, turns into a solid plinth around the base of the tree (Fig. 8d). The development of these additional roots goes on for a long time so that the plinth is continually strengthened.

In several species, the capacity of roots to enter into fusion can play a major role in the mechanical support of the plant. Strangling figs, for example, begin their life by germinating in the crown of a host tree (Fig. 9a). They quickly develop two or three tap roots which go down along the trunk, entwining it and branching (Fig. 9b). All these roots go into fusion and build something

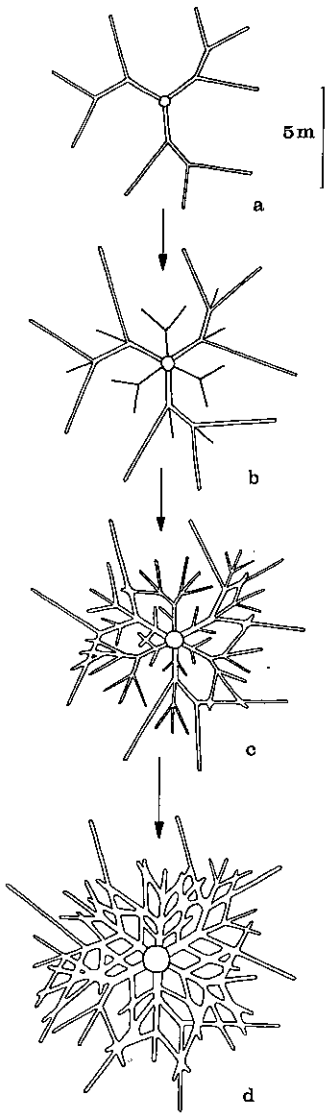


**Fig. 8.** Four stages in the development of the plane tree root system, showing the progressive grafting of roots.

like a framework around the host trunk, which gradually prevents its cambial growth and may eventually cause its death (Fig. 9c). In the same way, the entwining and the strengthening of these grafted roots lead to the formation of a root trunk whose rigidity allows the tree to be self-supported (Ng, 1975).

*Buttresses and Stilt Roots.* At the base of the trunk, roots can form some

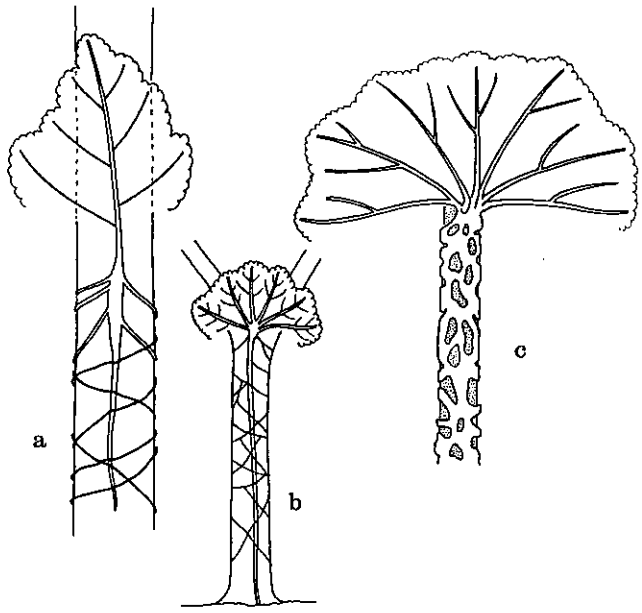


**Fig. 9.** Progressive grafting of roots allowing the strangling fig tree to self-support.

structures which prevent the tree from bending over. Buttresses are one example of such a structure (Fisher, 1982). Buttresses are a strip-like basal part of the perennial horizontal roots showing various shapes, which strengthen the meeting point between root and shoot. They are the result of an enhanced cambial growth of the upper part of the root, which leads to a vertical strip of wood joining the base of the trunk to that of these laterals. They have two origins: first, cambial growth concerns horizontal perennial roots already developed (Figs. 10a and b); and second, buttresses are formed from adventitious roots developing later at the base of the trunk (Fig. 10c). In these two cases the effect on tree support is the same. Some adventitious roots can act differently. *C. obtusa*, for example, strengthens its root system by developing stilt roots around the base of its trunk later. These roots are like arches and firmly hold up the trunk (Fig. 11).

## DISCUSSION AND CONCLUSION

This rapid survey has enabled us to present a few situations which may serve as models for biomechanics research. Many other situations occur, particularly those that are the result of trauma. We know that when a tree bends

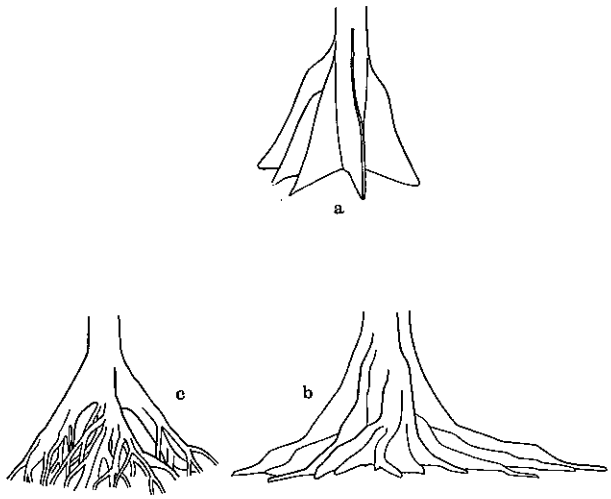


**Fig. 10.** (a, b) Various shapes of buttresses in tropical trees; (c) buttresses developed from adventitious roots.

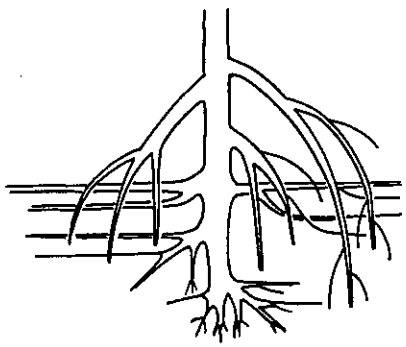

**Fig. 11.** Adventitious stilt roots in *Cecropia obtusa*.

as the result of an accident—say, when it has been partially uprooted—this deformation may cause the trunk and the branches to straighten up, and reaction wood is formed. Such an incident also has repercussions on the root system. On the other hand, when a part of the crown disappears after a drastic natural or artificial pruning, the tree reacts to reestablish harmony in the mass weighing on the crown. These phenomena are often mentioned, so we preferred to discuss less common situations. If we consider all these examples, we notice that the study of tree mechanics in the field must take into account two complementary aspects. First, we must analyze the static structure of the tree and understand

the forces which assure the stability of a shoot or root branched system spreading around one central axis. But this is not enough. The tree is an organism which undergoes constant changes. Its ontogeny is constantly creating new situations that the organism must control from a mechanical point of view by a specifically adapted production of wood according to problems that arise: development of the existing structures, changes in the growth direction of axes, torsion, etc. To understand tree mechanics, one must necessarily take these factors into account.

The study of trees shows how careful one must be in defining general models. Architecture and ontogenesis, cambial activity, and wood structure vary according to species, thus creating a great range of different mechanical problems and specifically adapted answers. The latter vary according to the organs involved. The ability to produce wood is not the same in the trunk, branches, or twigs, and the age and physiological state of the tree influence this faculty to a great extent. Faced with so much diversity and detail, engineers and botanists need to collaborate closely so that the study of tree mechanics in the field may give good results.

## ACKNOWLEDGMENT

This is a publication of the Institut des Sciences de l'Évolution.

## REFERENCES

Atger, C., and Edelin, C. (1994). Premières données sur l'architecture comparée des systèmes racinaire et caulinaire des arbres. *Can. J. Bot.* (in press).

Barthélémy, D., Edelin, C., and Hallé, F. (1991). Canopy architecture. In Raghavendra, A. S. (ed.), *Physiology of Trees*, John Wiley & Sons, New York, Chichester, pp. 1–20.

Edelin, C. (1991). The monopodial architecture: The case of some tree species from tropical Asia. *Research Pamphlet* **105**, Forest Research Institute Malaysia,, Kuala Lumpur, Malaysia.

Fischer, J. B. (1982). A survey of butresses and aerial roots of tropical trees for presence of reaction wood. *Biotropica* **14**(1):56–61.

Hallé, F., Oldeman, R. A. A., and Tomlinson, P. B. (1978). *Tropical Trees and Forest. An Architectural Analysis*, Springer Verlag, Berlin.

Kollmann, F. F. P., and Coté, W. A. (1968). *Principles of Wood Science and Technology*, Springer Verlag, Berlin.

Ng, F. S. P. (1975). A note on natural root grafts in Malaysian trees. *Malays. Forest.* **38**(2):153–159.

Raimbault, P. (1991). Quelques observations sur les systèmes racinaires des arbres de parcs et alignements: diversité architecturale et convergences dans le développement. In Edelin, C. (ed.), *L'Arbre. Biologie et Développement*, Naturalia Monspeliensia, H.S., pp. 85–96.

*Biomimetics, Vol. 2, No. 3, 1994*

# The Biomechanics of Leaf Rolling[1]

**Bruno Moulia**[1]

*The transverse rolling of the graminaceous leaves submitted to water depletion is studied from a biomechanical point of view. It is shown that the "poor" rolling of some species such as maize is not related to a local "low ability" of transverse curvature, but to a structural effect due to the coupling of curvatures within the shell structure made by the whole leaf. This is demonstrated through both an experimental study of free curvatures and a mechanical modeling of leaf rolling at the whole-leaf level. It is thus argued that the differences in the rolling response between species or cultivars may be linked to structural mechanical effects which have been overlooked in past studies, and which can be studied only by a biomechanical approach.*

**KEY WORDS:** leaf rolling; structure mechanics; water stress; Graminaceae.

## INTRODUCTION

Leaf movements are a common response to water depletion (Begg, 1980). In many graminaceous plants, the major change in leaf shape associated with water stress is a transverse rolling of the blade (Shield, 1951; Sobrado, 1987; O'Toole and Cruz, 1979, 1980; Hsiao *et al.*, 1984). Several authors have argued that leaf rolling is of adaptive value. Studies have demonstrated that it decreases the transpiration through changes of the "effective" leaf area (i.e., submitted to incident radiation) and of the boundary layer of the leaf (Lemée, 1950; O'Toole and Cruz, 1979; Begg, 1980). The efficiency of this water-saving mechanism may, however, vary with species (see for a minireview see Moulia, 1993). Thus, throughout the century, a research effort has been directed to the study of the

[1]This is the published version of a paper presented at the Plant Biomechanics Congress, Montpellier, France, September 5-9, 1994.

[2]U.R. Bioclimatologie, INRA, F-78 850 Thiverval-Grignon, France.



1059-0153/94/0900-0267$07.00/0 

relationship between rolling and water status of the leaf, both by botanists [to establish the anatomical basis of such an adaptation (e.g., Burström, 1942; Shield, 1951)] and by agronomists [to improve our knowledge of the behavior of crop canopies under water deficit (e.g., O'Toole and Cruz, 1979, 1980; Hsiao *et al.*, 1984; Matthews *et al.*, 1990)].

At the whole-leaf level, there seem to be two kinds of relations between the mean hydric status (usually measured as the leaf water potential $\Psi$; see Appendix) and leaf rolling [measured mostly by visual scoring; see Moulia (1993) for more details on the various measurements of leaf rolling]. These typical relations are sketched in Fig. 1. Some species, such as rice and tall fescue, display a rather complete rolling (type 1), whereas others, such as maize and some sorghum, roll much less (type 2). Moreover, both the range of water potential in which the leaf rolls and the shape of the rolling curve are clearly distinct; Type 1 leaves display an almost-linear increase in rolling over a large range of water potentials (approx 2 MPa, after an initial threshold), whereas type 2 leaves show a sigmoid curve, in which the rolling is limited to a much smaller range (approx. 0.6 MPa).

At the anatomical level, the focus has been mainly on the putative role of special motor cells, also called bulliform cells (Burström, 1942; Shield, 1951; Ellis, 1976). The discussion is based mainly on considerations of the correlation between the degree of leaf rolling and the amount and deformation of bulliform cells, that is, on a possible cellular basis for differences in the rolling response.

However, from a mechanical point of view, the leaf blade of the Graminaceae is a shell-like structure (not developable within a plane). Thus, there is a mechanical coupling of the changes in curvature within the leaf structure. If

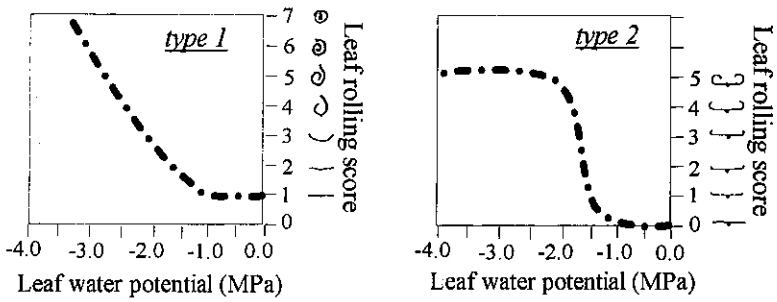


**Fig. 1.** The two types of relations between the mean water potential and the transverse rolling of graminaceous leaves. The degree of transverse rolling of the whole leaf is usually estimated by visual comparison to a scoring scale of typical transverse shapes (which are figured along the ordinate axis). The type 1 curve is redrawn from data for rice (O'Toole and Cruz, 1980; Hsiao *et al.*, 1984) and tall fescue (Viratelle, 1992), and the type 2 curve from data for maize (Sobrado, 1987) and sorghum (Begg, 1980). See Moulia (1993) for a more complete review of the literature on leaf rolling.

such coupling is important, it may prevent the display of the transverse rolling. As a matter of fact, it is noteworthy that type 1 rolling corresponds to species with very flexible blades, whereas type 2 plants have larger leaves with a stiff midrib.

The purpose of this paper is to report investigations of the importance of such structural effects in the determinism of leaf rolling. The general idea is to concentrate on the study of a type 2 plant, maize (*Zea mays* L.), and to try to determine the reasons for such a "poor" rolling behavior. The hypothesis to be tested is that the mechanical coupling of curvatures within the leaf structure is the major cause that explains the phenomenology of type 2 leaf rolling. Before going on to our results, however, it is necessary to recall the main features of the maize leaf.

## GENERAL MORPHOLOGY AND MECHANICS OF THE MAIZE LEAF

The mature (i.e., no longer growing) maize leaf is a slender structure, with bilateral symmetry. Its size varies with leaf rank (see Appendix) and also growing conditions. It is composed of a central thickened, curved midrib and of a much thinner part, on both sides of the midrib, which is henceforth referred to as the lamina (Fig. 2). Previous studies in our laboratory demonstrated that the midrib is the major stiffening element that influences the longitudinal bending rigidity of the leaf (Moulia *et al.*, 1994). It can be modeled as a tapered composite beam (Moulia and Fournier, 1994). Moreover, it has been demonstrated

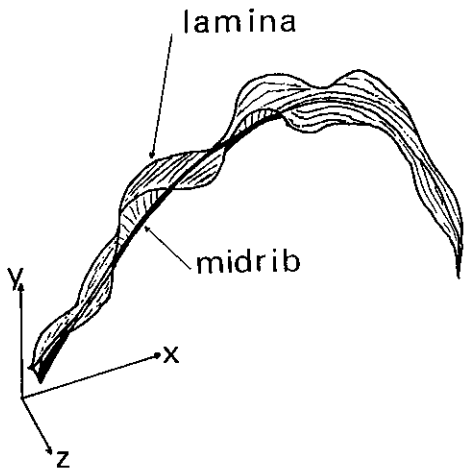


**Fig. 2.** General morphology of the mature maize leaf (redrawn from Moulia *et al.*, 1994).

(Moulia *et al.*, 1994) that, in mature leaves (see Appendix), the midrib is curved downward even when the instantaneous bending under its own weight is removed. More details on the morphology and the internal material structure (anatomy) of maize leaves are given by Sharman (1942) and Moulia (1993).

When submitted to water depletion, the maize leaf displays, as stated, type 2 transverse rolling. However, the amount of rolling at a given water status varies among the leaves, with the leaf rank (upper younger leaves usually roll more than lower ones), and within the leaf (the tip is usually more rolled than the middle of the leaf). Moreover, leaf rolling in maize is compounded with a trend to longitudinal straightening (seen mostly in the upper leaves), as seen in photographs of plants profiles and leaf habits (Downey and Miller, 1971; Viratelle, 1992). Notice that this empirical correlation is qualitatively in accordance with our hypothesis of mechanical coupling of the curvatures but could also be explained by a decrease in the self-weight loading due to water loss and, hence, concomitant to the rolling.

## EXPERIMENTAL STUDY OF LOCAL "FREE" CURVATURES

If our hypothesis is correct, then a corollary is that a piece of the lamina isolated from the leaf blade should display increased transverse rolling when submitted to water depletion. This corollary has been tested experimentally. A detailed description of this experiment is given by Moulia (1993) and is being published elsewhere. The general principle has been to submit a transverse specimen from the lamina to various controlled water statuses. The water conditioning has been obtained by bathing the specimens in solutions of polyethylene glycol (PEG 6000) of various known water potentials. The water potentials range from 0 to $-3.5$ MPa, as rolling typically occurs between these values. PEG was used, as it does not enter the cells, avoids respiration losses, and has been shown to have no toxic effects on maize tissues (Hohl and Schopfer, 1991). The transverse shape of the specimen at hydric equilibrium was recorded by photographs and two-dimensional (2D) digitizing (Fig. 3), and the transverse curvatures estimated using the sliding vicinity program Courb2D (Moulia *et al.*, 1994).

Figure 4 shows three typical transverse shapes at $\Psi = 0$, $-2.8$, and $-3.5$ MPa. It is clear that transverse rolling increases with drying. Moreover, at a given water potential, transverse rolling of a specimen isolated from the structure can be much more important than that observed in the whole leaf. This is particularly clear at $-3.5$ MPa, where rolling is almost complete and very similar to that observed in rice or tall fescue (compare with the sketches in Fig. 1).

When the curvatures along the specimen are calculated, there is no significant trend of change with the distance from the midrib (i.e., from the midrib

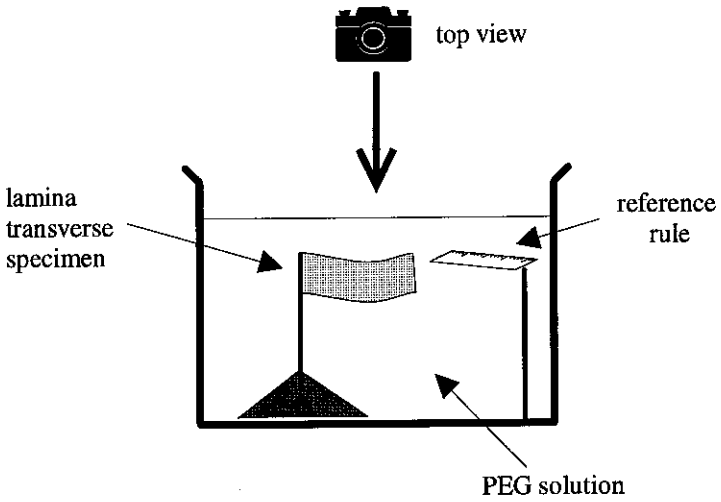


**Fig. 3.** Experimental design for the study of the free transverse curvatures related to changes in water status.

side to the edge of the transverse specimen). Thus the mean curvature can be estimated for each specimen. The graph of mean transverse curvature versus water potential is given in Fig. 5, showing an exponential relation. No effect of the initial position within the leaf or of the leaf of origin was detectable. Finally, the transverse curvatures are completely reversible (data not shown), so that the response curve of curvature vs potential at static water equilibrium is biunivocal (at least for the studied population of leaves, obtained under homogeneous growing conditions).

As a conclusion for this experimental study, our results are completely in accordance with our initial hypothesis. Free lamina transverse rolling is much more important than in the whole leaf structure and is homogeneous along the leaf, as between leaves. The next step is to study the mechanical (structural) effects within the leaf, to test if they can effectively explain the hindering of the rolling behavior in the whole leaf. This requires mechanical modeling.

## MECHANICAL MODELING OF LEAF ROLLING

Dealing with such a complicated structure as plant organs, there is *a priori* a very large number of material and structural characteristics that may play a part in the determination of their mechanical behavior. Much of the challenge of mechanical modeling is thus to incorporate enough complexity to be sufficiently realistic, but not too much, in order for the model to remain tractable

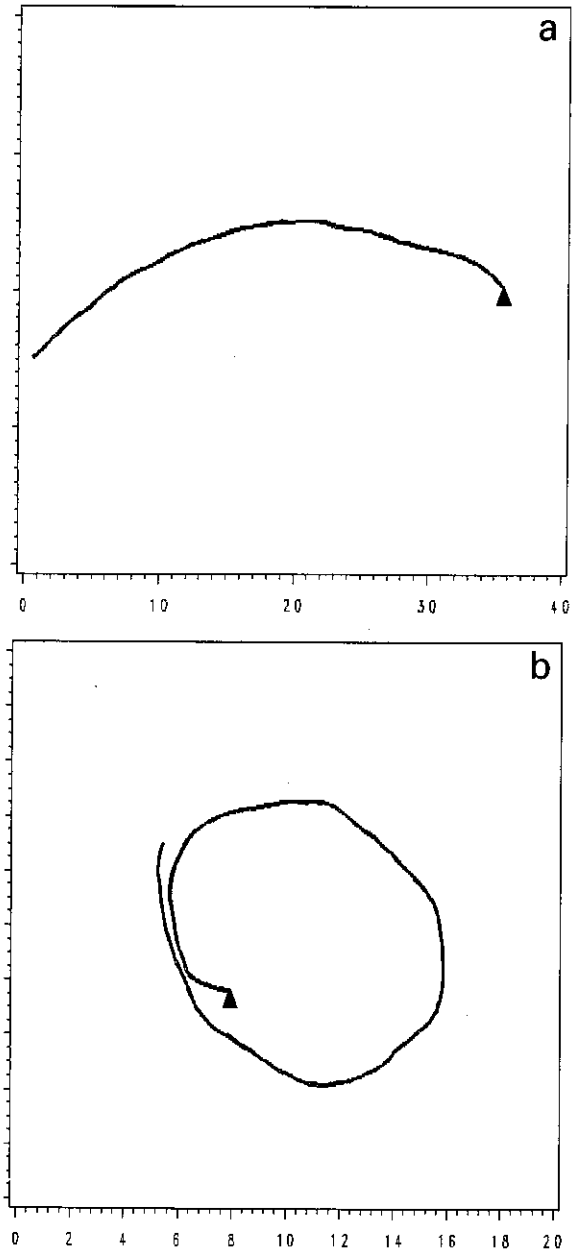


**Fig. 4.** Typical transverse shapes of the lamina specimens at three water potentials $\Psi$: (a) $\Psi = 0$ MPa (pure water); (b) $\Psi = -2.8$ MPa; (c) $\Psi = -3.5$ MPa. The shapes are obtained from the digitizing of the photographs. The black triangle represents the position of the midrib, with the top of the triangle directed to the upper (adaxial) part of the leaf.

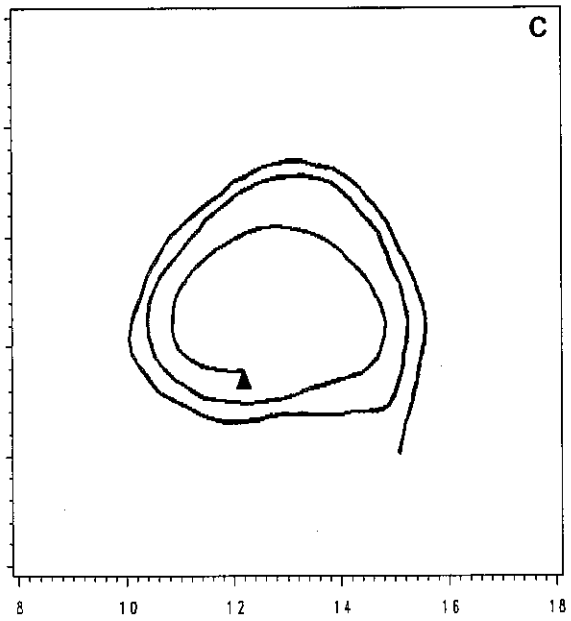


Fig. 4. Continued.

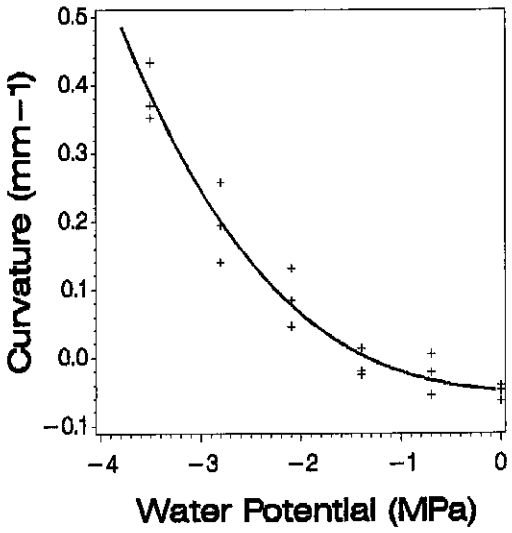


Fig. 5. Relation between mean transverse free curvature and mean water potential (at hydric equilibrium).

and understandable. It is worth discussing these underlying modeling choices, in order for the model to be understandable.

## Structural Geometry

The maize leaf has been modeled as a thin shell with a varying width, stiffened by a tapering and initially curved beam, representing the midrib. The lamina structure is thus seen as an assembly of shell elements, and the purpose of the mechanical model is to determine the behavior of the whole structure, given the constitutive laws of the shell elements of the "lamina" and of the beam elements of the "midrib." The whole structure is taken as symmetrical about the vertical plane. The width of the lamina is given by a biometrical model (Prevot *et al.*, 1991). No attempt has been made to model the wavy shape of its edges.

## Rheology of the Shell and Beam Elements

The constitutive law of the lamina has been considered as analogous to the linear thermoelastic rheological model. This is the simplest way to generalize the linear elasticity [described experimentally for grass lamina by Vincent (1982) and Moulia (1993) among others] to take into account the occurrence of the (previously described) free strains due to changes in the water status. It states only that any mechanical configuration in which the shape of a piece of the lamina differs from its free shape at a given local water status generates elastic internal stresses (which is called hydric autostresses). Such a thermoelastic analogy was also proposed by Vincent and Jeronimidis (1991), but at a tissue level. It is based on the underlying assumption that the present local water status is not influenced, at a first order, by the changes in the mechanical state.

The material within the lamina has been taken as axially anisotropic, in terms both of free strains and of elastic rigidities. The only water-induced free strain that has been retained in the model concerns the transverse curvature of the lamina, as described in the previous section (notice that the relation between water potential and free curvature is nonlinear).

No attempt was made to incorporate the effects of changes in lamina thickness, which were also reported to occur with changes in water status (Rashke, 1970). In thin shells, these former strains are thought to be geometrically compatible and, thus, of no autostressing effect. (Their only influence is thus on the linear transverse rigidities of the lamina, an effect that can be tested through the sensitivity analysis of the model.) As no longitudinal and transverse shrinkage has (to our knowledge) ever been reported within the ecophysiological ranges of water status, they have not been taken into consideration either.

The linear membrane and bending rigidities of the lamina are also taken as axially anisotropic, with a principal axis of anisotropy in the longitudinal

direction [the maize lamina, as other grass leaves, has longitudinal and parallel ribs, which makes the lamina similar to an oriented fibrous composite (Vincent, 1982; Moulia, 1993)]. The local elastic bending behavior of the midrib is given by a composite beam model (Moulia and Fournier, 1994). Here again, and for the same reasons as for the lamina, no transverse shrinking with water status has been retained.

## Loading

The only loads that have been taken into account is the occurrence of the autostress field related to changes in free curvatures due to changes in water status (i.e., a rheological autostressing). It is assumed also that the water status can vary only longitudinally (i.e., the water status is homogeneous along any transverse line going from the midrib to the lamina edge). Thus, the loading is also symmetrical about the vertical plane. Finally, for the sake of simplicity, self-weight has been neglected, as it can take action only as resisting bending moments and is, thus, equivalent to increased bending rigidity.

## Kinematics

When the maize leaf rolls, it is obvious that large rotations occur. Thus, for the model to provide morphologically realistic outputs, it is necessary to include the structural nonlinearity due to the large displacements. In other respects, it has been assumed in this first version of the model that the transverse shape of the lamina is always an arc of a circle (as free curvature was previously shown to be constant across the lamina). Moreover, we have assumed pure 2D bending [as the mechanical problem has a bilateral symmetry and as the whole leaf remains a very slender structure with a longitudinal aspect ratio (length/width) larger than 10]. As a consequence, the transverse bending plane is supposed to remain orthogonal to the central line of the midrib (no intralamina shearing).

## Mechanical Solving of the Problem

This mechanical problem cannot be handled analytically. The complexity of the structure forces to a discretization, to reduce the domain of possible strain fields. We have used semianalytical modeling. The basic element is presented in Fig. 6. It is truss, with a midrib subelement composed of articulated bars (discretizing the longitudinal beam in pure bending) and a lamina subelement with transverse curved beams (discretizing the transverse bending behavior) related by longitudinal ropes (representing the tensile behavior of the lamina). The whole structure is assembled as described in Fig. 7.

The total mechanical energy of the whole discretized structure at a given

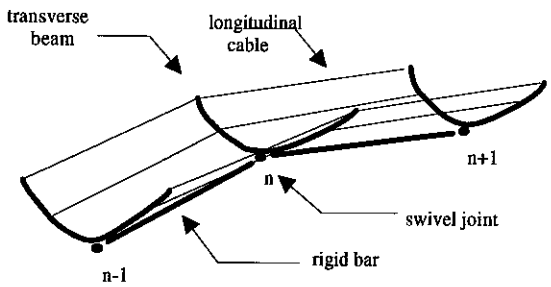


**Fig. 6.** Schematic drawing of the basic element of the leaf model (see text for explanations).

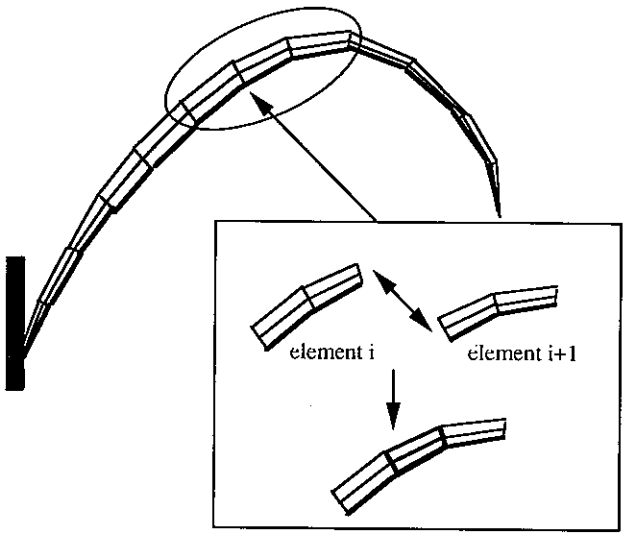


**Fig. 7.** The assembled whole structure (i.e., the modeled "leaf"). Two successive elements have one longitudinal bar and two transverse beams in common (C1 continuity).

"water status" can thus be calculated, given the initial "natural" (i.e., unloaded) geometry, the water-driven change in free curvature, and the rigidities of the midrib and of the lamina (transverse bending lineic rigidity and longitudinal tensile lineic rigidity). The mathematical expression of the model is not detailed here, and is given by Moulia (1993).

The equilibrium configuration is then determined through a numerical minimization of this total energy, the command variables being the longitudinal and transverse curvatures. Such an iterative method is required because of the nonlinearity of the problem related to large displacements (Curnier, 1993). Although

the numerical details are not given here (for a more complete discussion see Moulia, 1993), it should be noted that one of the main problems with a structurally nonlinear problem is that the equilibrium solution is not necessarily unique. The model has been implemented as a C program, called Leafroll.

## SIMULATION RESULTS

The ranges of realistic values for the lamina rigidities required for the model were estimated experimentally using a miniaturized testing machine [see Moulia (1993) for a description of the experiments and of the way to estimate the model parameters from them]. These data being obtained, a series of simulations has been done to test the sensitivity of the model outputs to changes in the various geometrical and material parameters. The only results presented here concern the study of the effect of the initial longitudinal shape (habit) of the leaf. Two initial (really observed) longitudinal habits have been compared (Fig. 8a). The first one is "weeping," corresponding to a typical leaf from the basal part of the plant; the second one is less curved, representative of leaves higher up the plant. All the other parameters of the model are the same in the two cases (including the values for numerical initiation). The loading corresponds to a change in water potential $\Psi$ from $-1.4$ to $-2.5$ MPa, which is the range in which rolling has been reported to occur in maize (see Fig. 1b). The related change in free curvature corresponds to a free rolling of one complete whorl in the part of the leaf with the largest width. Notice also that the potential (and hence the free curvature) has been taken as spatially homogeneous (no gradient of $\Psi$ along the leaf). The initial transverse geometry (i.e., at $\Psi = -1.4$ MPa) was supposed to be flat (i.e., corresponding to the free transverse curvature at this potential). The equilibrium configurations are presented in Fig. 8. Figure 8a shows the longitudinal habits, whereas Fig. 8b represents the width of the orthogonal projection of the lamina on the initial (flat) surface of the leaf. First it is clear that a large part of the transverse rolling cannot be expressed due to the structural shell effects. As stated, this is due to the structural coupling of transverse rolling and longitudinal straightening. Notice also that both the changes in longitudinal curvatures and the degree of transverse rolling are heterogeneous along the leaf. The tip (where the midrib is much less stiff) rolls and straightens much more than the rest of the leaf. Finally, there is a strong effect of the initial habit on both the transverse rolling and the longitudinal straightening. The initially curved leaf rolls and straightens less than the more erected one.

Thus, the shell structural effects existing on the maize leaf can explain (at least qualitatively) the observed morphology of leaf rolling in maize and its empirical correlation with a more or less important longitudinal straightening. Both the longitudinal changes in the degree of rolling along a given leaf and the changes in the degree of rolling between the droopy basal leaves and the upper,

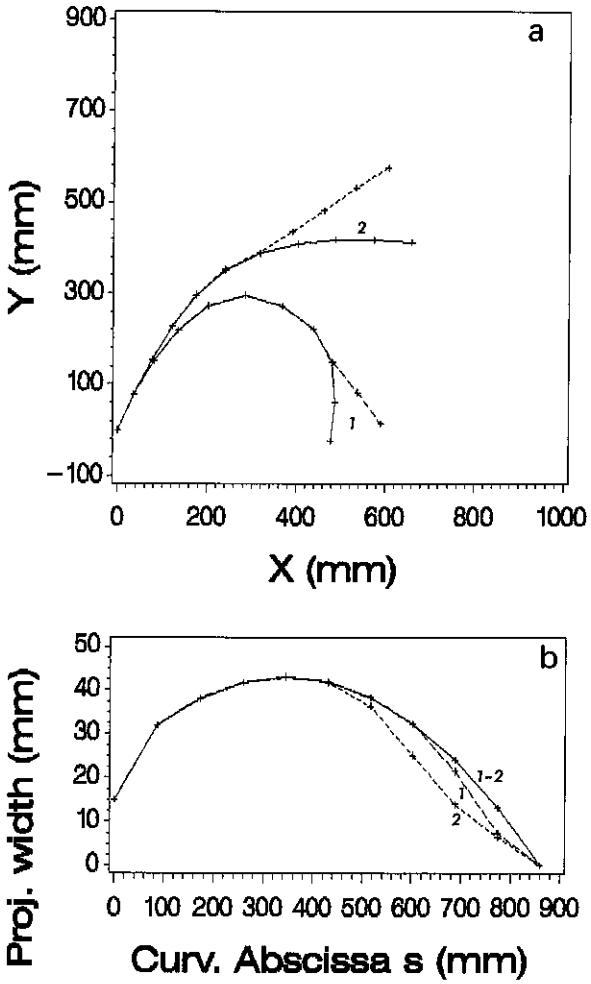


**Fig. 8.** Effect of the initial longitudinal habit of the leaf on leaf transverse rolling and longitudinal straightening: (a) leaf longitudinal profiles (i.e., habit of the midrib); (b) changes in the projected width of the lamina along the leaf (the position being measured by the curvilinear abscissa along the midrib, with the origin at the base of the leaf). (1) Leaf with a "weeping" initial longitudinal habit; (2) leaf with a more straight longitudinal habit. (+ —— +) Initial (unloaded) state; (+ - - - +) equilibrium state. See text for explanations about the values of the parameters.

more erect (but still adult) leaves can be simulated without any spatial gradient in the local water status of the lamina. Finally, the study of the sensitivity of the model to changes in its parameter values shows that the more important parameters are the initial longitudinal habit (as detailed above) and the bending stiffness of the midrib (data not shown; see Moulia, 1993). The more longitudinally curved and the stiffer the midrib, the less the observed rolling in the entire leaf.

## CONCLUSION

The initial purpose of the work reviewed here was to investigate the control of leaf rolling in graminaceous plants and to explain the "poor" rolling of maize- and sorghum-type leaves. It is demonstrated that this phenomenon is not related to some intrinsic inability of the maize lamina to roll (for example, an anatomical peculiarity). Moreover, it is shown that the structural mechanical effects within the leaf can explain the morphology of leaf rolling in maize. It is thought that this illustrates the usefulness of mechanical models in botany, to allow for a change of scale and to account for specific structural effects. Further work will concentrate on generalizing the discretized model (to test the effect of some assumptions concerning the transverse curvature or the shearing of the lamina), on microbiomechanical study of the determinism of free rolling, and also on the biomechanics of the curving of the midrib during the growth of the leaf.

## APPENDIX: DEFINITIONS OF THE MAIN TERMS USED

**Water potential:** This is one of the most popular variables used in plant sciences to characterize the hydric status. It is defined as the amount of work that must be given to 1 unit of volume of water in the considered system to bring it back to a reference state, called "free water" (i.e., pure water at the same temperature and normal atmospheric pressure), through an isothermal and quasi-static transformation. It is thus a local intensive variable, having the unit of a pressure (usual unit, MPa). Referring to "the water potential of a leaf" thus means a spatial homogenization, leading to an "equivalent water potential."

**Leaf rank:** The number of the leaf within the sequence of leaf emergence (the first leaf to emerge has rank 1).

**Mature leaf:** This is a leaf in which both growth and differentiation (especially lignification) are achieved.

## ACKNOWLEDGMENT

Drs. Meriem, Fournier, and Christine Girousse are particularly acknowledged for their contribution to the theoretical and experimental works that are reviewed here. I also thank Pr.D. Guitard for its useful suggestion of using a semianalytical approach for the model.

## REFERENCES

Begg, J. E. (1980). Morphological adaptations of leaves to water stress. In Turner, C. N., and Kramer, P. J. (eds.), *Adaptation of Plants to Water and High Temperature Stress*, J. Wiley & Sons, New York, pp. 33–42.

Burström, H. von (1942). Über Entfaltung und Einrollen eines mesophilen Grasblattes. *Botan. Notiser* **1942**:351–362.

Cumier, A. (1993). *Méthodes Numériques en Mécanique des Solides*, Presses Polytechniques et universitaires romandes, Lausanne.

Downey, L. A., and Miller, J. W. (1971). Rapid measurements of relative turgidity in maize (*Zea mays* L.). *New Phytol.* **70**:555–560.

Ellis, R. P. (1976). A procedure for standardizing comparative leaf anatomy in the Poaceae. I The leaf blade as viewed in transverse section. *Bothalia* **12**:65–109.

Hohl, M., and Schopfer, P. (1991). Water relations of growing maize coleoptiles: Comparison between mannitol and polyethylene glycol 6000 as external osmotica for adjusting turgor pressure. *Plant Physiol.* **95**:716–722.

Hsiao, T. C., O'Toole, J. C., Yambao, E. B., and Turner, N. C. (1984). Influence of osmotic adjustment on leaf rolling and tissue death in rice (*Oryza sativa* L.). *Plant Physiol.* **75**:338–341.

Lemée, G. (1950). Sur l'efficacité de l'enroulement des feuilles de graminées contre la transpiration. *C.R. Acad. Sci.* **230**:1201–1203.

Matthews, R. B., Azam-Ali, S. N., and Peacock, J. M. (1990). Response of four sorghum lines to mid-season drought. II Leaf characteristics. *Field Crop Res.* **25**:297–308.

Moulia, B. (1993). *Etude mécanique du port foliaire du maïs*, Thèse Doct. Univ. Bordeaux I, Bordeaux.

Moulia, B., and Fournier, M. (1994). Mechanics of the maize leaf: A composite beam model of the midrib (submitted for publication).

Moulia, B., Fournier, M., and Guitard, D. (1994). Mechanics and form of the maize leaf: *In vivo* qualification of the flexural behaviour. *J. Mater. Sci.* (in press).

O'Toole, J. C., and Cruz, R. T. (1979). Leaf rolling and transpiration. *Plant. Sci. Lett.* **16**:111–114.

O'Toole, J. C., and Cruz, R. T. (1980). Response of leaf water potential, stomatal resistance and leaf rolling to water stress. *Plant. Physiol.* **65**:428–432.

Prévôt, L., Ariès, F., and Monestiez, P. (1991). Modélisation de la structure géométrique du maïs. *Agronomie* **11**:491–503.

Raschke, K. (1970). Leaf hydraulic system: rapid epidermal and stomatal responses to changes in water supply. *Science* **167**:189–191.

Sharman, B. C. (1942). Developmental anatomy of the shoot of *Zea mays* L. *Ann. Bot.* **6**:245–282.

Shield, L. M. (1951). The involution mechanism in leaves of certain xeric grasses. *Phytomorphology* **1**:225–241.

Sobrado, M. A. (1987). Leaf rolling: A visual indication of water deficit in corn (*Zea mays* L.). *Maydica* **XXXII**:9–18.

Vincent, J. F. V. (1982). The mechanical design of grass. *J. Mater. Sci.* 17:856–860.
Vincent, J. F. V., and Jeronimidis, G. (1991). The mechanical design of fossil plants. In Rayner, J. M. V., and Wootton, R. J. (eds.), *Biomechanics and Evolution*, Cambridge University Press, Cambridge, pp. 21–36.
Viratelle, L. (1992). *Caractérisation de l'enroulement foliaire induit par la sècheresse chez deux graminées cultivées*, SEPF INRA, Lusignan.